

https://dspace.org/

Development and Evaluation of Adsorption coupling Biodesulphurization (AD/BDS) process for the desulphurization of South African Petroleum Distillates.

Sadare, Olawumi Oluwafokaleni

2018

https://hdl.handle.net/10539/26589

Downloaded from a DSpace repository. https://dspace.org/



Development and Evaluation of Adsorption coupling Biodesulphurization (AD/BDS) process for the desulphurization of South African Petroleum Distillates.

Olawumi Oluwafolakemi SADARE

(1592992)

A dissertation Submitted to the Faculty of Engineering and the Built Environment, University of the Witwatersrand, Johannesburg, South Africa, in fulfillment of the requirements for the degree of Doctor of Philosophy in Engineering.

Supervisor: Prof. M.O Daramola

October, 2018

Declaration

I declare that this dissertation is my own unaided work. It is being submitted for the degree of Doctor of Philosophy in Engineering to the University of the Witwatersrand, Johannesburg, South Africa. It has not been submitted before for any degree or examination to any other University



. …….. ……17th…… day of……October……../……2018……

Signature of Candidate Day Month Year

Dedication

I dedicate this dissertation to God almighty, the giver and sustainer of life, who has been my help from ages past, my hope for years to come, my glory and the lifter up of my head. This dissertation is also dedicated to my loving husband, Deacon Oluseye Sadare, my loving sons, Praise and Ifeoluwa and finally to my adorable daughter, Esther.

Abstract

Diesel is one of the most commonly used fuels, especially in the transport industry all over the world. During direct combustion of diesel, organic sulfur compounds are converted into SO_x. SO_x that form acid rain which cause damages to building, and loss of forests, resulting into destruction of ecosystem when it reacts with vapour in the atmosphere. Furthermore, the release of sulfur compounds into the atmosphere has resulted into health problems such as asthma, lung and heart disease and triggering of heart attack. Therefore, many countries have implemented regulations to refineries around the world to find a way of minimizing the emission of sulfur oxides into the environment. Currently, there is a stringent regulation that refineries in South Africa are expected to ensure a maximum specification of less than 5 ppm sulfur content in the petroleum distillates to levels equivalent to the Euro 5 emission standard by 2020. Therefore, there is a need to look for a better way of desulfurizing South African petroleum distillates to meet up with the stringent policies regarding emission of sulfur oxides. Research focus has been channeled towards hydrodesulfurization (HDS), adsorption (AD), biodesulfurization (BDS), oxidation and extraction. In addition, studies that will explore the combination of BDS with existing method e.g Adsorptive desulfurization (ADS) could be instrumental to achieving a higher reduction in sulfur-containing compounds in the petroleum distillates. In order to contribute to this research line, this study has focused on development and evaluation of adsorption coupling biodesulfurization (AD/BDS) process for the removal of sulfur-containing compounds from South African petroleum distillates.

The adsorbents (pomegranate and neem leaf powder) employed in the adsorptive desulfurization were successfully synthesized by activating with H_2SO_4 and then calcined at 500 ^oC. Carbon nanotubes were purified using HCl and acetic acid then functionalized using $KMnO_4$ and H_2SO_4. Activated carbon was used as-received for batch mode adsorption process, while it was immobilized with sodium alginate for use in continuous packed-bed adsorption experiments, so as to reduce clogging, pressure drop and increase adsorbent loading in the column.

The adsorbents were characterized using Fourier transform infrared (FTIR), Brunauer–Emmett–Teller (BET), scanning electron microscopy (SEM) equipped with energy dispersive x-ray (EDX), X-ray diffraction (XRD), and Raman spectroscopy for surface chemical functionalities, textural

property, morphological structure, chemical composition and structural and chemical information, respectively.

The adsorptive desulfurization experiments were carried out using a model diesel first and real diesel obtained from a typical refinery in South Africa. The model diesel was prepared by dissolving dibenzothiophene (DBT) in hexane. The desulfurized model diesel was analyzed using high performance liquid chromatography (HPLC) and gas chromatography/mass spectrometer (GC/MS). The adsorption performance of each adsorbent was evaluated in a batch mode and a continuous mode. Thereafter, the best adsorbent and operating parameters were used in AD/BDS coupling process. The mechanisms and the kinetic studies of the adsorption process were studied.

Biodesulfurization experiment was performed in a batch mode using growing and resting cells of *Pseudomonas aeruginosa* and *Pseudomonas putida* as biocatalysts. Model diesel used for biodesulfurization experiment was prepared by dissolving dibenzothiophene (DBT) in dimethylformamide (DMF). In addition, two different real South African diesel samples (diesel obtained before HDS (5200 mg/L) and diesel obtained after HDS (120 mg/L) were also used in this study. The best *Pseudomonas* strain, with highest desulfurization efficiency and best operating parameters were then used for the AD/BDS coupling process. The kinetic studies of the bacteria growth and diesel degradation were investigated as well.

In the AD/BDS experiment, real diesel was first transferred to a bed column packed with immobilized activated carbon as adsorbent, and then the desulfurized diesel obtained from the column was transferred into the bacteria basal medium consisting of resting cells of *Pseudomonas aeruginosa* for complete degradation. The desulfurized and the degraded diesel were analyzed using GC/MS. The adsorption performance of the packed-bed column and the degradation efficiency of *Pseudomonas aeruginosa* were evaluated. The kinetics of the AD/BDS process were studied

This dissertation has reported the adsorption performance evaluations of neem leaf powder (NLP) and pomegranate leaf powder (PLP), carbon nanotubes (CNTs), functionalized carbon nanotubes (FCNT) and activated carbon (AC) as promising adsorbents for removal of DBT from model diesel. The dissertation also reports for the first time in open literature the excellent percentage

DBT removal of PLP adsorbent and its adsorption mechanisms. The results show that PLP out-performed NLP by 9.88 %. PLP displayed 70.55 % percentage DBT removal and NLP displayed 65.78 % DBT removal.

As far as it can be ascertained, no study has been conducted on the use of $KMnO_4$/ H_2SO_4 treated-CNTs for removal of DBT from petroleum distillate. It can be concluded that the acid treatment of CNTs enhanced its surface affinity for DBT, thus contributed to the improved adsorption capacity of the adsorbent. Furthermore, the results show that functionalized CNTs out-performed the non-functionalized CNTs during the desulphurization by about 10 %, indicating that functionalization of the CNTs did improve the desulfurization performance of the CNTs. Therefore, the percentage performances of the adsorbents were 70.48 % and 60.88 % for FCNTs and CNTs, respectively. Furthermore, the results on adsorption of DBT onto activated carbon (AC) show that large surface area of AC contributed to its performance removal of the DBT in model oil. The percentage performance of the adsorbents was 83.84 %.

The results presented in this current study using different adsorbents, have demonstrated that AC out-performed all other adsorbents used in this study, owing to its exceptional higher surface area, micro structure and porosity. Therefore, AC was chosen for desulfurization of South African diesel samples. The results showed that large surface area of AC contributed to its performance removal of the DBT in the diesel samples. The percentage performance of the adsorbents for desulfurization of diesel obtained after HDS (99 %) was higher than that of the diesel obtained before HDS (60.41 %) at the same initial concentration of 120 mg/L.

The adsorption mechanisms of the adsorbents were extensively described using Langmuir and Freundlich isotherms. The adsorption kinetic studies were described using pseudo first-order, and pseudo second-order kinetic models. The results of the adsorption mechanism show that both Langmuir and Freundlich isotherm models could describe well the mechanism of the adsorption process for all adsorbents used in this study. The pseudo second-order kinetics described the adsorption kinetics of the adsorption process for all the adsorbents as well.

As it has been demonstrated in this current study, AC was successfully immobilized in sodium alginate for adsorption of DBT in model diesel in a continuous packedbed column. This is a

promising method of entrapping adsorbent for maximum performance. AC has been widely reported in literature for column adsorption of sulfur compound from petroleum distillates. However, there are only few studies on the immobilization of activated carbon in sodium alginate for use in bed column for desulfurization of petroleum distillate. Results show that adsorption of DBT in a packed-bed column are dependent on superficial velocity of the sorbate solution through the adsorption column. The best result was obtained at the lowest superficial velocity of 0.031 m/min (0.5 mL /min) at 15 cm bed height and lowest initial DBT concentration of 100 mg/L. Furthermore, breakthrough time was found to increase with decreasing DBT initial concentration, decreasing flow rate and increasing bed height. The initial region of breakthrough curve was well described by the Adams–Bohart model at all experimental conditions studied while the transient stage or working stage of the breakthrough curve was described well by the Thomas kinetics model.

The results presented in this current study have shown that, *Pseudomonas aeruginosa* and *pseudomonas putida* were successfully grown in basal salt medium. The growing and resting cells of both bacteria were used to degrade the DBT molecule in the model diesel. Results show that *Pseudomonas aeruginosa* showed better BDS performance than *pseudomonas putida* in all aspect. The results in this study also showed that *pseudomonas aeruginosa* and *pseudomonas putida* are capable of desulfurizing DBT in model diesels into less harmful compound, 2- HBP. The final product 2-HBP detected shows the specific activity of DBT desulfurization is 4S-pathway. Results showed BDS performance of 67.53 % and 50.02 %, by resting cells of *Pseudomonas aeruginosa* and *Pseudomonas putida*, respectively for 500 ppm initial concentration. In order to study desulphurization of diesel obtained from an oil refinery, resting cells studies by *Pseudomonas aeruginosa* were carried out which showed a decrease of about 30 % and 70.54 % DBT removal from 5200 ppm in diesel obtained before HDS and 120 ppm in diesel obtained after HDS, respectively. *P. aeruginosa* and *P. putida* selectively converted sulfur atom in DBT compound to 2-HBP. The results obtained in this study showed that biodesulfurization would be a better process to compliment HDS process rather than the main technique for desulfurization of organo-sulfur compounds in diesel.

As it has been demonstrated in this current study, adsorption coupling biodesulfurization process (AD/BDS) was used to remove sulfur compound from two different South African diesel samples. The bed column experiment showed that superficial velocity in the ascending order $0.031 < 0.063 < 0.094$ m/min, with flow rate in ascending order; $0.5 < 1.0 < 1.5$ mL /min. Results also show that adsorption of DBT in a packed-bed column is dependent on superficial velocity of the sorbate solution through the adsorption column. The best result was obtained at the lowest superficial velocity of 0.031 m/min (0.5 mL /min) at 15 cm bed height and lowest initial DBT concentration of 120 mg/L. This means that, a longer breakthrough time is needed for higher performance of the bed column which will successively result in higher adsorption capacity.

The kinetic models studied in this present work show that, Thomas and Bohart-Adam's model describe well the kinetics of the adsorption process for model diesel as well as for the South African diesel samples. The Bohart-Adam model described the initial region of the breakthrough curve, while the Thomas model described the transient stage of the breakthrough curve. First order kinetic model described well the microbial degradation of DBT in the model diesel and South African diesel samples and Michaelis-Menten kinetic model described well the microbial growth. Therefore, it was used to describe its kinetics. The results obtained in this study showed that AD/BDS coupling process is efficient for desulfurization of South African petroleum distillate (e.g diesel)

Acknowledgement

I give all the glory to God for the successful completion of my PhD degree programme. He has always been my provider, my all-sufficiency, my refuge and inspiration. He showed me mercy and stands by His promises concerning this journey. He has brought me this far and I will forever be grateful to Him.

My sincere appreciation goes to my supervisor, Professor Michael Olawale Daramola who has always been there for me, constructively criticizing my work, giving me scientific ideas and always ready to help with my research. I thank him for his moral and financial supports. I am indeed grateful sir. Thanks to his wife, Mrs Omotayo Daramola for her sisterly love and encouragements, at all times.

I will like to thank and appreciate Prof Samuel Afolabi for giving me the platform for my Masters Degree program which is a stepping stone to where I am today. Thanks for believing in me and for your moral and academic support always.

I am using this medium to thank the School of Chemical Engineering laboratory technicians, Bruce Mothibedi, Janet Smith and Motlatsi Phali for their constant assistance in providing me with all necessary equipment for my research work. Thanks to Prof Craig Sheridan, for giving me a space to work in his laboratory and to all postgraduate students working at Biochemical laboratory of School of Chemical and Metallurgical Engineering, University of the Witwatersrand for their assistance.

I will not fail to mention kindness of the workshop staffs towards me, Rodney Gurney, Hopewell Gumede, and Pathu Sikhwari, for always willing to go extra miles for me, to make sure I have everything I need on time.

To my research group, Sustainable Energy and Environment Research Unit (SEERU) thanks for your constructive criticism and share of scientific ideas. I appreciate Dr Tosin Bodunrin for his moral support and for being there when I needed someone to talk to at the time when my back was against the wall during the course of this journey. Thanks for your timely advice

Thanks to my friends, Funmi Oke, Segun, Toyin, Wale Oloye, Omolara and Funke, Aliki and Kelvin for their moral supports and encouragements at all times.

I acknowledge the spiritual supports of my spiritual fathers, Pastor (Dr) Oyekola, Prophet Isreal John, Pastor (Prof) Adeoluwa (your spiritual guidance brought forth this dream), Pastor Asunmo, Rev. (Dr) Adeniyi and Pastor Lekan Martins. In addition, I will not forget to show my appreciation to my spiritual mothers, Prophetess Jumoke Olakanmi and Pastor (Barr.) Olaseesi Martins for their moral, financial and spiritual supports.

Special appreciation goes to my sweet mother, Lady Evangelist Alice Oladunke Oladejo for her love and financial supports all through these years. I've always desired some of your unique personalities. You are a rare gem, mom. To my late father, Chief Oyeniyi Oladejo, you will forever live in my heart. Thanks for the trust you had in me, the encouragement and the smile of your face each time I came home with prize at the end of every school session. The smile keeps me going each time I wanted to give up. I'm very sure you'll still be smiling wherever you are now, I miss you my ever loving dad. To my father and mother in-law, Mr and Mrs Sadare, you are the best. Thanks for your love and patience. I can't have better parents. I also appreciate my sisters and brother in-laws, Mrs Raheem, Mr Tayo Sadare and Mr Tope Sadare, thanks for always having my back.

To my brothers, Dr Olayinka Oladejo, Dr Olatayo Oladejo, Dcn Abiodun Oladejo and Dr Titilola Oladejo, thank you so much for your love and supports at all times. My special thanks go to Dr Olatayo Oladejo, his wife, Lindiwe Skhosana and their children for their support morally and financially. Thanks bro Tayo, you always have a story to tell of your friends' achievements in the field of research, just to keep me going. The stories helped a lot. To my sisters, Fola Oguremi and Dcns Olaide Omotosho thanks for your words of encouragement and supports all through the years

To my ever caring, loving and supportive husband, words fail me to describe how much you mean to me. I can never repay you for what you have done. I will always be grateful to God for bringing you into my life. I cannot imagine a life without your love and support. It's been rough years for us. Thanks for the patience. You always had my back and take all the insults for allowing your wife to take the giant step. My God will reward you handsomely. To my loving and supportive

children, Praise, Ifeoluwa and Esther, you are the best. Mummy has to do what she has to do to make you to be proud of her. I have missed a part of your growing up years, but I promise to make up for the years I was not around to be with you. Thanks to Esther for keeping my company all through these 5 years in the Republic of South Africa.

Furthermore, my profound gratitude goes to University of the Witwatersrand for Postgraduate Merit Award and her financial support through the years.

I acknowledge the financial assistance of L'Oréal-UNESCO foundation for Women in Science, Sub-Saharan African Fellowship through the fellowship award for my PhD degree programme.

Publications and Presentations

The following journal articles and conference papers emanated from this study.

Journals:

1. **Olawumi O. Sadare**, Franklin Obasu and Michael O. Daramola. Biodesulfurization of petroleum Distillates–current status, opportunities and future challenges. Journal of Environments 2017, 4, 85; doi: 10.3390/environments4040085 (MPDI).
2. **Olawumi O. Sadare** and Michael Olawale Daramola. Adsorptive Removal of Dibenzothiophene (DBT) from Petroleum Distillates using Pomegranate leaf (*Punica Granatum)* powder as a Greener Adsorbent, Chemical Engineering Communications, https://www.tandfonline.com/doi/full/10.1080/00986445.2018.1488691 (In press).
3. **Olawumi O. Sadare,** Michael Olawale Daramola. Bio-catalytic degradation of dibenzothiophene (DBT) in South African Petroleum distillate (Diesel) by *Pseudomonas spp.* Biochemical Engineering Journal (Submitted).
4. **Olawumi O. Sadare,** Michael O. Daramola. Adsorptive Removal of Dibenzothiophene (DBT) from Petroleum Distillates using Activated Carbon and Novel green-Pomegranate leaf (*Punica granatum)* Adsorbent. Chemical Engineering Transactions (In preparation)

7. **Olawumi O. Sadare** and M.O Daramola. Development and Evaluation of Adsorption coupling Biodesulphurization (AD/BDS) process for the desulphurization of South African Petroleum Distillates. (In preparation)
8. **Olawumi O. Sadare** and M.O Daramola. Performance evaluation of functinalized carbon nanotubes in the removal of dibenzothiophene from model oil: Kinetic studies (In preparation).
9. **Olawumi O. Sadare** and M.O Daramola. Comparative study on activated carbon, functionalized carbon nanotubes, pomegranate leaf powder and neem leaf powder for adsorption of DBT from model petroleum distillates (In preparation)
10. **Olawumi O. Sadare** and M.O Daramola. Preparation of immobilized activated carbon and its kinetic studies for the removal of sulfur containing compounds (e.g DBT) from South African petroleum distillates (e.g diesel) (In preparation).

11. **Olawumi O. Sadare** and M.O Daramola. Desulfurization of hydrodesulfurized South African petroleum distillates (e.g diesel) by activated carbon in a bach process. (In preparation).
12. **Olawumi O. Sadare** and M.O Daramola. Kinetic study on desulfurization of sulfur-containing compounds in model oil using Neem leaf powder. (In preparation)
13. **Olawumi O. Sadare** and M.O Daramola. Kinetic studies for Removal of DBT from model diesel using immobilized activated carbon in a continuous packed-bed column; Bohart-Adam, Thomas and Yoon-Nelson models (In preparation).
14. **Olawumi O. Sadare** and M.O Daramola. Kinetic study on microbial degradation of DBT in South African petroleum distillates (e.g diesel), using *Pseudomonas aeruginosa* and *Pseudomonas putida* (In preparation)
15. **Olawumi O. Sadare** and M.O Daramola Adsorptive desulfurization of transportation fuel using low cost adsorbents current status, opportunities and future outlooks: A Review (In preparation).

Conferences:

1. Sadare, O.O., **Daramola, M.O.** (2018) Adsorption performance of functionalized carbon nanotubes during desulfurization of Dibenzothiophene (DBT) from model petroleum distillate, In: Proceedings of the 3rd International Conference on Integrated Environmental Management for Sustainable Development, May 2-5, Tunisia, pp. 72-74 (ISSN:1737-3638).

2. **Olawumi O. Sadare,** Mabafokeng Masitha, Michael O. Daramola, Removal of Sulfur (e.g DBT) from Petroleum Distillates using activated carbon in a continuous packed-bed adsorption column, In: Proceedings of the World Congress on Engineering and Computer Science 2018, October 23-25, San Franscisco, USA (Accepted).

Table of Contents

Title page……..i
Declaration…….……..ii
Dedication……...iii
Abstract……...…….....iv
Acknowledgement.…….……....ix
Publications and presentations……...xii
Table of contents…….....xiv
List of figures…….. xix
List of tables……..xxvii
Nomenclature…...…….xxxi
Chapter One……..……...1
1.0 Introduction……..……...……1
1.1. Motivation and background…….…….....1
1.2. Problem statement…….....4
1.3. Research aims, questions and objectives…….……11
1.4. Research benefits and novel contribution to knowledge…….....13
1.5. Thesis outline……..…….....14
1.6. References……16
Chapter Two……..…….....24
2.0. Literature review……...……...……24
2.1. World's perspective of diesel fuel and specifications…….....24
2.2 Environmental effects of sulfur oxides emission……....…….....29
2.3. Existing technologies for desulfurization and their challenges……..…….33
2.3.1. Hydrodesulfurization (HDS)…….…….....36
2.3.2. Oxidative desulfurization (ODS)……...……37
2.3.3. Adsorptive desulfurization (ADS)…….....38

2.3.4. Adsorbents for desulfurization……...40
2.3.5. Agro-waste adsorbents for desulfurization…...…….42
2.4. Adsorption isotherms and kinetics model……. …….....53
2.4.1. Continuous mode…….…….....53
2.4.2. Batch mode……...…...…….…… ……59
2.5. Regeneration of spent adsorbents……....65
2.6. Biodesulfurization……..…….....66
2.7. Potential of Biodesulfurization for industrial application…….....72
2.8. Kinetics of bacteria growth and diesel desulfurization……77
2.9. Summary……...……..……80
2.10. References……...……...82
Chapter Three……...106
3.0 Experimental procedure and analysis……..…….……...106
3.1. Investigation of adsorptive desulfurization (ADS) …….…….……..106
3.1.1. Preparations and characterization of adsorbents …….…….……....106
3.1.2. Evaluation of performance of adsorbents during desulfurization…...……..110
3.1.3. Study of effects of operating variables, optimization, isotherms and kinetic studies...114
3.2. Investigation of biodesulfurization (BDS)……..……....122
3.2.1. Inoculum preparation and investigation of biomass growth……...……..122
3.2.2. Evaluation of biodesulfurization efficiency of *Pseudomonas species*…..……....125
3.2.3. Investigations of operating variables, optimization and kinetic studies…….....125
3.3. Development of AD/BDS process and evaluation…….....130
3.4. Conclusion and recommendations……..……....132
3.4. References……133
Chapter Four……136
4.0. Adsorption performance of pomegranate and neem leaves powder during desulfurization
…...……...136
4.1. Introduction……136
4.2. Experimental……..…….…….....137
4.3. Results and discussion…….…….....138
4.3.1. Physico-chemical characterization of PLP and NLP adsorbents……..…….....138

4.3.2. Performance evaluation of PLP and NLP adsorbents during desulfurization ……144
4.4. Adsorption isotherms, kinetics and thermodynamics of PLP and NLP…….....149
4.5. Regeneration and re-usability of PLP and NLP……...…….....154
4.6. Concluding remarks……...159
4.7. References……..160
Chapter Five……....166
5.0. Desulfurization of model diesel using functionalized carbon nanotubes…….....166
5.1. Introduction…….……...166
5.2. Experimental……..……....167
5.3. Results and discussion…….……..168
5.3.1. Physico-chemical characterization of CNTs and FCNTs…..…..…….....168
5.3.2. Performance evaluation of functionalized carbon nanotubes during desulfurization..174
5.4. Adsorption isotherm, kinetics and thermodynamics of FCNTs for adsorption …...…….179
5.5. Regeneration and re-usability of FCNTs and CNTs….……...…….....185
5.6. Concluding remarks……..…….....188
5.7. References……...190
Chapter Six……...193
6.0. Desulfurization of model real diesel using activated carbon…….……193
6.1. Introduction……...…….....193
6.2. Experimental…….……....194
6.3. Results and discussion……...194
6.3.1. Physico-chemical characterization of activated carbon…..……...…….....194
6.3.2. Performance evaluation of activated carbon during desulfurization.…….……200
6.4. Isotherm, kinetics and thermodynamics of AC for adsorption …….211
6.5. Regeneration and re-usability of activated carbon……..…...…….....215
6.6. Concluding remarks……..……....219
6.7. References……..……....220
Chapter Seven……..224
7.0. Enhancement of desulfurization performance of AC in packed-bed column using immobilized activated carbon……..……....224
7.1. Introduction……224

7.2. Experimental…….....225
7.3. Results and discussion…….....226
7.3.1. Physico-chemical characterization of adsorbents…….....226
7.3.2. Performance evaluation of activated carbon in the packed-bed column ……..…....228
7.4. Kinetics for modelling adsorption behavior in a packed-bed column …….……...…..232
7.4.1. Modelling of experimental data……..238
7.5. Concluding remarks……...……....239
7.6. References……..……240
Chapter Eight…...…….....……244
8.0. Biodesulfurization using *Pseudomonas species*…..……..…….....244
8.1. Introduction……244
8.2. Experimental…….……....246
8.3. Results and discussion …….....245
8.3.1. Effect of pH and carbon sources on growth of bacteria …….…….....247
8.3.2. Effect of operating variables on growth of bacteria and biodesulfurization.…….....252
8.3.3. Biphasic effect on bacteria growth and biodesulfurization…….……....256
8.4. Kinetic of bacteria growth and degradation of model diesel……..……..……....260
8.4.1. Kinetic model for growth of bacteria……..…….260
8.4.2. kinetic model of DBT degradation in model diesel…….…....263
8.5. Evaluation of biodesulfurization efficiency of real diesel sample using resting cells of *Pseudomonas Sp*……..……266
8.6. Degradation kinetics of real diesel……..…….....270
8.7. Concluding remarks…….. ……...273
8.8. References……274
Chapter Nine……279
9.0. Performance of adsorption coupling biodesulfurization for desulfurization of petroleum distillate…….…….....279
9.1. Introduction……..……..……279
9.2. Experimental……...……..……....280
9.3. Results and discussion……...…….....281
9.3.1. Performance evaluation of immobilized AC during desulfurization of real diesel.....281

9.4. Adsorption kinetics study...……...283
9.5. Regeneration of spent adsorbent in a packed-bed column…….....290
9.6. Biodesulfurization of adsorptive-desulfurized real diesel sample…….....292
9.7. Kinetics of degradation of real diesel during biodesulfurization……..…….....299
9.8. Concluding remarks……...……301
9.9 References……...303
Chapter Ten……..307
10.0. Conclusions and recommendation……...…….…….....307
10.1. Conclusions…….....307
10.2. Recommendation……..……...311
Appendix…….....313
Appendix A: Experimental equipment……....313
Appendix B: Calculations of various adsorption parameters……...……...319
Appendix C: Adsorption experimental graphs……....323
Appendix D: Published, in-press articles and conference proceedings……..…….....348

List of Figures

Figure 1.1 4S-pathways for biodesulphurization of DBT adapted from Monticello, 2000 9

Figure 1.2 Process flow diagram of the (Adsorption/BDS) hybrid process 11

Figure 2.1 Percentage of diesel usage at various sectors (Adapted from EPA, 2017)…….. 25

Figure 2.2. Diesel sulfur level in South Africa (Adapted from SA Overview, 2018) 26

Figure 2.3 Chemical structure of organic sulphur compounds present in crude oils (Adapted from Hosseini et al., 2014). 36

Figure 2. 4 (a) Batch mode operation (b) Continuous mode operation 46

Figure 2.5. Representation of ideal breakthrough curve, (Adapted from Calero, 2000) 52

Figure 2.6 The percentage (%) desulfurizing ability of various microorganisms (Adapted from Kinoshi et al., 1999)..... 70

Figure 3.1. Overview of the procedures employed in this study…….107

Figure 3.2. Schematic of batch adsoption desulfurization experiments in a temperature regulated rotary shaker..... 111

Figure 3.3. Continous adsorption in a packed bed column: Experimental set-up 112

Figure 3.4. Schematic for ADS/BDS coupling technique process 132

Figure 4.1. Surface morphologies of (a) NLP (b) PLPadsorbent**……..…….**139

Figure 4.2. XRD pattern of PLP and NLP 140

Figure 4.3 FTIR spectra showing chemical functionalities of PLP before use and PLP after use. 143

Figure 4.4 FTIR spectra showing the chemical functionalities of neem leaves powder before use and neem leaves powder after use. 144

Figure 4.5. Effect of contact time on desulfurization by pomegranate leaf powder and neem leaves powder. Experimental conditions: Temperatures: 30 ^{o}C; Amount of adsorbents: g/0.02 L model diesel; Initial DBT concentration: 1000 ppm..... 145

Figure 4.6. Effect of temperatures on desulfurization of model petroleum distillate by (a) PLP adsorbent (b) NLP adsorbent. Experimental conditions: Amount of adsorbent 0.01 g/mL model diesel, DBT concentration 1000 mg/L..... 147

Figure 4.7. Effect of adsorbent amount on desulfurization of model oil by PLP and NLP at equilibrium temperature of 30 ^{o}C and varying adsorbent amount. Experimental conditions: Initial DBT concentration: 1000 mg/L; Temperature: 303 K; The amount of adsorbent: g/0.02L model diesel 148

Figure 4.8. Effect of initial concentration on adsorption of DBT. Experimental conditions: contact time 60 min, stirring speed 130 rpm, amount of NLP and PLP adsorbent 1.0 g, and temperature 30^{o}C 149

Figure 4.9. Freundlich isotherms for (a) PLP (b) NLP and Langmuir isotherms for (c) PLP (d) NLP. Experimental conditions: Initial DBT concentrations: 250-1000 mg/L; Temperature: 303 K, Amount of adsorbent: 1.0 g..... 151

Figure 4.10. Re-usability potential of PLP and NLP 155

Figure 5.1 Surface morphology of (a) CNTs (b) FCNTs……169

Figure 5.2. Adsorption-desorption isotherm plot of CNTs adsorbent 170

Figure 5.3. FTIR spectra of CNTs and FCNTs..... 172

Figure 5.4. Ramman spectra for CNTs and FCNTs..... 173

Figure 5.5. Effect of time on the adsorption of DBT onto the surface of CNTs and FCNTs. Experimental conditions: Time 180 min, Tempearture, 298 K, Initial DBT concentration 1000 mg/L, Volume of model oil 20 mL. 175

Figure 5.6. Effect of amount of adsorbent on the adsorption of DBT onto FCNTs and CNTs. Experimental conditions: Initial DBT concentrations 1000 mg/L, Temperature, 298 K. 176

Figure 5.7. Effect of initial concentration of DBT on its adsorption onto FCNTs and CNTs. Experimental conditions: Amount of adsorbent: 1.0 g; Temperature: 298 K..... 177

Figure 5.8. Effect of temperatures on the adsorption of DBT onto (a) CNTs and (b) FCNTs. Experimental conditions: Initial feed concentration: 1000 mg/L; Amount of adsorbent: 1.0 g. 179

Figure 5.9. Langmuir isotherms (a) FCNTs (b) CNTs and Freudlich isotherms of (c) FCNTs (d) CNTs. Experimental conditions: Temp: 298 K, amount 1.0 g. 181

Figure 5.10 Re-usability cycles of CNTs and FCNTs 186

Figure 6.1 Adsorption-desorption isotherm of fresh activated carbon……195

Figure 6.2 Surface morphology of commercial activated carbon (a) before adsorption and (b) after adsorption experiment 196

Figure 6.3.EDX spectrum for AC (a) Before desulfurization (b) After desulfurization..... 197

Figure 6.4 FTIR spectra of used and unused activated carbon 199

Figure 6.5 Effect of temperatures on adsorption of DBT onto Activated carbon. Experimental conditions: Initial DBT Concentration: 1000 mg/L; Amount of adsorbent: 0.2 g,..... 201

Figure 6.6 Effect of time on the adsorption of DBT onto AC. Experimental conditions: DBT concentration: 1000 mg/L; Amount of adsorbent: 1.0 g..... 202

Figure 6.7 Effect of amount of adsorbents on the adsorption of DBT onto AC. Experimental conditions: Temp.: 298 K, Initial DBT concentration: 1000 mg/L. 203

Figure 6.8 Effect of initial concentration on the adsorption of DBT onto activated carbon. Experimental conditions: Amount of adsorbent: 1.0 g; Temperature: 298 K..... 204

Figure 6.9 Performance of AC for removal of DBT from model diesel, diesel obtained after HDS and dieselobtained before HDS. Experimental conditions: Amount of adsorbent: 1.0 g; Initial DBT concentration: 120 mg/L, temperature 303 K. 206

Figure 6.10 Effect of temperature on adsorption of DBT onto activated carbon. Experimental conditions: Amount of adsorbent: 1.0 g; Initial DBT concentration: 120 mg/L. 207

Figure 6.11 Desulfurization of diesel obtained after HDS and diesel obtained before HDS. Experimental conditions: Initial concentrations of DBT: 120 mg/g; Amount of adsorbent: 1.0 g; Temperature: 318 K. 208

Figure 6.12 Chromatogram (a) Detection of peak and retention time of DBT using GC/MS (b) diesel obtained after HDS (c) diesel obtained before HDS 210

Figure 6.13 (a) Langmuir isotherm model for adsorption of DBT onto AC (b) Freudlich isotherm model for adsorption of DBT onto AC. Experimental conditions: Amount of adsorbents: 0.2 g; Temperatures: : 298 K; Initial concentrations: 250-1000 mg/L 212

Figure 6.14 Re-usability efficiency of AC adsorbents. Experimental conditions: Amount of adsorbent: 1.0 g; Temperature: 318 K; Initial DBT concentration: 120 mg/L. 216

Figure 7.1 (a) Sodium algilate pellets (b) immobilized actvated carbon entrapped in sodium algilate……..225

Figure 7.2 SEM images of (a) Fresh alginate-AC (a) Alginate-AC after use..... 227

Figure 7.3 FTIR spectra of alginate and alginate-AC..... 228

Figure 7.4 Effect of bed height on the adsorption of DBT in model oil in a packed bed column. Experimental conditions: Initial DBT concentration 100 mg/L, Flow rate 0.5 mL/min, Time 300 min 229

Figure 7.5 Effect of flow rate on adsorption of DBT in a packed-bed column. Experimental conditions: Bed height: 15 cm; Initial DBT concentration: 100 mg/L. 231

Figure 7.6 Effect of initial concentration on adsorption of DBT from a model oil in a packed-bed coulumn. Experimental conditions: Bed height: 15 cm; Flow rate: 0.5 mL/min. 232

Figure 7.7 Experimental and predicted breakthrough curve, using Bohart-Adam and Thomas model for adsorption of DBT onto immobilized activated carbon in a continuous fixed bed column. Experimental conditions: Bed height: 15 cm; Flow rate: 0.5 mL/min; Initial DBT concentration: 100 mg/L. 238

Figure 8.1 Effect of carbon source on the growth of (a) Psuedomonas Aeruginosa, (b) Pseudomonas Putida at. Experimental conditions: Initial DBT concentration: 25 mM, Temperatuure: 37 ^{o}C (PA), 30 ^{o}C (PP)……248

Figure 8.2 Biomass growth as a function of time during degradation of DBT and 2-HBP formation (a) with Pseudomonas Aeruginosa (b) with Pseudomonas Putida. Experimental conditions: Initial DBT concentration: 46 ppm; Temperature: 30 ^{o}C (PP) and (37 ^{o}C). 250

Figure 8.3 Effect of cell concentration of resting cells of PP and PA on DBT degradation and production of 2-HBP (a) 0.3 g DCW/L (b) 0.6 DCW/L (c) 0.9 g DCW/L (d)1.2 g DCW/L. Experimental conditions: Initial DBT concentrations: 500 ppm; Temperature 37 ^{o}C (PA) and 30 ^{o}C (PP). 252

Figure 8.4 Effect of initial DBT concentrations on the growth of (a) PA (b) PP. Experimental conditions: Oil: water ratio (1:4); Cell concentration: 1.2 gDCW/L; Temperature: 37 ^{o}C (PA), 30 ^{o}C (PP). 253

Figure 8.5 Effect of initial DBT concentration on DBT degradation by Pseudomonas aeruginosa and Pseudomonas putida (a) 250 ppm (B) 500 ppm (c) 750 ppm (d) 1000 ppm. Experimental conditions: Cell concentration: 1.2 gDCW/L; Temperature: 37 ^{o}C for PA and 30 ^{o}C for PP 254

Figure 8.6 Effect of biphasic (oil-water ratio) media on biomas growth (a) PA (b) PP Experimental conditions: Temperature: 37 ºC (PA); 30 ºC (PP); Initial DBT concentration: 500 ppm. 255

Figure 8.7 Effect of biphasic media on biodesulfurization of DBT and formation of 2-HBP by (a) PA (b) PP. Experimental conditions: Oil-to-water ratio: 1:4; Temperature: 37 ºC (PA), 30 ºC (PP); Initial DBT concentration: 500 ppm. 256

Figure 8.8 Michaelis-Menten growth kinetic model for growing cells of (a) PA (b) PP 261

Figure 8.9 First order kinetic model for DBT degradation by resting cells of PP at (a) 250 mg/L (b) 500 mg/L (c) 750 mg/L (d) 1000 mg/L. Experimental conditions: Cell mass: 1.2 gDCW/L, Temperature: 30 ºC. 263

Figure 8.10 First order kinetic model of DBT degradation in model diesel by resting cell of PA at (a) 250 mg/L (b) 500 mg/L (c) 750 mg/L (d) 1000 mg/L. Experimental conditions: Cell mass: 1.2 gDCW/L; Temperature: 37ºC. 264

Figure 8.11 Biodesulfurization of diesel obtained after HDS by PP and PA. Experimental conditions: Initial DBT concentrations: 120 ppm; Cell mass: 1.2 g DCW/L; Temperatures: 30 ºC (PP) and 37 ºC (PA). 266

Figure 8.12 Biodesulfurization of diesel obtained before HDS. Experimental conditions: Initial DBT concentrations: 5200 ppm. Cell mass: 1.2 g DCW/L, Temperatures: 30 ºC (PP) and 37 ºC (PA). 267

Figure 8.13 Chromatograms of (a) standard DBT and 2-HBP in ethyl acetate (b) Real diesel obtained before biodesulfurization (c) Biodesulfurized diesel 268

Figure 8.14 Kinetic model of DBT degradation in real diesel after HDS by resting cells of (a) *Pseudomonas putida* (b) *Pseudomonas aeruginosa*. Experimental conditions: Initial DBT concentration: 120 mg/L: Cell mass: 1.2 gDCW/L. 270

Figure 9.1 Breakthrough curve for desulfurization of diesel after HDS on AC in a packed-bed column, showing effect of initial concentration. Experimental conditions: Flow rate: 0.5 mL/min; Bed height: 15 cm……...….281

Figure 9.2 Breakthrough curve for desulfurization of diesel before HDS by immobilized activated carbon in a fixed bed column, showing effect of initial concentration. Experimental conditions: Flow rate: 0.5 mL/min; Bed height: 15 cm. 282

Figure 9.3. Regeneration of spent adsorbent using diesel obtained after HDS. Experimental conditions: Flow rate: 0.5 mL/min; Bed height: 15 cm; Initial Concentration: 40mg/L. 290

Figure 9.4 (a) Degradation of adsorptive-desulfurized diesel obtained after HDS from adsorption bed coulumn (AD coupling BDS system) by resting cell of PA (b) Chromatogram of diesel obtained after HDS, after complete desulfurization by AD/BDS hybrid process. Experimental conditions: Initial DBT concentration: 10 mg/L; Temperature: 37 ºC. 292

Figure 9.5 (a) Degradation of AD-desulfurized diesel obtained before HDS (AD/BDS coupling process) using resting cell of PA. (b) Chromatogram of diesel obtained before HDS, after complete desulfurization by AD/BDS hybrid process Experimental conditions: Initial DBT concentration: 10 mg/L; Temperature: 37 ºC. 294

Figure 9.6. Detection of peak of DBT in a pre-calibrated GC/MS 295

Figure 9.7. Chromatogram of diesel sample obtained before HDS 296

Figure 9.8. Chromatogram of diesel sample obtained after HDS 296

Figure 9.9. Chromatogram of biodesulfurized of diesel before HDS with the detection of 4S-pathway (2-HBP) 297

Figure 9.10. First order kinetic model for degradation of sulfur compound in (a) diesel obtained before HDS and (b) diesel obtained after HDS using PA. Experimental conditions: Initial DBT concentration: 10 mg/L; Temperature: 37 ºC. 299

Figure 10.1 Breakthrough curve for desulfurization of diesel after HDS on activated carbon in a fixed bed column, showing effect of initial concentration. Experimental conditions: Flow rate 0.5 mL/min, Bed height 15 cm. ……..……..….281

Figure 10.2 Breakthrough curve for desulfurization of diesel before HDS by immobilized activated carbon in a fixed bed column, showing effect of initial concentration. Experimental conditions: Flow rate 0.5 mL/min, Bed height 15 cm. 282

Figure 10.3. Regeneration of spent adsorbent using diesel after HDS. Experimental conditions: Flow rate 0.5 mL/min, Bed height 15 cm. Initial Concentration 40mg/L. 290

Figure 10.4 (a) Biodesulfurization of desulfurized South African diesel after HDS from adsorption bed coulumn (AD/BDS coupling technique) by resting cell of Pseudomonas aeruginosa. (b) Chromatogram of diesel after HDS, after completete desulfurization process by AD/BDS hybrid process Experimental conditions: Initial DBT concentration 10 mg/L, Temperature 37 ºC..... 292

Figure 10.5 (a) Biodesulfurization of desulfurized South African diesel before HDS from adsorption bed coulumn (AD/BDS coupling technique) using resting cell of Pseudomonas aeruginosa. (b) Chromatograph of diesel before HDS, after complete desulfurization by AD/BDS hybrid process Experimental conditions: Initial DBT concentration 10 mg/L, Temperature 37 ºC. 294

Figure 10.6. Chromatogram for detection of peak of DBT in GC/MC 295

Figure 10.7. Chromatogram of South African diesel sample after HDS 296

Figure 10.8. Chromatogram of South African diesel sample before HDS 296

Figure 10.9. Chromatogram of biodesulfurized of diesel before HDS with the detected of 4S-pathway (2-HBP) 297

Figure 10.10. First order model for degradation of sulfur compound in South African (a) diesel obtained before HDS and (b) diesel obtained after HDS using *Pseudomonas aeruginosa.* Experimental conditions: Initial DBT concentration: 10 mg/L; Temperature: 37 ºC. 299

Lists of Tables

Table 2.1 Status of clean fuel in South Africa till date 28

Table 2.2 Summary of today's world-class emission standards (with permission from ICCT)... 34

Table 2.3 Comparative characteristics of the efficiency of selected aerobic cultures in real fuel desulfurization..... 73

Table 2.4 Alkylated DBTs (Cx-DBT) desulfurization by some strains of bacteria and their end products..... 74

Table 3.1: Physical and chemical properties of a typical diesel fuel obtained from Refinery X, South Africa…….113

Table 4.1. Operating conditions for adsorption desulfurization of DBT by PLP and NLP…….137

Table 4.2: Elemental compositions of PLP ans NLP adsorbents before and after adsorption experiments 141

Table 4.3: Textural properties of NLP and PLP before and after adsorption experiments 142

Table 4.4: Langmuir and Fruendlich Isotherm parameters..... 150

Table 4.5: Kinetic parameters for pseudo-first and pseudo-second order adsorption model 153

Table 4.6: Results of this study compared with literature 158

Table 5.1: Surface area, pore volume and pore sizes determination of the adsorbents by Brunauer–Emmett–Teller (BET) analysis……..…….171

Table 5.2: Elemental compositions of Pomegranate powder by energy dispersive x-ray (EDX)…….170

Table 5.3: Langmuir and Fruendlich Isotherm parameters…….180

Table 5.4: Parameters for pseudo first and pseudo second-order kinetics……...183

Table 5.5: Themodynamic parameters for adsorption of DBT on PLP……..184

Table 5.6: Comparison of results with literature…….....188

Table 6.1: Surface area, pore volume and pore sizes determination of the adsorbents by Brunauer–Emmett–Teller (BET) analysis……...198

Table 6.2: Elemental composition of fresh activated carbon powder and used activated carbon powder by EDX spectroscopy……...……..198

Table 6.3: Langmuir and Fruendlich Isotherm parameters……..211

Table 6.4: Parameters for pseudo first and pseudo second order kinetics for activated carbon..213

Table 6.5: Themothynamic parameters for adsorption of DBT on activated carbon……..214

Table 6.6: Comparison of results with literature……..……...218

Table 7.1: Bohart-Adam's kinetic parameters for adsorption of DBT onto immobilized activated carbon in a continuous packed-bed column…….……...233

Table 7.2: Thomas' kinetic parameters for adsorption of DBT onto immobilized AC in a continuous packed-bed column..... 235

Table 7.3: Yoon-Nelson's kinetic parameters for adsorption of DBT onto immobilized activated carbon in a continuous fied bed column. 236

Table 7.4: Desulfurization of DBT in model diesel Adorption column and breakthrough capacity for adsorption of DBT in a continuous packed-bed column using immobilized AC 237

Table 8.1: Bohart-Adam's model parameters for adsorption of DBT onto immobilized activated carbon in a continuous fixed bed column……233

Table 8.2: Thomas model parameters for adsorption of DBT onto immobilized activated carbon in a continuous fixed bed column……235

Table 8.3: Yoon-Nelson parameters for adsorption of DBT onto immobilized activated carbon in a continuous fied bed column……...…...236

Table 8.4: Desulfurization of DBT in model oil Adorption column and breakthrough capacity for adsorption of DBT in a continuous fixed bed column using immobilized activated carbon…...237

Table 9.1: Bohart Adam's kinetic parameters for desulfurization of diesel obtained after HDS in a packed-bed column…….....283

Table 9.2: Bohart-Adam Kinetic parameters for desulfurization of diesel obtained before HDS in a packed-bed column. 284

Table 9.3: Thomas' kinetic parameter for desulfurization of diesel obtained after HDS in packed-bed column. 285

Table 9.4: Thomas' kinetic parameter for desulfurization of diesel before HDS in packed-bed column..... 286

Table 9.5: Yoon-Nelson's kinetic parameter for desulfurization of diesel obtained after HDS in packed-bed column. 287

Table 9.6: Yoon-Nelson kinetic parameter for desulfurization of diesel obtained before HDS in packed-bed column. 287

Table 9.7: Adorption column and breakthrough capacity parameters for desulfurization of DBT in SA diesel after HDS in a continuous fixed bed column 288

Table 9.8: Adorption column and breakthrough capacity parameters for desulfurization of DBT in diesel obtained before HDS in a continuous packed-bed column 289

Table 9.9: Regeneration of spent immobilized AC 290

Table 9. 10: X_{BDS}, Y_{BDS}, D_{BDS} and E parameters for BDS of diesel obtained after HDS and diesel obtained before HDS by resting cell of *PA* at the same initial concentrations of 10 mg/L. 298

Table 10.1: Bohart Adam parameter for desulfurization of South Africa diesel after HDS in fixed bed column……..….283

Table 10.2: Bohart Adam parameter for desulfurization of South Africa diesel before HDS in fixed bed column. 284

Table 10.3: Thomas parameter for desulfurization of South Africa diesel after HDS in fixed bed column 285

Table 10.4: Thomas parameter for desulfurization of South Africa diesel before HDS in fixed bed column 286

Table 10.5: Yoon-Nelson parameter for desulfurization of South Africa DIESEL after HDS sample in fixed bed column. 287

Table 10.6: Yoon-Nelson parameter for desulfurization of South Africa diesel before HDS in fixed bed column. 287

Table 10.7: Adorption column and breakthrough capacity parameters for desulfurization of DBT in SA diesel after HDS in a continuous fixed bed column 288

Table 10.8: Adorption column and breakthrough capacity parameters for desulfurization of DBT in SA diesel before HDS in a continuous fixed bed column 288

Table 10.9: Regeneration of spent immobilized activated carbon 290

Table 10.10: X_{BDS}, Y_{BDS}, D_{BDS} and E parameters for biodesulfurization of SA diesel after HDS and SA diesel before HDS by resting cell of *Pseudomonas aeruginosa* at the same initial concentrations of 10 mg/L. 298

Nomenclature

DBT	Dibenzothiophene
ADS	Adsorption desulfurization
HDS	Hydrodesulfurization
BDS	Biodesulfurization
PP	Pseudomonas putida
PA	Pseudomonas aeruginosa
V_{max}	Maximum specific growth rate
K_s	Half saturation constant
S	Substrate concentration
q_e	Amount of DBT adsorbed at equilibrium
C_o	Initial concentration of DBT
C_e	Concentration of DBT at equilibrium

Chapter One

1.0 Introduction

In this chapter, the motivation for this study and the research objectives are clearly defined. The benefits of the research effort to the scientific and industrial community are also highlighted.

1.1. Motivation and Background

In Petroleum refining, all crude oils are mainly comprised of aromatic, paraffinic and naphthenic groups with high molecular masses. The major products of the petroleum industry can be divided into three main groups: fuels such as gasoline, diesel oil, kerosene and jet fuel, refined non-fuel products for example asphalt, coke, grease, lubricating oils, solvent, petroleum wax and industrial feed stocks; such as butane, benzene, propane, ethane, naphtha, xylene and toluene (Mohebali and Ball, 2008). Diesel and fuel oil range are referred to as the middle-distillate fractions (Monticello, 2000). During direct combustion of diesel, significant quantities of sulphur-containing compounds such as sulphur oxides (gaseous particulate) e.g SO_2 and SO_3, sulphate particulate matter (PM) and sulphur-containing compounds (dibenzothiophene (DBT)) are released into the atmosphere which cause acid rain and environmental pollution that is detrimental to human health (Mei et al., 2003). As a result of these, a good number of countries have enforced policies to minimize the emission of these compounds. There are stringent restrictions to limit the amount of sulphur emission from power plants and on the amounts of sulfur allowable in power plants and fuels used in transportation such as diesel and jet fuel (Monticello, 2000). In South Africa, two different grades of diesel fuel are available since the beginning of 2006. Standard grade diesel has maximum sulphur levels of 500 ppm, while maximum for low sulphur grade diesel was 50 ppm. However, Sasol has been selling 10 ppm diesel to commercial and private diesel vehicles. Lately, sulfur in transportation fuel has been reported to poison the catalytic converters used for combustion of hydrocarbon on automobile exhaust systems which contribute considerably to urban environmental pollution. Therefore, the United States environmental protection agency (EPA) and other regulatory agencies have taken steps to remove sulfur permanently from transportation fuel so as to end the poisoning of these inorganic catalysts (Monticello, 2000). In order to meet up with the emission requirement, oxidation catalysts have been used in South Africa on diesel cars and

commercial vehicles since 2006. They have been found to be efficient in lowering the hydrocarbons residue after burning and carbon monoxide from the exhaust. However, soot particles in the exhaust still remain a major setback (Sasol, 2012). There is currently a stringent regulation that refineries in South Africa are expected to ensure a maximum specification of less than 5 ppm sulphur content in the petroleum distillates to levels equivalent to the Euro 5 emission standard by 2020 (Sasol, 2012). Therefore, there is a need to look for a better way of desulphurizing South African petroleum distillates to meet up with the stringent policies regarding emission of sulphur oxides. Equivalent of 70% sulphur in petroleum distillate exists as dibenzothiophene (DBT). DBT, an organosulphur compound commonly present in South African common diesel is difficult to desulphurize using the traditional method hydrodesulphurization (HDS) which is presently in use to obtain 500 ppm, 50 ppm and just of recent 10 ppm diesel in South Africa. Conversely, DBT has been considered the model compound for biodesulphurization (Monticello, 2000). Different methods of desulfurization have been employed for removal of sulfur-containing compounds from petroleum distiallets. In view of these challenges, desulfurization of petroleum distillates has been reviewed industrially in recent years with the aim of ensuring reduction in the emission of sulfur-containing compounds into the atmosphere and thus preventing environmental degradation (Gawande and Kaware, 2018). Sulfur-containing compounds, in the form of organic sulfur compounds, are present in some petroleum distillates like diesel. In fact, sulfur is reported to be the third most abundant element after hydrogen and carbon in diesel fuel (Daware et al., 2015). The fuel quality will be improved, if sulfur-containing compounds are removed from crude oil during refining by cheap and less energy intensive technique. This will contribute to the economy of crude oil refining remarkably (Agamuthu, 2009). Different techniques such as hydrodesulfurization (HDS), biodesulfurization (BDS), adsorption (ADS), extraction and oxidation have been investigated by various researchers to remove sulfur-containing compounds from petroleum distillates.

HDS is the most commonly used industrial technology for the removal of sulfur-containing compounds from transportation fuels. It is efficient for the removal of most of the Sulphur-containing compounds such thiols and sulphides, but very inefficient to remove refractory thiophenic compounds such as dibenzothiophenes, benzothiophene, and their derivatives (Babich and Moulijn, 2003). To meet the restrictive specifications and regulations set by Environmental

Protection Agency (EPA) on all transportation fuels, hydrodesulphurization process requires to be operated at elevated temperature and pressure which make the technique energy intensive. In addition, as huge amount of hydrogen is needed. This makes the process expensive (Fei et al., 2017). The need for cheap, less energy intensive and efficient technique for removal of sulfur compounds from petroleum distillate has necessitated research efforts all over the world for the past few years at both environmental and industrial levels. Therefore, exploring an effective technique for treatment of sulfur containing petroleum distillate is still highly desired.

Adsorption is the most economically attractive desulfurization technique (Al Zubaidi et al., 2015). It has been explored by many researchers owing to its applicability and low cost on large scale (Moosavi et al., 2012; Gawande and Kaware 2016). It is beneficial because the desulfurization process can be carried out at ambient temperature and pressure without consumption of hydrogen or oxygen consumption. Furthermore, there is possibility of adsorbent regeneration and reusability (Ahmed and Ahmaruzzaman, 2015).

Biodesulfurization offers the potential technique for reducing the sulfur content of petroleum products with benefits of low operating cost, lower capital and less greenhouse gasses (Linguist and Pacheco, 1999). Getting rid of enough sulphur to meet the imminent specification requires enzymes with wide-ranging specificities (Monticello, 2000). Therefore, biological desulphurization with the help of microorganisms is considered as the potential method for removal or reduction of sulphur in petroleum distillate.

There are only a few studies reported on the biodesulphurization of South African petroleum distillates. The use of *Pseudomona aeruginosa* (P. aeruginosa) and *Pseudomonas putida* (P. putida) bacteria strains for the biodesulphurisation of South African diesel has not been reported in literature. In addition, desulphurization by adsorption technique has been reported to be a promising approach in desulphurization of sulphur-containing compounds. Thus, this research effort will pave the way for the development of a hybrid process involving the use of adsorption and biological techniques for the desulphurization of South African petroleum distillates.

1.1.2 Problem Statement

Over a decade ago, significant efforts have been made in developing technological methods to eradicate sulfur from diesels and their feedstock. A lot of conventional processing plants can be used to eliminate sulfur and many new techniques have been developed to attend to the need for further economical desulfurization capability. Hydrodesulphurization is one of them. Petroleum distillates contain considerable quantity of heterocyclic sulfur compounds such as alkylated benzothiophenes (C_x-BTS) and alkylated dibenzothiophenes (C_x-DBTS), which are difficult to remove by traditional hydrodesulfurization (HDS) method due to high operating cost as a result of high pressure (1-20 MPa) and temperature between 290 and 450^{o}C which are required to reduce sulphur to hydrogen sulphide (Monticello, 1998). Owing to very high pressure and temperature required in HDS, there is reduction in some other chemical components which introduces some adverse effects on the quality of fuel (Folsom, 1999). These high operating conditions are obligatory to desulfurize the most recalcitrant molecules with HDS method (McFarland, 1999; Rashtchi et al., 2006). In addition, HDS results in reduction of catalyst life, higher consumption of hydrogen and higher cost of yield (Mei et al., 2003).

The HDS process conditions are not only useful in desulfurizing organosulfur compounds, they are used in removing metals and nitrogen from carbon-based compounds as well. In addition, HDS process is used in prompt saturation of carbon–carbon double bonds, removal of materials with unpleasant colour or odor, product clarification through drying, and improvement of the cracking qualities of the material (Swaty, 2005). Hence, with reverence to the advantages of HDS aside desulphurization, this study will consider BDS as a complementary step to HDS instead of only as a replacement to attain an ultra-low desulphurization.

Other types of desulphurization methods have been studied, such as desulphurization by oxidation. Oxidation of the divalent sulfur of the sulfide group to the hexavalent of the sulfone group makes oxidation desulphurization a promising approach, which upon thermal treatment can emit sulfur dioxide (Block, 1978). Although the sulphur is successfully removed, but the temperature needed for the decomposition of the sulfone is as high as 500^{o}C. In addition, large amount of oxidizing agents is needed and the activity and selectivity of the oxidant is low, hence the reaction takes a longer time to complete. Desulphurization by extraction is another potential method for removing

or reducing the amount of sulphur in petroleum distillate. Owing to the ability of sulphur to make the hydrocarbon molecules in which it occurs slightly more polar, the sulphur compounds can be selectively removed by solvent extraction method. Some extraction solvents have been used such as furfural and hydrogen fluoride. It was observed that high selectivity could be achieved in the removal of sulphur and the raffinate contains less sulphur than the original feedstock (Zannikos, 1995). However due to some setbacks in these methods of desulphurization, development of hybrid process of newly developed and efficient methods of desulphurization could be developed to obtain an ultra-low sulphur in South African diesel. Biodesulphurization, a new efficient method of desulphurization has been developed with cost effective operational conditions such as low temperature and pressure. Adsorption method of desulphurization has also been discovered to be cost effective and is carried out at ambient temperature using different types of adsorbents. However, selective choice of adsorbents has been the major concern to researchers. Activated carbon and carbon nanotubes have attracted much attention from researchers as promising adsorbent materials for adsorptive desulphurization due to their exceptional properties, for instance, large surface area, high pore structure, pore size distribution, high thermal stability as well as excellent physical and chemical stabilities. Therefore, this study seeks to investigate the development and evaluation of a hybrid process (adsorption coupling biodesulphurization, (AD/BDS)) for desulphurization of dibenzothiophene sulphur-containing compound, which constitute 70% of the components in South African petroleum distillates (e.g. diesel) obtained from hydrodesulphurizer (HDS) to 5 ppm.

Adsorption is the ability of a solid sorbent to selectively adsorb organosulphur compounds from refinery processing plant streams. Desulphurization by adsorption can be grouped into two: Adsorptive desulfurization and reactive adsorption desulfurization (Babich and Moulijn, 2003). These two depend upon the mechanism at which sulphur compounds relate with the sorbents. Adsorptive method of desulfurization depends on physical adsorption of organosulfur compounds on the surface of solid sorbent and this can be recovered by flushing the spent sorbent with a desorbent. This brings about a high concentration flow of organosulfur compound. However, desulphurization by reactive adsorption is all about chemical interaction between the sorbent and the organosulfur compounds. The sulfur removed is adsorbed on the surface of the sorbent in most cases as sulphide. This sorbent can be recovered by eliminating the SOx or H_2S depending on the

method employed. In order to achieve effective desulphurization, the following properties of the sorbent must be put into consideration; sorbent's adsorption ability, durability, selectivity for the organo-sulfur compounds and regenerability (Babich and Moulijn 2003).

In reactive adsorption desulfurization the process is in such a way that sulphur is removed from the molecule and attached to the sorbent. The sulphur-free distillate is then returned back to the final product without losing its original structure. (Meier et al., 2001; Babich and Moulijn 2003). Muzic et al., 2010 employed activated carbon and 13X type Zeolite as adsorbents in the removal of sulfur from diesel fuel. The result showed that activated carbon has a higher adsorbing ability when compared to Zeolite. Activated carbon and carbon nanotubes have attracted much attention from researchers as promising adsorbent materials for adsorptive desulphurization due to their exceptional properties, for instance, large surface area, high pore structure, pore size distribution, high thermal stability as well as excellent physical and chemical stabilities.

Adsorption is the most economically attractive desulfurization technique (Al Zubaidi et al., 2015). It has been explored by many researchers owing to its applicability and low cost on large scale (Moosavi et al., 2012; Gawande and Kaware 2016). It is beneficial because the desulfurization process can be carried out at ambient temperature and pressure without consumption of hydrogen or oxygen. Furthermore, there is possibility of adsorbent regeneration and reusability (Ahmed and Ahmaruzzaman, 2015). Capability of different kinds of adsorbents such as commercial activated carbon (CAC) (Zhou et al., 2009) metal–organic frameworks (Achmann et al., 2010; Khan and Jhung, 2013), mesoporous materials, activated carbon cloth (Fallah and Azizian, 2014), carbon nanoparticles (Fallah and Azizian 2012), zeolites (Xiao et al., 2008), and nano-porous activated carbon have been explored by researchers for the desulfurization of model and real transportation fuels. Commercial activated carbon, among others, has been widely used as an adsorbent because of its effectiveness due to its improved micro structures (Eddebbagh et al., 2016). Nevertheless, its procedure and application come with high expense (Ahmed and Ahmaruzzaman, 2015). Carbon nanotubes also come with the. short comings such as high cost of production. This motivates the alternative use of low-cost, readily available and environmentally friendly agro-waste adsorbent, such as neem leaf powder (NLP) and pomegranate leaf powder (PLP) for the desulfurization of petroleum distillate, especially diesel in this study.

It is estimated that about 998 million tonnes of agricultural waste is produced yearly (Agamuthu, 2009). Therefore, the use of agricultural waste materials for the treatment of sulfur-containing petroleum distillates will serve as a proof of concept in the development and application of green materials in sustainable, innovative and effective waste management for the abatement of environmental pollution. Agricultural waste materials are presently gaining attention as potential adsorbents for removal of various contaminants from wastewaters and fuels due to their availability and low cost (Ahmaruzzaman and Gupta, 2011). Low cost agricultural waste by-products such as palm kernel shell (Isam et al., 2013), neem leaf (Daware and Kulkami, 2015), and almond shell (Deniz, 2013) have been investigated by many researchers as adsorbents for removal of sulfur-containing compounds from petroleum distillates. Pomegranate peels have been utilized as adsorbent for the treatment of heavy metals in water (Bhattacharjee and Patel, 2017). However, PLP and NLP as adsorbents for the removal of DBT from model oil and petroleum distillates have not been reported until now. The leaves of pomegranate and neem are abundantly available locally. They are waste materials from which useful adsorbent materials can be developed for industrial application. From this point of view, PLP and NLP, which are agro-based wastes product, could be important materials for utilization in desulfurization of transportation fuels because they are cheap, readily available and will reduce environmental waste. Another technique that is currently being used recently is biodesulfurization.

Biodesulfurization offers the potential method for reducing the amount of the sulfur in petroleum products with benefits of low operating cost, lower capital and less greenhouse gases (Linguist and Pacheco, 1999). Dibenzothiophene (DBT) has been discovered to be a model polyaromatic sulfur heterocycle for the isolation and classification of bacteria proficient of converting organosulfur compounds found in a range of fossil fuels (Monticello, 2000). There are two major pathways for desulfurization of DBT; the Kodama pathway, in this case the initial attack, is focused towards one of the carbon atoms and 4S pathway (Figure 1.1), where the initial catalysis is directed towards the center of the sulfur atom (Kilbane and Bielaga, 1990). The 4S pathway is better and perfect for desulphurization because the carbon skeleton is not destroyed and the heating value of the fuel stays unchanged. Biodesulphurization is a promising application for producing biochemical since the reaction will be terminated before the last step to produce hydroxybiphenylbisulfinate (HPBS) (Monticello, 2000). The process is operational irrespective of the position or site of alkyl

substitution (Pacheco, 1999). Even though there has been a considerable development in the utilization of BDS process, there still remain so many challenges in the aspect of cost analysis of catalyst, design of reactor as well as separation of oil-water mixture (Guobin et al., 2006). In order to lower the operating cost of biocatalyst there is need for mass production of it in which the desulphurization capability will still be intact. This can be achieved by high cell density cultivation. At the moment, only few investigations have been carried out on cultivation of high cell density in BDS of organosulphur compounds (Guobin et al., 2006). In a BDS process, a bioreactor is used where fuel is mixed with an aqueous solution that contains bacteria and other elements required for the bacteria growth. The bacteria transform sulphur to sulphonate which can be used as feedstock for the surfactant production (Babich and Moulijn, 2003). Enzymes with wide-ranging specificities are needed in order to remove enough sulphur to meet the impending specification imposed on petroleum companies (Monticello, 2000). Therefore, biological desulphurization with the help of microorganisms is considered the potential method for removal or reduction of sulphur in petroleum distillates.

Microorganisms are microscopic living organisms which may be single celled or multicellular. Microorganism such as Pseudomonas, Rhodococcus and Mycobacterium species, have been used to degrade dibenzothiophene (DBT). DBTs are well known organosulfur compounds which usually exist in crude oil and fractions used in the production of diesel. DBT and its derivatives can account for a large fraction of the entire sulfur substance of a particular crude oils. The total amount of sulphur content remaining in a middle distillate fraction treated with HDS method is usually in form of C_x-DBT compounds. DBT and its derivatives are recalcitrant to desulfurization by HDS, and its alkyl derivatives are considered amongst the hardest to desulfurize by traditional methods. In addition, contrary to other substances, DBT is easy to control since it's not mutagenic or extremely hazardous to human health. Microorganisms have varying methods of removing sulfur atom from DBT. They can be categorized into four: carbon–carbon (C-C bonds) cleavage, sulphur oxidation and sulfur-specific cleavage (C-S bond). The last type, 4S- pathway is the most commonly studied owing to the fact that it released a sulfur atom from DBT, without the carbon chain broken, which is helpful in fuel biodesulfurization (Rashtchi et al., 2006).

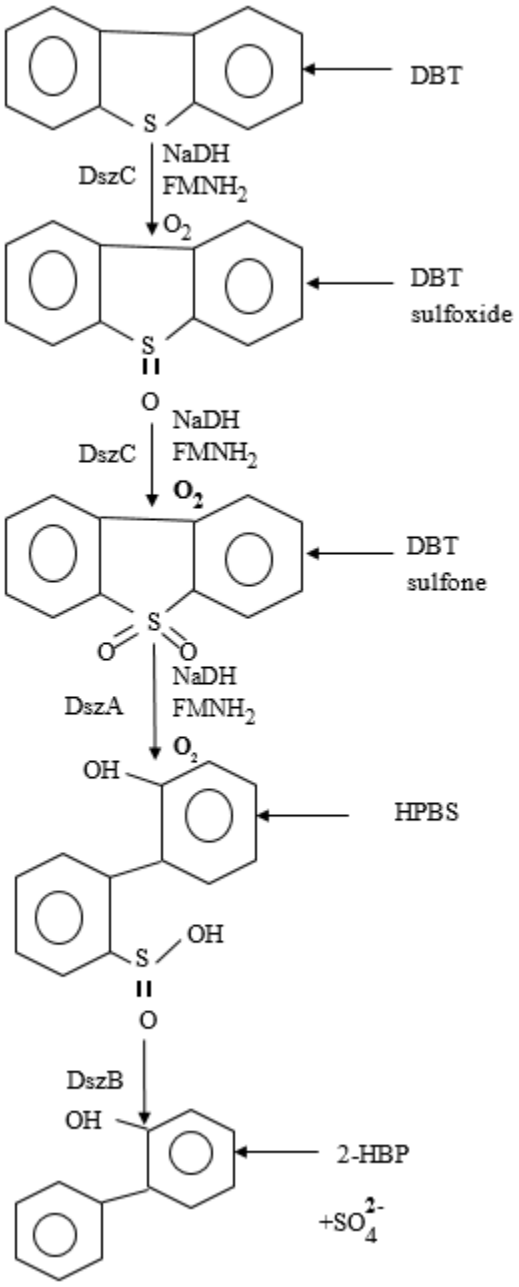


Figure 1.1 4S-pathways for biodesulphurization of DBT (Adapted from Monticello, 2000)

Rhodococcus erythropolis IGTS8 has been extensively used as bacterium in the biodesulphurization of DBT through a path way in which only the sulphur atom is attacked known as 4S-pathway (four steps). However, the process is not cost effective owing to high consumption

of the reducing equivalents which is required to arrive at the final stage. In this respect, the utilization of a new genetically advanced bacterial has received great consideration in the recent research drive. Therefore, *Pseudomonas putida and Pseudomonas aeruginosa* will be employed in this study because they can as well disulphurized DBT through 4S pathway. Many investigations have been successful reported on the desulfurization of organosulphur using Pseudomonas species, such as *Pseudomonas putida, pseudomonas aeruginosa* and so on (Md Noh et al., 2011; Caro et al., 2007). Biodesulfurisation of DBT with *Pseudomonas putida* CECT5279 by resting cells). *Pseudomonas aeruginosa* was used for desulphurization of crude oil before distillation as a form of pretreatment measure. The result showed that distillation time was greatly reduced and biodesulphurization of the crude oil was improved (Md Noh et al., 2011). Desulfurization of DBT has also been studied using Pseudomonas putida CECT5279. The growth rate of the microorganism was also investigated (Martins et al., 2004). The bacteria strains that will be used in this study namely *Pseudomonas aeruginosa and Pseudomonas putida* are known for their abilities to grow at optimum temperature of 37^{o}C and at a temperature as high as 47^{o}C. They have tolerance for a wide variety of conditions such as temperature and bacteriology. In addition, they are relatively available and can be easily cultured compared to other bacteria strains (Todar, 2016). Fig.1.2 represents the process flow diagram of the hybrid process (AD/BDS).

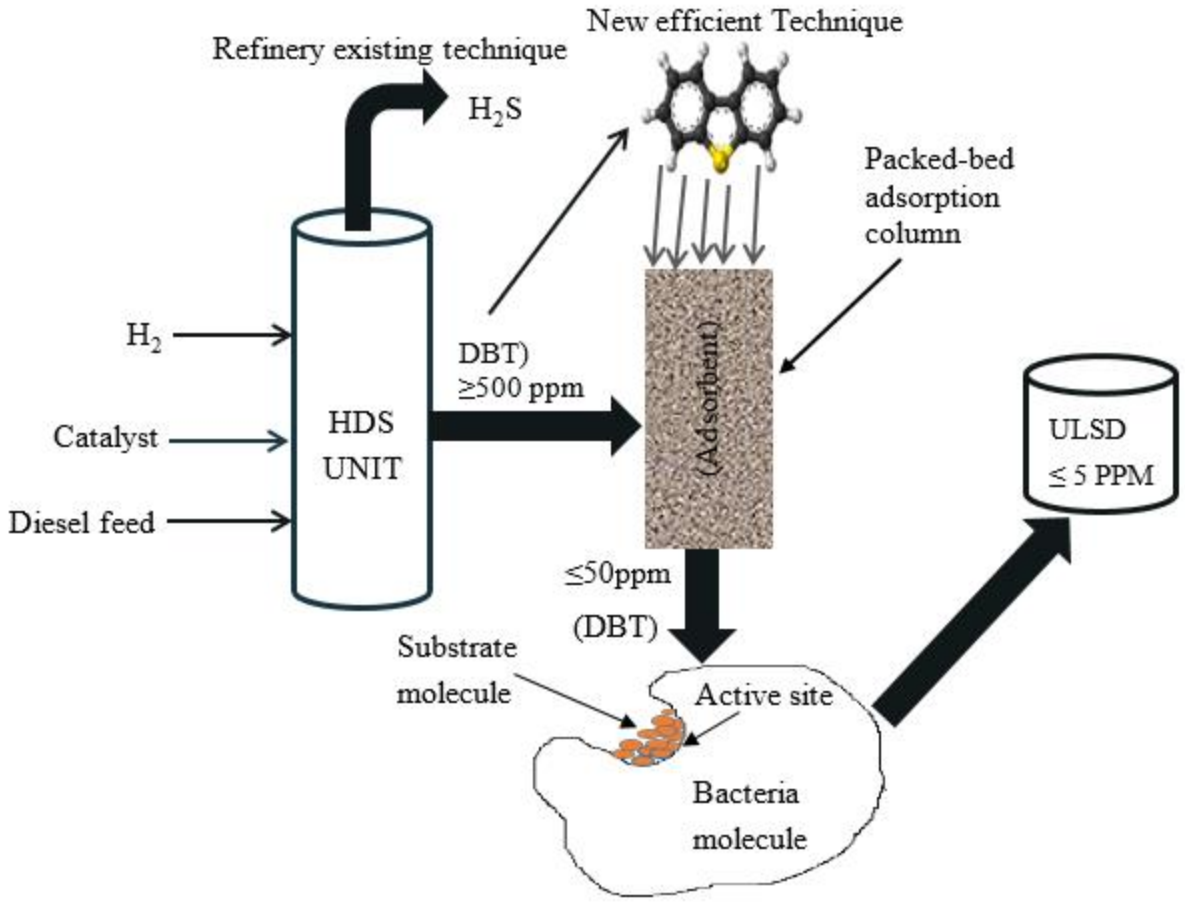


Figure 1. 2 Process flow diagram of the (Adsorption/BDS) hybrid process

1.3. Research aims, questions and objectives

The aim of this study is to develop and evaluate a hybrid process (AD/BDS) for the desulphurization of South African petroleum products (e.g. diesel) to obtain ultra-low sulphur content (≤ 5 ppm).

The following questions were addressed during the course of this study;

1. Could a hybrid process, combining adsorptive desulfurization (ADS) and biodesulphurization (BDS) be effective in reducing the level of sulfur-containing

compounds in South African petroleum distillates (e.g. diesel) obtained from hydrodesulphurizer (HDS) be reduced to 5 ppm?

2. What type of adsorbent will be required for the adsorption unit and what type of biocatalyst (whole cell or enzyme) will be required for the BDS to make the proposed hydrid process feasible?
3. What will be the effect of operating variables on the performance of the AD and BDS and the hybrid system for the removal of sulphur-containing compounds to ≤ 5 ppm in the South African petroleum distillates?
4. Can the kinetic and isothermal studies of the performance of the adsorbents be described using existing kinetic models and adsorption isotherms?

To profer solution to the above research questions, the following research objectives were considered:

1. To develop and evaluate the performance of ADS using some selected adsorbents (e.g. NLP, PLP, AC, CNTs and FCNTs) for the removal of sulphur-containing compounds from samples of South African petroleum distillates obtained from HDS unit and optimize the ADS performance.
2. To develop and evaluate BDS technique, using *Pseudomonas Putida* and *Pseudomonas Aeruginosa* as biocatalysts, for the removal of sulphur-containing compounds from samples of South African petroleum distillates obtained from HDS unit and optimize the process toward enhancing its performance.
3. To couple the two processes in (1) and (2) and evaluate the hybrid process for the removal of sulphur-containing compounds from samples of South African petroleum distillates
4. To conduct parametric optimization on the developed hybrid process in in (1) and (2) and apply it in (3).
5. To investigate whether the kinetics and isothermal adsoption exhibited by the adsorbents used in (1), (2) & (3) could be described by existing kinetic models and adsorption isotherms.

1.4. Research benefits and novel contribution to knowledge

As far as could be ascertained, no report on the application of a hybrid process combining AD with BDS has appeared in literature. This study was successfully conducted, with the following outcomes;

For the firsrt time, the study has reported the synthesis and performance evaluation of pomegranate for the removal of DBT in model oil and South African petroleum distillate. Further investigation was also carried out on neem leaf powder The kinetics, isotherm model and thermodynamics of the adsorption process of this adsorbents have also been reported. Furthermore, studies have shown that the performance efficiencies of these agro-waste adsorbents compared well to other adsorbents in literature. Therefore, the use of agricultural waste materials for the treatment of sulfur-containing petroleum distillates in this study may serve as a proof of concept in the development and application of green materials in sustainable, innovative and effective waste management for the abatement of environmental pollution. Therefore, results documented in this dissertation provide an avenue for further research development in the area.

Adsorption/biodesulfurization coupling technique is reported for the first time. This technique could serve as alternative method in the petroleum refinery to meet up with the stringent regulation to minimize the release of sulfur oxide into the atmosphere. Therefore, results documented in this dissertation could pave the way for the actualization of the benchmark set by the WHO on the minimum concentration of sulphur-contianing compounds in South African petroleum distillates.

There are only few reports on the development of hybrid process (AD/BDS) in desulfurizing South Africa petroleum distillate. The use of *Pseudomona aeruginosa (P. aeruginosa) and Pseudomonas putida (P. putida)* bacteria strains for biodesulphurisation of South African diesel oil has not been widely reported in literature as well. In addition, development of hybrid process (AD/BDS) for desulphurization of South Africa diesel diesel has not been well studied. Therefore, this study focused on this, building up on the literature and investigations that have already been carried out for BDS and adsorption separately on other diesel sources in other parts of the world. Existing Kinetics was used to predict the concentration time history of petroleum feedstock (diesel) and substrates (bacterial strains) using suitable growth kinetics. The results documented in this

dissertation could pave the way for the actualization of the benchmark set by the WHO on the minimum concentration of sulfur-contianing compounds in South African petroleum distillates. This could also contribute to scientific knowledge.

In summary, the outcome of this study provides a concept that could help in scaling up an adsorption-bioreactor plant for industrial application. The novel contributions have been communicated to the researchers working in similar research area and other related areas through publication of articles in international journal and conference proceedings. The published jurnals from this study can be found in Appendix C

1.5 Thesis Outline

Chapter One: This chapter presents an overall introduction, motivation on why the study was carried out. Its novel contribution to knowledge is highlighted. The aims and objectives are also stated. The overview of the whole dissertation is presented.

Chapter Two: This chapter contains a critical literature review describing the already existing techniques of desulfurization, their shortcomings and the new efficient techniques with their benefits. It also highlighted previous studies that have carried out on the subject. A review paper has been published on biodesulfurization and its state of art from this chapter. It has been included in Appendix C.

Chapter Three: This chapter presents the general methodology of the study. The materials and methods used in this study are described. This chapter also decribes the synthesis/preparation of the adsorbents used in this study, preparation and growth of bacteria used, characterization techniques used to analyze the samples are also decribed under this chapter. The performance evaluation of the adsorbent and the degradation of the DBT by the bacteria were described in detail under this chapter.

Chapter Four: In this chapter, agro-waste adsorbents (pomegranate leaf powder and neem leaf powder) were synthesized. Desulfurization experiment using model oil (DBT dissolved in hexane) was perfomed in batch operation mode. The best operating parameters (parametric optimization) such as temperature, time, amount of adsorbent were determined. The reusability performance of

the adsorbents so as to minimize wastage was studied. Furthermore, in order to understand the mechanism of the adsorption of DBT into these agro-waste adsorbents, first order and second order kinetics, isotherms model (Langmuir and Freundlich), and thermodynamics of adsorption process of these adsorbents, were described here.

Chapter Five: In this chapter, carbon nanotubes were funcionalized. Desulfurization experiment using model diesel (DBT dissolved in hexane) was perfomed in batch operation mode. The best operating parameters (parametric optimization) such as temperature, time, amount of adsorbent were determined. The regeneration and re-usability of the adsorbents were also studied. Furthermore, in order to understand the mechanism of the adsorption of DBT into carbon nanotubes (CNTs) and functionalized carbon nanotubes (FCNTs), first-order and second-order kinetics, isotherms model (Langmuir and Freundlich), and thermodynamics of adsorption process of these adsorbents, were described here. A manuscript has been written and published in conference proceeding from this chapter. The proceeding is attached in Apendix D at the end of the thesis.

Chapter Six: In this chapter, as-received activated carbon was used as adsorbent. Desulfurization experiment using model diesel (DBT dissolved in hexane) was perfomed in batch operation mode. The best operating parameters (parametric optimization) such as temperature, time, amount of adsorbent were determined. The reusability of the adsorbents in order to minimize wastage was carried out in cycles. Furthermore, in order to undesratnd the mechanism of the adsorption of DBT into activated carbon, first order and second order kinetics, isotherms model (Langmuir and Freundlich), and thermodynamics of adsorption process of these adsorbents, were described here. The desulfurization of real diesel using activated carbon as adsorbent in a batch mode was studied in this chapter. The best adsorbent with the highest % DBT removal and adsorption capacity from previous studies was chosen in this chapter to desulfurize South African real diesel (diesel obtained before HDS (5200 ppm) and diesel obtained after HDS (120 ppm), initially using the best operating paremeters from previous studies then modified the parameters to evaluate their effects on the adsorptive performance of the adsorbent on the real diesel samples.

Chapter Seven: The enhancement of desulfurization performance of AC in packed-bed column using immobilization technology extensively investigated and discussed using modelling and

experimental approaches such as; Bohart-Adams, Thomas and Yoon-Nelson models. The respective breakthrough curves, kinetics of adsorption were presented and discussed extensively. Validation of the models with experimental data was also carried out in this chapter.

Chapter Eight: This chapter discussed the biodesulfurization of DBT in model oil and South African diesel samples (diesel obtained after HDS and diesel obtained before HDS*). Pseudomonas aeruginosa* and *Pseudomonas putida* are used as biocatalysts in this Chapter. The growth of the bacteria was measured as well as the bio-degradation of the DBT and the formation of the 4S end product, 2-hydroxylbiphenyl (2-HBP). The kinetic of the bacteria growth and biodesulfurization were studied and discussed extensively under this chapter. The biodesulfurization experiment of resting cells of *Pseudomonas aeruginosa* and *Pseudomonas putida* for degradation of DBT in South African diesel samples and its kinetics were also discussed here. A manuscript from this chapter has been written and submitted for publication.

Chapter Nine: This chapter focused on the performance of adsorptive desulfurization coupling biodesulfurization for desulfurization of petroleum distillates (e.g diesel). The best parametric conditions obtained in Chapter 7 and 8 were used for this experiment. This experiment was carried out on South African diesel samples. The mechanism of the adsorption process was discussed extensively using kinetics models developd in chaper seven and eight. A manuscript has been written and submitted for publication.

Chapter Ten: This chapter reported a general summary of the study conducted and overall conclusions from preceding chapters as well as recommendations. References to all articles accessed in this study are presented at the end of each chapter in this dissertation.

1.6. References

Ademiluyi, F. T., Amadi, S. A., and Amakama, N. J. (2009) Adsorption and treatment of organic contaminants using activated carbon from waste Nigerian Bamboo. J. Appl. Sci. Environ. Manage, 13 (3), 39 - 47.

Achmann, S., Hagen, G., Hammerle, M., Malkowsky, I., Kiener, C., Moos, R. (2010) Sulfur removal from low-sulfur gasoline and diesel fuel by metal-organic frameworks. Chem Eng Technol., 33, 275–280.

Agamuthu, P. (2009) Challenges and opportunities in Agro waste management: An Asian perspective. Inaugural meeting of First Regional 3R Forum in Asia 11 -12 Nov., Tokyo, Japan.

Ahmaruzzaman, M. and Gupta, V.K. (2011) Rice Husk and Its Ash as Low-Cost Adsorbents in Water and Wastewater Treatment Ind. Eng. Chem. Res. 50, 13589–13613.

Al-Zubaidy, I. A. H. Tarsh, F.B., Darwish, N.-N., Majeed, Balsam S. S. A., Al-Sharafi, A. and Chacra, L.A. (2013) "Adsorption Process of Sulfur. Removal from Diesel Oil Using Sorbent.Journal of Clean Energy Technologies, 1(1), 66-68.

Ahmed, J. K. and Ahmaruzzaman, M. (2015) Adsorptive desulfurization of feed diesel using chemically impregnated coconut coir waste Int. J. Environ. Sci. Technol. 12, 2847–2856.

Ahmad, W., Ishaq, I.A.M., and Ihsan, K. (2014) Adsorptive desulphurization of kerosene and diesel oil by Zn impregnated monotmorollonite clay. American Journal of chemistry.

Alavi, S.A., and Hashemi, S.R. (2014) A Review on Diesel Fuel Desulfurization by Adsorption Process. International Conference on Chemical, Agricultural, and Biological Sciences (ICCABS'2014) Antalya (Turkey).

Alcon, A., Martin, A. B., Santos, V.E., Gomez, E., Garcia-Ochoa, F. (2008) Kinetic model for DBT desulphurization by resting whole cells of Pseudomonas putida CECT5279. Biochemical Engineering Journal, 39, 486–495.

Babich, I.V., and Moulijn, J.A. (2003) Science and technology of novel processes for deep desulfurization of oil refinery streams: a review. Fuel 82, 607–631.

Bhattacharjee, R. and Patel, R. (2017) Adsorption of chromium (vi) using neem leaves and pomegranate peels. Journal of Emerging Technologies and Innovative Research (JETIR), 4 (5).

Biswas, S.G.D., Bhattacharya, P., and Chowdhury, R. (2005) Bio-desulfurization of model organo-sulfur compounds and hydrotreated diesel—Experiments and modeling. Chemical Engineering Journal, 112, 145–151.

Block, E. (1978) Reactions of Organosulfur Compounds. Academic Press, New York, pp. 202-207.

Caro, A., Boltes, K., Leton, P., Garc´ıa-Calvo, E. (2007) Dibenzothiophene biodesulfurization in resting cell conditions by aerobic bacteria. Biochemical Engineering Journal, 35, 191–197.

Carter, P.T. (1954) Furfural refining of cat cycle gas oils. Oil Gas J., 52(46), 157.

Darzins, A., and Mrachko, G.T. (2000) Sphingomonas biodesulfurization catalyst, U.S. Patent No. 6,133,016.

Daware, G.B., Kulkarni, A. B. and. Rajput, A. A (2015) Desulphurization of diesel by using low cost adsorbent, International Journal of Innovative and Emerging Research in Engineering. 2 (6), 69-73.

Deniz, F. (2013) Adsorption Properties of Low-Cost Biomaterial Derived from Prunus amygdalus L. for Dye Removal from Water. The Scientific World Journal Volume 2013, Article ID 961671. 1-8.

Eddebbagh, M., Abourriche, A., Berrada, M., Zina, M.B. and Bennamara, A. (2016) Adsorbent material from pomegranate (Punica granatum) leaves: Optimization on removal of methylene blue using response surface methodology. J. Mater. Environ. Sci. 7 (6), 2021-2033.

Fallah, R. and, Azizian, S. (2012) Rapid and facile desulphurization of liquid fuel by carbon nanoparticles dispersed in aqueous phase. Fuel 95, 93–96.

Folsom, B.R., Schieche, D.R., Digrazia, P.M., Werner, J., and Palmer, S. (1999) Microbial Desulfurization of Alkylated Dibenzothiophenes from a Hydrodesulfurized Middle Distillate by Rhodococcus erythropolis I-19. American Society for Microbiology. 65 (11), 4967–4972.

Furuya, T., Kirimura, K., Kino, K. (2001) Thermophilic biodesulfurization of dibenzothiophene and its derivatives by Mycobacterium phlei WU-F1, FEMS Microbiology Letters, 204, 129-133.

Gawande, P. R and Dr. Kaware J. P. (2018). Isotherm and Kinetics of Desulphurization of Diesel by Batch Adsorption Studies International Journal of Chemical Engineering Research. 10 (1)), 1-16.

Grossman, M.J., Lee, M.K., Prince, R.C., Garrett, K.K., George, G.N., and Pickering, I.J. (1999) Appl. Environ. Microbiol. 65, 181.

Grossman, M.J., Lee, M.K., Prince, R.C., Minak-Bernero, V., G.N. and Pickering, I.J. (2001) Appl. Environ. Microbiol. 67, 1949.

Guobin, S., Huaiying, Z., Jianmin, X., Guo, C., Wangliang, L., and Huizhou, L. (2006) Biodesulfurization of hydrodesulfurized diesel oil with Pseudomonas delafieldii R-8 from high density culture. Biochemical Engineering Journal, 27, 305–309.

Khan, N.A. and Jhung, S.H. (2013) Effect of central metal ions of analogous metal-organic frameworks on the adsorptive removal of benzothiophene from a model fuel. J Hazard Mater 260, 1050–1056.

Hernández-Maldonado, A.J and Yang, R.T. (2004) Desulfurization of Transportation Fuels by Adsorption. Catalysis Reviews, 46, (2), 111-150.

Sasol (2012) on http://kiabuzz.co.za/2012/02/what-you-need-to-know-about-low-sulphur-50-ppm-diesel-fuel/#sthash.BsXoU1mo.dpuf. Accessed on the 20th of June, 2016.

Xamplified free online education source on http://www.chemistrylearning.com/adsorption. Accessed 29th, July, (2016).

Todar's online textbook of bacteriology on http://textbookofbacteriology.net/pseudomonas.html Accessed 8th of August, (2016).

Ishihara, A., Wang, D., Dumeignil, F., Amano, H., Qian, E.W., and Kabe., T. (2005) Oxidative desulfurization and denitrogenation of a light gas oil using an oxidation/adsorption continuous flow process. Applied Catalysis A: General, 279, 279–287.

Kim, J.H., Ma, X., Zhou, A., and Song, C. (2006) Ultra-deep desulfurization and denitrogenation of diesel fuel by selective adsorption over three different adsorbents: A study on adsorptive selectivity and mechanism, Catalysis today, 74–83.

Kim, Y.H., Woo, H.C., Lee, D., Lee, H.C. and Park, E.D. (2009). The effect of metal ions in MNaY-zeolites for the adsorptive removal of tetrahydrothiophene. Korean J. Chem. Eng. 26, (5), 1291-1295.

Irani, Z.A., Mehrnia, M.R., Yazdian, F., Soheily, M., Mohebali, G. and Rasekh, B. (2011) Analysis of petroleum biodesulfurization in an airlift bioreactor using response surface methodology. Bioresource Technology 102, 10585–10591.

Kilbane, J. J. & Le Borgne, S. (2004). Petroleum biorefining: the selective removal of sulfur, nitrogen, and metals. In Petroleum Biotechnology, Developments and Perspectives, pp. 29–65. Edited by R. Vazquez-Duhalt & R. Quintero-Ramirez. Amsterdam: Elsevier.

Le Borgne, S. and Quintero, R. (2003) Review Biotechnological processes for the refining of petroleum. Fuel Processing Technology. Vol. 81, pp. 155–169.

Lee, M.K., Senius, J.D. and Grossman, M.J. (1995) Sulfur-specific microbial desulfurization of sterically hindered analogs of dibenzothiophene. Appl. Environ. Microbiol. 61, (12), 4362-4366.

Lee, I.S., Bae, H., Ryu, H.W., Cho, K. and Chang, Y.K. (2005) Biocatalytic Desulfurization of Diesel Oil in an Air-Lift Reactor with Immobilized Gordonia nitida CYKS1 Cells. Biotechnol. Prog. 21, (15), 781-785.

Lien, A.P. and Evering, B.L. (1952) Hydrogen fluoride extraction of high-sulfur virgin petroleum stocks. Ind. Eng. Chem., 44, 874.

Linguist L, Pacheco M. (1999) Enzyme-based diesel desulfurization process offers energy, CO2 advantages. Oil Gas J, 97, 45-48.

Ma, X., Sun, L. and Song, C. (2002). A new approach to deep desulfurization of gasoline, diesel fuel and jet fuel by selective adsorption for ultra-clean fuels and for fuel cell applications. Catalysis Today 77, 107–116.

Marafi, M., Stanislaus, A. and Furimsky, E. (2010) Hand book of spent hydroprocessing—catalyst-regeneration, rejuvenation and reclamation. Elsevier. Linacre house, Jordan Hill, Oxford OX28DP, UK.

Martin, A. B., Alcon, A., Santos, V. E. and Garcia-Ochoa, F. (2004) Production of a Biocatalyst of Pseudomonas putida CECT5279 for Dibenzothiophene (DBT) Biodesulfurization for Different Media Compositions, Energy & Fuels, 18, 851-857.

Mehdizadeh, A. and Ahmadi, A.M. (2013) Deep desulfurization of fuel diesels using alkyl sulfate and nitrate containing imidazolium as ionic liquids. Journal of Applied Chemical Research, pp 75-85.

Mohebali, G and Ball, A.S. (2008). Biocatalytic desulfurization (BDS) of petrodiesel Fuels. Microbiology. 154, 2169–2183.

Monticello, D.J. (2000) Biodesulfurization and the upgrading of petroleum distillates. Current Opinion in Biotechnology 2000, 11:540–546.

Moosavi, E. S., Dastgheib, S.A. and Karimzadeh, R. (2012) "Adsorption of Thiophenic Compounds from Model Diesel Fuel Using Copper and Nickel Impregnated Activated Carbons "Energies, pp.4233- 4250.

McFarland, B.L (1999). Biodesulfurization, Curr. Opin. Microbiol. 2, 257–264.

Mei, H., Mei, B.W., Yen, T.F. (2003) A new method for obtaining ultra-low sulfur diesel fuel via ultrasound assisted oxidative desulfurization. Fuel 82, 405–414.

Meier, P.F, Reed, L.E, Greenwood, G.J. (2001) Removing gasoline sulphur. Hydrocarbon Engng. 1, 26.

Michlmayr, M.J. (1980). Selective Process for Removal of Thiophenes from Gasoline Using a Silver Exchanged Faujasite-Type Zeolite. U.S. Patent 4,188,285, February 12.

Monticello, D.J. (1998) Riding the fossil fuel biodesulfurization wave. ChemTech. 28, 38-45.

Monticello, D.J. (2000) Biodesulfurization and the upgrading of petroleum distillates, Curr. Opin. in Biotechnol. 11, 540–546.

Muzic, M., Sertic-Bionda, K., Gomzi, Z., Podolski, S. and Telen, S. (2010) Study of diesel fuel desulfurization by adsorption. Chemical Engineering Research and Design 88(4) 487–495.

Md Noh, N.A.., Salleh, S.M., Ibrahim M.M., and MohdYahya, A.R. (2011) International Conference on Biotechnology and Environment Management IPCBEE vol.18 (2011) © IACSIT Press, Singapoore). (Pseudomonas aeruginosa USM-AR2 culture containing biosurfactant facilitates crude oil distillation process.

Nazal, M.K., Oweimreen1, G.A., Khaled, M., Atieh, M.A., Aljundi, I.H and Abulkibash1, A.M. (2016) Adsorption isotherms and kinetics for dibenzothiophene on activated carbon and carbon nanotube doped with nickel oxide nanoparticles. Bull. Mater. Sci., 39, (2), 437–450.

Ohshiro, T., Hirata, T. and. Izumi, Y. (1996) Desulfurization of dibenzothiophene derivatives by whole cells of Rhodococcus erythropolis H-2. FEMS Microbiol. Lett. 142, 65.

Pacheco, M. A. (1999). Recent advances in biodesulfurization (BDS) of diesel fuel. Paper presented at the NPRA Annual Meeting, San Antonio, TX, pp. 21–23.

Rashed, M.N. (2013). Adsorption Technique for the Removal of Organic Pollutants from Water and Wastewater. Aswan Faculty of Science, Aswan University, Aswan, Egypt. Chap 7 ISBN 978-953-51-0948-8, DOI: 10.5772/54048.

Rashtchi, M., Mohebali, G.H., Akbarnejad, M.M., Towfighi, J., Rasekh, B., Keytash, A. (2006) Analysis of biodesulfurization of model oil system by the bacterium, strain RIPI-22. Biochemical Engineering Journal 29, 169–173.

Savage DW, Kaul BK, Dupre GD, O'Bara JT, Wales WE, Ho TC. US Patent 5,454,933.

Shimizu, Y., Kumagai, S. and Takeda, K. (2007) Adsorptive removal of sulphur compounds in kerosene by using rice husk activated carbon. Japan Energy Corporation, Today, pp 335-8502.

Swaty, T. E. (2005). Global refining industry trends: the present and future. Hydrocarbon Processing. pp. 35–46.

Topsøe, H., Clausen, B.S, Massoth, F.E. (1996) Catalysis: science and technology, 11, 310.

Xi, L., Squires, C.H., Monticello, D.J. and Childs, J.D. (1997) Biochem. Biophys. Res. Commun. 230, 73.

Vazquez-Duhalt, R., Torres, E., Valderrama, B. and Borgne, S.L. (2002) Will Biochemical Catalysis Impact the Petroleum Refining Industry? Energy Fuels, 16, (5), 1239–1250.

Yang, R.T., Arturo J. Herna´ndez-Maldonado, A.J. and Yang, F.H. (2003). Desulfurization of Transportation Fuels with Zeolites Under Ambient Conditions. Science 301, 79-80.

Zaheer, K and Syed, A. (2014) Oxidative desulphurization followed by catalytic adsorption method." South African Journal of Chemical Engineering, 18, (2), 14- 28.

Zannikos, F., Lois, E. and Stournas, S. (1995) Desulfurization of petroleum fractions by oxidation and solvent extraction. Fuel Processing Technology. 42 35-45.

Xiao, J., Li, Z., Liu, B., Xia, Q. and Yu, M. (2008) Adsorption of benzothiophene and dibenzothiophene on ion-impregnated activated carbons and ion-exchanged Y zeolites. Energy Fuels, 22,3858–3863.

Chapter Two

2.0. Literature review

In this chapter, related literature emphasizing the present trends in the evaluation and development of adsorption and biodesulfurization techniques and their applications are critically discussed.

2.1. World's perspective of diesel fuel and specifications

In the recent times, production of energy has remained a great challenge across the globe. Coal is a fossil fuel that plays an important role in the energy structure. Sulfur oxides are released into the atmosphere when coal containing high sulfur is combusted. This causes severe environmental problems, for example, air pollution and acid rain (Kan et al., 2010). The main concern in the refineries at the moment is the cleaning of the Sulphur-containing compounds from crude oil (Babich and Moulijn, 2003; Caitlin, 2012). Though, Pyrite has been investigated to be the major inorganic sulfur compound in high sulfur coal (Weerasekara et al., 2008). There has been a decrease in the fraction of energy derived from fossil fuel, although, the share of world energy from fossil fuels is about 82% (Duissenov, 2013). Crude oil is naturally present under the ground. It is mainly used as transportation fuels, such as diesel, gasoline, and jet fuels. The qualities of crude oil are significantly subjective to two properties viz.; American Petroleum Institute (API) gravity and sulfur content (Srivastava, 2012). Petroleum is one of the products of crude oil. It has prehistorically become part of human life. It contains hydrocarbons as the major components. Furthermore, insignificant amounts of sulfur, nitrogen, oxygen, and trace metals are also present. Diesel, among others, is one of the petroleum-derived fuels. Diesel comprises of a mixture of around 75% saturated hydrocarbons and 25% aromatic hydrocarbons (Alavi and Hashemi, 2014). Fig. 2.1 shows the percentage usage of of diesel at various sectors.

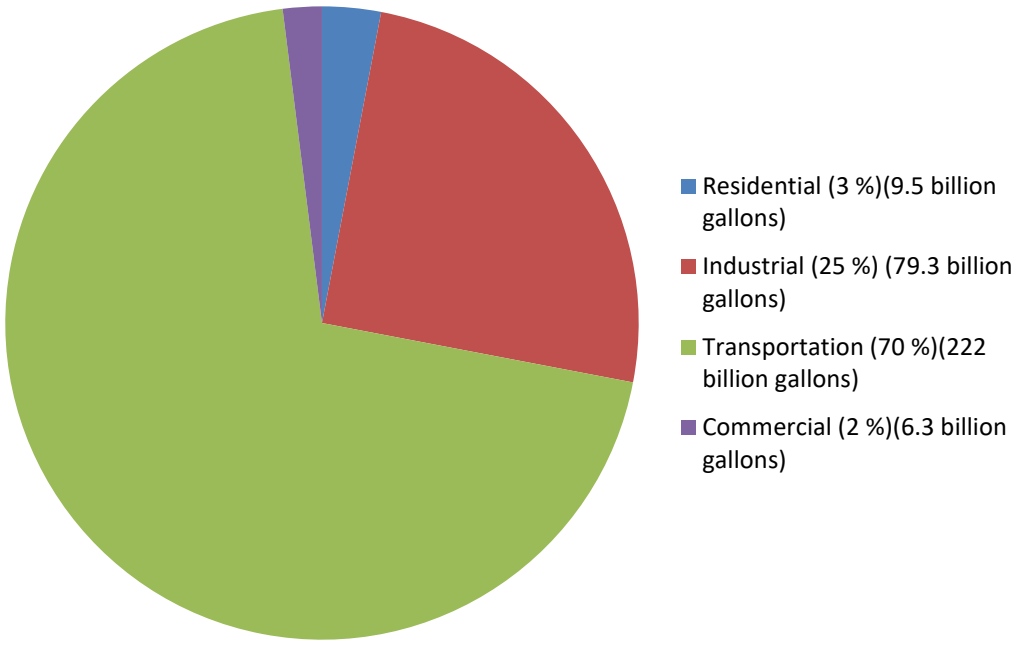


Figure 2.1 Percentage of diesel usage at various sectors (Adapted from EPA, 2017)

Diesel has been regarded as the larger and the most extensively used source of energy across the globe. Diesel consists of sulfur compounds which when combusted by direct method release toxic substances such as sulfur oxides (SO_x) into the atmosphere which contributed to acid rain, health diseases and environmental pollution (Kan et al., 2010). The world health organization estimated about 7 million deaths in 2012 alone (Babich and Moulijn, 2003). This was reported to be as a result of air pollution associated with particulate matter. This has become a major concern to law enforcement agency and environmental protection agency. Currently, a stringent guideline, by the environmental protection agency (EPA) has been passed to all refineries globally to reduce the emission of these harmful sulfur compounds into the atmosphere. South African government has recently passed a stringent law to all refineries to reduce the concentration of sulfur compounds in diesel to a minimum of 10 ppm to meet up with Euro V standard emission (Caitlin, 2012). This therefore has aroused the interest of researchers in this direction.

Different petroleum products are sold in South Africa such as; bitumen, petrol, diesel, jet fuel, illuminating paraffin, fuel oil and liquefied petroleum gas (LPG). However, petrol and diesel are most commonly used liquid fuels in South Africa, as reported by South African Petroleum Industry Association (SAPIA) bulletin (SAPIA, 2011). South African Independent online (IOL) business report on economy stated that SA's lagging behind on clean fuel specifications. For more than a decade, the standards of fuels in Europe and the US were ahead the fuel specifications in South Africa. Introduction of clean fuels which was supposed to be introduced in the country has now been postponed until after 2020. Clean fuels are essential for efficient and environmentally friendly products to the users (SAPIA, 2011).

Sulphur-containing compounds in diesel when released into the atmosphere causes lung disease and associated sicknesses. Therefore, South African administration is accountable for creating an environment that contributes to human health and safety (SA overview, 2018). Fig.2.2 shows the variations of low sulfur and standard grade sulfur levels of diesel in South Africa from 2001 to 2017.

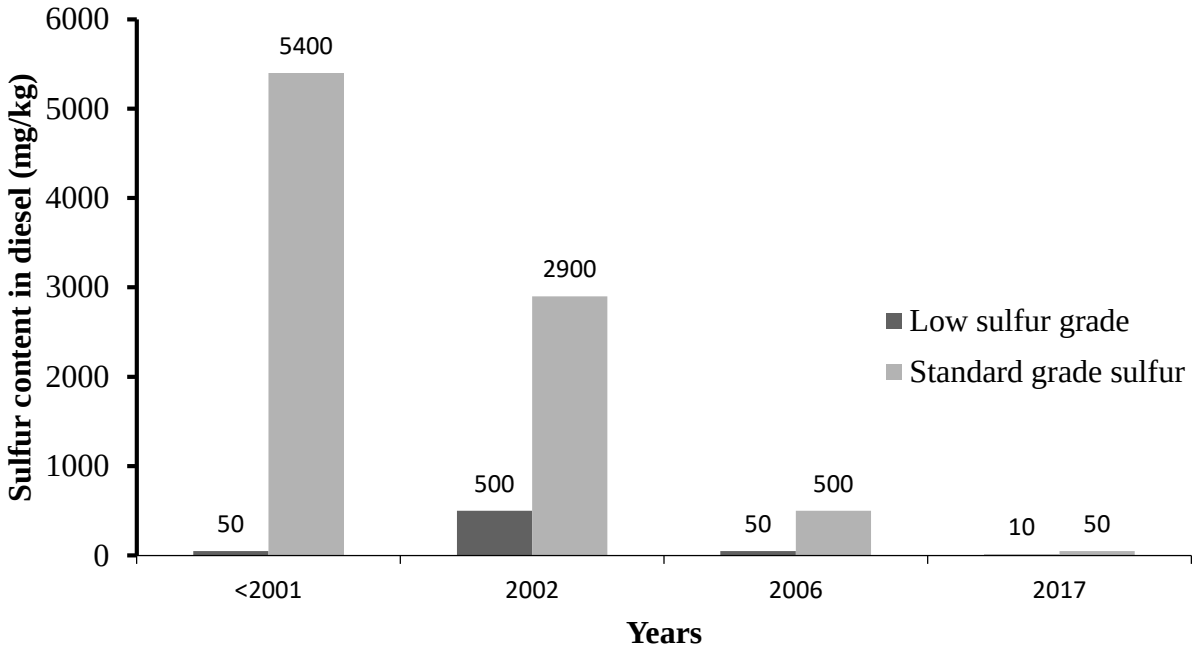


Figure 2.2. Sulfur level in South Africa diesel (Adapted from SA Overview, 2018)

Regulations concerning the introduction of Clean Fuels II were gazetted in June 2012 which specified its operation starting fully from 1st of July, 2017. This set date has been recently adjourned to a date to be affirmed in the future, as soon as other fininacial implications of the decision to introduce a cleaner fuel have been finalized. These regulations entail the reduction of sulphur levels to 10 ppm in both petrol and diesel. These also require other specifications conforming to those contained in the national standards for petrol and diesel that have been recently finalized (SAPIA, 2018). SAPIA has demanded the Department of Energy (DOE) to withdraw the regulations in connection to enactment of cleaner fuels by 1 July 2017. This is because of the uncertainty of the policy that generated delay in implementing cost recovery. DOE and SAPIA have agreed to launch a joint undertaking team to deliberate on several unresolved concerns related to cost recovery for cleaner fuels upgrades at the refineries. This is to ensure that the government in collaboration with the oil industries proffers solution to the issue regarding cost recovery. In addition, collaboration with other government strategy objectives, possible ways of implementating cost recovery mechanism, the effect on the existing refining fleet in case the cleaner fuels operation be deferred and environmental effect of cleaner fuels will be attended to. The work was near completion and the final report was expected to be available in 2016 (SAPIA, 2018). Table 2.1 shows the status of clean fuel in South Africa till date.

Sulfur compounds are present in various forms that can be classified into four groups namely: sulfides, disulfides, mercaptans and thiophenes (THs) (Srivastava, 2012). These compounds exist in significant quantities in natural gas (Chambers and Duffy, 2012). The tendency of corrosion of pipeleines and deactivation of catalyst during crude oil processing make sulfur compounds undesirable in refining process (Dunleavy, 2006; Srivastava, 2012; Ma et al., 2015). In addition, the existence of sulfur compounds in liquid fuels undesirably affects vehicles. This is responsible for lower efficiency of catalytic converters (Gap Forumn Policy, 2016). Naturally occurring sulfur compounds in fuels, when emitted reacts with water vapour in the air to form sulfates and acid rain that destroys buildings. In addition, it acidifies soil and eventually results in destruction of forests (Fang, 2004; Kan et al., 2010). Furthermore, the release of sulfur compounds has led to associated health concerns, for example, heart diseases, asthma, and respiratory illnesses.

Table 2.1 Status of clean fuel in South Africa till date

Years	Clean fuel development
1920	Introduction of cleaner fuels into South Africa and addition of lead to fuels
1970s	Banning addition of lead to fuel due to health effect
1986	Lead levels were reduced from 0.836 g Pb/L to 0.60 gPb/L in South Africa
1996	Unleaded petrol available throughout South Africa
2001	Initiation of fuel specification by Department of Minerals and Energy
2002	Sulfur in diesel reduced from 5500 to 3000 ppm
2005	Sulfur in ultra low petrol (ULP) reduced from 1000 to 500 ppm
2006	Leaded road fuel finally banned
2006	Sulfur in diesel was reduced from 500 ppm with a niche grade of 50 ppm
2010	New proposal for cleaner fuel was implemented
2011	DOE published amended regulation of petroleum products specification
2011	SAPIA commission KPMG to undertake a study on the impact of funding options of refinery upgrades to Clean Fuels II standards.
2013	Discussion between SAPIA and DOE in an attempt to finalize the cost recovery mechanism for the production and distribution of clean fuels.
2013	Discussion between SAPIA and DOE in an attempt to finalize the cost recovery mechanism for the production and distribution of clean fuels.
2014	Finalization of both the petrol and diesel CFI and CFII fuel specifications
2014	DOE confirmation of their proposal to delay the July 2017 CFII implementation date.
2015	SAPIA requested DOE to rescind the regulations pertaining to the implementation of cleaner fuels by 1 July 2017
2017	Reduction of low grade sulfur was implemented

A report by South African Petroleum Industry Association (SAPIA). (Available online at, http: www.sapia.org.za/overview/south-african-fuel-industry. Accessed on 5th April, 2018

There are various techniques of reducing sulfur content in transportation fuel. These techniques have been investigated with different levels of achievement. The most commonly used method is hydrodesulfurization (HDS) (Javadli and de Klerk, 2012). HDS has succeeded in removing aromatic sulfur-containing compounds such as sulfones, thiolates, thiols and sulfoxides. Despite the extreme conditions (high temperatures and pressures) that are involved in HDS, some of the sulfur-containing compounds still remained, resulting in the reduction in quality of the fuel (Ma et al., 1994). Therefore, the HDS method for deep desulfurization is expensive. In addition, some heterocyclic sulfur containing compounds, such as dibenzothiophene (DBT) and its alkyl substitutes, particularly 4, 6-dimethyldibenzothiophene (4, 6-DMDBT), are recalcitrant to HDS. Dimethyldibenzothiophene (DMDBT), being the least reactive of sulfur compounds also restricts HDS of petroleum distillates (Srivastava, 2012).

Other desulfurization techniques that are capable of producing ultra clean fuel are adsorptive desulfurization (AD), oxidation–extraction desulfurization (OEDS), desulfurization by oxidation (DO), and biodesulfurization (BDS).

Desulfurization by adsorption is the process whereby an active adsorbent with a large surface area selectively removes the sulfur-containing compound. Oxidative desulphurization is a chemical reaction that involves the use of oxidizing agents such as; H_2O_2, H_2SO_4, etc to oxidize sulfur-containing compounds to sulfone. Due to the higher polarity of the sulfone compound, it can be easily extracted from the fuel. BDS has attracted a lot of attention recently owing to its green processing of fossil fuel. Conversely, the major hindrance to its use, is slowness of the removal process. Recently, there are environmental regulations imposing a stringent limit for sulfur contents in transportation fuel. This is currently the strongest drive for the removal of sulfur in transportation fuels. In order to ensure the availability of energy at a lower cost by removing the sulfur from lower quality feed stocks there is urgent need for new efficient methods of desulphurization. This will also reduce its negative effects on the environment.

2.2. Environmental effects of sulfur oxides emission

Sulfur, when combust in air is toxic to humans, ecologically disastrous, and corrodes infrastructure. The existence of high sulfur-containing compounds in the process streams could

have a lot of damaging effects, which is dangerous to health. This section presents and discusses the effects of sulfur with respect to mankind and its environment.

Petroleum-based fuels, such as diesel and gasoline are used by internal combustion engines to power most automobiles. The emission of particulate matter (PM), nitrogen oxides (NOx), and carbon monoxide (CO), non-methane hydrocarbons, airborne toxins, and sulfur oxides (SOx) are usually caused by high temperature in cylinder of incomplete combustion of fuel. Some health issues and chronic diseases that are associated with exposure to these pollutants can eventually lead to early death (Sharaf, 2013).

Particulate matter (PM) is the most dangerous among the vehicle emissions. These categories of solid and liquid particles, lesser than 2.5 microns in aerodynamic diameter, ($PM_{2.5}$) can easily infiltrate into the lungs, stirring up inflammation and oxidative stress. In addition, the continuing exposure to $PM_{2.5}$ causes a series of chronic illnesses in adults. These include respiratory infections, aggravation of existing asthma, lung cancer, ischemic heart disease, chronic bronchitis, as well as cerebrovascular disease (Chambliss et al., 2013). Therefore, the reduction of sulfur-containing compounds from transportation fuel is essential in the petroleum industry. International Agency for Research on Cancer has confirmed that $PM_{2.5}$ is a recognized carcinogen, which is mainly caused by diesel exhaust in transportation fuel (McClellan et al., 2012). Exposure to high concentrations of $PM_{2.5}$ has been discovered to be connected to increase in hospital admissions that are related to infections of the respiratory organs, stroke, nonfatal heart attacks, and other acute outcomes (Lisabeth et al., 2008; Yu and Chien, 2016). Undesirable effects on reproduction, including reduced birth weight and increased death of children are also as a result of the emission of $PM_{2.5}$ (Woodruff et al., 2008; Geer and Weedon, 2012). New investigation into the impacts of black carbon on climate gives stronger proof that, if diesel particulate emissions can be controlled, it will reduce global warming (Jacobson, 2002). Over the years, diesel black carbon has been extensively reduced in carbon dioxide equivalent emission by diesel engine polices in the state of California (Air resource board, 2013). Therefore, the implementation of vehicle emission standards equivalent to Euro VI for the international fleet would reduce the rate of premature mortality to between 120,000 and 280,000 in 2030 at a worldwide standard (McClellan, 2012).

The quality of the air is seriously affected by the pollution emitted by vehicle engines. The vehicle manufacturers request for the removal of sulfur-containing compounds from petroleum, so as to reduce the global emissions of these compounds from vehicles (Parkinson, 2000). The emission-control devices in vehicles are affected since sulfur is intensely adsorbed onto the metal catalysts, which inhibit the reaction and the adsorption of carbon monoxide, Nitrogen oxide (NOx), and hydrocarbons (US EPA, 2016). Furthermore, production of the oxy-acids of sulfur from combustion products causes the internal combustion engines parts to corrode (Collins et al., 1997). Likewise, compounds of sulfur deactivate the catalysts that are used in hydrocarbon upgrading. In addition, they add to the formation of sticky deposits in petroleum products (Tam et al.,1990). Therefore, sulfur compounds are unwanted in refining processes and their removal from petroleum distillates is important to the refineries and to human welfare.

Some of the economic impacts of SO_x that are emitted due to the incomplete combustion of high-sulfur fuels have negative impacts on the economy of the nation. The acid rain as a result of this emission dissolves the calcium carbonate in monuments and buildings that are made with limestone and marble (Bravo et al., 2006). Sulfuric acid can cause huge economic loss owing to the occurrence of metal corrosion in machineries and vehicles in oil plants. Crude oils are refined and extracted by oil companies at varying levels. However, it is cheaper to refine crude that has lower sulfur content first, before refining crude with higher concentrations of sulfur. Since this is done the other way round, the oil reserves with lower sulfur contents would have been used up, leaving only high-sulfur concentrated crude oil to be used (Jones, 2011). From estimation, the use of low sulfur fuels would be economically useful since it will prevent hospital emergencies and thousands of hospital admissions, loss of working days, reduction of agricultural crop, and damage to commercial forest (UNEPA, 2017).

The reduction of sulphur content is anticipated to give room for the use of innovative emissions control methods that will significantly reduce PM emissions from diesel engines. The transformation started in the European Union and is now taking effect in North America. The need for greener fuels has made new emission standards to be implemented for automobiles in the United State of America since 2007 (Omidvarborna et al., 2014). Nevertheless, there remain numerous reasons for reducing the sulfur content in transportation fuel. The substances emitted

from by-products of combustion have also been connected to higher occurrences of bronchitis, lung and heart diseases and trigger asthma symptoms (Cackette, 1999; Gauderman etal., 2000). Therefore, in accordance with the international environmental law, sulfur compounds must be efficiently removed from fuels prior to release into the atmosphere (Sayyadnejad et al., 2008; Sekhavatjou et al., 2014).

It is also essential to remove sulfur content since it pollutes the advanced emission control systems (UEPA, 2016). The advanced emissions control systems have been aimed at furthering the reduction of PM and NOx. Conversely, as the quantity of sulfur used-up is reduced, they are contaminated by the sulfur contents and become caked, resulting in poor performance until they become ineffective and there will be a necessity for total replacement of the control system. This makes the whole less economical causing several companies to choose less effective systems owing to the foreseen effects of sulfur pollutants in exhaust gases (Sekhavatjou et al., 2014). The allowable sulfur in diesel fuel was 50 ppm for highway vehicles since 2005, agreeing with the Euro IV emission regulation (Shell global, 2016). Although, Sweden since 1990 has offered low sulfur diesel, according to the Euro IV regulation, of which low sulfur diesel had infiltrated almost 100% of the transportation fuel market in 2000. In addition, low aromatic diesel and zero sulfur have been obtainable since 2003 for use in extremely contaminated and confined regions (Lloyd and Cackette, 2001). In 2009, new Euro V standard was implemented for clean sulfur diesel (CSD) with a limit of 10 ppm for both highway and non-highway vehicles. Euro VI was the next standard implemented in 2013. This standard further restricts NOx and particulate matter missions, but is not affecting sulfur content directly (Lloyd and Cackette, 2001).

The majority of the transportation fuel obtainable in the United States in 2006 attains <15 ppm CSD limits. Non-highway automobiles such as marine, trains, and off-road vehicles have met the requirement for <500 ppm clean transportation fuel limit before 2008 and they were mandatory to attain the CSD requirement in 2012 (Barrett et al., 2012). Furthermore, in 2003, United States Environmental Protection Agency (US EPA) proposed a reduction of sulfur content in non-road diesel fuel from 3400 ppm to 500 ppm by the end of 2007, while the European Union enforced a policy for reduction of sulfur content in transportation fuel from 50 ppm to 10 ppm by 2009 [Song, 2003; Marcelis, 2003; Bailey et al., 2004). Many countries such as, USA, Australia, New Zealand,

Taiwan, Mexico, Singapore, Hong Kong, several Eastern and Central European countries, and other Asian countries have adopted reduction in sulfur limits in transportation fuels according to the enforced policies from individual country (Kilbane, 2006; Zietsman etal., 2007; Benerjee, 2011).

In May 2015, the International Council on Clean Transportation (ICCT) in a G20 briefing paper reviews today's world-class emission standards as shown in (Table 2.2). In addition, according to EPA assessments, implementation of the new fuel standards for diesel, e.g. emission of soot or particulate matter was reduced by 110,000 tons a year, while NO_x emissions were decreased by 2.6 million tons per year (Kodjak, 2015).

Some countries in Africa are already offering 50 ppm at filling stations. In 2009, Morocco launched 50 ppm diesel to fuel stations, likewise, several fuel stations stated offering 50 ppm by 2010 (AECC newsletter, 2016). Furthermore, in order to reduce environmental pollution in Mauritius, 50 ppm diesel has been standardized across all of the filling stations since June 2012 (United Nation Environmenta Programme, 2012). Early in 2006, a report showed that the South African Department of Minerals and Energy first legislated 50 ppm and since has been generally available and an overview of 10 ppm diesel to all filling stations was expected in December 2015. Sasol officially introduced 10 ppm diesel at few fuel stations in 2013. In 2017, South African government launched South Africa's Clean Fuels 2 standard, that will reduce the allowable sulphur content to 10 ppm (Industry news, 2016).

2.3. Existing Technologies for Desulphurization and their Challenges

Desulphurization is the removal or reduction of SO_2 level in distillates in order to meet the required standard. Numerous methods have been employed toward achieving this aim. Hydrodesulphurization (HDS) is one of the methods that are used to reduce the sulphur-containing compounds in transportation fuels (Shafi and Hutchings, 2000). Currently, most industries make use of HDS technique for sulphur removal from petroleum distillates.

Table 2.2 Summary of today's world-class emission standards (with permission from ICCT)

Policy Type	World-Class Emission Standard
Green Freight	• Heavy-duty vehicles: Measures that promote real-world, market-based performance improvements tracked through standardized and verifiable reporting mechanisms (e.g., SmartWay in the U.S. and Canada).
Clean, low-sulphur fuel	• 10 to 15 parts per million (ppm) sulphur for gasoline and diesel fuel plus Euro 6/VI, US Tier 2/HD2010, or equivalent fuel specifications
Fuel economy and CO_2 standards	• Passenger vehicles: 95 g CO_2/km, or measures to cut new vehicle fuel consumption by half in 2030 from a 2005 baseline • Heavy-duty vehicles: Measures to cut new vehicle fuel consumption by 35% by 2030 from a 2010 baseline.
Tailpipe emissions Standards	• Passenger vehicles: Euro 6 or US Tier 2 * • Heavy-duty vehicles: Euro VI or US HD2010 * • In-use compliance programs (inspection and maintenance, OBD, warranty and recall, etc.)

* Other equivalent standards include Japan PNLTES. Note that we expect US Tier 3 standards and California LEV III standards are expected. This is to establish a new level of world-class standards for passenger vehicles once they take effect in 2017 (Creative Commons Attribution-ShareAlike 3.0 Unported License).

In the HDS technique, there is the generation of H_2S gas, when a metal catalyst is used along with hydrogen gas (H_2) at elevated temperature and pressure in order to remove sulphur from organo-sulfur compounds in transportation fuels (Bachmann et al., 2014). Although, this method reduces the amount of sulphur in transportation fuels, however, there are numerous limitations that discourage its application. These include extreme operation conditions, such as high temperature and pressure (Bachmann et al., 2014)]. In addition, this method of desulphurization has difficulty

in removing recalcitrant heterocyclic sulphur compounds, such as dibenzothiophene (DBT) and its alkylated forms, such as 4-methyldibenzothiophene (4-DBT) and 4,6-dimethyldibenzothyiophene (4,6-DBT) (Zhang et al., 2013; Abin-Fuentes et al., 2014; Zeelani and Sundar, 2016; Startsev, 2017).

Currently, the strongest drive for the removal of sulphur in fuels is owing to the environmental guidelines, which are stringently imposing restrictions for sulphur levels in petroleum distillates. HDS technique is quite expensive because of the increase in the consumption of hydrogen gas, costly cobalt molybdenum catalyst, and severe operating conditions. Furthermore, it is difficult to lower the amount of sulphur in diesel to less than 15 ppm with HDS technique. Therefore, new cost effective methods are sought throughout the world. Attention has been shifted to biodesulfurization (BDS) as an alternative method or a complementary process of removing Sulphur-containing compounds from fuels (Boniek et al., 2015; Zhang et al., 2012). However, studies to improve the cost-effectiveness of the process are on-going. BDS technology is the future focus of most researchers throughout the world today because it employs microbes as bio-catalysts to remove sulphur-containing compounds that are recalcitrant to HDS. Although, BDS has shown lower capital cost of desulphurization over the HDS process, however its low rate of conversion coupled with difficulties encountered in monitoring the operating conditions of bacteria growth and desulfurization efficiencies hinder its commercial utilization (Hosseini and Hamidi, 2014). Better understanding of the fundamentals that are involved with the microbes and improvement in biotechnological equipment are recently assisting in alleviating this challenge. This could pave a way toward the realization of viable goals of BDS, hence its choice in this study. Chemical structures of organic sulphur compounds existing in crude oil are also presented in Fig. 2.3. Different existing desulfurization techniques and their shortcomings are discussed.

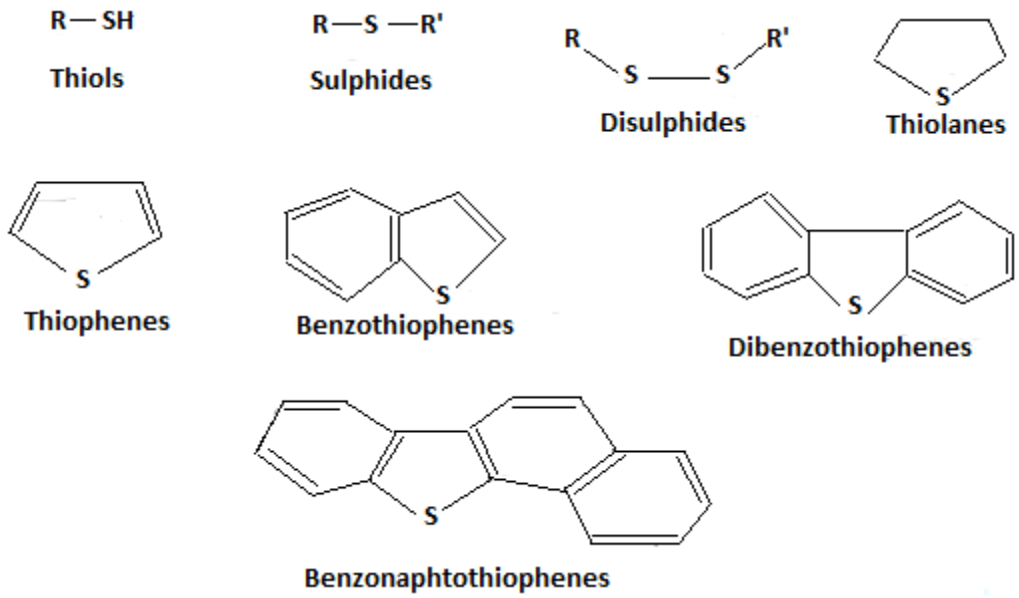


Figure 2.3 Chemical structure of organic sulphur compounds present in crude oils (Adapted from Hosseini et al., 2014).

2.3.1. Hydrodesulfurization (HDS)

Hydrodesulfurization (HDS) is a process that involves removal of sulfur compounds from the refined petroleum products with the use of a catalytic chemical process. HDS is a conventional way of reducing sulfur contents in fuel. This technology has been used since 1933, to reduce organo-sulfur compounds to lower levels by the use of metal catalyst (Bose, 2015). Easy availability of hydrogen from catalytic reformers initially stimulated the interest in HDS (Gary and Handwerk, 1984). Usually, the HDS process involves the conversion of a number of organo-sulfur compounds to H_2S and sulfur-free organic compounds. This can be done through catalytic treatment with hydrogen at elevated pressures, between 150 and 3000 psi, and elevated temperatures, between 290 and 455 °C with the help of metal catalysts such as $CoMo/Al_2O_3$ or $NiMo/Al_2O_3$ (Cattaneo et al., 2001; Hensen et al., 2003). This traditional HDS catalytic process for reducing sulfur content involves severe operation conditions, which makes the process expensive. In refineries, a modified version of the Claus process is used to convert the H_2S resulting from HDS process into elemental sulfur. (Shen et al., 2012). The shortcomings of HDS

process include: operation at elevated temperature and pressure, which eventually makes the process expensive and energy intensive. Also, some of the gas may not be reused again, which results into poor energy efficiency and the generation of environmental issues. The reactivity order of sulfur compounds from most to least reactive in HDS is as follows: thiophene > alkylated thiophene > BT > alkylated BT > DBT and MDBT > 4 or 6-MDBT > 4, 6-DMDBT (Gupta et al., 2005). Conclusively, the shortcomings of the HDS process has disadvantaged its practice, hence the reason for an alternative process. However, HDS still remains the artwork for desulfurization in petroleum refining industries.

2.3.2. Oxidative desulfurization (ODS)

Oxidative desulphurization (ODS) involves the oxidation of the sulfur compounds to their corresponding sulfoxides (1-oxide) and sulfones (1, 1-dioxide). This is contrary to the HDS method where sulfur compounds are reduced to form H_2S. ODS for the reduction of sulphur is carried out at a reduced temperature (~50 °C) and pressure. This makes the process a promising technology (Zhang et al., 2009). In ODS, appropriate oxidants are used to oxidize heavy sulfides into thio sulfone forms by the addition of one or two oxygen atoms to the sulphur, without altering the carbon–sulphur bonds, resulting in the sulfone and sulfoxide, respectively (Paniv et al. 2006). There are differences in the polarities of sulfoxides and sulfones that are produced, and the hydrocarbons of similar structure. Sulfoxides and sulfones are more polar than hydrocarbon. This difference in polarity enables the removal of the sulfones by the selective solvent extraction of solid adsorption. Many reagents have been employed as oxidizing agents. These include hydrogen peroxide (Hirai et al., 1996), organic hydroperoxides (Kocal and Branvold, 2002), and molecular oxygen. In order to accelerate the oxidation process, the use of catalyst has been introduced owing to the slow process of oxidation of sulphur compounds that are encountered in the absence of a catalyst. Various forms of catalysts have been investigated by different researchers (Cica et al., 2006; Wan Abu Barka, 2012; Sundararaman, 2012). ODS provides many advantages when compared to the traditional HDS method of desulphurization. It can be carried out using mild operation conditions of temperature and pressure, and there is no need for expensive hydrogen. Conversely, the technique involves huge amounts of oxidizing agent and involves the separation procedure to recover the catalysts. In addition, the reaction suffers from low selectivity and activity, and therefore an extended reaction time is required.

2.3.3. Adsorptive desulfurization (ADS)

Adsorption is a process which involves separation where gas or liquid molecules are adsorbed on the surface of an adsorbent. This process can be used for desulfurization of petroleum distillates based on the selective ability of the adsorbent to adsorb the organo sulfur compounds. In adsorption process, the solute penetrates into the porous structure of the adsorbent. Adsorptive desulphurization can be divided into two, namely; Physical adsorptive desulfurization, which involves the transfer of sulfur compound from the liquid phase to the surface of the adsorbent. In reactive adsorption desulfurization, the organo sulfur compounds react with chemical species on the surface of the adsorbent and the sulfur which usually is in form of sulphide is chemically bound to the surface of the adsorbent, and the newly produced hydrocarbon compound is released into the stream (Gawande et al., 2014). In adsorptive desulphurization technique, selectivity of adsorbent is very important.

This technique uses adsorbing agents (S-Zorb as they are called) having an affinity to adsorb sulfur containing compounds. S-Zorb sulfur reduction technique was created by ConocoPhillips to obtain ultra-low sulphur fuel. ConocoPhillips started operation in 2001 to market S-Zorb department at Borger refinery in Texas, USA due to a higher rate of production in thousands of barrels per day (Cheng, 2016). The adsorption could be of destructive type or what also could be termed as reactive adsorption, in which the adsorbed sulphur-containing compound is converted to a hydrocarbon after the stripping of its sulphur, which is left adsorbed on the adsorbing agent. On the other hand, adsorption could be of the non-destructive type (physical adsorption) i.e., one in which the chemical quality of the adsorbed Sulphur-containing species is preserved. In both cases, the adsorbing agent could be discarded or regenerated as convenient.

Reactive adsorption desulphurization involves the chemical reaction between the adsorbent and the sulfur compounds. The effectiveness of the method is dependent on the adsorbent properties which include: adsorption capacity, durability, selectivity for sulfur compounds, and adsorbent regeneration. The adsorbent can be regenerated after the adsorption process by eliminating the adsorbed sulfur compounds, subject to the method applied (Alavi and Hashemi, 2014). A study was conducted by Velu et al., (2003) on adsorbents that can be regenerated to selectively remove sulfur from fuel for fuel cell application. Authors stated that, desulfurization by adsorption could

be a potential approach for many novel processes, such as IRVAD and Philips S-Zorb processes. A novel S-Zorb process for obtaining ultralow sulphur in transportation fuel was developed by Conoco Phillips Petroleum Co. in Houston, Texas, in the United State by reactive adsorption of sulphur heterocyclic compounds using a solid adsorbent at high temperatures and low hydrogen pressure (Gislason, 2002; Ma et al., 2005; Zhanga et al., 2012). Reactive adsorption desulfurization utilizes the benefits of the adsorptive and HDS catalytic desulfurization, and therefore it is considered as an effective technique for deep desulfurization (Ryzhikov et al., 2008; Srivastav and Srivastava, 2009; Tawfik et al., 2015). Transition metals supported on basic oxides can form an ideal adsorption system for this purpose (Zhang et al., 2009). Ni supported on ZnO is the most suggested adsorbent for this process, because ZnO is identified as a sulfur-acceptor that is released by sulfided Ni species for the period of regeneration, as well as hydrogenation co-catalyst of organo-sulfur compounds on the surface of Ni particles (Kim et al., 2006; Bezverkhyy et al., 2008; Gawande et al., 2014).

Physical adsorptive desulfurization is the process whereby a solid adsorbent is used to remove a sulfur-containing compound from fuel through physical reaction (Alavi et al., 2014). In this method, molecules are adsorbed intact; therefore, the chemical characteristics of the sulfur-containing compounds in gasoline and diesel are preserved (Gawande and Jayant, 2014). Activated carbon and Ni-Al_2O_3 have been investigated to be good adsorbents for removal of hiophene, sulfide, and mercaptans, at moderate conditions of operation (Babich and Moulijn, 2003). In this technique of desulphurization, the adsorption strength for various thiophene compounds is in descending order: 4, 6-DMDBT > DBT > BT > 2-methyl thiophene> thiophene, which is the opposite for the HDS method. This is mainly because of the low sulfur uptake ability of the adsorbent material when the percentage of sulfur content in the oil fractions of interest is put into consideration. Another major setback of this adsorption method is the presence of competitive adsorption of aromatics and olefins, which results in a decrease in the sulfur uptake by the adsorbent (Yang et al., 2003; Moosavi et al., 2012; Liu et al., 2016). Therefore, studies have suggested the use of pre-adsorption treatment for removing larger organo-sulfur molecules. This will enhance the uptake capacity of the adsorbent used. Two major challenges must be overcome in adsorption desulfurization. Firstly, good adsorbents must be developed with a high adsorption capacity for sulfur compounds. Secondly, adsorbents that selectively adsorb mainly aromatic

sulfur compounds that are recalcitrant to HDS method must be developed over the other aromatic and olefinic compounds that are present in fuels from HDS units. Different adsorbents have been developed over the years for desulfurization of petroleum distillate. It is discussed in detail in the next section.

2.3.4 Adsorbent for desulfurization

Adsorbent materials are porous solids which bind liquid or gaseous molecules to their surface. They are mostly micro porous with high specific surface area (200-2000 m^2/g). Examples of adsorbent material include, Activated carbon, clay, silica gel, alumina, zeolite molecular sieves, carbon molecular sieves, carbon nanotubes, impregnated carbons, polymers, clays, and resins, (Alavi, 2004). The accessibility of adsorbate molecules to the internal adsorption surface is dependent on the size of the microspores. Therefore, the pore size distribution of microspores is a vital property for characterizing adsorptivity of adsorbents (Alavi et al., 2014).

The effectiveness of adsorption technique depends on the adsorbent properties, which includes: selectivity for sulfur compounds, adsorption capacity, regeneration of spent adsorbent and durability (Babich and Moulijn, 2003). In addition, adsorption of an adsorbate from a liquid solution to the surface of the adsorbent is dependent on; the molecular weight of solute, size, shape of the solute, shape of the adsorption site of the adsorbent, the electrostatic charge on the surface of solute molecule and matrix and the polarity of the adsorbate molecule (Alavi and Hashemi, 2013). Different adsorbents such as activated carbon, carbon nanotubes, pomegranate leave powder and neem leaf powder have been evaluated for desulfurization of sulfur-containing compound (DBT) from petroleum distillates in this study. They are therefore discussed as follow;

Activated carbon (AC) is made from various materials such as; bituminous coal, wood, lignite coal and coconut shell. Two major ways are common for the production of activated carbon. Firstly, they can be produced by placing the materials in a tank in the absence of oxygen and subjecting it to an extreme temperature between 600-900 ^oC (Colomba, 2015). This method produces a high purity and quality activated carbon. The carbon can then be treated with different chemicals, usually argon and nitrogen, and once more put in a tank and superheated to heating for 600-1200 ^oC. Afterwards, the carbon is placed in a tank and steam and oxygen is allowed to pass through it.

This creates holes or pore structure and usable increased surface area. The highly porous surface area of AC attracts and holds organic chemical on it (Shan, 2016). Organic chemicals are attracted to carbon the best. The undesirable substance adheres to the surface area of the adsorbent particles, while only few inorganic chemicals will be separated by adsorbent. The factors that affect the efficiency of adsorbent are; solubility in water, polarity, molecular weight, polarity, concentration of the adsorbate in the solution and temperature of the fluid stream.

Adsorption with AC appears to be the best prospect for removal of DBT molecules from petroleum distillates due to its excellent surface area and improved micro structures (Eddebbagh et al., 2016). However, regardless of its good efficiency, this adsorbent is costly with difficult regenerability after use. In addition, its procedure and application come with high expense (Ahmed and Ahmaruzzaman, 2015). Therefore, many researchers recently have focused on the application of different adsorbents as alternatives to activated carbon. CNTs have been discovered by researcher to be a good adsorbent, due to its large surface area and high porous structure.

CNTs can be termed as a hollow cylinder formed by rolling graphite sheets. Nanotubes bonding are basically sp^2. CNTs are mechanically stronger, electrically and thermally more conductive and chemically and biologically more reactive than graphite (Meyyappan, 2005). It was discovered in 1991 by Ijinma (Ijinma, 1991). Since then, CNTs have attracted attention of researchers mostly in the areas of science and engineering owing to their exceptional physical and chemical properties. The combnation of CNTs excellent properties such as, electrical, mechanical and thermal have made them to be ideal for wide range of applications, e.g as adsorbent (Baughman et al., 2002; Cao et al., 2004).

Currently, carbon nanofibres (CNFs) have been synthesized from vapour phase with diameters of 100 nm and lengths ranging from 20 and 100 μm. They have large surface area due to their small dimension in diameter and length, allowing excellent interaction between them and the adsrbate molecules. They also tend to have impressive mechanical properties with Young‘s modulus in the range 100–1000 GPa and strengths between 2.5 and 3.5 GPa (Tibbetts and Beets, 1987). Nanotubes can have diameters ranging from 1 to 100 nm and lengths of up to millimetres (Hata et al., 2004). The weakest types of CNTs have strengths of several GPa (Xie et al., 2000). CNTs have

been regarded as materials and most naturally related to the other obstinate carbon allotropes graphite and diamond (Ebbesen, 1998).

CNTs can be dvided into three types; single walled nanotubes (SWNT) (Bethune et al., 1993; Iijima and Ichihashi, 1993), consisting of a single sheet of graphene rolled flawlessly into a cylinder having 1 nm diameter and length of 1 cm. Double walled CNTs consist of two sheets of graphene rolled into a cylinder. Another type of CNTs is multi-walled nanotubes (MWNT). These consist of arrangement of cylinders concentrically formed and separated by 0.35 nm similar to the basal plane separation in graphite (Iijima, 1991). MWNTs can have diameters from 2 to 100 nm and lengths of tens of microns. Carbon nanotubes can either be a metal or a semi-conductor. They vary symmetrically and can differ in function owing to the way they are rolled up. CNTs are said to be stronger than stell per unit weight, even though, they are thinner 50,000 times than human hair (Ganesh, 2013). CNTs have been discovered to be promising adsorbent of organic compounds owing to their large surface area and porous structure. However, the adsorptive performance of carbon naotubes can be improved, if functional group is attached to the surface of the adsorbent. This can be achieved through chemical functionalization.

Functionalization of CNTs is a technique for surface modification of the available adsorption site of the adsorbent. Different techniques of functionalization of CNTs and the reaction mechanism between CNT and functional groups have been reported in literature (Hirsch and Vostrowsky, 2005; Tasis et al., 2006). Functionalization of CNTs can be classifed into physical and chemical functionalization depending on interaction between the acytive molecule and the carbon atoms on the CNTs. Functionalization of CNTs using covalent and non-covalent techniques can offer useful functional groups onto the CNT surface (Hirsch, 2002). However, these methods have two main shortcomings which damage the structure by creating defect on the CNTs sidewalls (Ma et al., 2010). Chemical functionalization has been employed by many researchers to modify the surface of carbon nanotubes. There are quite a lot of broad review papers that describe the interaction between the functionalized CNTs and the reaction path-way (Hirsch, 2002 and Hirsch, 2005). These can be achieved at the ends of the tubes or the sidewalls of the CNTs (Ma et al., 2010). Indirect covalent functionalization takes advantage of chemical alterations of carboxylic groups at

the open ends and holes in the sidewalls. The carboxylic groups may be attached during purification by oxidation and it might have existed on the as-grown CNTs.

Carbon nanotubes also come with its short comings such as high cost of production. This motivates the alternative use of low-cost, readily available and environmentally friendly agro-waste adsorbent, such as neem leaf powder (NLP) and pomegranate leaf powder (PLP) for the desulfurization of petroleum distillate, especially diesel in this study. Low cost adsorbents and agro-waste adsorbents were considered in this study.

2.3.5 Agrowaste adsorbents for desulfurization

It is estimated that about 998 million tonnes of agricultural waste is produced yearly (Agamuthu, 2009). Therefore, the use of agricultural waste materials for the treatment of sulfur-containing petroleum distillates serves as a proof of concept in the development and application of green materials in sustainable, innovative and effective waste management for the abatement of environmental pollution. Agricultural waste materials are presently gaining attention as potential adsorbents for removal of various contaminants from wastewaters and fuels due to their availability and low cost (Ahmaruzzaman and Gupta, 2011). Low-cost agricultural waste by-products such as palm kernel shell (Isam et al., 2013), neem leaf (Daware and Kulkami, 2015), and almond shell (Deniz, 2013) have been investigated by many researchers as adsorbents for removal of sulfur-containing compounds from petroleum distillates. However, further investigations are needed on the adsorption performance of neem leaf powder for desulfurization of DBT compound in petroleum distillates. Pomegranate peels have been utilized as adsorbent for the treatment of heavy metals in water (Bhattacharjee and Patel, 2017). However, PLP as adsorbent for the removal of DBT from model diesel and petroleum distillates have not been reported until now. The leaves of pomegranate and neem are abundantly available locally. They are waste materials from which useful adsorbent materials can be developed for industrial application. From this point of view, PLP and NLP, which are agro-based wastes product, could be important materials for utilization in desulfurization of transportation fuels because they are cheap, readily available and will reduce environmental waste. Hence, this study investigated the adsorption performance of PLP and NLP as green-based adsorbents for removal of DBT from petroleum distillates.

Neem leaves are regarded as waste when the tree sheds the leaves. Neem leaves powder has been explored to proffer solution to various challenges related to environmental pollution, health wisely and in agriculture (Sharma et al., 2009). Reports have shown that neem leaves powder has a wider range of useful product compared to other plants (Panhare and Dawande, 2013). Therefore, it can be used as an alternative low-cost adsorbent. Neem leaves powder has been used as an adsorbent in the removal of pollutants and colour from water and industrial effluents. Chromiun (VI) ion was adsorbed on NLP in an experiment conducted by Sharma and Bhattacharyya (2004). In addition, Sharma and Bhattacharyya, (2005) conducted an experiment using neem leaves powder as adsorbent to remove Cadmium (Cd) ion from aqueous medium. Jinturkar and Sadgir (2017) used neem leaf powder as adsorbent for removal of iron from aqueous solution. Activated neem powder prepared using phosphoric acid was used for removal of phenol, 4-nitro phenol, and 4-chlorophenol from aqueous solution by Ahmaruzzaman and Gayatri (Ahmaruzzaman and Gayatri, 2011). Padhare et al. (2013) synthesized an activated neem leave adsorbent using ortho-H_3PO_4 as an activating agent and only BET analysis was done on it. In addition, neem leaves powder was used for desulfurization of real diesel by Daware et al. (2015). However, there is a need for additional investigation on the mechanism and kinetics of adsorption desulfurization of DBT molecules which account for about 70 % of the sulfur organic compounds in diesel. Hence, this study investigated the adsorption performance of NLP as green-based adsorbent for removal of DBT from petroleum distillates.

The adsorption process generally depends on the following factors:

Contact time: The adsorption process can be fast or slow depending on the type of adsorption. In physical adsorption the time taken for adsorption to take place is slower than chemical adsorption because chemical adsorption requires high energy for operation. After the contact of sorbent with adsorbate, which is organosulphur compound adsorption, the adsorption of the adsorbate takes a very short time. Therefore, time is an important factor in adsorption in order for the adsorbate to have contact with the active site of the adsorbent (Saad, 2008).

Adsorbent particle size: As the adsorbent particle size increases, the surface area decreases and so adsorption capacity decreases. Likewise, adsorption capacity increases with decrease in particle size which results in larger surface area (Gao et al., 2009). Therefore, it can be said that adsorbent

particle size is inversely proportional to the adsorption capacity. Conversely, the adsorption capacity is directly proportional to surface area (Gao et al., 2009). Therefore, the surface area of adsorbents has immense importance for the adsorption process owing to the physicochemical properties (Long et al., 2009).

pH: Adsorbates have their own chemical characteristics. Therefore, the pH varies due to effect on each adsorbate in adsorption process.

Adsorbent dose: Adsorbed molecules increase as the adsorbent dose increase in the adsorption process. This means adsorbent dose is directly proportional to the adsorbate ions in the process. However, there is a reverse association among the value of adsorbed and the adsorbent dose (Veli and Alyüz, 2007; Saad, 2008).

There are two adsorption operation modes used in adsorption process; Batch operation mode and continuous operation mode (Seader and Heley, 1998). Batch mode operation involves an amount of adsorbent being mixed constantly with a definite volume of adsorbate till the solute of interest in the solution has been reduced to a chosen level. The adsorbent can then be removed by either discarding or regenerating for re-use with another volume of solution. Batch methods of adsorption are usually restricted to the treatment of small volume of effluents (Seader and Heley, 1998). However, in column or continuous mode type, there is a continuous contact of adsorbent with a fresh solution. At the end, the concentration in the solution in contact with a given layer of adsorbent in a column is relatively constant. There are two types of continuous mode adsorption systems, namely; packed-bed adsorption system and fluidized bed adsorption system (Seader and Heley, 1998). Several studies have reported the study batch and continuous mode adsorption processes of fuel desulphurization.

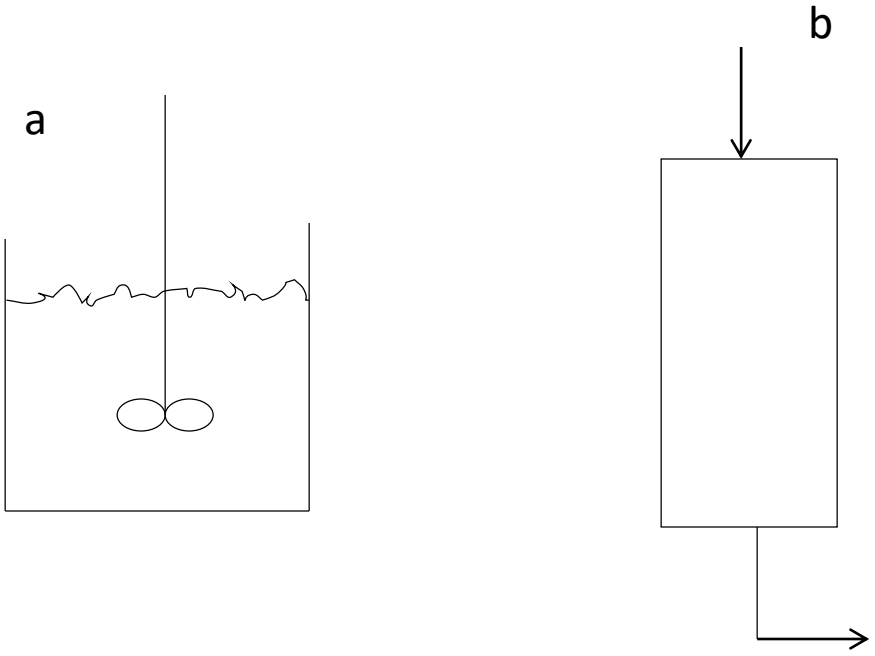


Figure 2. 4 (a) Batch mode operation (b) Continuous mode operation

Neran and Samar (2008) investigated desulfurization and kinetic study of diesel by batch adsorption on AC. The authors reported highest desulfurization efficiency of 57 % at best conditions of 50 ^{o}C, 0.8 mm AC particle size and 100 rpm. On the other study, Daware et al (2016) studied desulfurization of diesel using neen leaves on batch experiments. The authors concluded that with increase in time and temperature, concentration of sulphur removal also increases and maximum removal of sulphur is 65 % at 200 ^{o}C

Muzic el al (2009) used continuous fixed bed column for removal of organic sulfur compounds from diesel fuel by activated carbon. Authors reported that sulfur content of less than 0.7 mg/kg was attained for the lowest flow rate of 1 mL/min and highest bed height of 28.4 cm at 50 ^{o}C.

Artuo et al. (2012) studied desulphurization of a commercial diesel fuel by different adsorption in a fixed bed absorber at ambient temp and pressure. Investigators reported that the best adsorbent AC/Cu (I) –Y is capable of producing 30 cm^3 of diesel fuel per gram of adsorbent with a weighted average content of 0.15 ppm. It was recorded however from the studies that column type, the

continuous flow operation appears to have distinctive benefits over batch mode due to the fact that, rate of adsorption depends on the concentration of the adsorbate in the solution

Shakirullah et al., (2012) performed adsorptive desulfurization on three different types of petroleum distillates namely crude oil, kerosene and diesel oil using different clays obtained from indigenous sources, including Vermiculite, Kaolinite, Palygorskite and Montmorollinte. A batch experiment was performed at 40^{o}C at different time intervals of 1, 3, and 6 h. The result showed that Kaoinite displayed the highest desulfurization capability of 60 %, 76 % and 64 % in crude oil, kerosene, and diesel respectively. The adsorbents were characterized using, scannind electron microscope (SEM), electron dispersion x-ray (EDX) and Fourier transmission infra-red (FTIR). The FTIR analysis of the desulfurized fractions showed that thioles and thiophenic compounds with high molecular weight were completely removed during adsorption process

Ahmed and Ahmaruzzaman (2015) reported the usage of chemically impregnated coconut coir waste (CICCW) as a cheap adsorbent for treatment of diesel oil. The investigation was carried out at different temperatures and the adsorption of sulphur on the adsorbent was reported to be optimum at 20 ^{o}C, highest amount of 1 g/20 mL, and equilibrium was reached within 3 h.

Daware et al. (2015) studied adsorption desulphurization of diesel using neem leaves powder. The authors reported over 65% reduction in the amount of sulphur. This was achieved at optima conditions of time, 3.5 h, 2 g neem leave in 10 ml of diesel at temperature of 20 ^{o}C. According to kinetic studies experimental data were shown to be fitted to pseudo second-order isotherm. Kinetic equilibrium of Langmuir and Freundlich isotherms can also be studied for this experimentation.

Nazal et al. (2015) investigated the adsorption capacities of three different carbonaceous adsorbents namely CNT, AC and GO loaded with Al (5 % and 10.9 %) in the form of Al_2O_3 for the removal of DBT from n-hexane as a model diesel fuel. Activated carbon with 5% Al loading showed the highest adsorption capacity of 85 mg/g for DBT. The authors carried out selectivity study of DBT relative to thiophene and DBT relative to naphthalene was using AC with 5 % Al loading (ACAL5) and CNT with 5 % Al loading (CNTAL5). The result showed that selectivity factor for DBT/Thiophene and DBT/Naphthalene by ACAL5 and CNTAL5 were 255, 25, 127 and 7, respectively. The authors reported that modification of the CNT, AC and GO with Al_2O_3

enhanced the surface chemistry of adsorbents and consecutively improve their adsorption capabilities and selectivity for DBT from model diesel. This could be as a result of additional acidic sited introduced to the carbon surface rather than increase in pore volume or surface area. In conclusion, it was reported that the adsorbents could be reused for at least 5 times without losing its adsorption capacity.

Adsorptive desulfurization of diesel was studied by Al-Zubaidi et al. (2013) using seven different adsorbents namely; saw dust powder, Bentonite, date palm kernel powder, acid activated bentonite, acid activated date palm kernel powder, granules activated carbon and commercial powder. The study was conducted in batches at room temperature and contact time of 2 h with sorbents doses ranging from 0-5% by mass. Results showed that the commercial activated carbon and acid activated bentonite possessed the highest sulfur removal capacity. The sulfur content was reduced from 410.9 µg/g to 245.9 µg/g (40.10%) using 5% by mass commercial activated carbon and 278 µg/g (32.3%) using acid activated bentonite. In addition, authors stated that data followed Langmuir and Frendlich adsorption isotherms.

Blanc, et.al. (2010) studied the removal of refractory organic sulphur compounds in diesel using metal organic framework (MOF) compounds as adsorbents. Authors recommended improvement of adsorption capacity and regeneration of adsorbent by developing new porous substrate for desulfurization of a wider series of sulfur

Al-Zubaidy et al. (2013) explored the removal of organo-sulfur compounds from diesel with initial concentration of 410 ppm. A batch experiment was carried out using commercial activated carbon and carbonized palm kernel powder at ambient temperature. The results showed that there was over 54 % reduction in sulphur content with activated carbon, while carbonized palm kernel powder showed a lower desulphurization capability. Increasing the amount of adsorbent from 5 % to 10 % further reduced the sulphur contents in the diesel oil to 184.6 ppm. The authors concluded that this improved reduction will absolutely increase the emission quality and eradicate the detrimental outcome of the combustion process of diesel fuel to the environment.

In a batch reactor, activated carbon synthesized from black liquor was investigated by Patil et al. (2011). Results showed that stirring enhanced adsorption equilibrium to be reached within 1 h and

intra-particle diffusion resistance was overcome. AC showed high adsorption performance. In order to understand the adsorption nature, thermodynamics parameters such as ΔG, ΔH and ΔS were estimated and the author reported that experimental data obtained complied with Langmuir adsorption isotherm model.

Muzic et al. (2010) studied the removal of sulfur from diesel by adsorption on a 13X type zeolite and commercial activated carbon (CAC) in a batch reactor. Results showed that, CAC had higher adsorption capacity compared to Zeolite. Kinetic study on the experimental data of the adsorption technique was achieved by applying intraparticle diffusion models, Lagergren's pseudo first-order and pseudo second-order to determine the sulfur adsorption kinetics. The experimental data was perfectly described by Langmuir and Freundlich isotherms.

Alzubaidi et al. (2015) studied the adsorption desulfurization of diesel using granular activated carbon (GAC) at room temperature. The result showed good sulphur removal efficiency of 20.94 % which caused enhancement in all physical properties of the diesel and in particular the ignition quality. The diesel index, as well as the cetane number was improved in the process. The isotherm study of the desulphurization process was described by Langmuir isotherm.

Rosas et al. (2010) investigated the adsorption capabilities of four different commercial activated carbons (CAA, CAB, CAC, and CAD) using diesel oil as the feed stock containing the organosulphur with low sulfur content (72 ppmw). The experiment was carried out in batches at 30 ^{o}C, atmospheric pressure and 5-200 g-A/L-D, with magnetic stirring over 18 h. The result showered that the sulphur contents were reduced to 15 ppm. The author reported that, the adsorption isotherms were described by the Freundlich, Langmuir, Sips and Brunauer-Emmett-Teller (BET) models. The experimental and calculated adsorption isotherms data were of close values. However, the Sips and BET models gave the best correlation for the experiment.

Patil (2012) investigated unsteady state adsorption column using fixed-bed adsorber for the desulfurization of hydrocarbon liquid fuel. The authors used activated carbon as adsorbent in a continuous flow adsorption packed column. Parameters like feed flow rate, feed solution concentration, and adsorbent bed height on rate of adsorption were investigated. Result showed that, at all studied concentration, the adsorption zone height increased, as the feed flow rate

decrease. In addition, it was reported that increasing the flow rate of the feed solute increased the amount of adsorbate adsorbed, demonstrating an unstready state adsorption process.

Fallah and Azizian (2012) investigated the removal capacity of sulfur of BT, DBT and DMDBT in heptane using activated carbon cloths ACC-HNO_3 adsorbent. About 150 ppmw for each compound BT, DBT and DMDBT was dissolved in heptane for the preparion of the model oil. The experiment was carried out in batches where amount of adsorbent was varied from 0.02-0.05 g, at 30 ^oC. The researchers reported the removal percentage of total sulfur as a function of time that ACC-HNO_3 shows higher adsorption capacity than ACC for removal of total sulfur. Result also showed that as the mass of adsorbent increases from 0.02 to 0.05 g, the removal efficiency increased by 20 % for both ACC and ACC-HNO_3. In conclusion, it was reported that the maximum time for both adsorbents to reach optimum was 40 mins

Muzik et al. (2012) examined the desulphurizing capacities of different types of commercial adsorbents (activated carbon, 13X and Y zeolite, aluminum oxide) on model fuel comprising cyclo-hexane, n-heptane, n-octane and dibenzothiophene with concentration ranging from 0.48 to 42.91 mg/g. The experiment was carried out in a batch mode at 24.5 ± 0.7 ^oC. The authors reported that, Y-Zeolite had the highest adsorptive performance. The kinetic and equilibrium data analysis of the adsorption process showed that Ritchie and Sips models respectively were fitted in perfectly

In the packed-bed adsorption column, the solution can be fed in the packed-bed column by either down flow and up flow. However, the down flow is commonly used, when there is need for regeneration of the spent adsorbent in the column (Seader and Heley, 1998). For continuous feed flow, the mass transfer zone moves to the end of the bed column. The concentration of the solute in the bed increases while the efluent solute concentration eventually decreases (Seader and Heley, 1998). Based on the above point, the concept of breakthrough curve and breakthrough points come in use in designing the packed bed adsorption column (Seader and Heley, 1998). In the case of a downward flow fixed bed adsorber, the influent flows from the top of the adsorption column and usually in contact with the fresh adsorbent. Adsorption zone is the region where most of the adsorbate is removed (Senyangane, 2016). The upper layer of the fresh adsorbent becomes saturatedwith solute, as the fluid enters the column, and the adsorption zones moves towards the end of the column (Simate and Ndlovu, 2015). It will reach the point where the lower part of the

adsorption zone gets to the bottom of the column and the effluent solute concentration starts to rise rapidly. This point is called break point. It is said to be the point where the solute in the fluid cannot be adsorbed by the bulk of the bed (Simate and Ndlovu, 2015). The breakthrough curve is a plot of the adsorbate concentration at the column outlet (C_t / C_o) verse time (t). Column exhaustion time is the time at which the column exist concentration of adsorbate equals the influent adsorbate concentration (Senyangane, 2016). Fig. 2.7 is an idealized breakthrough curve expressed in terms of the mass concentration of the solute free in effluent, C and the total mass quantity of solute which has passed a unit cross sectional area of the absorber.

In adsorption process, a breakthrough curve is estimated in order to design an efficient column. Among many factors upon which the shape of a breakthrough curve is dependent on the individual transport processes of the adsorbent (Ahmed et al., 2010). It is a challenge to develop a mathematical model for breakthrough curve due to the complex flow and mass transfer all through the breakthrough process. Experimental equations, such as Dose-response model (Yan and Viraraghavan, 2001), and Yoon and Nelson model (Park et al., 2010) have been broadly used to describe column adsorption process. These equations can neither be reasonably extrapolated nor be deduced from batch studies. Alternatively, breakthrough models derived from basic mass transfer equations combined with adsorption isotherms can be established (Hatzikioseyian et al., 2001). This is based on the basic assumptions of fast local equilibrium and uniformly packed absorbents. Characteristic examples of such models are; overall rate model and its several basic types such as, lumped pore diffusion model, advection–dispersion–reaction equation, and transport–dispersive model. In these types of models description of mass transfer process depends on the intra-structure and morphology of the adsorbent. Adsorption isotherm can be easily obtained from breakthrough curve by inverse method, once mass transfer equations conforming to the control steps of mass transfer in the column are correctly given.

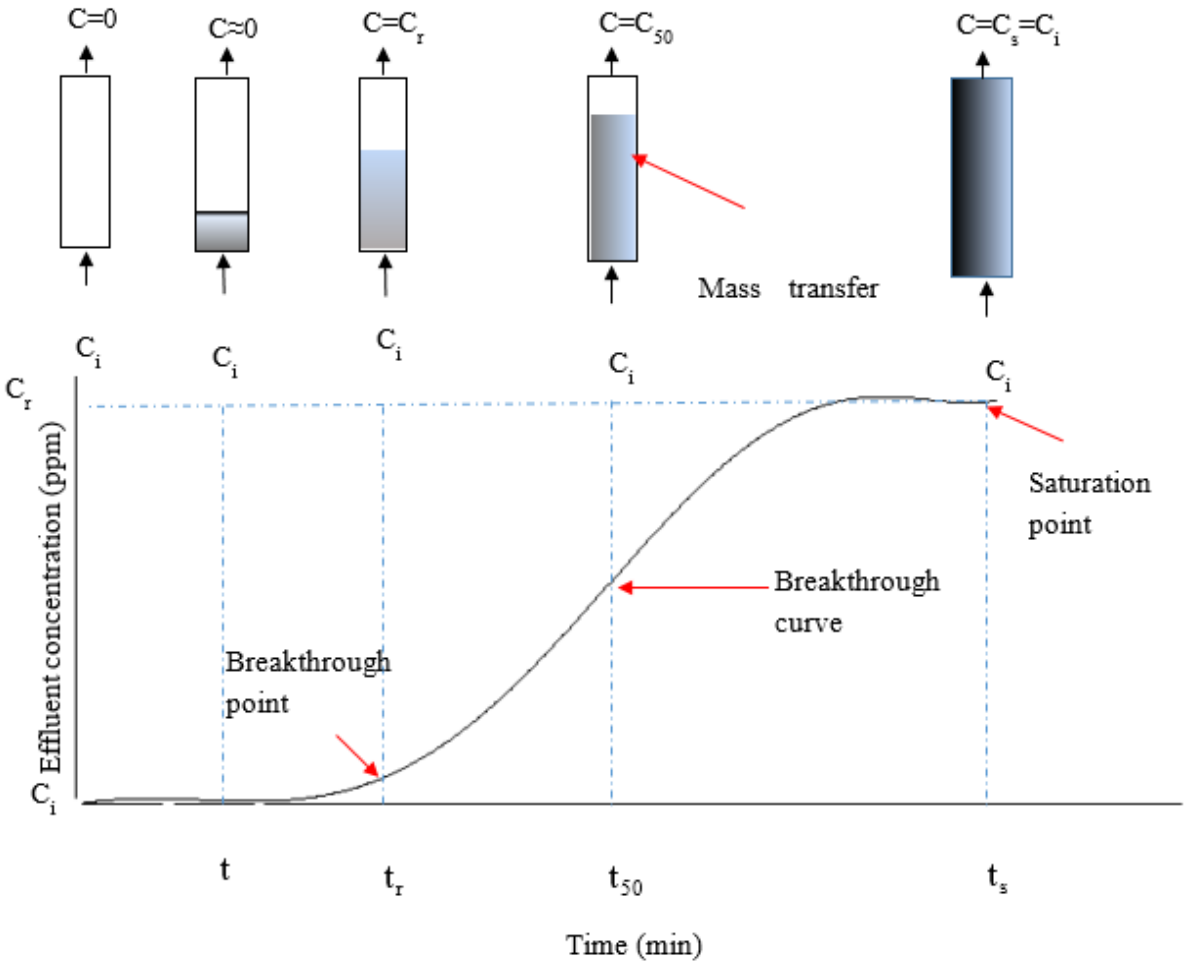


Figure 2.5. Representation of ideal breakthrough curve (Adapted from Calero, 2000)

Where t (min) is the time, t_s (min) is the saturation time, t_r (min) is the breakthrough time, t_{50} (min) is the time required to obtain 50 % breakthrough, C_i (mg/L) is the feed concentration, C (mg/L) is the effluent concentration, C_r (mg/L) is the influent concentration at breakthrough point, C_s (mg/L) is the solute concentration at saturation point, C_{50} (mg/L) is the solute concentration at 50 % recovery

2.4 Adsorption isotherm and kinetic models

2.4.1. Continuous mode

Langmuir model assumes monolayer coverage and constant binding energy between surface and adsorbate. The model is based on the assumption that maximum adsorption corresponds to a saturated monolayer (chemical adsorption) of solute molecules on the simulation of the adsorptive desulphurization of diesel fuel adsorbent surface, with no lateral interaction between the adsorbed molecules (Vijayaraghavan et al, 2006; Foo and Hameed, 2010). It refers to homogeneous adsorption and assumes all sites possess equal affinity for the adsorbate and the adsorption heat does not vary with the coverage. Adsorption is assumed to take place when a free adsorbate molecule collides with an unoccupied adsorption site and each adsorbed molecule has the same percentage to desorption (Langmuir, 1916).

The Langmuir isotherm has been found to fit well with most liquid/solid adsorption processes and specifically diesel desulphurization processes (Muzic et al, 2010b). Due to its simplicity and ability to well-fit most performances, the Langmuir isotherm has become one of the most popular models in adsorption studies (Xu et al, 2013).

The Langmuir model expression is given as;

$$q = \frac{\mathrm{K}Q_a C_e}{1+\mathrm{K}C_e} \qquad (2.1)$$

Where, Q_a is the maximum adsorption capacity g/mg, C_e is the concentration at equilibrium in mg/L, K is the Langmuir constant in L/mg

The kinetic performance of an adsorbent is of great value in the design of adsorption processes. The kinetic analysis provides the rate of solute uptake that determines the resident time needed to complete of adsorption process. Basically, adsorption kinetics is the core in determining the efficiency and performance of the fixed bed or any other flow-through system adsorption (Muzic

et al. 2016). Adsorption kinetics may be governed by various independent phenomena, either in parallel or series. These can be categorized into; chemical reaction, external mass transfer, bulk diffusion, and intra-particle diffusion (Senyangane, 2016)

Adsorption reaction models assume the rate of surface reaction to be the rate-limiting step. Specifically, for the adsorption of organic sulphur compounds, various articles have reported the use and application of adsorption reaction models (Muzic et al. 2016). Common models usually used by researcher are; Bohart-Adams, Thomas, Yoon-Nelson models and so on.

The Bohart-Adams model is based on the surface reaction theory and the model is based on the assumption that equilibrium is not reached promptly and the rate of adsorption is relative to the adsorption capacity of the adsorbent (Bohart and Adams, 1920). The Bohart-Adams model was fit to assess breakthrough behaviour in this study because its underlying assumption fit into the required assumptions considered in this study. It establishes the basic equation describing the relationship between C/C_o and time (t) in a continuous system. The model can then be used to describe the breakthrough curve in which the model parameters for instance, the maximum capacity of adsorption q_s and the adsorption coefficient K can be obtained.

The expression in Equation 2.2 is mass balance equation for the Bohart-Adams model and it it given as:

$$\frac{\partial c}{\partial t} + \frac{v\,\partial c}{\partial z} + \frac{(1-\varepsilon)\,\partial q}{\partial t} = 0 \qquad (2.2)$$

The Quasi-chemical law is used to describe the kinetics of adsorption and it is given in Equation 2.3;

$$\frac{\partial q}{\partial t} = KC(q_e - q) \qquad (2.3)$$

Where C in g/L is the concentration of adsorbate in the adsorbate solution, t is time in min, v is the superficial velocity of the sorbate solution, x is the distance from the column inlet, Ɛ is the bed porosity whiuch is dimensioness, qe is the concentration at equilibrium and q is the adsorbate concentration in the adsorbent in mg adsorbate/g adsorbent.

Some assumptions are made for Bohart-Adam's model, which are:

(i) Rectangle or step isotherm is assumed for the model and adsorption bed is homogenous
(ii) Gradients occur only in the axial direction and they are negligible
(iii) At time t=0, the bed is free of adsorbate (DBT)
(iv) The model assumes that equilibrium is not instantaneous
(v) Irreversible adsorption isotherm

The differential mass balance as proposed by Cooney, 1999 yields the expression in Equation 2.4, if a negligible axial dispersion as is assumed

$$\frac{C}{C_0} = \frac{e^T}{e^T + e^{\varepsilon} + 1} \tag{2.4}$$

$$\text{However, T} = K_{ab} C_0 \left(t - \frac{z}{\text{v}}\right) \tag{2.5}$$

$$\varepsilon = \frac{K_{ab} N_o Z}{\text{v}} \left(\frac{1-\varepsilon}{\varepsilon}\right) \tag{2.6}$$

K and N_o in can be can be obtained by fitting Equation 2.4 to a breakthrough data, T is the dimensionless time and ε is a dimensionless distance. Solving Equation 2.4 mathematically gives,

$$\frac{C_0}{C} = \frac{e^T}{e^T} + \frac{e^{\varepsilon}}{e^T} - \frac{1}{e^T} \quad (2.7)$$

$\frac{\mathbf{Z}}{\boldsymbol{v}}$ in Equation 2.4 can be neglected with time

$$ln\left(\frac{C_o}{C}\right) = \frac{K_{ab}N_oZ}{\mathrm{v}}\left(\frac{1-\varepsilon}{\varepsilon}\right) - K_{ab}C_o t \quad (2.8)$$

Subsequently, the bed is assumed to be homogenous, then the equation then becomes

$$ln\left(\frac{C_o}{C}\right) = \frac{K_{ab}N_oZ}{\mathrm{v}} - K_{ab}C_o t \quad (2.9)$$

The linearized form of Equation 2.2 yields Equation 2.10 which is the Bohart–Adam's model derived from mass balance Equations.

$$ln\left(\frac{C_o}{C}\right) = \frac{K_{ab}N_oZ}{\mathrm{v}} - K_{ab}C_o t \quad (2.10)$$

A plot of $ln\left(\frac{C_o}{C}\right)$ against time gives a linear graph from which the model parameters, maximum adsorption capacity, N_o and the adsorption coefficient, K can be obtained from the intercept and slope of the graph, respectively.

Thomas model is reported in literature as the frequently used kinetic model to evaluate the maximum adsorption capacity of the column in continuous mode in desulphurization of diesel model fuel (Muzic et al. 2010). The Thomas model is among the most commonly used methods in describing the performance of a fixed bed column. Thomas model was adapted in this study to investigate the breakthrough behaviour of novel adsorbents during desulfurization of DBT from South African petroleum distillate. The model described the breakthrough time and equilibrium concentration of DBT for the adsorption process in this study.

Thomas model assumptions are as follow;

(i) The radial and axial dispersion in the fixed bed column are negligible.
(ii) The column void fraction is constant.
(iii) The adsorption is described by a pseudo second-order reaction rate principle. This reduces to a Langmuir isotherm at equilibrium
(iv) Constant physical properties of the solid-phase and the fluid-phase;
(v) Isobaric and isothermal process conditions
(vi) During the mass transfer processes, the intra particle diffusion and external resistance are negligible.

Thomas model equation is given as;

$$\frac{C_o}{C_e} = \frac{1}{1+e^{\frac{K_{Th}}{V(q_o X - C_o t)}}} \tag{2.11}$$

The linearized form of Thomas model can be expressed as follow:

$$\ln\left(\frac{C_t}{C_o} - 1\right) = \frac{K_{Th} q_o w}{v} - K_{Th} C_o \, t \tag{2.12}$$

Where K_{Th} is the Thomas rate constant in mL/min.mg, q_o is the adsorption capacity, w is the amount of the adsorbent in g, Q is the feed flow rate in mL/min, C_o is the initial sorbate concentration in mg/L and C_t is the outlet solution concentration, in mg/L. A plot of $\ln(\frac{C_t}{C_o} - 1)$ against time gives a linear graph. The q_o and K_{Th} can be obtained from the intercept and slope of the graph using a linear regression analysis. This model is commonly employed to describe the performance of a bed column.

The value maximum column capacity, q_{total} (mg) for a given solute concentration and flow rate is equal to the area under the plot of the adsorbed sorbate concentration, C_R (C_R=C_o-C_t) (mg/l) vs t (min). This can be obtained by the expression in Equation (2.13):

$$q_{total} = \frac{Q}{1000} \int_{t=0}^{t=t_{total}} C_R \, dt \tag{2.13}$$

Where t total is the total time in min, Q is the flow rate in mL/min, C_R is the solute concentration in mg/L. The total amount of DBT (in mg) sent into the column, M_{total} can be calculated by the expression in Equation (2.14):

$$M_{total} = \frac{C_i Q t_{total}}{1000} \tag{2.14}$$

The percentage solute removal (% R) can be be calculated by the ratio of mass adsorbent (q_{total}) to the total amountof solute sent into the column (M_{total}) as shown in Equation (2.15):

$$\% \text{ R} = \frac{q_{total}}{M_{total}} \times 100 \quad (2.15)$$

The mass of solute adsorbed at equilibrium (q_e) in mg/g or adsorption capacity and equilibrium DBT concentration, C_e can be obtained using the following expressions in Equation (2.16) and (2.17), respectively.

$$q_e = \frac{q_{total}}{m} \quad (2.16)$$

$$C_e = \frac{M_{total} - q_{total}}{V_{eff}} \times 100 \quad (2.17)$$

Where m is the mass of the adsorbent in g.

2.4.2. Batch mode

The adsorption process is commonly investigated through a graph called adsorption isotherm. Adsorption isotherm is the graph of equilibrium relation between the amount of absorbed material on the surface of the adsorbent and the concentration or pressure in the bulk fluid phase at constant temperature. (Alavi and Hashemi, 2013). Various isotherms of adsorption have been studied, such as; Langmuir, Freundlich isotherms and BET theory.

Adsorption Isotherm which explained the variation of adsorption with pressure was proposed by Irving Langmuir in 1916. Following the concept of his theory, Langmuir Equation was derived which described the correlation between the number of binding sites of the adsorption surface and pressure. The Langmuir isotherm assumption is based a monolayer adsorption on to an adsorbent surface containing limited number of uniform adsorption sites, and it assumes no adsorbate

movement on the surface. Conversely, the Freundlich isotherm assumption is based on heterogeneous surface energies, whereby the Langmuir equation energy varies as a function of the surface coverage (Zhao et al., 2008). Comparing the coefficient of determination (R^2) can confirm the suitability of the existing adsorption isotherms to describe observations during any isothermal studies.

The linear form of the Langmuir's isotherm can be given by the following equation:

$$\frac{C_e}{q_e} = \frac{1}{K_l q_m} + \frac{C_e}{q_m} \quad (2.18)$$

Where C_e is the equilibrium concentration of solute in (mg/L), q_e and q_m are the equilibrium and maximum amounts adsorbed per unit mass of solute in (mg/mg), respectively, and K_l is the Langmuir constant related to the adsorption rate. From the plot of $\frac{C_e}{q_e}$ against C_e, if a straight line with slope $\frac{1}{q_m}$ is obtained, indicating that, the adsorption of solute on the adsorbent follows the Langmuir isotherm (Al-Zubaiby et al 2015).

The Freundlich model is given by Equation (2.19):

$$\text{Log } q_e = K_f \ (C_e)^{i/n} \quad (2.19)$$

And the linear form is given by:

$$\text{Log } q_e = Log\ K_f + \frac{1}{n} C_e \quad (2.20)$$

K_f and K_l and are the Freundlich constants showing the adsorption capacity of the adsorbents and the affinity between the adsorbent and solute, respectively. The plot of log q_e versus log C_e gives a straight line with slope '1/n'

Kinetics studies help in determining the time required for equilibrium to be attained during adsorption process (Mittal et al., 2006). Kinetics studies also determine the rates of adsorption at different experimental conditions. Resident time of the solute, dimensions of reactor and adsorption rate prediction are important factors in the design of an adsorption system (Ho et al., 2006). This allows to determine the effect of variables like sulphur concentration on the rates of reaction. The rate of adsorption of solute which controls the resident time of sorbate uptake at the solid-solution interface can be described by Kinetics studies. (Ho et al., 1999). In addition, the mechanism and effectiveness of the adsorption process can be concluded from their kinetic studies. Hence, the kinetic data is used, so as to know the dynamics of adsorption process in terms of order of rate constant.

The linear form of Lagergren pseudo-first-order kinetic model can be expressed

$$log(q_e - q_t) = logq_e - \frac{K_1}{2.303}\ t \qquad (2.21)$$

Where q_e is the amount of solute adsorbed (mg/g) at equilibrium while q_t denotes the mass of solute adsorbed at any time, t (min). K_1 is the pseudo-first-order equilibrium rate constant of adsorption in min^{-1}. A linear graph of log (q_e-q_t) versus t can be plotted where K_1 and q_e will be obtained.

Kinetic data can also be further obtained by typical pseudo second-order kinetic model and it can be expressed by a linear equation (Lam et al., 2008):

$$\frac{t}{q_t} = \frac{1}{k_2 {q_e}^2} + \frac{1}{q_e} t \quad (2.22)$$

Where K_2 is the equilibrium rate constant of pseudo-second-order model (g $mg^{-1}min^{-1}$). Steps in the adsorption process must be identified through mathematical methods, in order to enhance the interpretation of the kinetics. Sequential steps involved in the adsorption of an organic or inorganic by an adsorbent include (Mittal et al., 2006):

i) Transport of the adsorbate to the external surface of the adsorbent i.e. film diffusion.

ii) Transport of the adsorbate within the pores of the adsorbent except for a small amount of adsorption which occurs on the external surface i.e. particle diffusion.

iii) Adsorption of the adsorbate on the interior surface of the adsorbent. A quantitative treatment of the sorption dynamics was determined by the expression (Reichenberg et al., 1953):

$$B_t = 2\pi - \frac{(\pi^2 F)}{3} - 2\pi \left(1 - \frac{\pi F}{3}\right)^{0.5} \quad (2.23)$$

Where F is the fractional attainment of equilibrium at time t which can be obtained using Equation (2.24):

$$F = \frac{Q_t}{Q_\infty} \quad (2.24)$$

Where Q_t is the amounts of solute adsorbed after time t and Q_∞ is the amount adsorbed after an infinite time. Reichenberg's (1953) table and equation 2h can be used to determine F and corresponding B_t values. The linear plot of B_t versus t plots can be used to differentiate between

particle diffusion controlled rates and the film (Shady et al., 2012). Several studies have been investigated on the isotherms and kinetic studies during adsorptive desulfurization of petroleum distillates. The studies are therefore critically reviewed.

Muzic et al., (2015) investigated on two designs of experiments (DOE) by using activated carbon (Chemviron carbon) in a batch system to desulphurize a diesel fuel. Authors reported the process development of the statistical model, the effects of different factors and their interactions on concentration of sulfur and adsorption capacity. The behavior of the system was predicted by first-order models. Afterward, when a significant curvature was noticed authors developed second-order models which reasonably described well the system.

Patil, (2013) examined ultrasound-assisted desulfurization of commercial kerosene by adsorption using activated carbon and carbon nanotubes as adsorbents. The result of the ultrasonic irradiation for the sorption of hexyl mercaptan sulfur in kerosene showed that Carbon nanotubes show higher adsorptive capacity than activated carbon and the experimental data fitted to the Freundlich and Langmuir adsorption isotherm model.

Khodadia (2012) studied desulfurization capability of CuO nano particles adsorbent on diesel fuel. The result showed the best fit was observed with pseuso-second order model from the kinetic study of the adsorbent. The experimental data were fitted in Freundlich isotherm model.

The highest adsorption capacity for DBT using 5% Al-loaded activated carbon was reported by Nazal et al. (2015). The efficiency, adsorption capacities and removal selectivity of the adsorbents on DBT removal from model fuel are stated. The authors reported that the rate of adsorption of DBT followed pseudo-second order kinetics with correlation coefficients of nearly 1.0. The adsorbents were reported to be stable and can be reused for 5 times. In conclusion, the adsorption isotherms fitted into both the Langmuir and Freundlich models.

Bhattacharyulu (2015) employed a batch reactor to study desulphurization of hydrocarbon liquid fuels by adsorption. Activated carbon prepared from black liquor and phosphoric acid was employed as the adsorbent material. The result showed that experimental data were fitted in to Langmuir adsorption isotherm model. The author also reported that the intraparticle diffusion resistance was overcome by stirring.

Adsorption desuphurization capabilities of untreated, acid activated and magnetite nanoparticle loaded bentonite adsorbents were studied by Ishaq et al. (2017). The authors examined the experimental data using pseudo first and second order kinetics. The result showed that adsorption of the DBT into all the adsorbents was well described by pseudo second order kinetic. The adsorption isotherm data were examined using Langmuir and Freundlich isotherm models and the data fitted well into the Langmuir isotherm model.

Anbia and Karami (2015) studied the adsoptive desulphurization of DBT from gasoline fuel. The authors prepared ordered mesoporous carbon (OMC) adsorbents using spherical SBA-16 mesoporous silica, as a template. The authors reported that OMC showed higher sulfur adsorption due to high specific surface area and large mesopore volume. The equilibrium experimental data were examined by Langmuir and Freundlich isotherm models for OMC and result showed that the equilibrium results were best fitted into Langmuir isotherm.

Comparative investigation on desulphurizing ability of two metal oxides- activated zinc oxide and activated manganese dioxide, by Adeyi and Adekanmi (2012). The authors also stated that experimental data fitted into both Langmuir and Freundlich adsorption isotherm.

Rosas et al., (2010) investigated on adsorptive desulfurization of diesel fuel using different commercial activated carbons (CAA, CAB, CAC, and CAD). The adsorption isotherms were correlated by the Langmuir, Freundlich, Brunauer-Emmett-Teller (BET) and Sips models. Result showed that, there was correlation between the experimental and calculated adsorption isotherms. The experimental data was found to follow Sips and BET.

Fallah and Azizian (2012) investigated the adsorption capability of activated carbon cloth on DBT. The equilibrium adsorption of organosulfur compounds on the ACCs obeyed the Langmuir–Freundlich adsorption isotherm and their adsorption kinetic data were described by modified pseudo-n-order (MPnO) and mixed-order rate equation (MOE) models and both indicated the surface heterogeneity of the ACC surfaces.

2.5 Regeneration of spent adsorbents

Regeneration of the adsorbent is important in completing the adsorption process loop. Kim (2010) conducted experiments to study the efficiency of regenerated spent adsorbents. The saturated adsorbent was washed using toluene as solvent to remove the adsorbed sulphur compounds on the adsorbents. The existence of benzene ring methyl functional group on the toluene form a π-complexation with the metal halide in the used adsorbent (Kim et al., 2010). This aids in the removal of the sulphur compounds adsorbed from the spent adsorbents. The toluene treated adsorbent can be dried under vacuum and reactivated under high temperatures. Several studies on different regeneration and re-usability procedures have been investigated. Few of these different procedures and results are reviewed in this study.

Nejad et al., (2013) synthesized a magnetic mesoporous carbon (Ni-CMK-3) as an adsorbent for sulfur removal from model oil. Ni-CMK-3 was recovered by heating and extraction by solvent. The adsorbent regeneration was performed after adsorption of the DBT. In heating the adsorbent method, after separation of the adsorbent with the magnet, the adsorbent was put under temperature of 350 ^{o}C for 2 h under Ar atmosphere. The author reported that 67 % was recovered after the first cycle and 47 % after the second cycle. In solvent extraction method, 4 different solvents were used; namely, toluene, methanol, acetonitrile, or ethanol. 10 mL of each solvent was added and the mixture was agitated at room temperature for 1 h. The reports showed that desulphurization capability follows in the order toluene (97 %) ≫ acetonitrile ≅ methanol (36 %) > ethanol (23 %). Therefore, toluene was selected as the appropriate solvent for spent adsorbent regeneration. Percentage sulfur removal of 97 %, 94 % and 80 % were achieved for 1st, 2nd and 3rd cycles, respectively.

Safieh et al., (2015) studied adsorptive desulphurization of DBT by AC modified by MnO_2 adsorbent. The exhausted adsorbent (80.0 g) was regenerated using different organic solvents (n-hexane, toluene, o-xylene, phenol, n-octanol or n-pentanol) and the mixture was agitated at 250 rpm for 300 min at two temperatures. 20 ^{o}C and 65 ^{o}C. The authors reported that n-hexane achieved the best regeneration of the adsorbent of 66.4 % and 85.2 % of DBT at 20 ^{o}C and 65 ^{o}C respectively.

Regeneration of ACC-HNO_3 adsorbent was investigated by Fallah, and Azizian (2012) after it has been used to desulphurize DBT. The saturated adsorbent samples were washed with heptane in an ultrasonic or shaker bath at 30 °C and 65 °C. UV/Vis spectrometer was used to analyze the desorped amount of DBT as a function of time. The author reported that, the ultrasonic assisted method of regeneration is more efficient than the shaking method. In addition, high temperature enhanced regeneration of the adsorbent.

Adsorptive desulfurization process has been critically reviewed and discussed in detail in this chapter. Another desulfurization process that is employed in this study is biodesulfurization. It is therefore discussed in detail in the next section of this chapter.

2.6. Biodesulfurization

Biotechnology is the process whereby microorganisms are used to transform compounds for particular use. It is a vital instrument that is employed to develop new methods and to provide breakthroughs in numerous sectors, such as pharmaceutical, food, and agricultural industries. Biodesulfurization makes use of a biological catalyst to remove organo-sulfur from petroleum distillates. BDS technique results in a low energy cost, minimal generation of unwanted products, and low emissions of sulfur containing compounds. This is owing to the ability of the biological catalysts to operate at an ambient temperature and pressure with great capacity to remove sulfur compounds (Signh and Singh, 2005; Huang et al., 2010).

Petroleum refining is a process that employs physicochemical processes. Nevertheless, owing to the characteristics of the biotechnological method, it has been used as an alternative, or rather to complement the advancement of petroleum development in refining processes. Studies have been carried out on different types of microorganisms at both batch and industrial scales for refining process application, such as biological demulsification, denitrogenation, demetallation, and enhancement of oil recovery by microorganism, conversion of heavy crude to light crude, and biological control of reservoir souring (Gavrlescu and Chisti, 2005; Singh, 2010). There are still many opportunities to be exploited in this field, even though various biotransformation processes have been described (Ward et al., 2009; Voordouw, 2011).

In BDS, bacteria remove organo-sulfur from petroleum distillates, leaving the carbon chain of the organo-sulfur compounds undamaged. Therefore, BDS has often been used as an alternative method of desulfurization in place of HDS technique in refineries. The enzyme catalysed reaction method of removing sulphur from diesel fuel is now widely studied. There has been successful breakthrough in the use of biodesulfurization in the past 20 years. The first investigations were reported in the between 1950's and 1960's (Alves et al., 2005; Alves eta l., 2013). BDS removes the recalcitrant sulphur compounds that HDS cannot remove at low operating conditions of temperature and pressure. Therefore, the choice of enzymes that can use DBT and other PAHs as sulfur sources in their growth metabolism and transform them into a harmless compound is essential (Alves et al., 20130. In addition, studies have shown that the BDS technique is much cheaper than the HDS technique (Pacheco et al., 1999; Linguist, 1999). It has also been predicted that greenhouse gas emissions may be significantly reduced if the BDS process is used (Linguist, 1999).

Thiophenic compounds are used as carbon and sulphur sources by some of the isolated microorganisms, while some others used metabolized DBTs as a carbon source and they are converted after different steps of oxidation into a number of compounds that are soluble in water. However, the microbial growth and DBT oxidation rate could be significantly inhibited when the water-soluble end products accumulate (Abin-Fuentes, 2013). *Pseudomonas species* are used in this study as biocatalysts because of their ability to grow in biphasic medium.

Pseudomonas species are class of gram-negative bacteria. They are motile, polar-flagellate, non-spore-forming bacteria. They are generally found in nature such as; soil, fresh-water and marine environment and they are responsible for considerable decomposition of organic matter. *Pseudomonas aeruginosa* and *Pseudomonas putida* are the most common of the genus of *pseudomonas species.*

Pseudomonas aeruginosa is a motile, gram-negative, rod-shaped, asporogenous, and monoflagellated bacterium. *P. Aeruginosa* is a microorganism can be found everywhere and can live under a variety of environmental conditions. *P. aeruginosa* has the ability to grow well between temperatures of 25 °C to 37 °C. Optimum temperature being 37 ^{o}C, although, it can as well grow at 42 °C. This makes them to be exceptional compared to other *Pseudomonas species.*

The metabolism of *P. aeruginosa* is oxygen-based respiratory nevertheless, it grows in the absence of oxygen and in the presence of NO_3 (Wu et al., 2015)]. It is a rod shape micro-organism of 0.5–0.8 µm by 1.5–3.0 µm.

The typical *Pseudomonas* in nature exists in biofilm formats, attached to a substrate, or in a planktonic form, as a unicellular organism, swims actively with its flagellum. Actually, it can be found in samples from the wild or from patients (Colmer-Hamood et al., 2016). In order to grow well, *P. aeruginosa* requires a simple nutritional supply, even in ordinary deionized water. *P. aeruginosa* grows well in a medium containing acetate and ammonium sulphateas as carbon and nitrogen sourecs, respectively (nitrogen source). *P. aeruginosa* is resistant to most frequently used antibiotics, high salt concentrations, dyes and weak antiseptics, (Wu and Li, 2015). *Pseudomonas putida* is a genus of gram-negative bacterium which is usually found in water and soil, particularly around the roots of plants. It is motile with the aid of multiple 2 to 3 wavelengths long polar flagella. It grows well in the presence of oxygen between the temperature ranges of 25-30 ^{o}C with optimum temperature of 30 ^{o}C. It can be easily isolated. It can protect plants from disease from other microorganisms. It has a very complex aerobic metabolism with the ability to degrade a great variety of organic pollutants. This makes *P. putida* of commercial interest for degrading organic pollutants. Therefore, owing to the biological and chemical and biological applications of these *P. putida*, the DNA sequences of a number of strains have been sequenced. *Pseudomonas putida* has attracted the interest of researchers resently because of its strong appetite for organic pollutants (Kowalski, 2002). This bacterium is exceptional because it has the most genes needed for in breaking down harmful aromatic or aliphatic hydrocarbons released as a result of burning fuel, coal, tobacco, and other organic matter. (Marcus, 2003).

P. aeruginosa and P. putida are very closely related and share related sequenced genomes (approximately 85 % are shared), although, the gene for virulence determination of is lacking in *Pseudomonas putida. Pseudomonas putida* is very useful in research due to its nonpathogenic nature, ease of handling and high versatility (Kowalski 2002 and Marcus, 2003).

Several studies have been carried out on the use of microorganisms for the removal of sulfur from transportation fuel over the years. Refining processes by conventional methods have been carried out at an elevated temperature. Therefore, thermophilic BDS is required and could be easily

incorporated into the refining process without cooling the stock to 30 °C (Konishi et al., 1997). Thermophilic BDS makes the development of crude oil BDS more practicable since it also lowers the viscosity of crude oil (Borgne and Quitero, 2003). Currently a review paper was published by Soleimani et al. (2007) on BDS of refractory organo-sulphur compounds in transportation fuels. This paper focuses on the outcomes of the latest investigation on BDS. A study on the enzymatic oxidation of DBT by horseradish peroxidase (HRP) step was evaluated by Madeira et al. (2008). The result showed that about 60 % of DBT was transformed into dibenzothiophene sulfoxide (12 %) and 46 % dibenzothiophene sulfone at an optimum temperature, DBT concentration, molar ratio (DBT:H_2O_2), and reaction time of 45 °C, 0.267 mM, 1:20, and 60 min, respectively. Mohebali et al. conducted a BDS study on the removal of DBT from model oil, using both growth and resting stages of Gordonia lkanivorans (RIPI90A) bacterium, newly isolated (Mohebali, 2007). The result showed that cells that were harvested at the late exponential stage had higher DBT desulfurizing capacities. Alves et al. (2008) investigated on the enzymatic hydrolyzates of recycled paper sludge as suitable feedstock for BDS by *Gordonia alkanivorans strain 1B*. The result showed that, despite the increase in bacterial growth at non-dialyzed hydrolyzate, dialyzed-hydrolyzate obtained after enzymatic reaction displayed higher DBT desulfurization capacity. The maximum specific productivity of 2-hydroxybiphenyl (mol g/h) was achieved when 250 M DBT was used up after four days for dialyzed hydrolyzate. DBT was noticed to be completely consumed when phosphate and ammonia were added. A further increase in the production of 2-hydroxybiphenyl by 14 % was noticed. Caro et al. (2007) studied the BDS capability of aerobic *Rhodococcus erythropolis IGTS8* strain on DBT in oil–water emulsions. The result from the investigation showed that there was an increase in DBT diffusion into the aqueous phase when b-cyclodextrins was added, preventing HBP accumulation therefore improving the BDS yield. Furthermore, an increase in cell concentrations of biocatalyst decreased the rate of HBP production. This could be as a result of the limitation to mass transfer and inhibition effects. Chen et al. (2008) investigated the desulfurization ability of bacterium *Mycobacterium sp. ZD-19*. The result showed that TH and BTH were completely removed in 10 and 42 h, respectively. Also, about 100 % of DBT and 4, 6-DMDBT was removed in 50 and 56 h respectively. There was reduction in desulfurization efficiency when DBT and 4, 6-DMDBT were mixed together when compared to when they are desulfurized separately. This may be attributed to the existence of substrate competitive inhibition when DBT and 4, 6-DMDBT are mixed. The desulfurization activities of five substrates were

found to be in order of 4, 6-DMDBT < DBT < DPS < BTH < TH. Li et al. (2007) studied the removal of DBT in tetradecane using a facultative thermophilic bacterium Mycobacterium goodii X7B. There was almost a 99 % decrease in total sulfur level of DBT at 40 °C in 24 h. About 59 % of total sulfur was removed from Liaoning crude oil after 72 h treatment. Various studies of percentage sulfur removal from petroleum distillates by BDS techniques are summarized in Fig. 2.9, at optimum temperatures and DBT concentrations using different microorganisms. The microorganisms are abbreviated as follow; *Gordonia alkanivorans RIPI90A (GAR 190A), Gordonia alkanivorans strain 1B (GAS 1B), Rhodococcus erythropolis IGTS8 (RE IGTS8), Mycobacterium sp. ZD-19 (M sp ZD-19), Mycobacterium goodii X7B (MG X7B), Caldariomyces fumago (CF), Bacillus subtilis WU-S2B (BS WU-F1), Mycobacterium phlei WU-F1 (MP WU-F1), Rhodococcus sp. strain P32C1 (RS P32C1), Rhodococcus erythropolis ATCC 53968 (RE ATCC 53968), Mycobacterium sp. X7B (M sp. X7B), Microbacterium strain ZD-M2 (MS ZD-M2), Pseudomonas stutzeri UP-1 (PS UP-1), Sphingomonas subarctica T7b (SS T7b), Bacterium, strain RIPI-22 (SS RIPI-22), Pseudomonas delafieldii R-8 (PD R-8).*

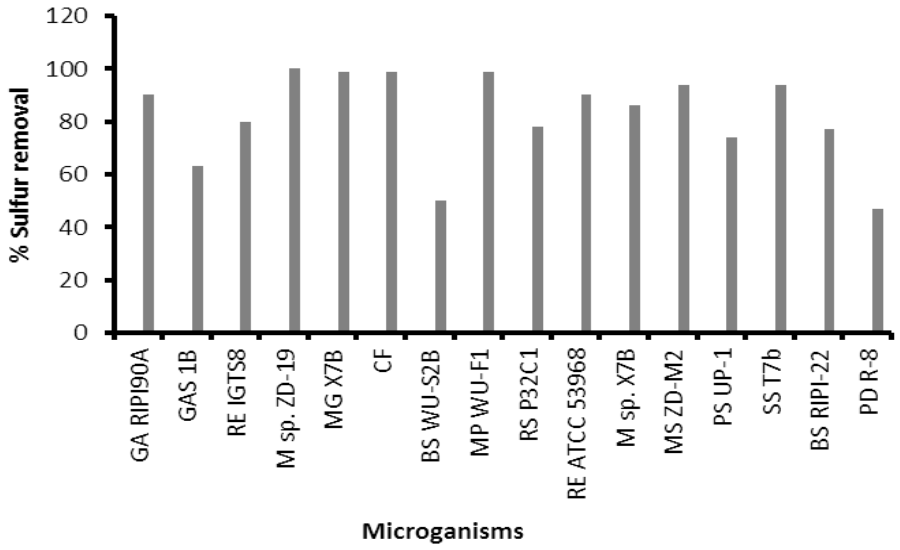


Figure 2.6 The percentage (%) desulfurizing ability of various microorganisms (Adapted from Kinoshi et al., 1999)

Recently, many bacteria species, such as *Arthrobacter, Brevibacterium, Pseudomonas, Gordona, and Rhodococcus* strains, and other related bacteria species have been discovered to be able to transform DBT or to use it as their only sulfur source for their growth metabolism (Grossman et al., 1999; Konishi et al., 1999). *Rhodococcus strains* are suitable for hydrocarbon metabolism. Many bacteria strains, such as *Rhodococcus, Mycobacterium, and Pseudomonas species* have transform organo-sulfur compounds in either of these three ways: one of three ways: C–S bond cleavage (reductive), C–C bond cleavage (oxidative), and C–S bond cleavage (oxidative). The latter attacks only the sulfur atom that is leaving the carbon chain intact, therefore preserving the quality of the fuel. There are a lot of reports on the desulfurizing capability of *Pseudomonas strains* through DBT C–C bond cleavage pathway. These results have shown about 90 % sulfur removal in 24 h by sulfur metabolising bacteria (Kim et al., 1990; Borole et al., 2002; Nehlsen, 2005). Dibenzothiophene has been investigated to be a model compound used in biodesulfurization of fuels.

Dibenzothiophene (DBT) is the most widely used typical organo-sulphur compound in biodegradation and biodesulfurization studies (Mohebali and Ball, 2008; Gün et al., 2015). Thus far, quite a few investigations have been carried out with DBT and alkyl-substituted DBTs using ring destructive DBT-degrading bacteria. DBT and its derivatives account for up to 70 % of the sulphur content and they are the main organo-sulphur compounds in diesel fuel (Kertesz and Wirtek, 2001). They are one of the compounds that are persistent and are mostly found in an oil contaminated environment (Yu et al., 2006). DBT and its derivatives are refractory to the HDS method (Bhatia and Sharma, 2012), surviving even to deep HDS treatment (Chen et al., 2009). Moreover, DBT can be easily manipulated unlike other substances, because it is not mutagenic, neither is it dangerous to human health (Pokethitiyooka et al., 2008)

In anaerobic BDS, there is conversion of organic sulfur into hydrogen sulfide, which is later transformed into a sulfur atom. This process follows for the reductive desulfurization order and may be of use at the refinery since unwanted end products, such as coloured and gum-forming products, due to oxidation of hydrocarbons to undesired compounds, such as colored and gum-forming products, is residual. Several anaerobic strains, such as Desulfovibrio desulfuricans, have demonstrated the ability to metabolize DBT during such a reductive desulfurization reaction. They

also remove organic sulfur from petroleum feedstocks by reductive C–S bond cleavage (anaerobic BDS) (Yamada et al., 2001). However, it is difficult to maintain an anaerobic process. (Amstrong et al., 1995).

Unlike anaerobic biodesulfurization, desulfurization by aerobic conditions occurs through oxidative pathways. These produce a water-soluble sulfate that is discarded alongside the unwanted aqueous phase. Desulfurization can occur in a different way depending on the substances present because the specificities of different strains differ for different sulfur compounds, and the pathway metabolism is not restricted to sulfur. This kind of desulfurization, however, comes with an associated carbon lost (Kirkwood et al., 2005; Kirkwood et al., 2007). The sustainability of BDS depends on the selectivity of sulfur over carbon. It is important to harvest the microorganisms if the carbon metabolism is high, in order to retrieve some of the carbon lost during desulfurization. Table 2.3 and Table 2.4 show the efficiency of aerobic cultures in real fuel desulfurization and desulfurization of alkylated dibenzothiophene with their end products, respectively.

2.7. Potential of biodesulfurization technique for industrial application

Over the years, there have been issues on the industrial application of BDS, although it serves as a complementary process to hydrodesulfurization. This is due to several challenges that are faced at both upstream and downsteam processes. One of the major problems hindering the useful application of BDS in the industries is the high cost of growing bacteria in a culture medium. In view of this, use of carbon sources that are obtained from industrial agricultural products can serve as alternatives so as to reduce capital expenses (Paixao et al., 2016; Rosenberg et al., 1980). Alves et al. (2014) investigated a fructose-rich carbon source using G. alkanivorans strain 1B to desulfurize sulfur heterocyclic compound in transportation fuel. The authors reported a higher desulfurizing capability of this strain on BT and DBT when compared with Rhodococcus erythropolis. The cost of microorganism can be another challenge for application of BDS in the industry. In other to overcome this challenge, the immobilization of cell has been suggested to be a feasible solution (Setti et al., 1996).

Table 2.3 Comparative characteristics of the efficiency of selected aerobic cultures in real fuel desulfurization.

Culture	**Type of petroleum distillate**	**Conc. of DBT (ppm)**	**(%) DBT removal**	**Ref.**
Gordonia sp. P32C1 (resting cells)	Light diesel fuel after hydrodesulfurization	303	48.5	Maghsoudi et al. (2001)
Mycobacterium sp. X7B (resting cells)	Diesel fuel after hydrodesulfurization	535	86.0	Li et al. (2003)
Pseudomonas delafieldii R_8 (growing cells)	Diesel fuel after hydrodesulfurization	591	47.0	Goubin et al. (2006)
Gordonia sp. CYKS1 (resting cells)	Middle distillate unit feed	1500	70.0	Rhee et al. (1998)
	Light gasoil	3000	50.0	
Gordonia sp. SYKS1 (resting cells)	Light gasoil not subjected to hydrodesulphurization	3000	35.0	Chang et al. (2001)
	Middle distillate unit feed	1500	60.0	
Gordonia sp. SYKS1 (resting cells)	Diesel fuel	250	76.0	Chang et al. (2001)
Rhodococcus sp. ECRD_1 (growing cells)	Medium fraction of light gasoil after catalytic cracking	669	92.0	Grossman et al. (2001)

Table 2.4 Alkylated DBTs (Cx-DBT) desulfurization by some strains of bacteria and their end products.

Bacterium	Sulphur Substrate(s)	End Product(s)	Ref.
Rhodococcus erythropolis KA2-5-1	Alkylated DBTs (C_2-DBTs and C_3-DBTs)	Corresponding hydroxylated Biphenyls	Kobashi et al. (2000)
Rhodococcus erythropolis H-2	2,8-DMDBT, 4,6-DMDBT	Corresponding hydroxylated biphenyl	Oshiro et al. (1996)
	3,4-Benzo-DBT	a-Hydroxy-b-phenylnaphthalene	
Bacterial strain RIPI-S81	4-MDBT	2-Hydroxy-3-methylbiphenyl, 2-hydroxy-3-methylbiphenyl	Rashidi et al. (2006)
	4,6-DMDBT	2-Hydroxydimethylbiphenyl	
Mycobacterium sp. G3	4,6-Dibutyl DBT, 4,6-dipentyl DBT; 4,6-DMDBT, 4,6-DEDBT	C–S bond cleavage products	Okada et al. (2002)
Paenibacillus sp. A11-2	Methyl, ethyl, dimethyl, trimethyl and propyl DBTs	Corresponding hydroxylated Biphenyls	Konish et al. (1997); Konishi et al. (1999)
Rhodococcus sp. ECRD-1	4,6-DEDBT	Hydroxydimethylbiphenyl	Lee et al. (1995)

The reported technique by Rosenberg et al. (1980) was adopted to study the affinity of *Pseudomonas* species towards some hydrocarbons. The results obtained indicated that an increase in adsorption of bacteria onto the hydrocarbon increases the percentage organic phase (Setti et al., 1996). Cell immobilization helps in the recovery of biocatalysts after treatment of microorganisms. The partial challenge that is encountered by BDS through the rate of transfer of sulphur heterocyclic compounds from oil phase into the microbial cell is also hindered during BDS, which affects the full application of BDS at industrial scale. Goubin et al. (2005) assembled γ-Al_2O_3 nano-sorbents on *Pseudomonas delafieldii R-8 strain*. It was shown from the result that adsorption rate was higher when compared to the rate of BDS. The assembly of the nano-adsorbent enhanced the transfer of the organo-sulfur (DBT) from the oil phase to the surface of the bacteria.

The biodesulfurization capacity (X_{BDS}), Conversion yield for DBT (Y_{BDS}), degree of desulfurization (D_{BDS}) and specific conversion rate (E) can be evaluated using the following equations:

Biodesulfurization capacity (%) evaluates the the efficiency of bacteria in biodesulfurization process

$$X_{BDS} = \frac{C_{2-HBP,(f)}}{C_{DBT,(i)}} \times 100\ \% \tag{2.24}$$

Where X_{BDS} is biodesulfurization capacity in (%), $C_{2\text{-}HBP(f)}$ in mg/L is the final concentration of 2-HBP formed during biodesulfurization of DBT, $C_{DBT(i)}$ in mg/L is the initial DBT concentration in the model oil before degradation.

Conversion yield of DBT (%) can be evaluated by using Equation (2.25);

$$Y_{BDS} = \frac{C_{DBT,(i)} - C_{DBT,(f)}}{C_{DBT,(i)}} \times 100\ \% \quad (2.25)$$

Where Y_{BDS} is the conversion yield for DBT degraded (%), $C_{DBT,(f)}$ is the final concentration of DBT after degradation in mg/L. X_{BDS} and Y_{BDS} indicate the efficiency of bacteria in the biodesulfurization process.

Degree of desulfurization (g DCW/L.h) is the degree to which desulfurization occurred during growth and resting process. This can be used to show relationship the biodesulfurization capacity of the bacteria and the biomass obtained within a specified period of growth time. Evaluation of D_{BDS} during bacteria growth provides information on optimum biocatalyst production process. D_{BDS} can be calculated using Equation (2.26):

$$D_{BDS} = \frac{X_{BDS} \cdot C_X}{t_G} \quad (2.26)$$

Where D_{BDS} in (g DCW/L) is the degree of desulfurization, X_{BDS} is the biodesulfurization capacity, C_x is the biomass concentration (g DCW/L), t_G (h) is the time required to attain the biomass concentration.

Specific conversion rate, E (L/g DCW.h) is the effectiveness of each bacterium. It can be determined by the expression in Equation (2.27):

$$E = \frac{X_{BDS\,(\max)}}{t_{G(\max)} \cdot C_X} \quad (2.27)$$

Where $t_{G\,(max)}$ (h) is the time required for maximum desulfurization.

2.8. Kinetics of bacteria growth and diesel desulfurization

Batch culture occurs in a closed system that contains an initial limited amount of substrate. The inoculated microorganism will pass through a number of growth phases. During the log phase, cell numbers increase exponentially at a constant maximum rate. In mathematical terms, we can write:

$$\frac{dX}{dt} = \mu X \tag{2.28}$$

Where X is the concentration of microbial biomass, t is the time in hours and μ is the specific growth rate in hours^{-1}. If we integrate between time t_o and time $t_1$when the concentrations of the cells are X_0 and X_1we obtain:

$$X_t = X_0 e^{\mu t} \tag{2.29}$$

Where x_o is the original biomass concentration, xt is the biomass concentration after a time interval t in hours and e is the base of the natural logarithm. On taking natural logarithms, the equation becomes:

$$lnX_t = lnX_0 + \mu t \tag{2.30}$$

Using this equation, a plot of the natural log of biomass concentration versus time should yield a straight line, the slope of which will equal the specific growth rate (μ).

The growth of a bacteria culture can be studied using the Minod expression as shown in Equation (2.31):

$$\mathrm{V} = \mathrm{V}_{max}\frac{[S]}{K_m+[S]} \tag{2.31}$$

Where V_{max} is the first order rate constant (mg/gDCW.h) particular to the exponential growth phase of culture described by the rate equation, V is the rate of bacteria growth (gDCW/L.h), [S] is the substrate concentration (mg/L), and K is a first-order constant (mg/L).

For a single substrate catalyzed reaction, Michaelis Menten equation is applied. Michaelis-Menten assumed that, a fast pre-equilibrium forming an enzyme-substrate complex precedes a slow, rate determining reaction of that complex. Michaelis-Menten can be considered satisfactory description of substrate utilization, only if the initial equilibrium can be considered in the context of the system as a whole and that the subsequent steps can be considered as occurring only within the cells.

$$\frac{-d[S]}{dt} = K[E_0]\frac{[S]}{K_m+[S]} \tag{2.32}$$

Where;

$$K_m = \frac{[E][S]}{[ES]}\ and\ [E_0] = [E] + [ES] \tag{2.33}$$

If $[E_o]$, the maximum concentration of available substrate-binding enzyme for a given cell concentration can be considered proportional to the bacteria density itself, and if also the rate of growth can be considered proportional to the rate of substrate utilization, then;

$$[E_0] = X[B]\ and\ \frac{d[B]}{dt} = -Y\frac{d[S]}{dt} \tag{2.34}$$

Where $\frac{d[B]}{dt}$ is the rate of growth of bacteria, X is a constant, and Y is a yield factor also considered to be constant throughout the period of substrate conversion. It follows that,

$$\frac{d[B]}{dt} = K'[B]\frac{[S]}{K_m+[S]} \tag{2.35}$$

Comparing Equation (2.31) with (2.35) shows that:

$$\mathrm{V} = K'\frac{[S]}{K_m+[S]} \tag{2.36}$$

This is the form of Minod equation.

Equation (2.35) shows that when S >> K the reaction is pseudo first order, but when S << K the reaction is second-order character predominate

$$\frac{d[B]}{dt} = \frac{K'}{K_m}\,[B][S] \tag{2.37}$$

The similarity of this second-order rate expression to that for an autocatalytic model where

$$S \rightarrow B \; and \; \frac{d[B]}{dt} = \mathrm{K}[B][S] \tag{2.38}$$

This is consistent with previous observation on the form of growth curves. K is said to be equivalent to the Michaelis-Menten constant, K_m. Linearized form of Michaelis mentel equation can be written as;

$$\frac{1}{V} = \frac{K_m}{V_{max}} . \frac{1}{S} + \frac{1}{V_{max}} \tag{2.39}$$

Plot of $\frac{K_m}{V_{max}}$ versus $\frac{1}{S}$ yields a straight line where the values of V_{max} and K_m can be calculated from the slope and intercept of the graph, respectively using a linear regression analyss. The differential method analysis can be used when when numerical values of the reaction rate have been obtained at different concentrations and at a constant temperature (Roberts, 2009).

2.9 Summary

This chapter has highlighted that sulphur has severe impacts on human life and its environment. A short overview of the state of the art of the application of different techniques for the removal of sulfur-containing compounds from petroleum distillates, especially adsorption and biodesulfurization processes have been presented. Several limitiations have also been highlighted. Most expecially, it has been shown that the use adsorbents such as; AC, FCNTs, PLP, NLP for diesel desulfurization could be promising. However, availability of high selective adsorbents for the removal of recalcitrant DBT compound from petroleum distillates is still a major problem. Furthermore, in-depth understanding of the fundamental behaviour of adsorbents during batch mode and continuous mode adsorption processes, during the adsorptive removal of DBT is essential.

In addition, only few studies have been carried out on local and waste adsorbents. Use of low-cost adsorbents could reduce cost of operation and enhance removal of waste products from our environment. In addition, cheap and easily available adsorbent will reduce the cost of adsorption process in the industry and may lead to maximum reduction of pollution to the environment. Furthermore, one of the properties of adsorbent upon which the efficiency of adsorption technique depends is the regeneration of spent adsorbent. This aspect of regenerability of adsorbents was not discussed in most of the reviewed papers. Therefore, reusability of the adsorbents for better efficiency is investigated in this study.

Regarding BDS, an in-depth understanding of how bacteria metabolize sulphur heterocycles requires extensive studies. Based on this review, the following suggestions need to be considered in the development of a new BDS process;

Indepth investigation into the understanding of the various microbial pathways that are involved in BDS is required towards the optimization and scale-up studies of the process. In addition, studies that will explore the combination of BDS with existing methods could be instrumental to achieving a higher reduction in sulphur-containing compounds in the petroleum distillates.

Based on the aforementioned problems, the remaining chapters of this dissertation will demonstrate the promising potentials of adsorption coupling biodesulfurization system for desulfurization of South African diesel through;

1. Development and evaluation of the performance of adsorption using a specific adsorbent (e.g. activated carbon, functionalized carbon nanotubes neem leaf powder and pomegranate leaf powder) for the removal of DBT compounds from model diesel and samples of South African diesel (diesel obtained before HDS and diesel obtained after HDS unit and investigating the operating variables on the process toward enhancing its performance. The results obtained from the studies might provide relevant information on the behavior of the adsorbents. More knowledge on the role played by the variables on the adsorption performance of the adsorbents could be instrumental in optimizing the operating conditions.
2. Development and evaluation of BDS system, using *Pseudomonas Putida* and *Pseudomonas Aeruginosa* as biocatalysts, for the removal of sulphur-containing

compounds from model diesel and samples of South African diesel obtained before and after HDS and investigating the operating conditions. This could assist in optimizing the parameters of the process toward enhancing its performance.

3. Coupling of the two processes in (1) and (2) and evaluation of the hybrid process for the removal of DBT from samples of South African diesel. The results obtained from this investigation could pave the way for the actualization of the benchmark set by the WHO on the minimum concentration of sulphur-contianing compounds in South African petroleum distillates.
4. Investigating whether the kinetics and isothermal adsoption exhibited by the adsorbents used in (1), (2) & (3) could be described by existing kinetic models and adsorption isotherms. The result from this exploration will affirm the observation from the experimental studies.

In order to disseminate this fundings as contained in this chapter to the research community, a review paper was published in a reputable research journal (see Appendix D for a copy of this paper).

2.10. References

Abín-Fuentes, A. (2013) Mechanistic Understanding of Microbial Desulfurization. Ph.D. Thesis, Massachusetts Institute of Technology, Department of Chemical Engineering, Cambridge, MA, USA.

Abin-Fuentes, A.; Leung, J.C.; El-Said Mohamed, M.; Wang, D.I.C.; Prather, K.L.J. (2014) Rate-limiting step analysis of the microbial desulfurization of dibenzothiophene in a model oil system. Biotechnol. Bioeng., 111, 876–884.

Adeyi, A., and Aberuaga, F. (2012) Comparative analysis of adsorptive desulfurization of crude oil by manganese dioxide and zinc oxide, Research Journal of Chemical Sciences, 8 (2),14-20.

Ahmed, J., and Ahmaruzzaman, M. (2015) "Adsorptive desulfurization of feed diesel using chemically impregnated coconut coir waste" Int. J. Environ. Sci. Technol. 2(9), 2847–2856.

Alves, L., Silva, T.P., Arez, B.F., Paixão, S.M. (2013) Enhancement of dibenzothiophene biodesulfurization by Gordonia alkanivorans strain 1B using fructose rich culture media. In Proceedings of the 1st International Congress on Bioenergy, Book of Abstracts, Portalegre, Portugal, 23–25 May, 48.

Alavi, S.A., Hashemi, S.H. (2014) A Review on Diesel Fuel Desulfurization by Adsorption Process. In Proceedings of the International Conference on Chemical, Agricultural, and Biological Sciences, Antalya, Turkey, 2–3 May, 33–36.

Alves, L., Salgueiro, R., Rodrigues, C., Mesquita, E., Matos, J., Girio, F.M. (2005) Desulfurization of dibenzothiophene, benzothiophene, and other thiophene analogs by a newly isolated bacterium, Gordonia alkanivorans strain 1B. Appl. Biochem. Biotechnol., 120, 199–208.

Alves, L., Marque, S., Matos, J., Tenreiro, R., Gírio, F.M. (2008) Dibenzothiophene Desulfurization by Gordonia alkanivorans Strain 1B Using Recycled Paper Sludge Hydrolyzate. Chemosphere, 70, 967–973.

Alves, L., Paixão, S.M. (2014) Enhancement of Dibenzothiophene Desulfurization by Gordonia alkanivorans Strain 1B Using Sugar Beet Molasses as Alternative Carbon Source. Appl. Biochem. Biotechnol., 31, 73–79.

Al-Zubaidy, I. A. H., Ali, Y. M., MeeraAl-Suwaidi, Al Shaihk, R., LeherFarooq, A, A., Al-Sulh, R. T., Zraqi, K. (year) “Kinetics of novel adsorption desulphurizationtechniques for diesel fuel using different sorbents”, International Conference on Chemical, Medical and Environmental Issues, pp 37.

Anastasia Colomba, A. (2015) Production of Activated Carbons from Pyrolytic Char for Environmental Applications. PhD Thesis submitted to the Department of Chemical and Biochemical Engineering. The University of Western Ontario London, Ontario, Canada, pp. 215.

Armstrong, S.M., Sankey, B., Voordouw, G. (1995). Conversion of diben-zothiophene to biphenyl by sulfate reducing bacteria isolated fromoil field production facilities. Biotechnol. Lett. 17, 1133–1136.

Ayala, M.; Tinoco, R., Hernandez, V., Bremauntz, P., Duhalt, R.V. (1998) Biocatalytic oxidation of fuel as an alternative to biodesulfurization. Fuel Process. Technol., 57, 101–111.

AECC Newsletter (2015) Available online: http://www.aecc.eu/en/content/pdf/AECC%20 Newsletter % 20 May-June % 202010.pdf (Accessed on 22 November 2016).

Air Resource Board. Black Carbon Emissions Reduced by ARB Regulations; Califonia Environmental Protection Agency: Sacramento, CA, USA, 2013, pp. 1–89.

Babich, I.V., Moulijn, J.A. (2003) Science and technology of novel processes for deep desulfurization of oil refinery streams: A review. Fuel 82, 607–631.

Bachmann, R.T., Johnson, A.C, Edyvean. R.G.J. (2014) Biotechnology in the petroleum industry: An overview International Biodeterioration & Biodegradation., 86, 225-237.

Bailey, D; Plenys, T; Solomon, G.M; Campbell, T.R; Feuer, G.R; Masters, J; Tonkonogy, B. (2004) Harboring pollution Strategies to Clean Up U.S. Ports. Natural Resources Defense Council, Pp 1-97.

Banerjee, S. (2017) The European Fuels Conference. Overview of the Asian fuel market. (2011) pp. 1–19.Available online: http://www.efoa.eu/documents/document/20110328145537-2011-03-09_overview_of_the_asian_fuel_ether_market_and_opportunities_for_europe.pdf (Accessed on 23rd, November 2017).

Barrett, S.R., Yim, S.H., Gilmore, C.K., Murray, L.T., Kuhn, S.R., Tai, A.P., Yantosca, R.M., Byun, D.W., Ngan, F. and Li, X. et al. (2012) Public Health, Climate, and Economic Impacts of Desulfurizing Jet Fuel. Environ. Sci. Technol., 46, 4275−4282.

Bergh Caitlin. (2012) Energy Efficiency in the South African Crude Oil Refining Industry: Drivers, Barriers and Opportunities. A thesis submitted for MSc Sustainable Energy Engineering at the University of Cape town.

Bezverkhyy, I., Ryzhikov, A., Gadacz, G., and Bellat, J.P. (2008) Kinetics of thiophene reactive adsorption on Ni/SiO2 and Ni/ZnO. Catal. Today, 130, 199–205.

Borgne, S.L. and Quintero, R. (2003) Biotechnological processes for the refining of petroleum. Fuel Process. Technol. 81, 155–169.

Berthou, F., Gourmelun, Y. Dreano, Y., and Friocourt, M.P. (1981) Application of gas chromatography on glass capillary columns to the analysis of hydrocarbon pollutants from the Amoco Cadiz oil spill. J. Chromatogr., 203, 279–292.

Borole, A.P., Kaufman, E.N., Grossman, M.J., Minak-Bernero, V., Bare, R. and Lee, M.K. (2002) Comparison of the emulsion characteristics of Rhodococcus erythropolis and Ecsherichia coli SOXC-5 cells expressing biodesulfurization genes. Biotechnol. Prog., 18, 88–93.

Bhatia, S.and Sharma, D.K. (2012) Thermophilic desulfurization of dibenzothiophene and different petroleum oils by Klebsiella sp. 13T. Environ. Sci. Pollut. Res. Int., 19, 3491–3497.

Bhattachryulu, Y. C., Patil, M., and Kamble, S. (2012) Unsteady state adsorption – Column studies. International Journal of Advanced Engineering Research and Studies, 1(I1), 179– 184.

Boniek, D., Figueiredo, D., Batista dos Santos, A.F., Maria Aparecida de Resende Stoianoff. (2015) Biodesulfurization: A mini review about the immediate search for the future technology. Clean Technol. Environ. Policy, 17, 29–37.

Blanco-Brieva, G., Campos-Martin, J.M., ALZahrani, S.M. (2010) "Removal of refractory organic sulphur compounds in fossile fuels using MOF sorbents", Global NEST Journal, Vol 12, pp 296-304.

Bose, D. (2015) Parameters for a Hydrodesulfurization (HDS) Unit for Petroleum Naphtha at 3500 Barrels per Day. World Sci. News, 9, 99–111.

Bouwens, S.M.A.M., van Zon, F.B.M., van Dijk, M.P., van der Kraan, A.M., de Beer, V.H.J., van Veen, J.A.R. and Koningsberger, D.C. (1994) On the structural differences between alumina-supported CoMoS type I and alumina-, silica-, and carbon-supported CoMoS type II phases studied by XAFS, MES, and XPS. J. Catal., 146, 375–393.

Bravo, A.H.; Soto, A.R.; Sosa, E.R.; Sánchez, A.P.; Alarcón, J.A.L.; Kahl, J.J.; Ruíz, B.J. (2006) Environ. Pollut., 144, 655–660.

Cackette, T. (1999) Importance of Reducing Emissions from Heavy-Duty Vehicles; California Air Resources Board: Sacramento, CA, USA, p. 15.

Cattaneo, R. Rota, F.and Prins, R. (2001) An XAFS Study of the Different Influence of Chelating Ligands on the HDN and HDS of γ-Al2O3-Supported NiMo Catalysts. J. Catal., 199, 318–327.

Chang, J.H., Chang, Y.K., Cho, K.S. and Chang, H.N. (2000) Desulfurization of model and diesel oils by resting cells of Gordona sp. Biotechnol. Lett., 22, 193–196.

Chang, J.H.; Kim, Y.J.; Lee, B.H.; Cho, K.S.; Rye, H.W.; Chang, Y.K.; Chang, H.N. (2001) Production of a desulfurization biocatalyst by two-stage fermentation and its application for the treatment of model and diesel oils. Biotechnol. Prog., 17, 876–880.

Chen, H. Cai, Y.B. Zhang, W.J. and Li, W. (2009) Methoxylation pathway in biodesulfurization of model organosulfur compounds with Mycobacterium sp. Bioresour. Technol., 100, 2085–2087.

Caro, A., Leton, P., Calvo, E.G. and Setti, L. (2007) Enhancement of dibenzothiphene biodesulphurization using β-cyclodextrins in oil-to-water media. Fuel, 86, 2632–2636.

Chen, H.; Zhang, H.W.J.; Chen, J.M.; Cai, Y.B.; Li, W. (2008) Desulfurization of various organic sulphur compounds and the mixture of DBT + 4,6-DMDBT by Mycobacterium sp. ZD-19. Bioresour. Technol., 99, 6928–6933.

Chambliss, S.; Josh Miller, J.; Façanha, C.; Minjares, R.; Blumberg, K. (2013) The Impact of Stringent Fuel and Vehicle Standards on Premature mortality and Emissions; ICCT'S Global Transportation Health and Climate Roadmap Series; International Council on Clean Transportation: Washington, DC, USA, pp. 1–89.

Cheng, S.S. (2008) Ultra Clean Fuels via Modified UAOD Process with Room Temperature Ionic Liquid (RTIL) & Solid Catalyst Polishing. Ph.D. Thesis, University of Southern California, Los

Angeles, CA, USA. Available online: http://cee.usc.edu/assets/025/85741.pdf (Accessed on 20 October 2016).

Chica, A.; Corma, A.; Dómine, M.E. (2006) Catalytic oxidative desulfurization (ODS) of diesel fuel on a continuous fixed-bed reactor. J. Catal., 242, 299–308.

Chu, X., Hu, Y., Li, J., Liang, Q., Liu, Y., Zhang, X., Peng, X., Yue, W. (2008) 'Desulfurization of diesel fuel by extraction with [BF4] —based ionic liquids', Chinese Journal of Chemical Engineering, 16(6), 881-884.

Collins, F.M. Lucy, A.R. Sharp, C.J. (1997) Oxidative desulfurization of oils via hydrogen peroxide and heteropolyanion catalysis. J. Mol. Catal. A Chem., 117, 397–403.

Colmer-Hamood, J.A., Dzvova, N., Kruczek, C., and Hamood, A.N. (2016) In Vitro Analysis of Pseudomonas aeruginosa Virulence Using Conditions That Mimic the Environment at Specific Infection Sites. Progress in Molecular Biology and Translational Science. 142, 151-191.

Diesel Fuel Specifications Korea. Diesel Fuel EN 590. Available online: https://en590.wordpress.com/ (Accessed on 21 November 2016).

Double–walled carbon nanotubes. Available online at https://www.google.com/search?q=single+walled+carbon+nanotubes+image. Accessed on 28th April 2018).

Dunleavy, J.K. (2006) Sulphur as a Catalyst Poison. Platin. Met. Rev., 50, 110.

Duissenov, D (2013) Production and Processing of Sour Crude and Natural Gas—Challenges due to Increasing Stringent Regulations; Norwegian University of Science and Technology. Faculty of Engineering Science and Technology Department of Petroleum Engineering and Applied Geophysics: Trondheim, Norway, p. 1.

Eber, J., Wasserstein, P., & Jess, A. (2004) Deep desulfurization of oil refinery streams by extraction with ionic liquids. Green chemistry, 6(7), 316-322.

Fang, W.L. (2004) Inventory of U.S Greenhouse Gas Emission and Sinks 1990–2003; Clear Air Market Division, United States Environmental Protection Agency: Washington, DC, USA.

Folsom, B.R.; Schieche, D.R.; DiGrazia, P.M.; Werner, J.; Palmer, S. (1999) Microbial desulfurization of alkylated dibenzothiophenes from a hydrodesulfurized middle distillate by Rhodococcus erythropolis I-19. Appl. Environ. Microbiol. 65, 4967–4972.

Furuya, T.; Kirimura, K.; Kino, K.; Usami, S. (2001) Thermophilic biodesulfurization of dibenzothiophene and its derivatives by Mycobacterium phlei WU-F1. FEMS Microbiol. Lett., 204, 129–133.

Fuel Quality in Australia, (2001) Available online: http://www.environment.gov.au/topics/ environment- protection/fuel-quality/standards/diesel (Accessed on 21 November 2016).

Gauderman, W.J.; Gilliland, G.F.; Vora, H.; Avol, E.; Stram, D.; McConnell, R.; Thomas, D.; Lloyd, A.C. and Cackette, T.A. (2001) Diesel Engines: Environmental Impact and Control. J. Air Waste Manag. Assoc., 51, 809–847.

Gary, J.H. and Handwerk, G.E. (1984) Petroleum Refining Technology and Economics, 2nd ed.; Marcel Dekker, Inc.: New York, NY, USA.

Gawande, P.R.and Dr. Jayant, P.K. (2014) A Review on Desulphurization of Liquid Fuel by Adsorption. Int. J. Sci. Res. 3, 2255–2259.

Gatan, R., Barger, P., & Gembicki, V. (2004) 'Oxidative desulfurization: a new technology for ULSD', ACS Division of Fuel Chemistry. 49 (2), 577-579.

Gatan, R., Barger, P., Gembicki, V., Cavanna, A., Molinari, D., & Enitecnologie, S. (2004) Oxidative desulfurization: A new technology for ULSD. Fuel Chem. 49, 577–579.

Gaurav, B., Daware R., Akshay, B., Kulkarni, A., Arti, A., & Rajput, T. (2015) "Desulphurization of diesel by using low cost adsorbent" International Journal of Innovative and Emerging Research in Engineering. 6 (2),69-73.

Gawan, P., and Kaware J. (2014) Desulphurization techniques for liquid fuel A Review. International of Engineering Technology Management and applied Science.2(7), 122-126.

Gawan, P., & Kaware J. (2016) Review of Research for Desulphurization of diesel by Adsorption. Journal of Engineering and Technology International Research. 3(12), 337-340.

Gawan, P., & Kaware J. (2016) Review on low cost Adsorbents for Desulphurization of Liquid Fuels. International Research Journal of Engineering and Technology. 2(1),108-112.

Gavrilescu, M. and Chisti, Y. (2005) Biotechnology a sustainable alternative to chemical industry. Biotechnol. Adv., 23, 471–499.

Geer, L.A.and Weedon, J.M.L. (2012) Ambient air pollution and term birth weight in Texas from 1998 to 2004. J. Air Waste Manag. Assoc., 62, 1285–1295.

Gislason, J. (2002) Phillips Sulfur removal process nears commercialization. Oil Gas J., 99: 74-76.

Grossman, M.J., Siskin, M., Ferrughelli, D.T., Lee, M.K. and Senius, J.D. (1999) Method for the Removal of Organic Sulfur from Carbonaceous Materials. U.S. Patent 5910440.

Guobin, S., Huaiying, Z., Jianmin, X., Guo, C., Wangliang, L. and Huizhou, L. (2006) Biodesulfurization of hydrodesulfurized diesel oil with Pseudomonas delafieldii R-8 from high density culture. Biochem. Eng. J., 27, 305–309.

Guobin, S. Jianmin, X. Huaiying, Z. and Huizhou, L. (2005) Deep desulfurization of hydrodesulfurized diesel oil by Pseudomonas delafieldii R-8. J. Chem. Technol. Biotechnol. 80, 420–424.

Guobin, S. Huaiying, Z. Weiquan, C. Jianmin, X. and Huizhou, L. (2005) Improvement of Biodesulfurization Rate by Assembling Nanosorbents on the Surfaces of Microbial Cells. Biophys. J., 89, L58–L60.

Grossman, M.J., Lee, M.K., Prince, R.C., Minak-Bernero, V., George, G.N. and Pickering, I.J. (2001) Deep desulfurization of extensively hydrodesulfurized middle distillate oil by Rhodococcus sp. strain ECRD-1. Appl. Environ. Microbiol., 67, 1949–1952.

Gunam, I.B.W., Yaku, Y., Hirano, M., Yamamura, K., Tomita, F., Sone, T., and Asano, K. (2006) Biodesulfurization of Alkylated Forms of Dibenzothiophene and Benzothiophene by Sphingomonas subarctica T7b. J. Biosci. Bioeng. 101, 322–327.

Gün, G. Yürüm, Y. and Doğanay, G.D. (2015) Revisiting the biodesulfurization capability of hyperthermophilic archaeon Sulfolobus solfataricus P2 revealed DBT consumption by the organism in an oil/water two-phase liquid system at high temperatures. Turk. J. Chem., 39, 255–266.

Gupta, N.; Roychoudhury, P.K.; Deb, J.K. (2005) Biotechnology of desulfurization of diesel: Prospects and challenges. Appl. Microbiol. Biotechnol., 66, 356–366.

Han, R., Yu W., Xin Z., Yuanfecy W., Fulng X., Cheng J., & Tang M. (2009) "Adsorption of Methyl Blue by Phoex Tree Leaf Power in a Fixed Bed Column: Experiments and Prediction of Breakthrough Curves. Desalination. 2(45)284-297.

Han, R.P., Wang, Y.F., Yu, W.H., Zou, W.H., Shiand. J. and Liu, H.M. (2007) Adsorption of methylene blue from by phoenix tree leaf power in a fixed-bed column. Hazard. Mater, 141, 713–718.

Hensen, E.J.M. de Beer, V.H.J. Van Veen, J.A.R. and van Santen, R.A. (2003) On the sulfur tolerance of supported Ni (Co)Mo sulfide hydrotreating catalysts. J. Catal., 215, 353–357.

Hosseini, H.; Hamidi, A. (2014) Sulfur Removal of Crude Oil by Ultrasound Assisted Oxidative Method. Proceedings of the International Conference on Biological, Civil and Environmental Engineering (BCEE-2014), Dubai, United Arab Emirates, 17–18 March.

Hirai, T., Ogawa, K. and Komasawa, I. (1996) Desulfurization process for dibenzothiophenes from light oil by photochemical reaction and liquid-liquid extraction. Ind. Eng. Chem. Res., 35, 586–589.

Hou, Y.; Kong, Y.; Yang, J.; Zhang, J.; Shi, D.; Xin, W. (2005) Biodesulfurization of dibenzothiophene by immobilized cells of Pseudomonas stutzeri UP-1. Fuel, 84, 1975–1979.

Huang, X.-F.; Guan, W.; Liu, J.; Lu, L.-J.; Xu, J.-C.; Zhou, Q. (2010) Characterization and phylogenetic analysis of biodemulsifier-producing bacteria. Bioresour. Technol., 101, 317–323.

"Incorporating Biotechnology into the Classroom What is Biotechnology?" from the Curricula of the "Incorporating Biotechnology into the High School Classroom through Arizona State University's BioREACH Program". Available online: http://www.public.asu.edu/~langland/biotech-intro.html (Accessed on 5 November 2016).

Industry News (2016) Available online: http://www.iol.co.za/motoring/industry-news/sasol-launches-10ppm-clean-diesel-1.1611081#.UpNbXsQW1KJ (accessed on 2 November 2016).

Isam, A., Zubaidy, H., Fatma, B., Noora, Naif D., Balsam, S., Sana, A., Aysha A., & Lamis, A. (2013) "Adsorption Process of Sulphur Removal from Diesel Oil Using Sorbent Materials" Journal of Clean Energy Technologies, 1(1), 66-68.

Isam A., Noora N., Yehya S., Zarook S., and Ziad S. (2015) "Adsorptive Desulfurization of Commercial Diesel oil Using Granular Activated Charcoal" Int'l Journal of Advances in Chemical Engineering., & Biological Sciences (IJACEBS).2(1),15-18

Ishii, Y., Kozaki, S., Furuya, T., Kino, K. and Kirimura, K. (2005) Thermophilic biodesulfurization of various heterocyclic sulphur compounds and crude straight-run light gas oil fraction by a newly isolated strain Mycobacterium phlei WU-0103. Curr. Microbiol., 50, 63–70.

Jones, J.A. (2011) Deep Desulfurization of Diesel Fuel Using a Single Phase Photochemical Microreactor. A Thesis Submitted to Oregon State University, in partial Fulfillment of the Requirements for the Degree of Master of Science.

Kabe, T., Ishihara, A. and Tajima, H. (1992) Hydrodesulfurization of sulfur-containing polyaromatic compounds in light oil. Ind. Eng. Chem. Res., 31, 1577–1580.

Kewale, A. and Babayemi, K. (2015) Design of Plot Packed Column for the Dehydration of water from ethanol-water Mixtures. Advance in Chemical Engineering and Science. 5(2) 152-157.

Kumar, A., and Banerjee, T. (2009) 'Thiophene separation with ionic liquids for desulphurization: A quantum chemical approach', Fluid Phase Equilibria. 5(278), 01-08.

Lurmann, F.; Margolis, H.G.; Rappaport, E.B. (2000) Association between Air Pollution and Lung Function Growth in Southern California Children: Results from a second cohort. Am. J. Respir. Crit. Care Med., 166, 76–84.

Policy Briefs on Global Atmospheric Pollution Forum. Available online: https://www.sei-international.org/gapforum/policy/effectshumanhealth.php (Accessed on 4 October 2016).

Jacobson, M.Z. (2002) Control of fossil fuel particulate black carbon and organic matter, possibly the most effective method of slowing global warming. J. Geophys. Res. 107, doi:10.1029/2001JD001376.

Javadli, R. and de Klerk, A. (2012) Desulfurization of heavy oil. Appl. Petrochem. Res., 1-4, 3–19.

Kertesz, M.A. and Wirtek, C. (2001) Desulfurization and desulfonation: Application of sulphur-controlled gene expression in bacteria. Appl. Microbiol. Biotechnol., 57, 460–466.

Konishi, J. Ishi, Y. Okumura, K. and Suzuki, M. (1999) High Temperature Desulfurization by Microorganisms. U.S. Patent 5,925,560, 20 July.

Kim, T.S., Kim, H.Y. and Kim, B.H. (1990) Petroleum Desulfurization by DesulfovibrioDesulfuricans M6 using electrochemically supplied reducing equivalent. Biotechnol. Lett., 12, 757–760.

Kirkwood, K.M.; Ebert, S.; Foght, J.M.; Fedorak, P.M.; Gray, M.R. (2005) Bacterial biodegradation of aliphatic sulfides under aerobic carbon- or sulfur-limited growth conditions. J. Appl. Microbiol., 99, 1444–1454.

Kirkwood, K.M. Andersson, J.T. Fedorak, P.M. Foght, J.M. and Gray, M.R. (2007) Sulfur from benzothiophene and alkylbenzothiophenes supports growth of Rhodococcus sp. strain JVH1. Biodegradation, 18, 541–549.

Kirkwood, K.M.; Foght, J.M.; Gray, M.R. (2007) Selectivity among organic sulphur compounds in one-and two-liquid-phase cultures of Rhodococcus sp. strain JVH1. Biodegradation, 18, 473–480.

Kodjak, D. (2015) Policies to Reduce Fuel Consumption, Air Pollution, and Carbon Emissions from Vehicles in G20 Nations; The International Council on Clean Transportation: Washington, DC, USA, pp. 1–22.

Kobayashi, M.; Onaka, T.; Ishii, Y.; Konishi, J.; Takaki, M.; Okada, H.; Ohta, Y.; Koizumi, K.; Suzuki, M. (2000) Desulfurization of alkylated forms of both dibenzothiophene and benzothiophene by a single bacterial strain. FEMS Microbiol. Lett., 187, 123–126.

Kan, H., Wong, C.M., Vichit-Vadakan, N. and Qian, Z. (2010) The PAPA project team's short term association between sulphur dioxide and daily mortality: The public health and air pollution in Asia (PAPA) study. Environ. Res. 110, 258–264.

Kirimura, K. Furuya, T. Nishii, Y. Ishii, Y. Kino, K. and Usami, S. (2001) Biodesulfurization of dibenzothiophene and its derivatives through the selective cleavage of carbon-sulphur bonds by a moderately thermophilic bacterium Bacillus subtilis WU-S2B. J. Biosci. Bioeng., 91, 262–266.

Kim, J.H., Ma, X., Zhou, A., Song, C. (2006) Ultra-deep desulfurization and denitrogenation of diesel fuel by selective adsorption over three different adsorbents: A study on adsorptive selectivity and mechanism. Catal. Today 111, 74–83.

Kilbane, J.J. (2006) Microbial biocatalyst development to upgrade fossil fuels. Curr. Opin. Biotechnol., 17, 305–314.

Koch, T.A., Krause, K.R., Manzer, L.E., Mehdizadeh, M., Odom, J.M. and Sengupta, S.K. (1996) Environmental challenges facing the chemical-industry. New J. Chem. 20, 163–173.

Kocal, J.A. and Branvold, T.A. (2002) Removal of Sulfur-Containing Compounds from Liquid Hydrocarbon Streams. U.S. Patent 6368495.

Kaufman, E.N., Harkins, J.B. and Borole, A.P. (1998) Comparison of batchstirred and electrospray reactors for biodesulfurization of dibenzothiophene in crude oil and hydrocarbon feedstocks. Appl. Biochem. Biotechnol. 73, 127–144.

Konishi, J., Ishii, Y. and Onaka, T. (1997) Thermophilic carbon-sulfur-bond-targeted biodesulfurization. Appl. Environ. Microbiol., 63, 3164–3169.

Kowalski, H. (2002) "U.S. – German Research Consortium Sequences Genome of Versatile Soil Microbe". J. Craig Venter Archive. December 2002.http://www.tigr.org/news/pr_12_02_02.shtml . Accessed November, 2017.

Lee, M.K., Senius, J.D. and Grossman, M.J. (1995) Sulfur-specific microbial desulfurization of sterically hindered analogs of dibenzothiophene. Appl. Environ. Microbiol. 61, 4362–4366.

Linguist, L.K. and Pacheco, M.A. (1999) Enzyme-based diesel desulfurization process offers energy, CO2 advantages. Oil Gas J., 97, 45–48.

Liu, B. Peng, Y. and Chen, Q. (2016) Adsorption of N/S-Heteroaromatic Compounds from Fuels by Functionalized MIL-101(Cr) Metal-Organic Frameworks: The Impact of Surface Functional Groups. Energy Fuels, 30, 5593−5600.

Laura C. L. and Duffy, M.L. (2003) Determination of Total and Speciated Sulfur Content in Petrochemical Samples Using a Pulsed Flame Photometric Detector Journal of Chromatographic Science, 41, 528-534.

Lisabeth, L.D. Escobar, J.D. Dvonch, J.T. Sanchez, B.N., Majersik, J.J., Brown, D.L., Smith, M.A., Morgenstern, L.B. (2008) Ambient air pollution and risk of ischemic stroke and TIA. Ann. Neurol. 64, 53–59.

Li, F.L., Xu, P., Ma, C.Q., Luo, L.L. and Wang, X.S. (2003) Deep desulfurization of hydrodesulfurization-treated diesel oil by a facultative thermophilic bacterium Mycobacterium sp. X7B. FEMS Microbiol. Lett. 223, 301–307.

Li, W., Zhang, Y., Wang, M.D. and Shi, Y. (2005) Biodesulfurization of dibenzothiophene and other organic sulphur compounds by a newly isolated Microbacterium strain ZD-M2. FEMS Microbiol. Lett., 247, 45–50.

Li, F., Zhang, Z., Feng, J., Cai, X. and Ping, X. (2007) Biodesulfurization of DBT in tetradecane and crude oil by a facultative thermophilic bacterium Mycobacterium goodii X7B. J. Biotechnol., 127, 222–228.

Ma, X., Sakanishi, K., Mochida, I. (1994) Three-stage deep hydrodesulfurization and decolorization of diesel fuel with CoMo and NiMo catalysts at relatively low pressure. Fuel, 73, 1667–1671.

Ma, Z., Wei, L., Zhou, W., Jia, L., Hou, B., Li, D; Zhao, Y. (2015) Overview of catalyst application in petroleum refinery for biomass catalytic pyrolysis and bio-oil upgrading. RSC Adv., 5, 88287-88297.

Wu, M. and Li, X. (2015). Klebsiella pneumoniae and Pseudomonas aeruginosa. Molecular Medical Microbiology (Second Edition).Volume 3. Chapter 87 – Pages 1547–1564.

Marcus, A. (2003) “Versatile soil-dwelling microbe is mapped”. Genome News Network. Available online at http://www.genomenewsnetwork.org/articles/01_03/soil_microbe.shtml. Accessed on January 2018.

Madeira, L., Santana, V., and Pinto, E. (2008) Dibenzothiophene oxidation by horseradish peroxidase in organic media: Effect of the DBT:H_2O_2 molar ratio and H_2O_2 addition mode. Chemosphere, 71, 189–194.

Maghsoudi, S., Vossoughi, M., Kheirolomoom, A., Tanaka, E., and Katoh, S. (2001) Biodesulfurization of hydrocarbons and diesel fuels by Rhodococcus sp. strain P32C1. Biochem. Eng. J. 8, 151–156.

Matsui, T. Onaka, T. Maruhashi, K. and Kurane, R. (2001) Benzothiophene desulfurization by Gordonia rubropertinctus strain T08. Appl. Microbiol. Biotechnol., 57, 212–215.

Mohebali, G. and Ball, A.S. (2008) Biocatalytic desulfurization (BDS) of petrodiesel fuels. Microbiology, 154, 2169–2183.

Monticello, D.J. (2000) Biodesulfurization and the upgrading of petroleum distillates. Curr. Opin. Biotechnol. 11, 540–546.

Mohebali, G., Ball, A.S., Rasekh, B. and Kaytash, A. (2007) Biodesulphurization potential of a newly isolated bacterium, Gordonia alkanivorans RIPI90A. Enzym. Microb. Technol., 40, 578–584.

Ma, X., Velu, S., Kim, J.H. and Song, C. (2005) Deep desulfurization of gasoline by selective adsorption over solid adsorbents and impact of analytical methods on ppm-level sulfur quantification for fuel cell applications. Appl. Catal. B Environ. 56, 137–147.

Marcelis, C. (2002) Anaerobic Biodesulfurization of Thiophenes. Ph.D. Thesis (Unpublished), Wageningen University, Wageningen, The Netherlands,

McClellan, R.O., Hesterberg, T.W. and Wall, J.C. (2012) Evaluation of carcinogenic hazard of diesel engine exhaust needs to consider revolutionary changes in diesel technology. Regul. Toxicol. Pharmacol., 63, 225–258.

Medici, L. and Prins, R. (1996) The Influence of Chelating Ligands on the Sulfidation of Ni and Mo in NiMo/SiO2 Hydrotreating Catalysts. J. Catal. 163, 38–49.

Monticello, D.J. (1998) Riding the fossil fuel biodesulfurization wave. ChemTech, 28, 38–45.

Omidvarborna, H., Kumar, A. and Kim, D.S. (2014) Characterization of particulate matter emitted from transit buses fueled with B20 in idle modes. J. Environ. Chem. Eng. 2, 2335–2342.

Montiel, C.; Quintero, R.; Aburto, J. (2009) Petroleum biotechnology: Technology trends from the future. Afr. J. Biotechnol., 8, 2653–2666.

Mohamed, M.E., Al-Yacoub, Z.H. and Vedakumar, V.J. (2015) Biocatalytic desulfurization of thiophenic compounds and crude oil by newly isolated bacteria. Front. Microbiol. 6, doi:10.3389/fmicb.2015.00112.

Muic, M. and Sertiæ-Bionda, K. (2010) A Design of ExperimentsInvestigation of Adsorptive Desulfurization of Diesel Fuel Gomzi Chem. Biochem. Eng. Q. 24 (3) 253–264

Moosavi, E.S. Seyed, A. Dastgheib, A.S. and Karimzadeh, R. (2012) Article Adsorption of Thiophenic Compounds from Model Diesel Fuel Using Copper and Nickel Impregnated Activated Carbons. Energies, 5, 4233–4250.

Muzic, M., Katica S. and Tamara A. (2009)" Kinetic Equilibrium and statistical analysis of diesel fuel adsorptive desulphurization" 4(9),373-394.

Mohebali, G., and Ball, A. (2008) 'Biocatalytic desulfurization (BDS) of petro diesel fuels". Microbiology, 54(1), 2169–2183.

Muzic, M., Sertic B., Adzamic T., Gomzi, Z. and Podolski, S. (2009) Optimization of diesel fuel desulfurization by adsorption on activated carbon, Chem. Eng. Trans., 17(5), 1549-1554.

Multiwalled carbon nanotubes. Available online at https://www.dreamstime.com/royalty-free-stock-image-multiwalled-carbon-nanotube-image25177276. (Accessed on 28th April 2018).

Neran, K., Ibrahim, A., Samar, K., and Aljanabi, S. (2015) "Desulfurization and Kinetic Study of Diesel Fuel by Batch Adsorption on Activated Carbon", Eng. & Tech. Journal, 7(33), 1901-1916.

Nehlsen, J.P. (2005) Developing Clean Fuels: Novel Techniques for Desulfurization. Ph.D. Thesis unpublished, Princeton University, Princeton, NJ, USA.

Oleimani, M., Bassi, A., & Margaritas, A. (2007) Biodesulphurization of refractory organic sulphur compounds in fossil fuels. Biotechnology Advances, 25(7), 570–596.

Oda, S. and Ohta, H. (2002) Biodesulfurization of dibenzothiophene with Rhodococcus erythropolis ATCC 53968 and its mutant in an interface bioreactor. J. Biosci. Bioeng., 94, 474–477.

Ohshiro, T., Hirata, T. and Izumi, Y. (1996) Desulfurization of dibenzothiophene derivatives by whole cells of Rhodococcus erythropolis H-2. FEMS Microbiol. Lett., 142, 65–70.

Okada, H., Nomura, N., Nakahara, T., and Maruhaski, K. (2002) Analysis of dibenzothiophene metabolic pathway in Mycobacterium sp. G3. J. Biosci. Bioeng. 93, 491–497.

Ohta, Y., Shimizu, T., Honma, T. and Yamada, M. (1999) Effect of chelating agents on HDS and aromatic hydrogenation over CoMo-and NiW/Al2O3. Stud. Surf. Sci. Catal., 127, 161–168.

Overview of Air Pollution from Transportation (2016). Available online: https://www.epa.gov/air-pollution-transportation/learn-about-air-pollution-transportation (Accessed on 2 November 2016).

Paixão, S.M., Silva, T.P., Arez, B.F. and Alves, K. (2016) Advances in the Reduction of the Costs Inherent to Fossil Fuels Biodesulfurization towards its Potential Industrial Application. In Applying Nanotechnology to the Desulfurization Process in Petroleum Engineering; IGI Global: Hershey, PA, USA, Chapter 13, pp. 390–425.

Pacheco, M.A.; Lange, E.A.; Pienkos, P.T.; Yu, L.Q.; Rouse, M.P.; Lin, Q.; Linguist, L.K. (1999) Recent advances in biodesulfurization of diesel fuel. In Proceedings of the 1999 National Petrochemical and Refiners Association, Annual Meeting, NPRA AM-99-27, San Antonio, TX, USA, 21–23 March; pp. 1–26.

Paniv, P.M. Pysh'ev, S.V. Gaivanovich, V.I. and Lazorko, O.I. (2006) Current Problems, Nontraditional Technologies, Noncatalytic oxidation desulfurization of the kerosene cut. Chem. Technol. Fuels Oils, 42, 159–166.

Patil, S., Kamble, S., Bhattacharyulu, Y.C. (2012) "Unsteady state adsorption steady state adsorption column studies," International Journal of Advanced Engineering Research and Studies, 1, 179-184.

Parkinson, G. (2000) Refiners crack down on sulphur. Chem. Eng., 107, 45–48.

Rashtchi, M., Mohebali, G.H., Akbarnejad, M.M., Towfighi, J., Rasekh, B., Keytash, A. (2006) Analysis of Biodesulphurization of model oil system by the bacterium strain RIPI-22. Biochem. Eng. J., 29, 169–173.

Rashidi, L. Mohebali, G. Towfighi darian, J. and Rasekh, B. (2006) Biodesulfurization of dibenzothiophene and its alkylated derivatives through the sulphur-specific pathway by the bacterium RIPI-S81. Afr. J. Biotechnol., 5, 351–356.

Rosenberg, M., Gutnick, D. and Rosenberg, E. (1980) Adherence of bacteria to hydrocarbons: A simple method for measuring cell-surface hydrophobicity. FEMS Microbiol. Lett., 9, 29–33.

Rhee, S.K., Chang, J.H., Chang, Y.K., Chang, H.N. (1998) Desulfurization of dibenzothiophene and diesel oils by a newly isolated Gordona strain, CYKS1. Appl. Environ. Microbiol., 64, 2327–2331.

Rob van Veen, J.A.R., Gerkema, E., van der Kraan, A.M., Hendriks, P.A.J.M. and Beens, H. (1992) A 57Co Mossbauer emission spectrometric study of some supported CoMo hydrodesulfurization catalysts. J. Catal., 133, 112–123.

Ryzhikov, A., Bezverkhyy, I. and Bellat, J.P. (2008) Reactive adsorption of thiophene on Ni/ZnO: Role of hydrogen pretreatment and nature of the rate determining step. Appl. Catal. B, 84, 766−772.

Ralph T. (2003) Adsorbents: Fundamentals & Applications. United State of America. John Wiley and Son Inc.8, 17-21,221-230.

Rang, H., Kann, J., and Oja, V. (2006) ‘Advances in desulfurization research of liquid fuel’, Oil Shale, 23 (2), 164-176.

Sam, A., Noora, N., Yehya S., Zarook S., and Ziad S., (2015) “Adsorptive desulfurization of Commercial diesel oil using granular activated charcoal” Int’l Journal of Advances in Chemical Engineering., & Biological Sciences (IJACEBS).2 (1), 15-18.

Shan, C. (2016) Removal of Toluene at Low Concentration with Activated Carbon Filter. Thesis unpublished submitted to the department of Environmental Engineering, Helsinki Metropolia University of Applied Sciences, pp 57.

Seader. J., and Heley, E. (1998) Separation process Principles. New York. John Wiley & Sons.inc. 90.681-682,781-810.

Seforo, R. (2016) Investigation of the desulphurization of Petroleum Distillate using Novel Ionic liquids. MSc. Wits University.

Senyangane, F. (2016) Simulation of the adsorption Desulphurization of Diesel fuel. MSc Thesis unpublished. Wits University.

Sharaf, J. (2013) Exhaust Emissions and Its Control Technology for an Internal Combustion Engine. Int. J. Eng. Res. Appl., 3, 947–960.

Sayyadnejad, M.A. Ghaffarian, H.R. Saeidi, M. (2008) Removal of hydrogen sulfide by zinc oxide nanoparticles in drilling fluid. Int. J. Environ. Sci. Technol., 5, 565–569.

Sekhavatjou, M.S., Moradi, R., Alhashemi, A.H. and Hejabi, T. (2014) A New Method for Sulphur Components Removal from Sour gas through Application of Zinc and Iron Oxides Nanoparticles. Int. J. Environ. Res., 8, 273–278.

Shafi, R. and Hutchings, G.J. (2000) Hydrodesulfurization of hindered dibenzothiophenes: An overview. Catal. Today 59, 423–442.

Shen, Y., Liu, X., Sun, T. and Jia, J. (2012) Recent advances of sodium boronhydride reduction in coal water slurry desulfurization: Integration of chemical and electrochemical reduction. RSC Adv., 2, 8867–8882.

Shell Global (2011) Available online: http://www.shell.com/.../sg-en/shell_for_motorists/fuels/diesel/ulsd_faqs_0914.html?LN=/leftnavs/zzz_lhn4_3_4.html. (Accessed on 10 October 2016).

Shiraishi, Y.; Hirai, T.; Komasawa, I. (1998) Deep Desulfurization Process for Light Oils by Photochemical Reaction in an Organic Two-Phase Liquid—Liquid Extraction System. Ind. Eng. Chem. Res., 37, 203–211.

Shong, R.G. (2015) Bioprocessing of crude oils. Texaco Exploration & Producing Technology Department Houston, Texas 77042 (Available online: https://web.anl.gov/PCS/acsfuel/ preprint%20 archive/Files/ Volumes/ Vol 44-1.pdf (Accessed on 23rd of November 2017).

Singh, A., Singh, B. and Ward, O. (2012) Potential applications of bioprocess technology in petroleum industry. Biodegradation, 23, 865–880.

Singh, B.K. (2010) Exploring microbial diversity for biotechnology: The way forward. Trends Biotechnol., 28, 111–116.

Soleimani, M.; Bassi, A.; Margaritis, A. (2007) Biodesulfurization of refractory organic sulphur compounds in fossil fuels. Biotechnol. Adv., 25, 570–596.

Song, C. (2003) An overview of new approaches to deep desulfurization for ultra-clean gasoline, diesel fuel and jet fuel. Catal. Today, 86, 211–263.

Srivastava, V.C. (2012) An evaluation of desulfurization technologies for sulphur removal from liquid fuels. RSC Adv., 2, 759–783.

Startsev, A.N. (2017) The Reaction Mechanisms of H_2S Decomposition into Hydrogen and Sulfur: Application of Classical and Biological Thermodynamics Journal of J Thermodynamics & Catalysis J Thermodyn Catal., 8, 2-8.

Srivastav, A. and Srivastava, V.C. (2009) Adsorptive desulfurization by activated alumina. J. Hazard. Mater. 170, 1133−1140.

Sundararaman, S. and Song, C. (2014). Catalytic Oxidative Desulfurization of Diesel Fuels Using Air in a Two-Step Approach. Ind. Eng. Chem. Res., 53, 1890–1899.

Tawfik, A., Saleh, G.I., and Danmaliki, T.D.S. (2015) Nanocomposites and Hybrid Materials for Adsorptive Desulfurization. Advances in Chemical and Materials Engineering (ACME); IGI Global: Hershey, PA, USA, pp. 129–153.

Tawara, K., Nishimura, T., Iwanami, H., Nishimoto, T. and Hasuike, T. (2001) New hydrodesulfurization catalyst for petroleum-fed fuel cell vehicles and cogenerations. Ind. Eng. Chem. Res., 40, 2367−2370.

Tawara, K. Nishimura, T. Iwanami, H. and Shi, S.G. (2000) Ultra-deep hydrodesulfurization of kerosene for fuel cell system. Part 2: Regeneration of sulfur-poisoned nickel catalyst in hydrogen and finding of autoregenerative nickel catalyst. J. Jpn. Petrol. Inst., 43, 114–120.

Tam, P.S. Kittrell, J.R. and Eldridge, J.W. (1990) Desulfurization of fuel oil by oxidation and extraction. 1. Enhancement of extraction oil yield. Ind. Eng. Chem. Res., 29, 321–324.

Tang, K., Song, L., Duan, L., Li, X., Gui, J. and Sun, Z. (2008) ″Deep desulfurization by selective adsorption on a heteroatoms zeolite prepared by secondary synthesis. Mater.145 (2007)331–335.

Thomas H.C. (1944) Heterogeneous ion exchange in a flowing system, J. Am. Chem. Soc., 66(1944) 1664–1466

Tanaka, H. Boulinguiez, M. and Vrinat, M. (1996) Hydrodesulfurization of thiophene, dibenzothiophene and gasoil on various Co-Mo/TiO2-Al2O3 catalysis. Catal. Today 29, 209–213.

The Info List—Ultra-Low Sulfur Diesel. Available online: http://www.theinfolist.com/php/SummaryGet.php?FindGo=Ultra-Low%20Sulfur%20Diesel (Accessed on 21 November 2016).

USEPA (2014). Available online: http://www. epa. Gov/sbrefaldocuments/pnl13f. Pdf. (Accessed on 25 October 2016).

UNEPA (2015). Report of the Partnership for Clean Fuels and Vehicles (PCFV), pp. 1–14. Available online:http://www.staging.unep.org/transport/pcfv/PDF/SulphurReport-Brochure.pdf (Accessed on 23rd of November 2017).

United States Environmental Protection Agency (UEPA) 2016. Available online: https://www.epa.gov/gasoline-standards/gasoline-sulfur (Accessed on 23rd November 2017).

United Nation Environment Programme (2012) Available online: http://www.unep.org/transport/pcfv/meetings/mauritius50ppm.asp (Accessed on 2nd November 2016).

Velu, S., Watanabe, S., Ma, X. and Song, C. (2003) Regenerable adsorbents for the adsorptive desulphurization of transportation fuels for fuel cell applications. Chem. Soc. Div. Fuel Chem. 48, 482–526.

Voordouw, G. (2011) Production-related petroleum microbiology: Progress and prospects. Curr. Opin. Biotechnol., 22, 401–405.

Ward, O.P. Singh, A. Van Hamme, J.D. and Voordouw, G. (2009) Petroleum microbiology. In Encyclopedia of Microbiology, 3rd ed.; Schaechter, M., Ed.; Elsevier: Amsterdam, The Netherlands; pp. 443–456.

Wan Abu Bakar, W. Rusmidah Ali, R. Abdul Kadir, A. and Wan Mokhtar, W. (2012) Effect of transition metal oxides catalysts on oxidative desulfurization of model diesel. Fuel Process. Technol., 101, 78–84.

Wang, W., Wang, S., Liu, H., Wang, Z. (2007) Desulfurization of gasoline by a new method of electrochemical catalytic oxidation. Fuel, 86, 2747–2753.

Weerasekara, N.S.; García Frutos, F.J.; Cara, J.; Lockwood, F.C. (2008) Mathematical modelling of demineralisation of high sulphur coal by bioleaching. Miner. Eng., 21, 234–240.

Wu, W., Jin, Y., Bai, F. and Jin., S. (2015) Pseudomonas aeruginosa. Molecular Medical Microbiology (Second Edition). Chapter 41. 2, 753–767.

Whitehurst, D.D., Isoda, I. and Mochida, I. (1998) Present state of art and future challenges in hydrodesulfurization of polyaromatic sulfur compounds. Adv. Catal., 42, 345–357.

Woodruff, T.J. Darrow, L.A. and Parker, J.D. (2008) Air pollution and postneonatal infant mortality in the United States, 1999–2002. Environ. Health Perspect. 116, 110–115.

Wijffels, R.H., Buitelaar, R.M., Bucke, C., and Tramper, J. (1996) In Progress in Biotechnology. Immobilized Cells: Basics and Applications; Eds.; Elsevier: Amsterdam, The Netherlands, 11, 777–784.

Yang, R.T., Hernandez-Maldonado, A.J. and Yang, F.H. (2003) Desulfurization of transportation fuels with Zeolites under ambient conditions. Science, 301, 79−81.

Yamada, K.O., Morimoto, M., Tani, Y. (2001) Degradation of dibenzothiophene by sulfate-reducing bacteria cultured in the presence of onlynitrogen gas. J. Biosci. Bioeng., 91, 91–93.

Yu, B., Ma, C., Zhou, W., Zhu, S., Wang, Y., Qu, J., Li, F. and Xu, P. (2006) Simultaneous Biodetoxification of S, N, and O Pollutants by Engineering of a Carbazole-Degrading Gene Cassette in a Recombinant Biocatalyst. Appl. Environ. Microbiol., 72, 7373–7376.

Yu, B. Xu, P. Shi, Q. and Ma, C. (2006) Deep desulfurization of diesel oil and crude oils by a newly isolated Rhodococcus erythropolis strain. Appl. Environ. Microbiol., 72, 54–58.

Pokethitiyooka, P., Tangaromsuk, J., Kruatrachue, M., Kalambaheti, C. and Borole, A.P. (2008) Biological removal of organic sulphur by bacterial strains isolated in Thailand. Sci. Asia, 34, 361–366.

Yu, H. and Chien, L. (2016) Short-term population-based non-linear concentration-response associations between fine particulate matter and respiratory diseases in Taipei (Taiwan): A spatiotemporal analysis. J. Expo. Sci. Environ. Epidemiol., 26, 197–206.

Zeelani, G.G.; and Dr. Sundar Lal Pal, S.L. (2016) A Review on Desulfurization Techniques of Liquid Fuels. Int. J. Sci. Res., 5, 2413–2419.

Zhang, G., Yu, F. and Wang, R. (2009) Research advances in oxidative desulfurization technologies for the production of low sulfur fuel oils. Pet. Coal, 51, 196–207.

Zhang, S., Chen, H. and Li, W. (2013) Kinetic analysis of biodesulfurization of model oil containing multiple alkyl dibenzothiophenes. Appl. Microbiol. Biotechnol., 97, 2193–2200.

Zhang, Y.; Wang, D.; Zhang, R.; Zhao, J.; Zheng, Y. (2012) ZSM-5-Ln(Pc)2 catalyzed oxygen oxidation of thiophene. Catal. Commun., 29, 21–23.

Zhao, H., Xia, S. and Ma, P. (2005) Use of ionic liquids as “green” solvents for extractions. Chem. Technol. Biotechnol., 80, 1089–1096.

Zhang, Y., Yang, Y., Han, H., Yang, M., Wang, L., Zhang, Y., Jiang, Z. and Li, C. (2012) Ultra-deep desulfurization via reactive adsorption on Ni/ZnO: The effect of ZnO particle size on the adsorption performance. Appl. Catal. B Environ., 119, 13–19.

Zietsman, J., Farzaneh, M., Storey, J.M.E., Villa, J., Ojah, M., Lee, D.W. and Bella, P. (2007) Emissions of Mexican-Domiciled Heavy-Duty Diesel Trucks Using Alternative Fuels; Texas Transportation Institute: College Station, TX, USA, pp. 4–70.

Chapter Three

3.0 Experimental procedures and analysis

The literature has been surveyed and reviwed in the previous study. Therefore, based on the identification of knowledge gap in this field, this study has been divided into several segements (see Fig. 3.1). The detailed description of adsorbents preparation, characterization techniques, bacteria growth, general experimental procedures and methods of analysis of results are presented and discussed in this chapter. Fig. 3.1 depicts an overview of the procedure employed in this study.

3.1 Investigation of adsorptive desulfurization (ADS)

The investigation of adsorptive desulfurizationreported in this dissertation involved preparations of some of the adsorbents while some of them were used as received in this study.

3.1.1 Preparations and characterization of adsorbents

As-received neem leaf powder was used for the acid-activation. Leaves of pomegranate were plucked from a nearby tree located at the East Campus of the University of the Witwatersrand, Johannesburg, South Africa. All other chemicals used were of analytical grade, commercially available and used without further purification. The leaves were washed thoroughly with distilled water, dried under sun for 24 hours and then ground. The adsorbent powder was then dried in the oven at 80 ^{o}C to remove moisture. About 20 g of PLP and NLP adsorbents were added to 10 mL of 0.5 M H_2SO_4. H_2SO_4 was used as the activating agent. The mixture was stirred at 70 ^{o}C for 2 h and dried at 110 ^{o}C in an oven. The samples were then carbonized in a furnace at 500 ^{o}C for 3 h. The adsorbents were washed severally with deionized water until a pH of 7 was reached so as to remove acid, and then dried at 70 ^{o}C for 24 h. The powdered adsorbents were sieved with a 150 µm sieve, kept in a dry air-tight container until for use in the adsorptive desulfurization experiment (Pandhare and Dawande, 2013; Nazal et al., 2016).

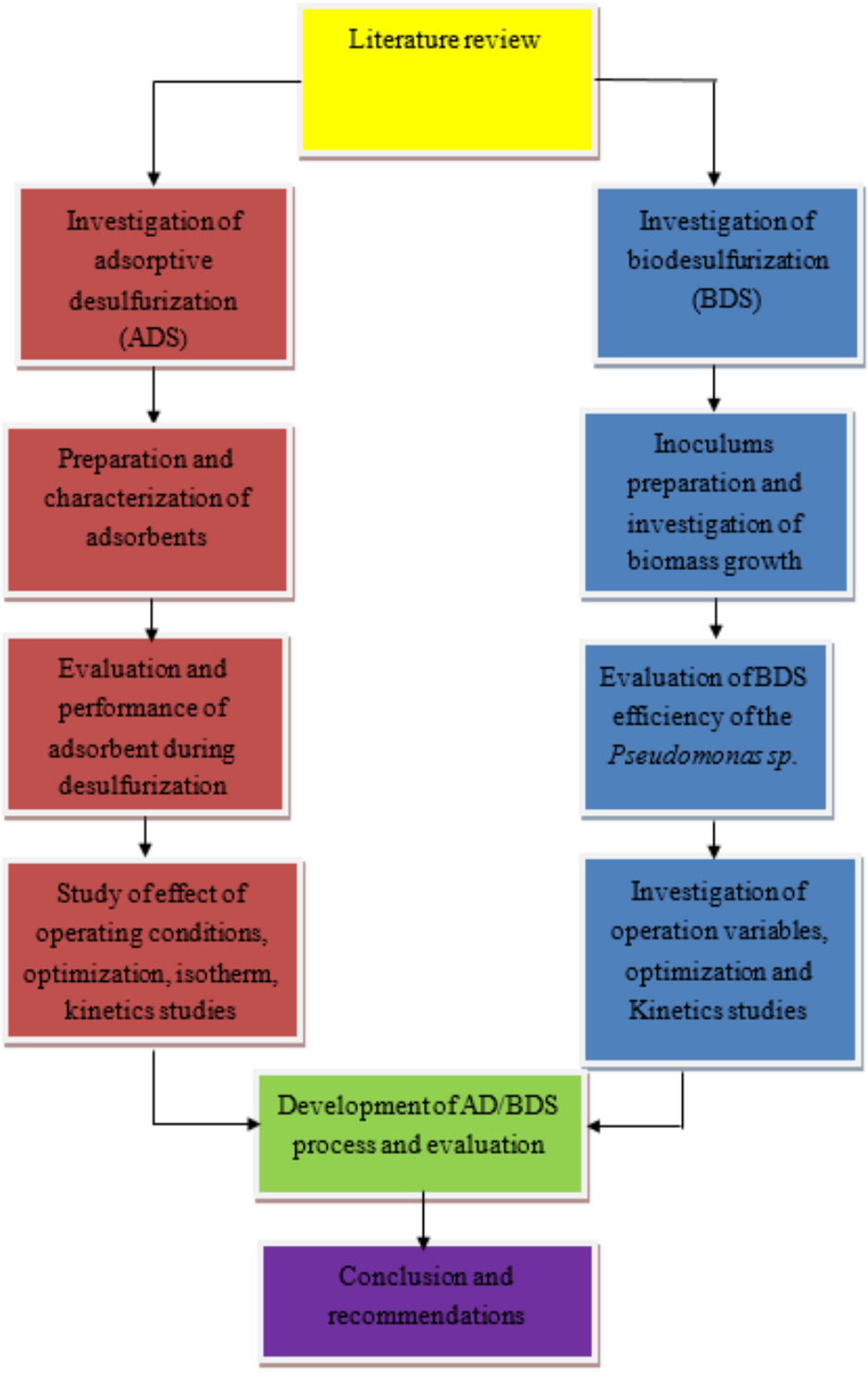


Figure 3.1. Overview of the procedures employed in this study

Activated carbon was purchased from Sigma Aldrich (Pty) Ltd., South Africa. Activated carbon was used as-received for batch experiments. In order to reduce disintegration of adsorbents in the continuous packed-bed column caused by high hydrostatic pressure, activated carbon was immobilized into pellets. Immobilization of adsorbent also offers better reusability, high adsorbent loading, and minimal clogging in continuous mode. Sodium algilate was purchased from Sigma Aldrich, (Pty) Ltd., South Africa. All other chemicals were of analytical grade, commercially available and used without further purification. About 5 g activated carbon was mixed with 250 mL of deionized water and allowed to hydrate for 10 min. 3 % (w/v) sodium algilate was added to the solution. 0.2 M Calcium chloride was prepared and the sodium algilate-adsorbent mixture was added dropwisely into the calcium chloride solution via a tube connected to a peristaltic pump so as to get even sized pellets. The droplets of sodium algilate-adsorbent forms pellets immediately they were in contact with calcium chloride solution, entrapping the adsorbent in it. The pellets were allowed to to solidify for about 30 min and washed with 0.9 % sodium chloride in order to remove excess calcium ion. The generated activated pellets had a diameter ranging from 3 mm to 4 mm (Simate and Ndlovu, 2016).

Multi-walled Carbon nanotubes (MWCNTs, purity: >98 % carbon basis). The dimension of the MWCNTs is (O.D × I.D × L): 10 nm (± 1 nm) ×4.5 nm (± 0.5 nm) × 3-6 µm were purchased from Sigma Aldrich Pty (Ltd), South Africa. All other chemicals used were of analytical grade, commercially available and used without further purification. As-received carbon nanotubes were functionalized in the laboration by using chemical method of functionalization. CNTs were first purified using solution of concentrated acetic acid and concentrated hydrochloric acid at ratio 3:1. The ratio of solid (CNTs) to liquid was 1:100. The solution was stirred on a magnetic stirrer at 400 rpm for 24 h at 80 ^{o}C. The CNTs was filtered and washed severally with deionized water until a neutral pH was achieved. The CNTs was dried at room temperature for 24 h, then in oven at 50 ^{o}C for 24 h. About 10 g of $KMnO_4$ was dissolved in 500 mL of 0.5 M H_2SO_4. The same operating measures were used as in purification of CNTs. The solution of CNTs was mixed on a magnetic stirrer using a reflux medium for 24 h. It was filtered and washed thoroughly with deionized water until pH of 7 was reached. The CNTs were dried for 24 h at room temperature and later oven dried at 50 ^{o}C to constant weight for 24 h (Olugbenga et al., 2018). It was then sieved through a 150 µm sieve.

The adsorbents used in this study were characterized using the following characterization techniques:

Fourier transform Infra-red analyzer, Bruker Tensor 27 at a spectra range of 500 cm^{-1} to 5000 cm^{-1} was used to determine the surface functionalities and the type of functional groups on the surfaces of the adsorbent samples.

N_2 physi-sorption experiments at 77 K were performed on the adsorbents for textural properties of the adsorbents. Micrometrics tristar 3000 static volumetric analysis unit was used to measure the surface area, cumulative pore volume and pore diameters of the adsorbents. This information was obtained from liquid nitrogen (@ -196 °C) equilibrium isotherms.

Scanning Electron Microscopy (SEM) equipped with energy dispersive x-ray (EDX) was used to check the morphology of the adsorbents. The samples were coated with 60 % palladium and 40 % gold (Pd/Au) prior to SEM analysis to prevent charge up. CARL ZEISS sigma field electronic scanning electron microscope (FESEM) was used to observe the surface morphology of the adsorbents CNTs, FCNTs, at different magnifications.

X-ray diffraction spectroscopy (XRD) was used to check the crystallinity of the adsorbents. The characterization was carried out on a Bruker D2 X-ray diffractometer was used to identify the phases of the adsorbent. The measurement range was 20 ^{o} to 100 ^{o} (2θ). The phases were confirmed using EVA software with PLU2018-pdf-4-2018RDB database.

The purity of the CNTs after functionalization was observed by Raman spectroscopy (J-Y T64000 micro-Raman spectrometer, Horiba Jobin-Yvon, Ltd., Stanmore, UK) equipped with a liquid nitrogen cooled charge coupled device detector. All samples were measured after excitation with a laser wavelength of 514.5 nm (Mhlanga et al., 2009).

3.1.2 Evaluation of Performance of adsorbent during desulfurization

The performance of the adsorbents was evaluated by conducting the adsorption experiments in batch mode and continuous mode. The batch mode experiment is further discussed in detail.

Acetonitrile, n-hexane 98 %, and Dibenzothiophene (DBT) were purchased from Sigma Aldrich (Pty) Ltd, South Africa. All other chemicals were of analytical grade, commercially available and used without further purification.

Adsorption performances of the (AC, CNTs, FCNTs, PLP and NLP) were evaluated by using a model diesel prepared in the laboratory by dissolving dibenzothiophene (DBT) in hexane because diesel consists of about 70 % of DBT in petroleum distillates obtained from hydrodesulphurizer (Kertesz and Wirtek, 2001). Model diesel was prepared by dissolving DBT (0.1 g) in 100 mL Hexane (100 mL). South African diesel samples (diesel obtained before HDS (5200 ppm) and diesel obtained after HDS (120 ppm)) were desulfurized using the best experimental parameters for model diesel desulfurization. Further dilutions were made from this solution to vary the concentration of DBT for use in this experiment. About 0.2 g adsorbent was weighed into an Erlenmeyer flask consisting of 20 mL of model oil/ South African diesel samples. The mixture was allowed to stir for 180 minutes on a rotary shaker at 298 K and 130 rpm.

There are more organo-sulfur compounds in typical real diesel. In order to increase the selectivity of DBT in the real diesel, the temperature, for real diesel in the adsorption desulfurization experiment was increased. In addition, for more availability and accessibility of the active vacant site of the adsorbent, contact time was increased. The temperature was varied (25-45 ^{o}C) and the time (0-120 minutes). The South African real diesel before HDS (5200 mg/L) was serially diluted using methanol to 120 mg/L. The results for desulfurization of real diesel samples are compared to results obtained for adsorptive desulfurization of model diesel

Aliquot samples were taken at interval and analyzed for DBT removal. All experiments were performed in triplicates so as to ensure accuracy and minimize errors. The mean values of these experiments were used in this study. The adsorption capacity and percentage DBT removal were calculated using Equation 3.1 and 3.2, respectively. Table 3.1 shows the physical and chemical

properties of a typical diesel fuel obtained from Refinery X, South Africa. The schematic of batch adsorption process is shown in Fig. 3.2.

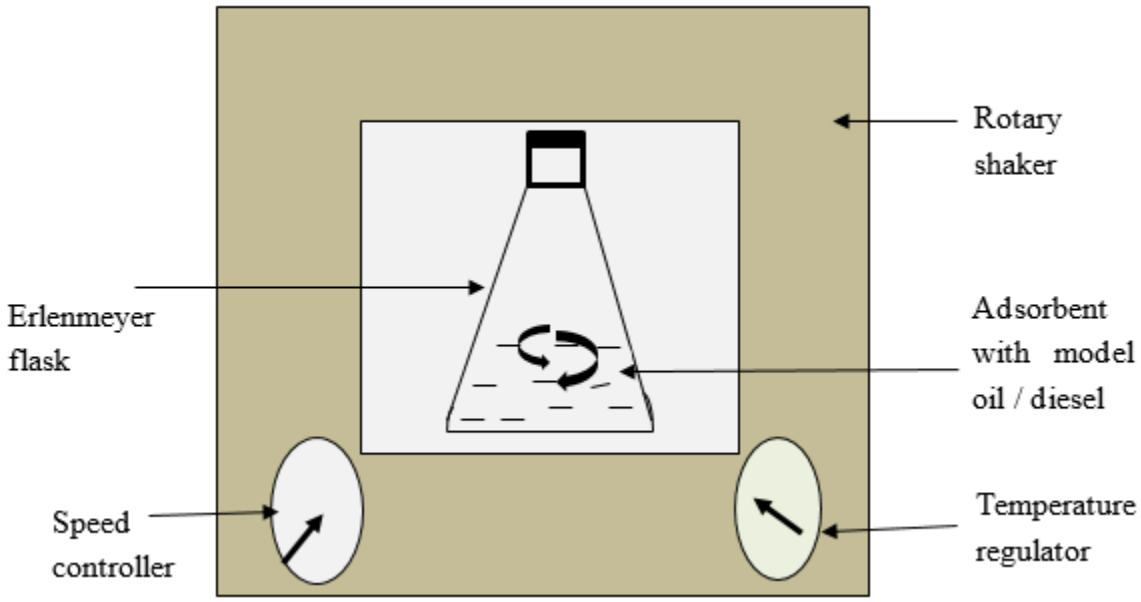


Figure 3.2. Schematic of batch adsoption desulfurization experiments in a temperature regulated rotary shaker.

In batch mode experiments, the spent adsorbents, loaded with sulfur were washed severally with hexane until they were back to their original state. Re-usability studies were carried out again on the regenerated adsorbents following adsorption–desorption for four cycles. The experimental runs were carried out with 1.0 g of the washed adsorbent and 20 mL of hexane, in a 250 mL Erlenmeyer flask and agitated vigorously at 130 rpm for 1 h. The initial concentration and concentration of the filtrate were analyzed for sulfur containing compound as mentioned earlier with HPLC.

The continoous mode experiments for adsorptive desulfurization of model oil and typical real diesel are discussed in detail;

Immobilized activated carbon was used for continuous packed-bed adsorption column to reduce adsorbent disintegration and pressure drop. Acetonitrile, n-hexane (98%) purity, and Dibenzothiophene (DBT) were purchased from Sigma Aldrich (Pty) Ltd, South Africa. All other chemicals were of analytical grade, commercially available and used without further purification. Desulfurization of diesel fuel was carried out in a lab-scale designed adsorption bed column as shown in Fig. 3.3. The column was made with a glass, with an internal diameter of 2.4 cm and a bed depth of 20 cm. The performance study of the colum was conducted at different DBT concentrations (100-500 mg/L), bed height (50-150 mm) and flow rate (0.5-1.5 mL). Adsorption reaction time was 3 hours. The immodilized activated carbon (pellets) was packed in the column with a layer of glass filter at the bottom. The DBT solutions was pumped in a downward direction using HLPC pump (HPLC Consta Metric 3500 MS. RIA VIS). Samples were taken at time intervals and analyzed.

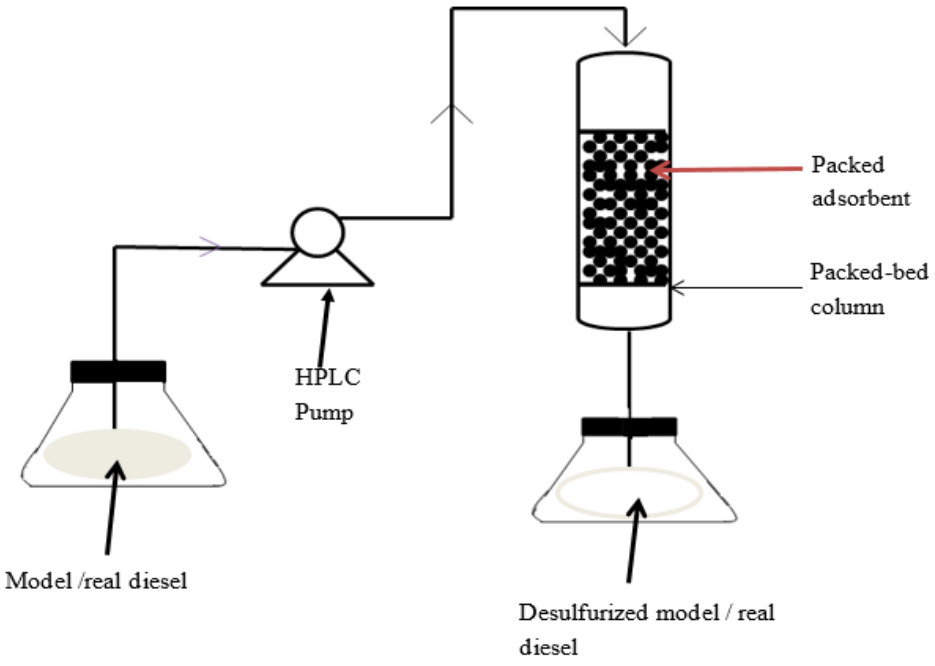


Figure 3.3. Continous adsorption in a packed bed column: Experimental set-up

In the continuous mode experiments, the saturated adsorbent with DBT molecules was regenerated by washing with methanol. The methanol was introduced into the column in a downward direction. The saturated beads were immersed in the methanol for 4 h, after which the adsorbents were washed thoroughly with deionized water and then allowed to drain off. The adsorption experiments were then conducted in three cycles. The performance efficiency of the adsorbent was evaluated.

The desulfurized model diesel samples were analyzed using Agilent high performance liquid chromatography (HPLC) equipped with an Eclipse C-18 column. Acetonitrile (55 %) was used as the mobile phase and the HPLC was operated at a wavelength of 234 nm, 1.0 µl/ min flow rate, and injection volume of 10 µl for 10 mins (Caro et al., 2008; Nazal 2015). The desulfurized South African diesel samples were analyzed using a Shimadzu (Japan) gas chromatography GC-MS unit equipped with fused silica column RXi-5MX. The dimension of the column was 0.25 µm thickness, 0.25 mm diameter and 30.0 mm length. The column temperature was set to hold at 90 ^{o}C for 2 minutes, and then increase to 300 ^{o}C at the rate of 10 ^{o}C/min and kept at 300 ^{o}C for 30 min. Helium was used as the carrier gas. MS ion source temperature was 200 ^{o}C. The pressure was set at 100 kpa with column flow of 1.39 mL/min, Linear velocity of 43.7 cm/sec, purge flow 3 mL/min and stop time of 10 min.

Table 3.1 Physical and chemical properties of a typical diesel fuel obtained from Refinery X, South Africa

Properties	Values
DBT (ppm)	5200 before HDS, 120 ppm after HDS
Density at 15 ^{o}C, kg/m^3	820.0
Ignition point	>55
Cetane index	46.0

3.13. Study of effects of operating conditions, optimization, isotherms and kinetic studies

Study of operating conditions is important in evaluating the performance of the adsorbents. The effect of operating variables such as temperature (^{o}C), time (min), DBT concentration (mg/L), and amount of adsorbents (g) on the performance of the adsorbents were studies in batch mode experiments. The operating variables were varied such as; time (0-180 minutes), temperature (298-308 K), amount of adsorbents (0.2-1.0 g) and initial DBT concentration (250-1000 mg/L). In the continuous mode adsorption experiments in a packed-bed column, effect of operating variables such as, flow rate (0.5-1.5 mL/min), bed depth (5-10 cm), and initial DBT concentration (100-500 mg/L) were studied at room temperature. The optimum operating conditions were obtained from these experiments and were used for adsorption coulpling bodesulfurization (AD/BDS) experiments.

The adsorption capacity for each run of the experiments was determined using Equation 3.1:

$$q_e = V\frac{C_o - C_e}{m} \tag{3.1}$$

Where V is the volume of the model oil (L), m is the amount of adsorbent in g, C_o and C_e are the initial and final concentration of DBT in the model oil in mg/L, respectively (Kiran and Kaushik, 2008).

The percentage sulfur removal (SR %) of adsorbent was calculated using Equation 3.2:

$$SR\ (\%) = \frac{C_o - C_e}{C_o} \times 100 \tag{3.2}$$

Where SR (%) is the percentage DBT removal, C_o and C_e are as decribed earlier in Equation 3.1 (Kiran and Kaushik, 2008).

Isotherm studies give detailed information on the nature of interactions between adsorbents and adsorbates (Wang and Wei, 2017). This is the most vital piece of information in understanding an adsorption process.

In the batch mode adsorption experiment in this study, equilibrium data were analyzed using Freundlich and Langmuir isotherm models. The linearized form of Langmuir isotherm model is given in Equation (3.3). Langmuir constants b, reflecting affinity of binding sites and the maximum monolayer coverage capacities, q_o (mg/g) can be calculated from the intercept and slope of the plot of $\frac{1}{q_e}\ versus\ \frac{1}{C_e}$.

$$\frac{1}{q_e} = \frac{1}{q_o} + \frac{1}{bq_oC_e} \tag{3.3}$$

Where C_e (mg/L) is the adsorbate equilibrium concentration, q_e is the amount of adsorbate in the adsorbent at equilibrium (mg/g). In order to determine the favourability of the Langmuir adsorption process, the separation factor (R_L) can be calculated using the expression given in Equation (3.4) (Langmuir, 1916; Wang and Wei et al., 2017)

$$R_L = \frac{1}{1 + bC_o} \tag{3.4}$$

Where b (L/mg) refers to the Langmuir coefficient and C_0 is the adsorbate initial concentration (mg/L) (Lam, 2008). For an adsorption system under study,

The values of R_L between 0 and 1 indicates favorable adsorption

$R_L > 1$ represents unfavorable adsorption

R_L = 1 represents linear adsorption

R_L = 0 indicates irreversible adsorption

The linearized form of Freundlich isotherm model is given in Equation (3.5). Freundlich constants K_f and n can be obtained from the intercept and slope of the plot of Log q_e versus log C_e.

$$Log\ q_e = Log\ K_f + \frac{1}{n}\ Log\ C_e \tag{3.5}$$

K_f (mg/g) and n represent Freundlich constants which relate to adsorption capacity and adsorption intensity respectively. Magnitude of exponent $\frac{1}{n}$ gives an indication of the favorability of adsorption.

Kinetic study on adsorption is important because it provides relevant information on the mechanism and the reaction pathways of adsorption interactions. Lagergren pseudo first-order kinetic model is the most useful and widely accepted amongst the models (Lagergren, 1998). Lagergren kinetic equation is given in Equation (3.6):

$$\frac{dq_t}{q_t} = K_1(q_{e-}\ q_t) \tag{3.6}$$

After applying the boundary conditions of qt = 0 at t = 0, the integrated rate law becomes;

$$Log\ (q_{e-}\ q_t) = Log\ q_e - \frac{K_1}{2.303}\ t \tag{3.7}$$

Where q_t is the amount of DBT adsorbed at time t and q_e is the amount of DBT adsorbed at time at equilibrium, k_1 (L/min) is the rate constant of the pseudo first order adsorption process. A straight line graph is obtained from the plot of log (q_e-q_t) versus t, from which the adsorption rate constant K_1, can be calculated.

Ho and McKay pseudo second order kinetics demonstrates how the rate depends on the sorption capacity, not on the concentration of the sorbate (Ho and McKay, 1999). The linearized form of second order kinetics is given in Equation (3.8):

$$\frac{t}{q_t} = \frac{1}{K_2 \ q_e 2} - \frac{1}{q_e} \ t \tag{3.8}$$

Where K_2 is the pseudo second order constant and q_e is the amount of DBT adsorbed at equilibrium. The q_e and the K_2 can be calculated from the slope and intercept of the plot of t/q_t versus t.

Intra-particle diffusion model describes the mechanism of adsorption process. It describes the multi-step process in adsorption when the solute molecules are transported from the aqueous phase to the surface of the solid adsorbent and then, the diffusion of the solute molecules into the interior of the pores. It can be expressed using Equation (3.9):

$$q_t = C + \mathrm{K}\, t^{0.5} \tag{3.9}$$

Where K in mg/g/min$^{0.5}$ is the intra-particle diffusion rate constant which can be obtained from the slope of plot of qt versus $t^{0.5}$.

The expression in Equation (3.10) was used to obtain the values for equilibrium adsorption constant (K_d) at different temperatures.

$$K_d = \frac{DBT\ amount\ in\ the\ adsorbent\ at\ equilibrium\ (q_e)(\frac{mg}{g})}{DBT\ concentration\ in\ the\ model\ oil\ at\ equilibrium\ (C_e)(\frac{mg}{mL})} \quad (3.10)$$

In order to determine the adsorption thermodynamics, the equilibrium constant values K_d, obtained at different temperatures from Equation (3.10) are used to calculate the thermodynamic parameter, ΔG^o, which is given in Equation (3.11) (Nejad et al., 2013).

$$\Delta G^o = -RTlnK_d \quad (3.11)$$

Where $\boldsymbol{\Delta} G^o$ is the standard free energy (kJ/mol); $\boldsymbol{\Delta} H^o$ is the standard enthalpy (J/mol). $\boldsymbol{\Delta} H^o$ can be determined from the slope of the linear plot of ln K_d versus 1/T, using the expression in Equation (3.12) $\boldsymbol{\Delta} S^o$ is the standard entropy which can be calculated using Equation (3.13):

$$lnK_d = \frac{\Delta S^o}{R} - \frac{\Delta H^o}{RT} \quad (3.12)$$

$$\Delta S^o = \frac{\Delta H^o - \Delta G^o}{T} \quad (3.13)$$

For column modelling and determination of kinetic parameters, the loading behavior of DBT molecule onto the surface of immobilized activated carbon in a continuous fixed bed coulumn was expressed in terms of C_t/C_o, where C_t is the effluent concentration of DBT in mg/L and C_o is the influent DBT concentration in mg/L. The breakthrough curve can be obtained by plotting C_t/C_o against time (Khan et al., 2011). The maximum column capacity, qt_{otal} (mg) for a given feed concentration and flow rate is equal to the area under the plot of the adsorbed DBT concentration. This can be obtained by the expression in Equation (3.14):

$$q_{total} = \frac{Q}{1000}\int_{t=0}^{t=t_{total}} C_R \, dt \tag{3.14}$$

Where t total is the total time in min, Q is the flow rate in mL/min, C_R is the concentration of DBT removal in mg/L

The total amount of DBT (in mg) sent into the column, M_{total} can be calculated by the expression in equation (3.15):

$$M_{total} = \frac{C_i Q t_{total}}{1000} \tag{3.15}$$

The percentage DBT removal (% R) can be be calculated by the ratio of DBT mass adsorbet (q_{total}) to the total amount sent into the column (M_{total}) as shown in Equation (3.16):

$$\% \text{ R} = \frac{q_{total}}{M_{total}} \times 100 \tag{3.16}$$

The amount of DBT adsorbed at equilibrium (q_e) in mg/g or adsorption capacity and equilibrium DBT concentration, C_e can be obtained using the following expressions in Equation (3.17) and (3.18):

$$q_e = \frac{q_{total}}{m} \tag{3.17}$$

$$C_e = \frac{M_{total} - q_{total}}{V_{eff}} \times 100\ \% \tag{3.18}$$

Where m is the mass of the adsorbent in g.

The development of a model that describes the concentration time profile is difficult in most cases, since the DBT concentration in the solution which moves across the bed continuously changes and therefore the process does not operate at steady state. Therefore, in order to successfully design design of a column adsorption bed, it is essential to predict the breakthrough curve for effluent parameters. Various kinetic models have been developed to predict the dynamic behavior of the fixed bed adsorption column. In this study, three major models such as Bohart-Adams, Thomas, and Yoon-Nelson models for the kinetic studies.

The Bohart-Adam model is used to descrie the initial part of the break through curve. The expression in Equation (3.19) is used to calculate the parameters of Bohart-Adaams model.

$$\ln\left(\frac{C_t}{C_O}\right) = K_{ab} C_O \mathrm{t} - \frac{K N_O \mathrm{Z}}{\mathrm{V}} \tag{3.19}$$

Where K_{ab} is the kinetic constant in L/mg.min, V is the linear flow rate (mL/min), Z is the bed height of the column (cm), N_o is the saturation concentration (mg/L) and t is time in min. The plot of $\ln(C_t/C_o)$ versus time yield a linear graph with slope and intercept, from with the Boahrt-Adam constants K_{ab} and N_o can be calculated, respectively (Bohart and Adama, 1920, Cooney 1999).

The Thomas adsorption model's expression is given as:

$$\ln\left(\frac{C_o}{C_t} - 1\right) = \frac{K_{Th} q_O \mathrm{w}}{\mathrm{V}} - K_{Th} C_O \mathrm{t} \qquad (3.20)$$

Where q_o is the equilibrium DBT uptake per g of the immobilized adsorbent (mg/g), K_{Th} is the Thomas constant (L./min.mg). A plot of $\ln\left(\frac{C_o}{C_t} - 1\right)$ against time yields a linear grapgh. The values of K_{Th} and q_o can be calculated from intercept and slope of the graph, using a linear regression analysis (Thomas,1942; Chu, 2010).

A model was developed by Yoon and Nelson (1984) based on the assumption that the rate of decrease in the probability of adsorption of adsorbate molecule is proportional to the probability of the adsorbate adsorption and the adsorbate breakthrough on the adsorbent. Therefore, the linearized form of Yoon-Nelson model equation can be expressed as in Equation (3.21);

$$\ln\left(\frac{C_t}{C_o - C_t}\right) = K_{Th} t - \text{ɽ}\, K_{Th} \qquad (3.21)$$

Where K_{YN} and ɽ are the rate velocity constant in min^{-1} and the time required for 50 % adsorbate breakthrough (min). K_{YN} and ɽ can be calculated from the intercept and slope of a linear graph of $\ln\left(\frac{C_t}{C_o - C_t}\right)$ versus time.

3.2. Investigation of Biodesulfurization (BDS)

3.2.1. Inoculum preparation and investigation of bacteria growth

Pseudomonas Putida, Pseudomonas Aeruginosa Kwik Stik, ATCC 27853 Microbiologics and 2-hydroxylbiphenyl (2-HBP) were purchased from Sigma Aldrich (Pty) Ltd., South Africa. Dibenzothiophene, acetonitrile (gradient grade for liquid chromatography) and N, N, dimethyl formamide (purity, GC) (99 %) were purchased from Merck (Pty) Ltd., South Africa. All other chemicals were of analytical grade without further purifications. Basal salt medium consisting of NaH_2PO_4. H_2O (4 g/L), K_2HPO_4. $3H_2O$ (3 g/L), $MgCl_2$. $6H_2O$ (0.0245 g/L), CaCl. $2H_2O$ (0.001 g/L), $FeCl_3$. $6H_2O$ (0.001 g/L) was prepared in the laboratory as described elsewhere (Rashtchi et al., 2006). All glass wares were sterilized in an autoclave at 121 ^oC, for 20 minutes. The chemicals were dissolved with deionized water in 1000 mL volumetric flask capacity and stirred till all chemicals were dissolved. The pH of the medium was maintained at 7.0 by adding drop wisely 0.5 M NaOH. The solution was sterilized in autoclave at the same conditions as for the glass wares mentioned earlier. The prepared BSM medium was stored at room temperature away from sunlight.

Luria-Bertani (LB) liquid medium was prepared by adding peptone (10 g), NaCl (5 g), yeast extract (5 g) to 950 mL deionized water and make up to 1000 mL. The medium was sterilized by autoclaving at 121 ^oC for 20 min. Frozen pellets of *Pseudomonas aeruginosa* and *Pseudomonas putida* each was taken with sterile forceps into a 250 mL Erlenmeyer flask consisting of 50 mL LB medium. 10 g/L of tetracycline was prepared and 150 µL was added to the inoculum to serve as antibiotics for the bacteria (Rashtchi et al., 20066). The mixture was incubated for 3 days at 30 ^oC, and 37 ^oC for *Pseudomonas putida* and *Pseudomonas aeruginosa*, respectively at 130 rpm. The prepared inoculum was kept at -80 ^oC.

0.1 M of (401 mL) potassium phosphate dibasic K_2HPO_4 (8.75 g/L) and 0.1 M (99 mL) of potassium phosphate mono basic KH_2PO_4 (13.6 g/L) was prepared. The initial pH of the buffer solution was 7.53 and was adjusted to 7.0 by adding 32 % 0.1 N (HCl) drop-wise. Potassium phosphate buffer was used in this study to wash the resting bacteria cells before storing in respective carbon source.

3.2.2 Evaluation of biodesulfurization efficiency of *Pseudomonas species*

Biodesulphurization (BDS) experiments with growing cell of *Pseudomonas aeruginosa* and *Pseudomonas putida* were conducted in batch mode. The bacteria of *Pseudomonas putida and Pseudomonas aeruginosa* previously inoculated in LB medium was used. 0.1 g of DBT was dissolved in dimethyl formamide (DMF) and serially diluted to vary the concentration as required. Glycerol 20 g/L was used as the only carbon source. 0.25 mL LB-frozen stock of bacteria was put into 50 mL of BSM in a 250 mL Erlenmeyer flask. The bacteria medium was supplemented with 1 mL of 0.25 mM (46 ppm) DBT as the only sulfur source with 150 µL tetracycline (Davoodi-Dehaghani et al., 2010). The flask was incubated at 30 ^{o}C and 37 ^{o}C for *Pseudomonas putida* and *Pseudomonas aeruginosa*, respectively, and agitated at 130 rpm for 10 days. The growth of bacteria was measured and desulfurization of DBT in model oil was monitored as well.

Biodesulphurization experiments with resting cells of *Pseudomonas aeruginosa* (*PA*) and *Pseudomonas putida* (*PP*) were performed in batch mode. The bacteria in growing cell experiment were harvested at late exponential phase. The bacteria medium was centrifuged at 7000 rpm for 5 min. The cells were washed thrice with potassium phosphate buffer solution. The washed PA and PP cells were then re-suspended into glycerol/ NaCl in ratio 1:1. The different cell concentrations (0.3-1.2 g DCW/L) of frozen resting cells of PA and PP in glycerol/NaCl solution was measured into 50 mL of BSM with 150 µL of tetracycline, 500 µL of glycerol and 1 mL of 500 ppm model oil. The initial concentrations of DBT were varied from 250 to 1000 ppm. The mixture was incubated for 8 h at 30 ^{o}C and 37 ^{o}C for *Pseudomonas putida and Pseudomonas aeruginosa,* respectively and the mixture was agitated at 130 rpm (Caro et al., 2008). Aliquots of samples were taken at intervals and the growth of bacteria was measured and the samples were analyzed for biodesulfurization efficiency as well.

Growth of bacteria and biodesulfurization of model oil in aqueous and biphasic media experiments were performed in batch mode. Hexadecane was chosen as organic phase in biphasic process owing to its presence in the diesel oil fraction. BSM was the aqueous medium. In this experiment the percentage of oil-to- water was varied 0 %, 20 % and 50 %. The organic phase was centrifuged and extracted with ethyl acetate from the aqueous phase oil. The final sulfur concentration and

produced 2-HBP end product of 4S pathway in the organic phase were determined (Caro et al 2007).

Resting cells of *Pseudomonas aeruginosa* and *Pseudomonas putida* were used for degradation of real diesel in this study. Diesel sample obtained before HDS with initial DBT concentration of 5200 ppm and diesel sample obtained after HDS with initial DBT concentration of 120 ppm were supplied by a refinery in South Africa. About 5 mL of diesel was measures into a 250 mL Erlenmeyer flask with 5 mL of resting cell in glycerol/NaCl (1:1) and 20 mL of BSM. The mixture was incubated for 8 h, at 30 ^{o}C and 37 ^{o}C and agitated at 130 rpm for *Pseudomonas putida* for *Pseudomonas aeruginosa, respectively.* Aliquots of samples were taken at intervals for analysis (Guobin et al., 2006).

The following analytical techniques were used for measurements of bacteria growth and desulfurization of model oil and typical real diesel during biodesulfurization experiments;

The pH was measured using a pH meter and a Spectroquant Pharo 300 Merck, (W210324), made in EU was used to measure the turbidity of the culture. The cell mass was determined by measuring the optical density (OD) at a wavelength of 660 nm. In order to measure the net dry cell weight (g DCW) of the biomass, 3 mL of the culture was centrifuged at 7000 rpm for 10 minutes and the concentrate was washed thoroughly with distilled water on a pre-weighed filter paper. The filter paper containing the bacteria was dried over-night at 100 ^{o}C and the weight of the bacteria was determined by subtracting the net weight from the initial weight of the filter paper. The relationship between the optical density ($OD_{660\,nm}$), dry mass and the absorbance was determined. A calibration curve was obtained and used in the determination of the unknown cell concentration (Rashtchi et al., 2006).

To obtain the final sulfur concentration in the desulfurized model oil, aliquots of samples were taken at intervals and concentration of DBT analyzed using a high performance liquid chromatography (HPLC). Acetonitrile (55 wt. %) was used as the mobile phase (Caro et al., 2008), with the UV detector at 254 nm. The incubated mixture was centrifuged at 7000 rpm for 10 min, and filtered. The aqueous phase was acidified with HCl in order to quench the desulfurization reaction before analyzing it with HPLC. The degraded DBT and the formed 2- HBP were extracted

with equal volume of ethyl acetate. In biphasic system, the DBT and the 2-HBP were extracted from the organic phase after centrifugation and analyzed using HPLC. The peak area of DBT and that of the 2-HBP of known concentrations at different elution time were used to calibrate the HPLC. The pre-calibration curve obtained during the calibration was used to determine the unknown concentration of DBT and 2-HBP in the desulfurized samples.

3.2.3 Investigation of operating variables, optimization and kinetic studies

Study of operating variables is important in evaluating the efficiency of the bacteria for degradation of DBT in model oil and typical real diesel. The effect of operating variables such as time (0-8 h), DBT concentration (250-1000 mg/L), and mass concentration of bacteria (0.3-1.2 gDCW/L), and oil-water ratio (0-50 %) on the biodegradation efficiency of the bacteria. The optimum operating conditions were obtained from these experiments and were used for ADS/BDS experiments.

The biodesulfurization capacity (X_{BDS}), conversion yield for DBT (Y_{BDS}), degree of desulfurization (D_{BDS}) and specific conversion rate (E) were evaluated using the following equations;

Biodesulfurization capacity (%) evaluates the the efficiency of bacteria in biodesulfurization process.

$$X_{BDS} = \frac{C_{2-HBP,(f)}}{C_{DBT,(i)}} \times 100 \qquad (3.22)$$

Where X_{BDS} is biodesulfurization capacity in (%), $C_{2\text{-}HBP(f)}$ in mg/L is the final concentration of 2-HBP formed during biodesulfurization of DBT, $C_{DBT(i)}$ in mg/L is the initial DBT concentration in the model oil before degradation.

Conversion yield of DBT (%) can be evaluated by using Equation (3.23) (Martins et al., 2004):

$$Y_{BDS} = \frac{C_{DBT,(i)} - C_{DBT,(f)}}{C_{DBT,(i)}} X\ 100 \qquad (3.23)$$

Where Y_{BDS} is the conversion yield for DBT degraded (%), $C_{DBT,(f)}$ is the final concentration of DBT after degradation in mg/L. X_{BDS} and Y_{BDS} indicate the efficiency of bacteria in the biodesulfurization process.

Degree of desulfurization (g DCW/L.h) is the degree to which desulfurization occurred during growth and resting process. This was used to show relationship the biodesulfurization capacity of the bacteria and the biomass obtained within a specified period of growth time. Evaluation of D_{BDS} during bacteria growth provides information on optimum biocatalyst production process. D_{BDS} was calculated using Equation (3.24) (Martins et al., 2004):

$$D_{BDS} = \frac{X_{BDS}.C_X}{t_G} \tag{3.24}$$

Where D_{BDS} in (g DCW/L) is the degree of desulfurization, X_{BDS} is the biodesulfurization capacity, C_x is the biomass concentration (g DCW/L), t_G (h) is the time required to attain the biomass concentration.

Specific conversation rate (L/g DCW.h) is the effectiveness of each bacterium. It was determined by the expression in Equation (3.25) (Martins et al., 2004):

$$E = \frac{X_{BDS\,(\max)}}{t_{G(\max)}.C_X} \tag{3.25}$$

Where $t_{G\,(max)}$ (h) is the time required for maximum desulfurization

Pseudo first order model was used to describe the degradation of DBT by *pseudomonas aeruginosa* and *pseudomonas putida* (Abin-Fuentes et al., 2014). The expression is described as follows:

$$C = C_0 e^{-kt} \tag{3.26}$$

Where C is the concentration of DBT at time (mg/L), t (h), C_o is the initial concentration of DBT in mg/L, K is the pseudo first order rate constant (h^{-1}), and t is the reaction time in hour. Linearizing this Equation (3.26) becomes;

$$lnC = lnC_0 - Kt \tag{3.27}$$

Plot of lnC versus time, t will give a straight line with ln C_o as the slope and K as the intercept. The value of C_o and K can then be determined from the slope and intercept of the graph, respectively using a linear regression analysis.

The growth of a bacteria culture can be studied using the Minod expression as shown in Equation (3.28):

$$\mathrm{V} = \mathrm{V}_{max}\frac{[S]}{K_m+[S]} \tag{3.28}$$

Where $V_{max\ is}$ the first order rate constant (mg/gDCW.h) particular to the exponential growth phase of culture described by the rate equation, V is the rate of bacteria growth (gDCW/L.h), [S] is the substrate concentration (mg/L), and K is a first order constant (mg/L).

For a single substrate catalyzed reaction, Michaelis Menten equation is applied. Michaelis-Menten assumed that, a fast pre-equilibrium forming an enzyme-substrate complex proceed a slow, rate determining reaction of that complex. Michaelis-Menten can be considered satisfactory description of substrate utilization, only if the initial equilibrium can be considered in the context of the system as a whole and that the subsequent steps can be considered as occurring only within the cells (Talaiekhozani et al., 2015).

$$\frac{-d[S]}{dt} = K[E_0]\frac{[S]}{K_m+[S]} \quad (3.29)$$

Where

$$K_m = \frac{[E][S]}{[ES]} \; and \; [E_0] = [E] + [ES] \quad (3.20)$$

If [E_o], the maximum concentration of available substrate-binding enzyme for a given cell concentration can be considered proportional to the bacteria density itself, and if also the rate of growth can be considered proportional to the rate of substrate utilization, then;

$$[E_0] = X[B] \; and \; \frac{d[B]}{dt} = -Y\frac{d[S]}{dt} \quad (3.31)$$

Where $\frac{d[B]}{dt}$ is the rate of growth of bacteria, X is a constant, and Y is a yield factor also considered to be constant throughout the period of substrate conversion. It follows that;

$$\frac{d[B]}{dt} = K'[B]\frac{[S]}{K_m+[S]} \quad (3.32)$$

Comparing Equation (3.28) with (3.32) shows that;

$$V = K' \frac{[S]}{K_m + [S]} \quad (3.33)$$

This is the form of Minod equation.

Equation (3.32) shows that when S >> K the reaction is pseudo first order, but when S << K the reaction is second order character predominate and

$$\frac{d[B]}{dt} = \frac{K'}{K_m}\,[B][S] \quad (3.34)$$

The similarity of this second order rate expression to that for an autocatalytic model where

$$S \rightarrow B \; and \; \frac{d[B]}{dt} = \mathrm{K}[B][S] \quad (3.35)$$

Linearized form of Michaelis mentel equation can be written as;

$$\frac{1}{V} = \frac{K_m}{V_{max}} \cdot \frac{1}{\mathrm{S}} + \frac{1}{V_{max}} \quad (3.36)$$

Plot of $\frac{K_m}{V_{max}}$ versus $\frac{1}{\mathrm{S}}$ yields a straight line where the values of V_{max} and K_m can be calculated from the slope and intercept of the graph, respectively using a linear regression analyss. The differential method analysis can be used when when numerical values of the reaction rate have been obtained at different concentrations and at a constant temperature (Roberts, 2009).

The experimental data was compared with the model data obtained. The percentage error between the experimanta data and the model parameters obtained was calculated using Equation (3.37)

In order to ensure accuracy, an error function was applied to each model employed in this study, based on the normalized standard deviation, as shown in Equation 3.37 (Yoro, 2016).

$$\%\ Error = \sqrt{\Sigma^{n=3}\left(\frac{\frac{Q_{exp}-Q_{mod}}{Q_{exp}}}{N-1}\right)^2} \times 100 \qquad (3.37)$$

3.3. Development of AD/BDS process and evaluation

In order to couple adsorption and biodesulfurization techniques, resulting in efficient and enhanced desulfurization of typical South African diesel samples to meet up with Euro V standard less than 10 ppm proposed by South African government to South African refineries, this study after determining the best operating conditions for both packed-bed column adsorption process and best operating condition for biodesulfurization process. The diesel obtained after HDS with initial concentration of 120 ppm sulfur compound and diesel obtained before HDS (5200 mg/L) obtained from a Refinery in South Africa were used in this section of the thesis. The diesel before HDS was serially diluted to reduce the concentration lower than South African standard diesel grade (500 mg/L) and higher than the current SA low diesel sulfur grade (50 mg/L). The effect of initial sulfur concentrations was studied. Kinetic model such as Bohart-Adam model, Thomas model and Yoon-Nelson model was used to describe the mechanism of adsorption of sulfur compound onto the surface of the immobilized adsorbent in a continuous fixed bed column. The initial concentrations of the DBT in the South African diesel samples were varied (40, 80 and 100 mg/L). Other operating parameters such as bed depth (15 cm), flow rate (0.5 mL/min) were kept contant at room temperature. The South African diesel samples were pumped into the packed-bed column by HPLC pump in a downward direction. Samples of desulfurized diesel were taken at intervals and analyzed using GC/MS equipment.

The samples were taken from packed-bed column experiment at 140 min, when the concentration of the SA diesel obtained after HDS was about 10 mg/L and 15 mg/L for SA diesel obtained before HDS. The samples were transferred into a 250 mL Erlenmeyer flask containing 20 mL of basal salt medium, with 75 µL of tetracycline as antibiotic for the bacteria, 5 mL of resting cells of Pseudomonas aeruginosa suspended in glycerol/NaCl (1:1). The mixture was incubated for 8 h, and agitated at 130 rpm at 37 ^{o}C and aliquots of samples were taken at intervals for analysis. The physical and chemical properties of the diesel oil are presented in Table 31. The samples were analysed in GC/MS. The degradation of DBT and formation of end product of 4S pathway were quantified. The schematic of the process is shown in Fig 3.4

Detection of sulfur containing compounds in diesel sample before HDS, diesel sample after HDS and the evolution of the 4S end product (2-HBP) was done by gas chromatography/mas spectroscopy (GC/MS) Shimadzu equipment with column Rx-SMX. Injection and detection temperature were set at 220 ^{o}C and 230 ^{o}C, respectively. Oven temperature at 80 ^{o}C, to 190 ^{o}C at 10 ^{o}C /min and 15 ^{o}C /min to 230 ^{o}C for 18 min in split-less mode. Helium was used as the carrier gas. In order to determine the calibration curve for HDS feed, and HDS outlet diesel. The diesel samples with known concentrations were diluted serially to vary their concentrations. The GC/MS was initially calibrated by plotting the peak areas detected form GC/MS against the known concentrations of the diesel. This was used to plot a calibration curve that was used to calculate the unknown concentrations of diesel in the samples. Physical and chemical properties of typical South African diesel oil are given in Table 3.1.

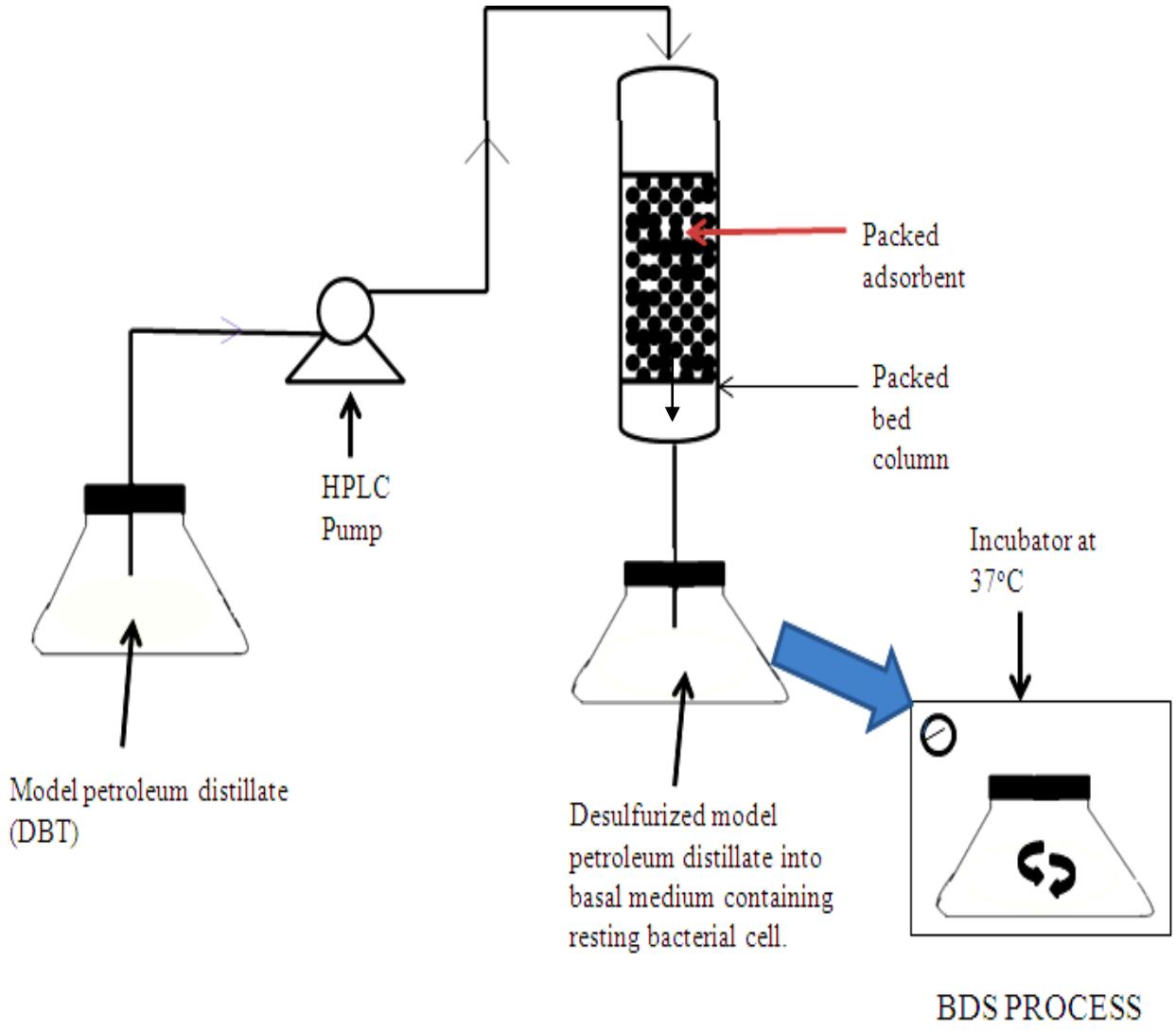


Figure 3.4. Schematic for ADS/BDS coupling technique process

3.4. Conclusion and recommendation

A sort overview of the methods used in the preparation and characterization of adsorbents for adsorptive desulfurization is presented in this chapter. In addition, series of experiments conducted in this study are described in detail. Also the techniques for growth of bacteria for

biodesulfurization experiment have been successfully highlighted. Results obtained from the experimental procedures described in this chapter are reported and discussed in later chapters.

3.5. References

Abin-Fuentes, A., Leung, J. C., Mohamed, M. E., Wang, D. I.C., and Prather, K. L.J. (2014) Rate-limiting step analysis of the microbial desulfurization of dibenzothiophene in a model oil system. Biotechnol Bioeng., 111(5), 876–884.

Bohart, G.S, Adams, E.Q. (1920) Some aspects of the behavior of charcoal with respect to chlorine, J. Am. Chem. Soc. Vol. 42, pp 523-529.

Caro, A. Leton, P., Garcia-Calvo, F., and Setti, L. (2007a) Enhancement of the DBT biodesulphurization by using β-cyclodextrins in oil-to water media. Fuel, 86, 2632-2636.

Caro A, Boltes K, Leto ´n P, Garcı ´a-Calvo, E. (2008b) Biodesulfurization of dibenzothiophene by growing cells of Pseudomonas putida CECT 5279 in biphasic media. Chemosphere 73, 663–669

Chu, K.H. (2010). Fixed bed sorption: Setting the record straight on Bohart-Adams and Thomas models. Journal of Hazardous Materials. Vol. 177, pp. 1006-1012.

Cooney, D.O. (1999). Adsorption design for wastewater treatment, Lewis publishers, Boca Raton.

Davoodi-Dehaghani, F., Vosoughi, M., Ziaee, A.A. (2010) Biodesulfurization of dibenzothiophene by a newly isolated Rhodococcus erythropolis strain. Bioresource Technology. Vol. 101, 1102-1105.

Guobin, S., Huaiying, Z., Jianmin, X., Guo, C., Wangliang, L., Huizhou, L. (2006) Biodesulfurization of hydrodesulfurized diesel oil with Pseudomonas delafieldii R-8 from high density culture. Biochemical Engineering Journal. Vol 27, 305-309.

Ho, Y. S., & Mckay, G. (1999) Pseudo-second order model for sorption processes. Process Biochemistry, 34, 451–465.

Khan, N., Yahaya, E.M., Abustan, I., Faizal, M., Latiff, P.M., Bello, O.S., Ahmad, M.A. (2011). Fixed-bed column study for Cu (II) removal from aqueous solutions using rice husk based activated carbon. International Journal of Engineering and Technology. Vol. II, No. 1, 248.

Kiran, B, Kaushik, A. (2008) Cyanobacteria biosorption of Cr (VI): Application of two parameter and Bohart Adams models for batch and column studies. Chemical Engineering Journal. Vol. 144, pp. 391-399.

Lam, M., Ridzuan, Z., (2008) Production of activated carbon from sawdust using fluidized bed reactor. International Conference on Environment, ICENV 2008.

Langmuir, I. (1916) The constitution and fundamental properties of solids and liquids. Journal of the Americal Chemical Society, 38(11), 2221–1195.

Martin, A. B., Alcon, A., Santos, V. E., and Garcia-Ochoa, F. (2004) Production of a Biocatalyst of Pseudomonas putida CECT5279 for Dibenzothiophene (DBT) Biodesulfurization for Different Media Compositions. Energy & Fuels, 18, 851-857.

Mhlanga, S. D., Mondal, K. C., Carter, R., Witcomb M.J., and Coville, N.J. (2009) The Effect of Synthesis Parameters on the Catalytic Synthesis of Multiwalled Carbon Nanotubes using Fe-Co/$CaCO_3$ Catalysts. S. Afr. J. Chem., 62, 67–76.

Nejad, N.F., Shams, E, Amini, M.K, Bennett, J.C. (2013) Synthesis of magnetic mesoporous carbon and its application for adsorption of dibenzothiophene. Fuel Processing Technology. Vol. 106, 376-384.

Oluwasina O.O., Daramola O.M., Iyuke S. (2018) Investigation on Purification Potential of Multiwalled Carbon Nanotubes Using Organic-Mineral Acid Mixture. Journal of Nanoscience and Nanoengineering Vol. 4, No. 1, pp. 1-8.

Rashtchi, M., Mohebali, G.H., Akbarnejad, M.M., Towfighi, J., Rasekh, B., Keytash, A. (2006) Analysis of biodesulfurization of model oil system by the bacterium, strain RIPI-22. Biochemical Engineering Journal. Vol. 29, 169-173.

Seepe, L. (2015) The use of cassava waste in the removal of cobalt, chromium and Vanadium ions from synthetic effluents. A dissertation submitted to the University of the Witwatersrand, South Africa.

Talaiekhozani, A., Jafarzadeh, N., Fulazzaky, M. A., Talaie, M. R., and Beheshti, M. (2015) Kinetics of substrate utilization and bacterial growth of crude oil degraded by Pseudomonas aeruginosa, Journal of Environmental Health Science and Engineering 13, pp. 64.

Thomas, H.C. (1944) Heterogeneous ion exchange in a flowing system. J. Am. Chem. Soc. Vol.66, pp. 1664-1666.

Yoon, Y.H., Nelson, J.H. (1984) Application of gas adsorption kinetics. I: Atheoretical model for respiratorcartridge service life. Am. Ind. Hyg. Assoc. J. Vol. 45,509-516.

Yoro, K.O. (2016**)** Numerical simulation of CO_2 adsorption behavior of polyspartamide adsorbent for post-combustion CO_2 capture. Master dissertation submitted to the University of the Witwatersrand, South Africa.

Chapter Four

4.0 Adsorption performance of pomegranate and neem leaf powder during desulfurization

In this chapter, effects of operating variables on the performance evaluation of pomegranate leaf and neem leaf powder adsorbents for removal of dibenzothiophene from a model diesel are reported and discussed. The results of mechanism, behavior and thermodynamics of the adsorbents are also reported

4.1 Introduction

Different types of adsorbents such as activated carbon, carbon nanotubes (CNTs) (Nazal et al., 2016), montmorillonite clay (Ahmad et al., 2017), bentonite (Ishaq et al., 2017), neem leaf powder (Daware and Kulkani, 2015), rice husk (Ahmaruzzaman, and Gupta, 2011) have been used for adsorptive desulfurization of DBT in petroleum distillate. Among these adsorbents, commercial activated carbon has been widely used due to its porous surface structure and high surface area, however, it is expensive to process (Fayazi et al., 2015; Nazal et al 2016). Agricultural wastes materials are presently gaining attention due to their ready availability and low cost as potential adsorbents for removal of various contaminants from wastewaters and fuels (Ahmarussaman and Gupta, 2011). Therefore, a new, green and agro-waste product can be employed in order to replace the expensive commercial activated carbon. Pomegranate leaf annually sheds its leaves and no useful materials have been developed from it for industrial application yet. Pomegranate leaf powder has been used by Battacharje and patel (2017) in the treatment of wastewater. However, its use in adsorptive removal of DBT from petroleum distillate has not been reported till date. Neem leaf has been used for the treatment of wastewater and as adsorbent for removal of sulfur compound in diesel (Daware et al., 2015). However, there is need for more exploration of the adsorbents in this field. In this chapter, synthesis and investigation of the adsorption performance of the pomegranate and neem leaf powder are presented. The potential re-usability performance of PLP nad NLP was studied due to growing concern for waste minimization, recovery, and reuse as well as for industrial applications. In order to understand the mechanisms and the kinetics of the adsorption process, the results of adsorption behavior of these adsorbents are presented as well.

4.2 Experimental

The materials for the preparation of adsorbents, characterization and the detailed description of experimental procedures employed in this chapter are provided in Chapter 3 (section 3.1.1) of this thesis. The performance evaluation of the adsorbents is also described in Chapter 3 (section 3.1.2) of this thesis. However, the operating conditions used are summarized in Table 4.1. In addition, the regeneration of adsorbent was discussed extensively in Chaper 3 section 3.1.2 of this thesis as well.

Equation 3.1 and Equation 3.2 were used to evaluate the adsorption capacity of the adsorbents and their DBT removal percentage, respectively. The adsorption behavior of the adsorbents was investigated as well, using isotherms and kinetic models described in Chapter 3.

Table 4.1. Operating conditions for adsorption desulfurization of DBT by PLP and NLP.

Quantity	Values
Amount of adsorbents (g)	0.2-1.0
Initial DBT concentrations (ppm)	250-1000
Adsorption temperature (^{o}C)	25-35
Time (min)	180

4.3 Results and Discussion

4.3.1 Physico-chemical characterization of PLP and NLP adsorbents

The SEM image of the as-prepared NLP, and that of the as-prepared PLP adsorbents are depicted Fig. 4.1 (a) and Fig. 4.1 (b), respectively.The SEM images show that the PLP and NLP possess irregular structural surfaces with well developed porous stuctures that could be instrumental to the good adsorption of DBT on the surface of the adsorbents. These obervations are in agreement with literature (Ghaneian et al., 2015). It could also be observed that the surface of NLP adsorbent is smoother than that of PLP adsorbent.

The difraction patterns of these adsorbents were obtained as described in Chapter 3 of this thesis and are shown in Fig. 4.2. The XRD patterns for PLP and NLP adsorbents are similar. It can be observed from the graph, that there are no diffraction peaks on the two XRD patterns except the bands observed at 2 θ values in the range of 20 ^{o}- 30 ^{o} for both PLP and NLP adsorbents. It can therefore be concluded that both adsorbents are amorphous in nature without any crystalline peaks. Results are in agreement with Prabhu et al. (2014) for NLP adsorbent.

Table 4.2 shows the elemental composition of PLP and NLP before and after adsorption experiments. The results in Table 4.2 show that PLP consists of 60.48 % carbon and 39.52 % oxygen before adsorption. However, there was 3.82 % sulfur on the surface of the used adsorbent, indicating the sulfur-containing compound was adsorbed on PLP adsorbent. It could be observed that NLP consists of C, O, Mg, Cl, Ca and K (Nazal et al., 2016). However, the elemental composition obtained from EDX on adsorbent after desulfurization showed the presence of sulfur on the surface of the adsorbent.

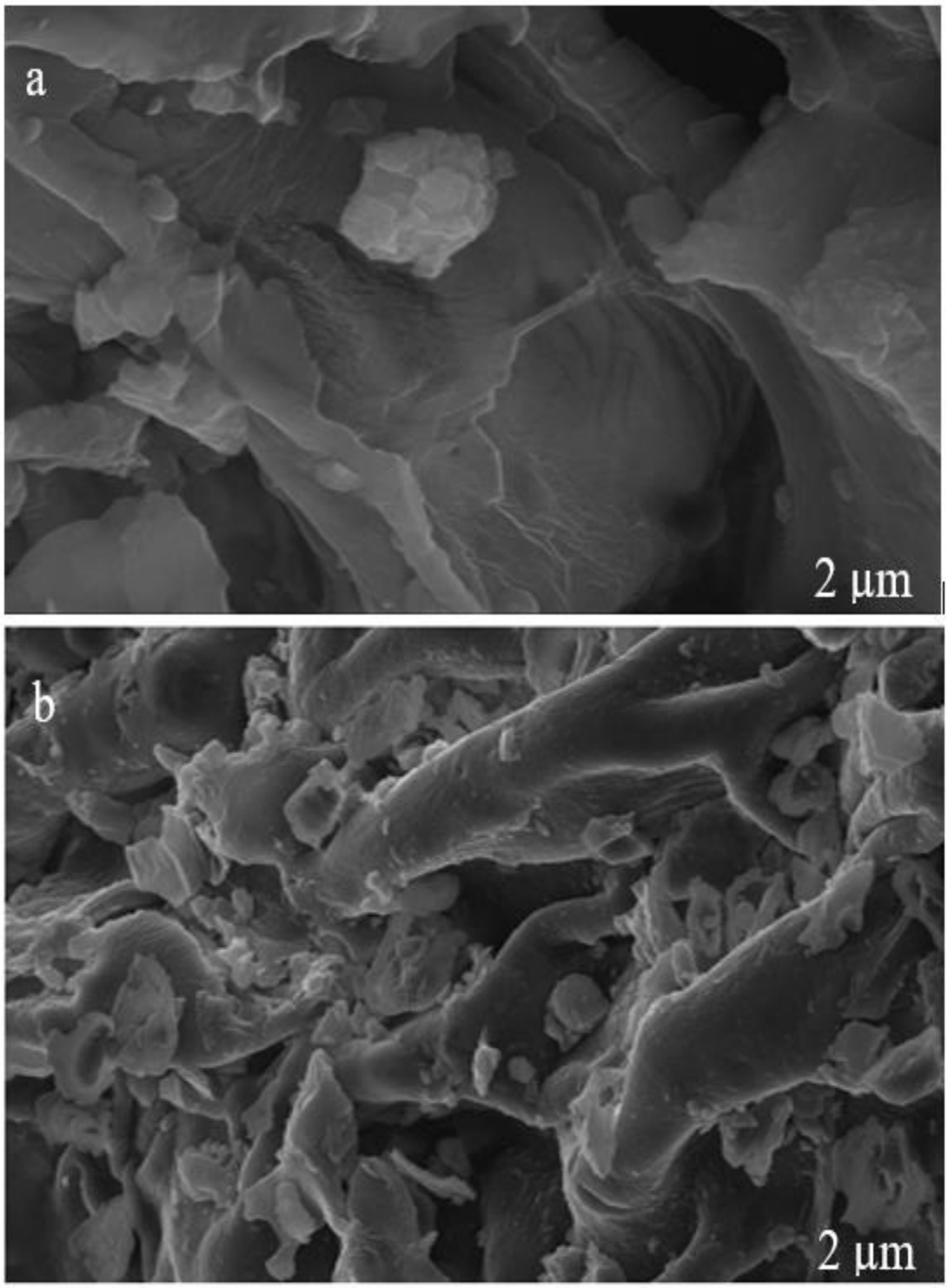


Figure 4.1. Surface morphologies of (a) NLP (b) PLP adsorbents

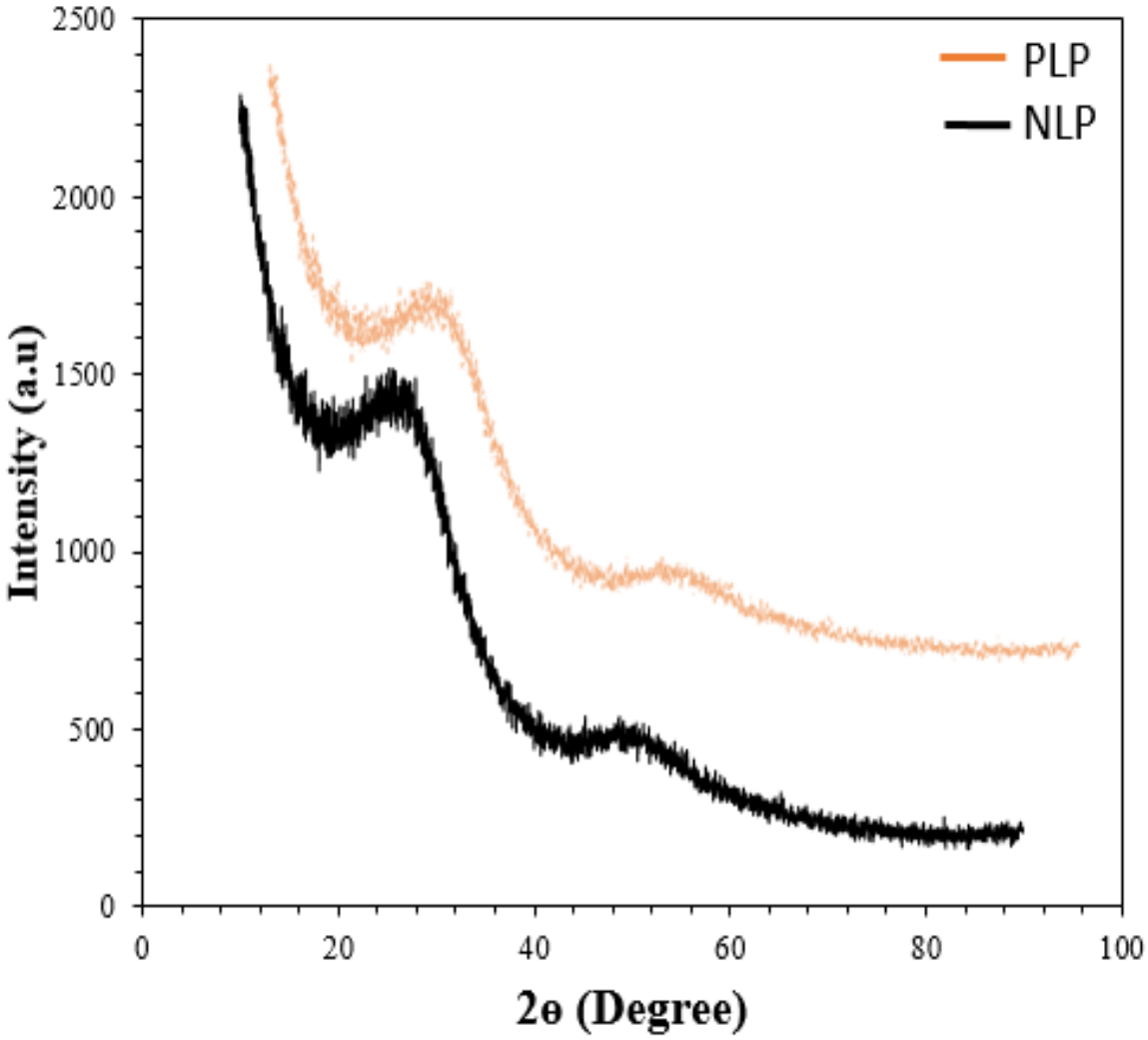


Figure 4.2. XRD pattern of PLP and NLP

Table 4.2: Elemental compositions of PLP ans NLP adsorbents before and after adsorption experiments

Element	Weight %				Atomic %			
	Fresh PLP	Used PLP	Fresh NLP	Used NLP	Fresh PLP	Used PLP	Fresh NLP	Used NLP
C	60.48	58.75	52.40	51.40	67.09	66.29	66.29	61.90
O	39.52	37.43	42.36	42.06	32.91	30.54	36.96	35.46
Mg	-	-	1.12	1.01	-	-	0.64	0.48
Cl	-	-	1.02	0.92	-	-	0.40	0.32
K	-	-	1.25	0.85	-	-	0.45	0.40
Ca	-	-	1.85	1.25	-	-	0.65	0.55
S	0.00	3.82	0.00	2.51	0.00	3.17	0.00	0.89
Total	100.00	100.00	100.00	100.00	100.00	100.00	100.00	100.00

Textural properties of NLP and PLP adsorbents were checked to understand their influence on the adsorption capacity of the adsorbent. N_2 Physio-sorption experiments were carried out and measured before and after adsorption experiments.

Results in Table 4.3 show that the surface area of PLP decreased from 94.16 m^2/g to 54.67 m^2/g, pore volume decreased from 0.185 cm^3/g to 0.088 cm^3/g and pore size decreased from 8.5 nm to 5.54 nm after the adsorption experiment. In the same vein, the surface area of NLP decreased from 73.21 m^2/g to 53.60 m^2/g, its pore volume decreased from 0.13 cm^3/g to 0.07 cm^3/g and its pore size reduced from 34 nm to 13.16 nm after the adsorption experiment. The observation indicates that some of the vacant adsorption sites of the adsorbents present before adsorption had been occupied with DBT molecules after the adsorption experiment.

Table 4.3: Textural properties of NLP and PLP before and after adsorption experiments

	PLP		NLP	
	Before adsorption	**After adsorption**	**Before adsorption**	**After Adsorption**
Surface area (m^2/g)	194.16	54.67	73.21	53.60
Pore volume (cm^3/g)	0.19	0.09	0.13	0.07
Pore size (nm)	8.50	5.54	34.00	13.16

Chemical functionalities of the adsorbents were checked as described in Chapter 3, in section 3.1.2 of this thesis. Fig. 4.3 shows the spectra of the raw PLP and the used PLP with different functional groups. The band located at 866 and 833 cm^{-1} is caused by C-H out-of-plane bending vibrations (Lua and Yang, 2004). The relatively pronounced band at 1231 cm^{-1} and a band at about 1020 cm^{-1} could be assigned to C–O stretching vibrations in alcohols, phenols, or ether or ester groups. The presence of a band at 1340 cm^{-1} can be ascribed to C–O stretching vibrations in carboxylate groups. The bands at around 1458 cm^{-1} and 1386 cm^{-1} correspond to the C–H in-plane bending vibrations in methyl and methylene group, while the band around 1617 cm^{-1} could be attributed to the stretching vibration of the aromatic ring or C═C (Eddebbagh et al., 2016). The peak at 1576 cm^{-1} is characterized by the C–C stretching of aromatic rings. The band around 1700 cm^{-1} is usually caused by the stretching vibration of C═O carboxyl groups. The spectra result show that a stretching has occurred after adsorption of DBT on the adsorbent, thereby causing the peak at 1729 cm^{-1} in the fresh PLP to be more pronounced and shifted to 1731 cm^{-1} after the adsorption (depicted with a red circle in Figure 4.3). The band at 2368 cm^{-1} is typically attributed to the C≡C stretching vibration of alkyne groups (Shaarani and Hameed, 2011; Ceyhan et al., 2013). The vibration of methyl and methylene could be observed at the bands located at 2936 cm^{-1} and 2858 cm^{-1}, respectively (Kaouah et al., 2013). Finally, the wide peak observed around 3332 cm^{-1} is usually attributed to hydroxyl groups or/and adsorbed water.

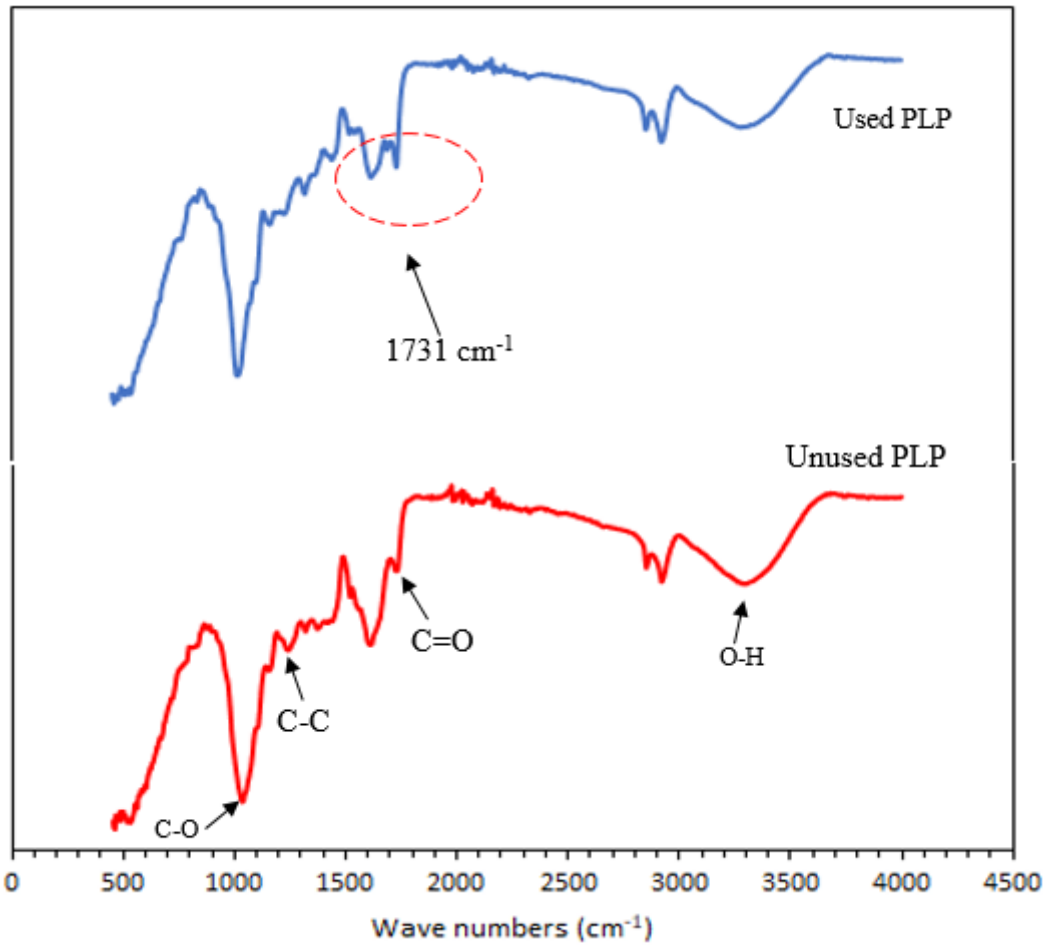


Figure 4.3 FTIR spectra showing chemical functionalities of PLP before use and PLP after use.

The FTIR spectra showing the functional groups in neem leaves powder before use and after use are shown in Fig. 4.4. The spectra indicated a peak at 1053 cm^{-1}, which corresponds to the stretching of C-O functional groups (Bharalia and Bhattacharyya, 2014). The existence of carbonyl (C-O) stretching vibration of amide groups from plant protein is indicated by the band at 1622 cm^{-1} The peaks observed at 1737 cm^{-1} correspond to the stretching vibration of carbonyl functional groups such as ketones, aldehydes and carboxylic acids. The band observed at 2927 cm^{-1} shows the existence of C-H stretching vibration of an aromatic aldehyde in neem powder as reported by

Noorjahan et al. (2015). The result also shows that, there was no chemical interaction between the adsorbent and the sulfur-containing compound in the model oil.

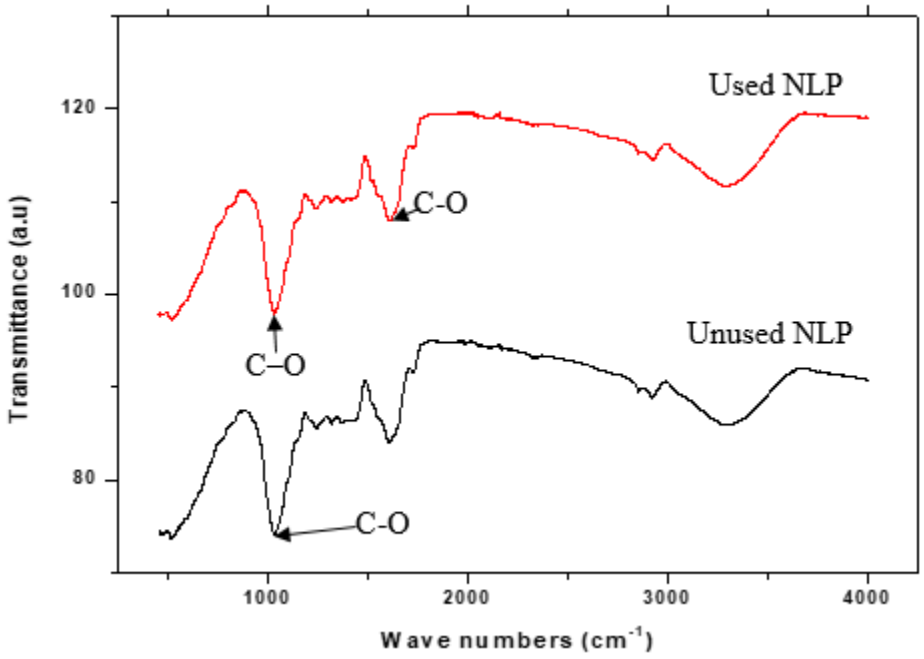


Figure 4.4 FTIR spectra showing the chemical functionalities of neem leaves powder before use and neem leaves powder after use.

4.3.2. Performance evaluation of PLP and NLP adsorbents during desulfurization

To understand the performance PLP and NLP adsorbents during desulfurization of DBT, effect of operating parameters on adsorption performance of the adsorbents for removal of DBT from the model oil was investigated. The detailed prodecure of this experiment is provided in Chapter 3 of this thesis.

Parametric effect of the operating variables such as contact time, amount of adsorbent, initial concentration of DBT and temperature on the removal efficiency of PLP and NLP was investigated. Fig 4.5 depicts the effect of contact time on the removal of DBT from the model diesel by PLP and NLP. The contact time was varied from 0-180 min, while all other parameters

such as the concentration (1000 mg/L), adsorbent amount (0.2 g) and temperature (30 ^{o}C) were kept constant. The results show that the intake of the DBT on the adsorbents surface was initially fast for the first 10 min during which about 30 % and 37 % of the DBT were adsorptively removed by NLP and PLP, respectively. This could be attributed to the large number of vacant sites on the adsorbent surface at the early stage of the adsorption process. Between 10 minutes and 60 minute the pace slowed down drastically due to the decrease in the number of adsorption sites on the surface of the adsorbent. The adsorptive removal reached equilibrium at 60 minutes during which the available adsorption sites on the surface of the adsorbent have been fully occupied with the DBT molecules, leaving no room for further adsorption. This observation is consistent with literature (Vadivelan and Kumar, 2005). At equilibrium, the adsorption capacity for PLP and NLP reached 39.8 mg/g and 53.46 mg/g, respectively. The nature of the adsorption behaviour of DBT onto the surface of the PLP and NLP (see Fig. 4.5) could indicate monolayer DBT coverage on the adsorbent surface as proposed by Namasiyayam (1993). The result showed that PLP adsorbent exhibited a higher adsorption performance compared to neem leaf adsorbent. This could be attributed to more adsorption sites available on the surface of PLP

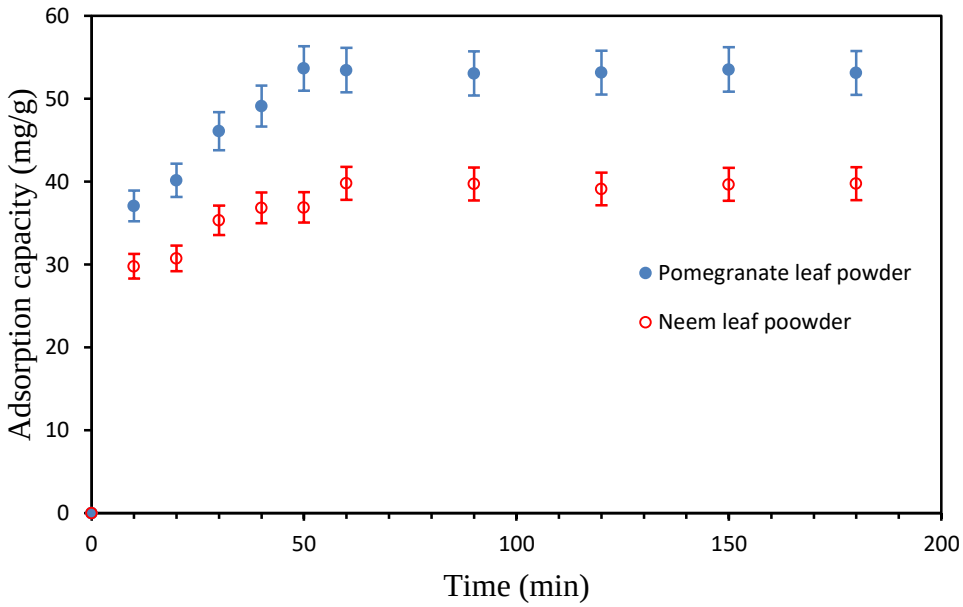


Figure 4.5. Effect of contact time on desulfurization by pomegranate leaf powder and neem leaves powder. Experimental conditions: Temperatures: 30 ^{o}C; Amount of adsorbents: 0.2 g/0.20 L model diesel; Initial DBT concentration: 1000 ppm.

Understanding effect of temperature during adsorptive desulfurization is essential to understanding the adsorption performance and mechanism of the adsorbent during the removal of DBT compounds from petroleum distillates. Effect of temperature on the performances of PLP and NLP as a function of contact time during the removal of DBT is depicted in Fig. 4.6 (a) for PLP and Fig. 4.6 (b) for NLP. Increase in temperature from 303 K to 308 K enhanced the adsorption efficiency of the adsorbent from 39.5 mg/g to 53.12 mg/g for PLP and 37.5mg/g to 39.8 mg/g for NLP. The increased adsorption capacity when the temperature was increase could be attributed to the broadening of adsorbent pores and formation of additional active sites on the adsorbent surface owing to cleavage of bond at higher temperature. These observations are in agreement with Betterman and Staudt (2009). Furthermore, the diffusion rate in the pore of adsorbent also increased with an increase in temperature (Ishaq et al., 2017). However, a decrease in adsorption efficiency from 53.12 mg/g to 31.01 mg/g with PLP adsorbent and from 39.8 mg/g to 33.8 mg/g with NLP was observed as the temperature further increased from 303 K to 308 K. This decrease could be attributed to weakening of the bonds between the DBT molecules and the active sites of pomegranate adsorbent (Ishaq et al., 2017).

Fig. 4.7 shows the effect of amount of adsorbent on the desulfurizing efficiency of PLP and NLP during removal of DBT from the model diesel when the amount of adsorbent was varied from 0.2-1.4 g. It could be seen that as the amount of adsorbent increase, the percentage removal of DBT also increased. This result could be attributed to an increase in available active adsorption sites accessible for the DBT. This is in agreement with literature (Srivastav and Srivastava, 2009; Daware et al., 2015; Ahmad et al., 2017). However, as the amount of PLP adsorbent increased from 1.0 to 1.4 g, there was no significant increase in the percentage removal. Also as the amount of NLP increased from 0.2 g to 0.8 g, the percentage DBT removal also increased. However, when the amount of adsorbent increased from 0.8 to 1.4 g, there was no further increase in DBT removal. This could be attributed to the inhibition of DBT onto the surface of PLP (Gonga et al., 2009; Marı´n-Rosas, 2010; Yasemin and Ayse, 2011). It could be observed that equilibrium was reached when amount of adsorbent was 1.0 g for PLP and 0.8 g for NLP adsorbent. These results show that the as-prepared PLP and NLP adsorbents could be employed as green adsorbents in the industry for removal of DBT from petroleum distillate, since the use of a small amount of the adsorbents could achieve about 70 % removal of DBT.

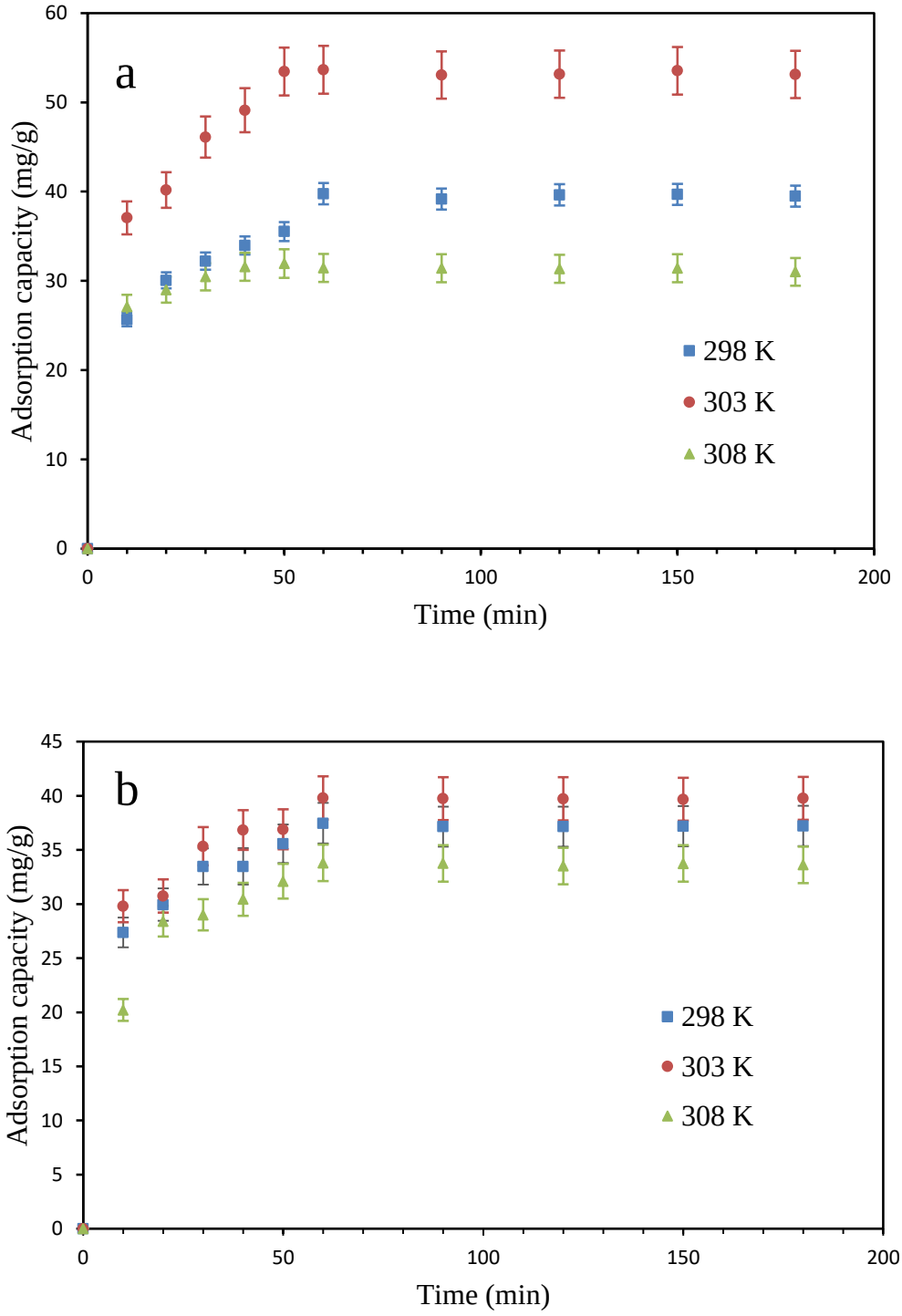


Figure 4.6. Effect of temperature on desulfurization of model petroleum distillate by (a) PLP adsorbent (b) NLP adsorbent. Experimental conditions: Amount of adsorbent: g/0.02 mL model diesel; Initial DBT concentration: 1000 mg/L.

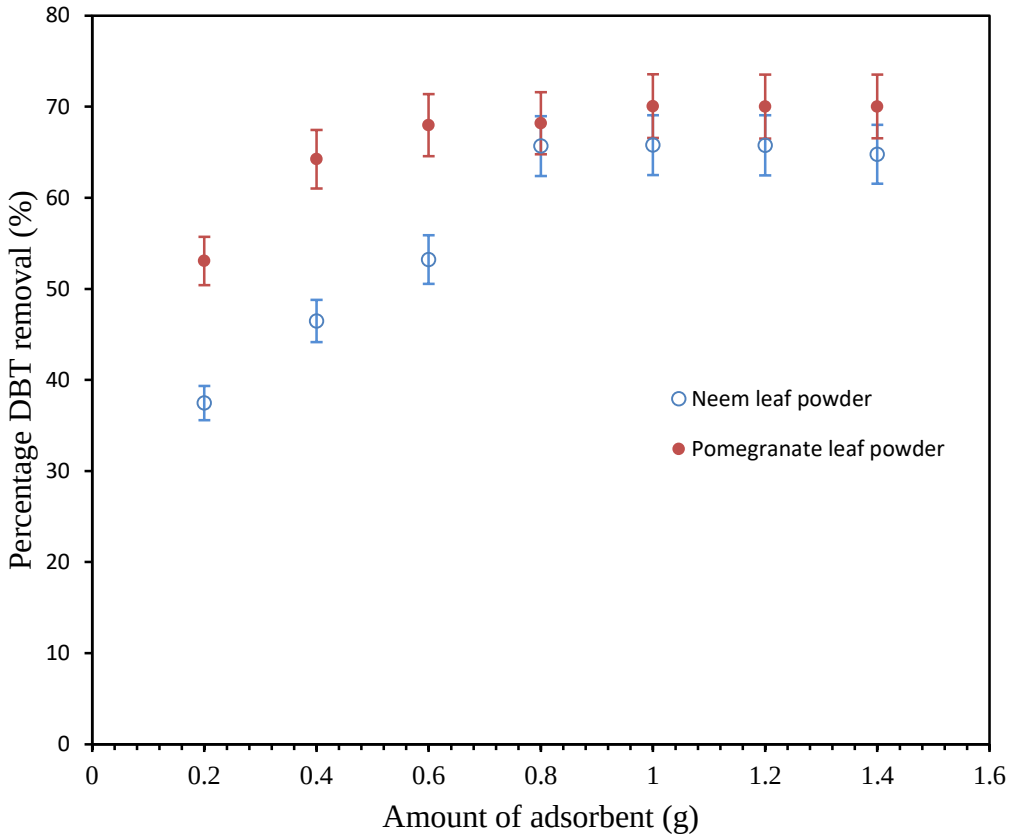


Figure 4.7. Effect of adsorbent amount on desulfurization of model oil by PLP and NLP at equilibrium temperature of 30 ^{o}C and varying adsorbent amount. Experimental conditions: Initial DBT concentration: 1000 mg/L; Temperature: 303 K.

Fig. 4.8 shows the effect of initial concentration of the model diesel on the adsorption efficiency of NLP and PLP. Effect of initial concentration on the adsorption efficiency was studied, because DBT concentration has an apparent effect on its removal from aqueous phase. The initial concentration of DBT was varied in the range 250-1000 mg/L while other variables such as temperature, adsorbent amount, and contact time were kept constant. Results show that the adsorption capacity of PLP (at equilibrium) increased from 2.73 mg/g to 14.11 mg/g with increase in the initial DBT concentration from 250 to 1000 mgL^{-1}. Also the adsorption capacity of NLP (at equilibrium) increased from 2.71 mg/g to 13.76 mg/g as the initial DBT concentration increased

from 250 mg/L to 1000 mg/L. This observation may be attributed to the high driving force for mass transfer at a high initial DBT concentration. Furthermore, if there is higher concentration of DBT in the solution, more DBT molecules will surround the active sites of adsorbents resulting in efficient adsorption. Therefore, results from this study confirm the explanation that adsorption increases with an increase in initial DBT concentration (Ishaq et al., 2017).

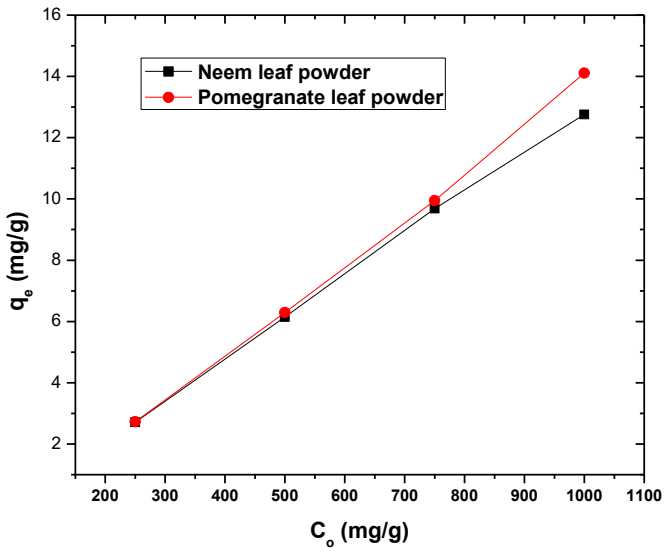


Figure 4.8. Effect of initial concentration on adsorption of DBT. Experimental conditions: contact time 60 min, stirring speed 130 rpm, amount of NLP and PLP adsorbent 1.0 g, and temperature 30 ^{o}C

4.4 Adsorption isotherms, kinetics and thermodynamics of PLP and NLP

After investigating the operating variables of the adsorption process, it is essential to understand the behavior of the adsorbents. Isotherm studies give information on the nature of the interaction between the adsorbents and the adsorbates. Thus, equilibrium data were analyzed using Langmuir and Freundlich isotherms. The results obtained are discussed:

Langmuir and Freundlich isotherm parameters for adsorption of DBT molecules onto PLP adsorbent are given in Table 4.4. Fig. 4.9 (a) and (b) depict the Freundlich isotherm for PLP and NLP respectively. Fig. 4.9 (c) and (d) depict the Langmuir isotherm for PLP and NLP, respectively.

It can be observed that adsorption of DBT onto PLP and NLP adsorbents were described well by both Langmuir and Freundlich isotherm models. They both have high coefficients of determination, R^2. (R^2) values for Langmuir isotherm and Freundlich isotherm model of PLP are 0.9952 and 0.9979, respectively. (R^2) values for Langmuir isotherm and Freundlich isotherm model of NLP are 0.9846 and 0.9881, respectively. The values of Langmuir separation factor, R_L which determines the favorability of the adsorption process for both PLP and NLP in Table 4.4 are 0.5 and 0.4, respectively. The values are below 1, indicating that adsorption process is favourable. The results show that the adsorption occured at specific homogeneous sites within the adsorbent creating monolayer DBT coverage at the surface of the PLP absorbent. This is in agreement with Wang and Wei (2017). The value of b in NLP, which reflects the activity of binding site is higher than the value of PLP. The values of adsorption intensity, n <1 for both NLP and PLP also indicate favorability of the adsorption process.

Table 4.4: Langmuir and Fruendlich Isotherm parameters

Adsorbents	**Langmuir Isotherm**				**Freundlich Isotherm**		
	Temp (K)	**R_L**	**b (L/mg)**	**R^2**	**K_f (mg/g)**	**n**	**R^2**
PLP	303	0.5	0.0010	0.993	0.0165	0.777	0.984
NLP	303	0.4	0.0015	0.985	0.0044	0.732	0.988

Where b is the Langmuir's constant, reflecting the activity of the binding site, K_f is the Freundlich's constant, n is the adsorption intensity and R is the coefficient of determination, R_L is the Langmuir separation factor.

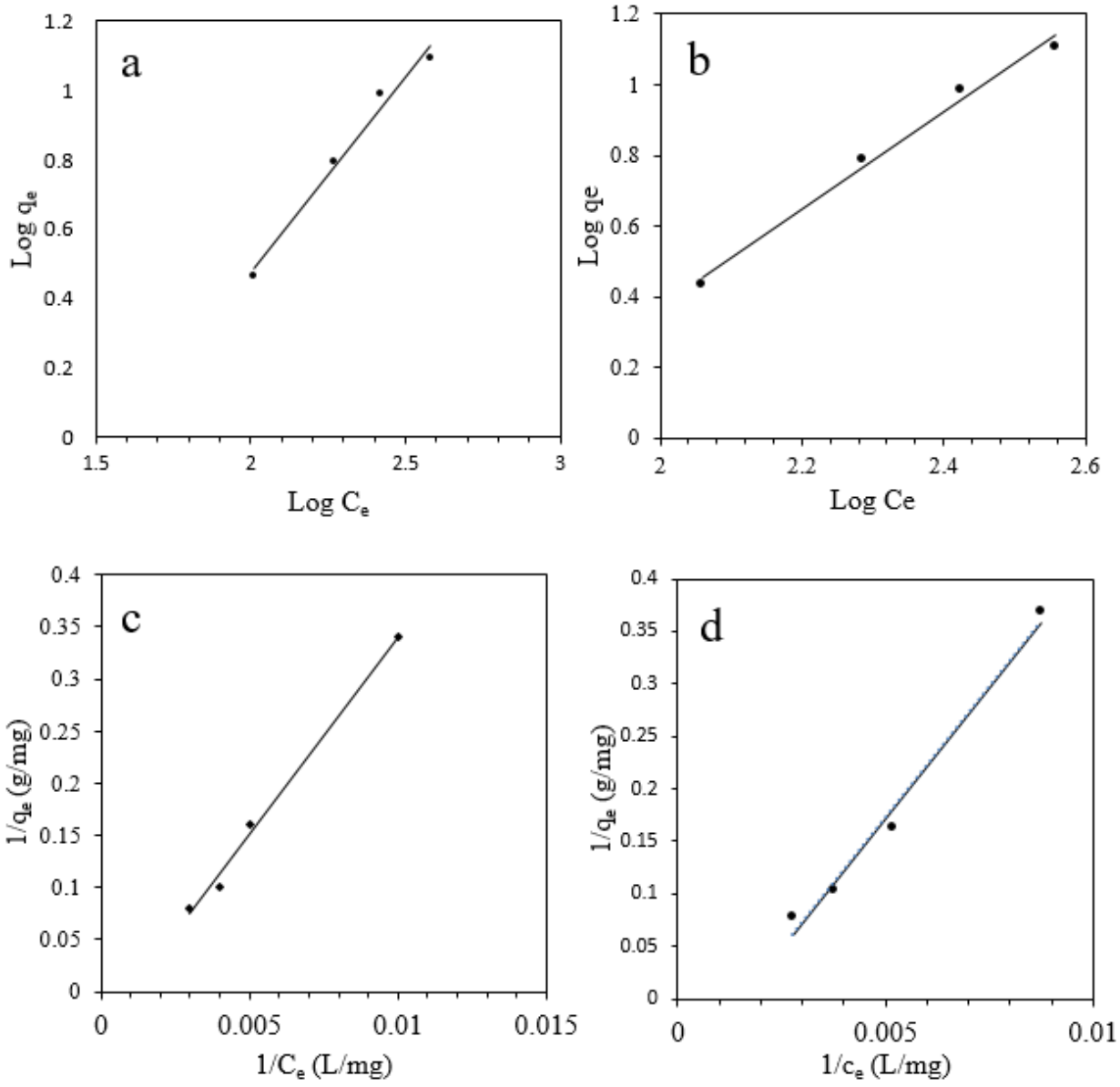


Figure 4.9. Freundlich isotherm model for (a) PLP (b) NLP and Langmuir isotherm model for (c) PLP (d) NLP. Experimental conditions: Initial DBT concentrations: 250-1000 mg/L; Temperature: 303 K, Amount of adsorbent: 1.0 g.

Kinetic studies provide information on the mechanism and the pathways of the adsorption interactions. Therefore, pseudo first and pseudo second-order kinetic models were used in this study and the results obtained are discussed.

Table 4.5 shows the parameters for pseudo first-order and pseudo second-order kinetics of DBT adsorption onto PLP and NLP. Comparing the coefficient of determination (R^2) of the kinetic models of PLP, the pseudo second-order model described the adsorption process well compared to pseudo first-order kinetic model. In addition the experimental q_e (33.65 mg/g) values obtained for pseudo-second order kinetics are very close to the calculated q_e (33.57 mg/g) compared to what were obtained for the experimental q_e (33.65 mg/g) and calculated q_e (23.44 mg/g) for the first-order kinetics (Table 4.5). Also, for NLP adsorbent, the correlation coefficients were higher in pseudo-second order kinetics (0.9992, 0.9991 and 0.9989) compared to pseudo first-order (0.8349, 0.8857, and 0.857) at 298, 303 and 308 K, respectively. The kinetic model value for q_e calculated (37.46 mg/g) was very close to experimental value obtained for q_e (38.46 mg/g) for psedo second-order kinetics. However, the model value calculated for q_e (38.46 mg/g) is lower than the value obtained in the experiment (10.69 mg/g) for pseudo first-order kinetics. It could be assumed that there were involvements of chemical interactions in the adsorption process. In addition, the adsorption rate may be controlled by the movement of DBT molecules in the pores of the PLP adsorbent. The result obtained in this study is similar to what was reported by Wang and Wei (2017). Lower correlation coefficient factor for pseudo first-order could be an indication that the rate of adsorption process is not dependent on concentration factor, but on both concentration and time. This is in agreement with Kumar and Tamilarasan (2017)

Table 4. 5: Kinetic model parameters for pseudo first and pseudo second-order adsorption model

Temp (K)	**Pseudo 1st-order (PLP)**				**Pseudo 2nd-order (PLP)**			
	$q_{e(expt)}$ (mg/g)	**$q_{e(calc.)}$ (mg/g)**	**K_1 (L/min)**	**R^2**	**$q_{e\ (expt)}$ (mg/g)**	**$q_{e\ (calc.)}$ (mg/g)**	**K_2 (g/mg.min)**	**R^2**
298	38.18	25.36	0.047	0.8349	38.18	40.49	0.0028	0.9999
303	53.66	33.07	0.0474	0.8857	53.66	55.55	0.0025	0.9959
308	33.65	23.44	0.0481	0.857	33.65	33.57	0.0035	0.9922
Temp (K)	**Pseudo 1st-order (NLP)**				**Pseudo 2nd-order (NLP)**			
	$q_{e(expt)}$ (mg/g)	**$q_{e(calc.)}$ (mg/g)**	**K_1 (L/min)**	**R^2**	**$q_{e\ (expt)}$ (mg/g)**	**$q_{e\ (calc.)}$ (mg/g)**	**K_2 (g/mg.min)**	**R^2**
298	38.46	10.69	0.0026	0.8349	38.46	37.46	0.0082	0.9992
303	39.80	14.78	0.0380	0.8857	39.80	39.80	0.0071	0.9991
308	33.80	6.76	0.0280	0.857	33.80	33.80	0.0078	0.9989

q_e is the amount of DBT adsorbed at equilibrium, R^2 is the coefficient of determination, K_1 is the pseudo first-order constant and K_2 is the pseudo second-order constant.

In order to understand the spontaneity and nature of the adsorption process, thermodynamics of the adsorption process were studies. The results obtained are discussed as follow;

The values of adsorption thermodynamics parameters, standard free energy ΔG^o, standard entropy, ΔS^o and and standard enthalpy, ΔH^o for PLP and NLP adsorbents are presented in Table 4.6. The negative values of ΔG^o and the positive values of ΔH^o indicate that DBT adsorption onto PLP and

NLP are spontaneous and endothermic in nature. Positive ΔS^o values of DBT adsorption process indicate an increase of the randomness at the PLPand NLP-solution interface during adsorption. This is in agreement with Fei et al. (2017) and Saini et al. (2017).

Table 4.6: Themothynamic parameters for adsorption of DBT on PLP and NLP

Adsorbent	**Temp.(K)**	***Δ*H (J/mol)**	***Δ*G (kJ/mol)**	***Δ*S (J/k/mol)**
PLP	298	+ 872.97	- 10.21	+37.21
	303		-11.97	+42.39
	308		-10.05	+35.38
NLP	298	+ 2036.9	- 10.14	+40.87
	303		-13.077	+49.88
	308		-10.069	+39.30

4.5 Regeneration and re-usability of PLP and NLP

To make NLP and PLP commercially suitable, there is need to carry out the re-usability process. About 0.25 g of NLP and PLP were mixed with 10 mL of solvent (hexane) and were stirred at 40^{o}C at 130 rpm for 5hrs. Hexane was used in this study as solvent, due to the favourable hydrophobic interactions with adsorbed DBT. Hexane has boiling point of 70^{o}C, therefore desorption was done at 40^{o}C to avoid boiling (Safieh et al., 2015). The same process was done three consecutive times until the adsorbent was back to its original state. Adsorption experiments were conducted at 30 ^{o}C, for 1 h with 1.0 g of adsorbents. The experiment was carried out in four

cycles. Initial and final concentration of the used adsorbent was analysed by HPLC. The results showed that the both NLP and PLP still retained their desulfurization capacities until the 4th cycle (Fig. 4.10). The percentage desulfurization of neem leaves powder decreased by 8.13 % at the fourth cycle and PLP decreased by 0.04 % which is negligible. This could be as a result of blocked adsorption sites by DBT after repeated use of the adsorbent. It could also be possible that the structure has been damaged with time, which prevented it from adsorbing DBT further. This however, indicated that NLP and PLP can be re-used four times before it slightly loses its adsorption efficiency for removing DBT compound from the model diesel. Therefore, NLP and PLP can be of great value for commercial application since they can be re-used up to four times without losing their efficiency of removing DBT from petroleum distillate.

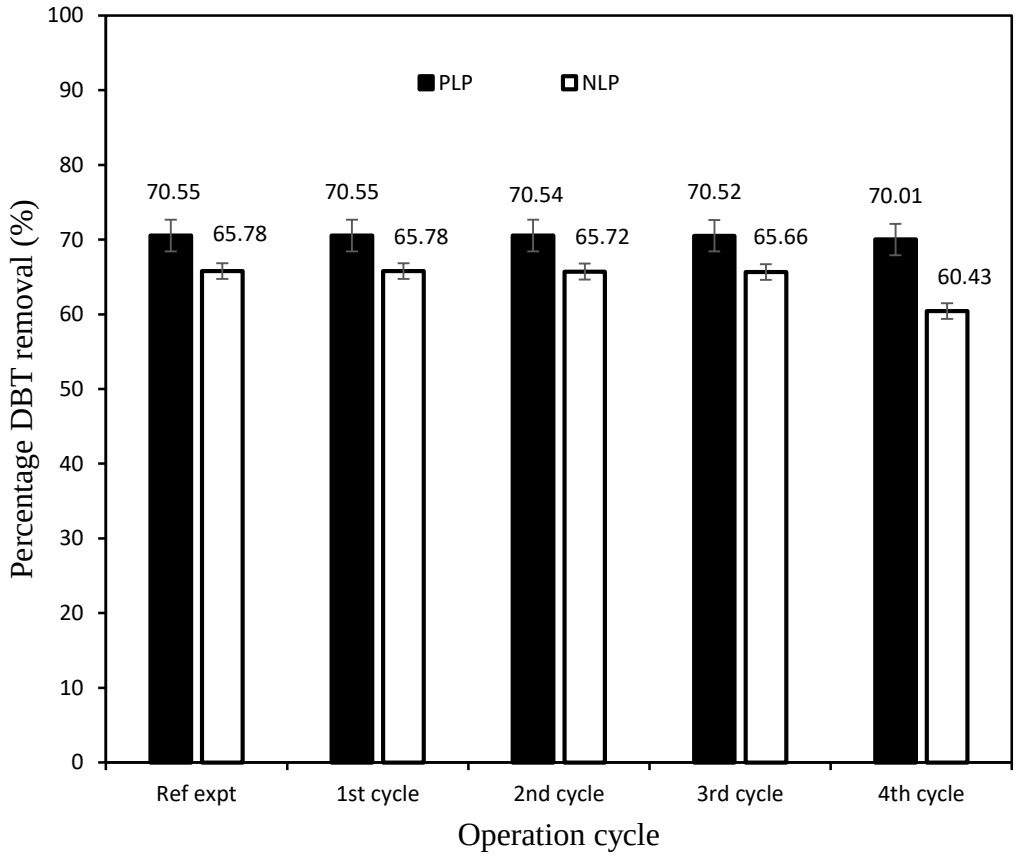


Figure 4.10. Re-usability potential of PLP and NLP. Experimental conditions: Amount of adsorbent: g/0.02 L model diesel; Temperature: 303 K; Initial DBT concentration: 1000 mg/L.

Table 4.7 shows the comparison of results of this study with literature. According to Table 4.7, Zinc impregnated on MMT clay was reported for the removal of DBT from model oil by Ahmad et al. (2017) and 81% of the DBT was removed at 25 ^{o}C when the initial concentration was 1000 mg/L. In addition, about 92 % DBT removal was reported by Anisuzzaman et al. (2017) when activated palm shell (APC) was used as the adsorbent. Percentage removal of DBT as reported by Ahmad et al. (2017) and Anisuzzaman et al. (2017) are about 81 % and 91 %, respectively. These results are higher than the percentage DBT removal obtained in this study for PLP (70.55 %) and NLP (65.68 %). The observable increase in the result of Ahmad et al. (2017) could be attributed to the surface modification of MMT clay with Zn and in the case of Anisuzzaman et al. (2017), the higher percentage DBT removal could be due to the high surface area of the APC. However, it is noteworthy to mention that the amount of adsorbent used by Ahmad et al. (2017) was 50 % more than what was used in this study for both adsorbents. It is expected that if the surface of the PLP and NLP are modified and the amount of the modified PLP and modified NLP is increased by 50 % (from 1.0 g used in this study to 1.5 g in the case of PLP and 0.8 g to 1.2 g in the case of NLP), adsorbents used in this study might out-perform the modified MMT clay.

Furthermore, it could be seen from Table 4.7 that DBT removal efficiency of the PLP and NLP are better than others reported in literature. For instance, about 44 % DBT removal was reported by Nazal et al. (2016) when CNTs impregnated with 15 % Ni was used as an adsorbent and the initial DBT concentration in their study was 4 times lower than what was used in this study (250 mg/L compared to 1000 mg/L). Nazal et al. (2016) also impregnated about 15 % Ni on AC to remove DBT from model oil. The result showed that desulfurization capacity of 76.4 % was achieved. Comparing their results with results obtained in this study, the activated carbon (76.4 %) out-performs the NLP and PLP by 10 % and 6 %, respectively. The better performance of the activated carbon used by Nazal et al. (2016) could be attributed to the higher surface area of the activated carbon. Moreover, a lower initial concentration of 250 ppm was used by the authors and this is 75 % lower than the concentration used in this study. Therefore, it cannot be concluded that the adsorbent used by Nazal et al. (2016) is capable of removing DBT at a higher initial concentration.

Daware et al. (2015) investigated on the performance of NLP for desulfurization of real diesel. About 65 % percentage DBT removal was achieved at initial DBT concentration of 20 mg/L. Comparing the result (65 % DBT removal) with what was obtained for NLP in this study, it can be observed that result of this study out-performed the result obtained in Daware et al. (2015). Considering the initial DBT concentration (20 mg/L) used by Daware et al. (2015) and the initial DBT concentration used in this study (1000 mg/L). The lower result obtained in Daware et al. (2015) despite lower initial DBT concentration could be as a result of many compounds of sulphur present in real diesel. Therefore, there might be a problem with selectivity of DBT removal. However, model diesel was used in this study which could be attributed to better performance of NLP in this study for removal of DBT compound.

Conclusively, it could be said that the performances of the PLP and NLP investigated in this study for the removal of DBT are comparable with results reported in literature. As far as could be ascertained, this is the first report on the use of PLP as an adsorbent for the desulfurization of petroleum distillate and the first report on the application of NLP for DBT model oil. Results documented in this study could provide a platform for further research efforts in this field.

Table 4.6: Results of this study compared with literature

Adsorbent	Model oil	Amount of ads.(g)	Time (min)	Temp (ºC)	C_o (mg/ L)	C_f (mg/L)	% SR	Ref.
Zn-MMT	DBT	1.50	60.0	25.0	1000	1.50	81.00	Ahmad et al. (2017)
Bentonite	DBT	0.05	160.0	25.0	100	2.00	98.00	Ishaq et al. (2017)
APC	BT	0.10	35.0	25.0	10	0.85	91.50	Anisuzzaman et al. (2017)
MSi	DBT	0.02	60.0	25.0	1000	825.00	17.5	Anbia and Karami (2015)
NLP	Diesel	0.25	0.1	65.0	20	3.50	2.00	Daware et al. (2015)
AC/15Ni	DBT	250	59.0	76.4	25	2.00	0.15	Nazal et al. (2016)
CNTs/15Ni	DBT	0.75	120.0	25.0	250	141.50	43.40	Nazal et al. (2016)
AC/γ-Fe_2O_3	DBT	0.08	60.0	25.0	600	320.00	46.67	Fayazi et al. (2015)
PLP	DBT	1.00	60.0	30.0	1000	294.50	70.55	This study
NLP	DBT	0.80	60.0	30.0	1000	342.2	65.78	This study

% SR: Percentage sulfur (DBT) removal; PLP: pomegranate leaf powder; APC: Activated palm shell; Msi: Mesoporous silica; Zn-MMT: Zinc impregnated on montmorollonite (MMT) clay; AC: activated carbon; CNTs/15Ni, AC/15Ni: 15 % Nickel on Carbon nanotubes and Activated carbon, respectively

4.6. Concluding remarks

As it has been established in this chapter, that NLP and PLP are promising candidates for removal of sulfur containing compound (DBT) from petroleum distillate (e.g diesel). As far as it can be ascertained, no study has been conducted on the use of PLP for removal of DBT from petroleum distillate. This chapter successfully investigated the adsorption performance of PLP and NLP for removal of DBT compound from model oil under different operating conditions. The best operating conditions for the adsorption process for each adsorbent were determined. Equilibrium was attained at 60 minutes for both adsorbents at 30 ^{o}C and 1.0 g PLP and 0.8 g NLP. The results also show that PLP out-performed NLP by 9.88 %. The adsorption mechanism of the adsorbent was extensively described by Langmuir and Freundlich isotherm models. The kinetics of the adsorption process was described by pseudo first-order and pseudo second-order. The adsorption kinetics for PLP and NLP were well described by pseudo second order. The negative values of ΔG^{o} and the positive values of ΔH^{o} indicate that DBT adsorption onto PLP and NLP are spontaneous and endothermic in nature. Positive ΔS^{o} values of DBT adsorption process indicate an increase of the randomness at the PLPand NLP-solution interface during adsorption.

Based on the outcome of the study documented in this chapter, it can be concluded that NLP and PLP are promising adsorbents for the removal of DBT from petroleum distillate (diesel), to meet up with the stringent policies regarding emission of sulfur oxides. The information in this chapter therefore provides a platform for further studies in this field. For quick dissemination of the novel contributions described in this chapter to the scientific community, two manuscripts are under review in a reputable journal and one has been published in Chemical Enginering Communications.

4.7. References

Achmann, S., Hagen, G., Hammerle, M., Malkowsky, I., Kiener, C., Moos, R. (2010) Sulfur removal from low-sulfur gasoline and diesel fuel by metal-organic frameworks. Chem Eng Technol., 33, 275–280.

Agamuthu, P. (2009) Challenges and opportunities in Agro waste management: An Asian perspective. Inaugural meeting of First Regional 3R Forum in Asia 11 -12 Nov., Tokyo, Japan. 2009.

Ahmaruzzaman, M. and Gupta, V.K. (2011) Rice Husk and Its Ash as Low-Cost Adsorbents in Water and Wastewater Treatment Ind. Eng. Chem. Res. 50, 13589–13613.

Ahmad, W., Ahmad, I. and Ishaq, M. and Ihsan, K. (2017) Adsorptive desulfurization of kerosene and diesel oil by Zn impregnated montmorollonite clay. Arabian Journal of Chemistry. 10 (2), S3263-S3269.

Al-Zubaidy, I. A. H. Tarsh, F.B., Darwish, N.-N., Majeed, Balsam S. S. A., Al-Sharafi, A. and Chacra, L.A. (2013) "Adsorption Process of Sulfur. Removal from Diesel Oil Using Sorbent.Journal of Clean Energy Technologies, 1(1), 66-68.

Anbia, M. and Karami. S. (2015) Desulfurization of gasoline using novel mesoporous carbon adsorbents. Nanostruct Chem 5, 131–137

Anisuzzaman, S. M., Abang, S., Krishnaiah, D. and Razlan, M.A.R. (2017) Adsorptive desulfurization of model fuel by activated oil palm shell. Indian Journal of Chemical Technology. 24, 206-212.

Babich, I. and Moulijn (2003) Science and Technology of Novel Processes for Deep Desulfurization of Oil Refinery Streams A Review. J. Fuel, 82, 607-631.

Bettermann, I. and Staudt, C. (2009) Desulfurization of kerosene pervaporation of benzothiophene/n-dodecane mixture, J. Membr. Sci. 343, 119–127.

Bharalia, K. R., Bhattacharyya, G.K. (2014). Kinetic and thermodynamic studies on fluoride biosorption by devdaru (polyalthia Longifolia) leaf powder, Oct. Jour. Env. Res. 2 (1), 22-31

Bhattacharjee, R. and Patel, R. (2017) Adsorption of chromium (vi) using neem leaves and pomegranate peels. Journal of Emerging Technologies and Innovative Research (JETIR), 4 (5)

Ceyhan, A.A., Sahin, Ö., Baytar, O. and Saka, C. (2013) Surface and porous characterization of activated carbon prepared from pyrolysis of biomass by two-stage procedure at low activation temperature and it's the adsorption of iodine. Journal of Analytical and Applied Pyrolysis 104, 378-383. J. Anal. Appl. Pyrol. 104, 378-383.

Daware, G.B., Kulkarni, A. B. and. Rajput, A. A. (2015) Desulphurization of diesel by using low cost adsorbent, International Journal of Innovative and Emerging Research in Engineering. 2 (6), 69-73.

Deniz, F. (2013) Adsorption Properties of Low-Cost Biomaterial Derived from Prunus amygdalus L. for Dye Removal from Water. The Scientific World Journal Volume 2013, Article ID 961671. 1-8

Eddebbagh, M., Abourriche, A., Berrada, M., Zina, M.B. and Bennamara, A. (2016) Adsorbent material from pomegranate (Punica granatum) leaves: Optimization on removal of methylene blue using response surface methodology. J. Mater. Environ. Sci. 7 (6), 2021-2033.

Fallah, R. and, Azizian, S. (2012) Rapid and facile desulphurization of liquid fuel by carbon nanoparticles dispersed in aqueous phase. Fuel 95, 93–96

Fallah, R.N. and Azizian, S. (2014) Removal of thiophenic compounds from liquid fuel by different modified activated carbon cloths. Fuel 93, 45–52

Fayazi, M., Taher, M.A., Afzali D. and Mostafavi, A. (2015) Removal of Dibenzothiophene Using Activated Carbon/γ-Fe2O3 Nano-Composite: Kinetic and Thermodynamic Investigation of the Removal Process Anal. Bioanal. Chem. Res., 2 (2), 73-84.

Fei, L. Rui, J., Wang, R., Lu, Y. and Yang, X. (2017). Equilibrium and kinetic studies on the adsorption of thiophene and benzothiophene onto NiCeY zeolites. loloo, 7, 23011-23020

Gawande, P. R and Dr. Kaware J. P. (2018). Isotherm and Kinetics of Desulphurization of Diesel by Batch Adsorption Studies International Journal of Chemical Engineering Research. 10 (1), 1-16

Ghaneian, M., Jamshidi, B., Dehvari, M.and Amrollahi, M. (2015) Pomegranate seed powder as a new biosorbent of reactive red 198 dye from aqueous solutions: adsorption equilibrium and kinetic studies. IsRes Chem Intermed. 41, 3223–3234.

Gonga, J., Wanga, B., Zenga, G., Yanga, C., Niua, C., Niua, Q., Zhoua, W. and Liang. Y. (2009) Removal of cationic dyes from aqueous solution using magnetic multi-wall carbon nanotube nanocomposite as adsorbent. Journal of Hazardous Materials 164, 1517–1522.

Ho, Y.S. and McKay, G. (1999) Pseudo-second order model for sorption processes. Process Biochem. 34, 451–465.

Ishaq, M., Sultan, S., Ahmad, I., Ullah, H., Yaseen, M. and Amir, A. (2017) Adsorptive desulfurization of model oil using untreated, acid activated and magnetite nanoparticle loaded bentonite as adsorbent Journal of Saudi Chemical Society. 21 (2), 143-151.

Kaouah, F., Boumaza, S., Berrama, T., Trari, M. and Bendjama, Z. J. (2013) Preparation and characterization of activated carbon from wild olive cores (oleaster) by H3PO4 for the removal of Basic Red 46. Clean. Prod. 54, 296-306.

Kertesz, M.A. and Wirtek, C. (2001) Desulfurization and desulfonation: Application of sulphur-controlled gene expression in bacteria. Appl. Microbiol. Biotechnol., 57, 460–466

Khan, N.A. and Jhung, S.H. (2013) Effect of central metal ions of analogous metal-organic frameworks on the adsorptive removal of benzothiophene from a model fuel. J Hazard Mater, 260, 1050–1056

Kumar and Tamilarasan (2017) Kinetics, equilibrium data and modeling studies for the sorption of chromium by Prosopis juliflora bark carbon Arabian Journal of Chemistry, 10, S1567–S1577

Lagergren, S. (1898) Zur theorie der sogenannten adsorption gelo ster stoffe. Kungliga Svenska Vetenskapsakademiens Handlingar, 24, 1–39

Lua, A.C. and Yang, T. (2004) Effects of vacuum pyrolysis conditions on the characteristics of activated carbons derived from pistachio- nut shells. J. Colloid. Interf. Sci. 276, 364-372

Md. Ahmed, J. K. and Ahmaruzzaman, M. (2015) Adsorptive desulfurization of feed diesel using chemically impregnated coconut coir waste Int. J. Environ. Sci. Technol. 12, 2847–2856

Marı´n-Rosas, C., Ramı´rez-Verduzco, L. F., Murrieta-Guevara, F. R., Herna´ndez-Tapia, G. and Rodrı´guez-Otal. L. M. (2010) Desulfurization of Low Sulfur Diesel by Adsorption Using Activated Carbon: Adsorption Isotherms. Ind. Eng. Chem. Res. 49, 4372–4374.

Moosavi, E. S., Dastgheib, S.A. and Karimzadeh, R. (2012) "Adsorption of Thiophenic Compounds from Model Diesel Fuel Using Copper and Nickel Impregnated Activated Carbons "Energies, pp. 4233- 4250.

Namasivayam, C., Kanchana, N. and Yamuna, R.T. (1993) Waste banana pith as adsorbent for the removal of rhodamine-B from aqueous solutions. Waste Manage. 13, 89–95.

Nazal, M.K., Oweimreen, G.A., Khaled, M., Atieh, M.A., Aljundi, I.H. and Abulkibash, A.M. (2016) Adsorption isotherms and kinetics for dibenzothiophene on activated carbon and carbon nanotube doped with nickel oxide nanoparticles. Bull. Mater. Sci., 39 (2), 437–450.

Noorjahan, C.M., Jasmine, S.K., Deepika, T., Rafiq, S. (2015) Green synthesis and characterization of zinc oxide nanoparticles from neem (Azadirachta indica), Int. J. Sci. Eng. Technol. Res. 4, 5751-5753.

Prabhu, M., Priscillia, S. R., Karitha, K., Manivasakan, P., Raj endian, V. and Kulandaivelu, P. (2014) Invitro bioactivity and anti-microbial tuning of bioactive glass nanoparticles added with

neem leaf powder. BioMed Research International. 2014, Article ID 950691, 1-10 http://dx.doi.org/10.1155/2014/950691

Sadare, O.O., Obazu, F and Daramola, M.O. (2017) Biodesulfurization of Petroleum Distillates—Current Status, Opportunities and Future Challenges. Environments, 4(4), 85- 104.

Safieh, K.A.A., Al-Degs, Y.S., Sanjuk, M.S., Saleh, A.I. and Al-Ghouti, M.A. (2015) Selective removal of dibenzothiophene from commercial diesel using manganese dioxide-modified activated carbon: a kinetic study. Environmental Technology. 36 (1-4), 98-105

Saini, S., Kumar, R., Chawla, J., Kaur, I. (2017) Punica granatum (pomegranate) carpellary membrane and its modified form used as adsorbent for removal of cadmium (II) ions from aqueous solution. DOI: 10.2166/aqua.2017.026

Salem, A.B.S.H. and Hamid, H.S. (1997) Removal of sulfur compounds from naphtha solutions using solid adsorbents, Chem. Eng. Technol., 20, 342-347

Shaarani, F.W. and Hameed, B.H. (2011) Ammonia modified activated carbon for the adsorption of 2, 4-dichlorophenol. Chem. Eng. J. 169, 180-185.

Srivastav, A. and Srivastava, V. C. (2009) "Adsorptive desulfurization by activated alumina," Journal of Hazardous Materials, 170 (2-3), 1133–1140,

Vadivelan, V., Kumar, K.V. (2005) Equilibrium, kinetics, mechanism, and process design for the sorption of methylene blue onto rice husk. J. Colloid Interf. Sci. 286, 90–100

Wu, L., Xiao, J., Xian, Y. S. K., Miao, G., Wang, H.H. and Li. Z. (2014) A combined experimental/computational study on the adsorption of organosulfur compounds over metal-organic frameworks from fuels. Langmuir, 30 (4), 1080-1088

Xiao, J., Li, Z., Liu, B., Xia, Q. and Yu, M. (2008) Adsorption of benzothiophene and dibenzothiophene on ion-impregnated activated carbons and ion-exchanged Y zeolites. Energy Fuels 22, 3858–3863.

Wang, J. and Wei, J. (2017) Selective and simultaneous removal of dibenzothiophene and 4-methyldibenzothiophene using double-template molecularly imprinted polymers on the surface of magnetic mesoporous silica Journal of Materials Chemistry A. 5, 4651-4659.

Yasemin, K. and Ayse, A.Z. (2011) Adsorption characteristic of the hazardous dye Brilliant Green, Chem. Eng. J. 172, 199– 206.

Zhou, A., Ma, X. and Song, C. (2009) Effects of oxidative modification of carbon surface on the adsorption of sulfur compounds in diesel fuel. Appl Catal B Environ, 87, 190–199.

Chapter Five

5.0 Performance of functionalized carbon nanotubes during desulfurization

In this chapter, the results of effect of operating variables on the performance of functionalized carbon nanotubes, during adsorptive desulfurization of model diesel are presented. The results of studies of isotherms, kinetics and thermodynamics of the adsorption process are also reported

5.1 Introduction

Adsorption has been considered as a promising option for desulfurization of sulfur compounds (DBT) in petroleum distillates. It has been employed by many researchers because it is relatively cheap and can be carried out at ambient temperature and pressure. (Moosavi et al., 2012; Gawande and Kaware, 2018). Furthermore, there is possibility of adsorbents regeneration and reusability (Ahmed and Ahmaruzzaman, 2015). Various adsorbents have been used by different researchers to remove sulfur containing compounds from transportation oil such as activated carbon (Zhou et al., 2009), carbon nanotubes (Saleh et al., 2014), zeolite (Xiao et al., 2008), bentonites and montmorillonite clay (Ahmad et al., 2017), and palm kernel shell (Al Zubaidy et al., 2013). Commercial activated carbon among others has been widely used as adsorbent because of its efficiency which is as a result of its improved micro structures (Eddebbagh et al., 2016). Nevertheless, its processing and application are expensive (Ahmed and Ahmaruzzaman, 2015).

CNTs have received a huge attention due to their chemically inert surfaces for physical adsorption, and their high specific surface areas with a strong Van der Waals binding energy for molecular adsorbates on well-defined adsorption. CNTs have more well-defined and uniform surfaces compared to activated carbon (AC) at the atomic scale. CNTs adsorption capacity can be quantified directly with the available adsorption sites, however efficiency of AC depends on the pore diameter distribution in order to quantify its adsorption properties. CNTs have been widely investigated owing to their extremely porous and hollow structures, high specific surface area, and their strong interaction with organic molecules. Khaled (1986) studied the adsorption performance of MWCNTs and graphene oxide (GO) for removal of thiophene and dibenzothiophene in model

diesel. Saleh et al., (2014) also investigated on the removal of DBT from model oil using a novel nanomaterial of multiwalled carbon nanotubes doped with Titania (CNT/TiO_2). Furthermore, DBT adsorption on CNTs supported by C_oM_oS/HDS catalyst was investigated by Chen et al. (2004). In order to improve the adsorption capacity of CNTs, the surface area needs to be modified. This can be achieved via acid treatment which purifies and causes attachment of functional group that enhances the adsorption of the organic molecule onto the surface of the adsorbent (Saleh et al., 2014). Only few studies have been conducted on the application of modification of CNTs surface by acid treatment for the removal of sulfur-containing compound from diesel. Therefore, for the first time, this study investigates the adsorptive desulfurization of model diesel, using acid treated carbon nanotubes as the adsorbent. The effect of surface modification on the desulfurization performance of CNTs was equally investigated. Furthermore, potential re-usability performance of CNTs and FCNTs was studied due to growing concern for waste minimization, recovery, and reuse as well as for industrial applications. To understand the mechanisms and nature of interaction between adsorbent and adsorbates, kinetics, isotherms and thermodynamics studies of the adsorbents are presented as well.

5.2. Experimental

The materials, the adsorbents preparation, adsorbent characterization and the detailed description of the experimental procedures are provided in Chapter three (i.e Section 3.1.1. to 3.1.3) of this thesis. Evaluation of performance of the adsorbents during desulfurization has been described in Chapter three (Section 3.1.2) of this thesis as well. However, the operating conditions used for experimentas described in this chapter are the same as those provided in Table 4.1 of this thesis. In addition, the procedures for the regeneration of adsorbent were described in Chaper three of this thesis.

5.3. Results and discussion

5.3.1 Physico-chemical characterization of CNTs and FCNTs

The surface morphology and elemental composition of the adsorbents were checked following the steps described in chapter 3 of this thesis. The Fig. 5.1 (a) and (b) show the surface morphology of CNTs and FCNTs, respectively. It can be observed that, there were agglomerates and bundles of CNTs clusterring together before functionalization. However, after acid-treatment the surface morphology of the FCNTs were well dispersed and spread out with much gaps between them compared to untreated CNTs. This could enhanced the adsorption surface of the purified CNTs therefore improving the adsorption capacity (Ishaq et al., 2017)

Table 5.1 depicts the elemental composition of carbon nanotubes (CNTs) and functionalized carbon nanotubes (FCNTs) before and after adsorption. The result in Table 5.1 show that CNTs consists of 97.28 % and 93.75 % of carbon before adsorption and after adsorption, respectively. It could be seen from Table 5.1 that the carbon content has been reduced from 97.28 to 90.88 % FCNTs contained 90.88 % after functionalization. This could be attributed to oxidation of the carbon nanotubes by acid treatment. The results agree with the observation of Deborah et al. (2014). In addition, it was observed that presence of sulfur was noticed after adsorption process for both adsorbents, indicating that DBT was adsorbed onto the surface of adsorbent.

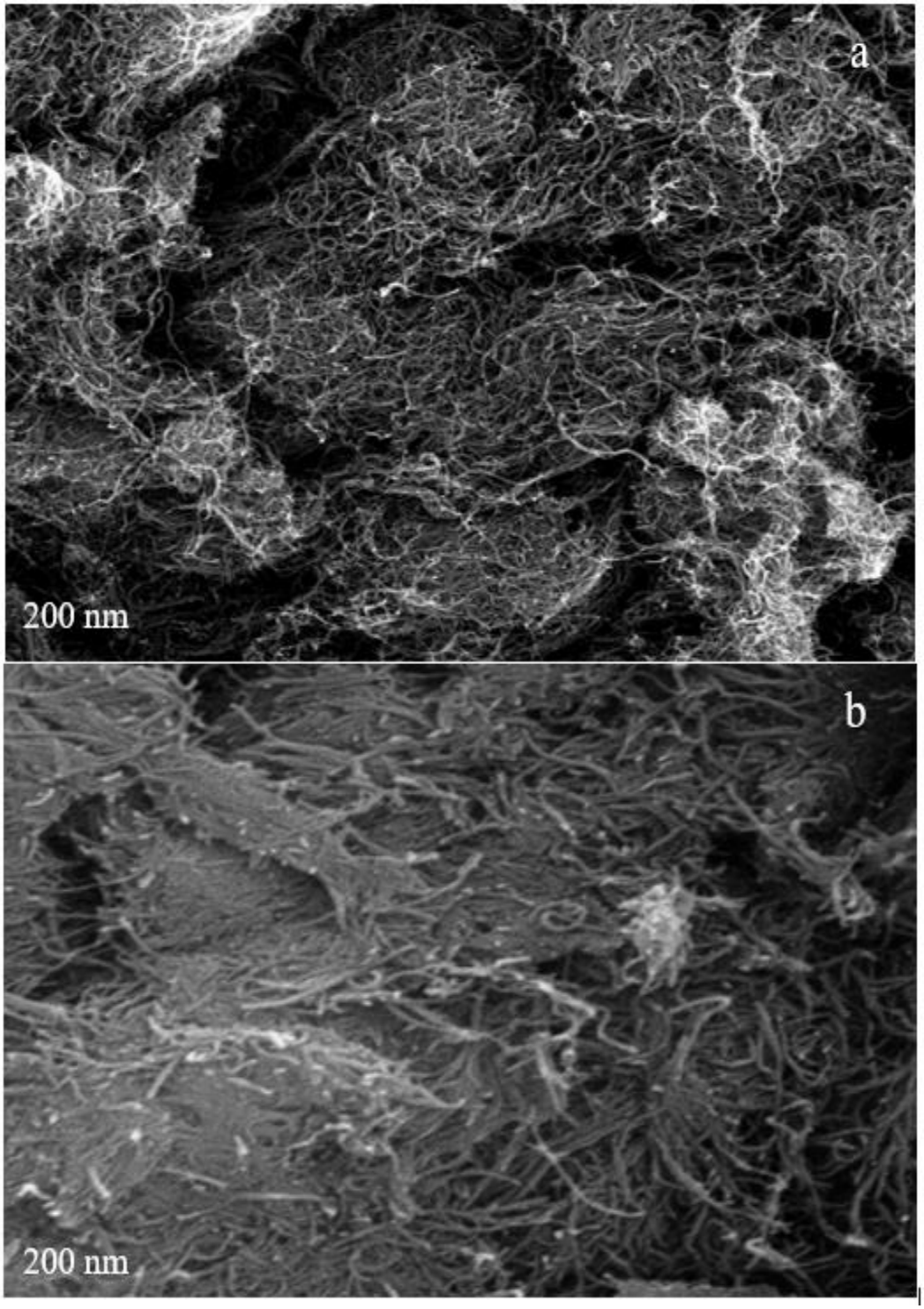


Figure 5.1 Surface morphology of (a) CNTs (b) FCNTs

Table 5.1: Elemental composition of CNTs and FCNTs

Element	Weight %		Atomic %		Weight %		Atomic %	
	Fresh CNTs	Used CNTs	Fresh CNTs	Used CNTs	Fresh FCNTs	Used FCNTs	Fresh FCNTs	Used FCNTs
C	97.28	93.75	95.44	90.29	90.88	89.95	88.10	87.29
O	2.72	3.43	4.56	4.54	9.12	5.23	11.90	6.54
S	0.00	2.82	0.00	5.17	0.00	4.82	0.00	6.17
Total	100.00	100.00	100.00	100.00	100.00	100.00	100.00	100.00

Fig. 5.2 depicts the adsorption-desorption isotherms of the adsorbent. It can be observed that the distance between adsorption and desorption plots was wide indicating pore condensation hysteresis with relatively weak attractive adsorbate-adsorbent interaction.

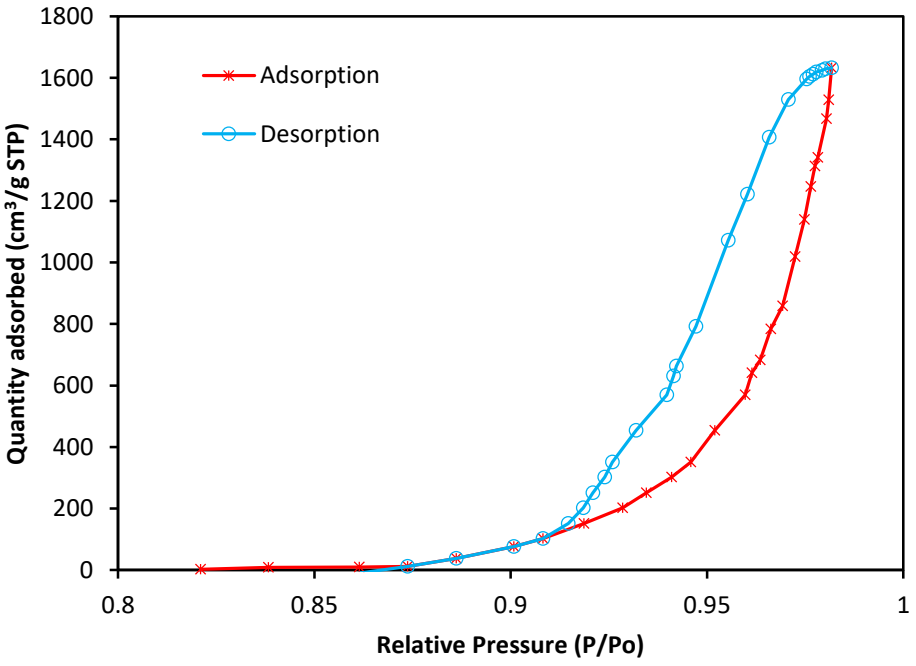


Figure 5.2. Adsorption-desorption isotherm plot of CNTs adsorbent

Table 5.2 shows the textural properties of the CNTs. It could be seen in the table that after surface modification, the surface area of CNTs decreased from 245.49 m^2/g to 224 m^2/g. This could be attributed to the blocking of some of the pores by functional groups introduced during the chemical modification. This is in agreement with results reported by Falah et al. (2005). The pore volume of CNTs also reduced after the chemical modification (See Table 5.2). Large pore diameter above 0.7 nm enhances the adsorption of DBTs in the adsorbents by reducing mass transfer resistance and hence increasing the rate of the adsorption process. As indicated in Table 5.2, pore diameter of CNTs has been reduced after surface modification; however, pore diameters of both adsorbents are >0.7 nm, which is necessary forenhancing access of DBT into the inner pores of the adsorbents. This observation is in agreement with literature (Jiang et al., 2003; Seredych et al., 2012).

Table 5.2: Surface area, pore volume and pore sizes of the adsorbents

Adsorbents	**Surface area (m^2/g)**	**Pore volumes (cm^3/g)**	**Pore diameter (nm)**
CNTs	245.49	2.365	47.87
FCNTs	225.05	1.090	16.72

Chemical functionalities of the CNTs and FCNTs adsorbents are checked following the steps described in chapter 3 of this thesis. Fig. 5.3 shows the chemical functionalities of the CNTs and FCNTs adsorbents. FTIR spectra from the CNTs show a broad peak at 3495 cm^{-1} which is a characteristic of the O-H stretch of hydroxyl group (Fig.5.3) which can be ascribed to the oscillation of carboxyl groups. Carboxyl group on the surface of CNTs could be due to the partial oxidation of the surface of CNTs during purification by the manufacturer. This feature moves to 1736 cm^{-1}, associated with the stretch mode of carboxylic groups as observed in the IR spectrum of the functionalized CNTs indicating that carboxylic groups are formed due to the oxidation of some carbon atoms on the surface of the CNTs by sulfuric acid. The FTIR spectra of functionalized CNTs show four major peaks, located at 3425, 1736, and 1560 cm^{-1}. The peak at 3495 cm^{-1} is attributed to free hydroxyl groups. The peak at 3425 cm^{-1} can be assigned to the O–H stretch from carboxyl groups (O=C−OH and C−OH) while the peak at 2361 cm^{-1} can be associated with the

O−H stretch from strongly hydrogen bonded −COOH. The peak at 1560 cm^{-1} is related to the carboxylate anion stretch mode (Deborah et al., 2014). It can be deducted that functionalization of the CNTs adsorbent with a hydroxyl group enhanced the adsorption capacity of the adsorbent (Sahebian et al., 2015). The role of aromatic structure and –OH substitution in the polar aromatic CNT system on the adsorption affinity of these compounds by CNTs increased with increasing number of aromatic rings and was greatly enhanced by –OH substitution. The spectrum of the FCNTs show that OH group was successfully attached to the surface of the CNTs adsorbent after treatment with acid (Le et al., 2013).

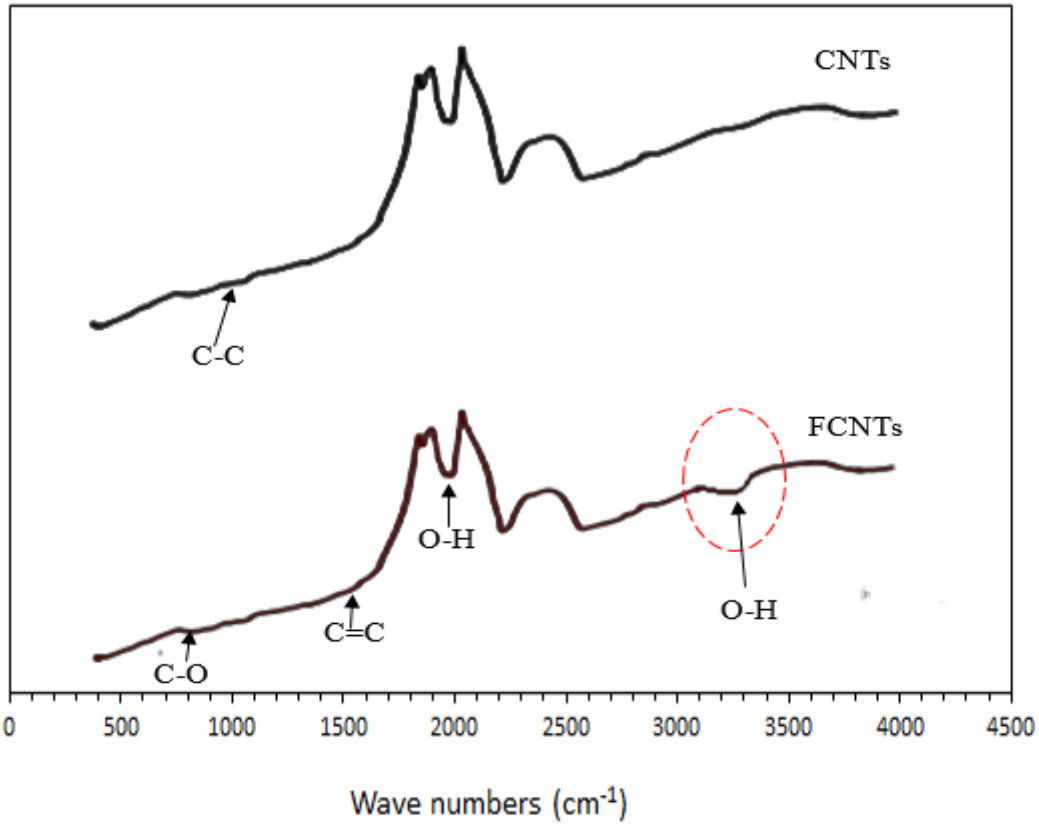


Figure 5.3. FTIR spectra of CNTs and FCNTs

The purity of the adsorbents was obtained as described in Chapter 3 of this thesis. Fig. 5.4 shows the Ramman spectroscopy of CNTs, FCNTs. The existence of disorder in sp^2-hybridized carbon

systems results in resonance Raman spectra. This D-mode is as a result of disordered structure of graphene. The D-band peaks are at 1354 cm^{-2} and 1381 cm^{-2} for FCNTs and CNTs, respectively and this corresponds to distortion of Sp^2 Crystal structure while the G-band which arises as a result of the stretching of the C-C bond in graphitic materials, and common to all sp^2 carbon materials are detected at 1636 cm^{-2} and 1635 cm^{-2} for FCNTs and CNTs, respectively. These bands are associated to the lattice vibration mode of all carbon (graphite) materials with sp^2 bonds (Misra et al., 2007; Liuiwen, et al., 2005). The value of I_G/I_D ratio of CNTs (1.35) is lower than the I_G/I_D ratio of FCNT (1.423). This is an indication that purification of carbon nanotubes resulted into fewer defect and higher structural quality of the FCNTs, enhancing the adsorption performance of the adsorbent.

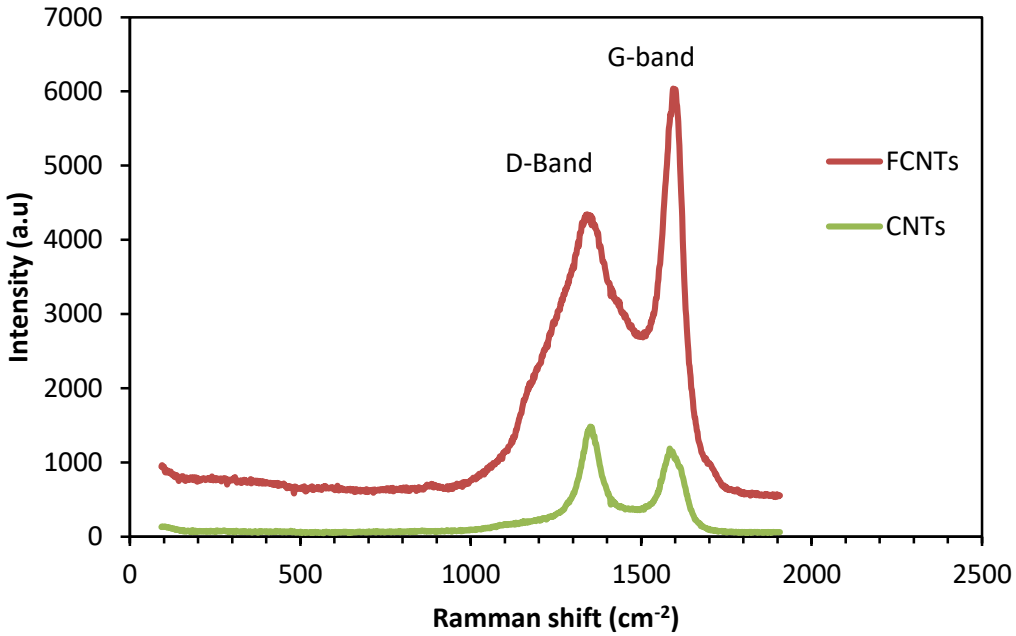


Figure 5.4. Ramman spectra for CNTs and FCNTs

5.3.2 Performance evaluation of CNTs and FCNTs during desulfurization

To understand adequately the performance of CNTs and FCNTs during adsorptive removal of DBT from model diesel, effect of operating parameters on adsorption performance of the adsorbents was investigated. The results obtained are hereby discussed.

Parametric effect of the operating variables such as contact time, amount of adsorbents, initial concentration of DBT and temperature was investigated. Determining the maximum operating time is important in adsorption process. The contact time was varied from 0-180 min, while other operating parameters such as initial DBT concentration 1000 mg/L, volume of model oil 20 mL, temperature 298 K, were kept constant. Fig 5.5 depicts the effect of contact time on the removal of DBT molecule from the model oil. It could be observed that the uptake of the DBT into the adsorbents (CNTs and FCNTs) was initially rapid for the first 10 minutes. Within this time about 13.3 % and 30.3 % of DBT had been removed by CNTs and FCNTs, respectively. This could be attributed to the large number of vacant sites on the surface of the adsorbents at the initial stage of the adsorption. The higher percentage of DBT removed by FCNTs at this stage compared to CNTs could be attributed to the functional group attached to the surface of the FCNTs after acid treatment, enhancing the removal of DBT from the model diesel. Between 10 minutes and 50 minute the pace slowed down drastically due to the decrease in the number of adsorption sites on the surface of the adsorbent. The adsorptive removal reached equilibrium at 50 minutes during which the available adsorption sites on the surface of the adsorbent have been fully occupied with the DBT molecules, leaving no room for further adsorption. This observation is consistent with literature (Vadivelan and Kumar, 2005). The nature of the adsorption behaviour of DBT onto the surface of the CNTs and FCNTs could indicate a monolayer DBT coverage on the adsorbent surface as proposed by Namasiyayam (1993). The results show that functionalization of CNTs enhanced the efficiency of the adsorbent for removal of DBT from model diesel.

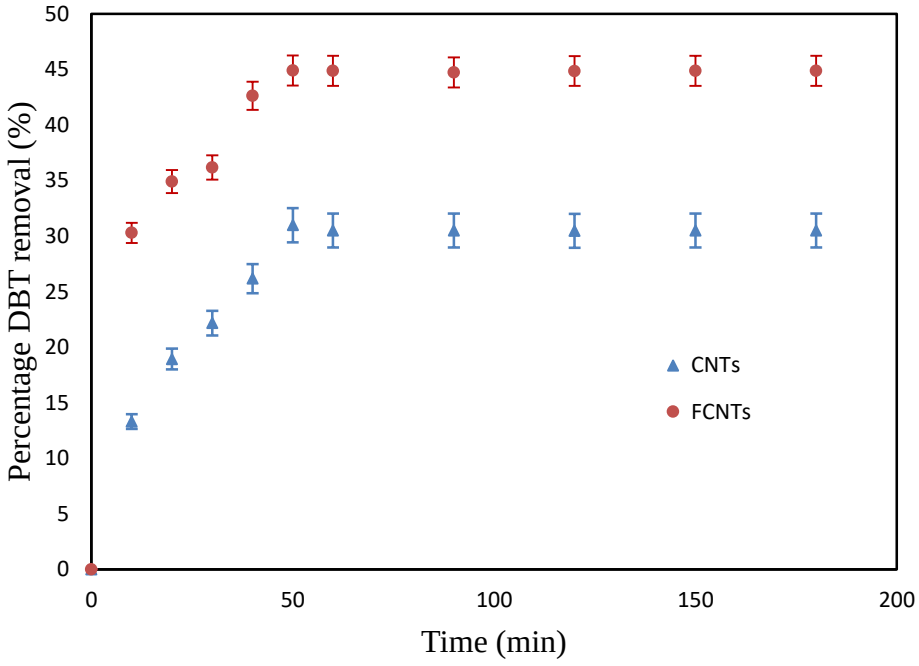


Figure 5.5. Effect of time on the adsorption of DBT onto the surface of CNTs and FCNTs. Experimental conditions: Temperature: 298 K; Initial DBT concentration: 1000 mg/L;

Fig. 5.6 shows the effect of amount of adsorbents on their adsorption capability. In order to determine the effect of amount of adsorbent for desulfurization of model diesel, the amount of adsorbents (CNTs and FCNTs) was varied from 0.2 -1.0 g. Other operating conditions, such as, initial DBT concentration (1000 mg/L), time 60 minutes, temperature 298 K were kept constant. The results show that, as the amount of adsorbent increases, the amount of DBT adsorbed on the surface of the adsorbents also increased. This observation could be attributed to the availability and accessibility of more adsorption sites and more surface area for DBT compound attachment on which adsorption process is dependent (Daware et al., 2015). It was observed for both FCNTs and CNTs that, as the adsorbent dosage increased the percentage yield increased until it reached 0.8 g (Khaled, 2015). About 70.84 % and 60.88 % DBT were adsorbed onto the surface of FCNTs and CNTs respectively. An additional increase in the adsorbent dosage from 0.8 g to 1.0 g for both adsorbents, showed no further obvious adsorption of DBT onto the surfaces of the adsorbents. This could result from inhibition of DBT molecules diffusion to the surface of the adsorbents (Gong et al., 2009). The result showed that percentage desulfurization performance for FCNTs was higher

that of the CNTs. The adsorption capacity of FCNTs (14.17 mg/g) was higher than that of CNTs with adsorption capacity of 12.18 mg/g. Equilibrium time was also reached at 50 minutes, when there was no further increase in adsorption of DBT as time increased. This is favorable in the commercial application of nanotubes powder since a higher adsorption capacity can be obtained at a minimum amount (0.8 g) for CNTs. In addition, decrease in percentage adsorption of CNTs compared to FCNTs powder may result from aggregation of adsorbent which prevented some active adsorbent sites from being exposed for the adsorption of DBT (Jiang et al., 2003). This is an indication that purification of CNTs enhanced the adsorption capacity of the adsorbent.

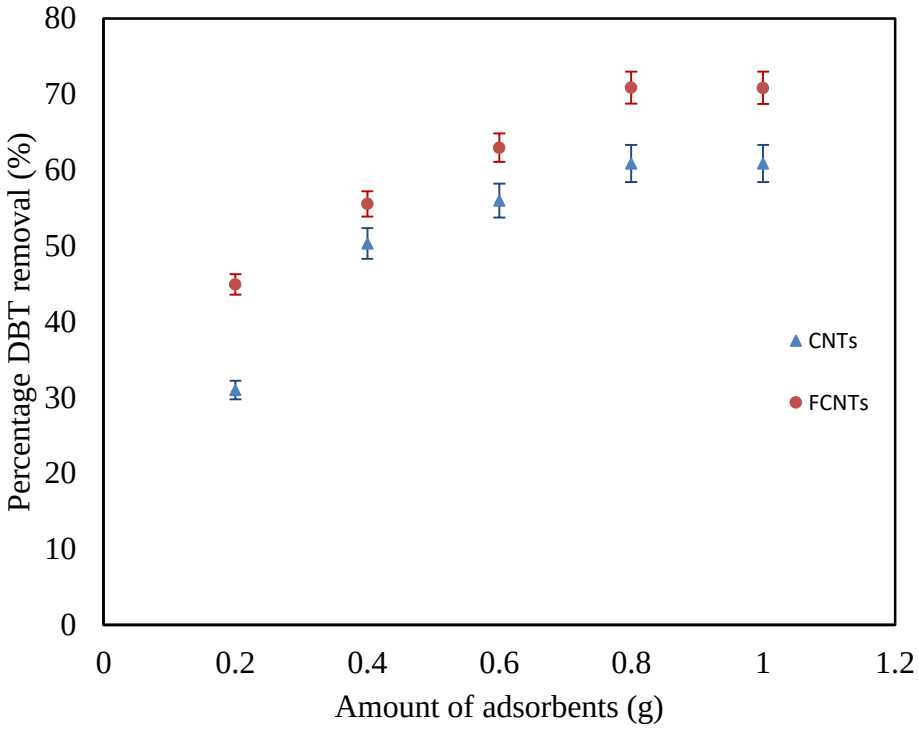


Figure 5.6. Effect of amount of adsorbent on the adsorption of DBT onto FCNTs and CNTs. Experimental conditions: Initial DBT concentrations: 1000 mg/L; Temperature: 298 K.

Fig. 5.7 shows the effect of initial concentration of DBT on the adsorption performance of the adsorbent. The concentration of DBT in the feed was varied in the model diesel. The initial

concentration was varied from 250 -1000 mg/L, while other operating conditions were kept constant; adsorbent amount (0.8 g), temperature (298 K), volume of model oil (20 mL), and contact time (60 min). From the results obtained at equilibrium in Fig. 5.7, it could be deduced that DBT adsorption per unit mass of adsorbent increased as the initial concentration increased. For CNTs, when the initial DBT concentration increased from 250-1000 mg/L, the adsorption capacity of CNTs also increased from 3.46-15.11 mg/g. The same trend was observed for FCNT where adsorption capacity increased from 3.75- 17.71 mg/g. This could be attributed to the concentration gradient developed on the surface of the adsorbent and the DBT solution which is as a result of increase in the driving force, resulting from increase in concentration The results obtained in this study are in agreement with literature (Fayazi et al., 2015; Ishaq et al., 2017).

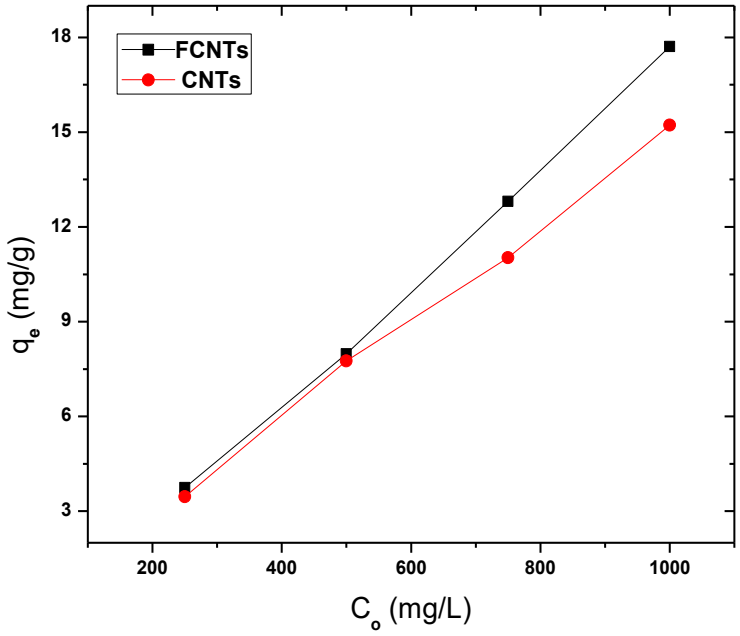
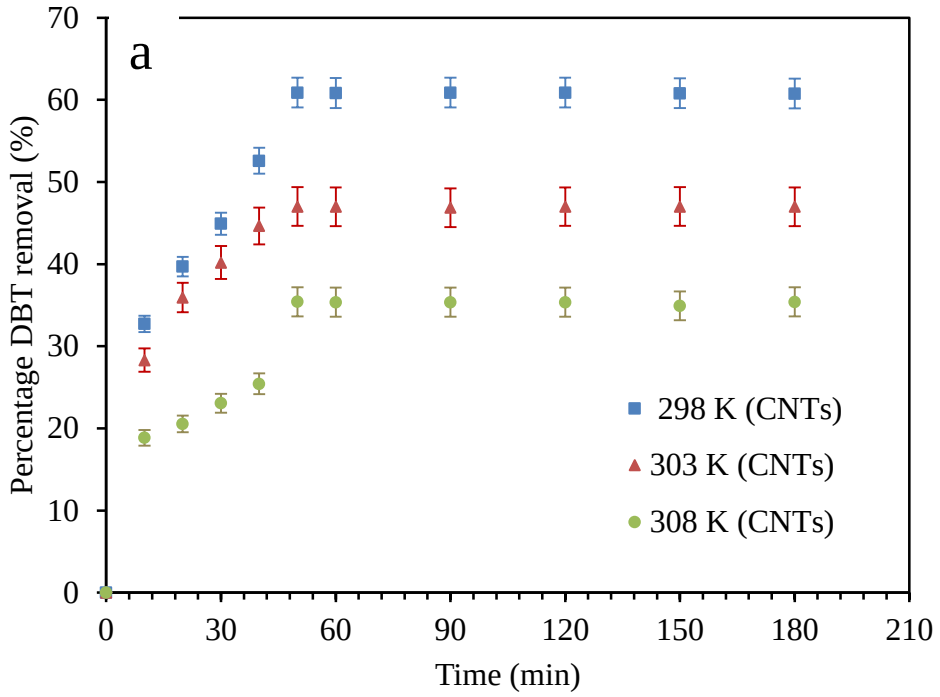


Figure 5.7. Effect of initial concentration of DBT on its adsorption onto FCNTs and CNTs. Experimental conditions: Amount of adsorbent 1.0 g, contact time 60 minutes, temperature 25 ^{o}C.

Fig. 5.8 (a) and 5.8 (b) show the effect of temperature on the adsorption process of CNTs and FCNTs, respectively. The temperature of the adsorption experiment was varied from 298 K-308

K. It can be deduced that, adsorption performance of the adsorbent decreased with increase in temperature from 298 K to 308 K for both CNTs and FCNTs adsorbents as the time increases. This behavior is expected since adsorption process is known to be an exothermic reaction where adsorption is favoured at lower temperature. Hence the highest adsorption capacity was obtained at 298 K. Maximum adsorption performances of 60.88 %, 47.01 % and 35.41 % by CNTs adsorbent at 298 k, 303 K and 308 K, respectively. In addition, about 70.84 %, 51.52 % and 43.86 % percentage DBT removal was achieved by FCNTs at 298 K, 303 K and 308 K (Nazal et al., 2015).



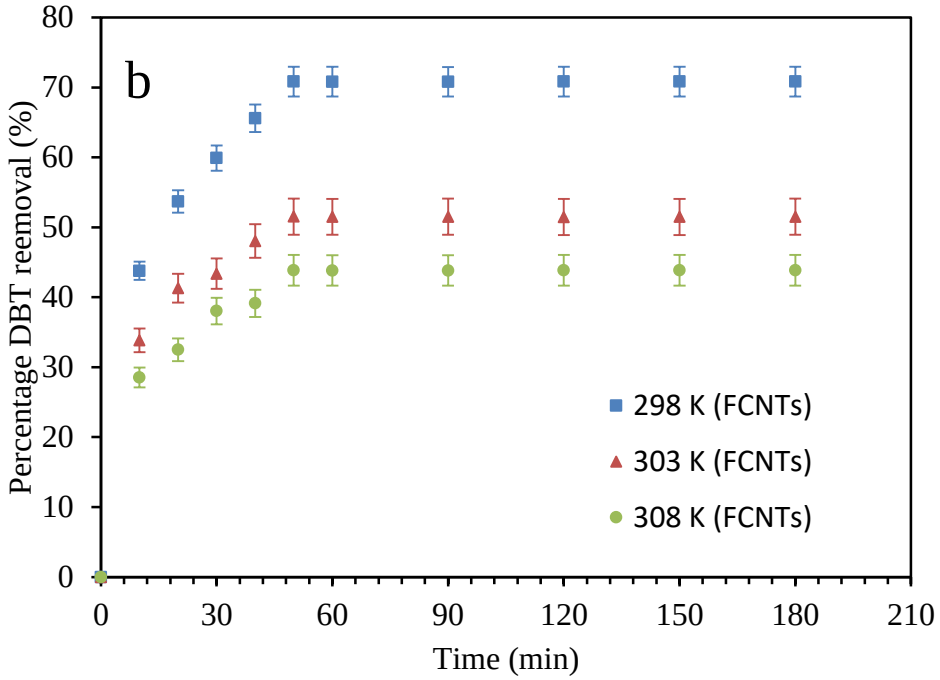


Figure 5.8. Effect of temperatures on the adsorption of DBT onto (a) CNTs and (b) FCNTs. Experimental conditions: Initial DBT concentration: 1000 mg/L; Amount of adsorbent: 1.0 g; Temperature: 298 K-308 K.

5.4 Isotherm, kinetics, and thermodynamics of CNTs and FCNTs for adsorption

Langmuir and Freundlich isotherms were used to the describe the behavior of the AC adsorbent. Table 5.3. represents the Langmuir and Freundlich isotherm parameters for adsorption of DBT molecules onto CNTs and FCNTs adsorbent. Fig. 5.9 (a) and (b) depict the Langmuir isotherms of FCNTs and CNTs, respectively. Fig. 5.9 (c) and (d) depict the Freundlich isotherms of FCNTs and CNTs, respectively. It can be observed that both langmuir and Freundlich isotherm models described well the adsorption of DBT onto CNTs and FCNTs. They both have high correlation coefficients (R^2) values. CNTs have R^2 values of 0.9764 and 0.9802 for Langmuir isotherm and Freundlich isotherm model, respectively (Al-Ghouti et al., 2017). FCNTs adsorbent also has high coefficient of determination for both Langmuir and Freundlich isotherms, 0.9995 and 0.9910, respectively. The values of Langmuir separation factor, R_L which determines the favorability of the adsorption process for both CNTs and FCNTs in Table 5.3 are 0.52 and 0.37, respectively. The

values are <1, indicating that the adsorption process is favourable. The results indicate that the adsorption took place at specific homogeneous sites within the adsorbent forming monolayer coverage of DBT at the surface of the CNTs and FCNTs absorbent. This is in agreement with Wang and Wei, (2017). The value of b in FCNTs, which reflects the activity of binding site is higher than the value of CNTs. The values of adsorption intensity, n <1 for both FCNTs and CNTs also indicate favorability of the adsorption process.

Table 5.3: Langmuir and Fruendlich Isotherm's model parameters for CNTs and FCNTs

Adsorbent	**Langmuir Isotherm**				**Freundlich Isotherm**		
	Temp (K)	**R_L**	**b (L/mg)**	**R^2**	**K_f (mg/g)**	**N**	**R^2**
CNTs	298	0.52	0.00019	0.9764	0.0125	0.864	0.9802
FCNTs	298	0.37	0.00230	0.9995	0.0038	0.690	0.9910

b is the Langmuir's contact, K_f is the Freundlich's constant, n is the adsorption intensity, R_L is the Langmuir separation factor and R is the correlation coefficient

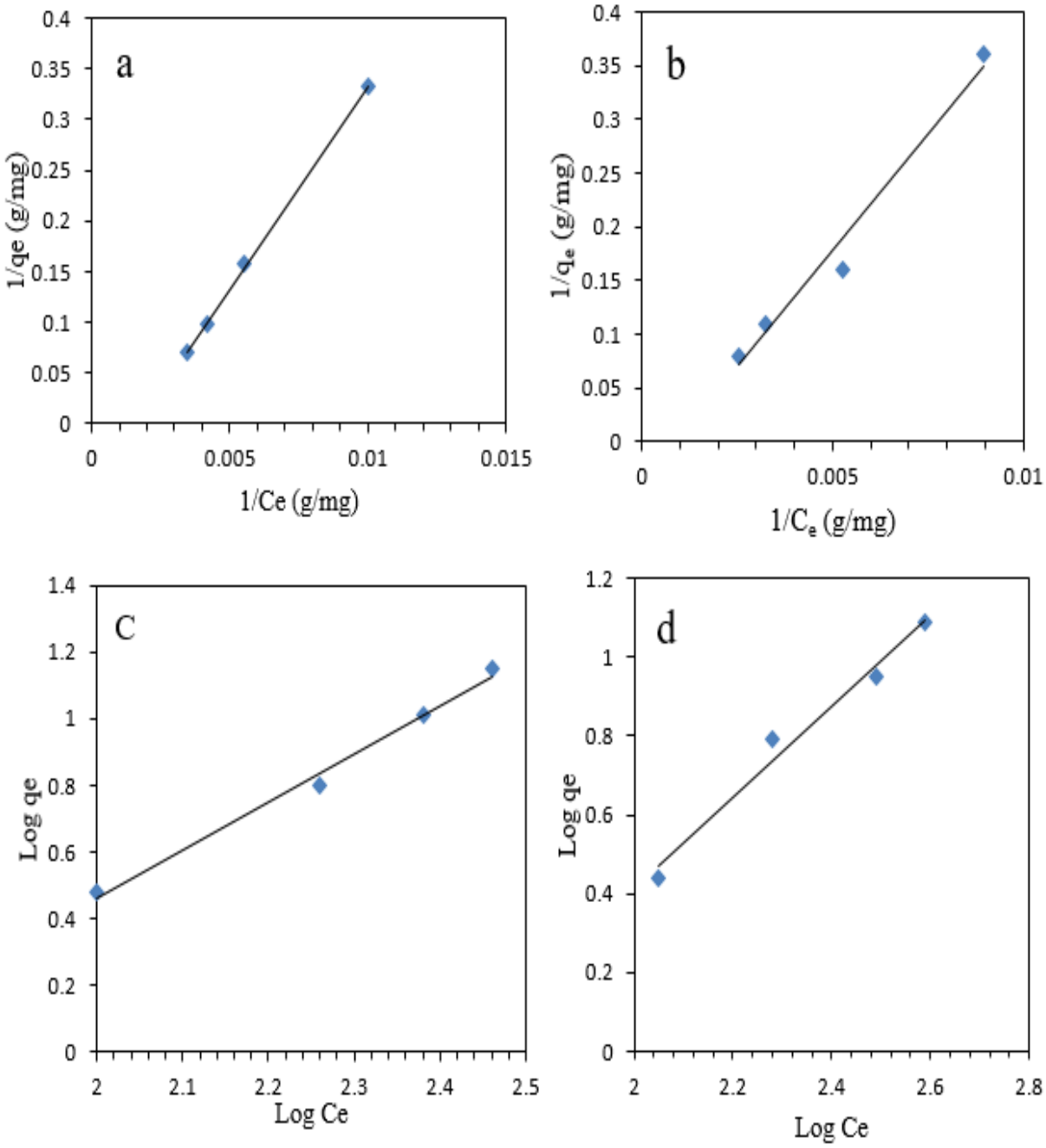


Figure 5.9. Langmuir isotherms model for (a) FCNTs (b) CNTs and Freudlich isotherms of (c) FCNTs (d) CNTs. Experimental conditions: Temp: 298 K; Amount of adsorbent: 1.0 g.

The kinetics of FCNTs anf CNTs are presented. Table 5.4 presents the parameters of pseudo first-order and pseudo second-order of DBT adsorption onto FCNTs and CNTs at 298, 303, and 308 K. Comparing the coefficient of determination (R^2) of the kinetic models of CNTs with pseudo first-order, it was observed that, the pseudo second-order model was better fitted into the experimental data with higher coefficient of determination (0.9985, 0.9989, 0.9885) than the coefficient of determination (R^2) (0.3192, 0.7156, 0.8293) for pseudo first-order model at 298 K, 303 K and 308 K, respectively. In addition the experimental q_e (12.18 mg/g) values obtained for pseudo secon-order kinetics are very close to the calculated q_e (12.44 mg/g) compared to what were obtained for the experimental q_e (12.18 mg/g) and calculated q_e (3.14) for the 1st orde kinetics (Table 5.4). Also, for FCNTs adsorbent, the coefficient of determination (R^2) was higher in pseudo second-order kinetics (0.9996, 0.9987, 0.9984) compared to lower coefficient of determination (R^2) obtained for pseudo fist order (0.5880, 0.5176, 0.7133) at 298, 303 and 308 K, respectively. The model value for q_e calculated (14.29 mg/g)was very close in experimental value obtained for q_e (14.17mg/g) for psedo second order kinetics for adsorption of DBT onto FCNTs. However, the model value calculated for q_e (23.06 mg/g) is higher than the value obtained in the experiment (14.17 mg/g) for pseudo first-order kinetics of DBT adsorption onto FCNTs. It could be assumed that there were involvements of chemical interactions in the adsorption process. In addition, the rate of adsorption may be controlled by the movement of DBT molecules within the pore of the CNTs and FCNTs adsorbents. The result obtained in this study is in agreement with what was reported by Wang and Wei, (2017). Lower coefficient of determination factor for pseudo first-order could be an indication that the rate of adsorption process does not depend on concentration factor, but depends on both concentration and time. This is in agreement with Kumar and Tamilarasan (2017)

Table 5.4: Kinetics model parameters for pseudo first and pseudo second-order kinetics

Temp (K)	**Pseudo 1st-order (CNTs)**				**Pseudo 2nd-order (CNTs)**			
	$q_{e(expt)}$ (mg/g)	**$q_{e(calc.)}$ (mg/g)**	**K_1 (L/min)**	**R^2**	**$q_{e\ (expt)}$ (mg/g)**	**$q_{e\ (calc.)}$ (mg/g)**	**K_2 (g/mg.min)**	**R^2**
298	12.18	3.14	0.020	0.3192	12.18	12.44	0.024	0.9985
303	9.40	2.24	0.032	0.7156	9.40	9.58	0.035	0.9989
308	6.99	4.54	0.039	0.8293	7.53	6.99	0.013	0.9885
Temp (K)	**Pseudo 1st-order (FCNTs)**				**Pseudo 2nd-order (FCNTs)**			
	$q_{e(expt)}$ (mg/g)	**$q_{e(calc.)}$ (mg/g)**	**K_1 (L/min)**	**R^2**	**$q_{e\ (expt)}$ (mg/g)**	**$q_{e\ (calc.)}$ (mg/g)**	**K_2 (g/mg.min)**	**R^2**
298	14.17	23.06	0.032	0.5880	14.17	14.29	0.042	0.9996
303	10.30	3.13	0.027	0.5176	10.30	10.48	0.076	0.9987
308	8.77	3.84	0.034	0.7133	8.77	8.94	0.030	0.9984

q_e is the amount of DBT adsorbed at equilibrium, R is the correlation coefficient, K_1 is the pseudo-first order constant and K_2 is the pseudo-second order constant.

The values of adsorption thermodynamics parameters, standard free energy ΔG^o, standard entropy ΔS^o and standard enthalpy, ΔH^o for CNTs and FCNTs adsorbents are presented in Table 5.5. The negative values of ΔG^o and the negative values of ΔH^o indicate that DBT adsorption onto pomegranate leaf and neem leaf are spontaneous and exothermic in nature. Negative ΔS^o values

of DBT adsorption process indicate a decrease of the randomness at the CNTs and FCNTs-solution interface during adsorption. In addition, the result show that the values of ΔS^o decreased with increase in temperature, while the values of ΔG^o increased with increase in temperature. The activation values obtained for both CNTs and FCNTs are 25.34 kJ/mol and 14.13 kJ/mol, respectively. These values are less than 65 kJ/mol. This si an indication that adsorption of DBT onto CNTs and FCNTs occurred more readily. In addition, the adsorption processes for both adsorbents could be said to be physical adsorption. This is in agreement with literature (Fei et al., 2017; Saini et al.,2017; Al- Ghouti et al., 2017).

Table 5.5: Adsorption themothynamics parameters for FCNTs and CNTs

	Temp.(K)	***Δ*H (kJ/mol)**	***Δ*G (kJ/mol)**	***Δ*S (J/k/mol)**	**E_A (kJ/mol)**
CNTs	**298**	-44.06	- 8.52	-119.27	25.34
	303		-7.26	-121.49	
	308		-6.09	-123.28	
FCNTs	**298**	-46.97	- 9.61	-125.37	14.13
	303		-7.71	-129.59	
	308		-7.04	-129.65	

ΔH: Standard enthalpy; ΔG: Standard free energy; ΔS: Standard entropy; E_A: Activation energy

5.5 Regeneration and re-usability of FCNTs and CNTs

Reusability performance of carbon nanoparticle adsorbents was studied due to growing concern for waste minimization, recovery, and reuse as well as for industrial applications. The used adsorbents loaded with sulfur were washed severally with hexane until they were back to their original states. In other to study the reusability capacities of these adsorbents, the regenerated adsorbents went through adsorption–desorption process for four cycles. The experimental runs were carried out with 1.0 g of the washed adsorbent and 20 mL of hexane, in a 250 mL Erlenmeyer flask and agitated vigorously at 130 rpm for 1 h. The initial concentration and concentration of the filtrate were analyzed for sulfur containing compound as mentioned earlier with GC/MS. Percentage sulfur removal capacities for each run were determined using eq. 3.2. In Fig. 5.10, the re-used adsorbent shows percentage sulfur removal of 70.77 % and 58 %, for FCNTs and CNTs at 4th cycle. The fourth cycle showing 99.9 % reusability efficiency of FCNTs compared to 95 % of CNTs after third cycle. The results show that acid treatment improved the reusability cycle of the FCNTs compared to non-functionalized CNTs after third cycle. The reusability cycle of CNTs decreased by 5 % while that of FCNTs only decreased by 0.1 %. The initial adsorption capacity of the adsorbent was retained till the third cycle. Therefore, commercial application of functionalized CNTs is possible due to its reusability strength for removal of DBT from petroleum distillate.

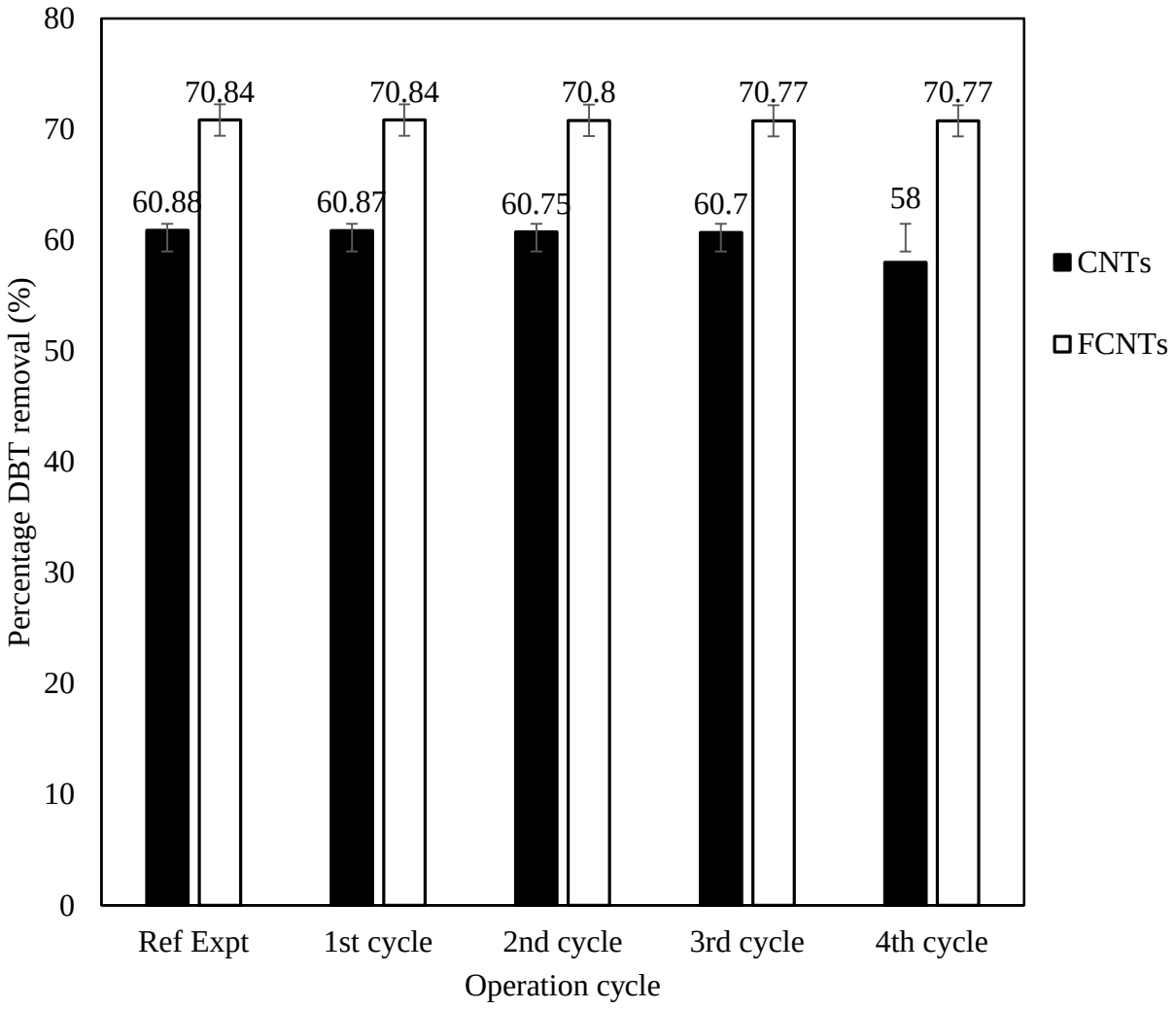


Figure 5.10 Re-usability cycles of CNTs and FCNTs. Experimental conditions: Amount of adsorbent: g/0.02 L model diesel; Temperature: 298 K; Initial DBT concentration: 1000 mg/L.

Table 5.6 shows the comparison of results of this study with literature. Nazal et al., (2015) modified the surface of CNTs with 5 % aluminium metal. 80 % adsorption performance was achieved at initial DBT concentration of 250 mg/L. Comparing this result with the result obtained in this study, their modified CNTs out-performed what was obtained for CNTs (60.88 %) and FCNTs (70.84 %) in this study. This could only be as a result of lower initial DBT concentration used which is 4 times lower than what was used in this study. In addition, 1.5 g of their adsorbent was used which

is almost two times what was used in this study. The result obtained will most likely be better than what was obtained by Nazal et al., (2015), if the same operating conditions are used. Saleh et al., (2014) also conducted an adsorptive desulfurization experiment to remove DBT from a model oil using CNTs modified with titanium oxide. Results showed 65 % desulfurization performance using 0.75 g adsorbent. The result obtained in this study for acetic and sulfuric acid-treated CNTs which was 70.88 %. However, out-performed the non-functionalized carbon naotubes used in this study by 5 %. This better performance of CNT/TiO_2 compared to non-functionalized CNTs could be as a result of the modifies surface of their adsorbent. About 87 % adsorptive removal of DBT was achieved in an experiment conducted by Khaled et al. (2015) using sulfuric acid treated 1.5 g of CNTs, at initial DBT concentration of 250 mg/L. The time for equilibrium to be reached in their study (160 min) was higher than the time equilibrium was reached in this study (60 min). In addition, a lower initial concentration was used which is 4 times lower than what was used in this study. In addition, about two times amount of adsorbent used in this study was used in Khaled et al. (2015). Therefore, it can not be concluded that their result is better than what was obtained in this study for both CNTs and FCNTs.

It can therefore be concluded that, the result obtained from this study is comparable with studies reported in literature. As far as could be ascertained, this is the first report on the use of acetic-sulfuric acid treated CNTs as an adsorbent for the desulfurization of petroleum distillate and the results documented in this study could provide a platform for further research efforts in this field.

Table 5.6: Comparison of results with literature

Adsorbent	Organo-sulfur	Temp. (°C)	Time (h)	C_o (mg/L)	C_f (mg/L)	Ads Amount (g)	% SR	Ref.
CNT/5 % Al	DBT	25	2.0	250	50	1.50	80.0	Nazal et al. (2015)
CNTs/TiO_2	DBT	23	1.0	-	-	0.75	65.0	Saleh et al. (2014)
FCNTs	DBT		2.5	250	32.75	1.50	86.9	Khaled et al. (2015)
CNTs	DBT	25	1.0	1000	60.88	0.80	65.0	This study
FCNTs	DBT	25	1.0	1000	70.48	0.80	70.0	This study

C_o is the initial concentration of DBT, C_f is the final concentration of DBT, Ads is adsorbent and % SR is the percentage of sulfur (DBT) removal.

5.6. Concluding remarks

As it has been established in this chapter, CNTs and FCNTs are promising candidates for removal of sulfur containing compound (DBT) from petroleum distillate (e.g diesel). As far as it can be ascertained, no study has been conducted on the use of $KMnO_4$/ H_2SO_4 treated-CNTs for removal of DBT from petroleum distillate. It can be concluded that the acid treatment of CNTs enhanced its surface affinity for DBT, thus contributing to the improved adsorption capacity of the adsorbent. CNTs tend to aggregate together as bundles because of Van der Waals interactions. Addition of -COOH group on the surface of the adsorbent improved the performance of the adsorbent, even though the surface area was decreased after functionalization. The results showed that functionalized CNTs outperformed the non-functionalized CNTs during the desulphurization by about 10 %, indicating that functionalization of the CNTs did improve the desulfurization performance of the CNTs. Therefore, the percentage performances of the adsorbents were 70.48 % and 60.88 %, for FCNTs and CNTs, respectively, at 0.8 g adsorbent dosage, temperature of 25

^{o}C and maximum contact time of 50 mins. FCNTs and CNTs can be of great value in commercial application since it can be re-used up to four times without losing its potential strength for removal of DBT from petroleum distillate. A higher adsorption capacity is obtained at reduced amount of FCNTs and CNTs. The results obtained in this study could promote the adsorbents for commercial application.

In understanding the mechanism of the adsorption process, the isotherm result showed that the adsorption isotherm fitted well into both Langmuir and Freundlich isotherm models and could well describe the mechanism of the adsorption process for both CNTs and FCNTs. The pseudo second-order kinetics described the adsorption mechanism of the adsorption process for carbon nanotubes and FCNTs with closer values of experimental data with the model parameters. The negative values of ΔG^{o} and the negative values of ΔH^{o} indicate that DBT adsorption onto CNTs and FCNTs are spontaneous and exothermic processes. Negative ΔS^{o} values of DBT adsorption process indicate a decrease of the randomness at the CNTs and FCNTs-solution interface during adsorption

Therefore, the results show that functionalized CNTs is an efficient and promising adsorbent for removal of DBT in petroleum distillate such as diesel, so as to meet up with the stringent policies regarding emission of sulfur oxides. However, there is need for further studies on how to improve the surface area of the FCNTs after the acid treatment. Therefore, the results documented in this studies could provide a platform for further studies in this field

In a nutshell, the use of functionalized carbon nanotubes adsorbent for the treatment of sulfur-containing petroleum distillates serves as a proof of concept in abatement of environmental pollution.

For quick dissemination of the novel contributions described in this chapter to the scientific community, a paper has been published in a conference proceeding of the 3rd International Conference on Integrated Environmental Management for Sustainable Development (ICIEM, 2018).

5.7. References

Al-Ghouti, M.A., Al-Degs, Y. S., Issa, A. A., Al Bakain, R. Z., and Khraisheh, M. A. (2017) Mechanistic and Adsorption Equilibrium Studies of Dibenzothiophene-Rich-Diesel on MnO_2-Loaded Activated Carbon: Surface Characterization Environmental Progress and Sustainable Energy (Vol.00, No.00) DOI 10.1002/ep

Ahmad, W., Ahmad, I. and Ishaq, M. and Ihsan, K. (2017) Adsorptive desulfurization of kerosene and diesel oil by Zn impregnated montmorollonite clay. Arabian Journal of Chemistry. 10 (2), S3263-S3269.

Ahmed, K. and Ahmaruzzaman, M. (2015) Adsorptive desulfurization of feed diesel using chemically impregnated coconut coir waste Md. J. Int. J. Environ. Sci. Technol., 12, 2847–2856

Al Zubaidy, I. A. H., Tarsh, F. B., Darwish, N. N., Abdul Majeed, B. S. S., Al Sharafi, A., and Chacra, L.A. (2013) Adsorption Process of Sulfur Removal from Diesel Oil Using Sorbent Materials Journal of Clean Energy Technologies, 1, (1), 66-68.

Chen, H., Zhou, X., Shang, H., Liu, C., Qiu, J., Wei, F. (2004) Adsorption properties of dibenzothiophene (DBT) on a CNT (carbon nanotube) support as well as on CoMoS/CNT and CoMoO/CNT catalysts. Journal of Natural Gas . 13 (4), 209-217.

Daware, G.B., Kulkarni, A. B., Rajput, A. A. (2015) "Desulphurization of diesel by using low cost adsorbent" International Journal of Innovative and Emerging Research in Engineering Volume 2, Issue 6, pp 69-73.

Deborah, M., Jawahar, A., Mathavan, T., Dhas, K. M. and Benial, A. M. F. (2014) Preparation and Characterization of Oxidized Multi-Walled Carbon Nanotubes and Glycine Functionalized Multi-Walled Carbon Nanotubes Fullerenes, Nanotubes and Carbon Nanostructures 23, 583–590

Eddebbagh, M., Abourriche, A., Berrada, M., Zina, M. B., and Bennamara, A. (2016) Adsorbent material from pomegranate (Punica granatum) leaves: Optimization on removal of methylene blue using response surface methodology. J. Mater. Environ. Sci. 7 (6), 2021-2033.

Gawande, P. R and Dr. Kaware J. P. (2018) Isotherm and Kinetics of Desulphurization of Diesel by Batch Adsorption Studies International Journal of Chemical Engineering Research. 10 (1)), 1-16

Gong, J., Wang, B., Zeng, G., Yang, C., Niu, C., Niu, Q., Zhou, W., Liang, Y. (2009) Removal of cationic dyes from aqueous solution using magnetic multi-wall carbon nanotube nanocomposite as adsorbent. Journal of Hazardous Materials 164, 1517–1522.

Ishaq, M., Sultan, S. Ahmad, I., Ullah, H., Yaseen, M., Amir, A. (2017) Adsorptive desulfurization of model oil using untreated, acid activated and magnetite nanoparticle loaded bentonite as adsorbent Journal of Saudi Chemical Society. 21 (2), 143-151.

Jiang, Z., Liu, Y., Sun, X., Tian, F., Sun, F., Liang, C., You, W., Han, C., and Li, C. (2003) Activated carbons chemically modified by concentrated H2SO4 for the adsorption of the pollutants from wastewater and the dibenzothiophene from fuel oils, Langmuir, 19, 731–736

Khaled, M. (2015) Adsorption performance of MWCNTs and multiwall carbon nanotubes and graphene oxide (GO) for removal of thiophene and dibenzothiophene in model diesel fuel. Res Chem Intermed. 41, 9817–9833 DOI 10.1007/s11164-015-1986-5.

Le, V. T., Ngo, C. L., Le, Q. T., Ngo, T. T., Nguyen, D. N. and Vu, M. T. (2013) Surface modification and functionalization of carbon nanotube with some organic compounds. Adv. Nat. Sci.: Nanosci. Nanotechnol. 4 035017. doi:10.1088/2043-6262/4/3/035017

Moosavi, E. S., Dastgheib, S. A. and Karimzadeh, R. (2012) "Adsorption of Thiophenic Compounds from Model Diesel Fuel Using Copper and Nickel Impregnated Activated Carbons "Energies, 4233- 4250.

Namasivayam, C., Kanchana, N., Yamuna, R.T., (1993) Waste banana pith as adsorbent for the removal of rhodamine-B from aqueous solutions. Waste Manage. 13, 89–95.

Nazal, M. K., Khaled, M., Atieh, M. A., Aljundi, I. H., Oweimreen, G. A., and Abulkibash, A.M. (2015) The nature and kinetics of the adsorption of dibenzothiophene in model diesel fuel

on carbonaceous materials loaded with aluminum oxide particles. Arabian Journal of Chemistry, https://doi.org/10.1016/j.arabjc.2015.12.003.

Sadare, O. O., Obazu, F. and Daramola, M. O. (2017) Biodesulfurization of Petroleum Distillates—Current Status, Opportunities and Future Challenges. *Environments 4*(4), 85-104.

Sahebian, S., Zebarjad, S. M., Khaki, J. V., Lazzeri. A. (2015) A study on the dependence of structure of multi-walled carbon nanotubes on acid treatment. Journal of Nanostructure in Chemistry, 5 (3), 287–293 .

Saleh, T. A., Siddiqui, M. N., and Al-Arfaj, A. A. (2014) Synthesis of Multiwalled Carbon Nanotubes-Titania Nanomaterial for Desulfurization of Model Fuel. Journal of NanomaterialsArticle ID 940639, 1-66.

Vadivelan, V., Kumar, K.V. (2005) Equilibrium, kinetics, mechanism, and process design for the sorption of methylene blue onto rice husk. J. Colloid Interf. Sci. 286, 90–100.

Xiao, J., Li, Z., Liu, B., Xia, Q., Yu, M. (2008) Adsorption of benzothiophene and dibenzothiophene on ion-impregnated activated carbons and ion-exchanged Y zeolites. Energy Fuels 22, 3858–3863.

Zhou, A., Ma, X. and Song, C. (2009) Effects of oxidative modification of carbon surface on the adsorption of sulfur compounds in diesel fuel. Appl Catal B Environ 87, 190–199.

Chapter Six

6.0 Desulfurization of model and real diesel using using activated carbon

This chapter reports the results of effects of operating variables on the adsorptive performance of activated carbon during desulfurization of model diesel and real diesel. The mechanisms and behavior of adsorbents during desulfurization are also studied.

6.1 Introduction

Hydrodesulfurization (HDS) is the current method used in the refineries. It can effectively remove sulfur compounds such as sulfides, thiophides. However, dibenzothiophene and its derivatives 4,6-dimethyldibenzothiophene has been found to be difficult to remove using HDS technique. In addition, HDS can only be operated at high temperatures and pressures, which make the technique high enery intensive. A lot of hydrogen is also expended during operation which makes the process expensive. Therefore, an efficient, less expensive and low energy intensive method is urgently needed. Adsorption technique has been found to fit this specification. It can be operated at moderate operating conditions, which makes the process to be less energy intensive. They are less costly and DBT selective adsorbent are readily available. Different adsorbents have been used to remove sulfur containing compounds from petroleum distillates. Among these adsorbents, activated carbon (AC) is the most commonly used, owing to its microstructure, high surface area and high porosity. Since there are many organo-sulfur components in the diesel which may affect selectivity of DBT compound, there is need to investigate the adsorption performance of AC on the removal of DBT from typical South African real diesel (diesel obtained before HDS, and diesel obtained after HDS, 120 ppm). AC is therefore adopted in this study to remove DBT from model diesel and typical South African real diesel. In this chapter performance of AC is evaluated and reported. Furthermore, due to growing concern for waste minimization, recovery, and reuse of AC for industrial applications, its potential re-usability performance was studied. It is essential to undesratand the mechanisms and nature of interaction between the adsorbent (AC) and the adsorbate (DBT). Therefore, kinetics, isotherms and thermodynamics studies of the adsorbents are presented as well.

6.2. Experimental

The materials, the adsorbents preparation, adsorbent characterization and the detailed description of this experimental procedures are provided in Chapter three (section 3.1.1. and 3.1.2) of this thesis. The performance evaluation and re-usability of the adsorbents is also described in Chapter three of this thesis.

6.3 Results and discussion

6.3.1 Physico-chemical characterization of adsorbents

Fig. 6.1 depicts the nitrogen adsorption-desorption isotherm of fresh activated carbon. It can be observed that the shape of the isotherm is of mixed type isotherm I and IV according to the IUPAC classification (Sing et al., 1985). A type I isotherm could be said to be associated with a microporous structure while type IV isotherm indicates a material having combination of microporous and mesoporous structures. The initial part of the isotherms could be seen to have a type I isotherm with a significant uptake at low relative pressures. This could be related to adsorption in micropores. However, at intermediate and relatively high pressures, the isotherms could be seen to be of type IV with a hysteresis loop associated with monolayer–multilayer adsorption, then followed by capillary condensation in narrow slit-like pores. The same trends were observed in studies reported by Sych et al. (2012) and Kumar and Jena. (2016).

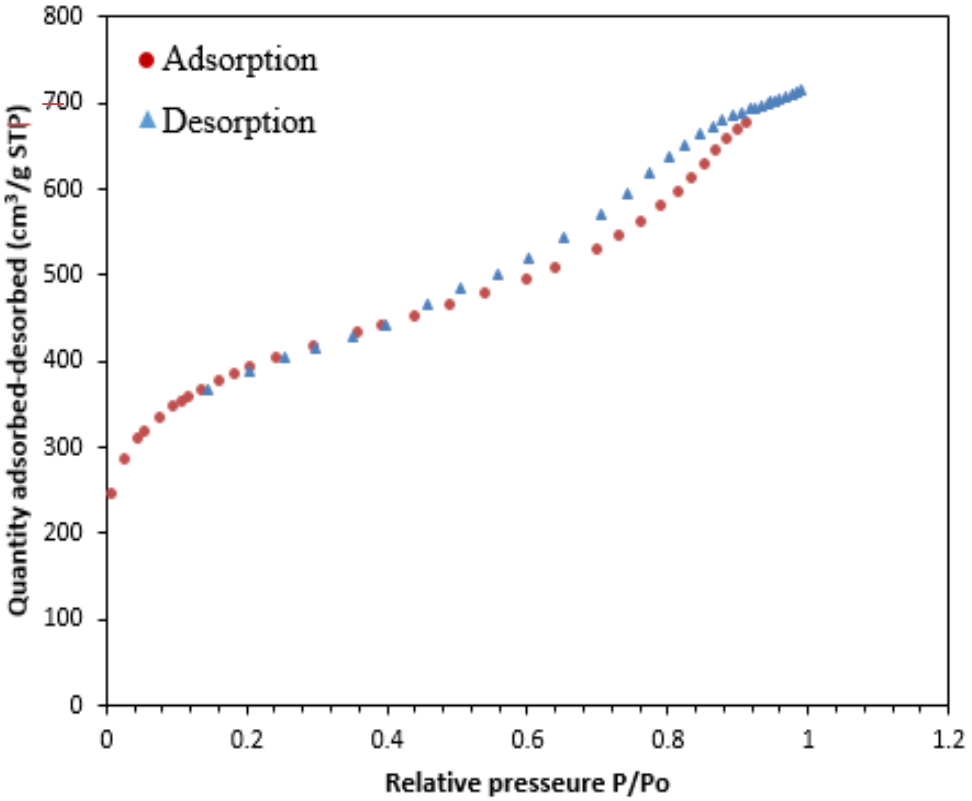


Figure 6.1 Adsorption-desorption isotherm of fresh activated carbon

The SEM images of the as-received (fresh) activated carbon before adsorption and SEM image of activated carbon after adsorption experiments are depicted in Fig. 6.2 (a) , Fig. 6.2 (b), respectively. The SEM images indicate that the AC posseses an irregular and heterogenous surface morphology with well developed porous stucture that is instrumental to the good adsorption of DBT on the surface of the adsorbent and this obervation is in agreement with literature (Ghaneian et al., 2015). In Fig. 6.2 (b), the SEM image after adsorption showed that some of the pores could have been occupied by DBT molecules after desulfurization. This observation is in agreement with literature (Shi et al., 2010; Eddebbagh et al., 2016).

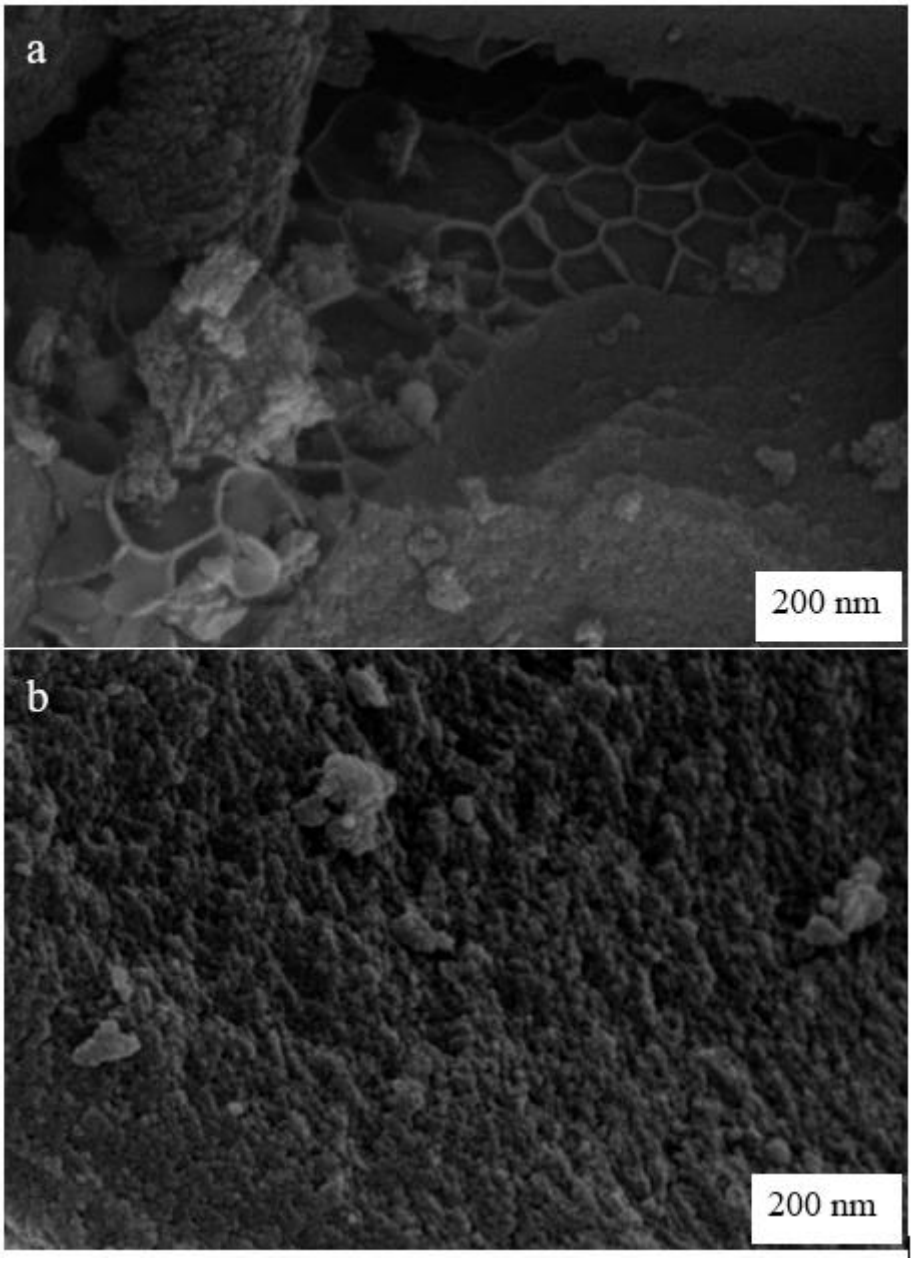


Figure 6.2 Surface morphology of commercial activated carbon (a) before adsorption and (b) after adsorption experiment .

Fig. 6.3 (a) and (b) show the EDX spectrum of fresh AC and used AC, respectively. Table 6.3 depicts the elemental compositions of AC as obtained from EDX. The result showed that fresh activated carbon before adsorption contains 81.80 % Carbon, 14.10 % Oxygen, 4.10 % Phosphorus and 0.0 % sulfur. The high percentage of sulfur could be as a result of the carbon tabe for mounting

the adsorbent sample before characterization. However, EDX result of used AC after adsorption showed 0.71 % of sulfur. This is an indication that sulfur-containing compound has been adsorbed on the surface of the AC adsorbents.

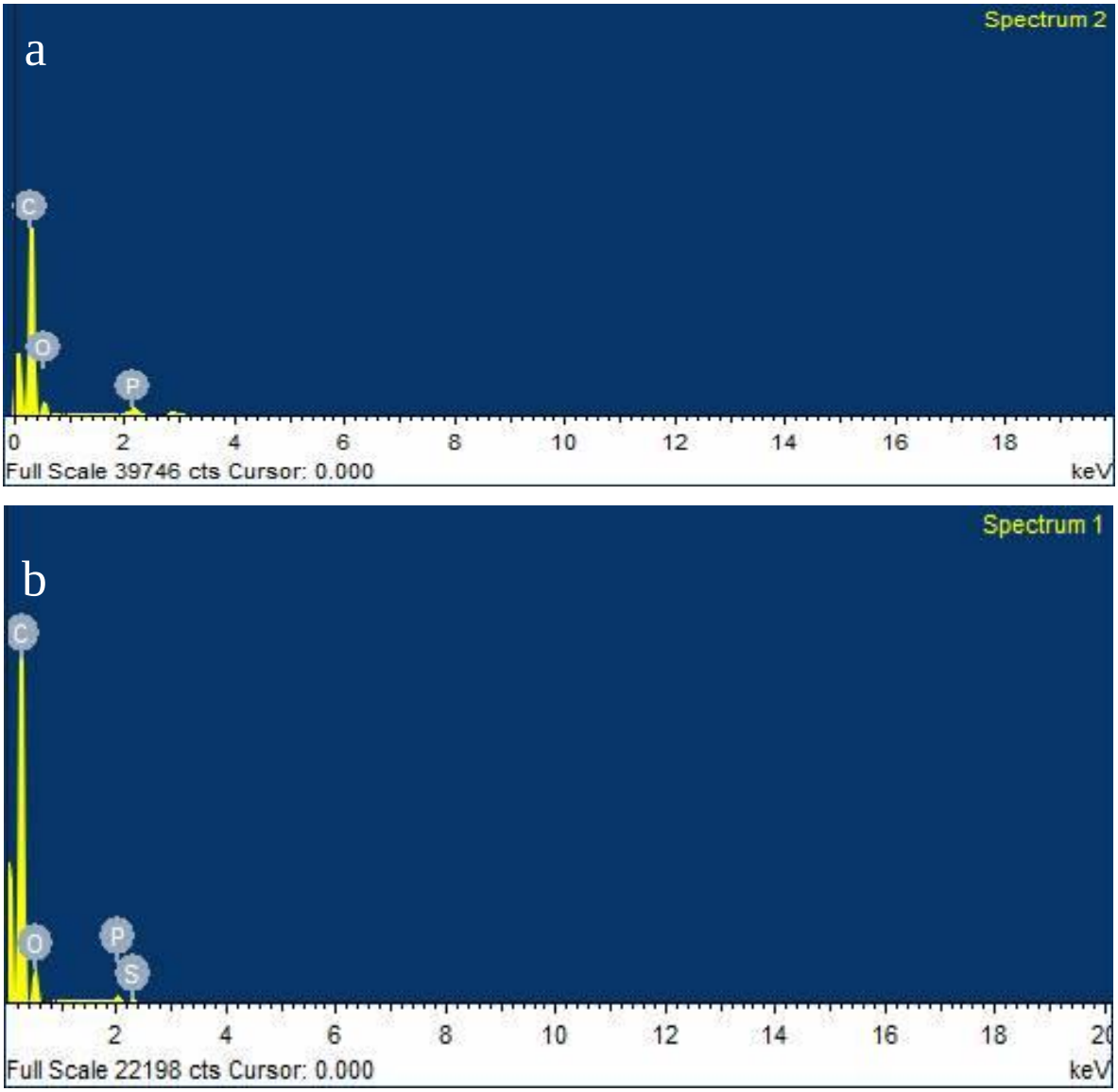


Figure 6.3.EDX spectrum for AC (a) Before desulfurization (b) After desulfurization

Table 6.1: Elemental composition of fresh activated AC and used AC

Element	Weight %		Atomic %	
	Fresh AC	Used AC	Fresh AC	Used AC
C	81.80	85.47	87.17	88.49
O	14.10	15.00	11.13	10.89
P	4.10	0.82	1.70	0.31
S	0.00	0.71	0.00	0.30
Total	100.00	100.00	100.00	100.00

Nitrogen adsorption-desorption experiment of the adsorbent at 77 K was conducted as described in chaper three of this thesis. Table 6.2 shows the textural properties of the adsorbents; Surface area, pore volume and pore size of the adsorbent were measured to be 1154.87 m^2/g, 1.02 cm^3/g and 3.45 nm for AC. AC has high surface area and pore colume and pore size. However, after adsorption, the surface area, pore volume and pose size were found to have decreased to 987.89 m^2/g, 0.761 cm^3/g, 1.83 nm, respectively. Adsorption perfomances of the adsorbents are dependent on their textural properties. Therefore, the high surface area of the adsorbent would enhanced its adsorption capacities.

Table 6.2: Surface area, pore volume and pore sizes of the adsorbents

Adsorbents	Surface area (m^2/g)	Pore volumes (cm^3/g)	Pore sizes (nm)
AC before adsorption	1154.87	1.020	3.45
AC after adsorption	987.89	0.761	1.83

Fig. 6.4 depicts the FTIR spectra of activated carbon before and after adsorption. The spectra showed the C–H out-of-plane bending vibrations in benzene derivative cause the bands at 848 cm^{-1} (Lua and Yang, 2004). The appearance of a band at 1365 cm^{-1} can be attributed to C–O stretching vibrations in carboxylate groups (Liu et al., 2010). The peak at 1570 cm^{-1} represented the C–C stretching of aromatic rings. While the band around 1600 cm^{-1} is ascribed to the aromatic ring or C═C stretching vibration (Shi et al., 2010). The band around 1753 cm^{-1} is usually caused by the stretching vibration of C═O carboxyl groups. The band at 3000 cm^{-1} can be attributed to the C-H stretching vibration (Yang and Qui, 2010). The broad peak at 3245 cm^{-1} is attributed to the O-H group or/ and absorbed water. It can be clearly seen that some of the peaks showed in the fresh activated carbon adsorbent shifted after adsorption had been carried out on the adsorbent. However, a peak is noticed on the used adsorbent at 2308 cm^{-1}. This band can be attributed to S-CΞN stretching vibration in thiocyanate. Thiocyanate is an analogue of Cyanate ion where oxygen is replaced by sulfur. This is an indication that sulfur has been attached to the surface of the activated carbon after adsorption.

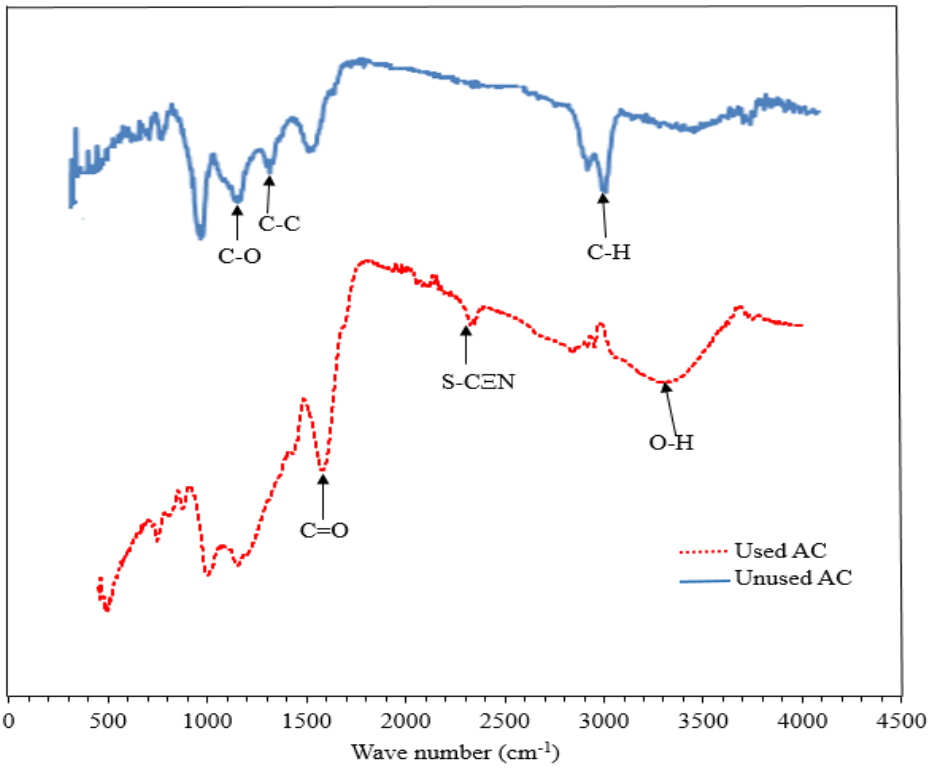


Figure 6.4 FTIR spectra of used and unused activated carbon

6.3.2 Performance evaluation of activated carbon during desulfurization

To understand adequately the performance of AC during adsorptive removal of DBT from model and real diesel, effect of operating parameters on adsorption performance of the adsorbents was investigated. The results obtained are hereby discussed.

It is essential to understand the effect of temperature on the adsorption of DBT molecules onto the surface of an adsorbent as it controls the adsorption mechanism and the adsorption performance of the adsorbent during adsorption process. Fig. 6.5 (a) depicted the effect of temperatures on the adsorption of DBT molecule onto the surface of activated carbon. From the results in Fig. 6.5, it can be observed that there was a decrease in the percentage removal of DBT by AC as the temperature increased from 298 K to 308 K. This situation explains the fact that adsorption is an exothermic process where adsorption is favoured with a decrease in temperature, therefore, enhancing the adsorption performance of the adsorbent. Another known fact is that increase in temperature favours desorption, which means desorption process occurred as the temperature increased from 298 K to 308 K. This result is similar to what was obtained in Nazal et al. (2015)

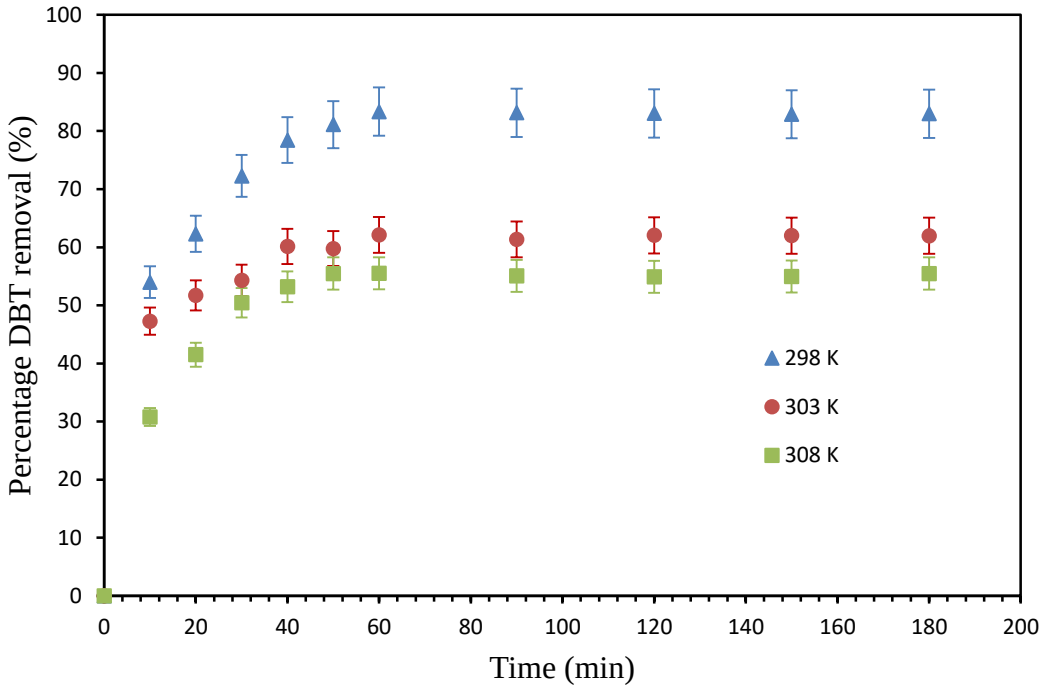


Figure 6.5 Effect of temperatures on adsorption of DBT onto Activated carbon. Experimental conditions: Initial DBT Concentration: 1000 mg/L; Amount of adsorbent: 1 g.

In order to determine the equilibrium contact time for the adsorption of DBT molecules from model oil onto AC adsorbents, the adsorption study was carried out in batch mode at different time intervals ranging from 0 to 180 min, while other experimental conditions such as: initial DBT concentration (1000 mg/L), model oil volume (20 mL), adsorbent dose (1.0 g) and temperature (298 K) were kept constant. Effect of contact time on the adsorption of DBT from model diesel onto activated carbon is shown in Fig. 6.6. The result showed rapid intake of the DBT molecules onto the surfaces of AC for the first 10 min. About 54 % DBT removal has been attained. This is attributed to the large number of vacant sites on the surfaces of the adsorbents at the earlier stage of the adsorption process. However, the adsorption performance slowed down from 10 min to 60 min due to decrease in the number of adsorption sites on the surface of the adsorbents since most of the sites have been occupied by DBT molecules. It can be concluded that 60 min is the equilibrium time for the removal of DBT by AC adsorbents where about 83 % DBT was removed from the model oil. After the equilibrium time, the results showed that there was no further decrease in the amount of DBT molecules adsorbed with increasing time; this is because of decreasing DBT concentration and a decrease in the number of active sites on the surface of the adsorbent (Vadivelan and Kumar, 2005; Namasivayam 1993). High DBT removal performance

by AC is expected considering the higher surface area and pore volume obtained from the N_2 adsorption-desorption experiment at 77 K (see Table 6.1).

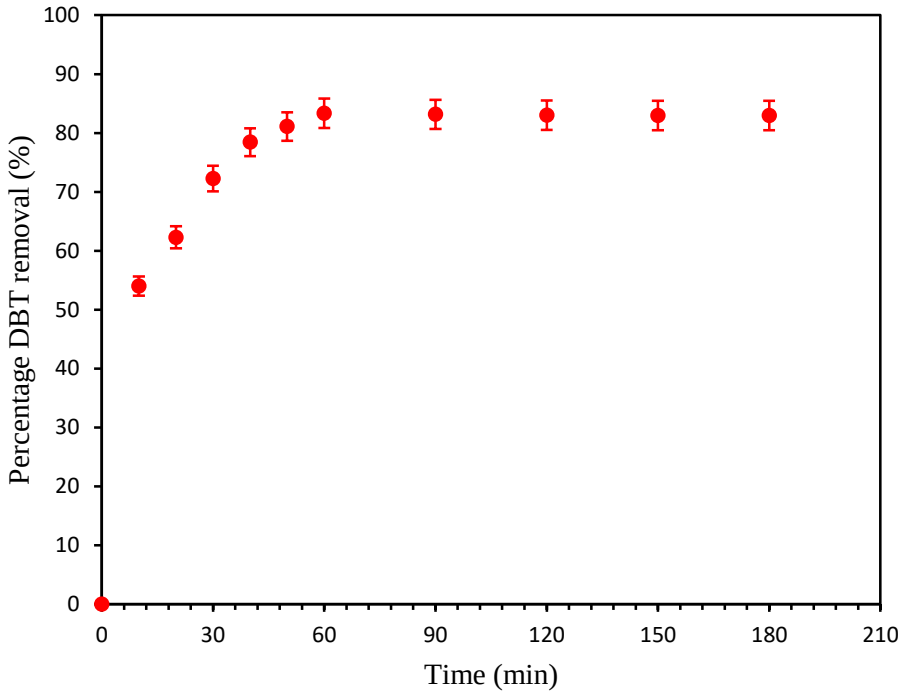


Figure 6.6 Effect of time on the adsorption of DBT onto AC. Experimental conditions: DBT concentration: 1000 mg/L; Amount of adsorbent: 1 g; Temperature: 298 K

Fig. 6.7 depicts the effect of amount of adsorbent on the adsorption of DBT onto AC adsorbent. It can be observed that percentage of sulfur removal increased with increase in amount of adsorbent (AC). This result could be as a result of increase in the number of adsorption site as the amount of adsorbent increases. The results show that, as the adsorbent dosage increases, the percentage of DBT adsorbed on the surface of the adsorbents also increased. This trend could also be attributed to the availability and accessibility of more adsorption sites and more surface area for DBT molecule attachment on which adsorption process is dependent. This result is comparable with literature (Dizge et al., 2008; Srivastav and Srivastav, 2009; Daware et al., 2015; Ahmad et al.,

2017). AC adsorbent attained equilibrium at 1.0 g with percentage sulfur removal of 83.34 %. There was no obvious increase in percentage sulfur removal when the amount of adsorbent increased from 1.0 g to 1.4 g (Graph not shown). Therefore, equilibrium is said to be reached for both adsorbents at 1.0 g of adsorbent amount.

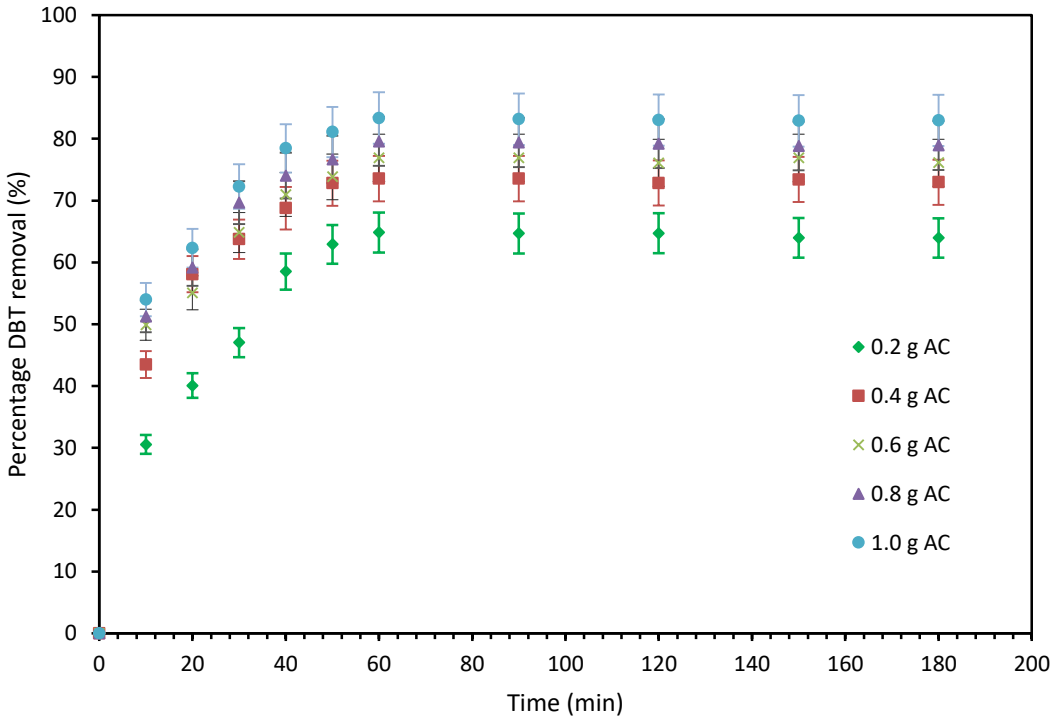


Figure 6.7 Effect of amount of adsorbents on the adsorption of DBT onto AC. Experimental conditions: Temp.: 298 K, Initial DBT concentration: 1000 mg/L; Amount of adsorbent:1 g.

Fig. 6.8 depicts the effect of initial concentration of DBT on its adsorption onto AC. Since diesel contains DBT in different concentrations, it is essential to carry out the adsorption study of DBT at different initial concentrations. Thus, the adsorption of DBT from model oil onto AC was carried out at different initial DBT concentrations, ranging from 250 mg/L to 1000 mg/L while other experimental conditions such as contact time (60 min), adsorbent dose (1.0 g), model oil volume (20 mL) and temperature (298 K) were kept constant. The results obtained for the desulfurization of model diesel at different DBT concentrations are depicted by Fig. 6.8. From the figure, it can be deduced that the adsorption of DBT per unit mass of the adsorbent increases with increasing

initial DBT concentration for AC. The increase of DBT adsorption with respect to its initial concentration is as a result of the increase in mass transfer driving force due to concentration gradient developed between the bulk solution and surface of the adsorbent (Anbia and Parvin, 2011). The DBT per unit mass of the adsorbent increased from 4.50 -16.67 mg/g as the initial concentration increased from 250 mg/L -1000 mg/L. The percentage adsorption of DBT on to AC decreased with increasing initial DBT concentration from 250 mg/L to 1000 mg/L. This decrease in percentage adsorption of DBT onto AC with increasing initial DBT concentration may be contributed to the saturation of available active sites of the adsorbent at higher DBT concentration. The result observed in this study is in agreement with literature (Nejad et al., 2013; Ishaq et al., 2015; Daware et al., 2015).

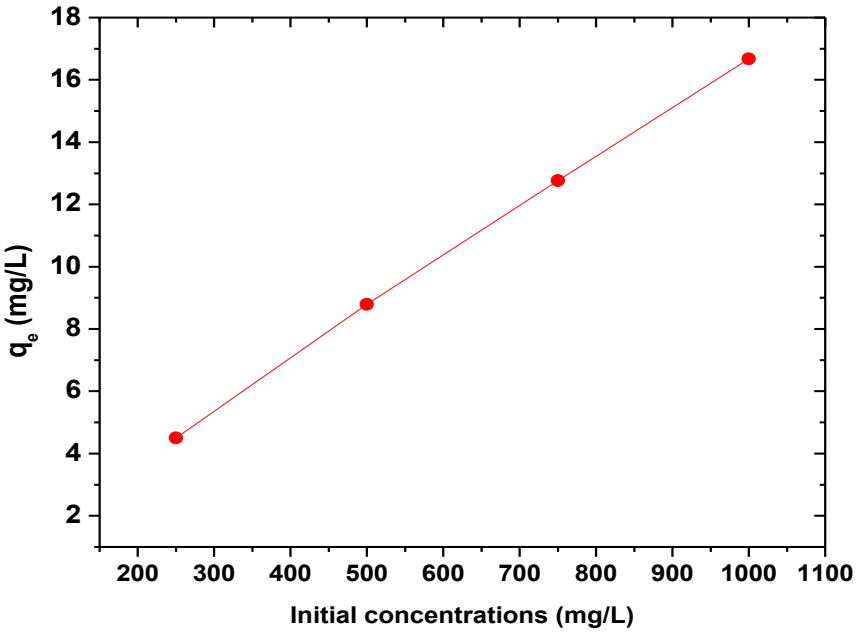


Figure 6.8 Effect of initial concentration on the adsorption of DBT onto activated carbon. Experimental conditions: Amount of adsorbent: 1.0 g; Temperature: 298 K; Time: 60 minutes.

The evaluation of the adsorbent was performed on South African real type diesel (diesel obtained before HDS and diesel obtained after HDS). The best operating conditions for model diesel experiment was used. Therefore, adsorption performance of the adsorbent was evaluated using model diesel and real diesel at the same conditions. Fig. 6.9 depicts the performance evaluation of AC for removal of DBT from real diesel and model diesel. Results show that, adsorption of DBT onto the surface of the adsorbent was initially rapid for both model diesel and real diesel samples. This could be as a result of more available active adsorption sites on the surface of the adsorbent. It could also be observed that AC adsorbed about 100 % of the DBT in the model diesel at equilibrium contact time of 40 minutes, after which no observable further decrese in DBT occurred. About 76.43 % removal of BDT was observed in the diesel after HDS. The lower adsorption performance of AC on diesel after HDS compared to model diesel could be attributed to other impurities present in it, which might affect the selectivity of the DBT for adsorption. A further decrease in adsorption performance was observed with diesel before HDS. About 30.28 % DBT was removed which is lower that the percentage DBT removed by model diesel and diesel after HDS. The higher performance of AC for removing DBT from diesel after HDS could be as a result of the hydrodesulfurization process that the diesel oil has undergone. This has been able to remove most of the heteroxyclic compounds in it. Results showed that the highest DBT removal by AC was achieved with model oil. This could be because there are no other compounds in the solution except DBT, therefore enhancing the adsorption of the DBT onto the active adsorption sites of the AC. For better performance of the AC for removal of DBT form typical South African diesel samples, the operating condition, such as temperature may be increased.

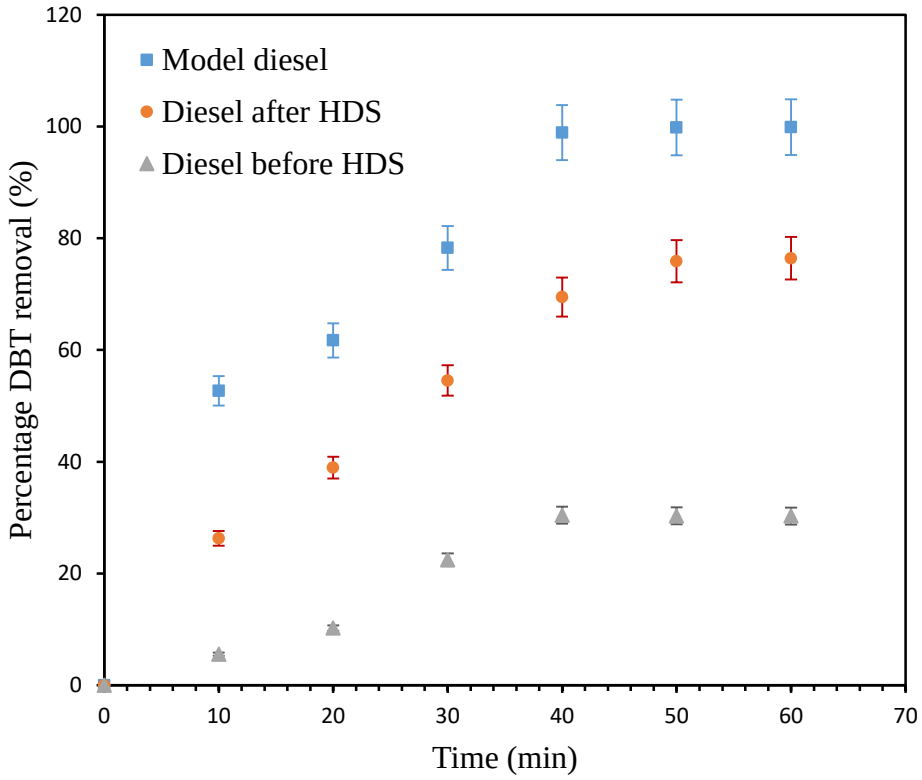


Figure 6.9 Performance of AC for removal of DBT from model diesel, diesel obtained after HDS and dieselobtained before HDS. Experimental conditions: Amount of adsorbent: 1.0 g; Initial DBT concentration: 120 mg/L, Temperature 303 K.

Evaluation of the performance of AC by increasing the contact time and temperature in the adsorption experiment for removal of DBT from typical South African real diesel samples are reported. The detailed procedure of the experimental is in the chapter 3 of this thesis

Fig 6.10 depicts the effect of temperatures on the desulfurization of diesel after HDS. In order to understand the effect of temperature on the desulfurization of diesel after HDS, temperature was varied from 298-318 K, while other experimental conditions such as, initial DBT concentration (120 mg/L), time (120 min), amount of adsorbent (1.0 g) remained constant. The results show that there was increase in adsorption capacity as the temperature increased. This could be as a result of pore widening as the temperature increased therefore enhancing the uptake of the sulfur compound onto the surface of the adsorbent. In addition, this could be due to the fact that the mobility of DBT molecules increased, in the porous structure of adsorbent, as the temperature increased, therefore, overcoming the activation energy barrier. The same observation was reported by Fayazi et al. (2015) and Ishaq et al. (2017)

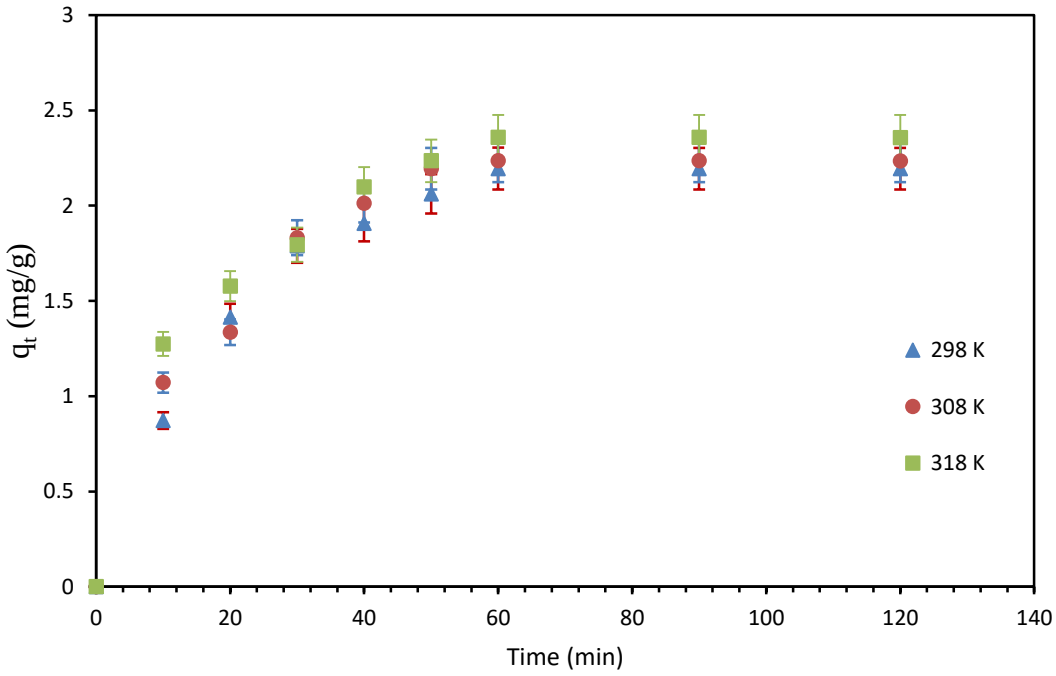


Figure 6.10 Effect of temperature on adsorption of DBT onto activated carbon. Experimental conditions: Amount of adsorbent: 1.0 g; Initial DBT concentration: 120 mg/L.

Fig. 6.11 shows the desulfurization and percentage DBT removal of from two diesel samples. SA diesel before HDS was diluted to 120 mg/L which is the initial concentration of diesel after HDS. This was considered necessary to understand the selectivity of DBT for adsorptive removal, since

diesel before HDS consists of many organic components. The chromatographs of SA diesel after HDS and SA diesel before HDS are shown in Fig 6.12 (a) and (b). It was observed that percentage desulfurization of diesel after HDS sample (98.24 %) was higher than than of diesel before HDS (60.93 %). Diesel after HDS showed 98.24 % desulfurization at 60 minutes, after which no further sulfur removal was observed. This could be because there was little or no DBT again in the diesel sample. However, at 50 min, only about 60 % sulfur removal was achieved for diesel before HDS and no further decrease in DBT removal was observed. This could be as a result of lower selectivity for DBT removal owing to present of other organo-sulfur components in the diesel. This results showed and improvement in the percentage removal of DBT when the temperature was increased from 303 K (see Fig. 6.9) to 318 K (see Fig. 6.11). This could be as a result of activation energy that is overcome due to increase in temperature which increase the movement of the DBT onto the surface of the AC

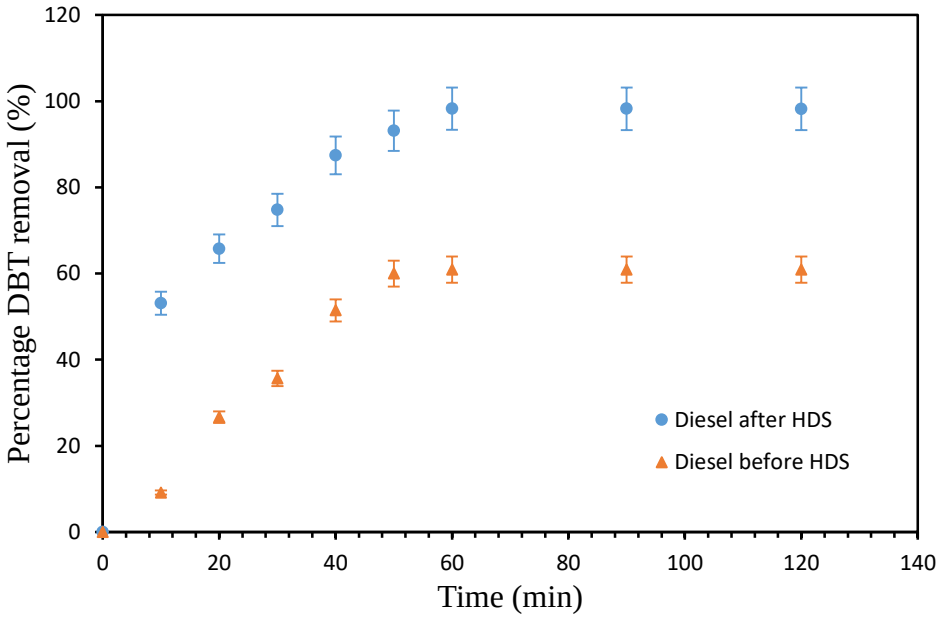


Figure 6.11 Desulfurization of diesel obtained after HDS and diesel obtained before HDS. Experimental conditions: Initial concentrations of DBT: 120 mg/g; Amount of adsorbent: 1.0 g; Temperature: 318 K.

Fig. 6.12 (a), (b) and (c) show the chromatograms for detection of retention time and peak of DBT compound, presence of DBT in hydrodesulfurized diesel sample and presence of DBT in the

hydrodesulfurizer feed sample, respectively. Fig. 6.12 (a) showed the elution time and peak of DBT at around 9 minutes as indicated by the mass spectrum showed MS spectrum of DBT with m/z 184 (Li et al., 2003). This is an indication that the compound at retention time of 9 minutes was DBT. The same peaks were observed in Fig. 6.12 (b) and 6.12 (c) at the same elution time. In Fig 6.12 (b), it could be observed that there are lesser organic components compared to the chromatographs of South African diesel before HDS with many organic components in Fig 6.12 (c). The fewer components in the diesel after HDS could be as a result of HDS process that this sample has undergone. The peak area of DBT at 9 minutes detection time as shown in Fig. 6.12 (b) was also observed to be lower than that of the diesel before diesulfurization in Fig 6.12 c). This showed that HDS of diesel reduced the amount of DBT in it, although not completely.

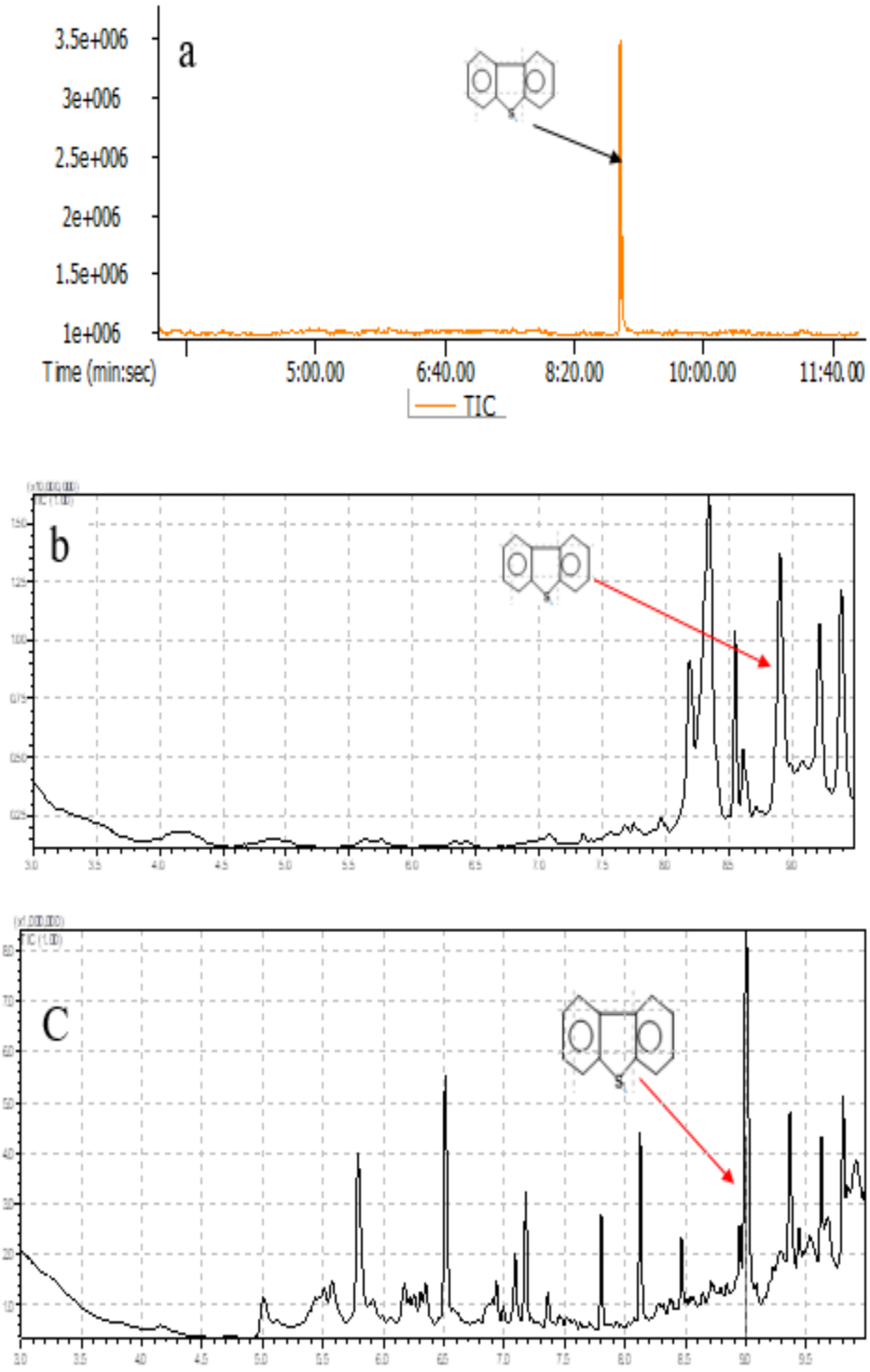


Figure 6.12 Chromatogram (a) Detection of peak and retention time of DBT using GC/MS (b) diesel obtained after HDS (c) diesel obtained before HDS

6.4 Isotherms, kinetics, and thermodynamics of AC for adsorption

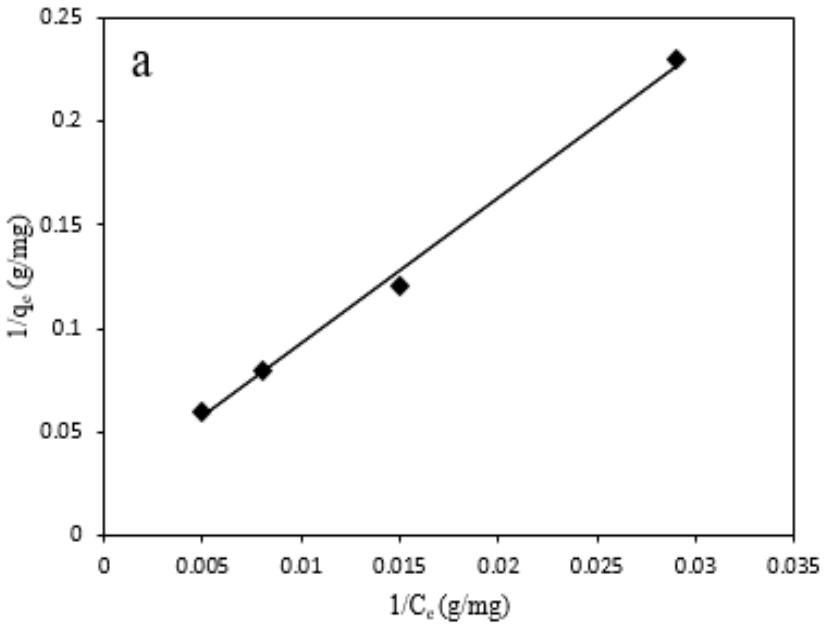
For better understanding of the mechanism and behaviour of adsorption process of DBT in model oil by AC, the results of isotherms and kinetics studies of this study are reported.

Langmuir and Freundlich isotherm parameters for adsorption of DBT in model diesel onto AC are given in Table 6.3. Fig. 6.13 (a) represents the Langmuir isotherm of DBT adsorption onto AC, Fig. 6.13 (b) depicts the Freundlich isotherm for DBT adsorption onto AC. It can be observed that both langmuir and Freundlich isotherm models described perfectly the behaviour adsorption of DBT onto AC perfectly. They both have high correlation coefficients (R^2) values. Langmuir isotherm model with R^2 value of 0.9952 and Freundlich isotherm model with R^2 value of 0.9693.. The values of R_L value was calculated to be 0.24 which is <1, indicating that the adsorption process is favourable. The result indicated that the adsorption took place at specific homogeneous sites within the adsorbent forming monolayer coverage of DBT at the surface of the activated carbon. This is in agreement with Wang and Wei, (2017). The value of b that reflects the activity of binding site is < 1 and the inverse of adsorption intensity, 1/ n is <1 which indicate favorability of the adsorption process.

Table 6.3: Langmuir and Fruendlich Isotherm model parameters for AC

Adosrbent	**Langmuir Isotherm**				**Freundlich Isotherm**		
	Temp (K)	**R_L**	**b (L/mg)**	**R^2**	**K_f (mg/g)**	**N**	**R^2**
AC	298	0.24	0.0031	0.9952	0.279	1.271	0.9693

b is the Langmuir's contact, K_f is the Freundlich's constant, n is the adsorption intensity, R_L is the Langmuir separation factor and R is the correlation coefficient



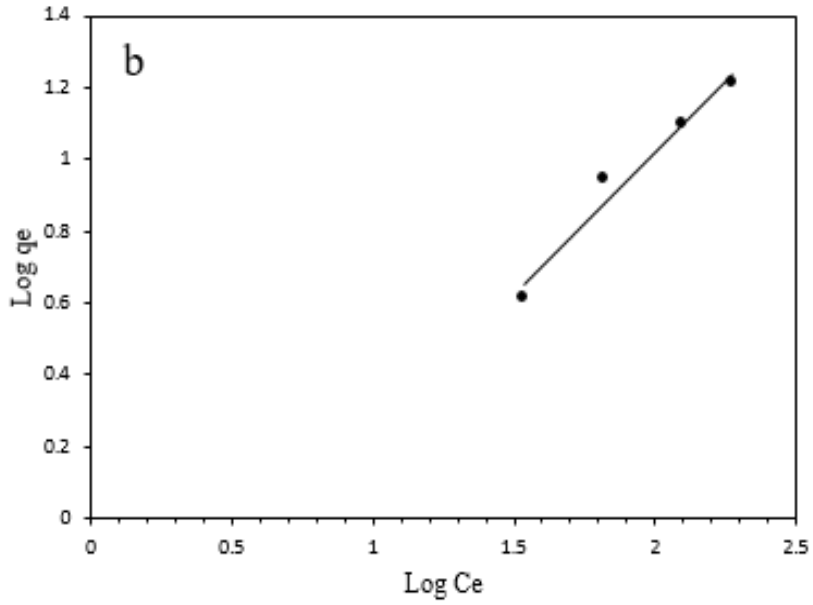


Figure 6.13 (a) Langmuir isotherm model for adsorption of DBT onto AC (b) Freudlich isotherm model for adsorption of DBT onto AC. Experimental conditions: Amount of adsorbents: 0.2 g; Temperatures: 298 K; Initial concentrations: 250-1000 mg/L

Adsorption kinetics for adsorption of DBT in model oil onto AC were described by pseudo first-order and pseudo second-order kinetic models. Table 6.4 presents the parameters of pseudo first-

order and pseudo-second order of DBT adsorption onto AC at 298, 303, and 308 K. Comparing the correlation coefficient (R^2) of the pseudo first-order kinetics with second-order kinetics, it it could be observed that, the pseudo second-order model described well the kinetics of the adsorption process. The correlation coefficients, R^2 of pseudo second-order were 1.0000, 0.9994, 0.9982 which are higher than the correlation coefficient (R^2) (0.7240, 0.8547, 0.5417) for pseudo first-order kinetic at 298 K, 303 K and 308 K, respectively. In addition the experimental adsorption capacity at equilibrium (qe) (16.67 mg/g) values obtained for pseudo second-order kinetics are very close to the calculated q_e (16.72 mg/g) compared to what was obtained for the experimental adsorption capacity at equilibrium (q_e) (16.67 mg/g) and calculated q_e (2.07) for the pseudo first-order kinetics (Table 6.4) at 298 Kat 298 K. It could be assumed that there were involvements of chemical interactions in the adsorption process. In addition, the rate of adsorption may be controlled by the movement of DBT molecules within the pore of the activated carbon. The result obtained in this study is in agreement with tresults obtained by Wang and Wei (2017). Lower correlation coefficient factor for pseudo-first order could be an indication that the rate of adsorption process does not depend on concentration factor, but depends on both concentration and time. This is in agreement with Kumar and Tamilarasan, (2017)

Table 6.4: Parameters for pseudo first and pseudo second-order kinetics for AC

Temp (K)	**Pseudo-firstst order**				**Pseudo-second order**			
	$q_{e\ (expt)}$ (mg/g)	**$q_{e\ (calc.)}$ (mg/g)**	**K_1 (L/min)**	**R^2**	**$q_{e\ (expt)}$ (mg/g)**	**$q_{e\ (calc.)}$ (mg/g)**	**K_2 (g/mg.min)**	**R^2**
298	16.67	2.07	0.033	0.7240	16.67	16.72	0.096	1.0000
303	12.42	4.06	0.035	0.8547	12.42	12.61	0.079	0.9994
308	11.10	2.58	0.031	0.5417	11.20	11.34	0.024	0.9982

q_e is the amount of DBT adsorbed at equilibrium, R is the correlation coefficient, K_1 is the pseudo-first order constant and K_2 is the pseudo-second order constant.

The values of adsorption thermodynamics parameters, standard free energy, ΔG^o, standard entropy, ΔS^o and standard enthalpy ΔH^o for AC adsorbent are presented in Table 6.5 The negative values of ΔG^o and the negative values of ΔH^o indicate that DBT adsorption onto AC is spontaneous and exothermic process. Negative ΔS^o values of DBT adsorption process indicate a decrease of the randomness at the AC-solution interface during adsorption. In addition, the result show that the values of standard entropy S decreased with increase in temperature, while the values of standard free energy G increased with increase in temperature. The activation values obtained for activated carbon is 57.78 2 kJ/mol. These values is less than 65 kJ/mol, which is an indication that adsorption of DBT onto AC occurred more readily. In addition, the adsorption processes for AC could be said to be physical adsorption. This is in agreement with Fei et al. (2017) and Saini et al. (2017).

Table 6.5: Themothynamic parameters for adsorption of DBT on AC

Adsorbent	**Temp.(K)**	**ΔH^o (kJ/mol)**	**ΔG^o (kJ/mol)**	**ΔS^o (J/k/mol)**	**E_A (kJ/mol)**
AC	**298**	-57.78	- 11.41	-155.61	57.78
	303		- 8.79	-161.68	
	308		- 8.25	-160.83	

ΔH^o : Standard enthalpy; ΔG^o: Standard free energy; ΔS^o: Standard entropy; EA: Activation energy.

6.5 Regeneration and re-usability of activated carbon

Fig. 6.14 depicts the re-usability efficiency of AC for adsorption of BDT in model diesel, diesel obtained after HDS and diesel obtained before HDS in reference to initial experiment (Ref expt). Adsorption-desorption cycle is essential in adsorptive desulfurization owing to the growing concern for waste minimization, recovery, and reuse of adsorbents that could promote their application in the refining industry. Results show that reusability efficiency of AC for removal of DBT in model diesel decreased gradually from 99.2% in the first cycle to 97.8 % in the 2nd cycle to 97.2 % in the 3rd cycle and to 95.2 % in the 4th cycle. This could be as a result obtained from the FTIR spectra of AC adsorbent where there was attachment of sulphur onto the surface of the adsorbent, making it difficult for the DBT molecule to be completely washed during desorption. Therefore, more spaces are occupied by the DBT molecules after each adsorption-desorption cycle. Even with the difficulty encounteded during adsorbent washing, only 4.6 % decrease in usability was obtained after the 4th cycle, with reference to the initial experiment. This result showed that AC can be reused which will promote its commercial application.

Re-usability of AC in diesel obtained after HDS show that the efficiency decreases for 98.23 %, 95.23 %, 90.01 %, 88.09 % and 85.11 % for 1st, 2nd, 3rd and 4th cycles, respectively. About 13.12 % decrease in efficiency was obtained in reference to the reference experiment. The decrease in the re-usability efficiency could be as a result of impurities remaining in it after HDS, hindering the adsorption of DBT. About 20.7 % decrease in re-usability efficiency of AC was noticed for removal of DBT from diesel before HDS. This decrease could be attributed to poor selectivity of DBT, owing to the numerous organo-sulfur compounds present in it.

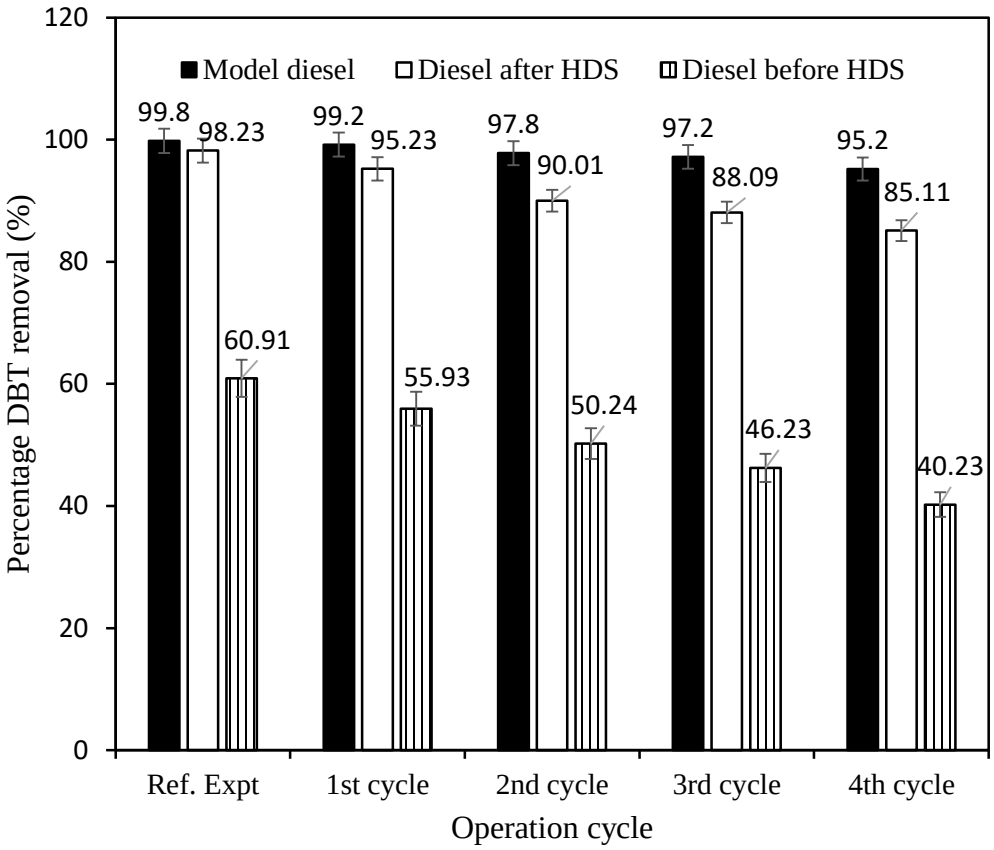


Figure 6.14 Re-usability efficiency of AC adsorbents. Experimental conditions: Amount of adsorbent: 1.0 g; Temperature: 318 K; Initial DBT concentration: 120 mg/L.

The results documented in this chapter are compared with literature. Table 6.6 summarizes comparison of the result in this study with literature. Xiao et al. (2010) also performed a batch experiment using AC-Ag/Cu/Fe for desulfurization of DBT in model oil at 30 ^{o}C, with an initial DBT concentration of 1843 mg/L, at contact time of 2880 min with 1.0 g amount of adsorbent and the percentage sulfur removal was 91.2 %. Anisuzzaman et al. (2017) investigated the adsorptive performance of activated palm kernel shell adsorbent for the removal of DBT from model oil. The percentage sulfur removal achieved was 91.5 % which was higher than the result obtained from this study. Although Anisuzzaman et al. (2017) started with a DBT concentration which is 100 % lower than the initial concentration used in this study. However, the initial DBT used by Xiao et

al., 2010 was higher than the initial concentration used in this study, yet the time for their equilibrium to be reached was 2880 min, against 60 min that was used in this study to reach equilibrium. The result in this study for activated carbon can be improved if the surface can be modified or treated before desulfurization. Although, Lin et al. (2012) started with a lower initial concentration compared with what was used in this study, yet the result in this study was better than their own with better adsorption performance. Lin et al. (2012) adsorbed DBT onto AC modified by Cerium starting with initial DBT concentration of 500 mg/L at 30 ^{o}C, contact time of 1080 min with 0.75 g amount of adsorbent. The adsorptive desulfurization achieved was 52.6 %. The percentage DBT removal from this study for AC is higher than the result obtained by Lin et al. (2012), although O.75 g adsorbent mass was used against 1.0 g that was used in this study. Considering the lower initial concentration (500 mg/L), and the equilibrium time (1080 min), the result from this study is better.

Comparing the results obtained for desulfurization of South African diesel in this study with Literature, it can be seen from Table 6.6 that the results are higher than most of the results obtained in literature. About 55 % sulfur removal was achieved by Al-Zubaidy et al., 2013, even when 41 g of adsorbent was used. The lower performance of desulfurization compared to this study could be as a result of higher initial DBT concentration (410 mg/L) used by the authors. Marin-Rosas studied the adsorption of DBT onto AC at initial DBT concentration of 72 mg/L. About 82 % desulfurization was achieved, which is higher than the result obtained for desulfurization of diesel obtained before HDS (60.91 %). This could be as a result of amount of adsorbent used by the author (200 g) which is higher than what was used in this study. However, the performance AC for desulfurization of diesel obtained after HDS (98.23 %) is higher than what was obtained by Marin-Rosas et al. (2013).

In conclusion, the performance of the AC documented in this study for the removal of DBT in model diesel and real diesel is comparable with results reported in literature. This results show that the use of AC as adsorbent for desulfurization of sulphur-containing compound in petroleum distillate could provide a platform for further research efforts in this field.

Table 6.6: Comparison of results with literature

Adsorbent	Type of PD	C_o (mg/L)	C_f (mg/L)	%SR	Temp (K)	Time (hr)	Amount of ads (g)	Ref.
AC/Ce	DBT	500	236.8	52.60	303	18	0.75	Lin et al. (2012)
AC-Ag/Cu/Fe	DBT	1843	162.6	91.20	303	48	1.00	Xiao et al. (2010)
APC	BT	10	0.85	91.50	298	35	0.10	Anisuzzaman et al. (2017)
AC	Diesel	410	194.6	55.00	30	2.0	41.00	Al-Zubaidi et al. (2013)
AC	Diesel	72	15	82.00	25	0.5	200.00	Marin-Rosas, (2010)
AC	DBT	1000	166.6	83.34	25	1.0	1.00	This study
AC	DBH	120	46.91	60.91	45	1.0	1.00	This study
AC	DAH	120	2.12	98.23	45	1.0	1.00	This study
AC	DBT	120	0.14	99.88	30	0.6	1.0	This study

C_o is initial DBT concentration, C_f -final DBT concentration, SR-sulfur (DBT) removal, PD-petroleum distillate, ads-adsorbent, DAH-diesel after HDS, DBH-diesel before HDS

6.6. Concluding remarks

As it has been established in this chapter, AC is a promising adsorbent for removal of sulfur containing compound (DBT) from model diesel and typical South African diesel. The result showed that large surface area of AC contributed to its performance removal of the DBT in model oil. The percentage performance of the adsorbents was 83.84 % at 1.0 g adsorbent dosage, temperature of 25 ^{o}C and maximum contact time of 1 h. Comparing AC with other adsorbents studied in this study, it has the highest performance for DBT removal from model diesel. The performance of AC on model diesel desulfurization was also compared to its performance on real diesel (Diesel obtained after HDS and diesel obtained befor HDS) desulfurization. The results show that AC effectively removed DBT from model oil than it did in diesel obtained after HDS and diesel obtained before HDS. Re-usability efficiency from AC for removal of DBT follows the descending order; model diesel > diesel after HDS > diesel before HDS. AC can be of great value in commercial application since it can be re-used up to four times without losing its potential strength for removal of DBT from petroleum distillate. A higher adsorption capacity is obtained at minimum amount of adsorbent and this could promote its commercial application.

In understanding the mechanism and behavior sof the adsorption process, both Langmuir and Freundlich isotherm models and could describe well the mechanism of the adsorption process for AC. The pseudo second-order kinetics described the adsorption mechanism of the adsorption process with closer values of experimental with the model parameters. Negative ΔS^{o} values of DBT adsorption process indicate a decrease of the randomness at the AC-solution interface during adsorption. In addition, the result show that the values of standard entropy ΔS^{o} decreased with increase in temperature, while the values of ΔG^{o} increased with increase in temperature. The ΔH value obtained for activated carbon is 57.78 2 kJ/mol.

The results show that AC is an efficient and promising adsorbent for removal of DBT in petroleum distillate such as diesel, so as to meet up with the stringent policies regarding emission of sulfur oxides. In a nutshell, the use of AC as adsorbent for the treatment of sulfur-containing petroleum distillates serves as a proof of concept in abatement of environmental pollution. The results documented in this study could pave the way for further R&D in this field

For speedy circulation of the novel contributions described in this chapter to the scientific community, a comparative study has been done on AC and PLP and the manuscript has been prepared to be submitted to the Journal of Chemical Engineering Transaction for possible publication.

6.7. References

Ahmaruzzaman, M., and Gupta, V. K. (2011) Rice Husk and Its Ash as Low-Cost Adsorbents in Water and Wastewater Treatment Ind. Eng. Chem. Res. 50, 13589–13613.

Anbia, M. and Parvin, Z. (2011) Desulfurization of fuel by means of nanoporous carbon adsorbent, Chem. Eng. Res. Des. 89, 641–647.

Al-Zubaidy, I. A. H. Tarsh, F. B., Darwish, N. N., Abdul Majeed, B. S.S., Al Sharafi, A., and Chacra. L. A. (2013) Adsorption Process of Sulfur Removal from Diesel Oil Using Sorbent Materials. Journal of Clean Energy Technologies, Vol. 1, No. 1, pp. 66-68.

Anisuzzaman, S. M., Abang, S., Krishnaiah, D. and Razlan, M.A.R. (2017) Adsorptive desulfurization of model fuel by activated oil palm shell. Indian Journal of Chemical Technology. 24, 206-212.

Bamufleh, H. S. (2011) Adsorption of Dibenzothiophene (DBT) on Activated Carbon from Dates' Stones Using Phosphoric Acid (H3PO4). JKAU: Eng. Sci., 22 (2), 89-105.

Bettermann, I. and Staudt, C. (2009) Desulfurization of kerosene pervaporation of benzothiophene/n-dodecane mixture, J. Membr. Sci. 343, 119–127.

Bhattacharjee, R. and Patel, R. (2017) Adsorption of chromium (VI) using neem leaves and pomegranate peels. Journal of Emerging Technologies and Innovative Research (JETIR), 4 (5)

Ceyhan, A.A., Sahin, Ö., Baytar, O. and Saka, C. (2013) Surface and porous characterization of activated carbon prepared from pyrolysis of biomass by two-stage procedure at low activation temperature and it's the adsorption of iodine. Journal of Analytical and Applied Pyrolysis 104, 378-383. J. Anal. Appl. Pyrol. 104, 378-383.

Daware, G.B., Kulkarni, A. B. and. Rajput, A. A. (2015) Desulphurization of diesel by using low cost adsorbent, International Journal of Innovative and Emerging Research in Engineering. 2 (6), 69-73.

Deniz, F. (2013) Adsorption Properties of Low-Cost Biomaterial Derived from Prunus amygdalus L. for Dye Removal from Water. The Scientific World Journal Volume 2013, Article ID 961671. 1-8

Eddebbagh, M., Abourriche, A., Berrada, M., Zina, M.B. and Bennamara, A. (2016) Adsorbent material from pomegranate (Punica granatum) leaves: Optimization on removal of methylene blue using response surface methodology. J. Mater. Environ. Sci. 7 (6), 2021-2033.

Fayazi, M., Taher, M.A., Afzali D. and Mostafavi, A. (2015) Removal of Dibenzothiophene Using Activated Carbon/γ-Fe2O3 Nano-Composite: Kinetic and Thermodynamic Investigation of the Removal Process Anal. Bioanal. Chem. Res., 2 (2), 73-84.

Folsom, B.R., Schieche, D.R., DiGrazia, P.M., Werner, J. and Palmer, S. (1999) Microbial desulfurization of alkylated dibenzothiophenes from a hydrodesulfurized middle distillate by Rhodococcus erythropolis I-19. Appl Environ Microbiol 65, 4967–4972.

Ishaq, M., Sultan, S., Ahmad, I., Ullah, H., Yaseen, M. and Amir, A. (2017) Adsorptive desulfurization of model oil using untreated, acid activated and magnetite nanoparticle loaded bentonite as adsorbent Journal of Saudi Chemical Society. 21 (2), 143-151.

Ishaq, M., Sultan, S., Ahmad, I., Ullah, H., Yaseen, M., Amir, A. (2015) Adsorptive desulfurization of model oil using untreated, acid activated and magnetite nanoparticle loaded bentonite as adsorbent Journal of Saudi Chemical Society, Pp.1-10

Javadli, R. de Klerk, A. (2012) Desulfurization of heavy oil. Applied Petrochemical Research, 1 (1) 3–19.

Kumar, A. and Jena, H. M. (2016) Preparation and characterization of high surface area activated carbon from Fox nut (*Euryale ferox*) shell by chemical activation with H_3PO_4, Results in Physics, 6, 651-658

Kaouah, F., Boumaza, S., Berrama, T., Trari, M. and Bendjama, Z. J. (2013) Preparation and characterization of activated carbon from wild olive cores (oleaster) by H_3PO_4 for the removal of Basic Red 46. Clean. Prod. 54 296-306.

Kertesz, M.A. and Wirtek, C. (2001) Desulfurization and desulfonation: Application of sulphur-controlled gene expression in bacteria. Appl. Microbiol. Biotechnol. 57, 460–466

Lua, A. C. and Yang, T. J. (2004) Characteristics of activated carbons prepared from pistachio-nut shells by physical activation. Colloid. Interf. Sci. 276, 364-372.

McFarland, B.L. (1999) Biodesulfurization, Curr. Opin. Microbiol. 2, 257–264.

Marı´n-Rosas, C., Ramı´rez-Verduzco, L. F., Murrieta-Guevara, F. R., Herna´ndez-Tapia, G., and Rodrı´guez-Otal, L. M. (2010) Desulfurization of Low Sulfur Diesel by Adsorption Using Activated Carbon: Adsorption Isotherms. Ind. Eng. Chem. Res. 49, 4372–4384.

Monticello, D.J. (2000) Biodesulfurization and the upgrading of petroleum distillates. Current Opinion in Biotechnology. 11, 540–546.

Nazal, M.K., Oweimreen, G.A., Khaled, M., Atieh, M.A., Aljundi, I.H. and Abulkibash, A.M. (2016) Adsorption isotherms and kinetics for dibenzothiophene on activated carbon and carbon nanotube doped with nickel oxide nanoparticles. Bull. Mater. Sci., 39 (2), 437–450.

Nejad, F.N. Amini, M.K. and Bennett, J.C. (2013) Synthesis of magnetic mesoporous carbon and its application for adsorption of dibenzothiophene, Fuel Process. Technol. 106, 376–384

Rashtchi, M., Mohebali, G.H., Akbarnejad, M.M., Towfighi, J., Rasekh, B., and Keytash, A. (2006) Analysis of biodesulfurization of model oil system by the bacterium, strain RIPI-22. Biochemical Engineering Journal 29, 169–173.

Seredych M, Xiong, L., Chen, F., Yan, X. and Mei, P. (2012) The adsorption of dibenzothiophene using activated carbon loaded with cerium J Porous Mater, 19, 713–719

Shaarani, F.W. and Hameed, B.H. (2011) Ammonia modified activated carbon for the adsorption of 2,4-dichlorophenol. Chem. Eng. J. 169, 180-185.

Shi Q. Zhang J. Zhang C. Li C. Zhang B. Hu W. Xu J and Zhao R. (2010) Preparation of activated carbon from cattail and its application for dyes removal. J. Environ. Sci. 22, 91-97.

Sing, K.S.W. Everett, D.H. Haul, R.A.W. Moscou, L. Pierotti, R.A. Rouquerol, J. *et al.* (1985) Reporting physisorption data for gas/solid systems with special reference to the determination of surface area and porosity. Pure Appl Chem, 57, 603-619.

Sych, N.V., Trofymenko, S.I. Poddubnaya, O.I., Tsyba, M.M., Sapsay, V.I. Klymchuk, D.O. P uziy, A.M. (2012) Porous structure and surface chemistry of phosphoric acid activated carbon from corncob, Appl Surf Sci, 261, 75-82.

Srivastav, A. and Srivastava, V. C. (2009) "Adsorptive desulfurization by activated alumina," Journal of Hazardous Materials, vol. 170, no. 2-3, pp. 1133–1140.

Wu, C.T, Brender, P., Ania, C.O., Vix-Guterl, C., and Bandosz, T.J. (2012) Role of phosphorus in carbon matrix in desulphurization of diesel fuel using adsorption process. Fuel, 92, 318–326.

Xiao, J., Bian, G., Zhang, W., and Zhong Li. J. (2010) Adsorption of Dibenzothiophene on Ag/Cu/Fe-Supported Activated Carbons Prepared by Ultrasonic-Assisted Impregnation Chem. Eng. Data 55, 5818–5823.

Yang, J. and Qiu, K. (2010) Development of high surface area mesoporous activated carbons from herb residues.Chem. Eng. J. 165, 209-217.

Chapter Seven

7.0 Enhancement of desulfurization performance of AC in packed-bed column using immobilized activated carbon

In this chapter, results of study of effect of operating variables on the enhancement of desulfurization performace of immobilized AC in a packed-bed column are reported. The kinetic models of the column adsorption study are presented as well.

7.1 Introduction

Activated carbon is the most commonly used adsorbent, owing to its large surface area and porous structure. Different researchers have investigated adsorption of activated carbon in batch adsorption mode. Although batch adsorption mode is needed for collecting basic data, but continuous adsorption modeis preferable in commercial application (Maftah et al., 2017). Furthermore, continuous adsorption process is feasible, cheap and requires less amount of adsorbent and can be easily controlled. High hydrostatic pressure causes disintegration of the adsorbent in the bed coulumn. This challenge can therefore be overcome by immobilizing the adsorbent. Furthermore, immobilization of adsorbent could overcome these challenges of column clogging and regeneration in a fixed bed column. The demands for sustainable techniques of entrapping adsorbent have increased in the recent times. Contribution of immobilization technology have attracted the attention of researchers in this direction. Immobolization technology also offers better reusability, high adsorbent loading, and minimal clogging in continuous mode (Jawad et al., 2018). Only few studies have been conducted on the removal of DBT from diesel using immobilized adsorbent in a fixed bed adsorption column. Therefore, activated carbon was immobilized into pellets for use in a continuous fixed bed adsorption column.

Breakthrough data obtained from continuous operation is instrumental to designing an industrial-scale desulfurization adsorption column. Furthermore, understanding the adsorption behavior and kinetics of the activated carbon in a packed bed column could pave way for its design and optimization. Therefore, Adams–Bohart model and Thomas model, being among the most commonly used models are used to represent breakthrough curve in adsorption studies. Hence, this chapter of the thesis reported the enhancement of AC in packed-bed column using immobilization

technology. In addition, the kinetics for modelling adsorption behavior of the adsorbent in a packed bed column using, Bohart-Adams, Thomas and Yoon-Nelson models were described as well.

7.2. Experimental

The material used, the preparation of the immobilization of adsorbent, adsorbent characterization and detailed experimental procedure were discussed in Chapter 3, (section 3.1.1 and 3.1.2) of this thesis. The evaluation of performance of the immobilized adsorbent during desulfurization has been described in Chapter 3 of this thesis. The analytical techniques used in this chapter have also been explained in Chaper 3 (section 3.1.2) Figure 7.1 (a) and Fig 7.1 (b) show the pictures of sodium alginate pellets and immobilized AC entrapped in sodium alginate, respectively. Model diesel and a typical real diesel obtained from a refinery in South Africa were desulfurized in this chapter in a contionous packed-bed adsorption column. The physical and chemical properties of the fuel were given in Table 3.1. The continuous fixed bed adsorption column set-up was described in chapter 3 in Fig. 3.3.

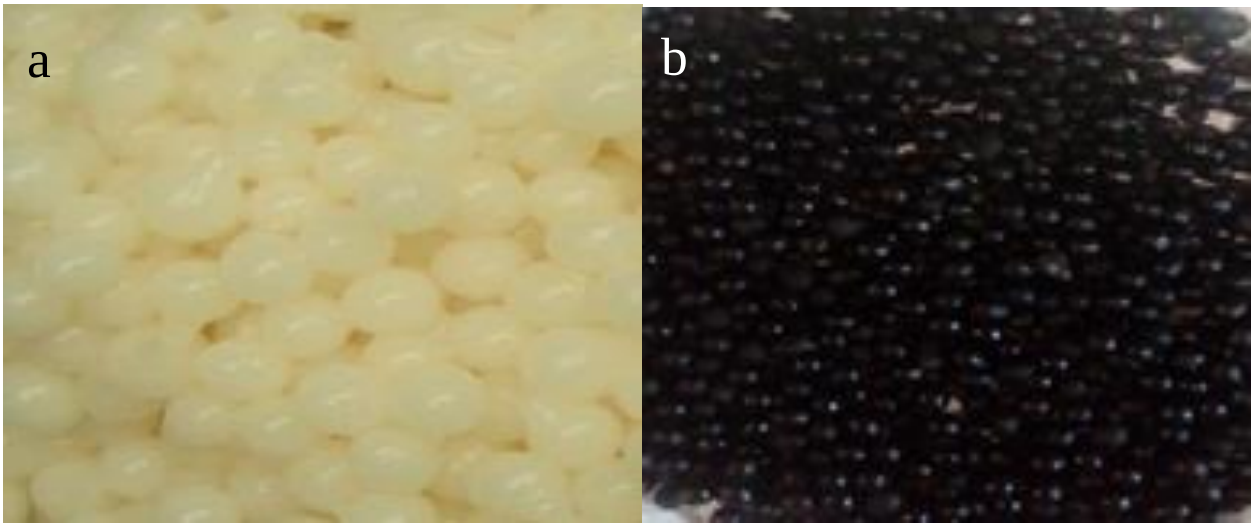


Figure 7.1 (a) Sodium algilate pellets (b) immobilized actvated carbon entrapped in sodium algilate

7.3 Results and discussion

7.3.1 Physico-chemical characterization of adsorbent

For detailed information about the results for physico-chemical characterization of adsorbent (AC), reference could be made to Chapter six of this thesis.

Fig. 7.2 depicts the surface morphology of (a) Fresh NaAlg-AC and (b) NaAlg-AC after use. It can be observed that the surface of the fresh NaAlg-AC was rough with well developed porous structure. However, after adsorption experiment, it could be observed that the pores on the surface of the adsorbent has been covered up. This could be due to the adsorption of DBT onto the surface of the adsorbent.

Fig. 7.3 shows the FTIR spectra of sodium alginate (NAalg) and AC trapped in sodium alginate (NaAlg-AC). The results show that, there was a stretching vibration of O-H bands appeared at band 3264 cm^{-1}. The stretching vibration of aliphatic C-H were also observed at 2992 cm^{-1} for both raw alginate and alginate-AC. The Observed band in 1596 cm^{-1} and 1416 cm^{-1} could be attributed to C=O symmetric stretching vibration and C-H in-plane deformation. The peaks at 1033 cm^{-1} could be attributed to the C-O stretching vibration and C-O stretching with contribution from C-C-H and C-OH deformation (Daemi et al., 2012). The FTIR spectrum showed a shift in the band around 1176 cm^{-1} and 1249 cm^{-1} in Alginate-AC which is absent in FTIR spectrum of raw alginate. This could be attributed to the C-C and C-O stretch as a result of the AC entrapped in it. It could also be obserbed that there was weakening of the band –OH group on the FTIR spectrum of alginate-AC. This could be due to utilization of some of –OH group on the NaAlg during the formation with the AC (Kummara et al., 2013)

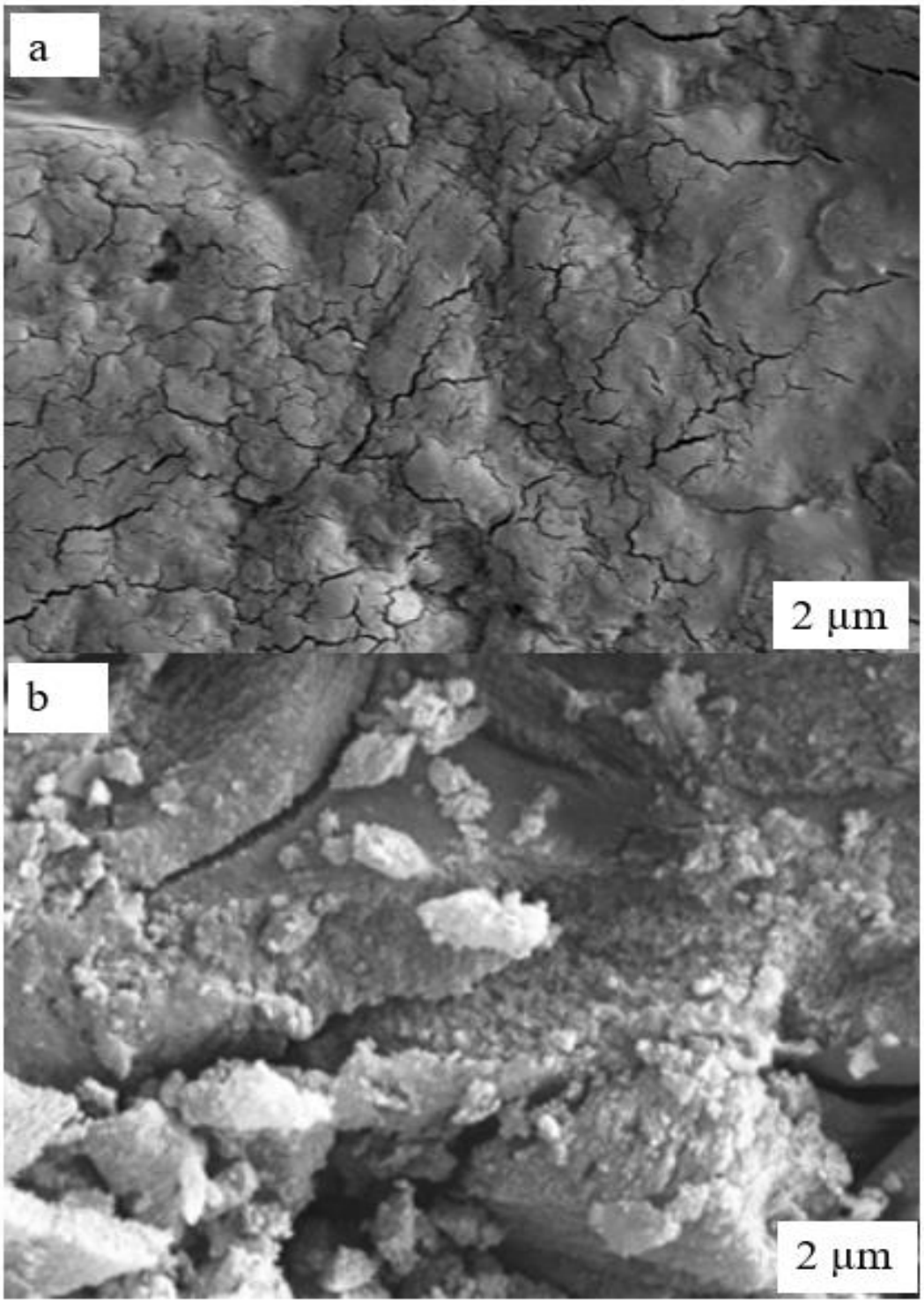


Figure 7.2 SEM images of (a) Fresh alginate-AC (B) Alginate-AC after use

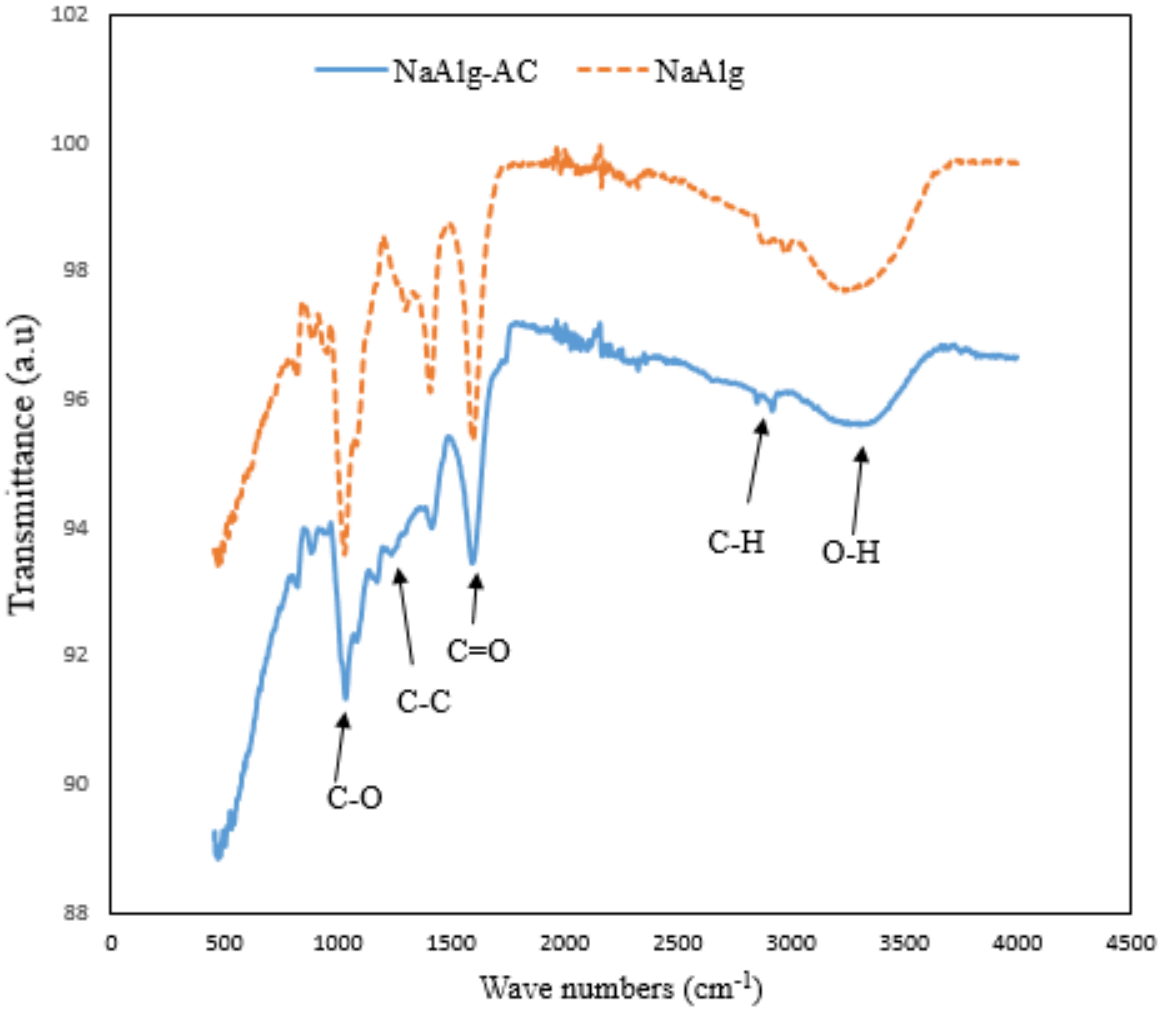


Figure 7.3 FTIR spectra of alginate and alginate-AC

7.3.2. Performance evaluation of adsorbent in the packed-bed column

To understand the performance immobilized AC adsorbents during desulfurization of DBT in a packed-bed column, effect of operating parameters such as; bed depth, flow rate, and initial DBT concentration on column performance for removal of DBT from the model diesel and typical real diesel was investigated. The detailed prodecure of this experiment is provided in chapter three of this thesis. The result obtained is hereby discussed;

DBT adsorption in a packed-bed column depends on the amount of adsorbent in the column. Column breakthrough experiments were conducted at a constant flow rate of 0.5 mL/min, constant DBT concentration of 100 mg/L and varying bed height of 5 cm, 10 cm and 15 cm. The breakthrough curve was obtained by plotting the ratio of DBT outlet concentration C to initial DBT concentration. Fig. 7.4 depicts the effect of bed height on the adsorption of DBT onto immobilized AC in a continuous packed-bed column. It could be observed from the results that breakthrough time increased with increasing bed height. This may be due to increase in number of active binding sites on the surface of the adsorbent in the column which broadens the adsorption transfer zone. The DBT adsorption capacity increased from 0.066 to 1.53 mg/g as the bed height increased from 5 cm to 15 cm. The adsorption capacity for DBT adsorption in this coulumn study was found to be maximum at 15 cm bed height. Therefore, this height was used in subsequent column experiments.

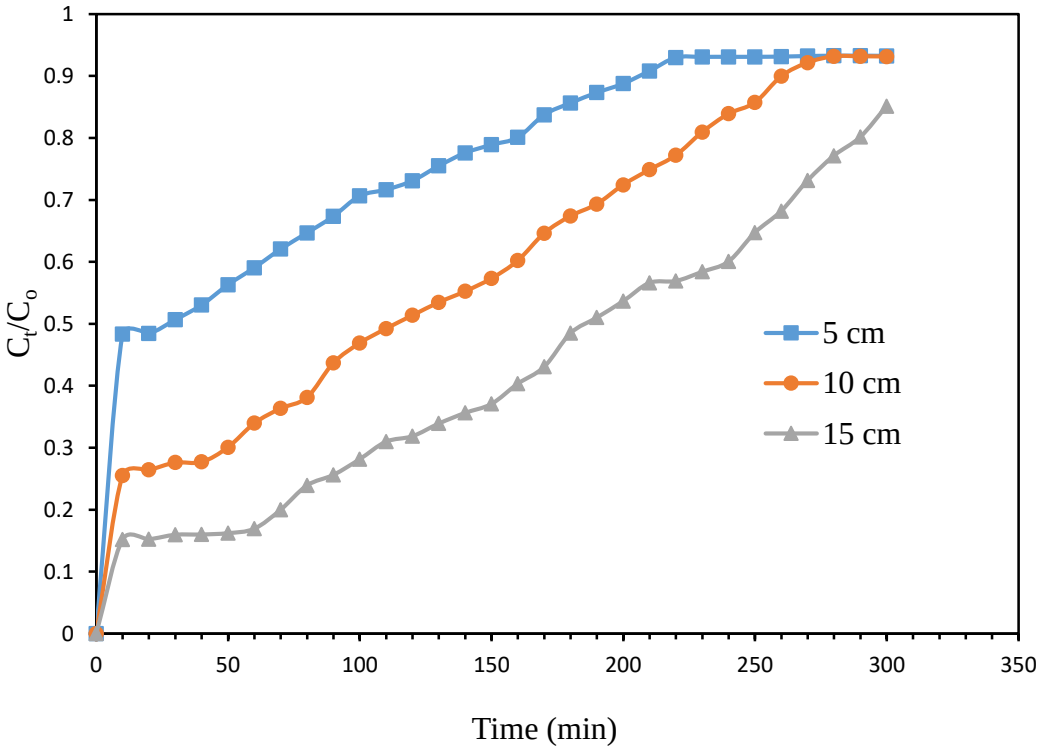


Figure 7.4 Effect of bed height on the adsorption of DBT in model oil in a packed-bed column. Experimental conditions: Initial DBT concentration: 100 mg/L; Flow rate: 0.5 mL/min

In ordet to evaluate the efficiency of adsorbent for a continuous packed-bed column studies on pilot or industrial scale, flow rate is an essential parameter to consider. Column experiments were conducted in this study at contant bed height of 15 cm, and constant initial DBT concentrations of 100 mg/L by varying the the flow rate from 0.5 mL/min-1.5 mL//min. Effect of flow rate is depicted in Fig. 7.5. The superficial velocity increased as the flow rate increased. The superficial velocities were calculated to be 0.031, 0.063 and 0.094 m/min at 0.5, 1.0 and 1.5 mL/min, respectively. Breakthrough curve is depicted in Fig. 7.5. It was observed that breakthrough time decreased from 60 min to 30 min with increasing flow rate from 0.5 mL/min to 1.5 mL/min. This could be due to the increase in occupancy of the adsorption zone as the influent velocity increased, which invariably resulted in decrease in time required to attain the specific breakthrough concentration. Flow rate also influenced the the adsorption of DBT onto immobilized activated carbon. The adsorption capacities of of activated carbon at different flow rate were found to be 0.066, 0.050 and 0.033 which is an indication that adsorption capacity decreased as flow rate increased from 0.5, 1.0 and 1.5 mL/min, respectively. This could be as a result of insufficient time for adsorption and diffusion limitation of DBT molecules on the surface of the adsorbent in the column at higher flow rate. Therefore, breakthrough time was reached faster at higher superficial velocity. The s obtained are in agree mentt with (Muzic 2011). Result also showed that there was higher removal of DBT at lower superficial velocity, because there was enough contact time for DBT with the immobilized activated carbon. This result is similar to what was obtained by other researchers with different sorbent-sorbate studies (Kiran and Kaushik 2008 and Auta 2012).

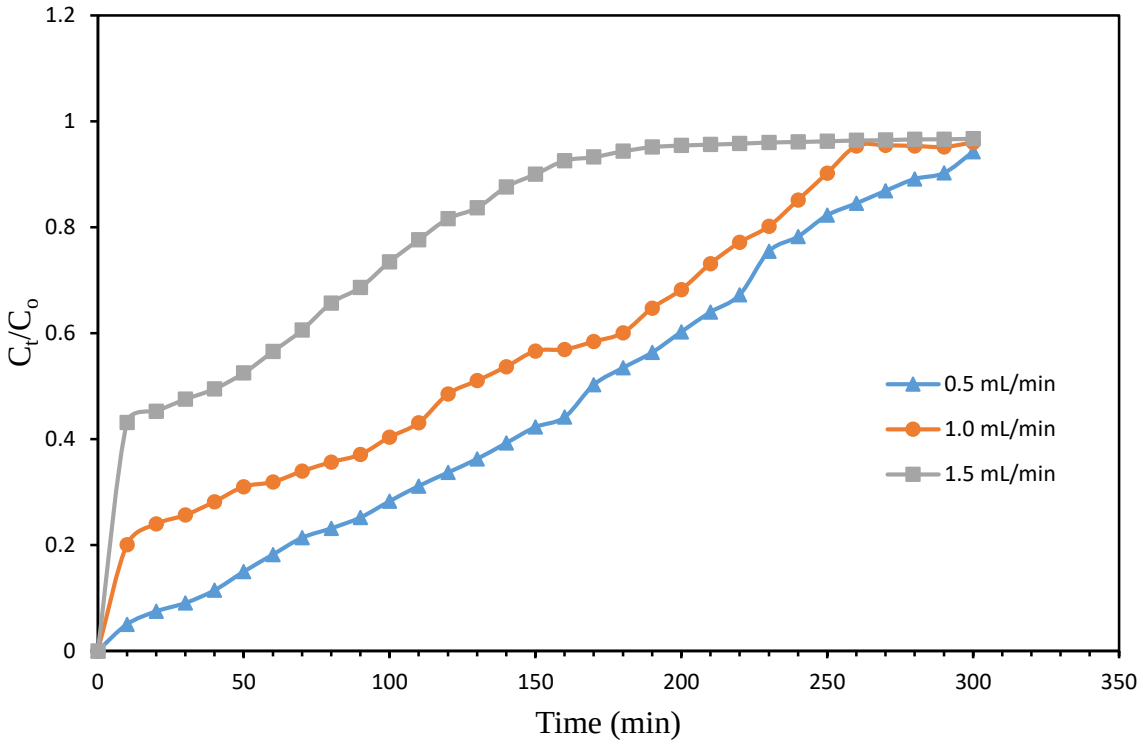


Figure 7.5 Effect of flow rate on adsorption of DBT in a packed-bed column. Experimental conditions: Bed height: 15 cm; Initial DBT concentration: 100 mg/L.

Fig 7.6 depicts the effect of initial concentration of DBT on its adsorption onto an immobilized AC in a continuous packed-bed column. Since the concentration of DBT vary in real diesel, it is important to understand its effect on its adsorption in a column study. The initial concentration of eefluent DBT solution was varied from 100-500 mg/L. Other operating conditions such as bed heigh (15 cm) and flow rate (0.5 mL/min) remained constant. The results show that breakthrough time decreased from 70 min to 40 min with increasing initial DBT concentration from 100 to 500 mg/L. This could be attributed to increase in DBT uptake rate, which result into decreas in adsorption zone length. In addition, these results explained that change of concentration gradient affects the saturation rate and breakthrough time. The resident time experienced at higher initial concentration affected its solid-phase concentration, resulting into reduction in adsorption capacity even as the concentration increased. The same trend was observed in studies reported by Han et al., (2009) and Muzic, (2011).

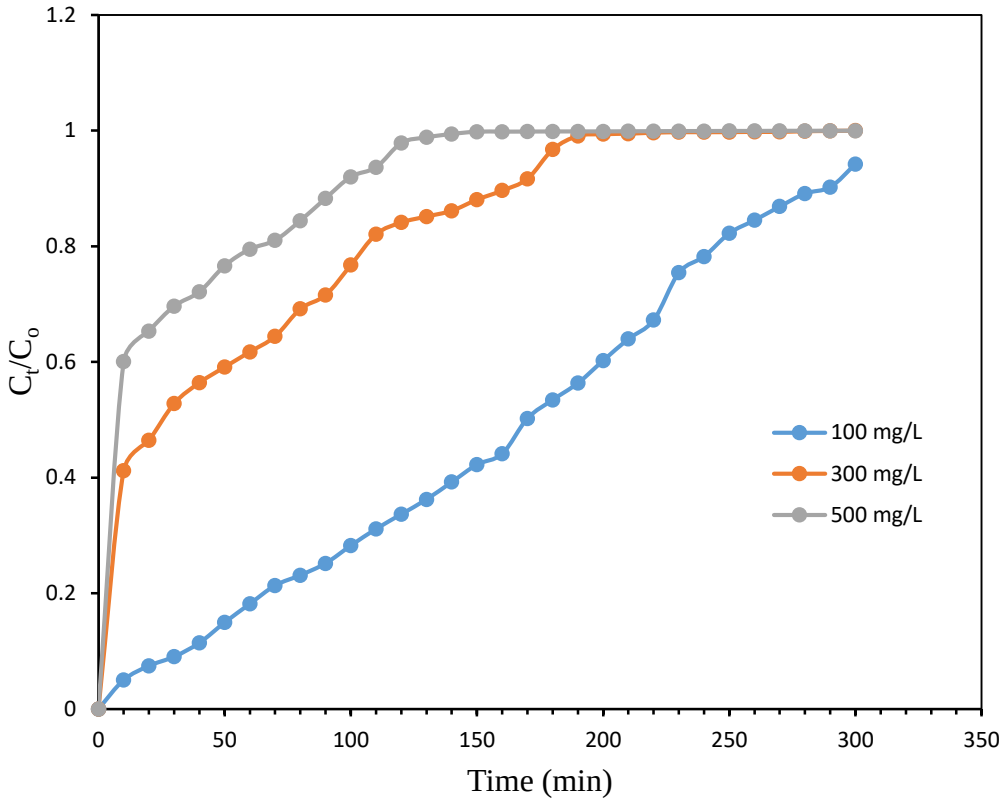


Figure 7.6 Effect of initial concentration on adsorption of DBT from a model oil in a packed-bed coulumn. Experimental conditions: Bed height: 15 cm; Flow rate: 0.5 mL/min.

7.4. Kinetics for modelling adsorption behavior in a packed-bed column

In this study, three major kinetic models such as Bohart-Adams, Thomas, and Yoon-Nelson models for the kinetic studies. The equations used for these kinetics were discussed in detail in Chapter 3 of this thesis.

The Bohart-Adam model was used to descrie the initial part of the break through curve. The expression in Equation (3.19) is used to calculate the parameters of Bohart-Adaams model. The plot of $\ln(C_t/C_o)$ versus time yielded a linear graph with slope and intercept, from with the Boahrt-Adam constants K_{ab} and N_o were calculated, respectively. Table 7.1 shows the Bohart-Adam parameters. The model produces the initial part of the breakthrough curve for all the concentrations

studied. Result showed that the maximum volumetric adsorption capacity, N_o were found to be 5.54, 14.31 and 22.71 x 10^{3} for 100, 300 and 500 mg/L, respectively. This is showing increase in volumetric adsorption capacity as the inlet concentration of DBT increased. This result is in agreementwith results obtained by other researchers studying different solute-adsorbate adsorption process. Result also showed that K_{ab} decreased from 0.88 to 0.28 x 10^{-5} mL/mg.min as the initial DBT concentration increased from 100-500 mg/L. It can also be observed that N_o increased from 5.54 to 15.13 x 10^{3} g/L as the flow rate increased from 0.5 to 1.5 mL/min, while the K_{ab} decreased from 8.8 to 2.8 x 10^{-5} mL/mg.min with increasing flow rate from 0.5-1.5 mL.min. However, the values of N_o were found to be The same trend was observed for increase in bed height. The N_o values were found to be 16.92, 8.62, 6.49 x 10^{3} g/L and for bed height 5 cm, 10 cm and 15 cm, respectively while K_{Th} values were found to be 2.4, 4.8 and 6.3 x 10^{-5} L/min.mg for bed depth of 5 cm, 10 cm and 15 cm, respectively. These results show that volumetric adsorption capacity, N_o decreased with increasing bed depth and the kinetic constant, K_{ab} increased with increasing bed depth. These results are comparable with Muzic (2009)

Table 7.1: Bohart-Adam's kinetic parameters for adsorption of DBT onto immobilized activated carbon in a continuous packed-bed column.

Flow rate (mL/min)	**Bed depth (cm)**	**Initial conc. (mg/L)**	**K_{ab} x 10^{5} (mL/mg/min)**	**N_o x 10^{-3} (g/L)**	**R^2**
0.5	15	100	8.80	5.54	0.9166
1	15	100	5.30	11.57	0.9767
1.5	15	100	2.80	15.13	0.8060
0.5	5	100	2.40	16.92	0.9053
0.5	10	100	4.80	8.62	0.9653
0.5	15	100	6.30	6.49	0.9801
0.5	15	100	8.80	5.54	0.9166
0.5	15	300	0.90	14.31	0.8176
0.5	15	500	0.28	22.71	0.6746

K_{ab} is Bohart-Adam's constant, N_o is adsorption capacity and R is the correlation coefficient.

Thomas adsorption model equation was given in Chapter 3 of this thesis in Equation (3.20). A plot of $\ln\left(\frac{C_o}{C_t}-1\right)$ against time yields a linear grapgh. The values of K_{Th} and q_o can be calculated from intercept and slope of the graph, using a linear regression analysis (Apendix C). Table 8.2 shows the parameters of Thomas model. The result showed that Thomas model has high correlation efficiency at higher flow rates of 1.5 mL/min than at 0.5 mL/min and 1.0 mL/min flow rates. Therefore, it can be concluded that Thomas model could best decribed the adsorption process at higher flow rate. in most cases. It could also be observed that, Thomas constant decreased from 1.54 to 1.45 x 10^{-4} mL/mg.min with increasing flow rate from 0.5 to 1.5 mL/min. The q_o was also observed to initially increase from 0.192 to 0.275 mg/g as the flow rate increased from 0.5 to 1.0 mL/min. The q_o later decreased as the flow rate was further increased to 1.5 mL/min. This could be as a result of the adsorption zone being rapidly saturated at higher flow rate of DBT solution into the bed column which resulted in shorter break through time. As the intial DBT (inlet) concentration inceased from 100 to 500 mg/L, the K_{Th} decreased from 1.54 to 0.59 mL/mg.min and the q_o decreased from 0.192 mg/g to 0.016 mg/g as the concentration increased from 100 to 500 mg/L. This could be as a result of the shorter resident time experienced by the column at higher initial DBT concentration which affected the solid-phase concentration resulting into lower adsorption capacity at higher concenytrations. The same result was obtained in Han et al., (2007) and Muzic (2009) The Thomas constant, K_{Th} initially increased from 1.08 to 1.25 x 10^{-4} mL/mg.min as the bed depth increased from 5 cm to 10 cm and then decreased to 1.01 x 10^{-4} mL/mg.min as the column bed was further increased to 15 cm.

Table 7.2: Thomas' kinetic parameters for adsorption of DBT onto immobilized AC in a continuous packed-bed column.

Flow rate (mL/min)	Bed depth (cm)	Initial conc. (mg/L)	K_{Th} x 10^{-4} (mL/mg/min)	q_o (mg/g)	R^2
0.5	15	100	1.54	0.192	0.8844
1	15	100	1.46	0.275	0.8843
1.5	15	100	1.45	0.079	0.9409
0.5	5	100	1.08	0.724	0.9719
0.5	10	100	1.25	0.197	0.9293
0.5	15	100	1.01	0.223	0.8495
0.5	15	100	1.54	0.192	0.8844
0.5	15	300	0.97	0.162	0.9356
0.5	15	500	0.59	0.016	0.9368

K_{Th}: Thomas' model constant; q_o: amount of DBT adsorbed; R is the correlation coefficient

The linearized form of Yoon-Nelson model equation can be expressed as in Equation (3.21), as described in Chapter three of this thesis. The rate velocity constant in min^{-1}, K_{YN} and the time required for 50 % adsorbate breakthrough (min), ţ were calculated from the intercept and slope of a linear graph of $\ln\left(\frac{C_t}{C_o - C_t}\right)$ versus time (see Apendix C). Table 7.3 shows the Yoon-Nelson parameters for adsorption of DBT in model oil onto immobilized activated carbon in a continuous fied bed column. The result showed that the $ţ_{mod}$ values according to Yoon-Nelson model 112.31 and 157.83 at different flow rates of 1.0 and 1.5 mL/min, respectively are very close to the $ţ_{expt}$ values as obtained from the experiment 121 and 160 min for flow rates of 1.0 and 1.5 mL/min, respectively. The $ţ_{expt}$ being the time required for 50 % adsorbate breakthrough time for the column experiment as shown in Table. The $ţ_{mod}$ values (183.24 min) for 15 cm bed depth is very close to what was obtained in the $ţ_{expt}$ (189 min). K_{YN} values are found to increase in order of 0.213, 0.322 and 1.851with increasing bed depth of 5, 10 and 15 cm, respectively. The same same trend goes for different flow rate. The result showed that K_{YN} values increased as the flow rate increased from 1.0 mL/min to 1.5 mL/min,

Table 7.3: Yoon-Nelson's kinetic parameters for adsorption of DBT onto immobilized activated carbon in a continuous fied bed column.

Flow rate (mL/min)	Bed depth (cm)	Initial concentration (mg/L)	Kyn (min^{-1})	τ_{mod} (min)	R^2
0.5	15	100	0.0144	21.13	0.9408
1	15	100	0.0144	112.31	0.8825
1.5	15	100	0.0154	157.83	0.8844
0.5	5	100	0.2130	19.86	0.9719
0.5	10	100	0.3220	10.59	0.9293
0.5	15	100	1.8501	183.24	0.8495
0.5	15	100	0.0154	157.83	0.8844
0.5	15	300	0.2910	4.440	0.9356
0.5	15	500	0.0296	2.640	0.9368

K_{Yn}: Yoon-Nelson's constant; $\tau_{mod:}$ Model breakthrough time

Table 7.4 shows the adsorption column capacity and breakthrough capacity parameters. The equations used for calculating these parameters were presented in Equation (3.16-3.18), in Chapter 3 of this thesis. The results show that breakthrough time decreased from 70 to 40 min with increasing initial influent concentration from 100 to 500 min. This could be attributed the saturation rate of the adsorbent at higher initial DBT concentration. In addition, the vacant adsorption sites of the adsorbent were rapidly filled up by the DBT molecule resulting in faster saturation of the adsorption zone of the adsorbent. Furthermore, it could also be observed that as the flow rate increases from 0.5, 1.0 and 1.5 mL/min, the breakthrough time decreased. This could be as a result of the rate of flow of the influent onto the adsorbent which did not give room for enough contact time of the the DBT molecule with the active vacant adsorption sites of the adsorbent. The breakthrough time increases with increasing bed height. This could be as a result of the more available adsorption site as the bed height increased resulting in increase in breakthrough time as the column bed height increased. This obtained in this study are in agreement to what was obtained in literature by Auta, (2012).

The amount, q_{total} of DBT molecule sent into the bed column increased from 1.0 to 1.48 g as the flow rate increased from 0.5 to 1.5 mL/min. This is because as the flow rate increased the amount of DBT sent into the bed coulumn also increased. The adsorption capacity of the of the immobilized activated carbon decreased with increasing flow rate. This could be as a result of longer breakthrough time involved with lowest flow rate of 0.5 mL/min, there was enough time for the DBT molecule to be in contact with the immobilized activated carbon in the bed column. This resulted into highest adsorption capacity at 0.5 mL/min. It can be seen from the table that the equilibrium adsorption capacity increased from 0.067 to 0.153 mg/g as the column bed height increased from 5 cm to 15 cm. This could be as a result of more available active adsorption site on the sirface of the adsorbent, giving room to longer breakthrpough time. Therfore, resulting in increased adsorption capacity. The same trend was obtained from literature (Auta, 2012).

Table 7.4: Desulfurization of DBT in model diesel Adorption column and breakthrough capacity for adsorption of DBT in a continuous packed-bed column using immobilized AC

Initial conc (mg/L)	**Bed depth (cm)**	**flow rate (mL/min)**	**Q_B (mg/g)**	**q_{total} (g)**	**q_e (mg/g)**	**t_b (min)**
100	15	0.5	85.36	0.8570	0.0570	70
300	15	0.5	209.51	0.0045	0.0001	60
500	15	0.5	243.00	0.0204	0.0003	40
100	15	0.5	73.00	1.0000	0.6600	60
100	15	1.0	98.00	1.2000	0.5000	40
100	15	1.5	11.00	1.4800	0.0330	20
100	5	0.5	110.00	0.0010	0.0670	30
100	10	0.5	93.00	0.0010	0.0690	50
100	15	0.5	97.00	0.0023	0.1530	80

Q_B is the breakthrough capacity, qtotal is the total amount of adsorbate sent into the packed-bed column, q_e is the amount of DBT adsorbed at equilibrium and t_b is the breakthrough time.

7.4.1 Modelling of experimental data

Adsorption behavior for packed-bed column experiment performed in this study was described by Thomas, Bohart-Adam andYoon-Nelson models.

Fig. 7.7 shows the comparison of experimental data with Bohart Adam and Thomas model. Result shows that Thomas model fitted well with the experimental data, until around 240 min, when there was a little deviation in the fitting as the time increased further. It could be observed that the model described the intial part of the curve. The result agreed with other reaserches although with different solute-solvent system (Tarty-Costodes et al., 2005; Calero et al., 2009) Bohart Adam model also fitted well into the experimental data The model has been reported in literature to describe the initial part of the breakthrough curve and the same was confirmed in this study (Calero et al., 2009). There was a large deviation between experimental data and Yoon-Nelson model (Result not shown). Thereore, it could not be used to describe the breakthrou curve in this study for all the concentrations used.

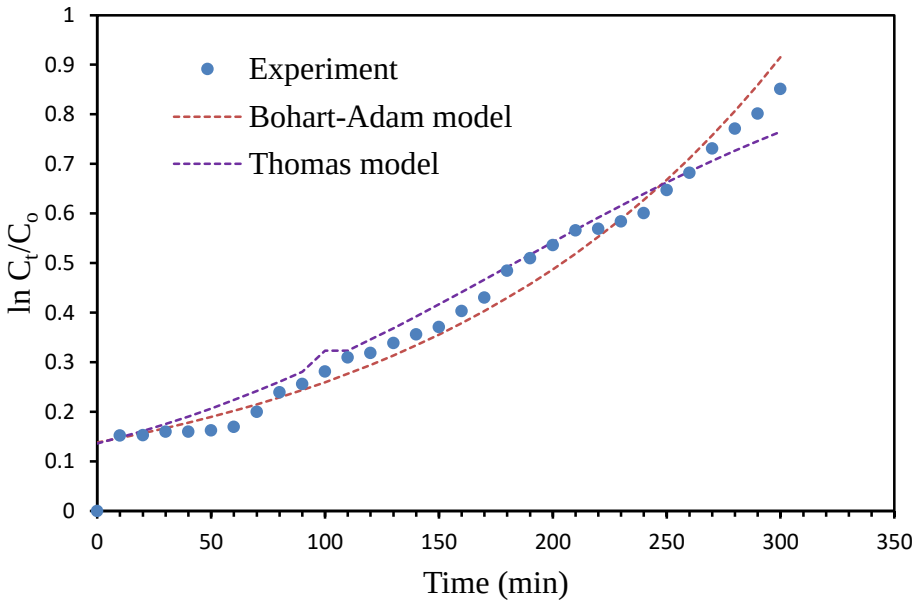


Figure 7.7 Experimental and predicted breakthrough curve, using Bohart-Adam and Thomas model for adsorption of DBT onto immobilized AC in a continuous packed-bed column. Experimental conditions: Bed height: 15 cm; Flow rate: 0.5 mL/min; Initial DBT concentration: 100 mg/L.

The results documented in this chapter are comparable with literatue. Muzic et al. (2010) studied adsorption of DBT in diesel in a continuous fixed bed column with initial DBT concentration of 27 mg/L, in a bed column of height 28.4 cm and internal diameter 2.2 cm. The breakthrough time was reported to be 11.8 h when the feed flow rate was 1.0 mL/min at reaction temperature of 50 ^{o}C. The final concentration achieved at the various operating conditions was 0.7 mg/L. Comparing this result with what was obtained in this study (bed height 15 cm, at room temperature, initial DBT concentration 100 mg/L, flow rate 0.5 mL/min), the results show that the breakthrough time was about 2 h. It could be observed that the breakthrough time obtained int hius study is lower than what was obtained in Muzic et al. (2010). This could be attributed to lower initial sulfur concentration in the diesel used in their study. In addition, the bed height used by Muzic et al. (2010) was almost twice what was used in this study which could also favour the adsorption breakthrough time in their study. Meanwhile a reasonable effluent concentration was achieved in this study accounting for about 90 % adsorption performance of the bed column.

7.5. Concluding remarks

As it has been demostrated in this chapter, activated carbon was successfully immobilized in sodium algilate for adsorption of DBT in model diesel in a continuous packed-bed colomn. This is a promising method of entrapping adsorbent for maximum performance. Activated carbon has been widely reported in literature for column adsorption of sulfur compound from petroleum distillates. However, there are only few studies on the immobilization of AC in sodium algilate for use in bed column for desulfurization of petroleum distillate. Results show that adsorption of DBT in a packed-bed column is dependent on superficial velocity of the sorbate solution through the adsorption column. The best result was obtained at the lowest superficial velocity of 0.031 m/min (0.5 mL /min) at 15 cm bed height and lowest initial DBT concentration of 100 mg/L. Furthermore, breakthrough time was found to increase with decreasing DBT initial concentration, decreasing flow rate and increasing bed height.

Increasing the superficial velocity of the DBT solution decreased the breakthrough time needed for the contact of adsorbate solution with the adsorbent in the bed column resulting in decreased amount of DBT adsorbed by the immobilized adsorbent. This means that, a longer breakthrough

time is needed for higher performance of the bed column which will successively result in higher adsorption capacity.

The amount, q_{total} of DBT molecule sent into the bed column increased from 1 to 1.48 g as the flow rate increased from 0.5 to 1.5 mL/min. In addition, it was observed that the equilibrium adsorption capacity increased from 0.067 to 0.153 mg/g as the column bed height increased from 5 cm to 15 cm. The adsorption capacities of the adsorbents were founs to be very low, this may be attributed to the minimum amount of AC that the sodium algilate could entrap. Only a small amount of adsorbent was immobilized by the algilate. Therefore, more studies are need to increase the ration of activated carbon to sodium algilate and study the influence of algilate ration of the performance of an immobilized activated carbon in a packed-bed column experiment

At all experimental conditions, Adams–Bohart model described well the initial region of breakthrough curve, while Thomas modelsdescribed the transient stage or working stage of the breakthrough curve. In order to share the novel contribution of this work with the scientific community, a manuscript has been submitted for publication in a conference Proceedings of the World Congress on Engineering and Computer Science, 2018 Francisco USA.

7.6. References

Adeyi, A., Aberuaga, F. (2012) Comparative analysis of adsorptive desulfurization of crude oil by manganese dioxide and zinc oxide, *Research Journal of Chemical Sciences*, (*2*)8,14-20.

Ahmed, J. and Ahmaruzzaman, M. (2015) "Adsorptive desulfurization of feed diesel using chemically impregnated coconut coir waste" *Int. J. Environ. Sci. Technol. 2*(9), 2847–2856

Alavi, S. A. and Hashemi, S. R. (2014) A Review on Diesel Fuel Desulfurization by Adsorption Process. International Conference on Chemical, Agricultural, and Biological Sciences (ICCABS'2014). 9-10.

Auta, M. (2012) Fixed bed adsorption studies of Rhodamine B dye using oil palm empty fruits bunch activated carbon. Journal of Enineering research and studies. Vol 3, issue 3, 03-06.

Bhattachryulu, Y. C., Patil, M. and Kamble, S. (2012) Unsteady state adsorption – Column studies. International Journal of Advanced Engineering Research and Studies, *1*(I1), 179– 184.

Calero, M., Hernainz, F., Blazquez, G., Tenorio, G. and Martin-Lara, M.A. (2009) Study of r (III) biosorption in a fixed bed column. Journal of Hazardous Material, 171, 886-893.

Daemi, H. and Barikani, M. (2012) Synthesis and characterization of Calsium alginate nanoparticles, sodium honopolymannuronate salt and its calcium nanoparticles. Scientia Iranica. Vol. 19, Issue 6, pp 2023-2026.

Eber, J., Wasserstein, P., and Jess, A. (2004) Deep desulfurization of oil refinery streams by extraction with ionic liquids. *Green chemistry*, *6* (7), 316-322.

Fayazi, M. Taher, M.A., Afzali, D. and Mostafavi. A. (2015) Removal of Dibenzothiophene Using Activated Carbon/γ-Fe_2O_3 Nano-Composite: Kinetic and Thermodynamic Investigation of the Removal Process. Anal. Bioanal. Chem. Res., Vol. 2, No. 2, 73-84.

Gawan, P., and Kaware, J. (2014) Desulphurization techniques for liquid fuel A Review. *International of Engineering Technology Management and applied Science.2*(7), 122-126.

Gawan, P., and Kaware J. (2016) Review of Research for Desulphurization of diesel by Adsorption. *Journal of Engineering and Technology International Research. 3*(12), 337-340.

Gaware, P., and Kaware J. (2016) Review on low cost Adsorbents for Desulphurization of Liquid Fuels. *International Research Journal of Engineering and Technology. 2*(1),108-112.

Han, R., Wang, Y., Zou, W, Wang, Y, Shi, J. (2007) Comparison of linear and non-linear analysis in estimating the Thomas model parameters for methylene blue adsorption onto natural zeolite in fixed bed coulumn. Journal of Harzadous Materials. 145, 331-335.

Han, R., Yu W., Xin Z., Yuanfecy W., Fulng X., Cheng J., and Tang M. (2009) "Adsorption of Methyl Blue by Phoex Tree Leaf Power in a Fixed Bed Column: Experiments and Prediction of Breakthrough Curves. Desalination. 2(45), 284-297.

Han, R.P., Wang, Y.F., Yu, W.H., Zou, W.H., Shiand, J. and Liu, H.M. (2007) Adsorption of methylene blue from by phoenix tree leaf power in a fixed-bed column. *Hazard. Mater, 141,* 713–718.

Jawad, R.J., Ismail, M. H. S., Siajam, S.I. (2018) Adsorption of heavy metals and residual oil from palm oil mill effluent using a novel adsorbent of alginate and mangrove composite beads coated with chitosan in a packed bed column IIUM Engineering Journal, Vol. 19, (1), pp. 1-14.

Kummara, M.R., Basetty, M., K., Rao, K. S.V., Subha, M.C.S. (2013) Synthesis and characterization of pH sensitive poly- (hydroxyl ethyl methacrylate co accrylamidoglycolic acid) based hydrogels of controlled release studies of 5-fluorouracil. Journal of Applied Pharmaceutical Science. Vol. 3 (06), pp. 061-069.

Muzic, M., Sertic B., Adzamic T., Gomzi, Z., Podolski, S. (2009) Optimization of diesel fuel desulfurization by adsorption on activated carbon, *Chem. Eng. Trans., 17(5),* 1549-1554.

Muzic, M., Gomzi, Z., Sertic-Bionda, K. (2010) Modeling of the Adsorptive Desulfurization of Diesel Fuel in a Fixed-Bed Column. Chem. Eng. Technol. Vol. 33, No. 7, 1137–114.

Muftah, H. E., Manal, A. A., & Sulaiman, A. (2017) Evaluation of an activated carbon packed bed for the adsorption of phenols from petroleum refinery wastewater. *Environ Sci Pollut Res, 24*:7511–7520. DOI 10.1007/s11356-017-8469-8.

Muzic, M., Katica S., Tamara A. (2009)" Kinetic Equilibrium and statistical analysis of diesel fuel adsorptive desulphurization*" 4*(9), 373-394.

Muzic, M., Sertic B., Adzamic T., Gomzi, Z., Podolski, S. (2009) Optimization of diesel fuel desulfurization by adsorption on activated carbon, *Chem. Eng. Trans., 17(5),* 1549-1554.

Tarty-Costodes, V.C., Fauduet, H., Porte, C., Ho, Y.S. (2005) Removal of lead (II) ions from synthetic and real efflunts using immobilized pinus sylvestris sawdust; adsorptionon a fixed bed column. J. Hazard. Mater. 123, 135-144.

Chapter Eight

8.0 Biodesulfurization using *Pseudomonas species*

This chapter discusses the results of biodesulfurization efficiencies of *Pseudomonas Aeruginosa* and *Pseudomonas Putida* during degradation of DBT from model diesel and real diesel. The results of effects of operating variables on the growth of bacteria and biodesulfurization performance of the bacteria are presented. Furthermore, the kinetics of bacteria growth and degradation of model diesel and real diesel are reported.

8.1 Introduction

Different techniques such as hydrodesulfurization, adsorption, oxidation, extraction, and biodesulfurization have been studied by researchers to reduce the amount of sulfur-containing compound in petroleum distillates. Conventional hydrodesulfurization (HDS) is the most commonly used technique in the refineries to reduce the sulfur content with huge success recorded. Though, HDS is capable of reducing sulfur content in diesel such as heterocyclic sulfur compounds like benzothiophene and sulfones from diesel, but the technique is inefficient to desulfurize refractory sulfur compounds such as dibenzothiophene and its derivatives, especially 4, 6-dimethyldibenzothiophene (4, 6-DMDBT). In addition, this technology suffers from high capital and operating costs due to the fact that it is operated at high temperature and pressure, thereby making it energy intensive (Babich and Moulijn, 2003). Furthermore, a lot of hydrogen is used, making the process highly risky in terms of safety. This situation has provoked the thoughts of many researchers worldwide to urgently explore alternative methods for desulfurization of petroleum distillates.

Biodesulfurization (BDS) is a promising method that could be efficient, cheap and less energy intensive technique for desulfurization. BDS involves the use of biocatalyst for the degradation of the sulfur compound in petroleum distillates to a less harmful compound without altering the quality of the fuel. In addition, it can be operated at low temperature under mild conditions. Different bacteria strains such as *Rhodococcus erythropolis Sp. SHT87(*Fatemeh et al., 2010), *Pseudomonas Sp., and Gordona alkanivorous RIPI90A (*Li et al., 2008*)*, *Microbacterium sp. NISOC-06 (*Papizadeh et al., 2010), *Pseudomonas putida CECT 527* (Caro et al., 2008a*)* have been

employed for degrading sulfur compounds. For instance, *Pseudomonas* strains are very prolific and could survive in biphasic media and metabolic diversity (Tao et al., 2006). They are known to thrive in conditions with or without oxygen, although they are classified as aerobic. They are readily available since they are present naturally in soil and water. Among the *Pseudomonas strains, Pseudomonas aeruginosa* is the most common.

In BDS, only C-S oxidative bond cleavage occurs to release the sulfur atom as sulfate and the carbon skeleton of the thiophenic compound is not affected as a phenolic end product. Consequently, in the BDS process the thiophenic sulfur compound serves only as the sole sulfur source for bacteria growth and the calorific value of the fuel is preserved by the final end product 2-HBP (Monticello, 2000; Kilbane, 2003; Aggarwal et al., 2013). A variety of sulfur containing compounds have been reported, but the HDS recalcitrant sulfur compound accounts for 70 % of the sulfur compounds in diesel and it is considered as a model compound for biodesulfurization (Rhee et al., 1998; Oshiro and Izumi, 1999). The recalcitrant DBT is considered as the only sulfur-containing compound in the model diesel used in this study.

Vast investigations have been reported on the use of pseudomonas strains, at different conditions to degrade DBT. Al-Faraas et al. (2015) isolated *Pseudomonas Aeruginosa* from Iraqi Soil for desulfurization of Dibenzothiophene. Effect of different sulfur sources on the degradation efficiency of *Pseudomonas Sp*. has been reported (Al-Faraas et al., 2015). However, detailed desulfurization activity of the bacteria is very limited in literature. Davoodi-Dehaghani et al. (2010) investigated the desulfurization ability of *Rhodococcus Erythropolis* for degradation of DBT. Mingfang et al. (2003) desulfurized DBT and 4,6-dimethyldibenzo thiophene in dodecane and straight run diesel using lyophilized cell of R-8. As far as it can be ascertained, limited studies have been conducted on the biodegradation of DBT in South African diesel using *Pseudomonas strains*. It is essential to monitor the pH of the bacteria medium, so as to ensure that the condition is not toxic for the growth of the bacteria. Different carbon sources have been employed in biodesulfurization. Carbon source is a requirement because it enhances the growth of bacteria Farhama et al. (2011). Therefore, effect of carbon sources on the growth of bacteria was investigated in this study. The bacteria are growth before utilization for desulfurization experiment

in this study. This helps to know the exponential phase of the bacteria, at which the resting cells are harvested.

Since diesel and bacteria basal medium form 2-phase (Biphasic) medium during BDS experiment, it is important to study effect of biphasic media on the growth and degradation of sulfur-containing compunds in diesel. In addition, to overcome the challenge of low bacteria growth that is usually encountered during desulfurization of petroleum distillate (Tao et al., 2011), effect of biophasic media is investigated in this chapter. To investigate the efficiency of bacteria for degradation of DBT in model diesel, effect of operating varaiables are investigated and the results obtained are reported in this chapter. The bacteria with higher degradation efficiency, and the best operating variables are chosen for degradation of DBT in real diesel samples.

Against this background, this chapter reports the results of investigation of biodegradation of DBT and compares the biodegradation effeciency of growing and resting cells of *Pseudomonas Aeruginosa* (*PA*) and *Pseudomonas Putida (PP).* It is important to understand the kinetics of the biodesulfurization process. Kinetic studies of bacteria growth give information on behavior of the bacteria during growth and BDS process. Therefore, the kinetics that governs the growth of the bacteria and the DBT degradation are also provided.

8.2. Experimental

The materials, detailed description of experimental procedure, analytical techniques for this chapter have been extensively described in Chapter 3 of this thesis (section 3.2.1 and 3.2.2). The physical and chemical properties of the real diesel obtained from a typical refinery located in South Africa is provided in Table 3.1.

8.3 Results and discussion

To evaluate the efficiency of the bacteria for degradation of DBT model diesel and real diesel, there is need to study effect of operating variables. The results obtained are discussed in this section of the chapter.

8.3.1 Effect of pH and carbon sources on the growth of bacteria

Table 9.1 shows the effect of pH on the growth of bacteria. It could be observed that there was no obvious change in the pH value of the control medium without bacteria and the bacteria medium within the given priod of growth. This is an indication that the pH of the medium did not change during the growth of bacteria. The change in the pH of the bacteria medium is insignificantly noticeable.

Table 8.1: pH measurement of *PA* and *PP* medium and control (without bacteria) during growth

Time (Hour)	**pH**		
	Control	***PA***	***PP***
0	7.05	7.04	7.03
24	7.02	7.19	7.05
28	7.11	7.13	7.07
72	7.13	7.14	7.1
96	7.16	7.16	7.1
120	7.12	7.14	7.09
144	7.16	7.15	7.11
168	7.14	7.19	7.07
192	7.11	7.13	7.08
216	7.15	7.17	7.12
240	7.11	7.16	7.10

Fig. 8.1 (a) and Fig. 8.1 (b) show the effect of carbon sources on the growth of *PA* and *PP*, respectively. Carbon source is a requirement for enhancement of bacteria growth, therefore, its effect is studied in this chapter. Glucose and glycerol were used as the sources of carbon for the growth of the bacteria. In Fig 9.1 (a), it could be observed that *PA* grew faster when glycerol was

used as the carbon source compared to when glucose was used. It can be seen that the rate of growth of *PA* increased with glycerol as the carbon source to 1.0 gDCW/L, in 120 h. Then, there was a decrease in the growth of the bacterial from 1.0 to about 0.9 g DCW/L at 144 h and remained almost constant till 240 h. The first stage of the growth from 0 h to 120 h represents the initial lag phase (accelerating growth phase). The point at which the growth showed the highest dry cell weight of bacteria could be regarded as the exponential growth phase of the bacteria. The later stage represents the decelerating growth phase of the bacteria growth. The growth of the bacteria using glucose was found to be below the control medium without carbon source. The results obtained show indicate that *PA* grows better in glycerol than in glucose. Therefore, glycerol was used for the rest of the experiment performed in this study to grow *PA*. In Fig. 9.1 (b), it could be observed that the *PP* grew better in glucose as the source of carbon compared to when glycerol was used. The results show that the *PP* consistently grew from 0 h to 120 h, where it reached its maximum dry cell weight of 1.01 gDCW/L. Its progression then decreased as the time increased from 120 h to 210 h, then became constant from 210 h to 240 h. However, the growth of control experiment without glucose showed a decrease in growth compared to when carbon source was added. This result showed that carbon sources enhanced the growth of the bacteria compared to when no carbon souce was added to the bacteria medium. The results obtained in this study is in agreement with results were reported by Fontes et al. (2013) and Nikel et al. (2015).

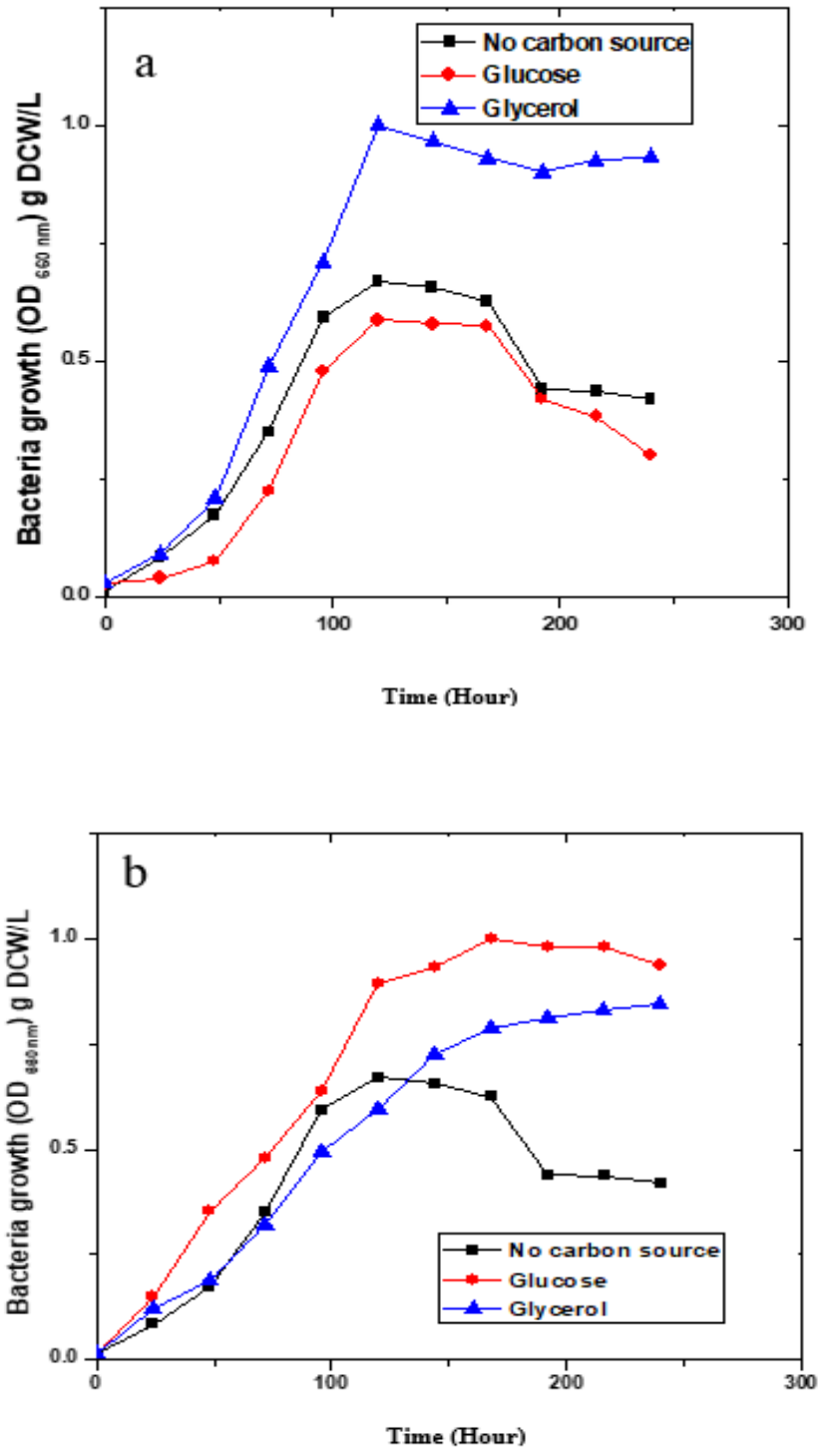


Figure 8.1 Effect of carbon source on the growth of (a) *Psuedomonas Aeruginosa*, (b) *Pseudomonas Putida* at. Experimental conditions: Initial DBT concentration: 25 mM, Temperatuure: 37 ^{o}C (*PA*), 30 ^{o}C (*PP*).

Fig. 8.2 (a) and Fig. 8.2 (b) depict the growth of *PA and PP* with degradation of DBT and formation of 2-HBP as a function of time. The results show that growth of the bacteria increased with time. Growth of PP began to decrease slightly after 120 h while the growth of *PP* began to decrease after 168 h. At 120 h, optical density of *PA* reached 1.00 g DCW/L and that of *PP* was 0.998 g DCW/L. It can be observed that as the growth of bacteria increased there was simultaneous increase in the degradation of DBT from 46 ppm to 0.21 ppm for *PA* and from 46 ppm to 0.51 ppm for *PP*. Likewise, amount of 2-HBP increased from 0 ppm to 32.5 ppm for *PA*, and amount of 2-HBP increased from 0 ppm to 24.5 ppm for *PP*. It was observed in all experiments that the growth of bacteria stopped before the DBT was completely degraded to 2-HBP. In addition, the production of 2-HBP, as a final metabolite of 4S pathway, was less than the consumption of DBT in both cases. This could be as a result of intra and extra cellular accumulation of 4S compounds. These results are in agreement with the results reported by Caro et al. (2008) and Davodii-Dehaghani et al. (2010). The desulfurization of DBT to 2-HBP through 4S pathway could be the reason why there was no further growth of the bacteria at 120 h for PA and 168 h for *PP*.

The major 4S pathway metabolite identified during the batch cultivation was 2-HBP. This was also confirmed by Rhee et al. (1998). Approximately 99.5 % of DBT and 98 9 % of DBT was degraded by *PA* and PP, respectively. However, 2-HBP could accumulate up to concentration of 33.06 ppm for PA and 22.99 ppm for PP which account for 71.9 % and 50 % formation of 2-HBP for *PA* and *PP*, respectively. The results show that the amount of 2-HBP formed was not equivalent to the amount of DBT degraded. In addition, no sulfate or sulfite accumulation was detected during growth of bacteria. Therefore, it could be assumed that the sulfur content has been assimilated by the cells.

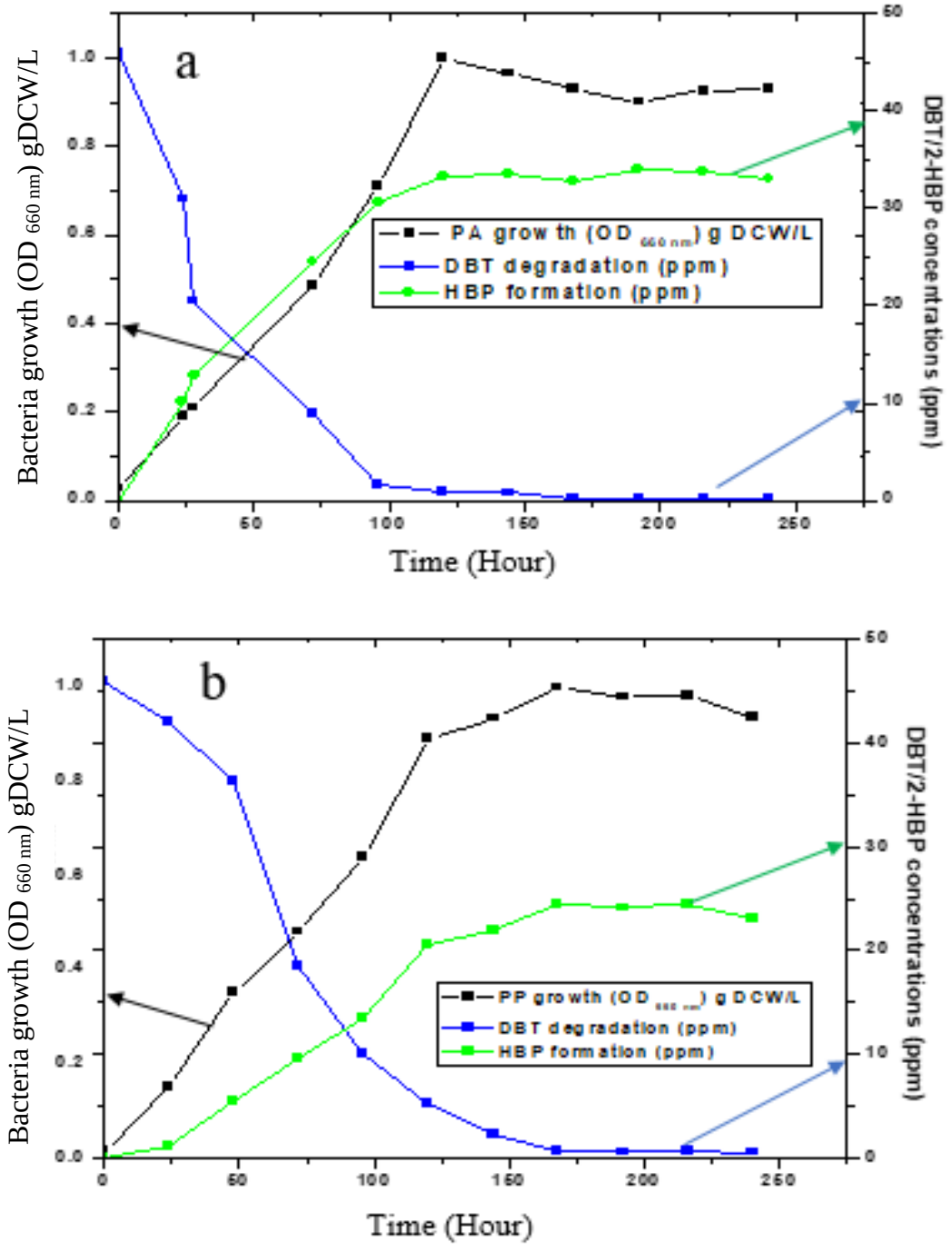


Figure 8.2 Biomass growth as a function of time during degradation of DBT and 2-HBP formation (a) with *Pseudomonas Aeruginosa* (b) with *Pseudomonas Putida*. Experimental conditions: Initial DBT concentration: 46 ppm; Temperature: 30 ^{o}C (*PP*) and 37 ^{o}C (*PA*).

8.3.2 Effect of operating variables on the growth of bacteria and biodesulfurization

The results in Fig 8.3 show the degradation of DBT and the production of 2-HBP. The results show that as the concentration of the bacteria in the medium increased, desulfurization of DBT and production of 2-HBP are enhanced. This could be as a result of more available bacteria to feed on the DBT which in return increase the production of 2-HBP. The lowest desulfurizing capacity of 55 % for *PA* and 32 % for *PP* was recorded when the cell concentration was 0.3 g DCW/L. In addition, the concentration of 2-HBP produced for *PA* and *PP* at 0.3 g DCW/L was 117.34 ppm and 81.04 ppm, respectively. Enhancement in degradation of DBT and formation of 2-HBP at increased concentration of bacteria could be attributed to the availability of more bacterial to feed on the DBT. It could be observed that formation of 2-HBP was lower than the degradation of DBT in all the cases. This could be attributed to inhibition caused as a result of 2-HBP accumulation in the medium, that is, production of 2-HBP inhibits the growth of the bacteria. Enzymes of 4S pathway also undergo feedback inhibition exerted by 2-HBP, thus limiting the cell growth, and hence, in low degradation efficiency These results are in agreement with results reported by Mohebali and Ball (2008).

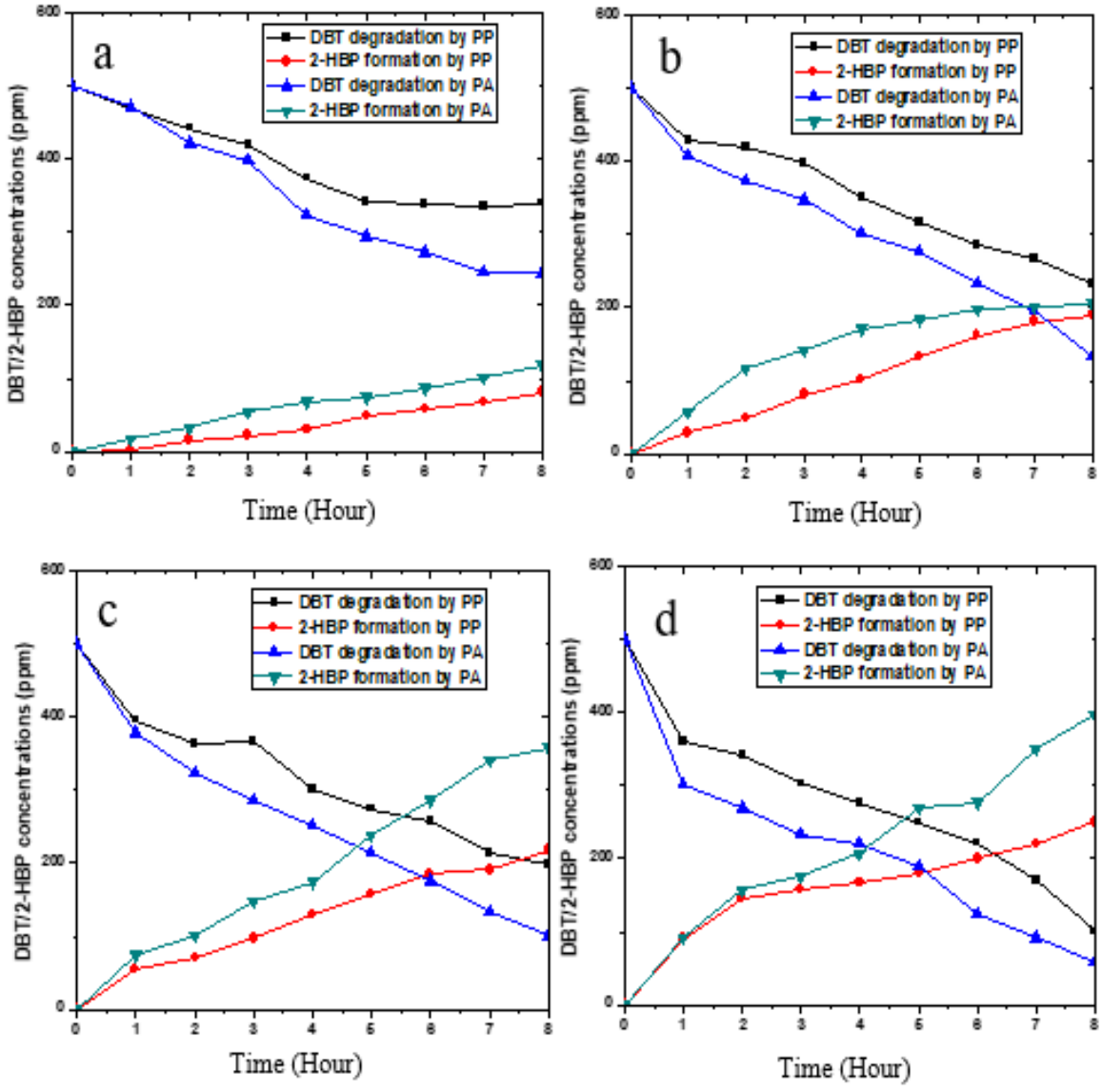


Figure 8.3 Effect of cell concentration of resting cells of *PP* and *PA* on DBT degradation and production of 2-HBP (a) 0.3 g DCW/L (b) 0.6 DCW/L (c) 0.9 g DCW/L (d)1.2 g DCW/L. Experimental conditions: Initial DBT concentrations: 500 ppm; Temperature 37 ^{o}C (P*A*) and 30 ^{o}C (*PP*).

Fig. 8.4 (a) and Fig. 8.4 (b) depict the effect of initial DBT concentration on the growth of *PP* and *PA*. The initial concentrations of DBT were varied from 250-1000 ppm. The result showed that increase in initial concentration of DBT resulted in an increase in the growth of bacteria (*PA* and *PP*). This could be as a result of presence of more DBT for the metabolism of the cell in the

medium resulting thereby in enhanced growth. It was discovered that growth stopped before the final or complete desulfurization of the DBT. This could be attributed to the accumulation of 4S compounds in the medium that inhibited further growth of the cells at 7 h. This is in agreement with the result of Maxwell et al. (2000). Other products of 4S pathway were detected in negligible amount, except 2-HBP (no data is provided for other negligible products in this study). Other authors also confirmed that, other metabolites of 4S pathway could not be detected in the experiment. However, they are indicated as assumed metabolites (Maxwell et al., 2000; Gunam et al., 2013).

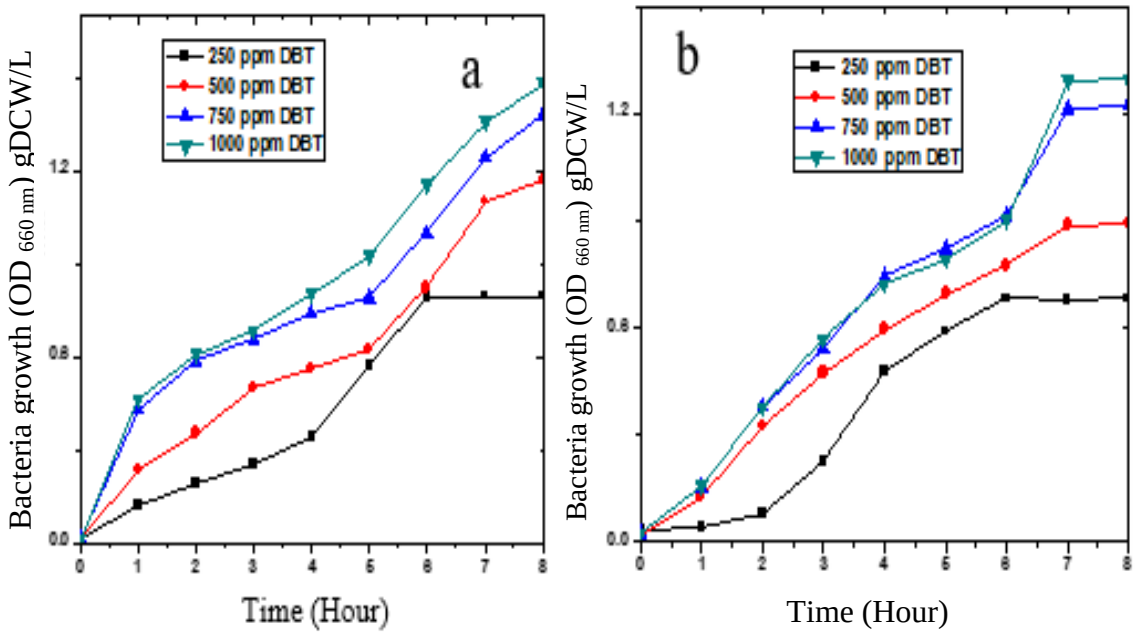


Figure 8.4 Effect of initial DBT concentrations on the growth of (a) *PA* (b) *PP*. Experimental conditions: Oil: water ratio (1:4); Cell concentration: 1.2 gDCW/L; Temperature: 37 ^{o}C (*PA*), 30 ^{o}C (*PP*).

Fig. 8.5 (a - d) depict the effect of DBT initial concentrations on the biodesulfurization of DBT by *PA* and *PP*. The initial concentration of DBT was varied from 250-1000 ppm, in order to evaluate their effect on the growth, DBT desulfurization and 2-HBP formation. The results show that increase in initial concentration of DBT increased the growth of bacteria, thereby increasing the

biodesulfurization of DBT which also resulted in increase in 2-HBP production. About 47.57 %, 48.17 %, 59.89 % and 68.82 % BDS efficiencies were achieved at 250, 500, 750, and 1000 ppm, respectively, when *PA* was used as the biocatalyst. About 39.85 %, 45.97 %, 58.93 %, and 56.31 % degradation efficiency were achieved biocatalyst at 250 ppm, 500 ppm, 750 ppm and 1000 ppm, respectively, when *PP* was used as biocatalyst. A slight decrease in desulfurization efficiency was noticed as the initial DBT was further increased to 1000 mg/L.

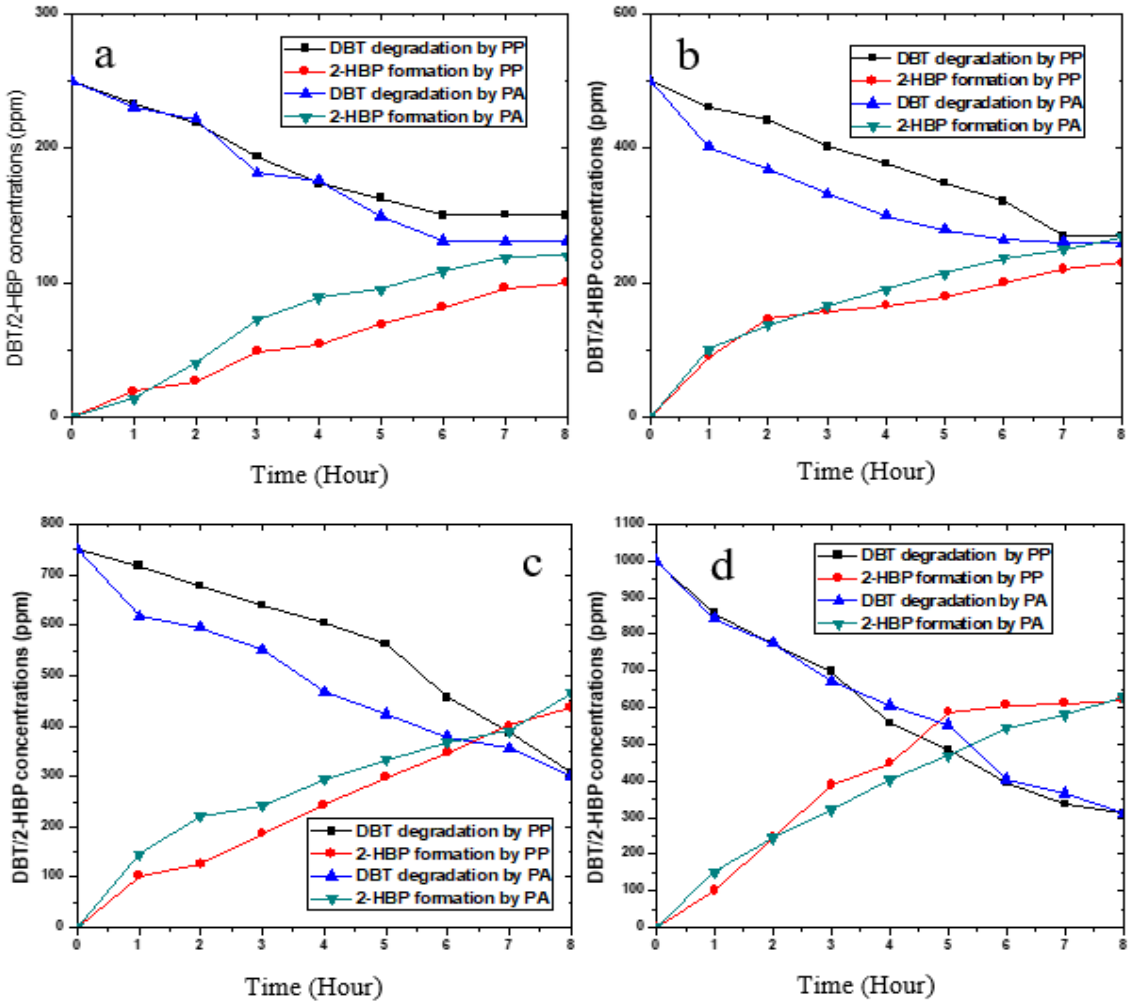


Figure 8.5 Effect of initial DBT concentration on DBT degradation by *Pseudomonas aeruginosa and Pseudomonas putida* (a) 250 ppm (B) 500 ppm (c) 750 ppm (d) 1000 ppm. Experimental conditions: Cell concentration: 1.2 gDCW/L; Temperature: 37 ^{o}C for *PA* and 30 ^{o}C for *PP*

8.3.3. Biphasic effect on growth of bacteria and biodesulfurization

Fig. 8.6 (a), (b), (c) and (d) described the effect of biphasic and aqueous medium on the growth of bacteria *PA* and *PP*. It could be observed from the result in Fig. 8.6 that the optical densities of both *PA* and *PP* in g DCW/L decreased with increase in percentage of oil to water at 50 %. Results show best growth rate when 20 % oil phase was used compared to aqueous medium without the oil phase and 50 % oil phase. The lower growth rate at 50 % could be as a result of hydrophilicity of DBT, owing to the reduced concentration of DBT when oil phase increased because the same initial concentration of DBT was used in all. It is assumed that transfer of DBT from the oil phase to the aqueous phase is an important parameter especially when biocatalyst that has lower capability to adhere at the interface is used (Montecello, 2000; Caro et al., 2008). Another reason this could be so is that, there might be mass transfer limitation of DBT from the oil phase to the aqueous phase where the cells are present. And it has been discovered that the cells use DBT as its sulfur source for it metabolic growth, since bacteria use the DBT in the model diesel for its growth. It could also mean that there was lower supply of oxygen as the oil phase increased. This result is in agreement with Caro et al. (2007 b).

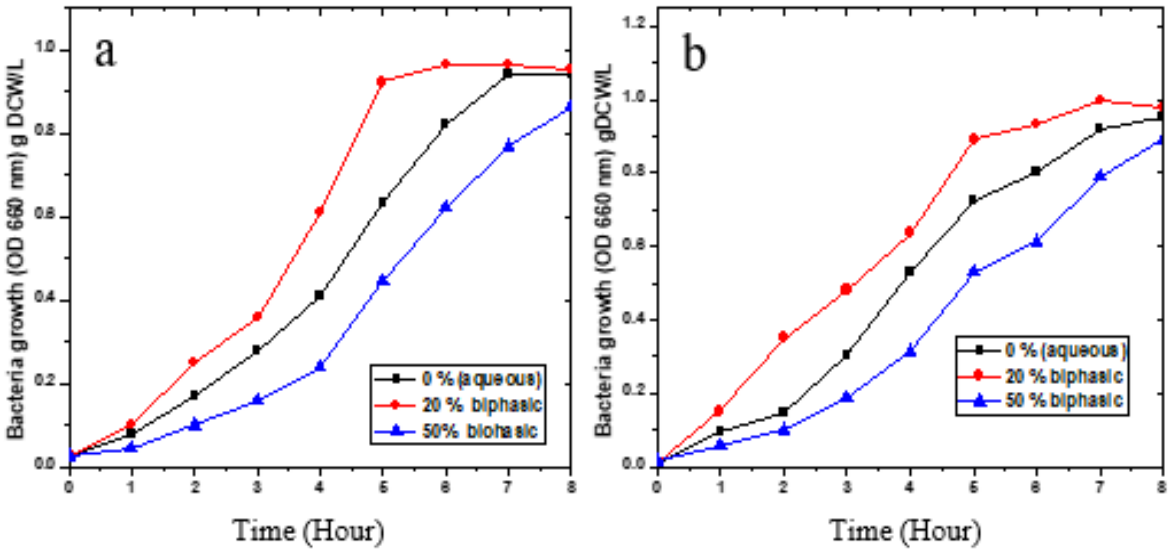


Figure 8.6 Effect of biphasic (oil-water ratio) media on biomas growth (a) *PA* (b) *PP* Experimental conditions: Temperature: 37 ^{o}C (PA); 30 ^{o}C (PP); Initial DBT concentration: 500 ppm.

Fig. 8.7 (a) and Fig. (b) depict the effect of biphasic media on the biodesulfurization of DBT using *PA* and *PP*. The oil-water ratio is an essential factor in defining the production of the reactor as well as the volume of the reactor. The ratio of volume of oil to water (O/W) affects the bioavailability of DBT when BDS takes place at the interface between the aqueous and the organic phases. Result showed better DBT degradation of 2-HBP production in the biphasic medium than in the aqueous medium. This could be as a result of better growth achieved in the result discussed in Fig. 8.6. Enhanced desulfurization was achieved with resting cells of *PA* and *PP* in biphasic media compared to aqueous media. Hence, the amount of 2-HBP production was more than in aqueous phase for both bacteria. This could be attributed to substrate availability and reduced end product inhibition, since 2-HBP which causes feed-back inhibition is in the organic phase. The inhibition effect of 2-HBP was therefore avoided by directing the DBT molecule to the organic phase permitting the desulfurization process to continue unobstructed in the aqueous phase. These results is in agreement with literature (Caro et al., 2007 a; Gunam et al., 2013; Nuhu, 2013).

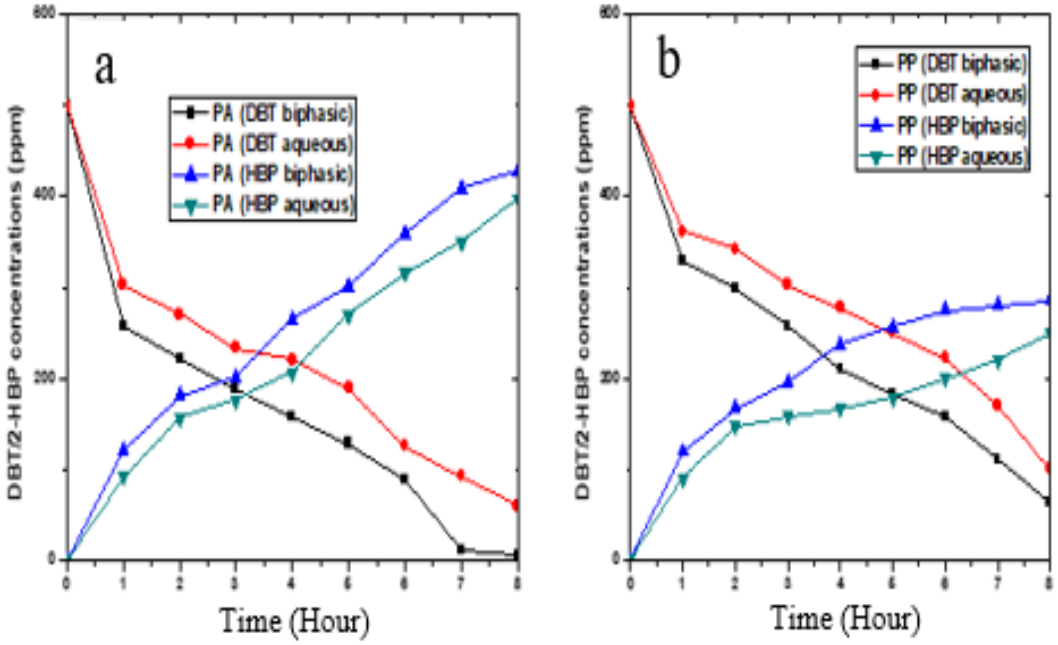


Figure 8.7 Effect of biphasic media on biodesulfurization of DBT and formation of 2-HBP by (a) *PA* (b) *PP*. Experimental conditions: Oil-to-water ratio: 1:4; Temperature: 37 ^{o}C *(PA*), 30 ^{o}C (*PP*); Initial DBT concentration: 500 ppm.

The evaluation of biodesulfurization capacity (X_{BDS}), Conversion yield for DBT (Y_{BDS}), degree of desulfurization (D_{BDS}) and specific conversion rate (E) were obtained using Equation (3.22-3.24) in chapter three of this thesis. Table 8.2 shows X_{BDS}, Y_{BDS}, D_{BDS} and E values for the degradation of DBT in model diesel using resting cells of *PA* and *PP* at different initial DBT concentrations of 250, 500, 750 and 1000 ppm. The results show increase in the order, 48.06 %, 53.53 %, 62.07 % and 62.97 % biodesulfurization efficiency as the initial DBT concentration increased from 250 ppm to 1000 ppm. This could be attributed to availability of the sulfur source needed for the growth and metabolism of the bacteria. Furthermore, the desulfurization yield (Y_{BDS}) were found to be 47.57 %, 48.17 %, 59.89 % and 68.82 % which showed that the yield increased with increasing initial DBT concentrations. Since increase in initial concentration increased the groth rate, therefore the yield of biodesulfurization of DBT also increased. The degree of desulfurization to were found to increase (4.78, 7.84, 10.72 and 11.69 g DCW/L.h) as the intial concentration increased from 250 to 1000 ppm. However, the specific conversion rate decreased as the initial DBT concentrations.

The same trend was observed for biodesulfurization using pseudomonas putida. The results show increase in the order, 40.06 %, 46.02 %, 61.60 % and 62.21 % biodesulfurization efficiency of *PP* as the initial DBT concentration increased in the order 250, 500, 750 and 1000 ppm. This could be attributed to availability of the sulfur source needed for the growth and metabolism of the bacteria. Furthermore, the desulfurization yields (Y_{BDS}) values of *PP* were recorded to be 39.85 %, 45.97 %, 58.93 % and 56.31 % which showed that the yield increased with increasing initial DBT concentrations from 250 to 750 ppm. Since increase in initial concentration increased the growth rate, the yield of biodesulfurization of DBT also increased. However, the biodesulfurization yield was observed to decrease to 56.31 when the initial DBT concentration increased to 1000 ppm. The degrees of desulfurizations of *PP* were found to increase (3.40, 5.13, 9.40 and 10.09 g DCW/L.h) as the intial concentration increased from 250 to 1000 ppm. However, the specific conversion rate decreased as the initial DBT concentrations. In all respect, the X_{BDS}, Y_{BDS}, D_{BDS} and E values for *PA* were found to be higher than that of *PP*.

Table 8.2: X_{BDS}, Y_{BDS}, D_{BDS} and E parameters for biodesulfurization of DBT in model oil by resting cells of *Pseudomonas aeruginosa and Pseudomonas putida*

	Pseudomonas Aeruginosa				***Pseudomonas Putida***			
C_{DBT} (ppm)	**X_{BDS} (%)**	**Y_{BDS} (%)**	**D_{BDS} (g DCW/L.h)**	**E_{BDS}(L/h.g DCW)**	**X_{BDS} (%)**	**Y_{BDS} (%)**	**D_{BDS}(g DCW/L.h)**	**E_{BDS}(L/h.g DCW)**
250	48.06	47.57	4.78	7.55	40.06	39.85	3.40	7.37
500	53.53	48.17	7.84	5.71	46.02	45.97	5.13	6.45
750	62.07	59.89	10.72	5.61	61.60	58.93	9.40	6.31
1000	62.97	68.82	11.69	5.31	62.21	56.31	10.09	6.00

Table 8.3 illustrates the results obtained in this study compared with literature. Resting cells of Lyophilized R-8 was utilized to degrade DBT in model oil by Mingfang et al. (2003) with an initial concentration of 1807 ppm. The result showed 55.23 % BDS performance at BDS rate of 8.75 Mm (g DCW/L)$^{-1}h^{-1}$. Comparing this with the result obtained in this study, when the initial DBT concentration in this study was 500 ppm in a model oil, a BDS performance and BDS rate of 67.53 % at 21.25 mM (g DCW/L)$^{-1}h^{-1}$, respectively by resting cells of *pseudomonas aeruginosa* and 50. 02 ppm and 13.90 mM (g DCW/L)$^{-1}h^{-1}$ by resting cells of *pseudomonas putida* were obtained. The BDS performance results obtained in this study are better than what was obtained by Mingfang et al. (2003). This could be due to a higher initial concentration used in their study. Alcon et al. (2005) desulfurized DBT in a model diesel using *Pseudomonas putida CECT 5259* for 10 h with an initial

DBT concentration of 1.84 ppm. About 86 % desulfurization efficiency was achieved by the bacteria. The result obtained in their study was higher than the result obtained in this study. This could be attributed to higher initial DBT concentration of 500 ppm used in this study.

Table 8.3: Results of degradation of DBT in model diesel compared with literature.

Bacteria	**Sulfur compound**	**Reaction time (h)**	**C_o (ppm)**	**C_f (ppm)**	**% BDS**	**DZ rate (mM g (DCW/L)$^{-1}$h^{-1}**	**Ref.**
Lyophilized cell of R-8	DBT	24	1807.00	808.90	55.23	8.75	Mingfang et al. (2003)
PP CECT 5279	DBT	10	1.84	0.26	86.00	0.12	Alcon et al. (2005)
Pseudomonas Putida	DBT	8	500.00	250.10	50.02	13.90	This study
Pseudomonas aeruginosa	DBT	8	500.00	162.35	67.53	21.25	This study

C_o is the initial DBT concentration, C_f is the final DBT concentration, DZ is desulfurization.

8.4 Kinetics of bacteria growth and degradation model diesel

8.4.1. Kinetic model for growth of bacteria

The growth of bacteria in a culture was studied using the Michaelis-Menten expression in Equation 3.36 in chapter three of this thesis. The experimental data was compared with the model data obtained. The percentage error between the experimanta data and the model parameters obtained was calculated using Equation (3.37). Fig. 8.8 depicts the fitting of the model data with the experimental. Michaelis-Menten equation (see Eq. 3.36) was used to describe the growth of bacteria strains used in this study using Lineweaver-Burk plot. The maximum velocity, V_{max} and

Michaelis-Menten's constant, K_m parameters were calculated from the intercept and the slope of the straight line graph. The The percentage errors were calculated using the expression in Equation 3.37. Table 8.4 shows the parameters obtained, and the percentage error calculated. It can be seen that the reaction rate increased with increasing initial DBT concentration for both bacteria. The observation was consistent with data obtained initially in the experiment. This obviously showed a change in DBT distribution with the degree of desulfurization. The rate of DBT desulfurization by growing cells of *PP* are 0.102, 0.116, 0.156 and 0.163 gDCW/L.h at 250, 500, 750 and 1000 ppm initial DBT concentration. This indicates that the rate of growth of *PP* increased with increasing initial DBT concentrations. This could be due to enough availability of DBT for the metabolism of the cell in the medium which resulted in increase in their growth. This is in agreement with the result of Maxwell et al. (2000). The maximum specific growth rate obtained for *PP* was 0.192 mgDBT/g DCW.h. and the Michaelis-Menten constant, K_m obtained was 234.28 ppm. The percentage error calculated were 0.92 %, 3.76 %, 1.99 % and 1.5 % at 250, 500 750, and 1000 mg/L, respectively.

The rate of DBT desulfurization by growing cells of *PA* are 0.111, 0.138, 0.148 and 0.165 gDCW/L.h at 250, 500, 750 and 1000 ppm initial DBT concentration. This indicates that the rate of growth of *PA* increased with increasing initial DBT concentrations. This could be due to enough availability of DBT for the metabolism of the cell in the medium which resulted in increase in their growth. This is in agreement with the result of Maxwell et al. (2000). The maximum specific growth rate obtained for *Pseudomonas putida* was 0.187 mg DBT/g DCW.h. and the Michaelis Menten constant, K_m obtained was 174.12 mg/L. The percentage error calculated were 0.23 %, 0.17 %, 0.15 % amnd 0.16 % at 250, 500 750, and 1000 ppm, respectively. Comparing the percentage error in first order model of *PA* with that of *PP*, it can be seen that the % error in pseudomonas aeruginosa were smaller compared to *PP*. Thereore, Michaelis-Menten model described well the kinetics that govern the growth of *PA* than it did for *PP*. The observations in this model were consistent with data obtained initially in the experiment. This obviously demonstrated a shift in DBT distribution with the extent of desulfurization. The results obtained in this study are comparable with literature. A *Gordonia CYKS1* desulfurizing bacterium was reported by Rhee et al., (1998). The bacterium was reported to transform DBT into 2-HBP at the rate of 27.6 mg/gDCW.min. The rate of transformation of DBT into 2-HBP in this study is lower

that what was obtained in Rhee et al study. Folsom et al., 1999 also investigated the desulfurization of DBT by R. erythropolis I-19. The rate of desulfurization by this bacterium was 920 mg/gDCW.min. Although 36.8 mg/gDCW/L was previously reported by Holda et al., (1999) using wild type *R. erythropolis IGTS8* for conversion of DBT to HBP. *PP* used in this study has the same gene as *the R. erythropolis* used in their studies. The Michaelis constant (K_m) estimated by Abin-Funtes et al. (2014) for degradation of DBT by R. erythropolis KA2-5-1 was 1840 mg/L and 4784 mg/L was obtained by Kobayashi et al. 2001. In this study, the Michaelis Menten constant, (Km) parameters obtained were 4536.5 mg/L and 2639.40 mg/L for *PA* and *PP*, respectively for DBT degradation in diesel. These are very close to what was reported by Albin-Funtes et al (2014) and Kobanashi et al. (2001), respectively. Therefore, these results are comparable with literature.

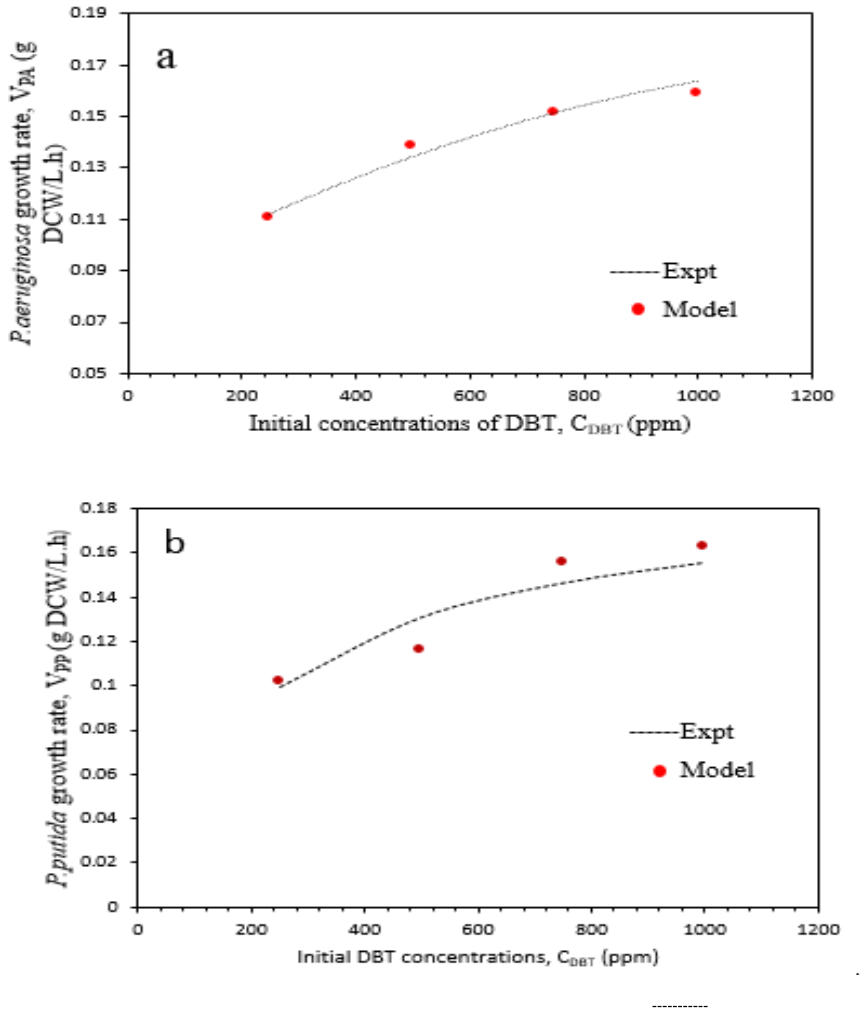


Figure 8.8 Michaelis-Menten growth kinetic model for growing cells of (a) *PA* (b) *PP*

Table 8.4: Michaelis-Menten Kinetic model parameters for growth of *PA* and *PP*

PA				***PP***			
CDBT (mg/L)	**V_{exp} (g DCW/L.h)**	**V_{mod} (g DCW/L.h**	**% Error**	**CDBT (mg/L)**	**V_{exp} (g DCW/L.h**	**V_{mod} (g DCW/L.h)**	**% Error**
250	0.111	0.110	0.232	250	0.102	0.099	0.942
500	0.138	0.139	0.168	500	0.116	0.131	3.758
750	0.148	0.152	0.827	750	0.156	0.146	1.992
1000	0.165	0.159	1.158	1000	0.163	0.156	1.522

C_{DBT}: Initial DBT concentration; V_{exp}: Experimental value for maximum reaction velocity; V_{mod}; Model value for maximum reaction velocity.

8.4.2. kinetic model of DBT degradation in model diesel

Pseudo-first order model was used to describe the degradation of DBT by *PA* and *PP*. The expression is described in Equation (3.27) in chapter three of this thesis. The kinetic of DBT degradation by resting cell of *PA* and *PP* under aqueous condition in this study was described by Pseudo-first order model. Fig. 8.9 and 8.10 (a-d) depict the first order model and experimental data of DBT degradation in model oil by *PA* and *PP* at initial DBT concentrations of 250, 500, 750, and 1000 mg/L. Desulfurization of DBT in this study followed first order kinetics model and fitted well into experimental data. The apparent first order kinetic constants obtained for different DBT concentrations of 250, 500, 750 and 1000 mg/L, were 0.071, 0.081, 0.105 and 0.15 3 h^{-1}, respectively for PP (see Table 8.5). It could be observed that kinetic constant increased with increasing initial DBT concentration. The apparent first order kinetic constant for *PA* at different DBT initial concentrations of 250, 500, 750 and 1000 mg/L were 0.092, 0.079, 0.108 and 0.104 h^{-}

[1], respectively (see Table 8.5). The first order model described well the degradation of DBT at all initial DBT concentrations, for both *PA* and *PP*. All the results obtained here show that *PP* and *PA* could utilize DBT as sole carbon sources for growth and desulfurization of DBT compound in model diesel. Nevertheless, the rate of degradation was still slow and the time taken was long. Therefore, increasing the rate of degradation is important for biodegradation of DBT. About 62.21 % and 62.97 % were degraded by *PP* and *PA* respectively. The DBTcould not be degraded further by the microorganisms owing to large size, great hydrophobicity, and high molecular weight of DBT which invariably resulted to its low bioavailability and limited mass transfer rate. The results obtained in this study were comparable to literature (Talaiekhozani1 et al., 2015).

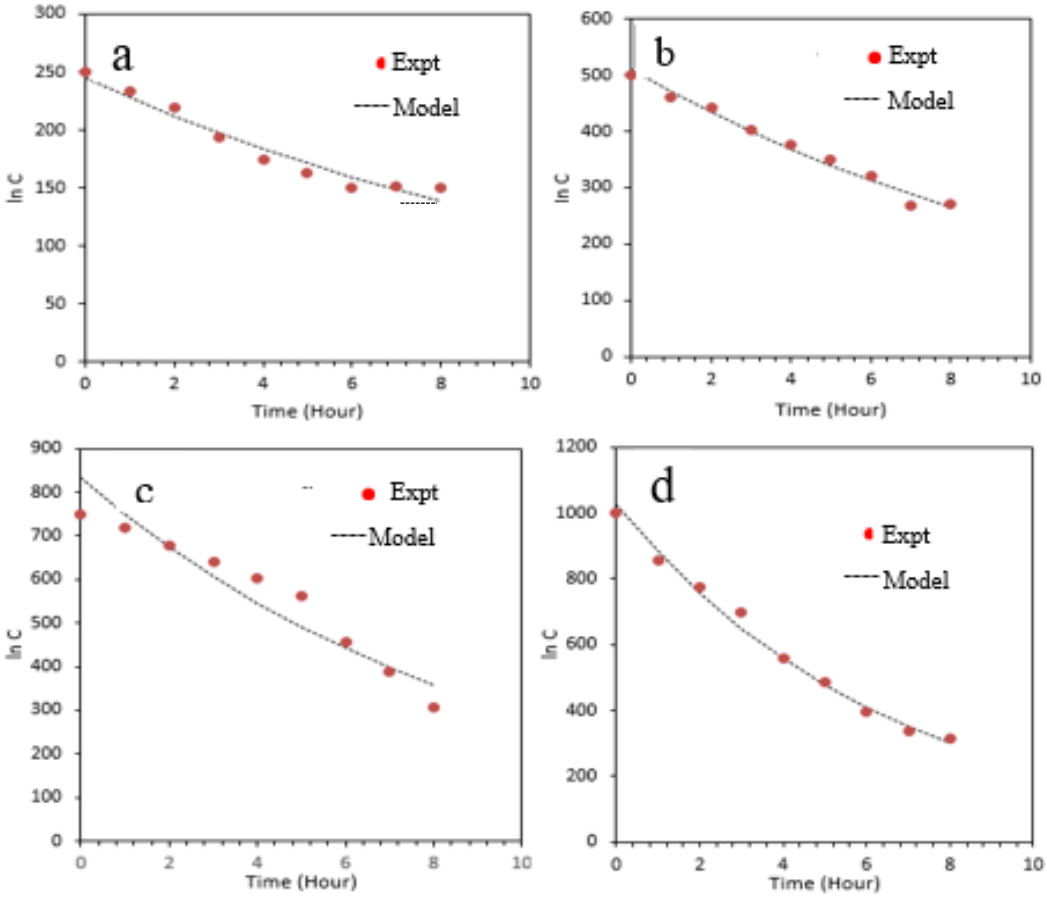


Figure 8.9 First order kinetic model for DBT degradation by resting cells of *PP* at (a) 250 mg/L (b) 500 mg/L (c) 750 mg/L (d) 1000 mg/L. Experimental conditions: Cell mass: 1.2 gDCW/L, Temperature: 30 ^{o}C.

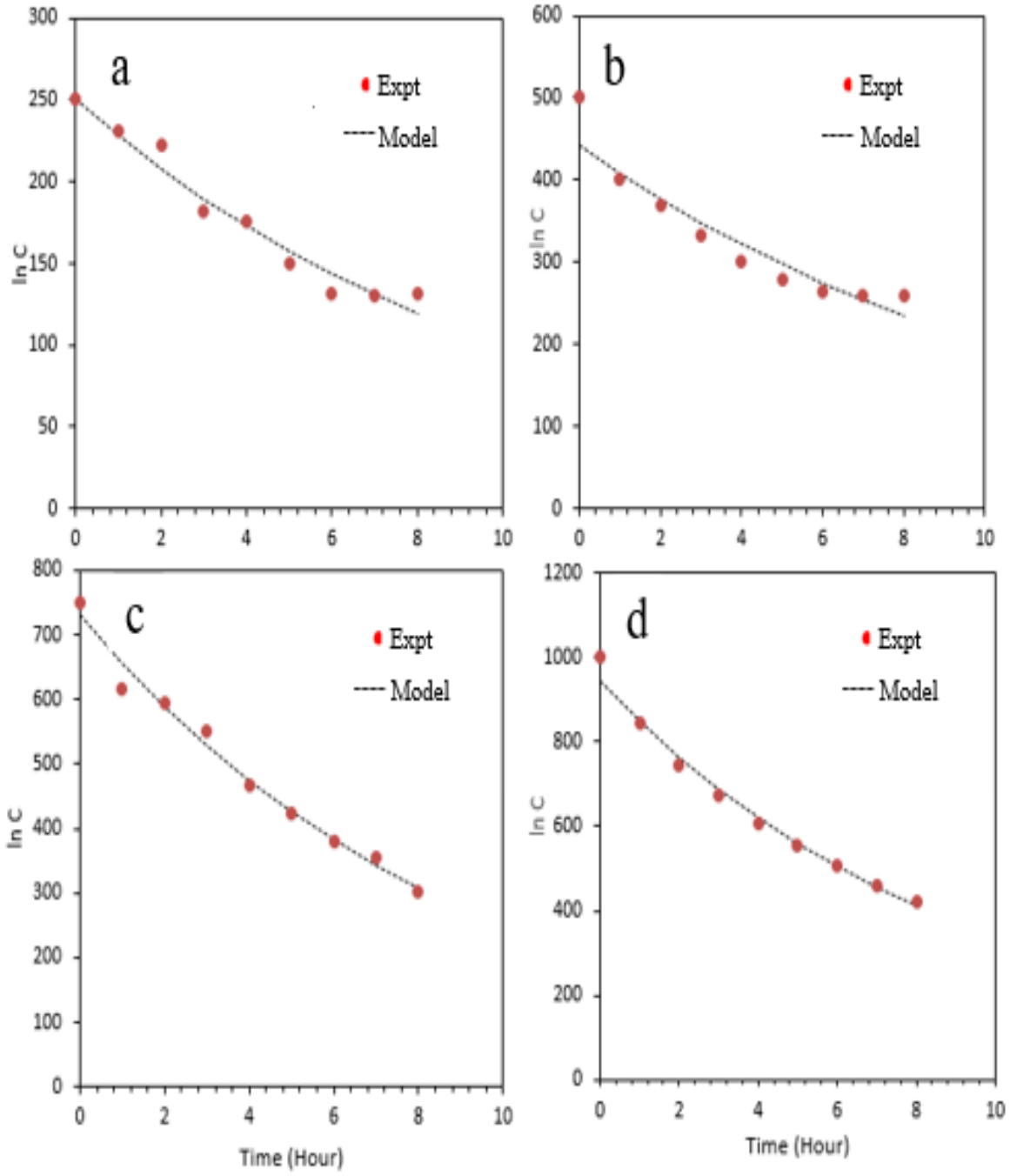


Figure 8.10 First order kinetic model of DBT degradation in model diesel by resting cell of PA at (a) 250 mg/L (b) 500 mg/L (c) 750 mg/L (d) 1000 mg/L. Experimental conditions: Cell mass: 1.2 gDCW/L; Temperature: 37^{o}C.

Table 8.5: First order kinetic constants for degradation of DBT by *PA* and *PP* at different initial DBT concentrations.

C_{DBT} (mg/L)	K_{PA} (h^{-1})	K_{PP} (h^{-1})
250	0.0922	0.0809
500	0.0795	0.1054
750	0.1078	0.1527
1000	0.104	0.1705

K_{PA} and K_{PP} are the first order constant for *PA* and *PP*, respectively; C_{DBT} is the initial concentration of DBT

8.5. Evaluation of biodesulfurization efficiency of real diesel samples using resting cells of *Pseudomonas Sp.*

Results of Biodesulfurization of real diesel samples obtained from a typical South African refinery are shown in Fig. 8.11 and Fig 8.12. Fig. 8.11 depicts the desulfurization of diesel sample after HDS with initial DBT concentration of 120 ppm. The results show that there was an appreciable increase in degradation of diesel sample after HDS from initial DBT concentration of 120 ppm to 35.35 ppm for *PA* and from 120 ppm DBT to 38.99 ppm for *PP*. This accounted for about 70.54 % and 67.50 % degradation capacity for *PA* and *PP*, respectively. It could be observed as well that 36 % 2-HBP was produces when *PA* was used as biocatalyst and 33 % of 2-HBP was formed for biodesulfurization of diesel by *PP*. This result is lower compared to what was obtained in biodesulfurization of model diesel. This could be because a lot of compounds are present in the real diesel which might affect selectivity of DBT for biodegradation (Samokhvalov 2012)

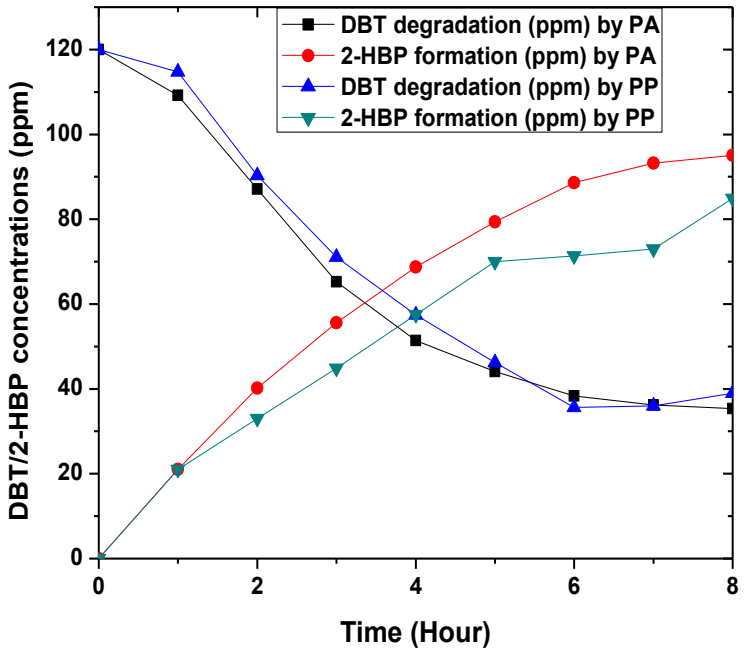


Figure 8.11 Biodesulfurization of diesel obtained after HDS by *PP* and *PA*. Experimental conditions: Initial DBT concentrations: 120 ppm; Cell mass: 1.2 g DCW/L; Temperatures: 30 ^{o}C (*PP*) and 37 ^{o}C (*PA).*

Fig 8.12 depicts the biodesulfurization of DBT in diesel sample obtained before HDS with initial DBT concentration 5200 ppm by *PA* and *PP*. The results show that about 36 % and 33 % desulfurization of the diesel was achieved by *PA* and *PP*, respectively. After 8 h of biocatalyst activity at resting stage, the DBT content of the diesel reduced from its initial value of 5200 ppm to 3328 ppm for *PA*, and from 5200 ppm to 3440 ppm for *PP*. This low desulfurizing efficiency could be attributed to the presence of other organosulfur present in the feed stock diesel (diesel sample obtained before HDS). In addition, high concentration of sulfur content could hinder the growth of bacteria i.e the concentration might be too toxic for the enhanced growth of the bacteria. This will invariably affect the degradation efficiency of the DBT compound in the diesel. The

formation of 2-HBP was also observed during the experiment as shown in Figure 8.10 b, and the production was significantly low (e.g about 21.53 % and 20.17 % for *PA* and *PP*, respectively) (Samokhvalov, 2012).

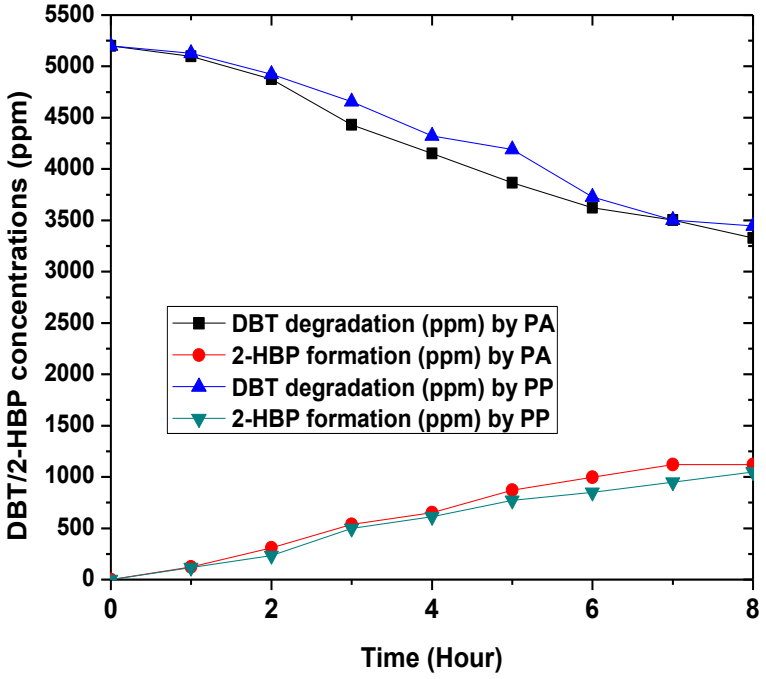


Figure 8.12 Biodesulfurization of diesel obtained before HDS. Experimental conditions: Initial DBT concentrations: 5200 ppm. Cell mass: 1.2 g DCW/L, Temperatures: 30 ^{o}C *(PP)* and 37 ^{o}C (*PA*).

Fig. 8.13 (a) shows the GC/MS chromatogram of DBT and 2-HBP standard in ethyl acetate, Fig. 8.13 (b) GC/MS chromatogram of diesel obtained after HDS and (c) GC/MS chromatogram of biodesulfurized diesel. Fig 8.13 (a) indicates that DBT was obtained at m/z 184 and 2-HBP at m/z 170 (Li et al., 2003). The chromatogram in Fig. 8.13 (c) show decrease in the peak area of DBT compared to the control sample before biodesulfurization (see Fig. 8.13 b). Also there was an

appearance of a peak at 7.5 minutes (Fig. 8.13 c) retention time which indicates the formation of 2-HBP in the desulfurized diesel.

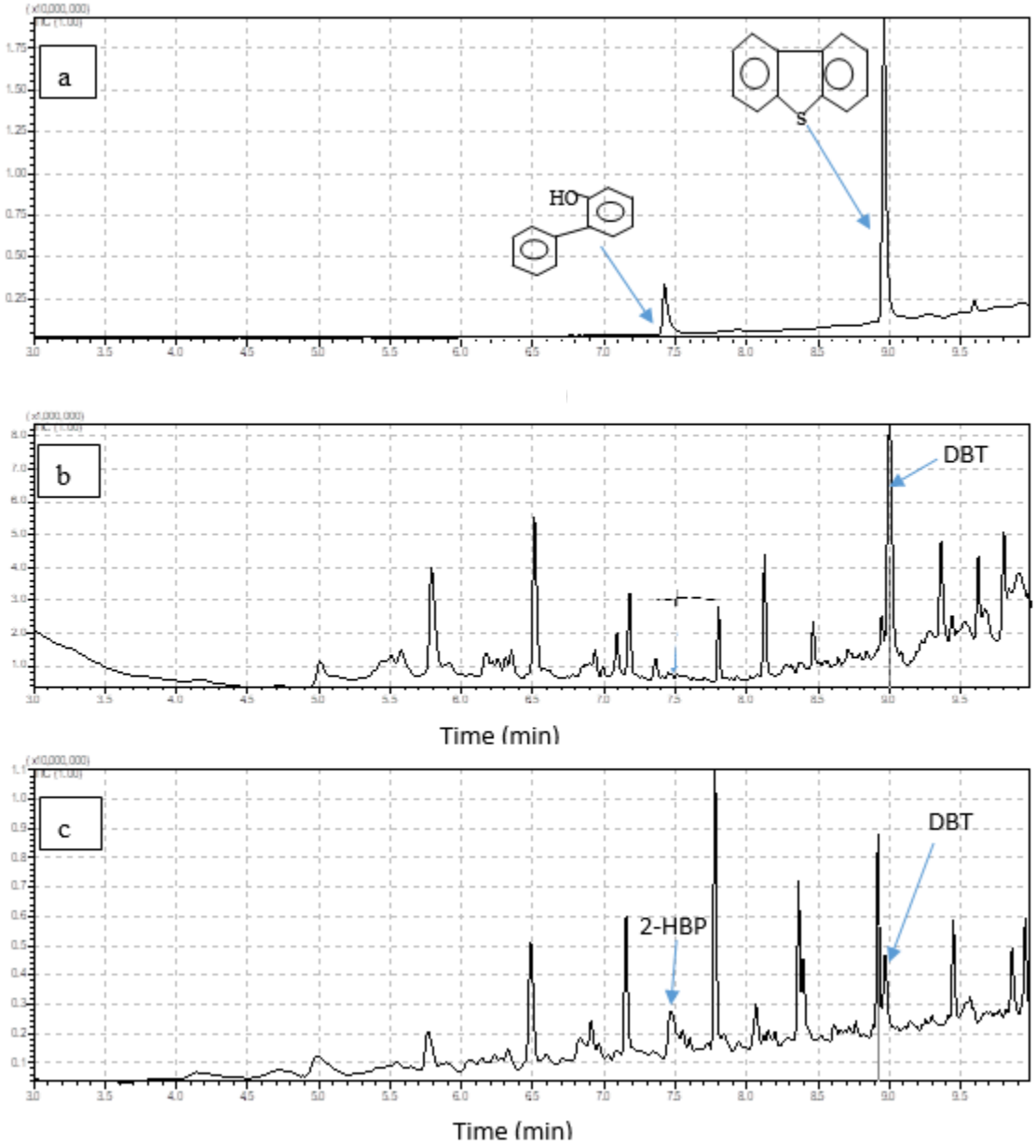


Figure 8.13 Chromatograms of (a) standard DBT and 2-HBP in ethyl acetate (b) Real diesel obtained before biodesulfurization (c) Biodesulfurized diesel

8.6 Degradation kinetics of real diesel

Only DBT degradation kinetic model was described here for desulfurization of real diesel. First order kinetic model for used for degradation DBT in South African real diesel. Fig. 8.14 (a) and (b), depict the first-order model and experimental data of DBT degradation of South African diesel after HDS by *Pseudomonas aeruginosa* and *Pseudomonas putida*, respectively at initial DBT concentrations of 120 mg/L. Desulfurization of DBT in this study followed first order kinetics model and fitted well into experimental data. The apparent first order kinetic constants obtained were 0.1705 h^{-1} and 0.711 h^{-1}, for SA diesel after HDS at 120 mg/L initial sulfur concentration by *PA* and *PP*, respectively. The values are both close because their desulfurizing activities are also close. The model shows perfect fits at all initial DBT concentrations with experimental data. The results are comparable with Talaiekhozani1 et al. (2015).

Table 8.6 illustrates the comparison of results of biodesulfurization of DBT in model diesel and real diesel documented in this chapter with literature. It could be observed that Chang et al. (2000) desulfurized middle distillate diesel using cells *Gordona CYKS1* for 10 h with an initial DBT concentration of 1500 ppm. Results show that the bacteria were able to degrade 53 % of the DBT, which is higher that the result obtained in this study. The bacteria *(PA)* used in this study could only degrade 30 % of the DBT with an initial concentration of 5200 ppm. This could be due to the toxic effect of the DBT at higher concentration on the growth of the bacteria, which invariably affected the degradation and production of 2-HBP at the same time. However, when diesel sample obtained after HDS was used, with an initial concentration of 120 ppm, a higher biodesulfurization efficiency of 70.54 % was obtained which was higher than the result obtained by Chang and his co-authors. In addition, the DBT in the middle distillate was degraded after 10 h, which is higher than 8 h recorded in this study to degrade the DBT in the diesel sample obtained before HDS and diesel sample obtained after HDS. These results were also compared the report of Verma et al. (2016).

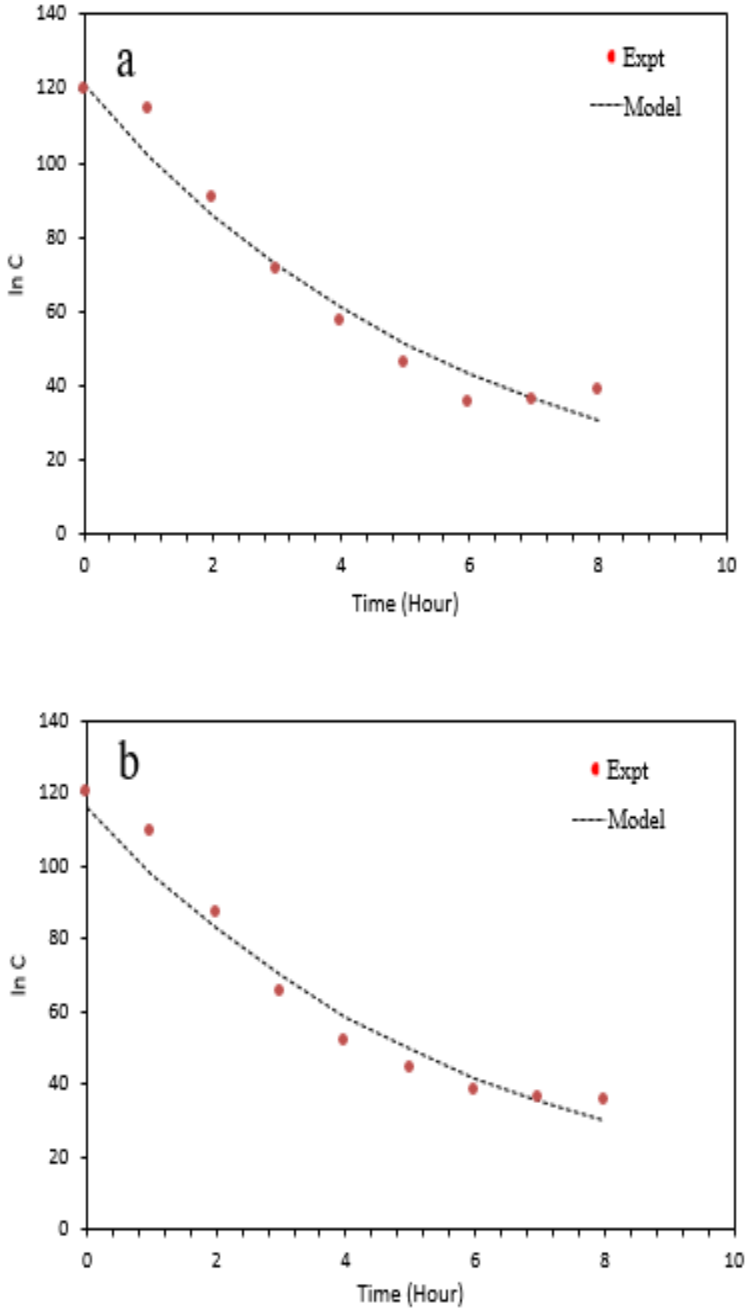


Figure 8.14 Kineic model of DBT degradation in real diesel after HDS by resting cells of (a) *Pseudomonas putida* (b) *Pseudomonas aeruginosa*. Experimental conditions: Initial DBT concentration: 120 mg/L: Cell mass: 1.2 gDCW/L.

Verma et al. (2016) reported that about 88 % DBT was degraded by an isolate E1 bacteria with an initial concentration of 368 ppm at 72 h. It can be seen that the result obtained in this study was lower than what was reported by Verma et al. (2016). This could be as a result of short reaction time (8 h) used in this study. In addition, the exact concentration of bacteria (2 %) used by Verma et al. (2016) was not disclosed. Increasing the reaction time of this study from 8 h to 72 h could increase the degradation efficiency of the bacteria.

Resting cells of Lyophilized R-8 was utilized to degrade DBT in model diesel by Mingfang et al. (2003) with an initial concentration of 1807 ppm. The results showed 55.23 % BDS efficiency at BDS rate of 8.75 Mm (g DCW/L)$^{-1}$h^{-1}. Comparing this with the results documented in this study, when the initial DBT concentration in this study was 500 ppm in a model diesel, a BDS efficiency and BDS rate of 67.53 % at 21.25 mM (g DCW/L)$^{-1}$h^{-1}, respectively by resting cells of *PA*. The BDS performance and DBS rate results reported in this study are better than what was obtained by Mingfang et al. (2003). This could be due to a higher initial concentration used in their study. The results obtained in this study are comparable to the results obtained in the literature. However, further investigations are required to detect all the metabolites in the 4S pathway.

Table 8. 6: Comparison of results of BDS of model diesel and real diesel literature

Bacteria	Sulfur compound	Time (h)	C_o (ppm)	C_f (ppm)	% BDS	DZ rate (mM g $(DCW/L)^{-1}h^{-1}$	Ref.
Lyophilized cell of R-8	DBT	24	1807	808.90	55.23	8.75	Mingfang et al. (2003)
Gordona CYKS1	Diesel	10	1500	610.00	59.30	94.00	Chang et al. (2003)
PA	DBT	10	1.84	0.26	86.00	0.12	Alcon et al. (2005)
Isolate E1	Crude oil	72	368	18.40	88.00	-	Verma et al. (2016)
PA	DBH	8	5200	3444.00	30.00	12.96	This study
PP	DBT	8	500	250.10	50.02	13.90	This study
PA	DBT	8	500	162.35	67.53	21.25	This study

PA: *Pseudomonas Aeruginosa; PP: Pseudomonas Putida*; C_o: Initial DBT concentration; C_f: final DBT concentration; DAH: diesel obtained after HDS; DBH: diesel obtained before HDS.

8.7. Concluding remarks

As it has been demonstrated in this chapter, *PA* and *PP* were successfully grown. The growing and resting cells of both bacteria were used to degrade the DBT molecule in the model oil. Results showed that *PA* showed better BDS performance than *PP* in all aspect. The results in this study show that *PA* and *PP* are able to desulfurize DBT into less harmful compound, 2- HBP. However, further studies are required to determine their desulfurization potential for other sulfur organic compounds in real diesel.

The final product 2-HBP detected shows the specific activity of DBT desulfurization is 4S – pathway. However, more investigations are still required in this field to detect all the various metabolites in the 4S pathway. In addition, introduction of sufficient oxygen could improve the

biodesulfurization efficiency of these bacteria. Results show BDS performance of 67.53 % and 50.02 %, by resting cells of *PA* and *PP*, respectively for 500 ppm initial concentration. In order to study desulphurization of diesel oils obtained from an oil refinery, resting cells studies by *PA* were carried out which showed a decrease of about 30 % and 70.54 % DBT removal from 5200 ppm in diesel before HDS and 120 ppm in diesel after HDS, respectively. *PA* and *PP* selectively converted sulfur atom in DBT compound to 2-HBP. First order kinetic model was used for growth of bacteria and it fitted well into the experimental data. Likewise, Micaelis-Menten fitted described well the behavior of the bacteria for degradation of DBT in model diesel and real diesel samples.

The result obtained in this study showed that biodesulfurization would be a better technique to compliment HDS technique rather than the main technique for desulfurization of organo-sulfur compounds in diesel oil. Furthermore, *PA* and *PP* could be better biocatalysts for degrading harmful sulfur compound in South African diesel. This will assist the refineries to meet up with the stringent regulation to minimize the emission of sulfur compounds which cause environmental pollution and health problems in South Africa and all over the world.

In order to communicate the novel contribution of this work to the scientific community, one manuscript has been submitted to an international reputable journal for publication (Biochemical Engineering Journal). One or more manuscripts are in preparation for submission in reputable international journals for possible publication.

8.8. References

Abin-Fuentes, A., Leung, J. C., Mohamed, M. E., Wang, D. I.C., and Prather, K. L.J. (2014) Rate-limiting step analysis of the microbial desulfurization of dibenzothiophene in a model oil system. Biotechnol Bioeng., 111(5), 876–884.

Aggarwal, S., Karimi, I. A., Ivan, G. R. (2013) *In silico* modeling and evaluation of *Gordonia alkanivorans* for biodesulfurization.*Mol. Biosyst.* 9, 2530–2540.

Alcon, A., Santos, V.E., Martins, A.B., Yustos, P., and Garcia-Ochoa, F. (2005) Biodesulfurization of DBT with Pseudomonas putida CECT 5279 by resting cells: Influence of cell growth time on

reducing equivalent concentration and HpaC activity. Biochemical Engineering Journal 26, 168-175.

AL-Faraas1, A. F., AL-Jailawi1, M. H., and Yahia. A. I. (2015) Desulfurization of Dibenzothiophene by Pseudomonas aeruginosa Isolated from Iraqi Soils. Iraqi Journal of Biotechnology, 14 (1) 37-43.

Babich, I. V., and Moulijn, J. A. (2003) Science and technology of novel processes for deep desulfurization of oil refinery streams: a review. *Fuel* 82, 607–631.

Caro, A. Boltes, T. Leton, P. and Garcia-Calvo, E. (2007b) Dibenzothiphene desulfurization in resting cell condition by aerobic bacteria. Biochem Eng. J. 35, 191-197.

Caro, A. Leton, P., Garcia-Calvo, F., and Setti, L. (2007a) Enhancement of the DBT biodesulphurization by using β-cyclodextrins in oil-to water media. Fuel, 86, 2632-2636.

Caro A, Boltes K, Leto ´n P, Garcı ´a-Calvo, E. (2008b) Biodesulfurization of dibenzothiophene by growing cells of Pseudomonas putida CECT 5279 in biphasic media. Chemosphere 73, 663–669.

Caro , A., Boltes , K., Letón, P. and García-Calvo . E. (2008b) Description of by-product inhibiton effects on biodesulfurization of dibenzothiophene in biphasic media. Biodegradation. 19 (4), 599-611.

Chang. J.H., Chang, Y.K., Cho, K.S. and Chang, K.N. (2000) Desulfurization of model oil and diesel oil by resting cells of Gordon asp. Biotechnol. Lett. 22, 193.

Davoodi-Dehaghani, F., Vosoughi, M., and Ziaee, A.A. (2010) Biodesulfurization of dibenzothiophene by a newly isolated Rhodococcus erythropolis strain. Bioresour. Technol. 101, 1102–1105.

Farhana, M.S.N., Bivi, M.R., Khairulmazmi, A. (2011) Effect of carbon sources on bacterial production of metabolites against Fusarium oxysporum and Colletotrichum gloeosporioides. Int. J. Agric. Biol., 13: 1–8.

Fatemeh, D.D., Vosoughi, M. and Ziaee, A.A. (2010) Biodesulfurization of dibenzothiophene by a newly isolated Rhodococcus erythropolis strain. Biores Technol 101, 1102–1105.

Folsom, B. R., Schieche, D. R., Digrazia, P. M., Werner, J. and Palmer, S. (1999) Microbial Desulfurization of Alkylated Dibenzothiophenes from a Hydrodesulfurized Middle Distillate by Rhodococcus erythropolis I-19. Applied and Environmental Microbiology, Vol. 65, No. 11. p. 4967–4972.

Fonte, E.S., Amado, A.M., Meirelles-Pereira, F., Esteves, F.A., Rosado, A.S., Farjalla, V.F. (2013) The combination of different carbon sources enhances bacterial growth efficiency in aquatic ecosystems. Microb Ecol. , 66(4), pp. 871-878.

Gunam, I.B.W., Kenta, Y., Nengah, I.S., Nyoman, S.A., Wayan, R.A., Michiko, T., Fusao, T., Teruo, S., and Kozo, A. (2013) Biodesulfurization of DBT and its derivatives using resting and immobilized cells of Sphingomonas Subarctica T7b. J. Microbiol. Biotechnol., 23, 473-482.

Honda, H., Sugiyama, H. Saito, I. and Kobayashi, T. (1998) High cell density culture of Rhodococcus rhodochrous by pH-stat feeding and dibenzothiophene degradation. J. Ferment. Bioeng. 85:334–338.

Kilbane, J. J. (2006) Microbial biocatalyst developments to upgrade fossil fuels. *Curr. Opin. Biotechnol.* 17, 305–314.

Kobayashi, M., Horiuchi, K., Yoshikawa, O., Hirasawa, K., Ishii, Y., Fujino, K., Sugiyama, H., Maruhashi, K. (2001) Kinetic analysis of microbial desulfurization of model and light gas oils containing multiple alkyl dibenzothiophenes. Biosci Biotechnol Biochem.; 65(2), 298–304.

Li, G.Q., Li, S.S., Qu, S.W., Liu, Q.K., Ma, T. et al (2008) Improved biodesulfurization of hydrodesulfurized diesel oil using Rhodococcus erythropolis and Gordonia sp. Biotechnol Lett 30, 1759–1762.

Li, F. L., Xu, P., Ma, Q. C., and Luo, L. L., Wang, X. S. (2003) Deep desulfurization of hydrodesulfurization-treated diesel oil by a facultative thermophilic bacterium Mycobacterium sp. X7B. FEMS Microbiology Letters 223, 301-307.

Maxwell, S., Yu, J. (2000) Selective desulfurization of DBT by a soil bacterium. Biochem. 35 551-556.

Mingfang, L., Jianmin, X., Zhongxuan, G., Huizhou, L., and Jiayong, C. (2003) Microbial desulfurization of DBT and 4,6- dimethyldibenzothiophene in dodecane and straight run diesel oil. Korean J. Chem.Eng. 20(4), 702-704.

Mohamed, M. E.,.Zakariya, H. A., and Vedakumar J. V. (2015) Biocatalytic desulfurization of thiophenic compounds and crude oil by newly isolated bacteria. Front Microbiol. 6, 112-124.

Mohebali, M. and Ball, A. S. (2008) Biocatalytic desulfurization (BDS) of petrodiesel fuels. *Microbiology* 154, 2169–2183.

Monticillo, D. J. (2000) Biodesulfurization and the upgrading of petroleum distillates. *Curr. Opin. Biotechnol.* 11, 540–546.

Nikel, P. I. Romero-Campero, F. J. Zeidman, J . A., Goñi-Moreno, Á., de Lorenzo, V. (2015) The Glycerol-Dependent Metabolic Persistence of *Pseudomonas putida* KT2440 Reflects the Regulatory Logic of the GlpR Repressor. The American Society for Microbiology, 6 (2).

Nuhu, A. (2013) Biocatalytic desulfurization of fossiel fuels: a mini review. Rev. Environ. Sci. Biotechnol.; 12, 9-23.

Ohshiro, T., and Izumi, Y. (1999) Microbial Desulfurization of Organic Sulfur Compounds in Petroleum, Bioscience, Biotechnology, and Biochemistry, 63 (1), 1-9.

Papizadeh, M., Ardakani, MR., Ebrahimipour, G. and Motamedi H. (2010) Utilization of dibenzothiophene as sulfur source by Microbacterium sp. NISOC-06. World J Microbiol Biotechnol 26, 1195–1200.

Rhee, S., Chang, J.H., Chang, Y.K. and Chang, H.N. (1998) Desulfurization of Dibenzothiophene and diesel oil by a newly isolated Gordona strain, CYKSI. Applied and Environmental Microbiology, 2327–2331.

Sadare, O. O., Obazu. F. and Daramola, M. O. (2017) Review Biodesulfurization of Petroleum Distillates—Current Status, Opportunities and Future Challenges Environments 4 (85), 1-20.

Samokhvalov, A. (2012) Desulfurization of Real and Model Liquid Fuels Using Light: Photocatalysis and Photochemistry.Journal of Catalysis Reviews Science and Engineering 54 (3), 281-343.

Tao, F., Yu, B., Xu, P. and Ma, C. (2006) Biodesulphurization in biphasic system containing organic solvents. Appl. Environ. Microb. 72, 4604-4609.

Talaiekhozani, A., Jafarzadeh, N., Fulazzaky, M. A., Talaie, M. R., and Beheshti, M. (2015) Kinetics of substrate utilization and bacterial growth of crude oil degraded by Pseudomonas aeruginosa, Journal of Environmental Health Science and Engineering 13, pp. 64.

World health organization (W.H.O) (2015) Global health observatory data repository. Geneva, Switzerland. Available online at http://www.teriin.org/projects/teddy/pdf/air-pollution-health-discussion-paper.pdf (Accessed on 28th, May 2018).

Chapter Nine

9.0 Performance of adsorptive desulfurization coupling biodesulfurization (AD/BDS) process for desulfurization of petroleum distillate

In this chapter, the results of evaluation of performance of adsorption coupling biodesulfurization (AD/BDS) system is presented. The kinetics governing adsorption this system is also reported.

9.1 Introduction

Adsorptive desulphurization (ADS) technique has been reported to be a promising approach in the removal of sulphur-containing compounds from petroleum distillates. It has a faster rate of reaction compared to biodesulfurization. However, biodesulfurization (BDS) converts the sulfur-containing compound in the petroleum distillate into a less harmful compound without altering the quality of the fuel. Therefore, BDS technique serves as a complimentary technique to other methods of desufurization. In other to achieve a less harmful compound in the prtroleum distillate rather than having the sulfur oxides in the fuel reduced, this chapter explores the hybrid system, namely ADS/BDS in the desulfurization of diesel.

Adsorption coulpling biodesulfurization (AD coupling BDS) has advantages of enhancing BDS selectivity and achieving high rate of adsorptive performance (Song et al., 2003; Zhang et al., 2008). Zhang et al. (2008) studied in-situ coupling desulfurization process by assembling nano γ-Al_2O_3, Na-Y molecular sieves, and active carbon onto the surface of *Pseudomonas delafieldii R-8*. Wang et al. (2015) also studied reactive ADS coupling aromatization on Ni/ZnO-$Zn_6Al_2O_9$, in order to achieve a higher adsorption performance. Furthermore, a novel study on reactive ADS of Ni/MnO adsorbent coulpling hydrodesulfurization was carried out by Tang et al, (2015). The results showed that, breakthrough time of the coupled process was 5 times longer than when real diesel desulfurizared using only ADS techcnique. Yitzhaki' and Aharoni (1987) also studied adsorption coupled with hydrogenation. Results showed that, Ni-Mo catalyst did not promote the

adsorption of the sulfur compounds, but inhibit cracking and other hydrocarbon reactions. The experiment was carried out at temperature of 650 K and pressure of 20 MPa. As far as it could be ascertained, no studies have been reported on AD coupling BDS process.

To study the performance of the AD coupling BDS system, the optimum operating parameters obtained from previous experiments as reported in previous chapters (chapter 7 and chapter 8) are used. Thus, in this chapter, the South African diesel samples (diesel obtained before HDS and diesel obtained after HDS) were desulfurized by AD coupling BDS system in a packed-bed column using immobilized activated carbon (AC) as adsorbent and BDS process using resting cells of *Pseudomonas Aeruginosa (PA).* DBT in South African diesel are present in different concentration, therefore for better understanding of the behavior of the process, effect of initial DBT concentrations was studied and reported in this chapter. It is essential to understand the behaviour of the ADS process and the kinetics that governs the biodegradation of the DBT in the real diesel samples. Thereofore, kinetics studies of the AD coupling BDS process were investigated as well. This new concept could pave the way for the development of a hybrid process involving the use of adsorption and biological techniques for the desulphurization of petroleum distillates worldwide, most especilally in South Africa.

9.2 Experimental

The materials used in this chapter for ADS, characterization, analytical techniques have been decribed in chapter three. Likewise, the growth of *Pseudomonas Aeruginosa Sp* used in this chapter are mentioned in chapter three. The preparation, regeneration of the immobilized adsorbent and the detailed experimental procedures of each technique were extensively discussed as well in chapter three (section 3.1.1 and 3.1.2). In addition, the experimental procedure for AD coupling BDS system was extensiveny discussed in chapter three (section 3.3). The schematic of the experimental procedure for desulfurization of South African real diesel is shown in Fig. 3.4.

9.3 Results and discussion

9.3.1 Performance evaluation of immobilized AC during desulfurization of real diesel

To understand adequately the performance immobilized AC for removal of DBT from real diesel in packed-bed column, effect of initial DBT concentration was investigated. Optimum operating conditions reported in chaper seven were used. The results obtained are hereby discussed.

Fig 9.1 depicts the effect of initial DBT concentrations on its removal from diesel after HDS onto an immobilized AC in a continuous packed-bed column. Since the concentration of DBT vary in real diesel, it is important to understand its effect on its adsorption in a column study. The initial concentration of diesel obtained after HDS and diesel obtained before HDS were varied from 40-120 mg/L. Other operating conditions such as bed height (15 cm) and flow rate (0.5 mL/min) remained constant at room temperature. The results show that breakthrough time decreased from 40 min to 10 min with increasing initial DBT concentration from 40 to 80 mg/L. This could be attributed to increase in DBT uptake rate, resulting into decrease in adsorption zone length. In addition, these results show that, the saturation rate and breakthrough time are affected by change in concentration gradient. The resident time experienced at higher initial concentration affected its solid-phase concentration which resulted into reduction in adsorption capacity even as the concentration increased. The same trend was observed in literature, by Han et al. (2007)

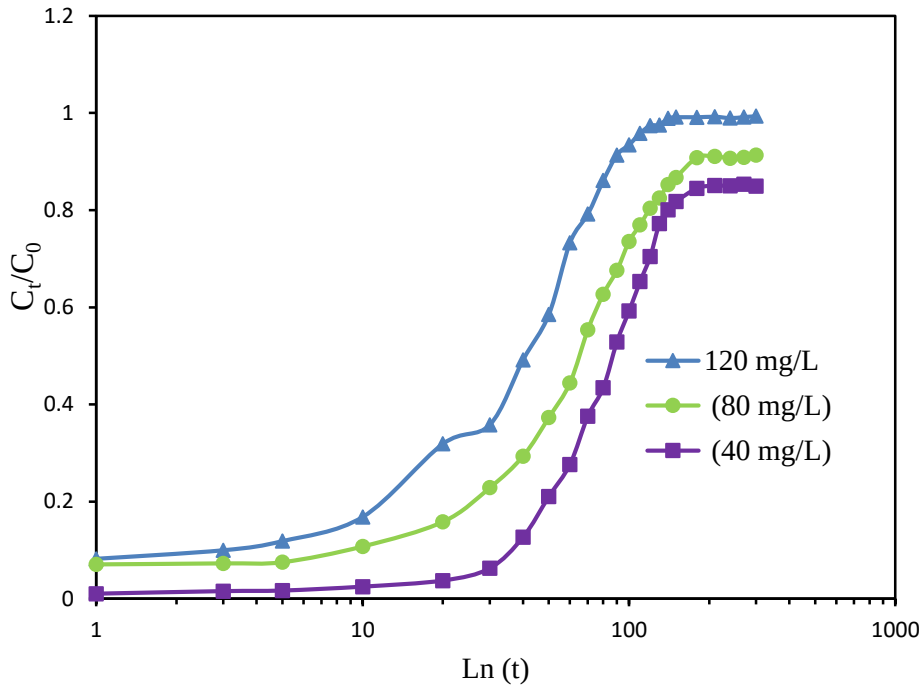


Figure 9.1 Breakthrough curve for desulfurization of diesel after HDS on AC in a packed-bed column, showing effect of initial concentration. Experimental conditions: Flow rate: 0.5 mL/min; Bed height: 15 cm.

Fig 9.2 depicts the effect of initial DBT concentration in diesel before HDS, on its adsorption onto an immobilized activated carbon in a continuous fixed bed column. Since the concentration of DBT vary in real diesel, it is important to understand its effect on its adsorption in a column study. The initial concentration of effluent diesel solution was varied from 80-120 mg/L. Other operating conditions such as bed heigh (15 cm) and flow rate (0.5 mL/min) remained constant. The result showed that breakthrough time decreased from 40 min to 5 min with increasing initial DBT concentration from 40 to 120 mg/L. This could be attributed to increase in DBT uptake rate, which result into decreased in adsorption zone length. Furthermore, these results show that the saturation rate of saturation and breakthrough time are affected by change in concentration gradient. The resident time experienced at higher initial concentration affected its solid-phase concentration which resulted into reduction in adsorption capacity even as the concentration increased. The same trend was observed in literature by Han et al. (2007) and Cao (2017)

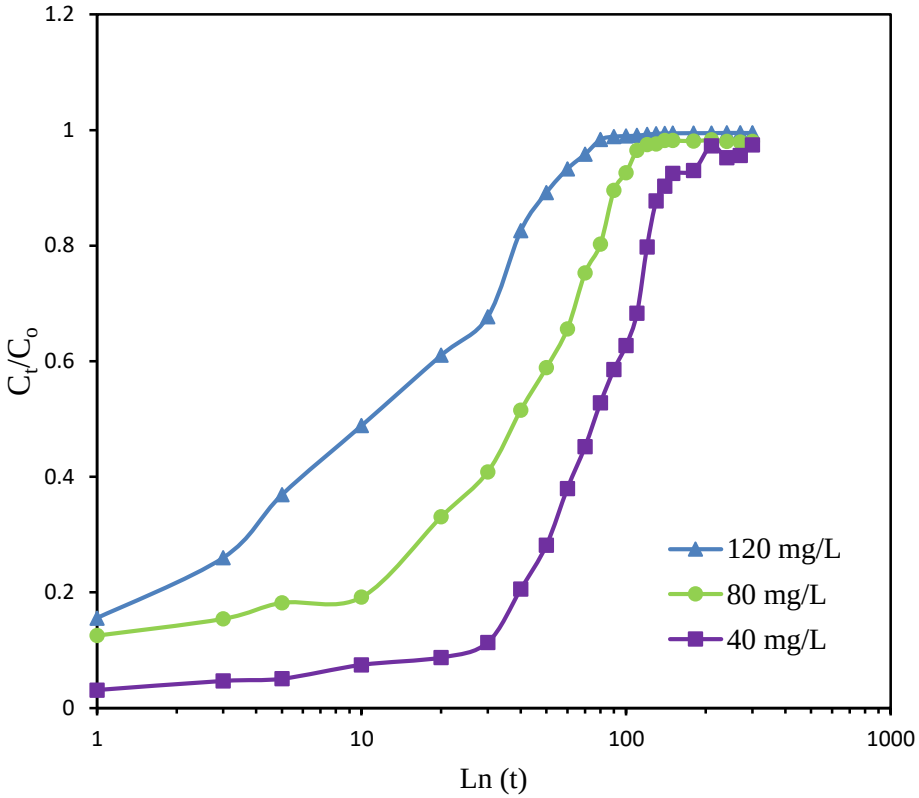


Figure 9.2 Breakthrough curve for desulfurization of diesel before HDS by immobilized activated carbon in a fixed bed column, showing effect of initial concentration. Experimental conditions: Flow rate: 0.5 mL/min; Bed height: 15 cm.

9.4 Adsorption kinetics study

Column modelling and determination of kinetic parameters were studied using Equations (3.16-3.18) in chapter three. In this study, three major models such as Bohart-Adams, Thomas, and Yoon-Nelson models were studied to describe the mechanism of the adsorption bed column. The Bohart-Adam model is used to descrie the initial part of the break through curve. The expression in Equation (3.19) is used to calculate the parameters of Bohart-Adaams model. The plot of $\ln(C_t/C_o)$ versus time yielded a linear graph with slope and intercept, from with the Boahrt-Adam constants K_{ab} and N_o can be calculated, respectively.

Table 9.1 shows the Bohart-Adam parameters for adsorption of DBT diesel after HDS in a fixed bed column by immobilized activated carbon. The operating conditions of the column experiment

for this section was limited to effect of initial sulfur concentration in the diesel. The Bohart-Adam model produces the initial part of the breakthrough curve for all the concentrations studied (Appendix C). Result showed that the maximum volumetric adsorption capacity, N_o were found to be 1.56, 3.42, 5.12 X 10^3 mL/mg.min for 40, 80 and 120 mg/L, respectively. This is showing increase in volumetric adsorption capacity as the inlet concentration of DBT increased. This result is similar to results obtained by other researchers studying different solute-adsorbate adsorption process. Result also showed that K_{ab} decreased from 1.7 to 1.16 x 10^{-4} mL/mg.min as the initial DBT concentration increased from 40-120 mg/L (Calero et al., 2009).

Table 9.1: Bohart Adam's kinetic parameters for desulfurization of diesel obtained after HDS in a packed-bed column.

Flow rate (ML/min)	**Bed depth (cm)**	**Initial conc.(mg/L)**	**K_{ab} X 10^4 (mL/mg/min)**	**N_o X 10^{-3} (g/L)**	**R^2**
0.5	15	40	1.70	1.56	0.5140
0.5	15	80	1.04	3.42	0.6266
0.5	15	120	1.16	5.12	0.6287

K_{ab} is Bohart-Adam's model constant, N_o is capacity of adsorption, R^2 is the coefficient of determination.

Table 9.2 shows the Bohart-Adam kinetic parameters for adsorption of DBT in diesel before HDS in a fixed bed column by immobilized activated carbon. The Bohart-Adam model produces the initial part of the breakthrough curve for all the concentrations studied (Appendix C). Results show that the maximum volumetric adsorption capacity, N_o was recorded to be 1.68, 3.21, 4.53 X 10^3 mL/mg.min for 40, 80 and 120 mg/L, respectively. This is showing an increase in volumetric adsorption capacity as the inlet concentration of the sulfur compound in the diesel increased. This result is similar to results obtained by other researchers studying different solute-adsorbate adsorption process. The result also showed K_{ab} values of 2.68, 0.75, 0.29 x 10^{-4} mL/mg.min at 40,

80 and 120 mg/L, respectively showing a decreased in K_{ab} as the initial DBT concentration increased from 40-120 mg/L. (Muzic et al., 2008; Han et al., 2009).

Table 9.2: Bohart-Adam Kinetic parameters for desulfurization of diesel obtained before HDS in a packed-bed column.

Flow rate (mL/min)	**Bed depth (cm)**	**Initial conc. (mg/L)**	**K_{ab} X 10^4 (mL/mg/min)**	**N_o X 10^{-3} (g/L)**	**R_2**
0.5	15	40	2.68	1.68	0.6626
0.5	15	80	0.75	3.21	0.5511
0.5	15	120	0.29	4.53	0.3728

K_{ab} is Bohart-Adam's model constant, N_o is capacity of adsorption, R^2 is the coefficient of determination.

The expression for Thomas model is given in Equation 3.20, where a plot of $\ln\left(\frac{C_o}{C_t} - 1\right)$ against time yields a linear graph. The values of K_{Th} and q_o were calculated from intercept and slope of the graph (Apendix C), using a linear regression analysis.

Table 9.3 shows the parameters of Thomas model for adsorption of DBT in diesel after HDS in a continuous fixed bed column. It could be observed that, Thomas constant values were calculated to be 5.53, 2.25, 2.23 x 10^{-4} mL/mg.min at 40, 80 amd 120 mg/L. This shows that the values of K_{TH} constants decreased with with increasing initial sulfur concentration. The q_o was also observed to initially increased from 0.063, 0.085 as the DBT concentration in the influent concentration increased from 40 to 80 mg/L. However, further increase in the initial sulfur concentration in the inlet diesel sample decreased the adsorption capacity to 0.051 mg/L. This could be as a result of the adsorption zone being rapidly saturated at higher initial of DBT solution into the bed column which resulted in shorter breakthrough time. In addition, shorter resident time was experienced by the column at higher initial DBT concentration which affected the solid-phase concentration

resulting into lower adsorption capacity at higher concentrations. The result is in agreement to reslt reported by Han et al. (2007) and Patil et al. (2012).

Table 9.3: Thomas' kinetic parameter for desulfurization of diesel obtained after HDS in packed-bed column.

Flow rate (mL/min)	**Bed depth (cm)**	**Initial conc. (mg/L)**	**K_{Th} X 10^{-4}(mL/mg/min)**	**q_o (mg/g)**	**R^2**
0.5	15	40	5.53	0.063	0.7640
0.5	15	80	2.25	0.085	0.8118
0.5	15	120	2.23	0.051	0.8166

K_{th} is Thomas' model constant, q_o is the adsorption capacity and R^2 is the coefficient of determination.

Table 9.4 shows the parameters of Thomas model for desulfurization of diesel obtained before HDS in a fpacked-bed column. It could be observed that, Thomas constant values were calculated to be 6.18, 2.76, 1.91 x 10^{-4} mL/mg.min at 40, 80 amd 120 mg/L, respectively. This shows that the values of K_{TH} constants decreased with with increasing initial sulfur concentration. The q_o was also observed to initially increased from 0.046, 0.072 as the DBT concentration in the influent concentration increased from 40 to 80 mg/L. However, further increase in the initial sulfur concentration (120 mg/L) in the inlet diesel sample decreased the adsorption capacity to 0.047 mg/L. This could be as a result of the adsorption zone being rapidly saturated at higher initial of DBT solution into the bed column which resulted in shorter break through time. In addition, shorter resident time was experienced by the column at higher initial DBT concentration which affected the solid-phase concentration resulting into lower adsorption capacity at higher concentrations. The same trend was obtained in Han et al. (2007) and Muzic et al. (2008). Results show that adsorption capacity for diesel obtained after HDS at different initial concentrations were higher than that of the diesel obtained before HDS. This could be attributed to early saturation of the

vacant adsorption sites on the immobilized AC adsorbent due to the presence of other organic compounds in disel before HDS. Previous hydrodesulfurization of diesel obtained after HDS could be the reason why its adsorption capacities at all initial DBT concentrations were higher than that of diesel obtained before HDS.

Table 9.4: Thomas' kinetic parameter for desulfurization of diesel before HDS in packed-bed column.

Flow rate (mL/min)	Bed depth (cm)	Initial conc. (mg/L)	K_{Th} X 10^{-4} (mL/mg/min)	q_o (mg/g)	R^2
0.5	15	40	6.18	0.046	0.8870
0.5	15	80	2.76	0.072	0.7607
0.5	15	120	1.91	0.047	0.6928

K_{th} is Thomas' model constant, q_o is the adsorption capacity and R^2 is the coefficient of determination.

The linearized form of Yoon-Nelson model equation was expressed in Equation (3.21) in chapter 3 of this thesis. Table 9.5 shows the Yoon-Nelson's kinetic parameters for adsorption of DBT in diesel obtained after HDS onto immobilized AC in a continuous packed-bed column. The results show that the τ_{mod} values recorded according to Yoon-Nelson's kinetic model are; 129.46, 85.07 and 34.10 min at different initial sulfur concentrations of 40, 80 and 120 mL/min, respectively are not close to the τ_{expt} values as obtained from the experiment 87, 65 and 41 min for initial DBT concentration of 40, 80 and 120 mg/L, respectively. K_{YN} values are found to decrease from 0.0221 to 0.0189 min^{-1} as the concentration increased from 40 mg/L to 80 mg/L, respectively.

Table 9.5: Yoon-Nelson's kinetic parameter for desulfurization of diesel obtained after HDS in packed-bed column.

Flow rate (mL/min)	Bed depth (cm)	Initial concentration (mg/L)	Kyn (min^{-1})	τ (min)	R^2
0.5	15	40	0.0221	129.46	0.7640
0.5	15	80	0.0180	85.07	0.8118
0.5	15	120	0.0268	34.10	0.8166

K_{YN} is Yoon-Nelson's model constant, τ predicted breakthrough time and R^2 is the coefficient of determination.

Table 9.6 shows the Yoon-Nelson's kinetic parameters for adsorption of DBT in diesel obtained before HDS onto immobilized AC in a continuous packed-bed column. The results show that the τ_{mod} values recorded according to Yoon-Nelson's kinetic model were calculated to be 93.43, 27.95, 32.17 min at different initial sulfur concentrations of 40, 80 and 120 mL/min, respectively. This showed a wide variation with τ_{expt} values as obtained from the experiment 78, 39 and 11 min for initial DBT concentration of 40, 80 and 120 mg/L, respectively. K_{YN} values are found to decrease from 0.02219 to 0.0227 min^{-1} as the concentration increased from 40 mg/L to 80 mg/L, respectively.

Table 9.6: Yoon-Nelson kinetic parameter for desulfurization of diesel obtained before HDS in packed-bed column.

Flow rate (mL/min)	Bed depth (cm)	Initial conc. (mg/L)	Kyn (min^{-1})	τ (min)	R^2
0.5	15	40	0.0229	93.43	0.8870
0.5	15	80	0.0247	27.95	0.7607
0.5	15	120	0.0229	32.17	0.6928

Adsorption column capacity and breakthrough capacity for desulfurization of DBT in diesel obtained after HDS in a continuous packed-bed column were evaluated. Table 9.7 and 9.8 show the values of adsorption column capacities and breakthrough capacities for diesel obtained after HDS and diesel obtained before HDS, respectively. In Fig 9.7, results show that breakthrough time decreased from 40 to 10 min with increasing initial feed concentration from 40 to 120 mg/L This could be attributed the saturation rate of the adsorbent at higher initial DBT concentration. In addition, the vacant adsorption sites of the adsorbent were rapidly filled up by the DBT molecule resulting in faster saturation of the adsorption zone of the adsorbent. These results are comparable to literature (Xia et al., 2009; Patil et al., 2012).

The amount, q_{total} of DBT molecule sent into the bed column decreased from 0.91 to 1.04 g as the initial sulphur concentration in the diesel obtained after HDS increased from 40 to 80 mg/L, as can be seen in Table 9.7. Further increase from 80 to 120 mg/L decreased the adsorption capacity to 0.119 mg/g. This is because as the initial sulphur concentration increased the adsorption zone is rapidly saturated. The breakthrough time is also observed to be shortened. This has a negative effect on the adsorption capacity of the adsorbent. The same trend was observed for diesel obtained before HDS in Table 9.8. This is in agreement with the results reported by Xia et al., 2009, Patil et al. 2012 and Cao, 2017.

Table 9.7: Adorption column and breakthrough capacity parameters for desulfurization of DBT in SA diesel after HDS in a continuous fixed bed column

Initial conc (mg/L)	Bed depth (cm)	flow rate (mL/min)	Q_B (mg/g)	q_{total} (g)	q_e (mg/g)	t_b (min)
40	15	0.5	19.51	0.91	0.152	40
80	15	0.5	19.51	1.04	0.087	20
120	15	0.5	14.63	0.119	0.006	10

Q_B is the breakthrough capacity, qtotal is the total amount of adsorbate sent into the packed-bed column, q_e is the amount of DBT adsorbed at equilibrium and t_b is the breakthrough time.

Table 9.8: Adorption column and breakthrough capacity parameters for desulfurization of DBT in diesel obtained before HDS in a continuous packed-bed column

Initial conc (mg/L)	Bed depth (cm)	flow rate (mL/min)	Q_B	q_{total}	q_e	t_b
40	15	0.5	19.51	0.155	0.077	40
80	15	0.5	19.51	0.233	0.019	20
120	15	0.5	27.27	0.089	0.0049	5

9.5 Regeneration of spent Adsorbent in a packed-bed column

Fig. 9.3 depicts the breakthrough curve of reference experiment and regenerated-spent adsorbents at three different adsorption-desorption cycles at the same experimental conditions. Table 9.9 shows the breakthrough uptake, breakthrough time, exhaustion time and the % DBT removal from the immobilized AC with reference to the first experiment (Ref. expt). The results show that adsorption capacity of the adsorbent decreased as the adsorbents are been re-used, which resulted into early breakthrough for the re-used adsorbents. In addition, it could be observed that the percentage DBT removal also decreased as the adsorbent is been re-used from 1st cycle (64.08 %) to the 3rd cycle (20.96 %). The exhaustion time and breakthrough capacity at 50 % breakthrough time also decreased after each cycle (See Table 9.9). This could be as a result of unavailable adsorption sites on the surface of the adsorbents after each cycle. The results obtained in this study is in agreement with results reported by Li et al. (2001) and Chowdhury et al. (2015)

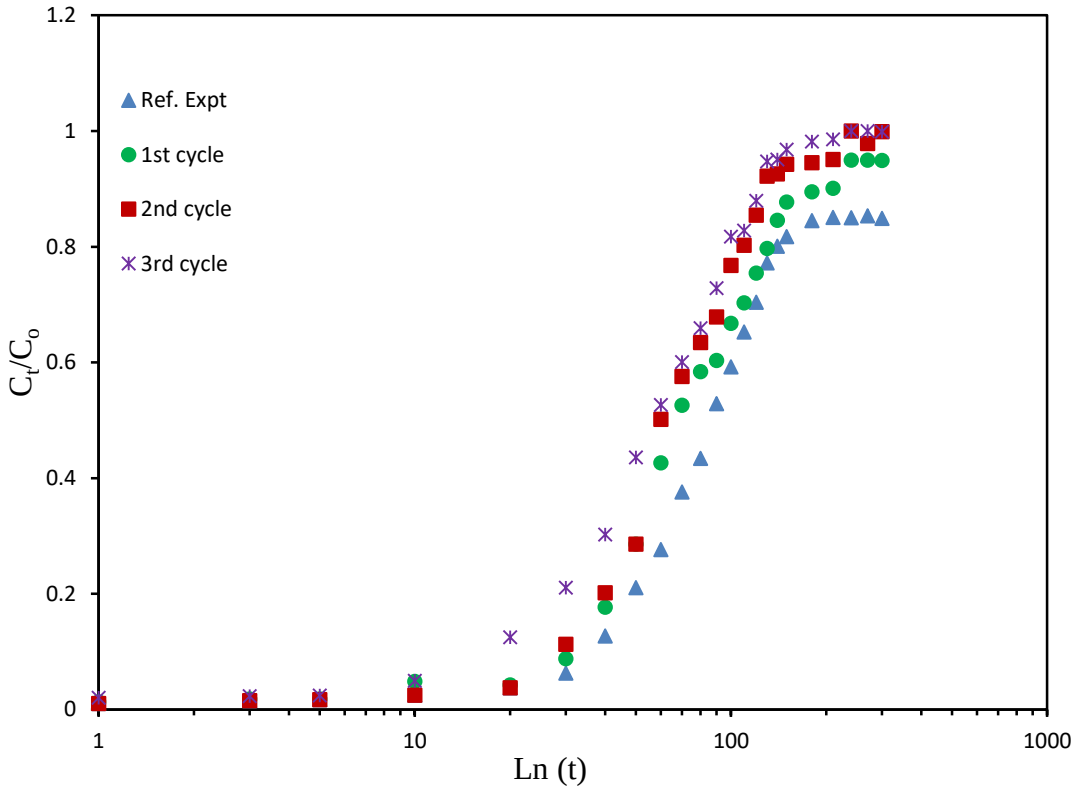


Figure 9.3. Regeneration of spent adsorbent using diesel obtained after HDS. Experimental conditions: Flow rate: 0.5 mL/min; Bed height: 15 cm; Initial Concentration: 40mg/L.

Table 9.9: Regeneration of spent immobilized AC

Cycle No.	Breakthrough uptake (mg/g)	Breakthrough time (min)	Exhaustion time (min)	% SR
Ref Expt	0.155	87	180	Original
1st cycle	0.099	68	150	64.08
2nd cycle	0.055	60	130	35.48
3rd cycle	0.033	57	120	20.96

SR: Sulfur (DBT) removal

9.6 Biodesulfurization of adsorptive-desulfurized real diesel samples

The detailed experimental procedure was decribed in chapter three. The operating conditions are, initial DBT concentration 10 mg/L, temperature 37 ^{o}C, time 8h at 130 rpm and 5 mL of resting cell of *Pseudomonas putida* suspended in glycerol/Nacl. Fig. 10.4 (a) depicts the growth of bacteria and biodesulfurization of South African diesel obtained after HDS and Fig. 10.4 (b) depicts the chromatogram of SA diesel obtained after HDS after complete desulfurization by AD/BDS hybrid process. Results show that desulfurization of DBT occurred gradually and at the same time there was formation of 2-HBP. It could also be observed that as the bacteria grows, there was degradation of DBT. This is an indication that DBT was used up by the bacteria as its only source of carbon. Furthermore, it was discovered that growth stopped before the final or complete desulfurization of the DBT. This could be attributed to accumulation of 4S compounds in the medium which inhibited the further growth of the cells at 5 h as a result of inhibition effect. This is in agreement with the result of Maxwell et al. (2000). Other products of 4S pathway were not detected (no data is provided due to negligible amount of other 4s-pathways products detected), except 2-HBP that was quantifiable. Other authors also confirmed that, other metabolites of 4S pathway could not be detected in the experiment. However, they are indicated as postulated metabolites (Maxwell et al., 2000). About 99.9 % degradation was achieved on 10 mg/L South African diesel obtained after HDS, with 81.3 % yield for 2-HBP (see Figure 10.4 b). The degree of desulfurization was found to be 20.08 gDCW/L.h while the conversion rate was 13.17 L/g DCW.h. This result showed that adsorption coupled with biodesulfurization (AD/BDS) is a perfect system for reducing the amount of DBT in South African petroleum distillate. Biodeslfurization could serve as suplimentary process for desulfurization in the refineries. This will enable the refineries to meet up with the stringent regulation on emission of sulfur compounds during combustion of diesel into the atmosphere.

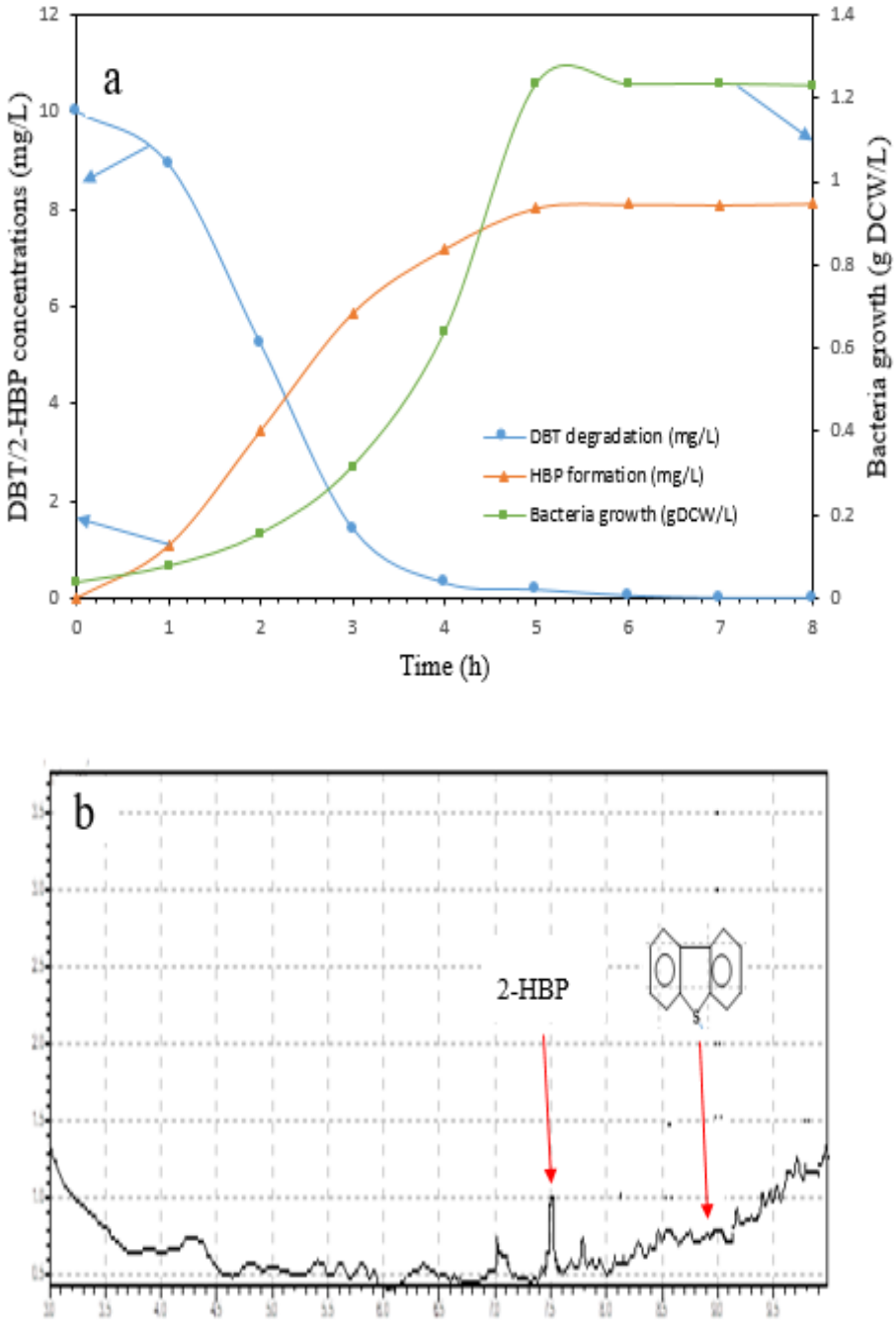
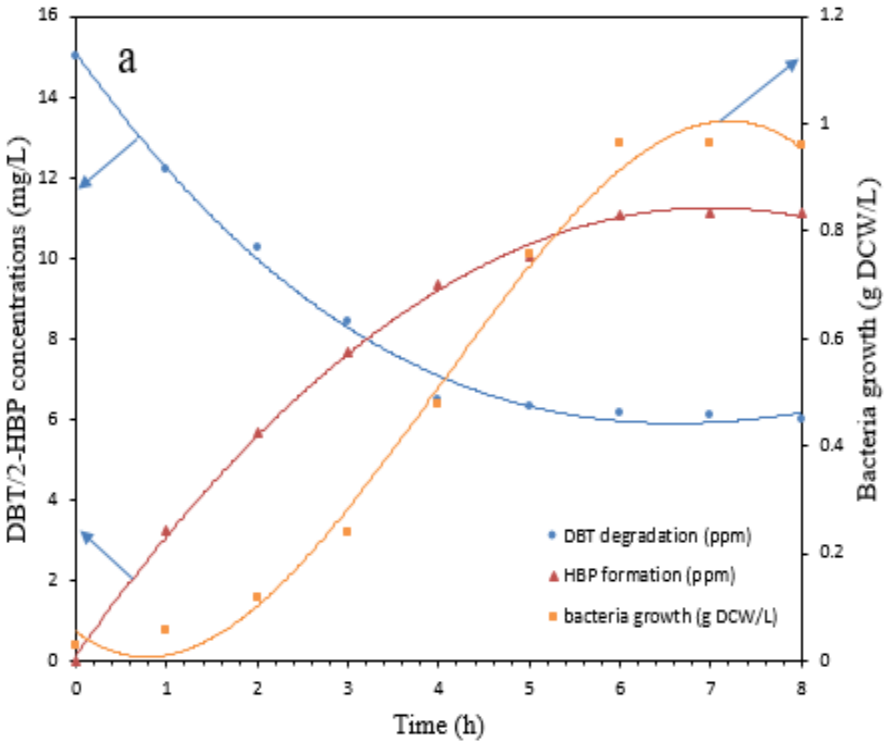


Figure 9.4 (a) Degradation of adsorptive-desulfurized diesel obtained after HDS from adsorption bed coulumn (AD coupling BDS system) by resting cell of *PA* (b) Chromatogram of diesel obtained after HDS, after complete desulfurization by AD/BDS hybrid process. Experimental conditions: Initial DBT concentration: 10 mg/L; Temperature: 37 ^{o}C.

Fig. 9.5 (a) depicts the growth of bacteria and BDS of diesel obtained before HDS and Fig. 9.5 (b) depicts the chromatogram of diesel obtained before HDS, after complete desulfurization by AD/BDS hybrid process. Results show that desulfurization of DBT occurred gradually and at the same time there was formation of 2-HBP. It could also be observed that as the bacteria grows, there was degradation of DBT. This is an indication that DBT was used up by the bacteria as its source of sulfur. Furthermore, it was discovered that growth stopped before the final or complete desulfurization of the DBT. This could be as a result of accumulation of 4S compounds in the medium which inhibited the further growth of the cells at 6 h as a result of inhibition effect. This is in agreement with the result of Maxwell et al. (2000). Other products of 4S pathway were not detected (no data provided due to negligible amount of other 4S-pathway products detected), except 2-HBP that was quantifiable (see Fig. 9.5 b). Other authors also confirmed that, other metabolites of 4S pathway could not be detected in the experiment. However, they are indicated as postulated metabolites (Maxwell et al., 2000). About 65.73 % degradation was achieved on 15 mg/L diesel obtained before HDS, with 34.27 % yield for 2-HBP. The degree of desulfurization was found to be 4.34 gDCW/L.h while the conversion rate was 7.47 L/g DCW.h. This results show that adsorption coupling biodesulfurization (AD/BDS) system is perfect process for reducing the amount of DBT in South African petroleum distillate. BDS could serve as suplimentary technique for desulfurization in the refineries. This could enable the refineries to meet up with the stringent regulation on emission of sulfur compounds during combustion of diesel.

Comparing the AD coupling BDS process results of diesel obtained after HDS and diesel obtained before HDS, it could be observed degradation rate was lower for diesel obtained before HDS at 7.47 L/g DCW.h compared to diesel obtained after HDS with degradation rate of 20.08 gDCW/L.h. The ADS/BDS efficiency of diesel obtained after HDS was higher than diesel obtained before HDS. The lower percentage of degradation of DBT in diesel before HDS by AD/BDS coupling process could be as a result of many organic components that were present in the sample. This hindered the selectivity of DBT for biodegradation.



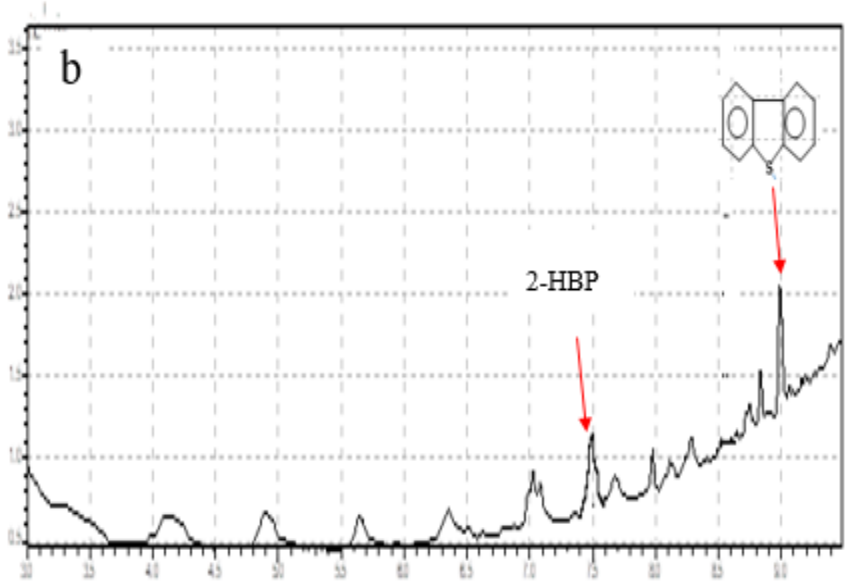


Figure 9.5 (a) Degradation of AD-desulfurized diesel obtained before HDS (AD/BDS coupling process) using resting cell of PA. (b) Chromatogram of diesel obtained before HDS, after complete desulfurization by AD/BDS hybrid process Experimental conditions: Initial DBT concentration: 10 mg/L; Temperature: 37 ^{o}C.

Fig. 9.6 shows the detection of elution time of DBT compound by a pre-calibrated GC/MS. This was found to be at around 9 minutes. Fig. 9.7 depicts the chromatogram of diesel obtained before HDS. Fig. 9.8 shows the chromatogram of diesel obtained after HDS. It could be observed that there are lesser organic components compared to the chromatogram of diesel obtained before HDS with many organic components (Fig 9.7). The lower components in the diesel obtained after HDS could be as a result of HDS process that this sample has undergone. The peak area of DBT at 9 minutes elution time (Fig. 9.8) was also observed to be lower than that of the non-desulfurized diesel sample in Fig (9.7). This showed that pre-HDS of diesel reduced the amount of DBT in it, although not completely.

Fig 9.7 show that there was no 2-HBP compound in the diesel before biodesulfurization. Fig 9.9 is the microgram of diesel sample after biodesulfurization with detection of 2-HBP. This is a confirmation that biodesulfurization followed 4S- pathway.

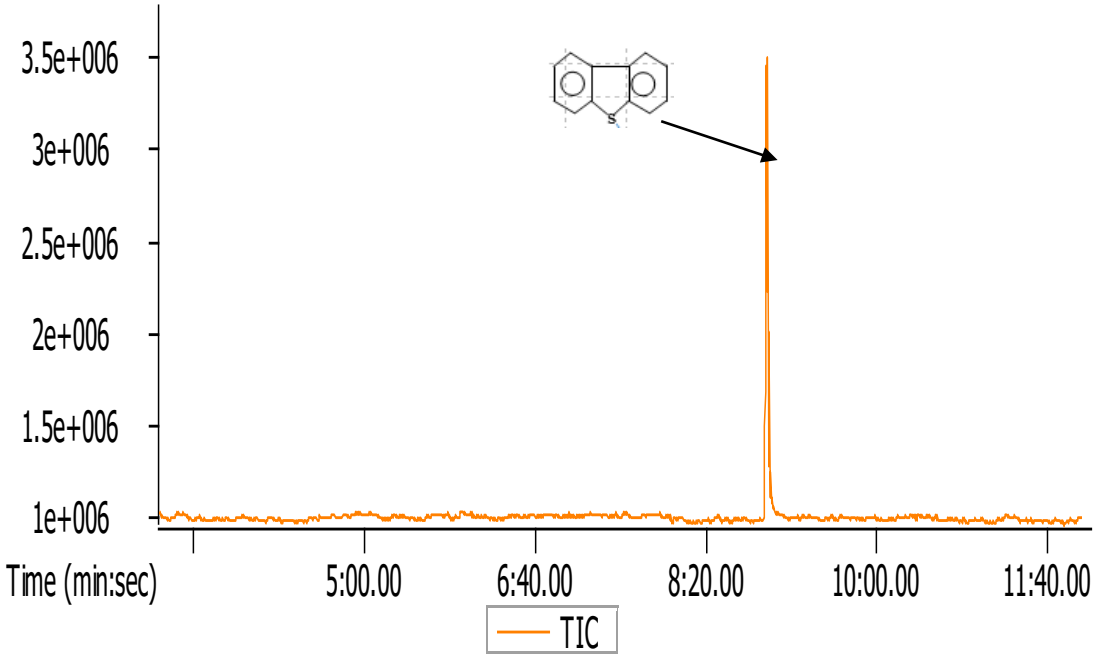


Figure 9.6. Detection of peak of DBT in a pre-calibrated GC/MS

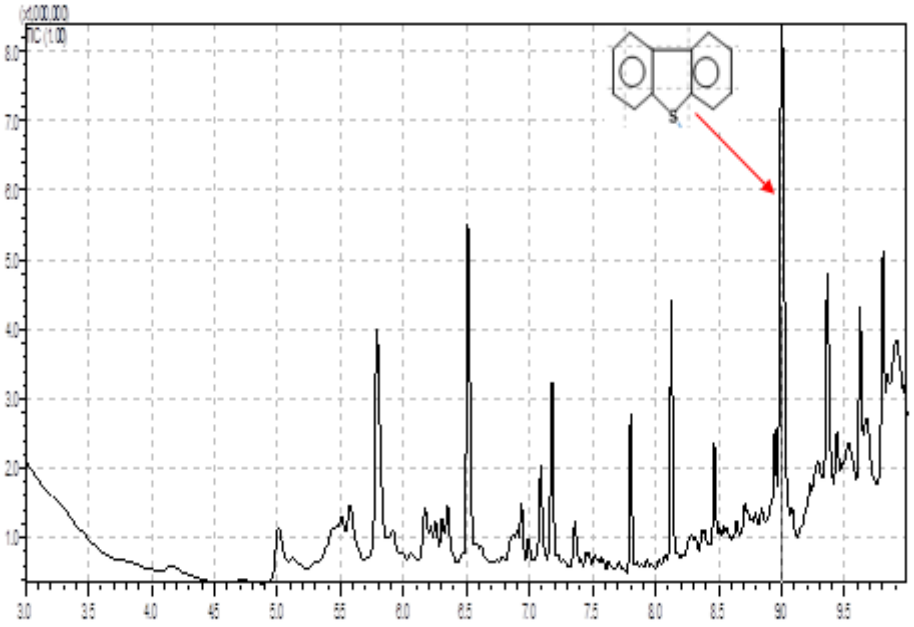


Figure 9.7. Chromatogram of diesel sample obtained before HDS

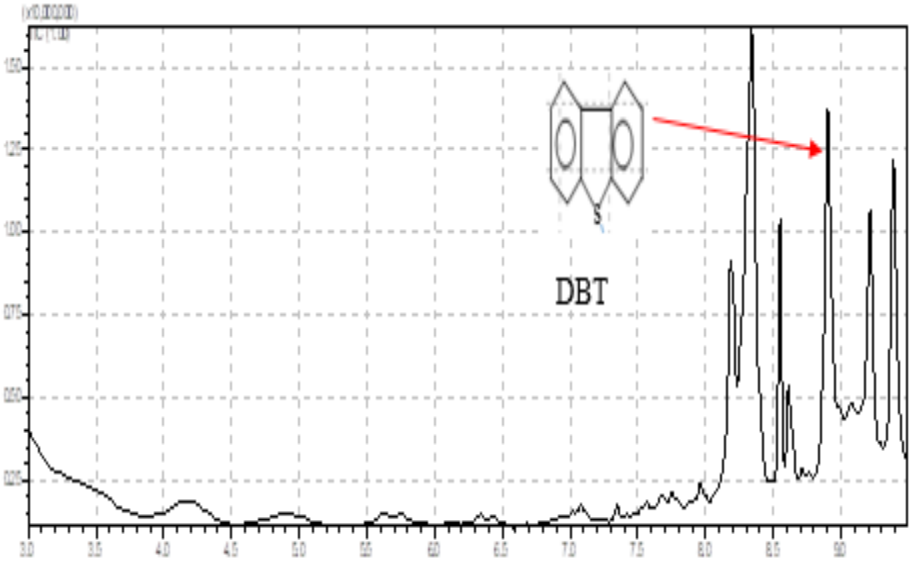


Figure 9.8. Chromatogram of diesel sample obtained after HDS

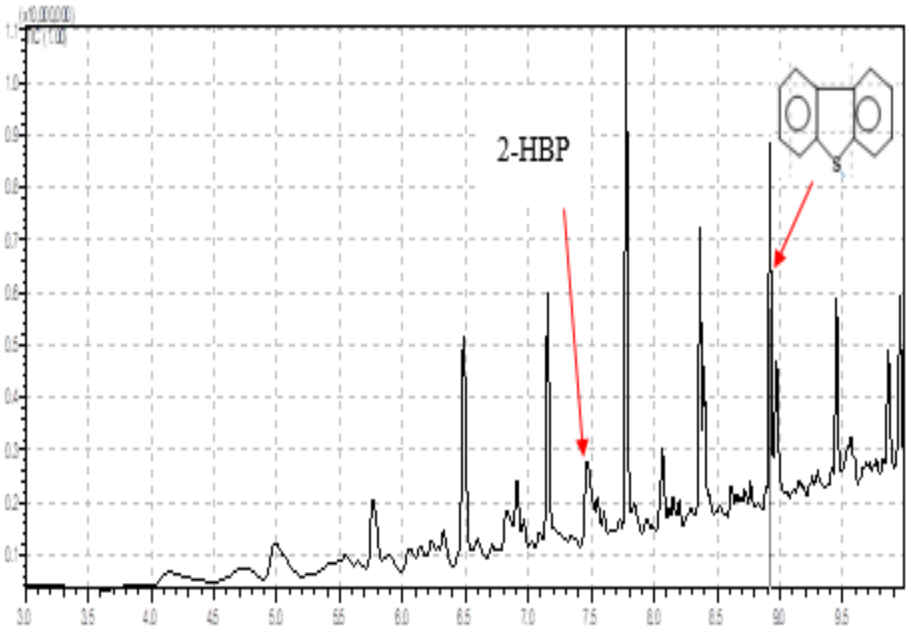


Figure 9.9. Chromatogram of biodesulfurized of diesel before HDS with the d etection of 4S-pathway (2-HBP)

Biodesulfurization capacity (X_{BDS}), Conversion yield for DBT (Y_{BDS}), degree of desulfurization (D_{BDS}) during growing cell and specific conversion rate (E) were evaluated using Equation (3.22 - 3.34) in chapter three of this thesis. Table 9.10 shows the parameters obtainded for biodesulfurization capacity (X_{BDS}), Conversion yield for DBT (Y_{BDS}), degree of desulfurization (D_{BDS}) during growing cell and specific conversion rate (E) during ADS/BDS coupling process for desulfurization of diesel obtained after HDS and diesel obtained before HDS at the same initial DBT concentration. The results show that biodesulfurization capacity (81.3 %), conversion yield (99.9 %), degree of desulfurization (20.08 gDCW/L.h) and specific converaion rate (13.17 L/g DCW/L.h) of diesel obtained after HDS are higher than diesel obtained before HDS (74.27 %, 93 %, 11.94 gDCW/L and 12.83 L/gDCW.h, respectively). The lower values of dieselobtained before HDS compared to diesel obtained after HDS could be as a result of other organic sulfur compounds present in it.

Table 9. 10: X_{BDS}, Y_{BDS}, D_{BDS} and E parameters for BDS of diesel obtained after HDS and diesel obtained before HDS by resting cell of *PA* at the same initial concentrations of 10 mg/L.

	Diesel obtained after HDS	**Diesel obtained before HDS**
X_{BDS} (%)	81.30	74.27
Y_{BDS} (%)	99.90	93.00
D_{BDS} (g DCW/L.h)	20.08	11.94
E (L/g DCW.h)	13.17	12.83

X_{BDS}: Biodesulfurization capacity; Y_{BDS}: Conversion yield for DBT; D_{BDS}: Degree of desulfurization; E: Specific conversion rate

It is important to consider the percentage of DBT removed from South African diesel obtained after HDS by individual process, results show that adsorption desulfurization process contributed to about 91.67 % DBT removal, while BDS contributed to about 8.33 % DBT removal in the overall desulfurization. It can therefore be concluded that BDS could serve as a complimentary process rather than the main process for desulfurization of sulfur compounds in petroleum distillate.

9.7 Kinetics of degradation of diesel during biodesulfurization

First order kinetic model was employed to describe the bacterial degradation of DBT in South African diesel samples, using the expression in Equation (3.27). Fig. 9.10 depicts the First order kinetic model for degradation of DBT from (a) South African diesel obtained before HDS and (b) diesel obtained after HDS. The results show that the first order constants are 0.1175 h^{-1} and 0.3003 h^{-1} for diesel obtained after HDS and diesel obtained before HDS samples, respectively. The model described well the degradation of diesel samples by the bacteria. The model parameters perfectly fitted into the experimental data. The first order model fitted perfectly well into experimental data of diesel obtained after HDS than it did for diesel obtained before HDS (Talaiekhozani1 et al., 2015).

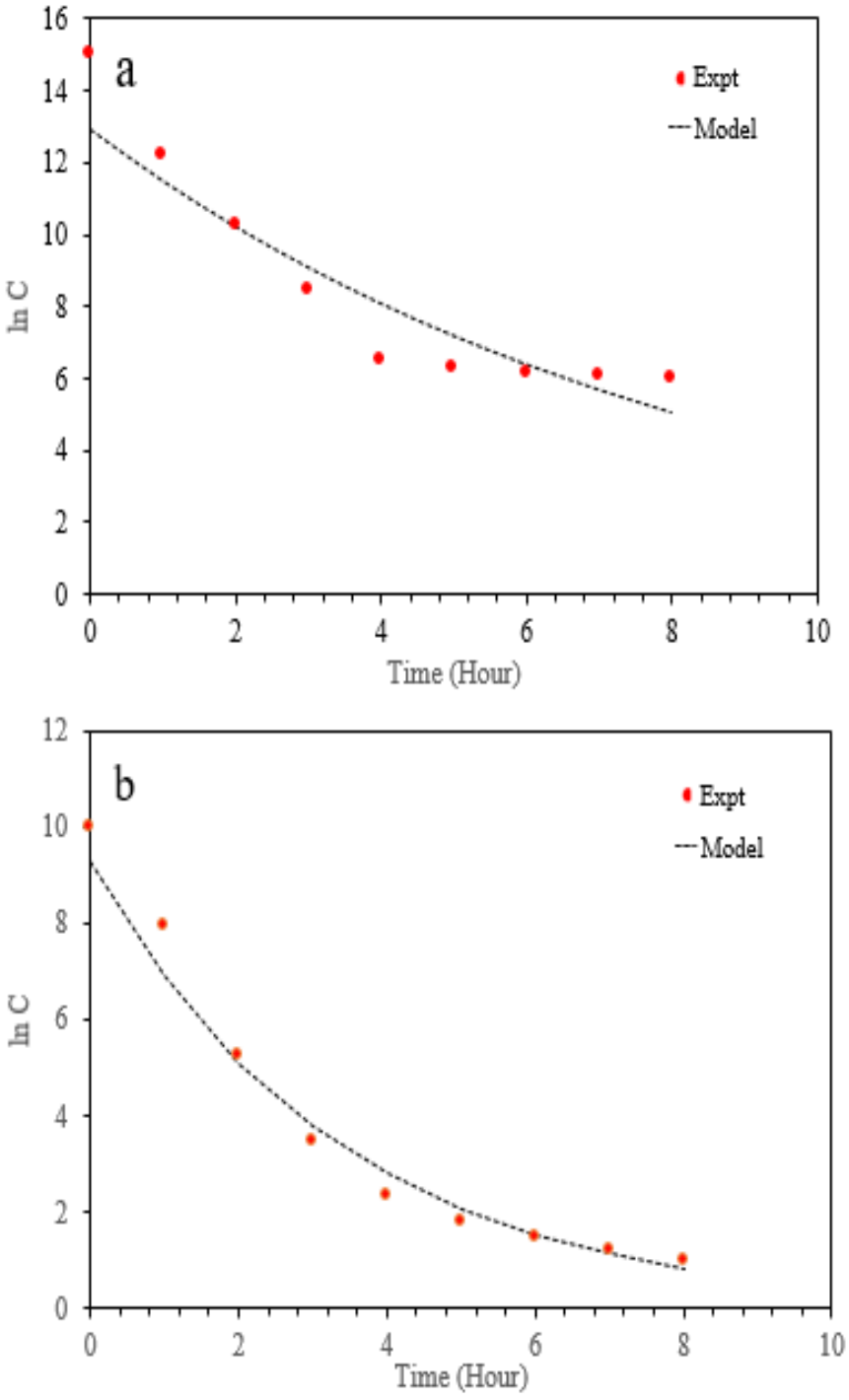


Figure 9.10. First order kinetic model for degradation of sulfur compound in (a) diesel obtained before HDS and (b) diesel obtained after HDS using *PA*. Experimental conditions: Initial DBT concentration: 10 mg/L; Temperature: 37 ºC.

Results of AD/BDS coupling process are comparable with literature. Zhang et al. (2008) studied in-situ coupling desulfurization technique by assembling nano γ-Al_2O_3, Na-Y molecular sieves, and active carbon onto the surface of Pseudomonas delafieldii R-8. Wang et al. (2015) also studied reactive adsorption desulfurization coupling aromatization on Ni/ZnO-$Zn_6Al_2O_9$, in order to achieve a higher adsorption performance. Furthermore, a novel study on reactive adsorption desulfurization Ni/MnO adsorbent coulpling hydrodesulfurization was carried out by Tang et al., (2015). The results showed that, breakthrough time of the coupled technique was 5 times longer than when real diesel without hydrodesulfurization technique was not coupled with adsorption technique. Yitzhaki' and Aharoni (1987) also studied adsorption coupled with hydrogenation. Results showed that, Ni-Mo catalyst did not promote the adsorption of the sulfur compounds, but inhibit cracking and other hydrocarbon reactions. The experiment was carried out at temperature of 650 K and pressure of 20 MPa. However, in this study the experiments were performed under moderate temperature and atmospheric pressure. The results show complete (99.9 %) desulfurization of the sulfur-containing compound in the real diesel.

9.8. Concluding remarks

As it has been demostrated in this chapter, adsorption coupling biodesulfurization technique (AD/BDS) was used to remove sulfur compound from two different South African diesel samples. The diesel was first transferred to a bed column filled with immobilized adsorbent, and then the desulfurized diesel was transferred into the bacteria basal medium consisting of resting cells of *Pseudomonas aeruginosa* for complete degradation. The bed column experiment showed that superficial velocity increased in the order 0.031, 0.063, 0.094 m/min, with increasing flow rate at 0.5, 1.0 and 1.5 mL /min. Result showed that adsorption of DBT in a fixed bed column is dependet on superficial velocity of the sorbate solution through the adsorption column. The best result was obtained at the lowest superficial velocity of 0.031 m/min (0.5 mL /min) at 15 cm bed height and lowest initial DBT concentration of 120 mg/L. Furthermore, breakthrough time was found to increase with decreasing DBT initial concentration, decreasing flow rate and increasing bed height. Increasing the superficial velocity of the DBT solution decreased the breakthrough time needed

for the contact of adsoebate solution with the adsorbent in the bed column resulting in decreased amount of DBT adsorbed by the immobilized adsorbent. This means that, a longer breakthrough time is needed for higher performance of the bed column which will successively result in higher adsorption capacity. The adsorption capacities of the adsorbent were found to bw 0.152, 0.087, 0.006 mg/g, decreasing with increasing initial sulphur concentration in SA diesel before HDS sample from 40, 80, 120 mg/L. Adsorpton capacities for diesel obtained after HDS were found to be 0.077, 0.019, 0.0049 mg/g as the initial concentration increased at 40, 80 and 120 mg/L. The adsorption capacities of the adsorbents were founs to be very low, this may be attributed to the minimum amount of activated carbon that the sodium algilate could entrap. Only a small amount of adsorbent was immobilized by the algilate. Therefore, more studies are needed to increase the ratio of activated carbon to sodium algilate and study the influence of algilate ratio on the performance of an immobilized activated carbon in a packed-bed column experiment. At all experimental conditions investigated, Adam-Bohart model described well the initial region of the breakthrough curve, while Thomas models described the the transient stage or working stage of the breakthrough curve.

In the biodesulfurization experiment, the result showed that the resting cells of the bacteria were able to degrade completely the DBT compound in the South African hydrodesulfurizer outlet diesel (diesel obtained after HDS) at initial sulfur (DBT) concentration of 10 mg/L after 8 h of reaction. The results in this study show that *Pseudomonas Aeruginosa* was able to desulfurize sulfur compound in real diesel (DBT) into less harmful compound, 2- HBP. However, further studies are needed to determine their desulfurization capability for other sulfur organic compounds in real diesel.

The final product 2-HBP detected shows the specific activity of DBT desulfurization is 4S – pathway. However, more investigations are still required in this field to detect all the various metabolites in the 4S pathway. In addition, introduction of sufficient oxygen could improve the biodesulfurization performance of these bacteria cells.

First-order kinetic model was employed for DBT desulfurization in SA diesel samples. The model fitted with the experimental data. This is an indication that first order kinetic can be used to describe the microbial degradation of DBT in SA diesel samples.

The result obtained in this study showed that biodesulfurization could be a better technique to compliment HDS technique rather than the main technique for desulfurization of organo-sulfur compounds in diesel oil.

In conclusion, *Pseudomonas aeruginosa* and *Pseudomonas putida* could be better catalysts for desulfurizing harmful sulfur compound in South African diesel. This will assist the refineries to meet up with the stringent regulation to minimize the emission of sulfur compounds which cause environmental pollution and health problems in South Africa and all over the world.

In order to share the novel contribution of this work with the scientific community one paper has been submitted to an international reputable journal for possible publication (Biochemical Engineering Journals).

9.9. References

Adeyi, A., Aberuaga, F. (2012) Comparative analysis of adsorptive desulfurization of crude oil by manganese dioxide and zinc oxide, *Research Journal of Chemical Sciences*, 8 (*2*), 14-20.

Ahmed, J. and Ahmaruzzaman, M. (2015) "Adsorptive desulfurization of feed diesel using chemically impregnated coconut coir waste" *Int. J. Environ. Sci. Technol. 2* (9), 2847–2856

Alavi, S. A. and Hashemi, S. R. (2014) A Review on Diesel Fuel Desulfurization by Adsorption Process. International Conference on Chemical, Agricultural, and Biological Sciences (ICCABS'2014). pp. 9-10.

Auta, M. (2012) Fixed bed adsorption studies of Rhodamine B dye using oil palm empty fruits bunch activated carbon. Journal of Engineering Research and Studies. 3 (3), 03-06

Bhattachryulu, Y. C., Patil, M. and Kamble, S. (2012) Unsteady state adsorption – Column studies. International Journal of Advanced Engineering Research and Studies, *1* (I1), 179– 184.

Calero, M., Hernainz, F., Blazquez, G., Tenorio, G. and Martin-Lara, M.A. (2009) Study of r (III) biosorption in a fixed bed column. Journal of Hazardous Material, 171, 886-893.

Cao, Y. (2017) Activated Carbon Preparation and Modification for Adsorption South Dakota. A dissertation submitted in partial fulfillment of the requirements for the Doctor of Philosophy, South Dakota State University.pp. 1-160.

Chowdhury, Z.Z., Abd Hamid, S.B., Mohd Zain, S. (2015). Evaluation design parameters for breakthrough curve analysis and kinetics of fixed bed column for Cu (II) cations using lignocellulosic wastes, BioResources. 10 (1), 732-749.

Eber, J., Wasserstein, P., and Jess, A. (2004) Deep desulfurization of oil refinery streams by extraction with ionic liquids. Green Chemistry, *6* (7), 316-322.

Fayazi, M. Taher, M.A., Afzali, D. and Mostafavi. A. (2015) Removal of Dibenzothiophene Using Activated Carbon/γ-Fe_2O_3 Nano-Composite: Kinetic and Thermodynamic Investigation of the Removal Process. Anal. Bioanal. Chem. Res., 2 (2), 73-84.

Gawan, P., and Kaware, J. (2014) Desulphurization techniques for liquid fuel A Review. International of Engineering Technology Management and applied Science *2* (7), 122-126.

Gawan, P., and Kaware J. (2016) Review of Research for Desulphurization of diesel by Adsorption. Journal of Engineering and Technology International Research. *3* (12), 337-340

Gaware, P., and Kaware J. (2016) Review on low cost Adsorbents for Desulphurization of Liquid Fuels. International Research Journal of Engineering and Technology, *2* (1),108-112.

Han, R., Wang, Y., Zou, W, Wang, Y, Shi, J. (2007) Comparison of linear and non-linear analysis in estimating the Thomas model parameters for methylene blue adsorption onto natural zeolite in fixed bed coulumn. Journal of Harzadous Materials, 145, 331-335.

Han, R., Yu W., Xin Z., Yuanfecy W., Fulng X., Cheng J., and Tang M. (2009) "Adsorption of Methyl Blue by Phoex Tree Leaf Power in a Fixed Bed Column: Experiments and Prediction of Breakthrough Curves. Desalination, 2 (45)284-297.

Han, R.P., Wang, Y.F., Yu, W.H., Zou, W.H., Shiand, J. and Liu, H.M. (2007) Adsorption of methylene blue from by phoenix tree leaf power in a fixed-bed column, Hazard. Mater., *141*, 713–718.

Li, P., Xiu, G., Jiang, L. (2001) Adsorption and desorption of phenol on activated carbon fibers in a fixed bed. Separation Science and Technology, 36 (10), 2147-2163.

Muzic, M., Sertic B., Adzamic T., Gomzi, Z., Podolski, S. (2009) Optimization of diesel fuel desulfurization by adsorption on activated carbon, Chem. Eng. Trans., *17 (5)*, 1549-1554.

Muftah, H. E., Manal, A. A., & Sulaiman, A. (2017) Evaluation of an activated carbon packed bed for the adsorption of phenols from petroleum refinery wastewater. Environ Sci Pollut Res, *24*:7511–7520. DOI 10.1007/s11356-017-8469-8.

Muzic, M., Katica S., Tamara A. (2009) Kinetic Equilibrium and statistical analysis of diesel fuel adsorptive desulphurization, *4* (9),373-394

Muzic, M., Sertic B., Adzamic T., Gomzi, Z., Podolski, S. (2009) Optimization of diesel fuel desulfurization by adsorption on activated carbon, Chem. Eng. Trans., 17 (5), 1549-1554.

Patil, M.S., Kamble, S., Bhattacharyulu, Y.C. (2012) Unsteady state adsorption – column studies International Journal of Advanced Engineering Research and Studies, I, Issue II, 179-184

Song C S. (2003) An overview of new approaches to deep desulfurization for ultra-clean gasoline, diesel fuel and jet fuel, Catal Today, 86.

Tang, M., Zhou, L., Du, M., Lyu, Z., Wen, X., Li, X., Ge, H. (2015) A novel reactive adsorption desulfurization Ni/MnO adsorbent and its hydrodesulfurization ability compared with Ni/ZnO. Catalysis Communications, 61, 32-40.

Tarty-Costodes, V.C., Fauduet, H., Porte, C., Ho, Y.S. (2005) Removal of lead (II) ions from synthetic and real efflunts using immobilized pinus sylvestris sawdust; adsorptionon a fixed bed column. J. Hazard. Mater., 123, 135-144.

Wang, T., Wang, X., Gao, Y., Su, Y., Miao, Z., Wang, C., Lu, L., Chou, L., Gao, X. (2015) Reactive adsorption desulfurization coupling aromatization on Ni/ZnO-$Zn_6Al_2O_9$ prepared by ZnxAly$(OH)_2(CO_3)$ z·xH_2O precursor for FCC gasoline. Journal of Energy Chemistry. http://dx.doi.org/10.1016/j.jechem.2015.07.002 2095-4956.

Xia, Q., Yu, M.X., Ji, Q.N., Li, Z.S. (2009) Adsorption capacity of super surface area activated carbon for thiophenic sulfur in real diesel. Journal of Functional Materials, 40 (10), 1730.

Yitzhaki' D., C. Aharoni. (1987) Kinetics and Mechanism of Catalytic Hydrodesulfurization of Gas Oil: Adsorption and Hydrogenation of the Sulfur Compounds Journal of Catalysis, 107, 255-262.

Zhang, H.Y., Liu, Q.F., Li, Y.G., Li, W.L., Xiong, X.C., Xing, J.M., Liu, H.Z. (2008) Selection of adsorbents for in-situ coupling technology of adsorptive desulfurization and biodesulfurization Sci China Ser B-Chem 51 (1), 69-77.

Chapter Ten

10.0. Conclusion and recommendation

10.1. Conclusion

Based on the objectives highlighted chapter 1 of this dissertation, the following studies have been carried out and reported:

1. Development and evaluating the performance of adsorption using a specific adsorbent (e.g. activated carbon, functionalized carbon nanotubes neem leaf powder and pomegranate leaf powder) for the removal of DBT compounds from model diesel and samples of South African diesel (diesel obtained before HDS and diesel obtained after HDS unit and parametric optimization on the process toward enhancing its performance.
2. Development and evaluation of BDS system, using *Pseudomonas Putida* and *Pseudomonas Aeruginosa* as biocatalysts, for the removal of sulphur-containing compounds from model diesel and samples of South African diesel obtained before and after HDS and parametric optimization on the process toward enhancing its performance
3. Coupling of the two processes in (1) and (2) and evaluation of the hybrid process for the removal of DBT from samples of South African diesel
4. Parametric optimization on the developed hybrid process in (3)
5. Investigating whether the kinetics and isothermal adsoption exhibited by the adsorbents used in (1), and Kinetics of biodesulfurization used in (2) & (3) could be described by existing adsorption isotherms and adsorption and degradation kinetic models.

The results obtained from the above-mentioned studies have produced the following novel contributions toward further research efforts on the development and evaluation of AD/BDS coupling process for desulfurization of South African petroleum distillate (e.g diesel):

- The adsorbents (AC, FCNTs, PLP and NLP) used in this study were successfully developed and evaluated for their adsorptive desulfurization performances. The dissertation also reports for the first time in open literature the excellent desulfurization performance of PLP. The results show that PLP out-performed NLP by 9.88 %. PLP displayed 70.55 % DBT removal and NLP showed 65.78 % DBT removal. As it has been established in this study, CNTs and FCNTs are promising candidates for removal of sulfur containing compound (DBT) from petroleum distillate (e.g diesel). As far as it can be ascertained, no

study has been conducted on the use of CNTs functionalized with $KMnO_4$/ H_2SO_4 for removal of DBT from petroleum distillate. It can be concluded that the acid treatment of CNTs enhanced its surface affinity for DBT, thus contributed to the improved adsorption capacity of the adsorbent. The results show that functionalized CNTs out-performed the non-functionalized CNTs during the desulphurization by about 10 %, indicating that functionalization of the CNTs did improve the desulfurization performance of the CNTs. It is noteworthy to mention that, the removal of DBT the adsorbents were 70. 48 % and 60.88 for FCNTs and CNTs, respectively, at 0.8 g adsorbent dosage, temperature of 25 ^oC and maximum contact time of 50 mins.

The results show that large surface area of AC contributed to its performance removal of the DBT in model diesel. The percentage performance of the adsorbents was 83.84 % at the following optimum operating variables; 1.0 g adsorbent dosage, temperature of 25 ^oC and contact time of 1 h. The optimized parameters and the best adsorbent were used in the performance evaluation of the adsorbent for removal of DBT from typical real diesel. Results show that AC out-performed all other adsorbents used in this study, owing to its exceptional higher surface area and micro structure and porosity. Therefore, AC was chosen for desulfurization of typical sreal diesel samples. The results show that large surface area of AC contributed to its performance removal of the DBT in the diesel samples. The percentage performance of the adsorbents for desulfurization of diesel obtained after HDS (99 %) was higher than that of the diesel obtained before HDS (60.41 %) at the same initial concentration of 120 mg/L.

As it has been demostrated in this study, AC was successfully immobilized in sodium algilate for adsorption of DBT in model oil in a continuous packed-bed column. This is a promising method of entrapping adsorbent for maximum performance. AC has been widely reported in literature for column adsorption studies of sulfur compound from petroleum distillates. However, there are only few studies on the immobilization of AC in sodium algilate for use in packed-bed column for desulfurization of petroleum distillate. Results show that adsorption of DBT in a packed-bed column is dependet on superficial velocity of the sorbate solution through the adsorption column. The best result was obtained at the lowest superficial velocity of 0.031 m/min (0.5 mL /min) at 15 cm bed height and lowest initial DBT concentration of 100 mg/L. Furthermore, breakthrough time was found to

increase with decreasing DBT initial concentration, decreasing flow rate and increasing bed height.

- In order to develop a BDS process and evaluate the degradation efficiencies of the bacteria, *Pseudomonas aeruginosa* (*PA*) and *pseudomonas putida* (*PP*) were successfully grown in this thesis. The growing and resting cells of both bacteria were used to degrade the DBT molecule in the model oil. Results show that *PA* showed better BDS performance than *PP* in all aspect. The results in this study show that *PA* and PP are able to desulfurize DBT into less harmful compound, 2- HBP. The final product 2-HBP detected shows the specific activity of DBT desulfurization is 4S–pathway. Furthermore, BDS performance of 67.53 % and 50. 02 %, by resting cells of *PA* and *PP*, respectively for 500 ppm initial concentration. In order to study desulphurization of diesel oils obtained from an oil refinery, BDS studies using resting cells by *PA* were carried out, which shows a decrease of about 30 % and 70.54 % DBT removal from 5200 ppm in diesel obtained before HDS and 120 ppm in diesel obtained after HDS, respectively. *PA* and *PP* selectively converted sulfur atom in DBT compound to 2-HBP. The results obtained in this study show that BDS would be a better technique to compliment HDS rather than the BDS being the main technique for desulfurization of organo-sulfur compounds in diesel.
- Studies on development and evaluation of AD/BDS coupling system for desulfurization of petroleum distillate has not been widely reported. Therefore, for the first time in open literature, the development and evaluation of AD/BDS coupling system will be reported. As it has been demostrated in this study, adsorption coupling biodesulfurization system (AD/BDS) was used to remove sulfur compound from two different South African diesel samples. The results obtained from the ADS experiment in a packed-bed showed that superficial velocity increased in the order 0.031, 0.063, 0.094 m/min, with increasing flow rate at 0.5, 1.0 and 1.5 mL /min. Results show that adsorption of DBT in a packed-bed column is dependent on superficial velocity of the sorbate solution through the adsorption column. The best result was obtained at the lowest superficial velocity of 0.031 m/min (0.5 mL /min) at 15 cm bed height and lowest initial DBT concentration of 120 mg/L. This means that, a longer breakthrough time is needed for higher performance of the packed-bed column which will successively result in higher adsorption capacity.

- It is important to consider the percentage of DBT removed from South African diesel obtained after HDS by individual process, results show that adsorption desulfurization process contributed to about 91.67 % DBT removal, while BDS contributed to about 8.33 % DBT removal in the overall desulfurization. It can therefore be concluded that BDS could serve as a complimentary process rather than the main process for desulfurization of sulfur compounds in petroleum distillate.
- In understanding the mechanisms and behavior of the adsorbents used in this study in batch mode ADS process, isotherm model and kinetics model, respectively were studied. Results show that Langmuir and Freundlich isotherm isotherm models described the adsorption mechanism perfectly for all the adsorbents used in this study. Kinetic studies were performed to understand the adsorption behaviuor of the adsorption process. Results show that, pseudo-first order described well the adsorption behavior of all adsorbents used in this study. Thermodynamics of the adsorption process was also studied. The negative values of ΔG^o and the positive values of ΔH^o indicate that DBT adsorption onto PLP and NLP are spontaneous and endothermic processes. Positive ΔS^o values of DBT adsorption process indicate an increase of the randomness at the PLP and NLP-solution interface during adsorption.

  The negative values of ΔG^o and the negative values of ΔH^o indicate that DBT adsorption onto CNTs and FCNTs are spontaneous and exothermic process. Negative ΔS^o value of DBT adsorption process indicate a decrease of the randomness at the CNTs and FCNTs-solution interface during adsorption

  Negative ΔS^o values of DBT adsorption processon AC indicates a decrease of the randomness at the AC-solution interface during adsorption. In addition, the results show that the values of standard entropy ΔS^o decreased with increase in temperature, while the values of standard free energy G increased with increase in temperature.

  In understanding the behaviour of adsorbents used in desulfurization of DBT in model diesel and real diesel during continous mode adsorption process, kinectics using Bohart-Adam, Thomas and Yoon-Nelson's kinetic models was studied. The results showed that, Bohart-Adam and Thomas kinetic models described well the behaviour of the adsorbent. The initial region of breakthrough curve was well described by the Bohart–Adams kinetic

model at all experimental conditions studied while the transient stage or working stage of the breakthrough curve was described well by the Thomas kinetic model.

The kinetics governing the removal of DBT compound from South African diesel by hybrid process was investigated. Results show that, Thomas and Bohart-Adam's kinetic models decribed well the behavious of adsorbent in the ADS while first-order kinetic model and Michaelis-Menten kinetic models were used to describe the mechanism of DBT degradation and bacteria growth, respectively in the AD/BDS coupling process. The results showed that the models fitted well into experimental data.

In summary, the encouraging results, as documented in this dissertation and also communicated to researchers in the area of adsorption and biodesulfurization (in the form of four peer-reviewed international scientific publications and two conference proceedings), could provide a platform for developing a scaled-up, energy efficient and less-expensive AD/BDS coupling system for industrial process, for the complete removal of sulfur-containing compounds from petroleum distillates.

10.2 Recommendations

Based on the observations from this study, the following suggestions need to be considered in the development of a new adsorption and BDS process.

(i) Adsorption process in batch process: It may be required that effect of pH and particle sizes be carried out on the adsorption performances of the adsorbents

(ii) Adsorption process in continuous mode: It is essential to investigate the effect of temperature on the performance of the packed-bed column. The set-up used in this study did not give room for checking or investigating the effect of temperature in the column, making it impossible to study the thermodynamics of the packed-bed column. In addition, more studies on the effect of pressure on the adsorption column should be carried out.

(iii) Supply of oxygen into the bacteria medium could enhance the growth of the bacteria, and thereby enhance the biodesulfurization efficiency. This should be looked into in future studies.

(iv) Thorough exploration into the understanding of the different microbial pathways that are involved in BDS is required towards the optimization and scale-up studies of the process. More studies should be conducted in order to determine the other 4S-pathway products of biodesulfurization.

(v) During the AD/BDS system, the aspect of allowing a continous coupling process should be considered in future studies.

(vi) At the same time, the development of new strains or the modification of sulphur degrading strains via recombinant DNA technology or genetic engineering could be essential to enhancing the degrading performance of the existing bacteria.

(vii) Finally, almost all research efforts involving the use of hybrid process for removal of sulfur-containing compounds from petroleum distillates are still limited to laboratory scale studies. In view of this, scale-up studies are essential for future investigation of AD/BDS coupling system.

Appendix

Appendix A: Experimental equipment



Figure A 1 Photograph of GC/MS connected with the monitor

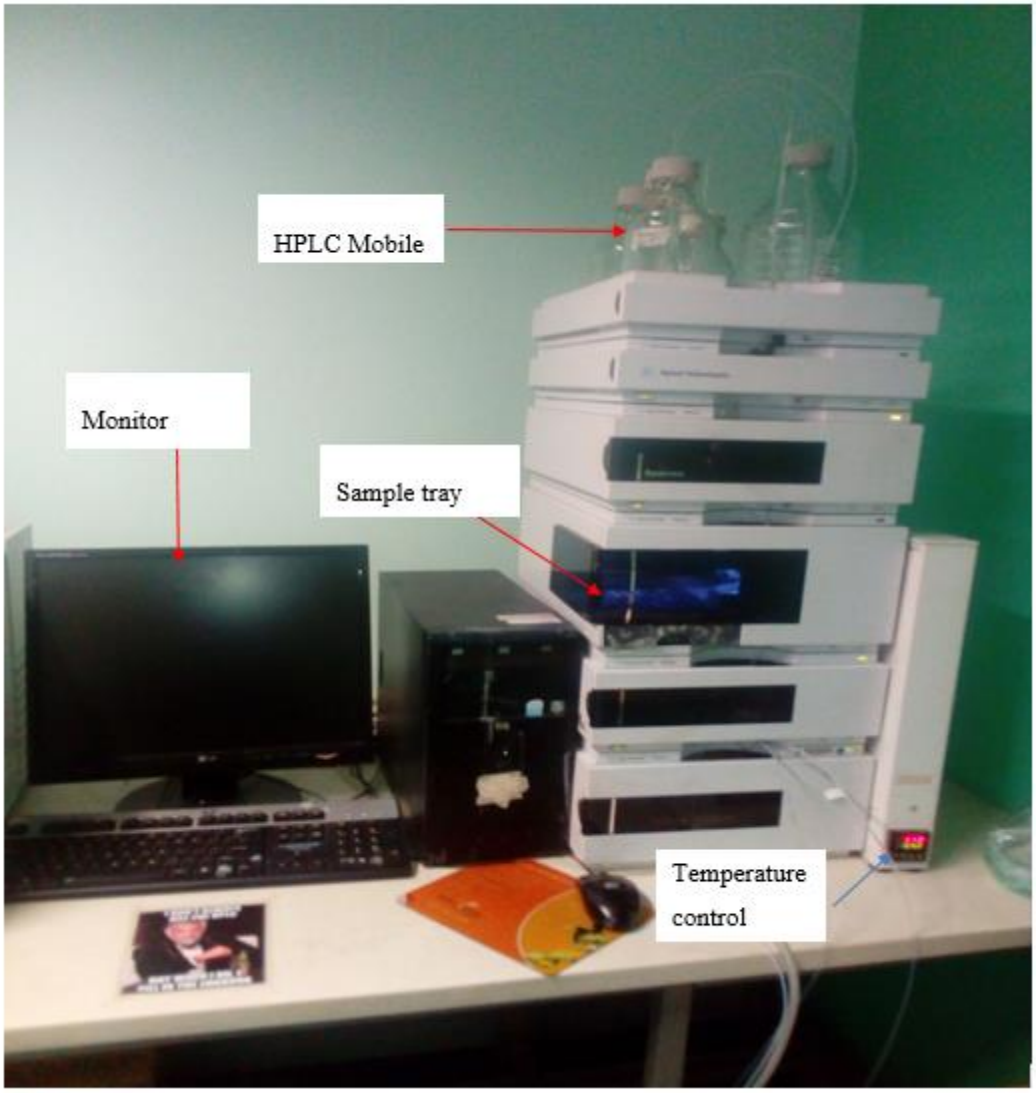


Figure A 2 Photograph of high performance liquid chromatography (Agilent technologies)

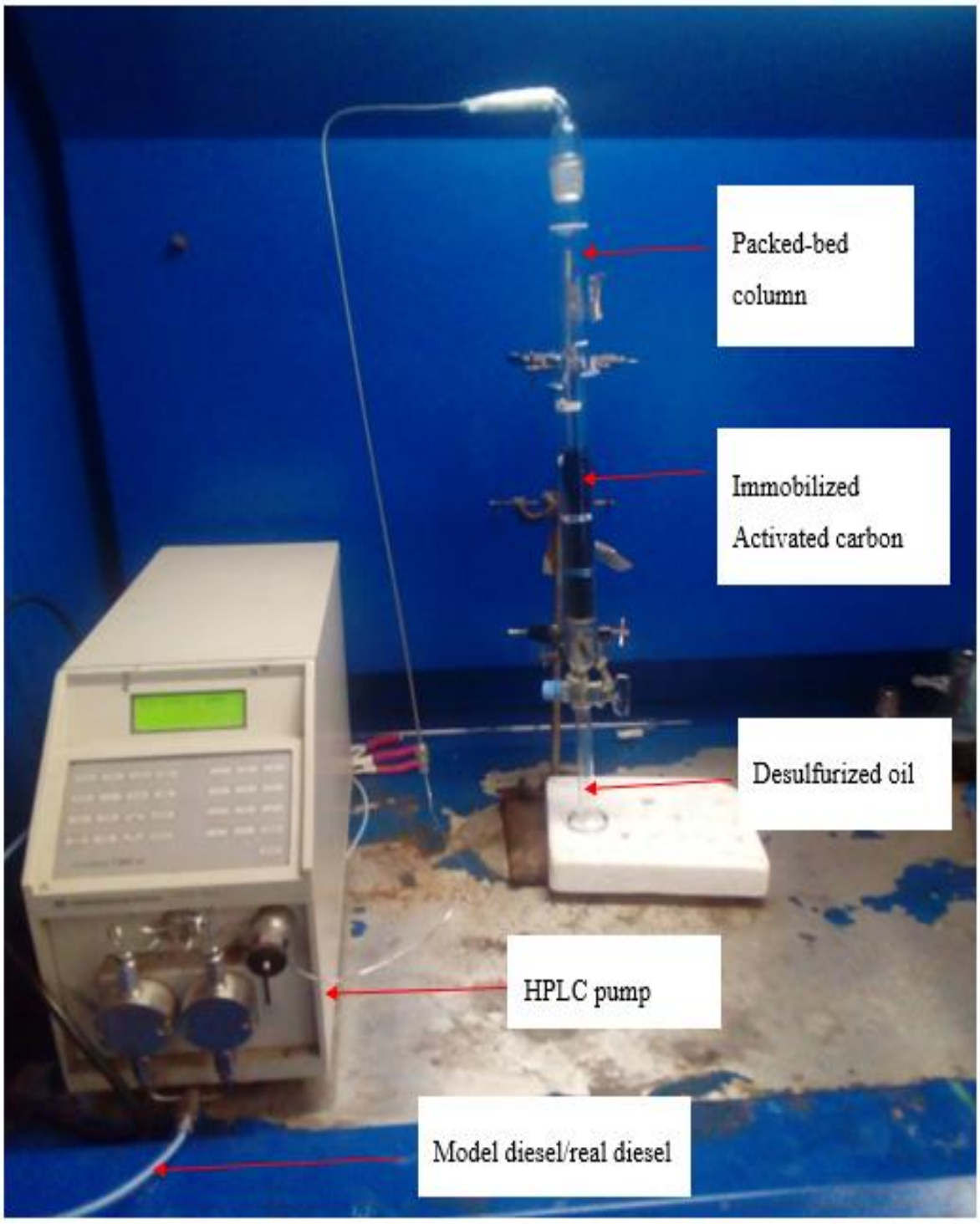


Figure A 3 Photograph of continuous packed bed column experimental set-up



Figure A 4 Photograph of Incubator



Figure A 5 Photograph of autoclave



Figure A 6 Photograph of spectroquant

Appendix B: Calculations of various adsorption parameters

(1) Langmuir isotherm

For FCNTs,

$$\frac{t}{q_t} = \frac{1}{q_o} + \frac{1}{bq_o} . \frac{1}{C_e}$$

Y= 40.238X - 0.0681

$$\frac{1}{q_o} = 0.0681$$

$$q_o = 14.68\, mg/g$$

$$\frac{1}{bq_o} = 40.238$$

b= (14.68 X 40.238)

(2) Freundlich isotherm

$$Log q_e = Log\ K_f - \frac{1}{\mathrm{n}}\ Log\ C_e$$

For CNTs

Y=1.1572 X-1.9048

$$Log\ K_f = \text{-}1.9048$$

$K_f = 10^{-1.9048}$

$K_f = 0.0125$

$$\frac{1}{\mathrm{n}} = 1.1572$$

n =0.864

(3) Pseudo 2nd order kinetics

At 25 ^{o}C,

Y= 0.0316x +0.0075

$$\frac{t}{q_t} = \frac{1}{K_2 q_e 2} - \frac{1}{q_e} t$$

Y = C + MX

$$\frac{1}{q_e} = 0.0316$$

$$q_e = \frac{1}{0.0316}$$

$$q_e = 34.64\ mg/g$$

$$\frac{1}{K_2 q_e 2} = 0.0075$$

$$K_2 = 0.0075\ X 34.64\ X\ 34.64$$

K_2 = 0.133 L/mg.min

(4) Pseudo 1st order kinetics

$$Log(q_e - q_t) = Log\ q_e - \frac{K_1}{2.303}\ t$$

For PLP at 25 ^{o}C,

Y= - 0.0204X + 1.4042

$$Log\ q_e = 1.4042$$

$$q_e = 10^{1.4042}$$

$$q_e = 25.36\ mg/g$$

$$-\frac{K_1}{2.303} = \text{-}0.0204$$

$$K_1 = 2.303\ X\ 0.0204$$

K_1=0.04698 L/min

(5) Bohart-Adam model

$$ln\frac{C_t}{C_o} = K\ C_o t - \frac{\mathrm{K}N_o Z}{\mathrm{V}}$$

At 0.5 mL/min

Y= 0.0088 X -2.384

$$K\ C_o = 0.0088$$

C_o=100 mg/L

K= 100 X 0.0088

K = 8.8 X 10^{-5}

$$-\frac{\mathrm{K}N_o Z}{\mathrm{V}} = -2.3584$$

Bed height 15 cm = Z =0.15 m^2

$$\mathrm{V} = \frac{\text{Flow rate}}{\text{Area}} = \frac{0.0005}{0.016}$$

V = 0.031L/m^2/min

N_o= 2.3584 X 0.031/ (8.8 X10^{-5} X 0.15)

$N_o = 5.54 \text{ X } 10^3$

(6) Thomas model

$$ln\left(\frac{C_0}{C_t} - 1\right) = \frac{K_{Th} q_0 w}{\text{V}} - K_{Th} C_0 t$$

At 40 mg/L,

Y=-0.0221 X + 2.8611

$$\frac{K_{Th} q_0 w}{\text{V}} = 2.8611$$

$$At\ 0.5 \frac{mL}{min},$$

Mass of adsorbent at 15 cm bed height = 41 g, flow rate =0.5 mL/min= 0.0005L/min

$$\frac{w}{\text{V}} = \frac{41}{0.0005}$$

$q_o = 2.8611 / (5.53 \text{ X } 10^{-4} \text{ X } 82000)$

$q_o = 0.063$ mg/L.

(7) Yoon-Nelson model

$$ln\left(\frac{C_t}{C_0 - C_t}\right) = K_{YN} t - K_{YN} \tau$$

At 40 mg/L

Y=0.0221 X – 2.8611

$$K_{YN} = 0.0221$$

$$-K_{YN} \tau = -2.8611$$

$\tau = 2.8611/0.0221 = \tau = 129.46$ min.

Appendix C Adsorption experimental graphs

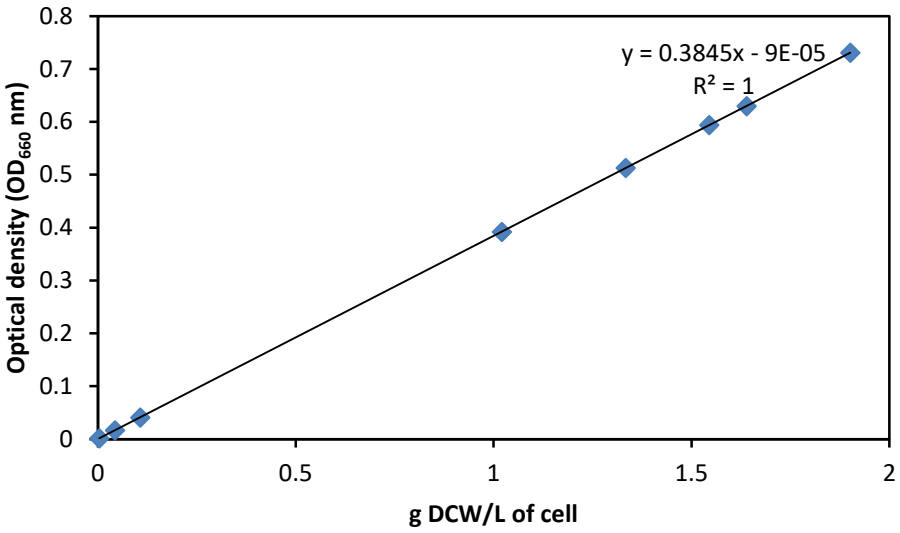


Figure C 1 Optical desnsity of cell growth converted to g dry cell weight /L of cell

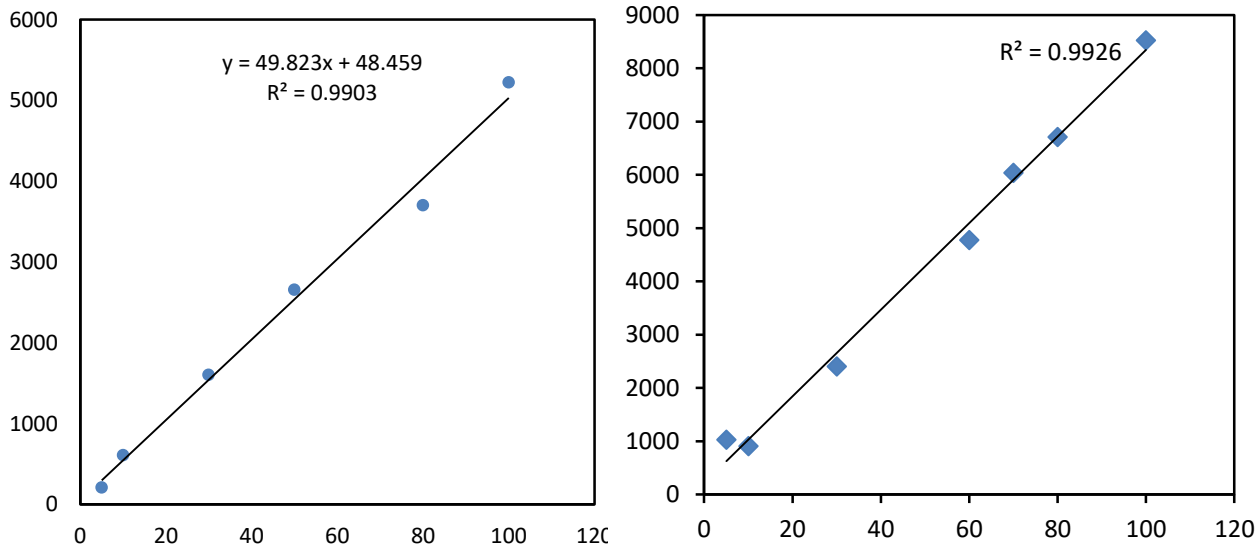


Figure C 2 Calibration curve for (a) DBT/acetate and (b) HBP/ethyl acetate at retention time of 7.497 and 2.649, respectively in HPLC

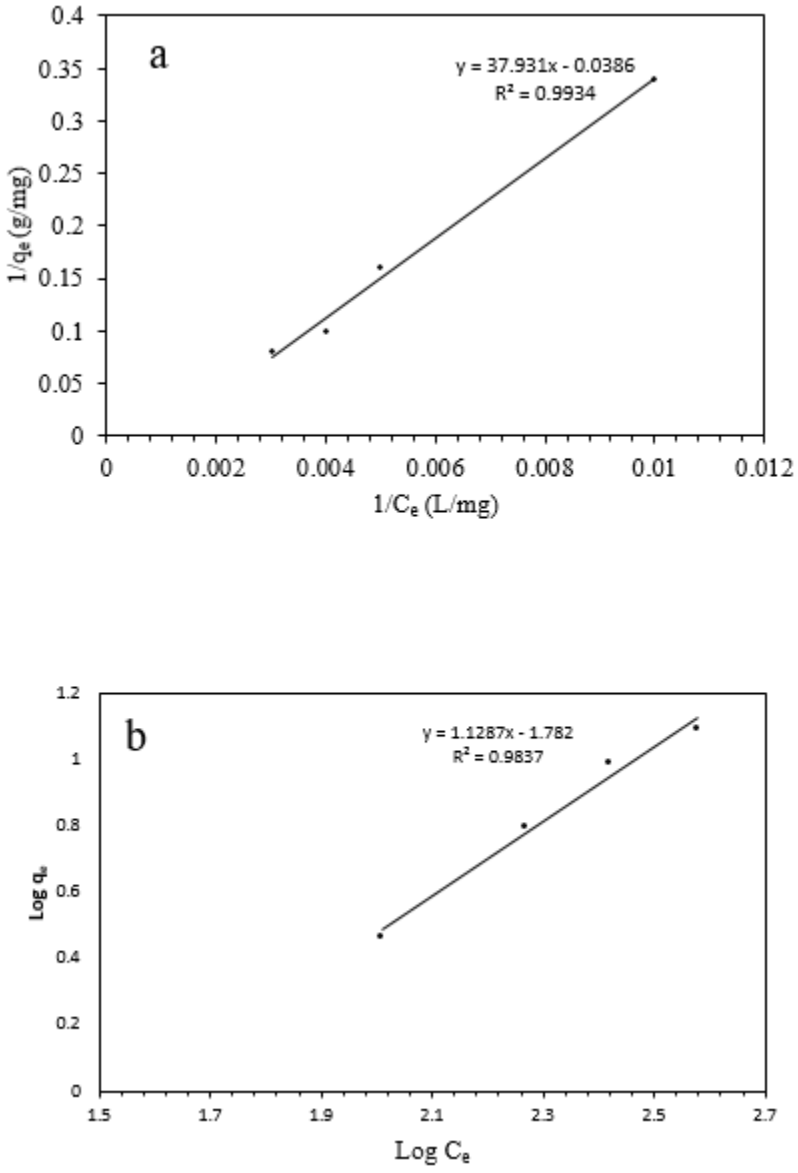


Figure C 3 (a) Langmuir and (b) Freundlich isotherm models of DBT adsorption onto PLP adsorbent

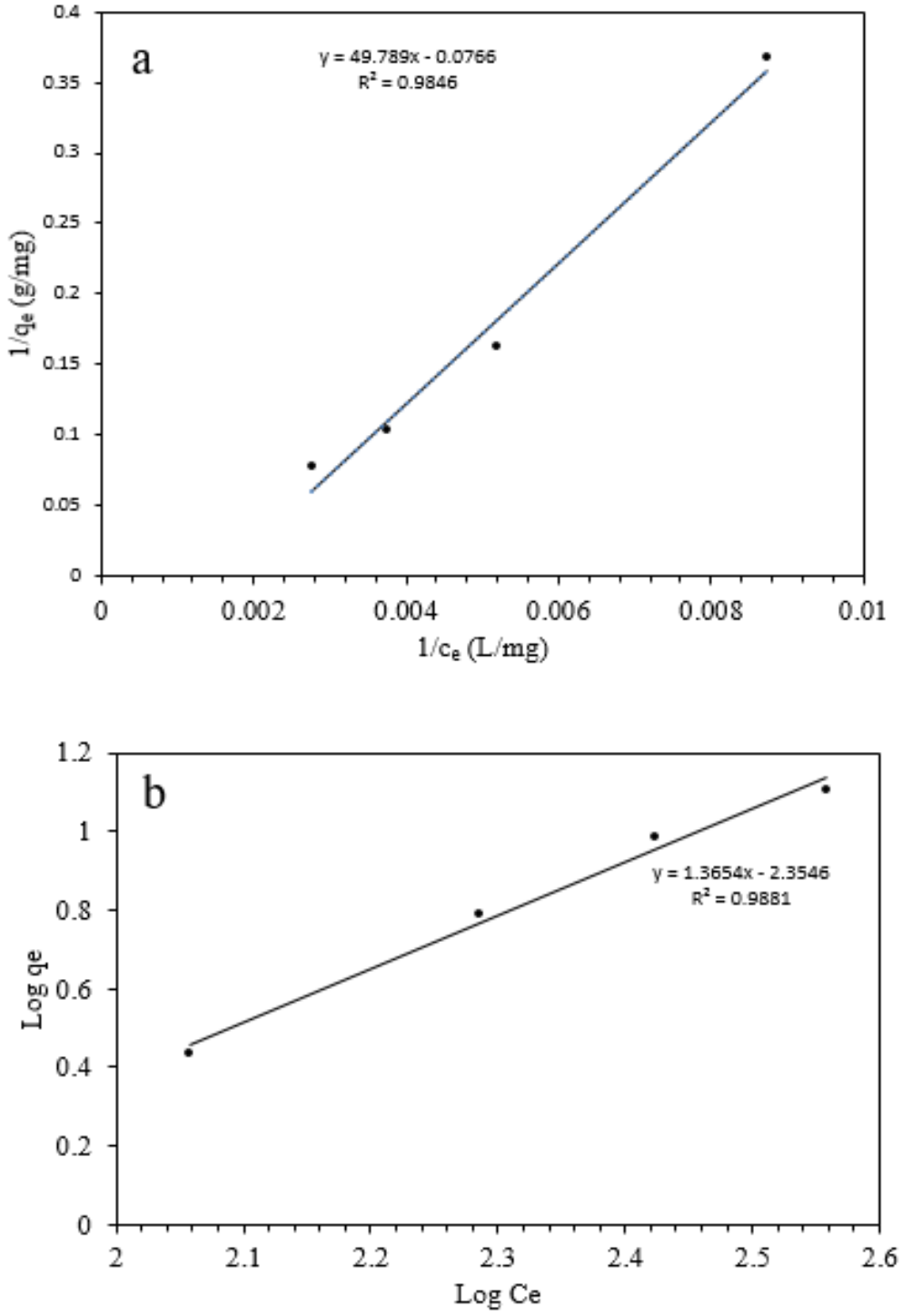


Figure C 4 (a) Langmuir and (b) Freundlich isotherms for NLP adsorbent

Figures of Asorption Isotherms, Kinetics and themodynamics

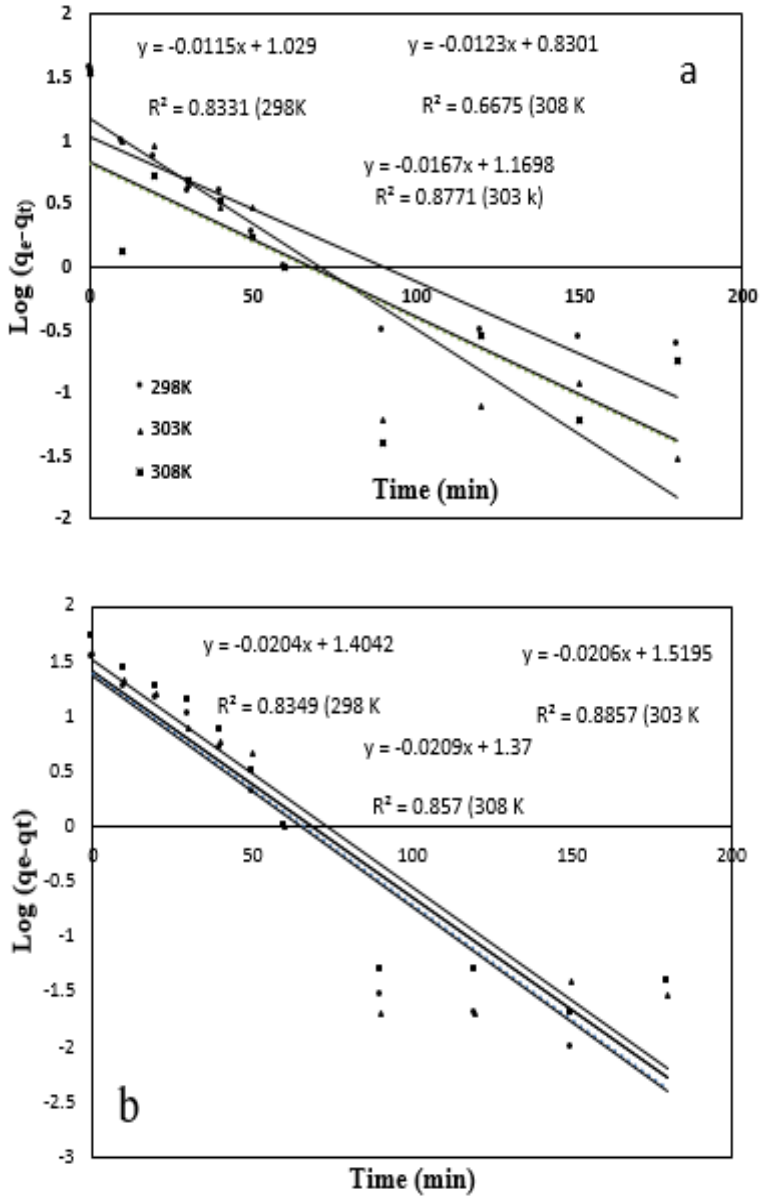


Fig. C 5 Pseudo first order for (a) NLP (b)PLP adsorbent for adsorption of DBT in model diesel

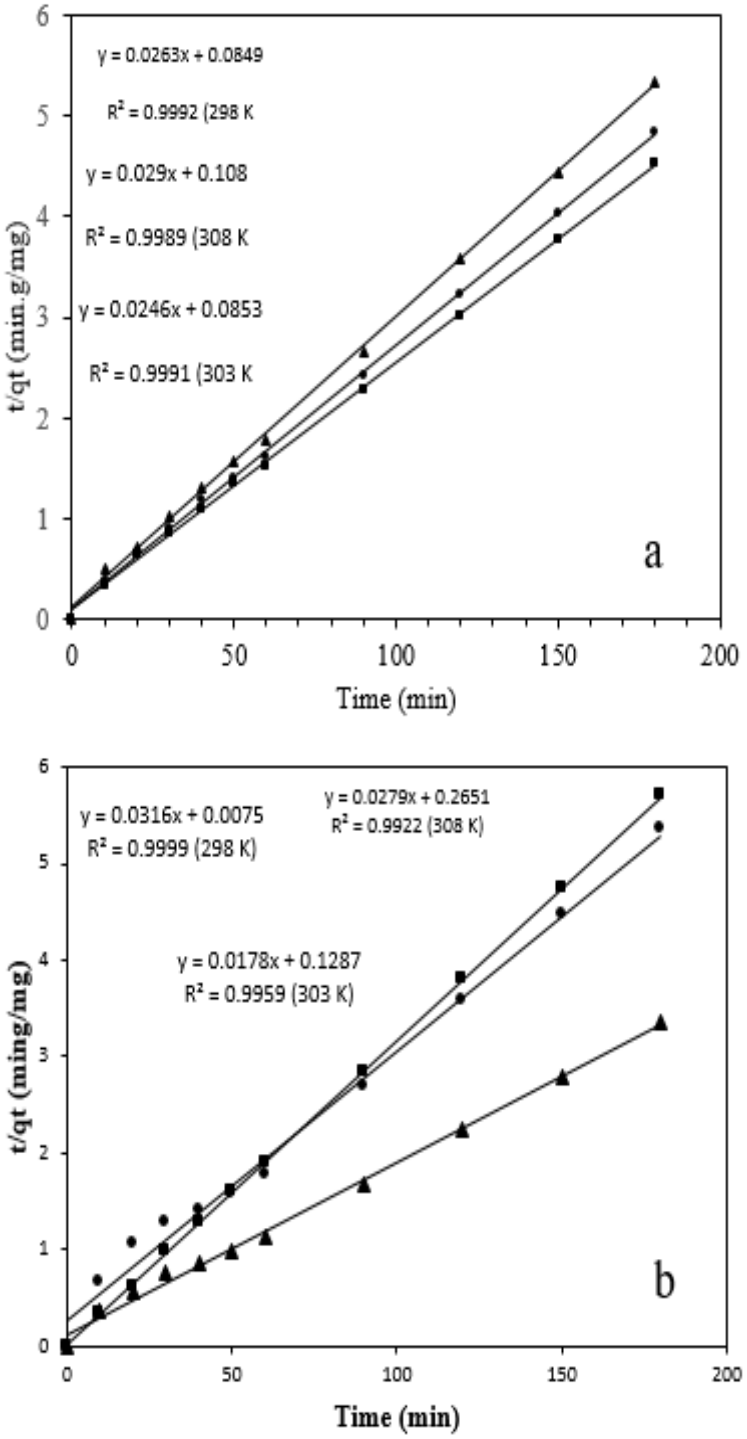


Fig. C 6 Pseudo second order kinetics of DBT adsorption onto (a) NLP adsorbent (b) PLP adsorbent at 298, 303, and 308 K. Circle (298 K) Square (303 K) and triangle (308 K).

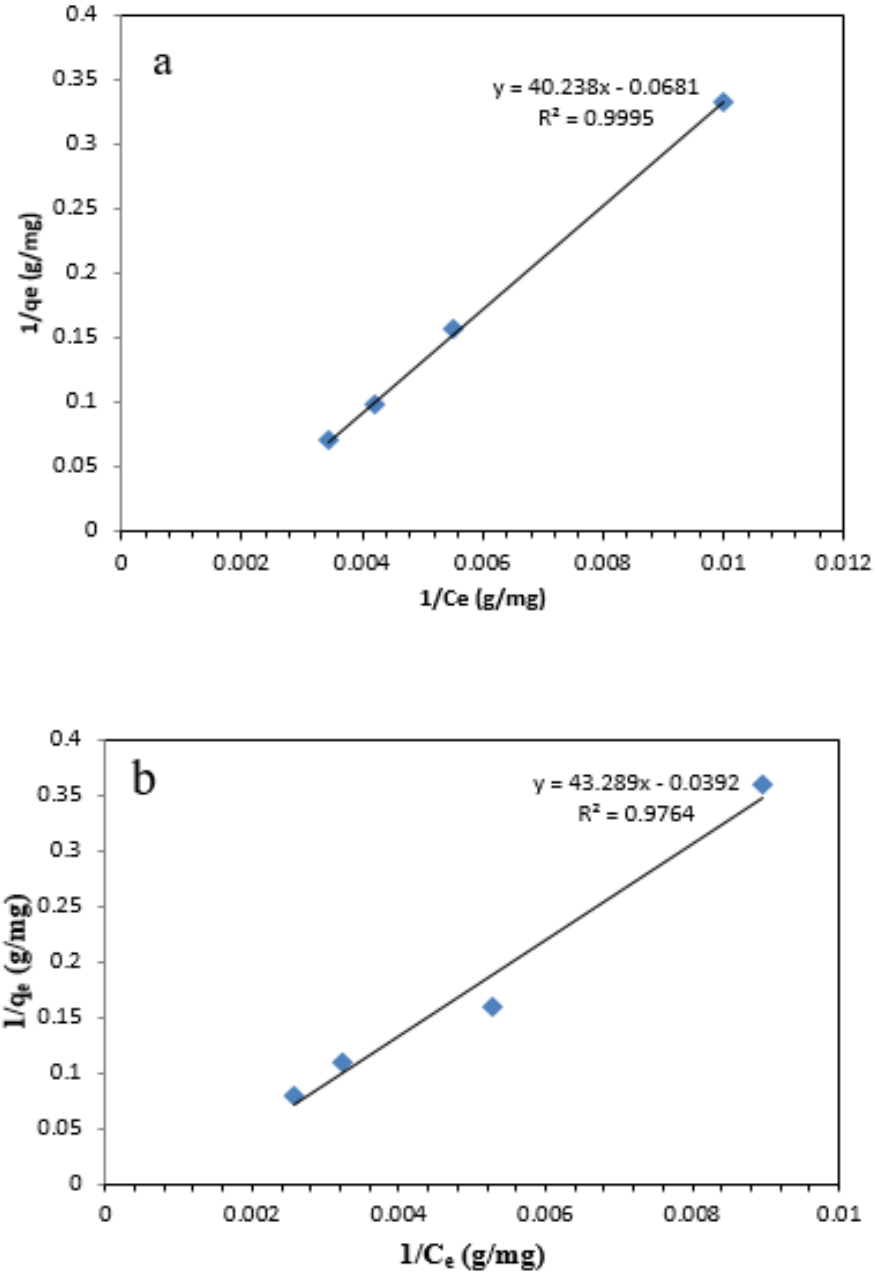


Fig. C 7 (a) Fig. Langmuir isotherm of adsorption of DBT over (a) FCNTs. (b) CNTs. Operating conditions: Temp: 298 K, amount 1.0 g, and equilibrium time of 50 min.

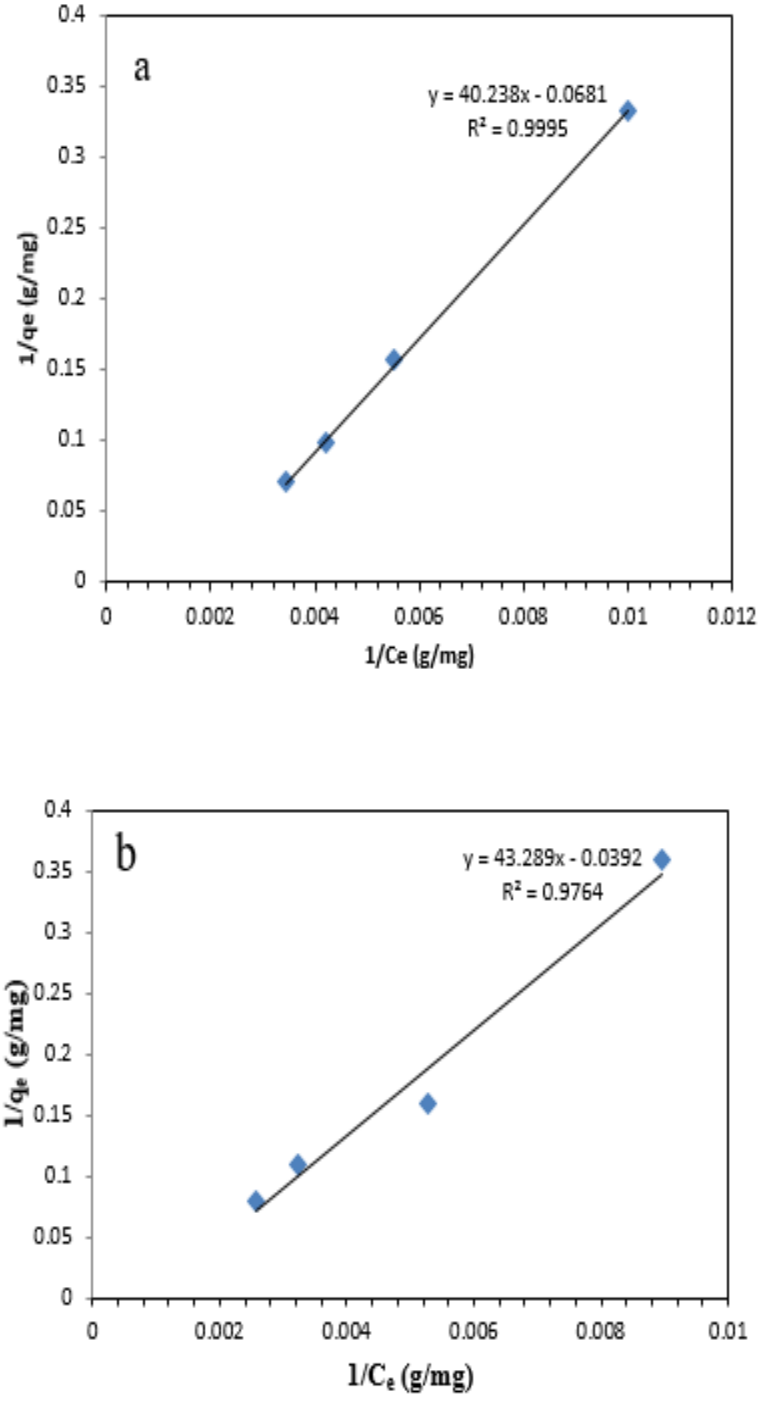


Fig. C 8 (a) Freudlich isotherm of adsorption of DBT over FCNTs (b) CNTs. Experimental conditions: Temp: 298 K; Amount of adsorbent: 1.0 g

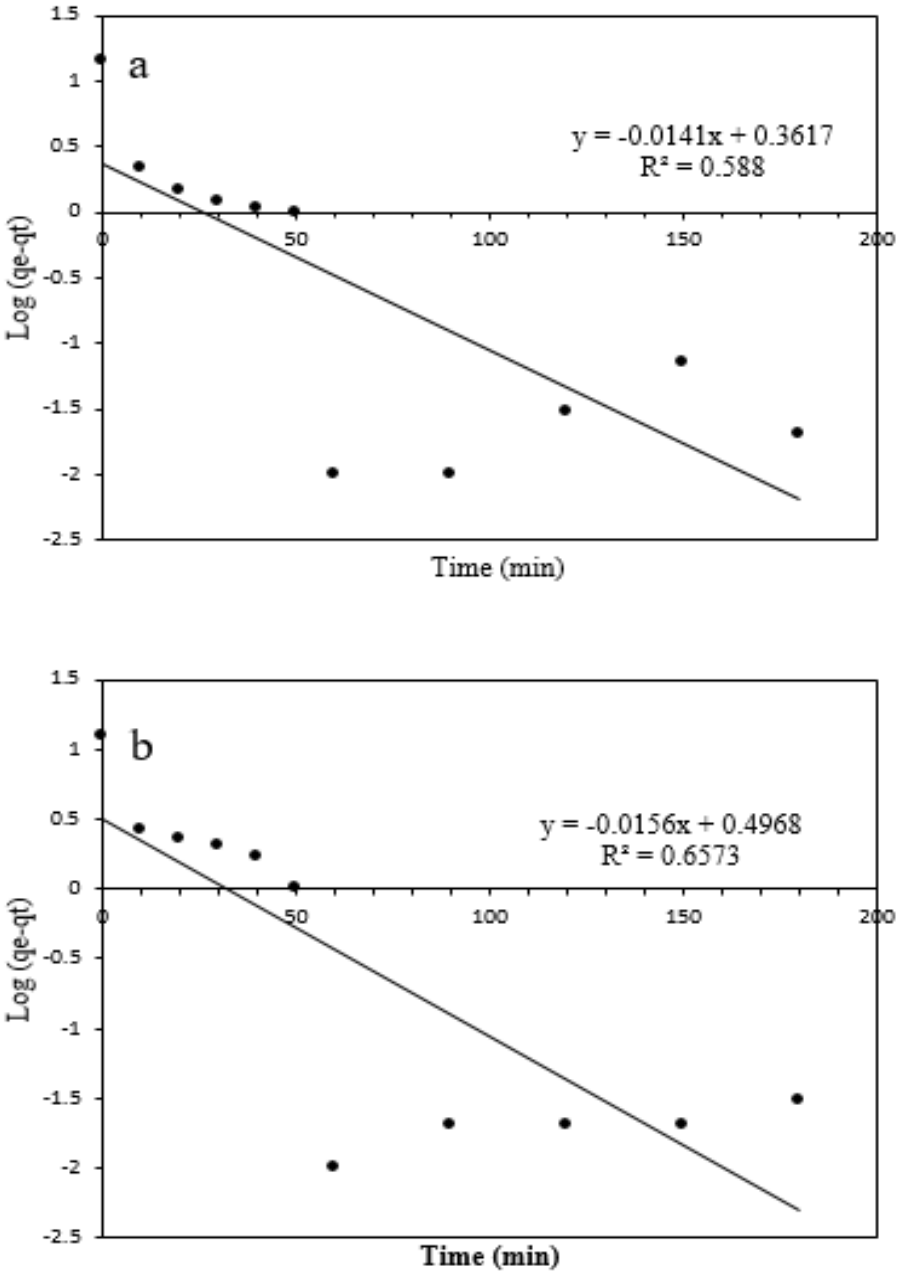


Fig. C 9 Pseudo first-order of DBT adsorption on (a) FCNTs (b) CNTs. Experimental conditions: Temp. 25 ^{o}C, amount of adsorbent; 1.0 g.

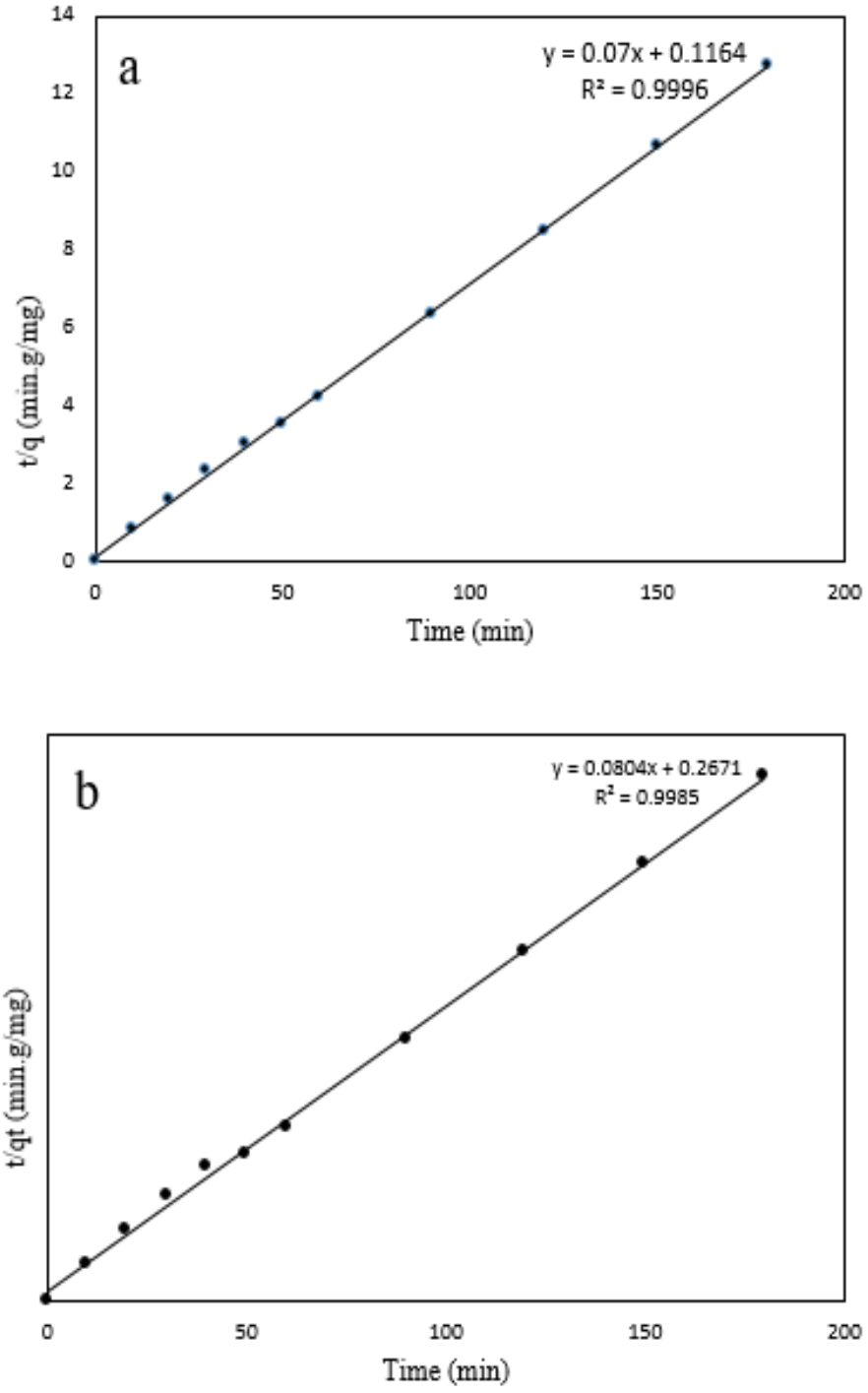


Fig. C 10 Pseudo second order of DBT adsorption on (a) FCNTs (b) CNTs. Experimental conditions: Temp: 298 K; Amount of adsorbent: 1.0 g.

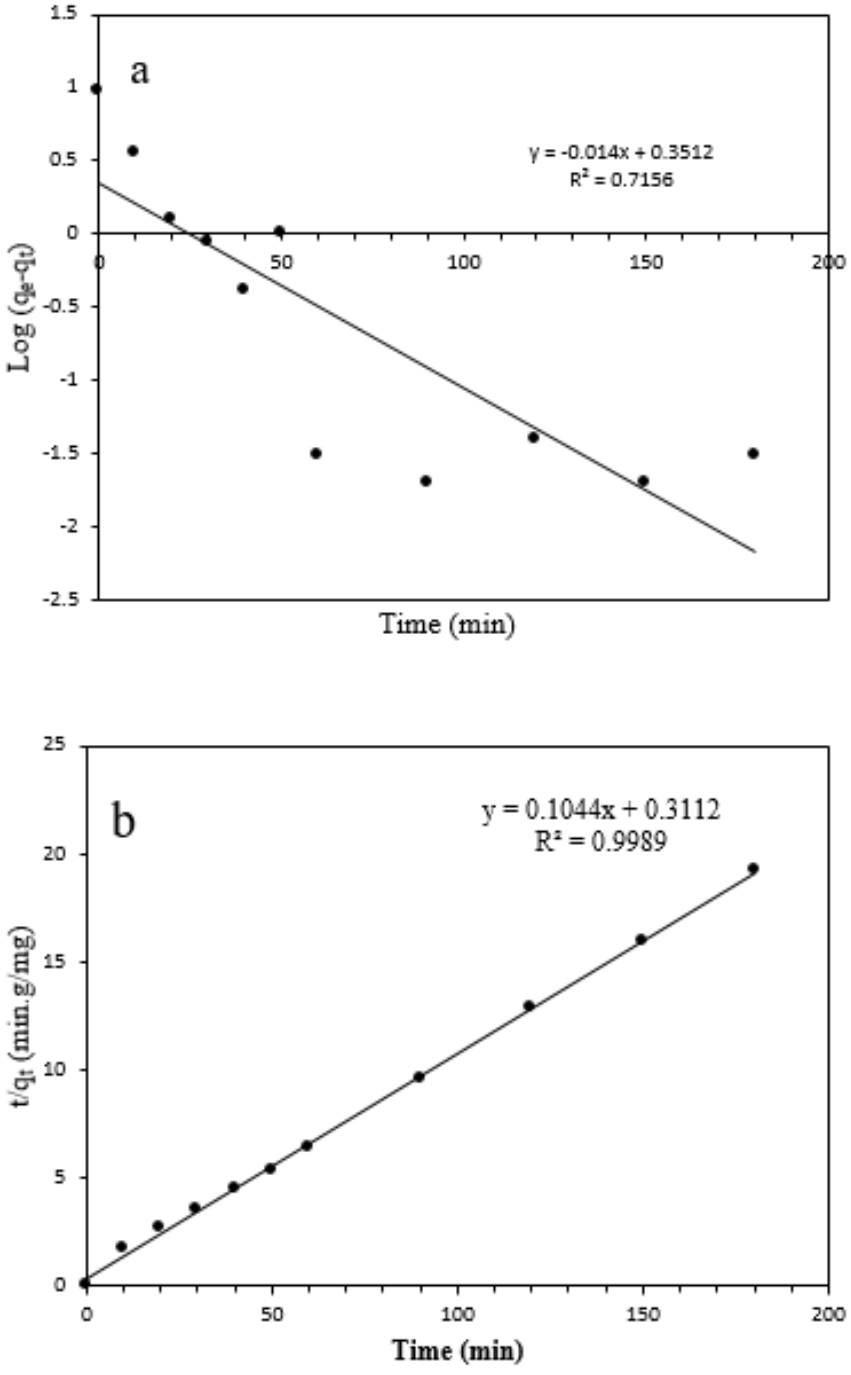


Fig.C 11 (a) Pseudo first-order of DBT adsorption on CNTs (b) Pseudo second-order of DBT adsorption on CNTs. Experiment conditions: Temp: 303 K; Amount of adsorbent: 1.0 g.

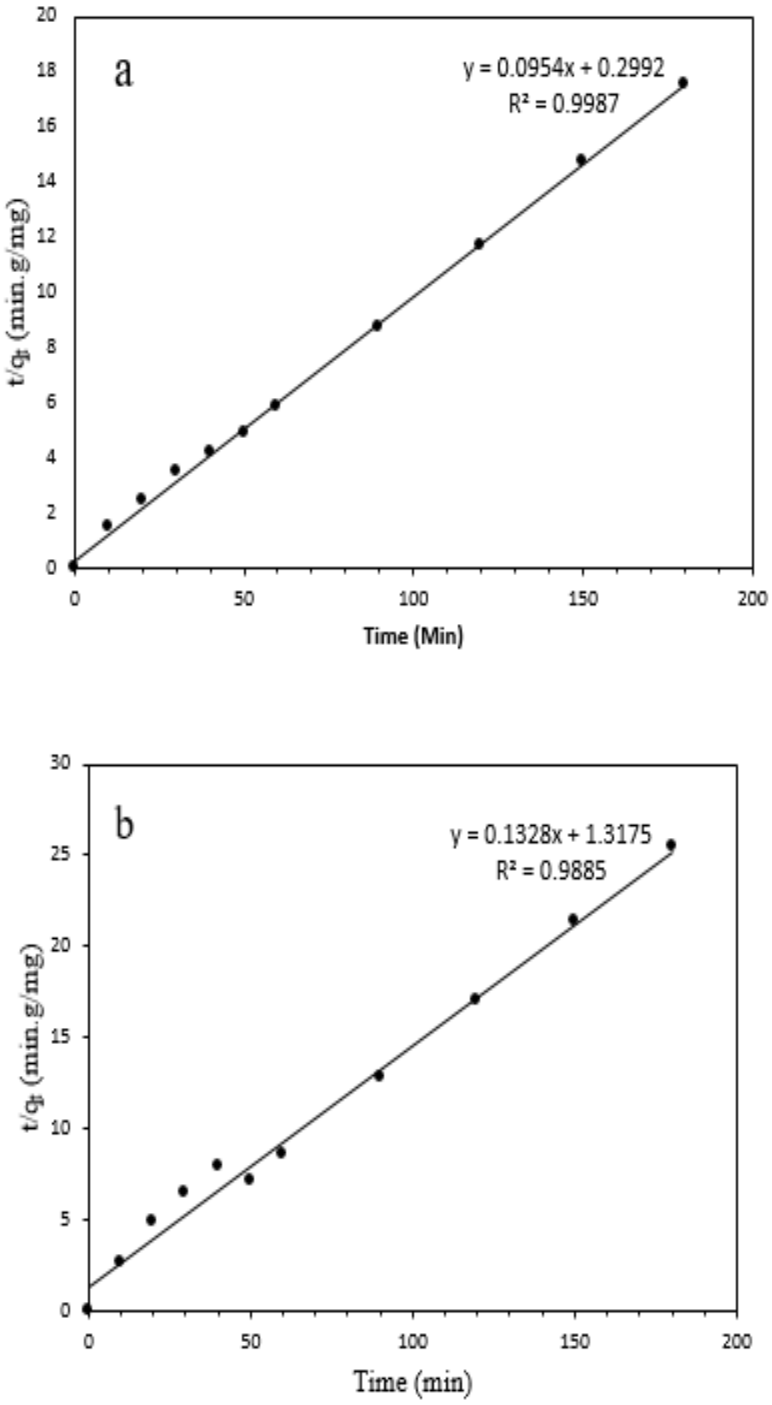


Fig C 12 Pseudo second order of DBT adsorption on (a) FCNTs (b) CNTs. Experimental conditions: Temp. 318 K; Amount of adsorbent: 1.0 g.

Adsorption thermodynamics

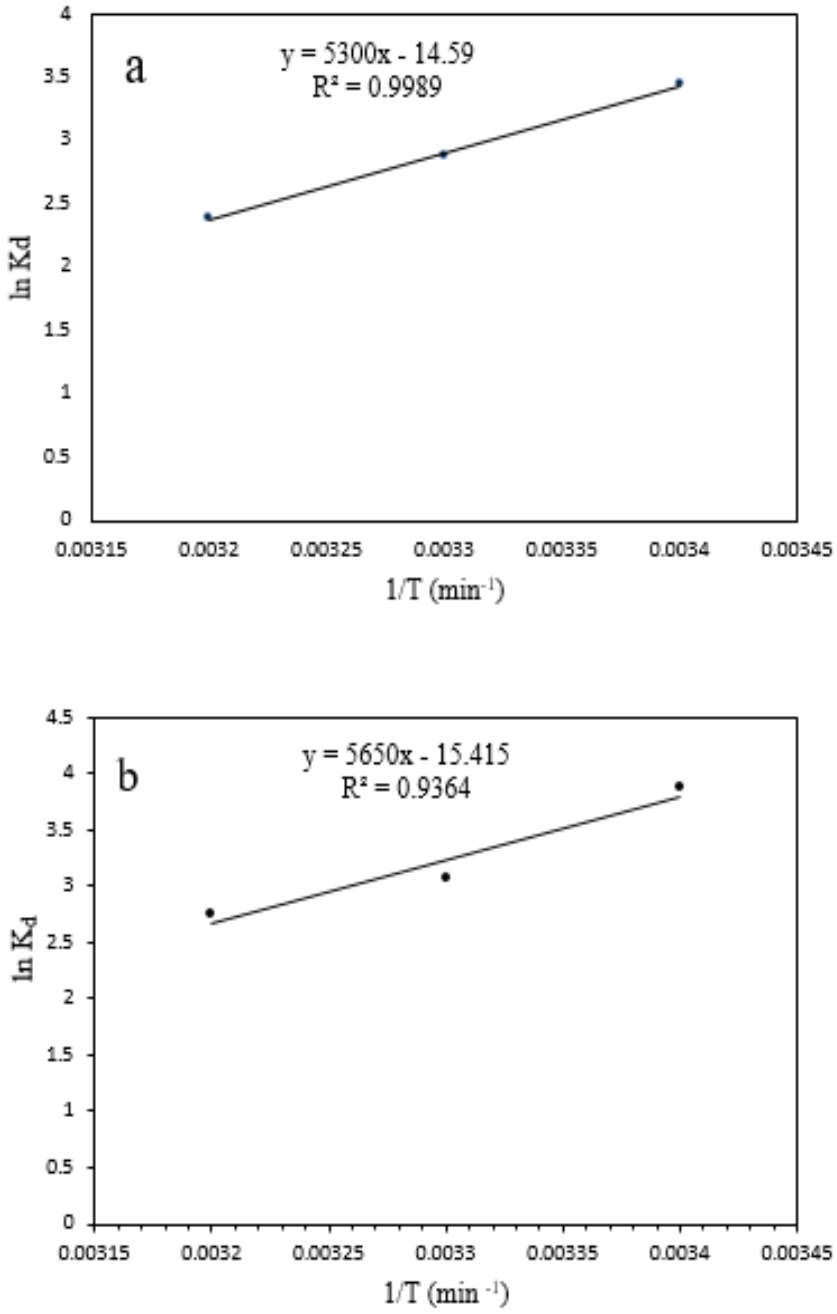


Fig. C 13 Plot of ln Kd versus 1/T for adsorption of DBT onto (a) CNTs (b) FCNTsadsorbent for determination of enthalpy

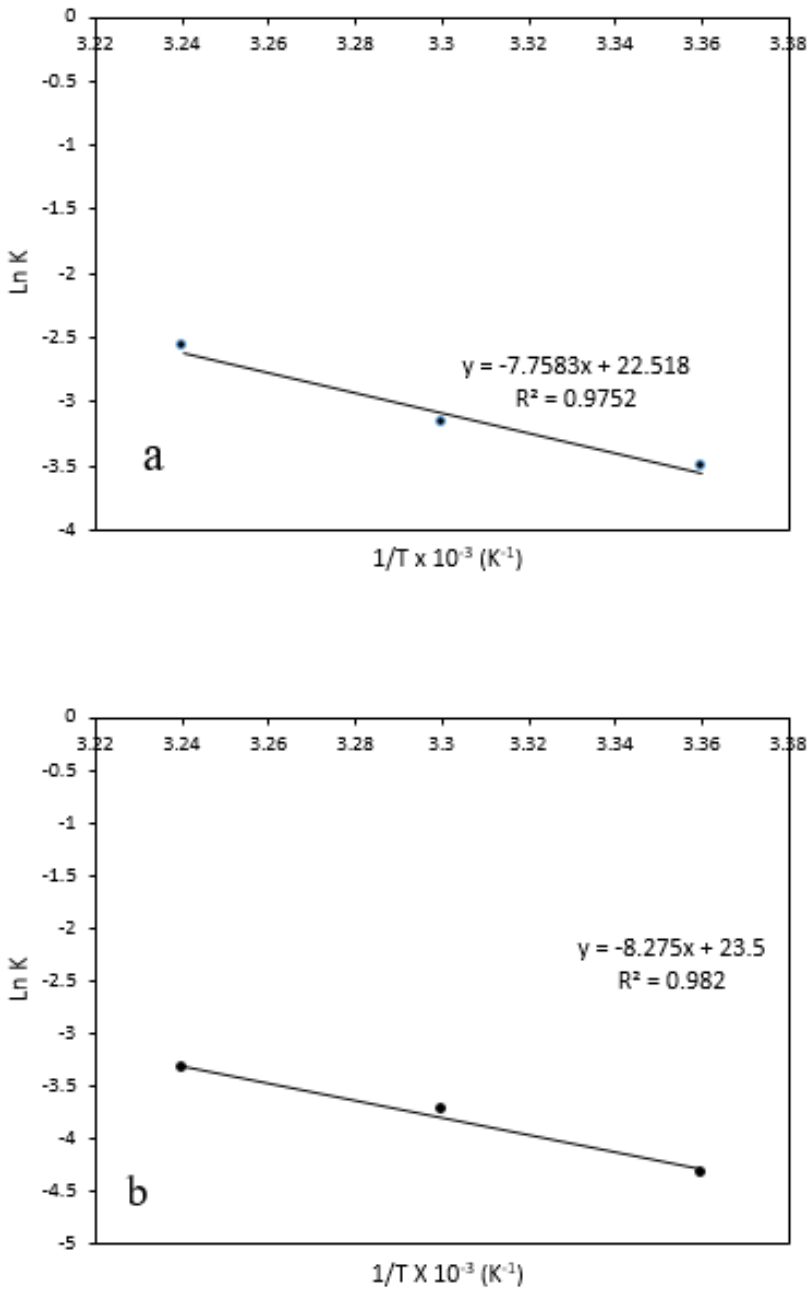


Fig. C 14 Determination of activation energy for adsorption of DBT onto (a) FCNTs (b) CNTs

Adsorptive desulfurization of DBT onto Activated carbon

Adosrption isotherms, kinetics and thermodynamics of activated carbon

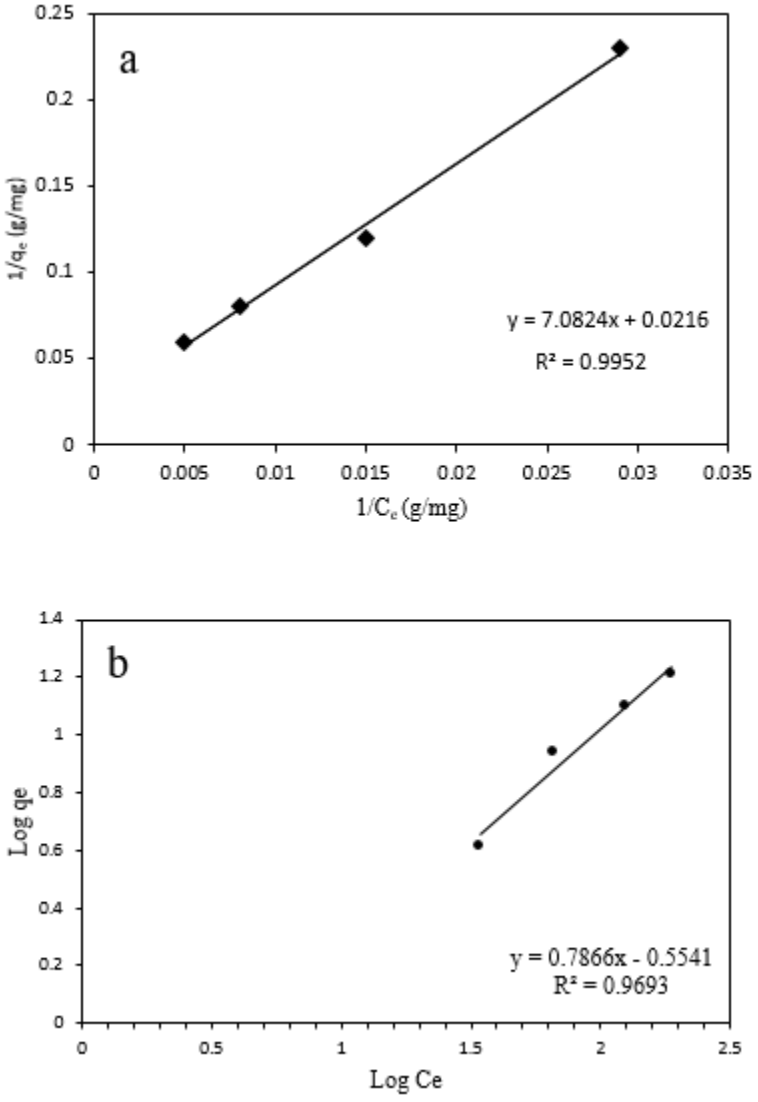
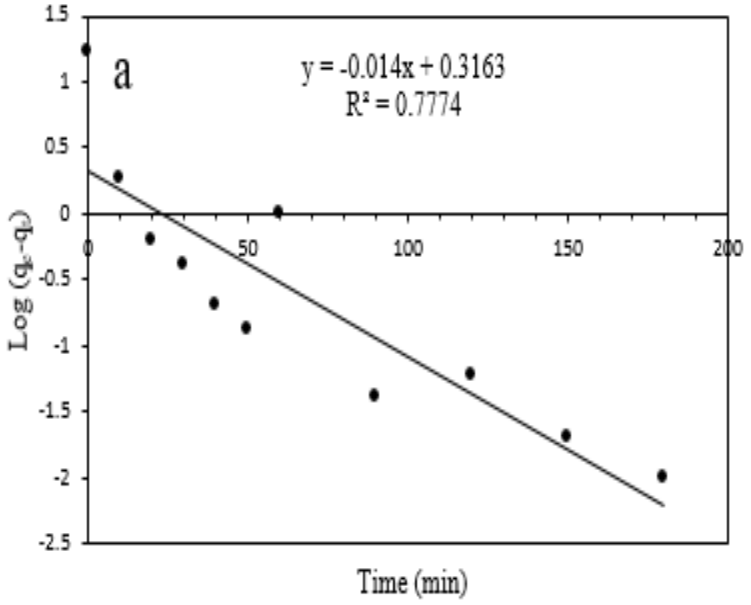


Fig. C 15 (a) Langmuir isotherm of adsorption of DBT onto AC (b) Freudlich isotherm of adsorption of DBT onto AC. Experimental conditions: Amount of adsorbents: 0.2 g; Temperatures: 298 K; Initial concentrations: 250-1000 mg/L.



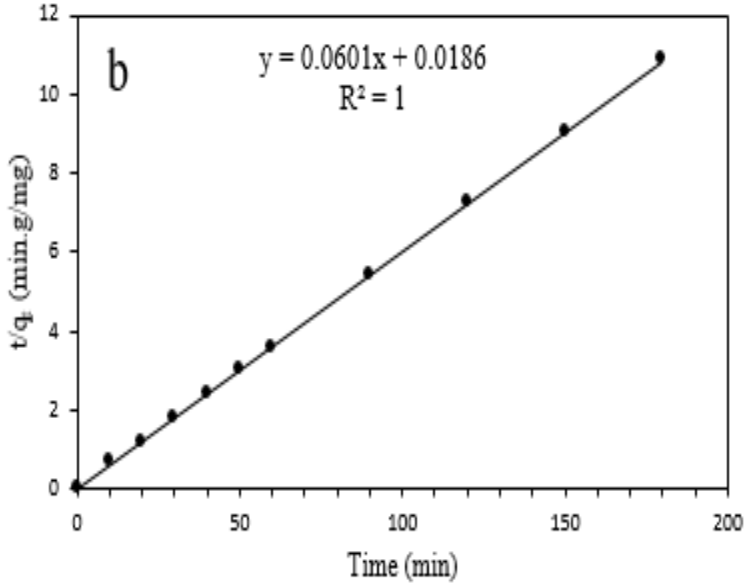


Fig.C 16 (a) Pseudo first-order for adsorption of DBT onto activated carbon (b) Pseudo second-order for adsorption of DBT onto activated carbon. Experimental conditions: Temperature 298 K; Amount of adsorbent: 1.0 g; Initial feed concentration: 1000mg/L.

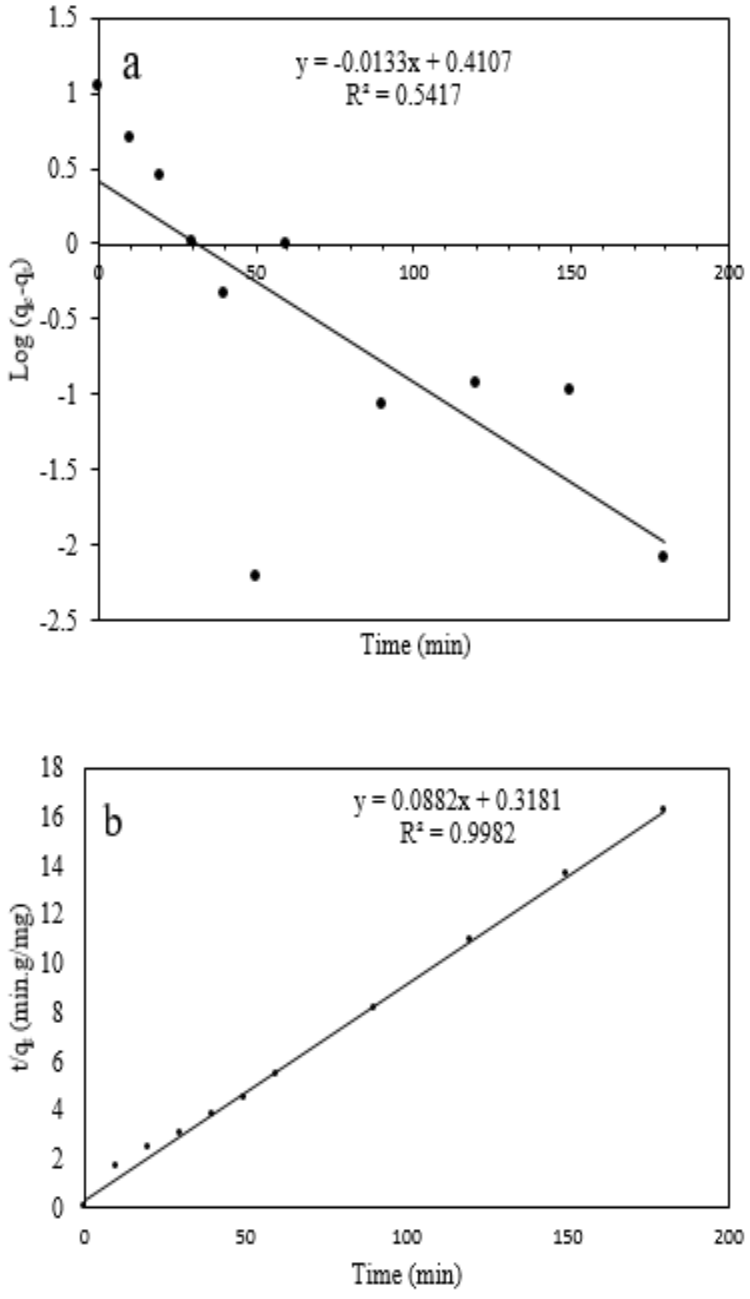


Fig. C 17 (a) Pseudo first order for adsorption of DBT onto activated carbon (b) Pseudo second order for adsorption of DBT onto activated carbon. Operating conditions: Temperature: 308 K; Amount of adsorbent :1.0 g; Initial feed concentration: 1000mg/L.

Adsorption isotherms and kinetics of desulfurization of South African diesel

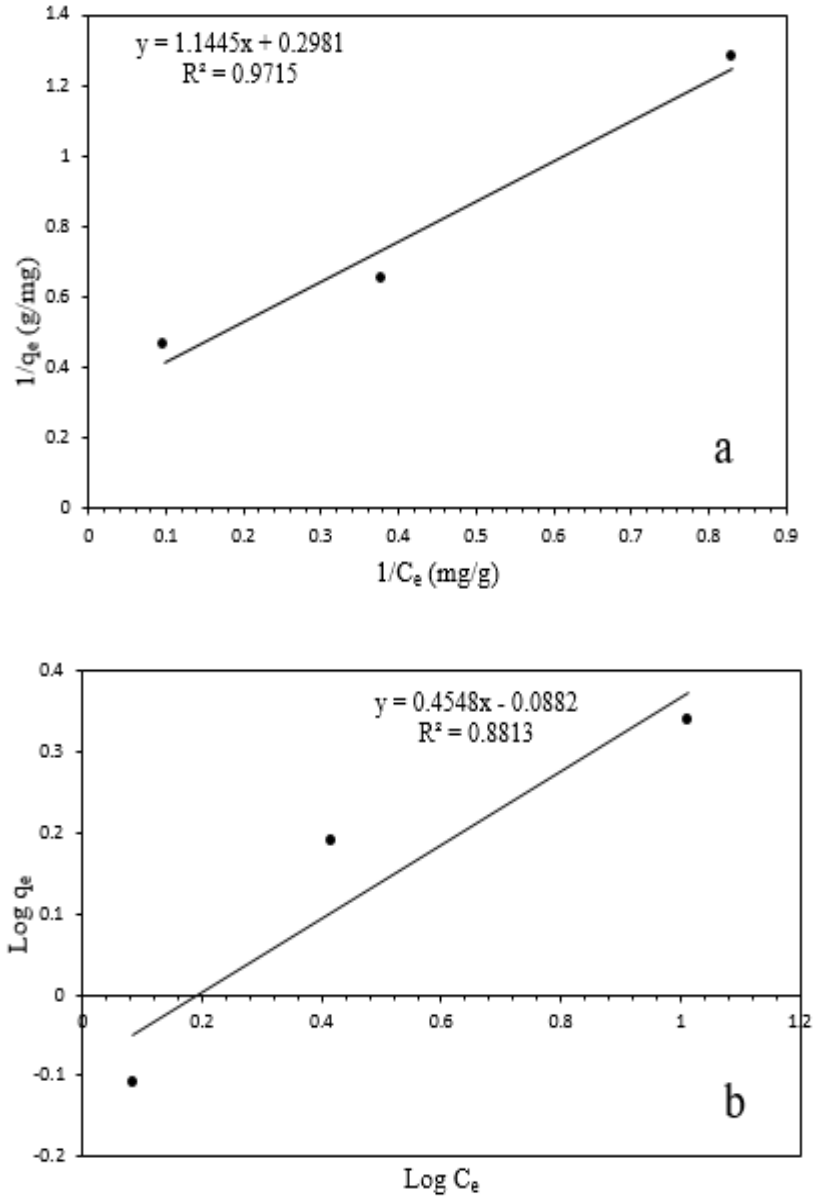


Fig. C 18 (a) Langmuir isotherm for adsorption of sulfur content in diesel obtained after HDS (b) Freundlich isotherm for adsorption of sulfur content in diesel obtained after HDS. Experimental conditions: Initial conc.: (40, 80, 120, mg/L); Amount of adsorbent: 1.0 g; Temperatures 298 K.

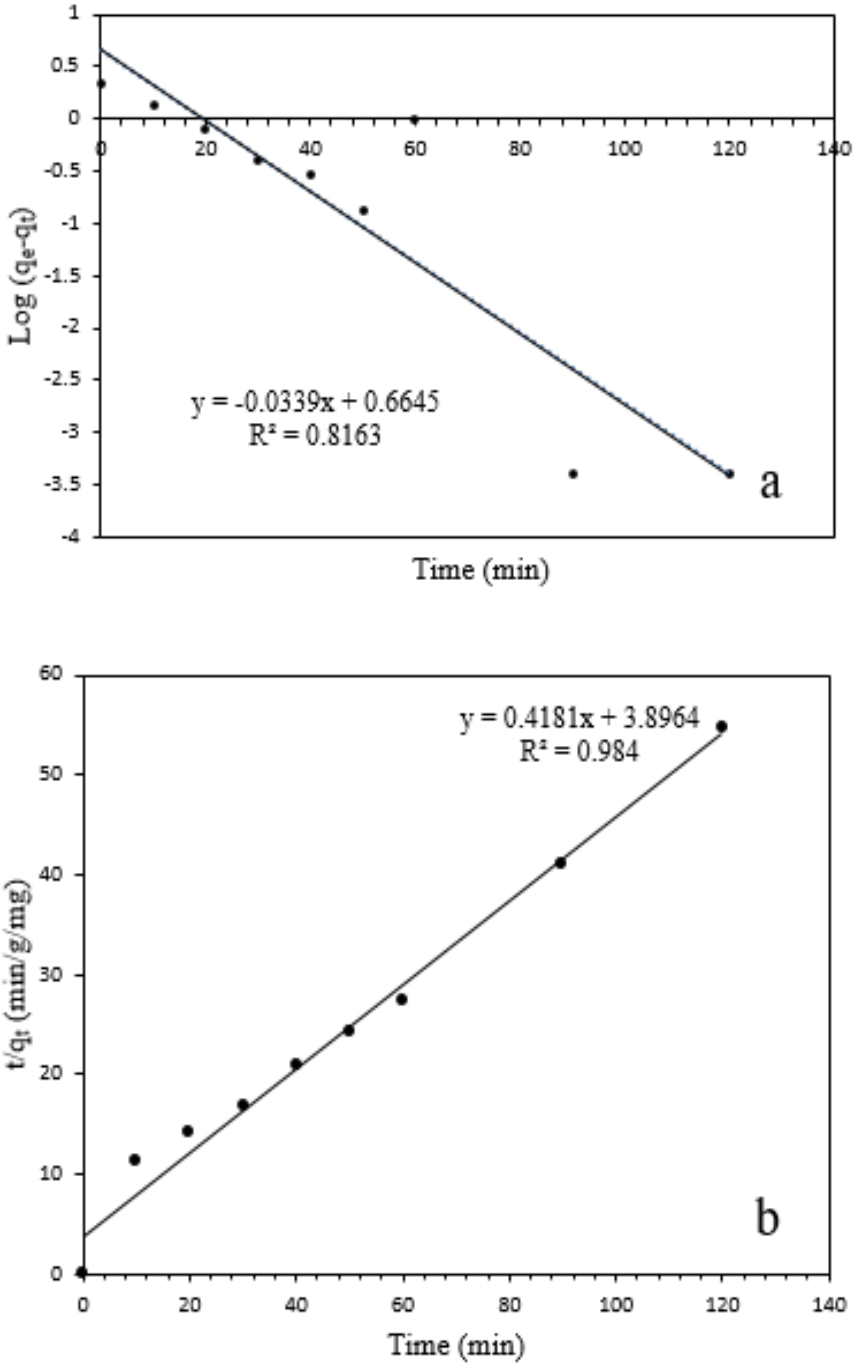
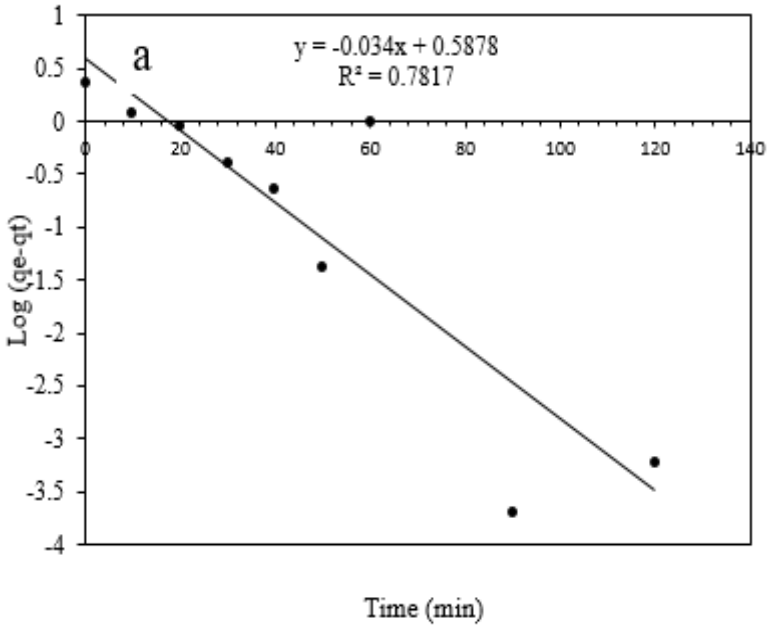


Fig. C 19 Pseudo first-order of adsorption of DBT in diesel before HDS (b) Pseudo second-order of adsorption of DBT in diesel obtained before HDS. Experimental conditions: Temperature 298 K, amount of adsorbent: 1.0 g; Initial DBT concentration: 120 mg/L.



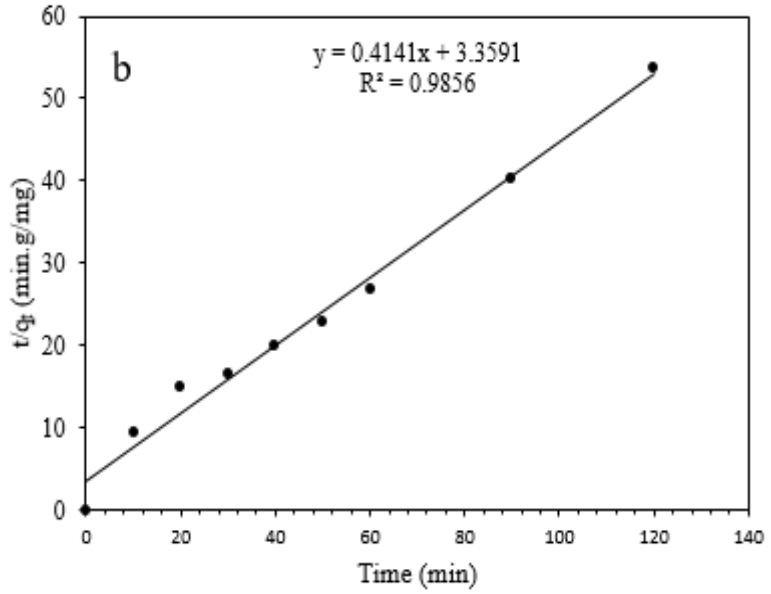


Fig C 20 (a) Pseudo first order of adsorption of DBT in diesel obtained after HDS (b) Pseudo second order of adsorption of DBT in diese after HDSl. Experimental conditions: Temperature: 308 K; Amount of adsorbent: 1.0 g; Initial sulfur concentration: 120 mg/L.

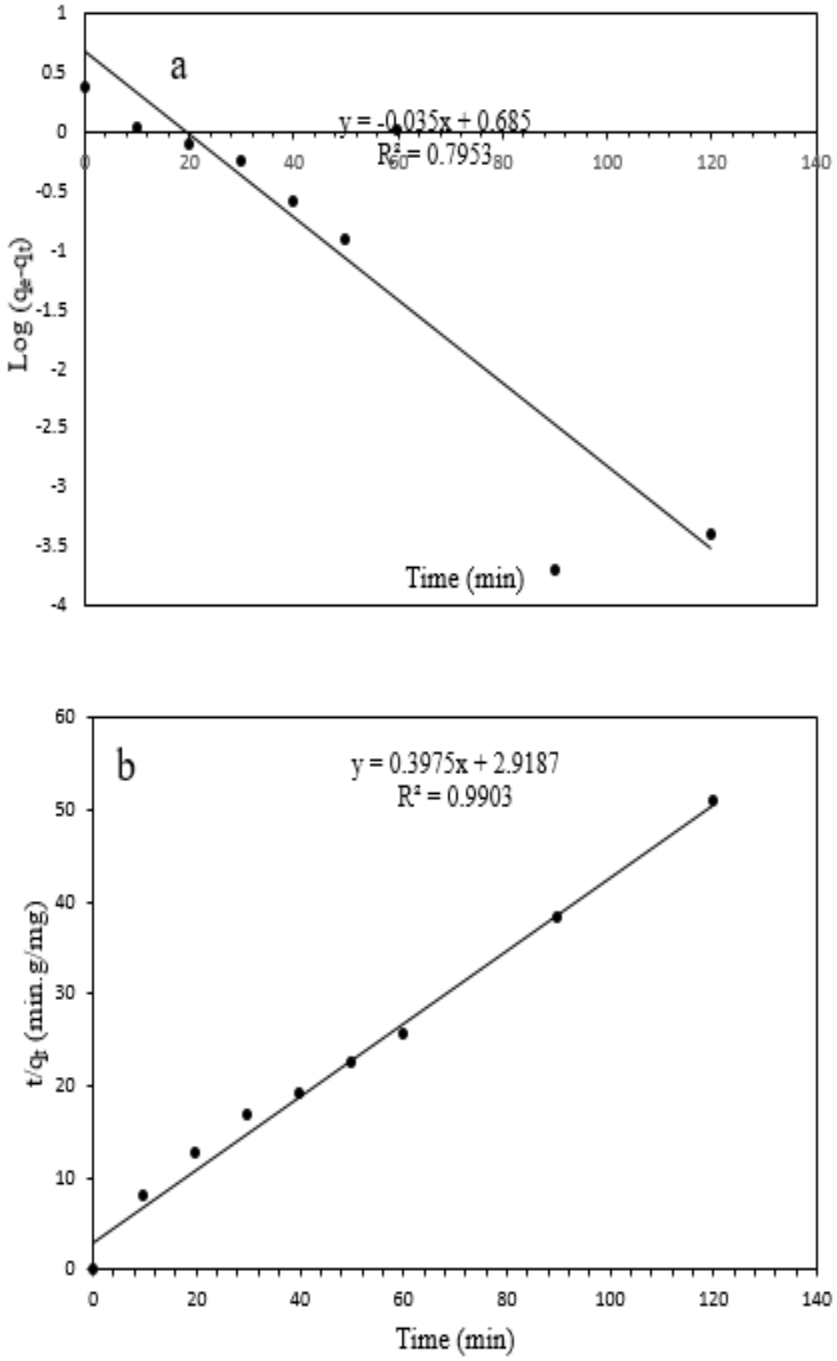


Fig. C 21 (a) Pseudo first-order of adsorption of DBT in diesel obtained before HDS (b) Pseudo second-order of adsorption of DBT in diesel obtained before HDS. Experimental conditions: Temperature 318 K, amount of adsorbent, 1.0 g, Vol of HDFD 20 mL, Initial sulfur concentration 120 mg/L

Continous packed bed model column

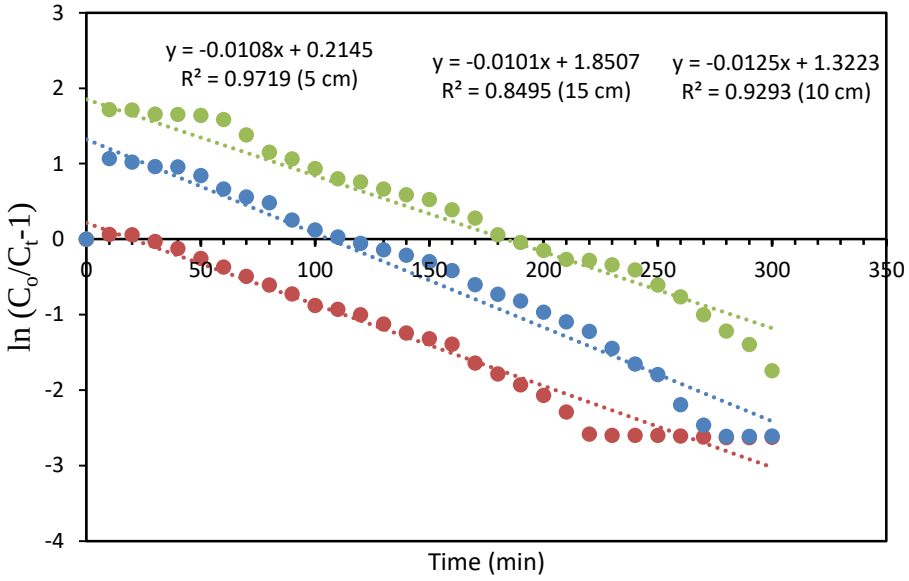


Fig. C 22 Thomas model for effect of bed height. Experimental conditions: Initial concentration: 100 mg/L; Flow rate 0.5 mL

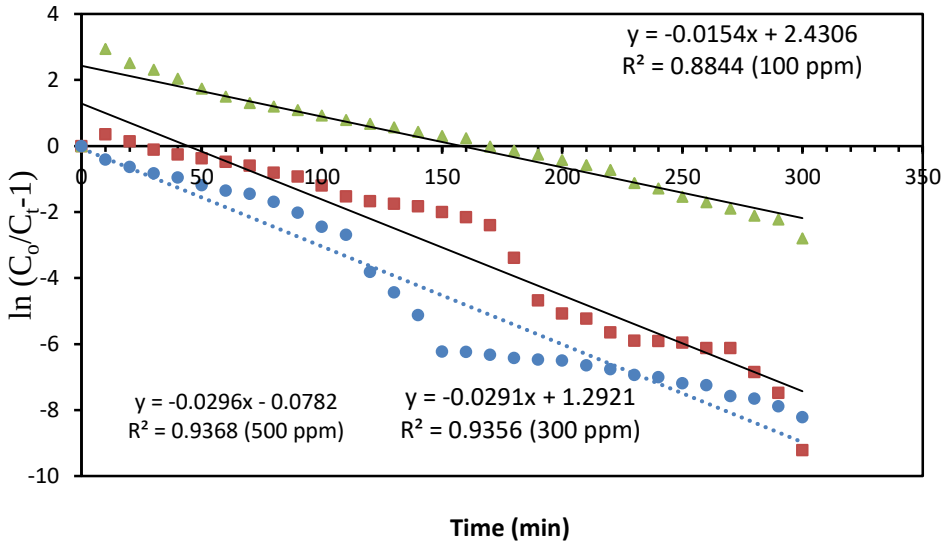


Fig. C 23 Thomas model for effect of initial concentrations. Experimental conditions: Bed height: 15 cm; Flow rate: 0.5 mL/min.

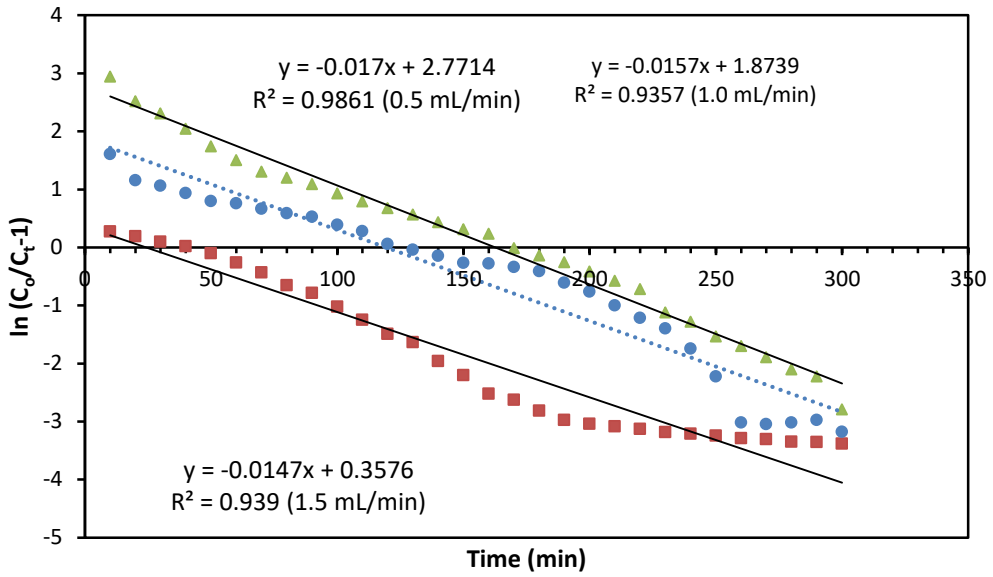


Fig. C 24 Thomas model for effect of flow rate. Experimental conditions: Bed height: 15 cm; Initial DTB concentration; 100 mg/L.

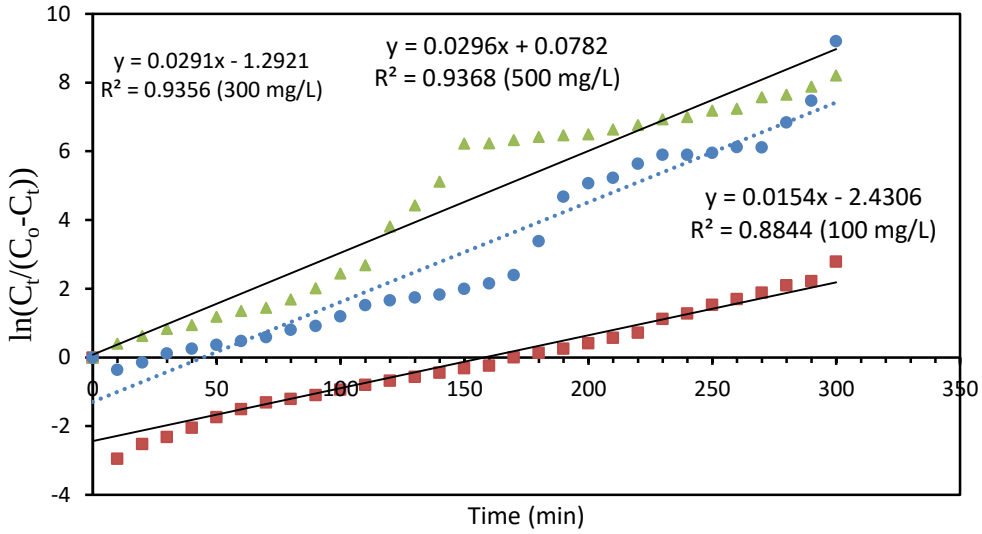


Fig C 25 Yoon-Nelson model for effect of initial concentration. Experimental conditions: flow rate 0.5 mL/min

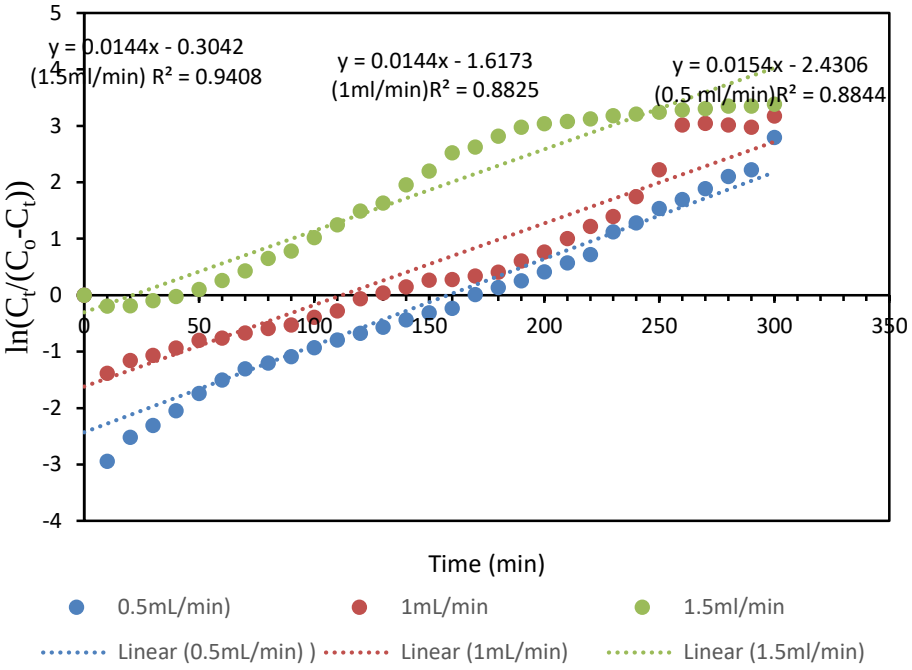


Fig. C 26 Yoon –Nelson model for effect of flow rate

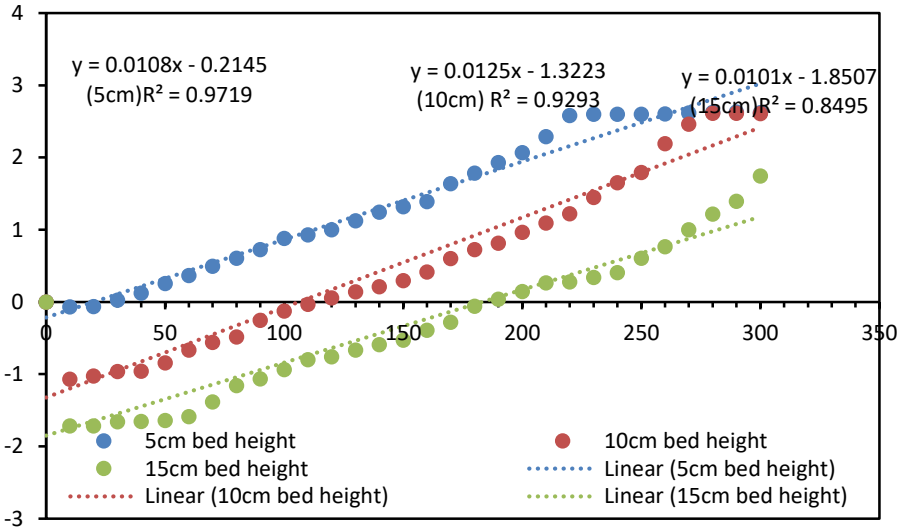


Fig. C 27 Yoon-Nelson model for effect of bed height

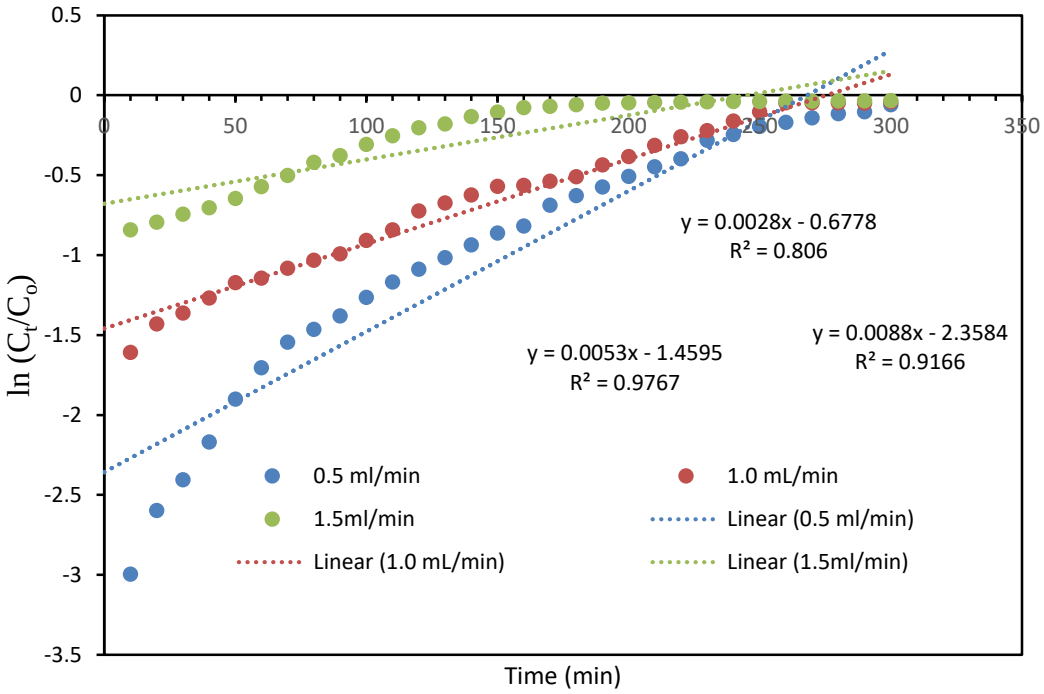


Fig. C 28 Bohart Adams model for effect of flow rate

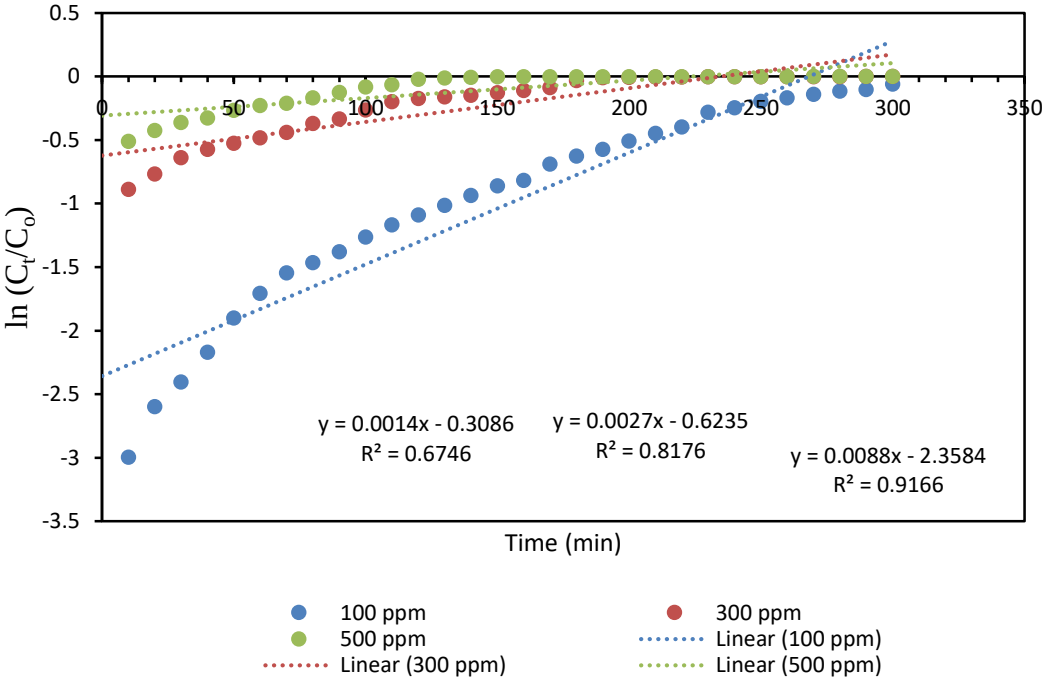


Fig. C 29 Bohart Adams model for effect of initial concentration

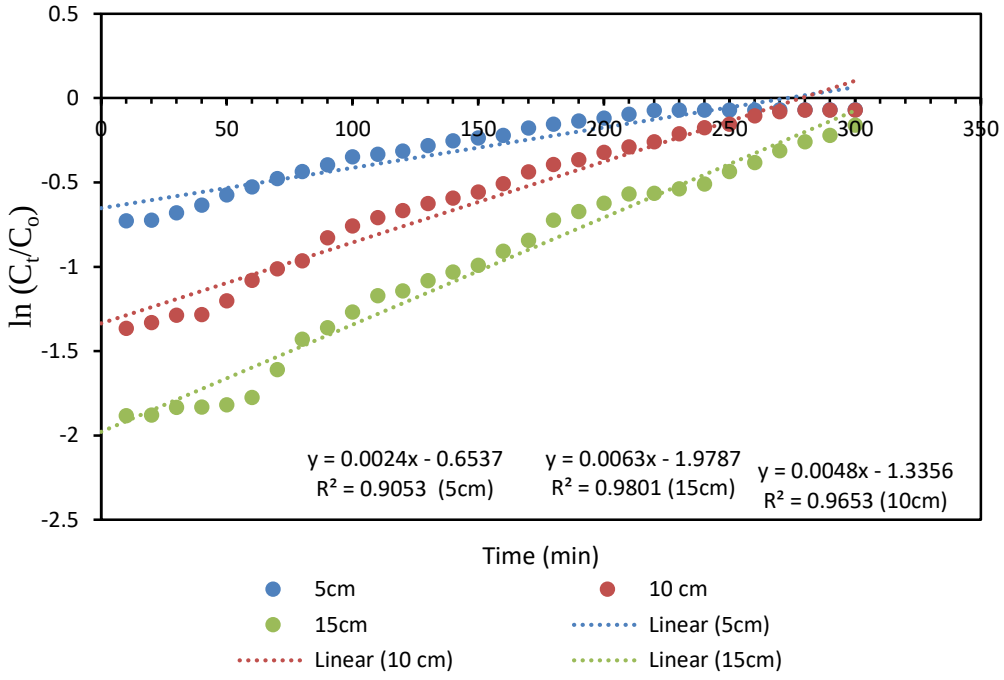


Fig. C 30 Bohart Adams model for effect of bed height

Appendix D: Published, in press articles and conference processdings